frontiers | Research Topics

Checkpoint immunotherapy: reshaping the landscape of gastrointestinal cancer treatment

Edited by
Stavros P. Papadakos, Stamatios E. Theocharis, Georgios Germanidis and Elias Kouroumalis

Published in
Frontiers in Immunology

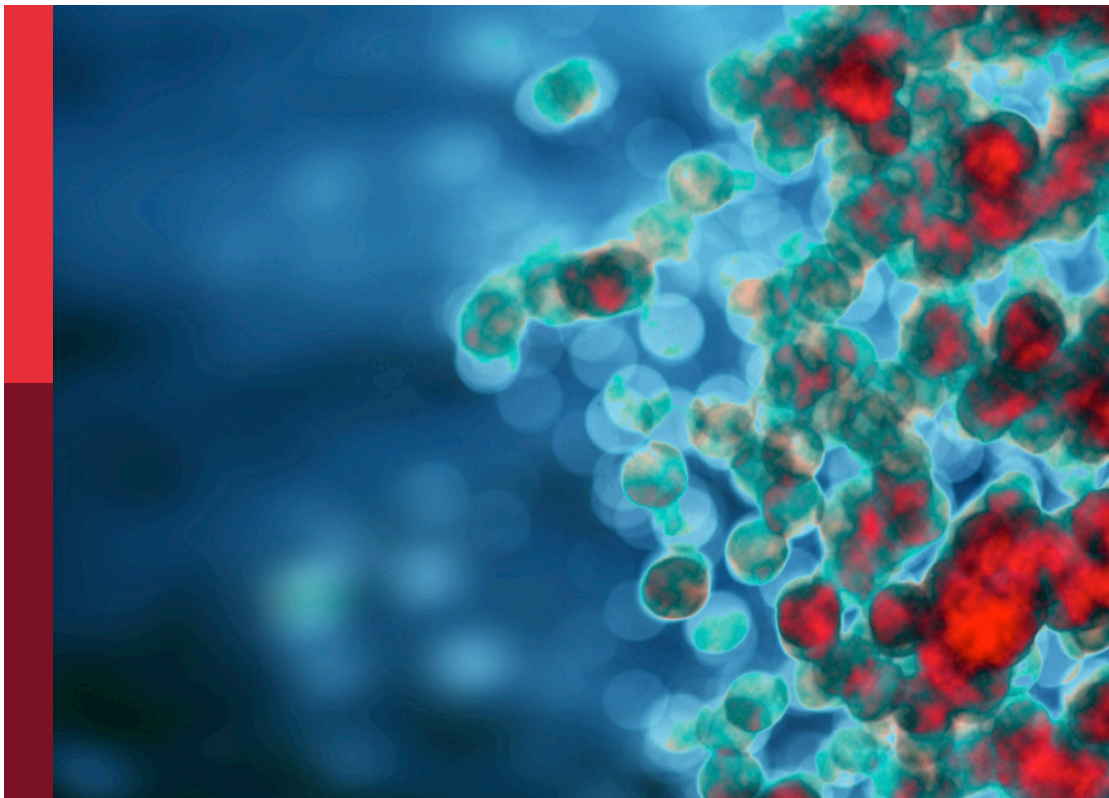

ISSN 1664-8714
ISBN 978-2-8325-7303-7
DOI 10.3389/978-2-8325-7303-7

Generative AI statement
Any alternative text (Alt text) provided alongside figures in the articles in this ebook has been generated by Frontiers with the support of artificial intelligence and reasonable efforts have been made to ensure accuracy, including review by the authors wherever possible. If you identify any issues, please contact us.

About Frontiers

Frontiers is more than just an open access publisher of scholarly articles: it is a pioneering approach to the world of academia, radically improving the way scholarly research is managed. The grand vision of Frontiers is a world where all people have an equal opportunity to seek, share and generate knowledge. Frontiers provides immediate and permanent online open access to all its publications, but this alone is not enough to realize our grand goals.

Frontiers journal series

The Frontiers journal series is a multi-tier and interdisciplinary set of open-access, online journals, promising a paradigm shift from the current review, selection and dissemination processes in academic publishing. All Frontiers journals are driven by researchers for researchers; therefore, they constitute a service to the scholarly community. At the same time, the *Frontiers journal series* operates on a revolutionary invention, the tiered publishing system, initially addressing specific communities of scholars, and gradually climbing up to broader public understanding, thus serving the interests of the lay society, too.

Dedication to quality

Each Frontiers article is a landmark of the highest quality, thanks to genuinely collaborative interactions between authors and review editors, who include some of the world's best academicians. Research must be certified by peers before entering a stream of knowledge that may eventually reach the public - and shape society; therefore, Frontiers only applies the most rigorous and unbiased reviews. Frontiers revolutionizes research publishing by freely delivering the most outstanding research, evaluated with no bias from both the academic and social point of view. By applying the most advanced information technologies, Frontiers is catapulting scholarly publishing into a new generation.

What are Frontiers Research Topics?

Frontiers Research Topics are very popular trademarks of the *Frontiers journals series*: they are collections of at least ten articles, all centered on a particular subject. With their unique mix of varied contributions from Original Research to Review Articles, Frontiers Research Topics unify the most influential researchers, the latest key findings and historical advances in a hot research area.

Find out more on how to host your own Frontiers Research Topic or contribute to one as an author by contacting the Frontiers editorial office: frontiersin.org/about/contact

Checkpoint immunotherapy: reshaping the landscape of gastrointestinal cancer treatment

Topic editors

Stavros P. Papadakos — Laiko General Hospital of Athens, Greece
Stamatios E. Theocharis — National and Kapodistrian University of Athens, Greece
Georgios Germanidis — University General Hospital of Thessaloniki AHEPA, Greece
Elias Kouroumalis — University of Crete, Greece

Citation

Papadakos, S. P., Theocharis, S. E., Germanidis, G., Kouroumalis, E., eds. (2026). *Checkpoint immunotherapy: reshaping the landscape of gastrointestinal cancer treatment*. Lausanne: Frontiers Media SA. doi: 10.3389/978-2-8325-7303-7

Table of contents

frontiers | Frontiers in Immunology

TYPE Editorial
PUBLISHED 08 December 2025
DOI 10.3389/fimmu.2025.1723645

OPEN ACCESS

EDITED AND REVIEWED BY
Adriana Albini,
European Institute of Oncology IEO (IRCCS), Italy

*CORRESPONDENCE
Stavros P. Papadakos
stavrospapadakos@gmail.com

RECEIVED 12 October 2025
ACCEPTED 21 October 2025
PUBLISHED 08 December 2025

CITATION
Papadakos SP, Kouroumalis E, Germanidis G and Theocharis S (2025) Editorial: Checkpoint immunotherapy: reshaping the landscape of gastrointestinal cancer treatment. *Front. Immunol.* 16:1723645. doi: 10.3389/fimmu.2025.1723645

Editorial: Checkpoint immunotherapy: reshaping the landscape of gastrointestinal cancer treatment

Stavros P. Papadakos[1,2*], Elias Kouroumalis[3], Georgios Germanidis[4,5] and Stamatios Theocharis[1]

[1]First Department of Pathology, Medical School, National and Kapodistrian University of Athens, Athens, Greece, [2]First Academic Department of Gastroenterology, Medical School of National and Kapodistrian University of Athens, General Hospital of Athens "Laiko", Athens, Greece, [3]Department of Gastroenterology, Panepistimiako Geniko Nosokomeio Irakleiou (PAGNI) University Hospital, University of Crete Medical School, Heraklion, Greece, [4]Division of Gastroenterology and Hepatology, First Department of Internal Medicine, American Hellenic Educational Progressive Association (AHEPA) University Hospital, Aristotle University of Thessaloniki, Thessaloniki, Greece, [5]Basic and Translational Research Unit, Special Unit for Biomedical Research and Education, School of Medicine, Faculty of Health Sciences, Aristotle University of Thessaloniki, Thessaloniki, Greece

KEYWORDS

immune checkpoint inhibitors, gastrointestinal cancers, tumor regression, organ preservation, biomarkers

Editorial on the Research Topic
Checkpoint immunotherapy: reshaping the landscape of gastrointestinal cancer treatment

Immune checkpoint inhibitors (ICIs) targeting PD-1, PD-L1, and CTLA-4 have become standard treatments for advanced gastric, biliary tract, and colorectal cancers, significantly extending survival, achieving tumor regression, and enhancing organ preservation, particularly in dMMR/MSI-H subtypes (1–4). These therapies enable conversion of unresectable to resectable disease, as seen in gastric and colorectal cancers, and improve quality of life by reducing recurrence and supporting organ-sparing approaches. This editorial synthesizes contributions from recent studies in *Frontiers in Immunology*, highlighting the clinical utility of ICIs across key GI cancers, including gastric/gastroesophageal junction (GC/GEJ) cancer, hepatocellular carcinoma (HCC), biliary tract cancer (BTC), colorectal/rectal cancer (CRC/RC), and esophageal squamous cell carcinoma (ESCC). This editorial also situates these advancements within the broader immunotherapy landscape.

Clinical utility of immunotherapy in GI cancers

ICIs have demonstrated robust clinical benefits across GI cancers, transforming treatment strategies and outcomes.

Gastric/gastroesophageal junction cancer

ICIs significantly enhance outcomes in advanced GC/GEJ. Xu et al. demonstrated that first-line ICI plus chemotherapy extends progression-free survival (PFS) to 357 days versus 270 days for chemotherapy alone, with a disease control rate (DCR) of 38% versus 14.5% and manageable adverse events (AEs). Neoadjuvant immunochemotherapy achieves remarkable responses: Sun et al. reported the first pathological complete response (pCR) in synchronous multiple gastric cancer (SMGC) using tislelizumab plus SOX, enabling R0 resection. Similarly, Li et al. documented tumor regression in hepatoid adenocarcinoma of the stomach (HAS), reducing serum AFP levels from 52,951.56 ng/mL to 241.04 ng/mL with sintilimab plus SOX, facilitating curative surgery. Li et al. demonstrated that hyperbaric oxygen therapy (HBOT) with CAPOX and sintilimab yields a clinical complete response (cCR) in advanced HAS with peritoneal metastasis, highlighting a novel approach to overcoming therapeutic resistance in advanced gastric cancer. Yang et al. identified blood-based biomarkers (e.g., CA125, CA199, and PLR) that predict ICI response, improving patient selection. These findings underscore the role of ICIs in prolonging survival, addressing mechanisms of therapeutic resistance in GC/GEJ.

Hepatocellular carcinoma

ICIs improve HCC outcomes when combined with targeted therapies. Liang et al. reported that postoperative hepatic arterial infusion chemotherapy (HAIC) with lenvatinib and PD-1 inhibitors significantly enhances disease-free survival (DFS) in solitary, large HCC, with no increase in hepatic toxicity, leveraging systemic immune activation to reduce recurrence. Hochnadel et al. identified novel T-cell inhibitory targets (Ngp, Hba-a1, and S100a8) via RNAi screening, with S100A8/S100A9 upregulated in human HCC, offering new immunotherapeutic possibilities. These studies highlight ICIs' ability to extend survival and introduce novel targets in HCC.

Biliary tract cancer

ICIs are a cornerstone of advanced BTC treatment. Zheng et al. reported a median overall survival (OS) of 15.7 months and a PFS of 8.4 months with first-line ICIs, with an 8.6% incidence of grade 3–4 immune-related AEs, indicating manageable toxicity. Durvalumab shows numerically superior OS compared to sintilimab, suggesting subtype-specific efficacy. These results affirm the robust survival benefits of ICIs in BTC, particularly in first-line settings.

Colorectal/rectal cancer

Immunotherapy excels in dMMR/MSI-H CRC, with Deng et al. reporting a 75% pCR rate with neoadjuvant ICI therapy, particularly with dual PD-1/CTLA-4 blockade (nivolumab plus ipilimumab), which enables organ preservation. Zhang et al. extended these benefits to pMMR/MSS rectal cancer, achieving a 37% pCR rate and a 77% anal preservation rate with neoadjuvant immunotherapy, thus expanding its utility to a resistant subtype. These findings emphasize the role of ICIs in achieving tumor regression and supporting organ-sparing strategies in CRC/RC.

Esophageal squamous cell carcinoma

Feng et al. demonstrated that adjuvant immunotherapy after neoadjuvant immunochemotherapy and esophagectomy improves DFS (38.5% vs. 23.9%) and OS (61.5% vs. 37.0%) in ypT+N+ ESCC patients, reducing the risk of recurrence. This sequential approach highlights the value of ICI in improving long-term outcomes in ESCC.

Key research themes

Combination therapies

Combining ICIs with other modalities enhances efficacy. Zhang et al. reported a 33.3% tumor regression grade (TRG) 0/1 rate with trastuzumab plus chemoimmunotherapy in HER2-positive gastric cancer, supporting its neoadjuvant role. Wei et al. proposed a phase II trial of nab-paclitaxel plus cadonilimab for second-line GC post-immunochemotherapy failure, exploring immune rechallenge to restore anti-tumor responses. This trial investigated potential biomarkers, such as ctDNA and TMB, to identify responsive patients. Li et al. introduced HBOT as an immunosensitizing strategy, achieving cCR in HAS by alleviating tumor hypoxia, which suppresses immune responses in the tumor microenvironment (TME). These studies demonstrate how combinations address resistance and improve outcomes.

Biomarker discovery

Biomarker identification is pivotal for precision medicine. Wen et al. developed a four-gene liquid-liquid phase separation (LLPS) signature (DACT1, EZH2, PAK2, and PSPC1) for gastric cancer prognosis, with PSPC1 knockdown inhibiting tumor proliferation, suggesting it could be a therapeutic target. Hochnadel et al. identified Ngp, Hba-a1, and S100a8 as T-cell inhibitors in HCC. These inhibitors were validated in human samples and open new immunotherapeutic avenues. Yang et al. used peripheral blood markers (e.g., pre-IBIL, post-CA125, and CA199) to predict ICI outcomes in GC/GEJ cancer, enhancing patient stratification. These advances enable tailored treatment by identifying responsive patients.

Cost-effectiveness

Economic analyses address ICI accessibility. Lang et al. found that cadonilimab plus chemotherapy is cost-effective for GC

patients with PD-L1 CPS ≥5 in China (ICER: $37,499.27/QALY), but not without price reductions. Zhou et al. reported similar findings for HER2-negative GC/GEJ cancer, with ICERs exceeding willingness-to-pay thresholds, highlighting the need for pricing reforms to ensure equitable access, particularly in resource-limited settings.

Systematic reviews

Zhang et al. conducted a meta-analysis of neoadjuvant immunotherapy in pMMR/MSS rectal cancer, reporting a 37% pCR rate and a 77% anal preservation rate, with short-course radiotherapy and PD-1 inhibitors outperforming alternative treatment options. This study supports the broader application of immunotherapy in challenging subtypes, complementing clinical findings with robust evidence.

Broader context and future directions

These studies highlight the transformative impact of ICIs on GI cancer management, achieving prolonged survival, tumor regression, and organ preservation across diverse malignancies. Combination therapies, such as ICIs with chemotherapy, targeted agents, or HBOT, address resistance mechanisms, particularly in immunologically "cold" tumors, such as HAS, where hypoxia and immunosuppressive TMEs limit efficacy (Li et al., Li et al.). Neoadjuvant and adjuvant strategies, as seen in ESCC and CRC, reduce recurrence rates and enable organ-sparing surgeries, improving quality of life. Biomarker research, including LLPS signatures and novel T-cell targets, advances precision medicine, while real-world studies validate clinical trial findings in diverse populations.

However, challenges persist, including tumor heterogeneity, ICI resistance, and high costs. Heterogeneity, as seen in SMGC and HAS, complicates treatment responses due to interlesional variability (Sun et al.). Resistance, driven by immunosuppressive TMEs and low tumor mutational burden, limits efficacy in pMMR/MSS cancers, necessitating strategies such as HBOT or immune rechallenge (Wei et al.). High costs, as noted by Lang et al. and Zhou et al., restrict access, particularly in low-resource settings, requiring pricing reforms and global health policy initiatives.

Future research should focus on overcoming resistance through TME modulation. This can be achieved through HBOT, vascular normalization, or novel immune agonists to enhance ICI penetration and immune activation. Validating biomarkers such as TMB, MSI, ctDNA, and peripheral blood markers will improve patient selection, as emphasized by Yang et al. and Wen et al.,. Prospective trials, such as those proposed by Wei et al. and Li et al., are critical to confirming the efficacy of immune rechallenge and adjuncts such as HBOT Multi-omics approaches integrating genomics, transcriptomics, and proteomics will refine personalized treatment, while real-world evidence will validate these approaches in clinical practice.

Conclusion

This Research Topic underscores the profound impact of checkpoint immunotherapy on GI cancer management, demonstrating significant clinical benefits, innovative combination strategies, and biomarkers for personalized care. By addressing efficacy, safety, and accessibility, these findings pave the way for more effective and equitable treatments, inspiring continued innovation to improve outcomes for GI cancer patients worldwide.

Author contributions

SP: Writing – review & editing, Writing – original draft. EK: Writing – original draft, Writing – review & editing. GG: Writing – original draft, Writing – review & editing. ST: Writing – original draft, Writing – review & editing.

Conflict of interest

The authors declare that the research was conducted in the absence of any commercial or financial relationships that could be construed as a potential conflict of interest.

Generative AI statement

The author(s) declare that Generative AI was used in the creation of this manuscript. Generative AI was used solely for language polishing to enhance clarity and readability.

Any alternative text (alt text) provided alongside figures in this article has been generated by Frontiers with the support of artificial intelligence and reasonable efforts have been made to ensure accuracy, including review by the authors wherever possible. If you identify any issues, please contact us.

Publisher's note

References

1. Gao Z, Wang X, Song T, Wu S, Jin X. Real world effectiveness of chemotherapy plus bevacizumab with immunotherapy in colorectal cancer. *Sci Rep*. (2025) 15:29170. doi: 10.1038/s41598-025-13701-0

2. Chan SL, Lamarca A, Hsu C, Moreno V, Chan LL, Keenan BP. New targets and new drugs for hepatobiliary cancers. *J Hepatol*. (2025). doi: 10.1016/j.jhep.2025.08.018 [Epub ahead of print].

3. Papadakos SP, Argyrou A, Michailidou E, Papatheodoridis GV. C-Reactive Protein and Management of Hepatocellular Carcinoma: Bridging Systemic Inflammation and Clinical Prognosis. *Liver Int*. (2025) 45:e70278. doi: 10.1111/liv.70278

4. Wang Z, Wang T. Mechanisms, advances, and challenges of immunotherapy in gastric cancer. *Front Immunol*. (2025) 16:1639487. doi: 10.3389/fimmu.2025.1639487

frontiers | Frontiers in Immunology

TYPE Original Research
PUBLISHED 27 September 2024
DOI 10.3389/fimmu.2024.1466497

OPEN ACCESS

EDITED BY
Stavros P. Papadakos,
Laiko General Hospital of Athens, Greece

REVIEWED BY
Mariana Pavel-Tanasa,
Grigore T. Popa University of Medicine and Pharmacy, Romania
Guillaume Mestrallet,
Icahn School of Medicine at Mount Sinai, United States

*CORRESPONDENCE
Cheng Luo
figaro123@126.com
Bo Song
bo_yuejun@163.com

†These authors have contributed equally to this work

RECEIVED 18 July 2024
ACCEPTED 12 September 2024
PUBLISHED 27 September 2024

CITATION
Deng Z, Luo Y, Chen X, Pan T, Rui Y, Hu H, Yan J, Zhang K, Luo C and Song B (2024) Pathological response following neoadjuvant immunotherapy and imaging characteristics in dMMR/MSI-H locally advanced colorectal cancer. *Front. Immunol.* 15:1466497. doi: 10.3389/fimmu.2024.1466497

Pathological response following neoadjuvant immunotherapy and imaging characteristics in dMMR/MSI-H locally advanced colorectal cancer

Zijian Deng[1†], Yajun Luo[1†], Xiaoli Chen[2], Tao Pan[1], Yuanyi Rui[1], Hai Hu[1], Jin Yan[1], Ke Zhang[1], Cheng Luo[3*] and Bo Song[1*]

[1]Department of Colorectal Surgery, Sichuan Cancer Hospital & Institute, Sichuan Cancer Center, Cancer Hospital Affiliated to University of Electronic Science and Technology of China, Chengdu, China, [2]Department of Imaging Department, Sichuan Cancer Hospital & Institute, Sichuan Cancer Center, Cancer Hospital Affiliated to University of Electronic Science and Technology of China, Chengdu, China, [3]Department of Pharmacy, West China Second University Hospital, Sichuan University, Chengdu, China

Background: In recent years, there has been significant research interest in immunotherapy for colorectal cancer (CRC). Specifically, immunotherapy has emerged as the primary treatment for patients with mismatch repair gene defects (dMMR) or microsatellite highly unstable (MSI-H) who have colorectal cancer. Yet, there is currently no data to support the practicality and safety of neoadjuvant immunotherapy for colorectal cancer with dMMR or MSI-H. Therefore, a study was conducted to identify the postoperative pathology, safety profile, and imaging features of patients with dMMR or MSI-H CRC following neoadjuvant immunotherapy.

Methods: The retrospective study was carried out on patients with locally advanced or metastatic CRC who received immunotherapy at Sichuan Cancer Hospital, with approval from the hospital's ethics committee. The study aimed to assess the short-term effectiveness of immunotherapy by focusing on pathological complete response (pCR) as the primary outcome, while also considering secondary endpoints such as objective response rate, disease-free survival, and safety profile.

Results: Twenty patients with dMMR/MSI-H CRC who underwent neoadjuvant immunotherapy as part of the treatment were enrolled between May 2019 and February 2024 at Sichuan Cancer Hospital. Out of these patients, eight patients received PD-1 blockade monotherapy as neoadjuvant treatment, while 12 were administered a combined therapy of anti-CTLA-4 and anti-PD-1. 12 patients received Nivolumab plus Ipilimumab regimen and 8 patients received PD-1 blockades (2 patients were Pembrolizumab, 2 patients were Sintilimab, 4 patients were Tislelizumab) monotherapy. Additionally, 19 patients underwent surgery after immunotherapy and of these, 15 (75.0%) achieved complete pathological response (pCR), 8 (66.7%) achieved the same on Nivolumab plus Ipilimumab immunotherapy while 7 (87.5%) achieved on PD-1 antibody monotherapy. The overall response rate (ORR) was 75%, with 45.0% of patients experiencing grade I/II immunotherapy-related adverse events. The most

frequent adverse event observed was increased ALT i.e. 20%. Notably, no postoperative complications were observed.

Conclusion: Based on the findings, neoadjuvant immunotherapy for colorectal cancer may be both safe and effective in clinical practice. Furthermore, the study suggested that dual immunotherapy could potentially increase the immunotherapy cycle and contribute to a superior pCR rate. However, the conclusion emphasized the need for further prospective clinical trials to validate these results.

KEYWORDS

colorectal cancer, mismatch repair gene defects, microsatellite highly unstable, PCR, neoadjuvant immunotherapy, PD-1

1 Introduction

Colorectal cancer (CRC) is the third most common form of cancer and the second leading cause of cancer-related deaths worldwide (1). Mismatch repair deficiency (dMMR) occurs in 4–5% of all metastatic colorectal cancers (mCRC) (2, 3). Patients with dMMR/MSI-H CRC have certain characteristics such as poor differentiation, mucinous histology, increased tumor-infiltrating lymphocytes, and a Crohn's like lymphocytic reaction (4–6). Previous studies have shown that neoadjuvant immunotherapy for CRC is safe and efficacious (7). Neoadjuvant immunotherapy demonstrated promising outcomes in dMMR or MSI-H CRC, especially in rectal cancer patients. Neoadjuvant immunotherapy may lead to a sustained clinical complete response, allowing for organ preservation and avoiding adverse effects on fertility, sexual function, bowel and bladder function after surgery and radiotherapy.

These immunogenic traits make dMMR/MSI-H CRC respond well to treatment with anti-programmed death-1 (PD-1) checkpoint inhibitors. In 2018, PD-1 blockades gained approval for treating metastatic dMMR/MSI-H CRC after standard chemotherapy in the United States (7). The KEYNOTE-016 study showed that dMMR mCRC might benefit from Pembrolizumab (PD-1 inhibitor) monotherapy (5). Subsequently, the CheckMate142 study showed that recurrent dMMR and MSI-H mCRC could benefit from Nivolumab (a PD-1 inhibitor) and Ipilimumab (a CTLA-4 inhibitor) (8). Based on these studies, the Chinese Society of Clinical Oncology guidelines recommend an immune checkpoint inhibitor (ICI) as the second and third-line treatment of dMMR and MSI-H mCRC (9). Following the results of the KEYNOTE-177 study, pembrolizumab was proven to be an effective first-line treatment option in patients with dMMR/MSI-H CRC (10).

Regarding, immunotherapy in perioperative treatment among dMMR CRC, the results of the NICHE 2 study showed high rates of pathological response i.e. 95% (105/111), and complete response 68% (75/111) (11). PD-1 blockade for 6 months alone yields durable recurrence-free responses and provides the potential feasibility for dMMR colon cancer patients to enter a wait-and-watch strategy after neoadjuvant immunotherapy, thereby enabling patients to obtain the benefits of organ function preservation and avoiding the injury and complications caused by surgery (12).

However, data on neoadjuvant immunotherapy for locally advanced or metastatic CRC remained limited. The pCR rate in different clinical trials varied, and whether it was related to the immunotherapy use cycle is still unknown. Here, we presented a study reporting subjects of neoadjuvant immunotherapy for dMMR/MSI-H CRC in our institution. This study was designed to evaluate the clinical features and short-term efficacy of neoadjuvant PD-1 blockade therapy in patients with locally advanced or resectable dMMR/MSI-H CRC. Our study aimed to elucidate the factors contributing to the discrepancy in pCR rate between single-agent and two-drug immunotherapy.

2 Methods

2.1 Patient selection

The following study was conducted in accordance with the STROBE guidelines (13). It retrospectively included patients with locally advanced or metastatic colorectal cancer (CRC) who received immunotherapy at Sichuan Cancer Hospital. The study was approved by the ethical committee of the Sichuan Cancer Hospital (Ethics Approval Number: SCCHEC-02-2024-069) and informed patient consent for this retrospective analysis was waived. The study enrolled 20 patients with dMMR/MSI-H CRC who underwent neoadjuvant immunotherapy between May 2019 and February 2024 at Sichuan Cancer Hospital. The main inclusion criteria included the pathological diagnosis of CRC with dMMR or MSI-H, clinical stage II~Iva, ECOG performance status of 0 or 1, and patients at least 18 years of age. The exclusion criteria included metastatic lesions that could not be resected prior to radiation therapy, chemotherapy, or surgery for a tumor, and active

autoimmune disease requiring systemic treatment or previous treatment with immune checkpoint inhibitors.

2.2 Data collection

The clinical features of the patients such as gender, age, family and personal history of malignant tumor, tumor site, degree of differentiation, clinical stage, pathological stage, MMR/MSI status, tumor regression grade (TRG), immunotherapy regimen, adverse events, postoperative complication were collected. All stages were performed following the eighth edition of the American Joint Committee on Cancer (AJCC) (14). Tumor specimen demonstrating mismatch repair deficiency by immunohistochemistry or microsatellite instability as demonstrated by Next Generation Sequence (NGS) or PCR (15).

2.3 Outcomes

The primary outcome of the study was pCR, defined as an absence of vital tumor cells in the sampled specimen after resection by pathological examination. Secondary endpoints included the objective response rate by the Response Evaluation Criteria in Solid Tumors RECIST Version 1.1 (RECIST 1.1), disease free survival, and adverse effects as per Common Terminology Criteria for Adverse Events version 5.0 criteria (16).

2.4 Immunotherapy regimen

Nivolumab was administered 3mg/kg for 2 cycles and ipilimab 1mg/kg for 1 cycle according to NICHE-2 study protocol. Patients using single-agent immunotherapy received 200mg intravenous infusion every three weeks until the tumor regressed to undergo radical resection. Surgery was performed within 4-6 weeks after the end of medication. PD-1 inhibitors were used in this study including pembrolizumab, sindillizumab and tislelizumab.

2.5 Treatment response

The efficacy of neoadjuvant immunotherapy was assessed by RECIST 1.1. Endoscopy and selective biopsy were performed to determine the presence of residual tumor. The pathologic efficacy indexes were ypTNM and TRG scores after immunotherapy. TRG pathological diagnostic criteria for rectal cancer were obtained based on the AJCC system (14). TRG MRI diagnostic criteria for rectal cancer were obtained based on pathological Mandard diagnostic criteria (17).

2.6 Statistical analysis

All continuous data was expressed as median with range, presenting other discrete variables as counts and percentages, and using the software program SPSS version 29 (SPSS Inc., Chicago, IL, version 26.0 for Mac) for statistical analysis. Student's t-test was used to analyze imaging size changes of tumor and lymph nodes before and after treatment. Univariate analyses were performed to analyze the relationship between baseline characteristics and pCR using a logistic regression model. The expected sample size was calculated according to the alternative hypothesis that the PCR with neoadjuvant immunotherapy would be 60% or higher (H1 = 60%) and the null hypothesis that the PCR after nCRT was 25% (H0 = 25%) (18, 19). With α of 5% and power of 90%, 18 cases would be recruited. A total of 20 patients were recruited with dropout incidence of 10%. $P<0.05$ was considered statistically significant.

3 Results

3.1 Characteristics of the patients

A total of 20 patients with dMMR/MSI-H CRC were included in the study. There was one patient with stage II disease, 16 with stage III, and 3 with stage IV. 85% of the patients had adenocarcinoma and 65% had colon cancer. Among the stage IV patients: one had postoperative recurrence of colon cancer with liver metastasis, where both the primary lesion and metastasis were resected. Another presented with isolated retroperitoneal lymph node metastasis following right hemicolectomy and the third had colon splenic carcinoma with isolated liver metastasis. 20 patients were diagnosed with dMMR by IHC and 12 patients were detected as MSI-H by PCR. Detailed characteristics are outlined in Table 1.

All patients underwent immunohistochemical testing for dMMR, and some also underwent MSI gene or NGS testing to confirm MSI-H status. Eight patients received PD-1 blockade monotherapy as neoadjuvant treatment, while 12 patients received a combination of anti-PD-1 and anti-CTLA-4 treatment (Table 2). Patients receiving nivolumab plus ipilimumab underwent surgery after 2 treatment cycles, whereas median cycle of single-agent immunotherapy was 5.14 (95%CI, 2.00-8.28). Five patients underwent preoperative chemotherapy, lasting 1-3 cycles, and three patients had received chemotherapy at other hospitals before admission. Additionally, two patients underwent preoperative chemotherapy while awaiting genetic test results. Multiple organ resection was performed in two cases. Notably, Patient 1 had concurrent ascending colon and rectal cancer; pathological and genetic tests showed pMMR and MSS in a patient with elevated colon cancer post-surgery.

3.2 Efficacy of neoadjuvant immunotherapy

Out of the 20 patients enrolled, 19 underwent radical surgery. One patient with anorectal carcinoma achieved imaging PR and opted for observation due to anal retention issues before proceeding with surgical treatment. Among the surgical patients, 15 out of 20 achieved a complete pathological response (Figure 1A). Specifically, 7 out of 8 (87.5%) patients who received PD-1 blockades monotherapy achieved a complete pathological response. The

TABLE 1 Baseline clinicapathological characteristic of total patients.

Characteristic	NO. (%)
Age (year)	56 (27–71)
Sex	
Male	11 (55)
Female	9 (45)
Tumor site	
Colon	13 (65)
Rectum	5 (25)
Multiple primary colorectal cancer	2 (10)
Histological Grade	
Medium or Well-differentiated	NA
Poor differentiated	6 (30)
Pathological type	
Adenocarcinoma	17 (85)
Mucinous adenocarcinoma	3 (15)
Drug of ICB	
Single-agent	8 (40)
Two-drug	12 (60)
Loss of expression of MMR proteins	
MSH2 only	4 (20)
PMS2 only	2 (10)
MLH1 and PMS2	7 (35)
MSH2 and MSH6	4 (20)
MSH1, MSH2 and PMS2	2 (10)
MSI status	
MSI-H	12 (60)
Not tested	8 (40)
Pathological TNM Stage	
II	1 (5)
III	16 (80)
IVa	3 (15)
Liver only	2
Distant Lymph Node only	1

NA, not avaliable.

radiological and pathological responses of patient 2 in Table 2 following immunotherapy adjuvant therapy are illustrated in Figure 2. Univariate analyses were performed to analyze the relationship between baseline characteristics and pCR by using a logistic regression model, and the results showed no statistical significance (Table 3). Additionally, 8 out of 12 (66.7%) patients achieved a complete pathological response with Nivolumab plus Ipilimumab therapy. Patient 9 in Table 2 attained complete pathological response, and the radiological and pathological response to nivolumab plus ipilimumab adjuvant therapy were depicted in Figure 3.

3.3 Imaging response of tumor after neoadjuvant immunotherapy

The changes in imaging for the maximum length diameter and thickness of the primary lesion, as well as the short diameter of the largest lymph node, for the patients before and after treatment are presented in Table 4 and Figure 4. Out of 20 patients, 18 were assessable for the efficacy of neoadjuvant immunotherapy, resulting in an overall response rate (ORR), with 2 complete responses (75%) and 13 partial responses (65%) (Figure 1B). Imaging data was unavailable for 2 patients who were examined in other hospitals before treatment. The imaging evaluation was consistent with the pathological evaluation. In addition, one case (Patient 12 in Table 2) showed ineffective neoadjuvant immunotherapy, as indicated by tumor progression in a patient with mucinous adenocarcinoma, which was observed in the preoperative MRI. The radiological, colonoscopic, and pathological manifestations of this patient are illustrated in Figure 5 and were completely consistent with the postoperative pathology.

3.4 Safety and feasibility

Details of adverse events are mentioned in Table 5. All adverse events reported spontaneously by the patients or observed by the investigator were recorded during the period of study, with assessments conducted at each treatment cycle, regular follow-up visits, and through patient self-reports. Imaging and laboratory tests were conducted as clinically indicated to identify and grade immunotherapy-related adverse events (irAEs). Among the patients, 45.0% (9/20) experienced grade 1-2 irAEs. The most frequent irAE was ALT increased (20%). Among patients receiving PD-1 blockade monotherapy, 1 out of 8 (12.5%) experienced immune-related adverse reactions, while this rate was 8 out of 12 (66.6%) for patients receiving anti-PD-1 + anti-CTLA-4 immunotherapy. No perioperative deaths were reported, and no postoperative complications were found.

4 Discussion

The study examined colorectal cancer (CRC) patients with dMMR/MSI-H who received preoperative neoadjuvant immunotherapy at a single center through retrospective analysis. Among the 12 patients treated with dual immunotherapy, the rate of pathological complete response (pCR) was 66.7%, which is consistent with findings from the NICHE-2 study and prior research (11, 20, 21). Notably, the pCR rate was significantly high in patients receiving single-agent immunotherapy (87.5%). The adverse events were generally acceptable (Grade 1-2) and predominantly related to thyroid dysfunction. Thus, preoperative neoadjuvant immunotherapy seemed to be a beneficial and promising strategy.

10.3389/fimmu.2024.1466497

TABLE 2 Details of the 20 patients with neoadjuvant ICB therapy.

Patient	Age	Gender	MSI context	RAS/ RAF Mutation	Clinic TNM	Drug of ICB	Dose of ICB(mg)	Neoadjuvant Chemotheropy	Surgery
1	56	male	Lynch syndrome, dMMR	NA	cT3N0M0 and cT4aN1M0	Pembrolizumab	200 q3w*3	XELOX +Rectal radiotherapy	Anterior resection + Right hemicolectomy
2	53	female	Lynch syndrome, dMMR, MSI-H	NA	cT4aN2M0	Pembrolizumab	200 q3w*8	NO	Anterior resection + Hysterectomy and double adnexectomy
3	46	male	Sporadic, dMMR,	NA	cT4NxM1	Sintilimab	200 q3w*10	NO	Left hemicolectomy
4	37	male	Sporadic, dMMR,	NA	cT4bN1M1	Sintilimab	200 q3w	NO	Left hemicolectomy
5	50	female	Sporadic, dMMR,	NA	cT3-4aN1M0	Tislelizumab	200 q3w*2	XELOX*1	Right hemicolectomy
6	68	female	Sporadic, dMMR, MSI-H	KRAS	Retroperitoneal lymph node metastasis	Tislelizumab	200 q3w*2	FOLFIRI*1	Retroperitoneal lymphadenectomy
7	48	male	Sporadic, dMMR, MSI-H	NA	cT4bN1M0	Tislelizumab	200 q3w*8	XELOX*3	Radical resection of sigmoid carcinoma + partial cystectomy
8	27	female	Lynch syndrome, dMMR,	NA	cT3N1M0	Tislelizumab	200 q3w*3	NO	Watch and wait
9	71	male	Sporadic, dMMR, MSI-H	KRAS	cT3N1M0	Nivolumab plus ipilimumab	200 + 50	NO	Laparoscopic robot-assisted anterior rectal resection
10	59	male	Lynch syndrome, dMMR, MSI-H	NA	cT4aN1M0	Nivolumab plus ipilimumab	240 + 80	NO	Right hemicolectomy
11	35	male	Lynch syndrome, dMMR, MSI-H	NA	cT3N1M0	Nivolumab plus ipilimumab	240 + 50	NO	Right hemicolectomy
12	67	male	Lynch syndrome, dMMR, MSI-H	KRAS	cT4N1M0	Nivolumab plus ipilimumab	200 + 50	NO	Anterior resection
13	50	female	Sporadic, dMMR, MSI-H	NO	cT3N2M0	Nivolumab plus ipilimumab	200 + 50	FOLFOX*1 Before immunotherapy	Laparoscopic left hemicolectomy
14	34	female	Sporadic, dMMR, MSI-H	NA	cT3N1M0	Nivolumab plus ipilimumab	200 + 64	NO	Laparoscopic right hemicolectomy
15	47	male	Sporadic, dMMR, MSI-H	NA	cT4aN1M0	Nivolumab plus ipilimumab	200 + 65	NO	Laparoscopic left hemicolectomy
16	53	male	Sporadic, dMMR, MSI-H	KRAS	cT4aN1M0	Nivolumab plus ipilimumab	240 + 74	NO	Laparoscopic left hemicolectomy
17	57	female	Sporadic, dMMR, MSI-H	NA	cT4aN1M0	Nivolumab plus ipilimumab	150 + 50	NO	Laparoscopic left hemicolectomy

(Continued)

TABLE 2 Continued

Patient	Age	Gender	MSI context	RAS/ RAF Mutation	Clinic TNM	Drug of ICB	Dose of ICB(mg)	Neoadjuvant Chemotheropy	Surgery
18	42	male	Sporadic, dMMR, MSI-H	NA	cT3N1M0	Nivolumab plus ipilimumab	200 + 50	NO	Laparoscopic anterior rectal resection
19	34	male	Sporadic, dMMR, MSI-H	NA	cT3N1M0	Nivolumab plus ipilimumab	195 + 50	NO	Laparoscopic right hemicolectomy
20	37	female	Sporadic, dMMR, MSI-H	NA	cT4aN1M0	Nivolumab plus ipilimumab	200 + 44	NO	Laparoscopic right hemicolectomy

ICB, Immune Checkpoint Block; pCR, pathological complete response; PR, partial response; TRG, tumor regression grade; MSI, microsatellite instability; dMMR, mismatch repair-deficient. NA, not avaliable.

In a recent study, 16 dMMR patients with locally advanced rectal cancer were treated with dostarlimab (a PD-1 inhibitor) monotherapy for six months (22). All twelve patients who completed the entire treatment regimen achieved complete clinical response (cCR) without requiring chemoradiotherapy or surgery, and there was no reported progression or recurrence during 6-25 months of follow-up (22). Another study enrolled 34 patients with dMMR or MSI-H locally advanced CRC, and they were randomized to receive either Toripalimab (a PD-1 inhibitor) monotherapy (17 cases) or triplimumab combined with Celecoxib (a COX-2 inhibitor) (17 cases) (23). The pCR was notably high at 88% in the triplimumab combined with the Celecoxib group and 65% in the triplimumab monotherapy group (23). Our study demonstrated a pCR of 75.0% among 19 patients who underwent surgery. These findings suggested that neoadjuvant immunotherapy plus COX-2 inhibitors might be a promising option for CRC patients, particularly those for whom anus preservation is challenging. Notably, a female patient, aged 27, with anorectal carcinoma is currently undergoing treatment, and the possibility of adding COX-2 inhibitors to neoadjuvant immunotherapy is

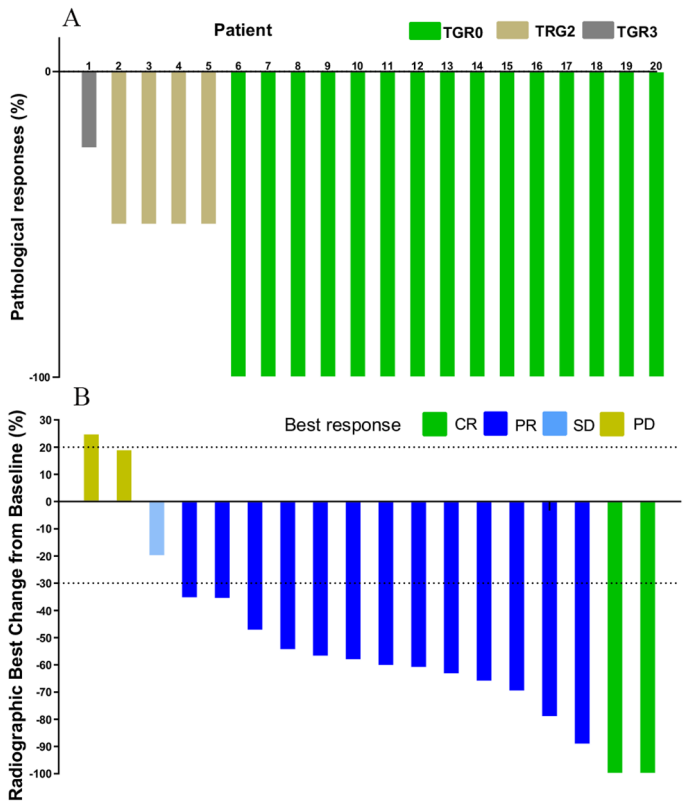

FIGURE 1
Waterfall plot of efficacy evaluation of neoadjuvant immunotherapy in dMMR/MSI-H CRC. **(A)** Pathological responses(n=20); **(B)** Radiographic responses (n=18).

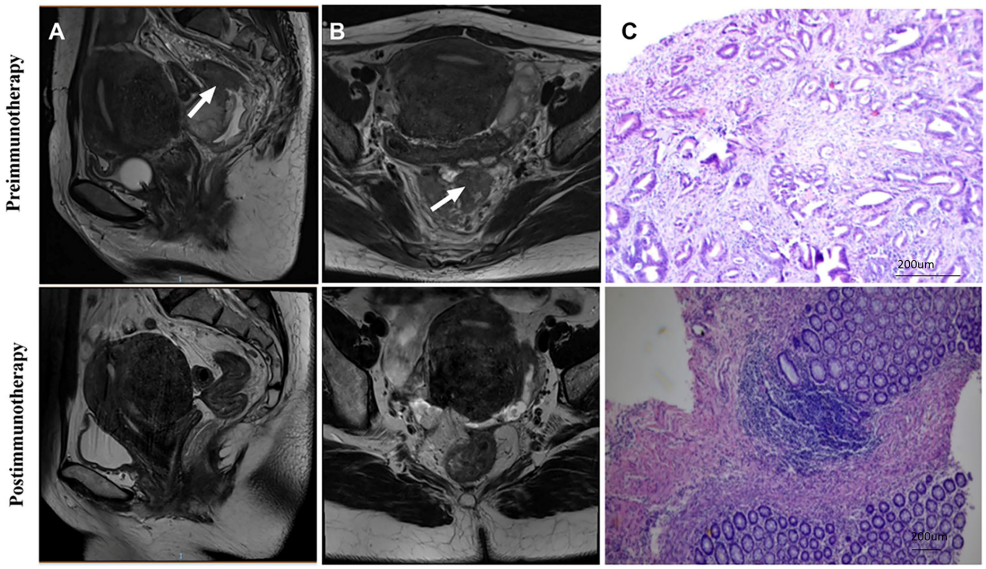

FIGURE 2
Radiological and pathological responses of 1 pCR patient to monotherapy immunotherapy neoadjuvant therapy (Patient 2 in Table 2). **(A)** Sagittal MR View of the pelvis: before immunotherapy VS after immunotherapy; **(B)** MR View of the axial plane of the pelvis: before immunotherapy VS after immunotherapy; **(C)** Pre-biopsy (HE) VS post-biopsy (HE): pre-immunotherapy vs post-immunotherapy. pCR, pathological complete response; MR, magnetic resonance; HE, hematoxylin-eosin.

under consideration pending further discussions by our multidisciplinary team, as 4 patients in our study did not achieve a complete pathological response despite multidisciplinary team deliberations.

Moreover, none of these patients achieved cCR based on imaging evaluations, and two patients showed disease progression according to imaging assessments. This underscores the importance of comprehensive pre-treatment evaluations, especially in genetically confirmed MSI-H patients. For patients with radiographically evident mucinous adenocarcinoma, the likelihood of poor treatment response should be anticipated. In such cases, adding chemotherapy during immunotherapy or expediting surgery might be warranted.

Interestingly, the pCR among CRC patients treated with nivolumab plus ipilimumab was lower compared to single-drug immunotherapy. Patients receiving nivolumab plus ipilimumab underwent surgery after 2 treatment cycles, whereas median cycle of single-agent immunotherapy was 5.14, potentially reflects insufficient treatment duration with nivolumab plus ipilimumab. Our study results aligned with the NICHE-2 study, showing a 66.7% pathological response rate with ipilimumab plus nivolumab (The NICHE-2 study reported 68% (11, 20)). Currently, there is no consensus regarding the optimal neoadjuvant immunotherapy duration.

In this study, 7 out of 8 (87.5%) patients achieved complete pathological response with -PD-1 blockades monotherapy (including two patients receiving Pembrolizumab, two receiving Sintilimab, and four receiving Tislelizumab). Notably, all 7 patients who received monotherapy achieved complete pathological response. As one patient had not undergone surgery yet, the possibility of a complete pathological response cannot be ruled out. Among patients receiving nivolumab plus ipilimumab, surgery was performed after 2 treatment cycles, with the longest treatment duration reaching 10 cycles. Tailoring treatment cycles according to individual patient characteristics might enhance the pCR rate and implementation of a wait-and-watch strategy is deemed acceptable subsequent to neoadjuvant immunotherapy. Neoadjuvant immunotherapy for patients with early-stage dMMR CRC exhibited a high response rate and low recurrence rate in previous studies (24), but randomized phase III trial with a larger sample size and longer follow-up is warranted to observe the duration of response. The lack of CR detected by imaging in our

TABLE 3 Univariate analysis of clinical variables for the prediction of pCR.

Characteristic	pCR	Non-pCR	P value
Age (year)			0.157
Sex			
Male	9	3	0.422
Female	6	2	
Tumor site			
Colon	10	3	0.999
Rectum	4	1	
Pathological type			
Adenocarcinoma	13	4	0.998
Mucinous adenocarcinoma	2	1	
TNM Stage			
III	12	5	0.998
IVa	3	0	

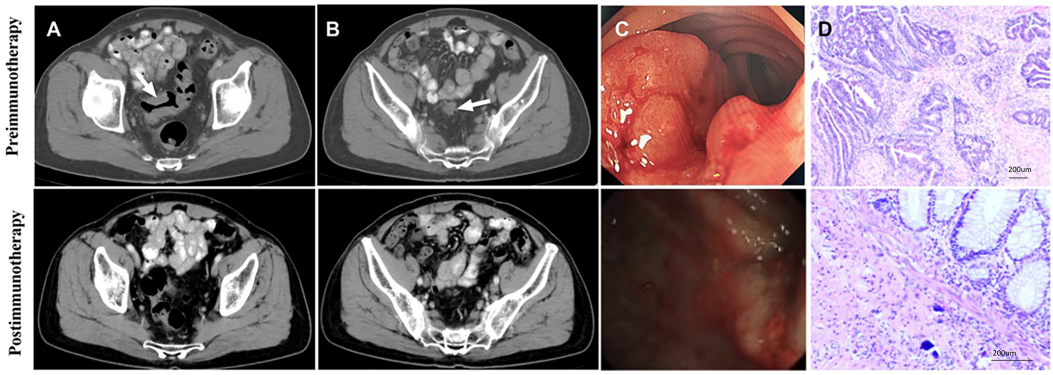

FIGURE 3
Radiology, colonoscopy, pathological reactions, and postoperative specimens of 1 pCR patient to dual drug immunotherapy and neoadjuvant therapy (Patient 9 in Table 2). **(A)** CT view of sagittal tumor: pre-immunotherapy VS post-immunotherapy; **(B)** CT view of lymph nodes around sagittal tumor: before immunotherapy VS after immunotherapy; **(C)** Colonoscopy: pre-immunotherapy VS post-immunotherapy; **(D)** Pre-biopsy (HE) and post-biopsy (HE): pre-immunotherapy VS post-immunotherapy.

TABLE 4 Imaging size changes of tumor and lymph nodes before and after treatment.

patient	Tumor maximum diameter before treatment (cm)	Tumor thickness before treatment (cm)	Tumor maximum diameter after treatment (cm)	Tumor thickness after treatment (cm)	Lymph node maximum diameter (short diameter) before treatment(cm)	Lymph node maximum diameter (short diameter) after treatment(cm)	clinical Response	Tumor Response
1	7.2	2.4	1.5	0.5	0	0	1*	rectum PCR
2	6.3	2.9	2.5	0.4	2.4	1.2	1*	PCR
3	NA	NA	5.2	2	NA	NA	NA	PCR
4	9.3	3.6	1	0.5	0.8	0.4	PR	PCR
5	4.1	2.2	1.5	0.2	0.7	0.5	PR	PCR
6	2.8	2.4	1.8	1.7	NA	NA	PR	PCR
7	NA	NA	5	0.7	NA	NA	NA	PCR
8	6	1.8	NE	1.2	0.5	0.5	2*	PR
9	3.1	1.2	2	0.7	1.1	0.5	1*	PCR
10	6.7	3.5	2.8	2.1	1	0.4	PR	PCR
11	5	2.3	4	0.8	0.7	0.5	SD	PR
12	7.3	5.5	8.7	4.6	0.6	0.6	PD	PD
13	5.9	1.9	1.5	0.9	0.5	0.4	cCR	PCR
14	5.8	2.3	2.5	0.4	1.3	1.0	PR	PCR
15	7.6	2.9	2.3	2	0.8	0.6	PR	PCR
16	7.7	2.7	3	0.6	0.6	0.4	PR	PCR
17	11	2.1	5	1.5	0.7	0.5	PR	PCR
18	5.9	2.5	2	1.5	0.7	0.5	1*	PCR
19	7.6	3.2	4	1.5	1.3	2	PR	PR
20	4	1.5	5	1.5	1.8	1.3	PD	PD

PR, partial response; SD, stable disease; PD, progressive disease; cCR, clinical complete response; *TRG, tumor regression grade; NA, not available; NE, not evaluable.

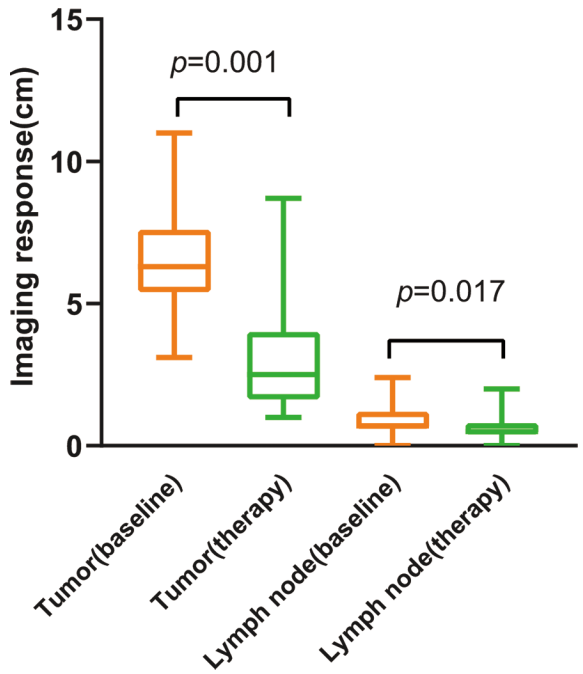

FIGURE 4
Imaging size changes of tumor and lymph nodes before and after treatment.

study, compared to previous studies, may be attributed to several factors, including patient heterogeneity, variability in immunotherapy regimens, differences in imaging and response assessment criteria, and the timing of response evaluations. These factors highlight the complexity of assessing response rates in real-world settings and underscore the need for prospective studies to better characterize CR in diverse patient populations.

The findings of the CheckMate 8HW Phase 3 study (NCT04008030), presented at the 2024 American Society of Clinical Oncology Digestive Oncology Symposium, demonstrated a 79% reduction in disease progression or mortality risk following four to six doses of dual-agent immunotherapy (25). For instance, a patient with mucinous adenocarcinoma progressed despite dual immunotherapy following 2 years of pembrolizumab treatment, indicating the need for individualized immunotherapy strategies.

Immunotherapy has shown promising results in clinical practice but requires careful safety monitoring. A particular concern is immune-related adverse events (irAE), whose mechanisms remain unclear and which commonly affect the lungs, skin, endocrine glands and liver. irAE could manifest with delayed onset, even occurring up to a year after treatment cessation (26). The KEYNOTE-177 study reported a 9% irAE incidence, compared to 13% in the conventional chemotherapy group (10, 27). Timely prediction, identification, and management of irAEs are crucial, with guidelines issued by ASCO, ESMO, and NCCN to assist clinicians in irAE management. Although our study observed immune-related adverse reactions in 12.5% of PD-1 monotherapy patients and 6.6% of anti-PD-1 + anti-CTLA-4 immunotherapy patients, further research is needed to fully understand these outcomes.

Our study has limitations due to its retrospective nature and small sample size, which may result in biases. The diversity of immunotherapy regimens among patients complicates our findings' interpretation. Therefore, caution is necessary when applying these findings to broader populations. We found no specific clinical variable related to the prediction of pCR, possibly due to the total number of events and sample size, affecting the validity of our logistic model (28). Large studies with extended follow-up durations are needed to understand the correlation between pathological responses and survival rates. While

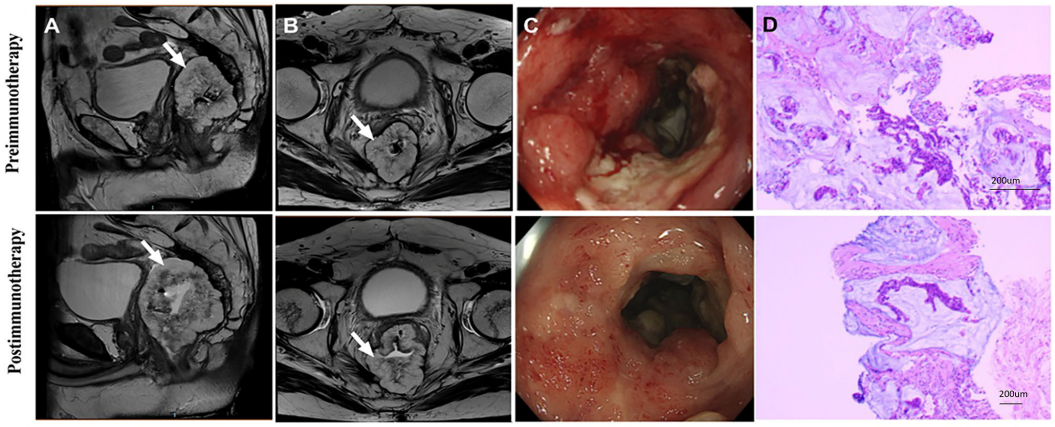

FIGURE 5
Radiological and pathological reactions of one patient who progressed after receiving dual-drug immunoneoadjuvant therapy (patient 12 in Table 2). **(A)** Sagittal MR View of the pelvis: before immunotherapy VS after immunotherapy; **(B)** MR View of the axial plane of the pelvis: before immunotherapy VS after immunotherapy; **(C)** Colonoscopy: pre-immunotherapy VS post-immunotherapy; **(D)**Pre-biopsy (HE) VS post-biopsy (HE): pre-immunotherapy vs post-immunotherapy. MR, magnetic resonance; HE, hematoxylin-eosin.

TABLE 5 Adverse events.

Adverse Events	Grade 1-2 (%)	Grade 3-4 (%)
Any	9 (45)	1 (5)
ALT increased	4 (20)	1 (5)
Rash	2 (10)	0 (0)
Thyroid dysfunction	3 (15)	0 (0)
autoimmune myocarditis	1 (5)	0 (0)
gastrointestinal reaction	1 (5)	0 (0)
surgery-related	0 (0)	0 (0)
Anastomotic leak	0 (0)	0 (0)
Obstruction/Ileus	0 (0)	0 (0)
Surgical Site infection	0 (0)	0 (0)
Urinary Retention	0 (0)	0 (0)
Chylous Ascites	0 (0)	0 (0)

our study highlighted the significance of achieving complete or near-complete pathological responses with neoadjuvant immunotherapy, prospective studies are needed to validate the findings. Some dMMR tumors exhibit resistance to immune checkpoint blockade (ICB) due to various mechanisms, such as an immunosuppressive tumor microenvironment and alterations in antigen presentation pathways. Additionally, genetic alterations beyond dMMR, such as mutations in interferon signaling pathways, and activation of intrinsic tumor cell pathways like WNT/β-catenin, can further contribute to immune evasion. Understanding these resistance mechanisms is crucial for developing combination strategies to overcome resistance and improve the therapeutic outcomes of dMMR tumors. Although our study aimed to replicate existing findings in the context of ICB therapy, we also recognize the importance of providing new insights into the immune dynamics during treatment. Although we did not conduct sequencing of tumor biopsies to assess neoantigen immunoediting directly, immunohistochemistry analysis of pre- and post-treatment samples could indicate trends in immune cell infiltration that correlate with treatment response. Future studies in our cohort will include comprehensive genomic and immune profiling techniques, such as neoantigen sequencing, flow cytometry, and spatial transcriptomics, to better characterize the evolution of immune responses during ICB therapy and identify novel mechanisms of resistance.

In summary, neoadjuvant immunotherapy might be safe and efficacious, but individualized treatment approaches are crucial. For patients exhibiting suboptimal treatment responses, prompt identification and modification of treatment plans were imperative. Ongoing research endeavors are expected to further advance the field of neoadjuvant immunotherapy.

Data availability statement

The original contributions presented in the study are included in the article/supplementary material. Further inquiries can be directed to the corresponding authors.

Ethics statement

The studies involving humans were approved by ethics committee of the Sichuan Cancer Hospital. The studies were conducted in accordance with the local legislation and institutional requirements. The ethics committee/institutional review board waived the requirement of written informed consent for participation from the participants or the participants' legal guardians/next of kin because informed patient consent for this retrospective analysis was waived.

Author contributions

ZD: Conceptualization, Data curation, Formal analysis, Investigation, Methodology, Project administration, Resources, Software, Supervision, Validation, Visualization, Writing – original draft, Writing – review & editing. YL: Conceptualization, Data curation, Formal analysis, Investigation, Methodology, Project administration, Resources, Software, Supervision, Validation, Visualization, Writing – original draft, Writing – review & editing. XC: Methodology, Project administration, Writing – review & editing. TP: Methodology, Project administration, Writing – review & editing. YR: Methodology, Project administration, Writing – review & editing. HH: Methodology, Project administration, Writing – review & editing. JY: Methodology, Project administration, Writing – review & editing. KZ: Methodology, Project administration, Writing – review & editing. CL: Resources, Software, Supervision, Validation, Visualization, Writing – original draft, Writing – review & editing, Conceptualization, Data curation, Formal analysis, Investigation, Methodology, Project administration. BS: Conceptualization, Data curation, Formal analysis, Funding acquisition, Investigation, Methodology, Project administration, Resources, Software, Supervision, Validation, Visualization, Writing – original draft, Writing – review & editing.

Funding

The author(s) declare financial support was received for the research, authorship, and/or publication of this article. Supported from the National Natural Science Foundation of China: 82302993.

Conflict of interest

The authors declare that the research was conducted in the absence of any commercial or financial relationships that could be construed as a potential conflict of interest.

Publisher's note

References

1. Sung H, Ferlay J, Siegel RL, Laversanne M, Soerjomataram I, Jemal A, et al. Global cancer statistics 2020: globocan estimates of incidence and mortality worldwide for 36 cancers in 185 countries. *CA: Cancer J Clin*. (2021) 71:209–49. doi: 10.3322/caac.21660

2. Cercek A, Dos Santos Fernandes G, Roxburgh CS, Ganesh K, Ng S, Sanchez-Vega F, et al. Mismatch repair-deficient rectal cancer and resistance to neoadjuvant chemotherapy. *Clin Cancer Res*. (2020) 26:3271–9. doi: 10.1158/1078-0432.Ccr-19-3728

3. Venderbosch S, Nagtegaal ID, Maughan TS, Smith CG, Cheadle JP, Fisher D, et al. Mismatch repair status and braf mutation status in metastatic colorectal cancer patients: A pooled analysis of the cairo, cairo2, coin, and focus studies. *Clin Cancer Res*. (2014) 20:5322–30. doi: 10.1158/1078-0432.Ccr-14-0332

4. Le DT, Durham JN, Smith KN, Wang H, Bartlett BR, Aulakh LK, et al. Mismatch repair deficiency predicts response of solid tumors to pd-1 blockade. *Sci (New York NY)*. (2017) 357:409–13. doi: 10.1126/science.aan6733

5. Le DT, Uram JN, Wang H, Bartlett BR, Kemberling H, Eyring AD, et al. Pd-1 blockade in tumors with mismatch-repair deficiency. *New Engl J Med*. (2015) 372:2509–20. doi: 10.1056/NEJMoa1500596

6. Jenkins MA, Hayashi S, O'Shea AM, Burgart LJ, Smyrk TC, Shimizu D, et al. Pathology features in bethesda guidelines predict colorectal cancer microsatellite instability: A population-based study. *Gastroenterology*. (2007) 133:48–56. doi: 10.1053/j.gastro.2007.04.044

7. Zhang X, Wu T, Cai X, Dong J, Xia C, Zhou Y, et al. Neoadjuvant immunotherapy for msi-H/dmmr locally advanced colorectal cancer: new strategies and unveiled opportunities. *Front Immunol*. (2022) 13:795972. doi: 10.3389/fimmu.2022.795972

8. André T, Lonardi S, Wong KYM, Lenz HJ, Gelsomino F, Aglietta M, et al. Nivolumab plus low-dose ipilimumab in previously treated patients with microsatellite instability-high/mismatch repair-deficient metastatic colorectal cancer: 4-year follow-up from checkmate 142. *Ann oncology: Off J Eur Soc Med Oncol*. (2022) 33:1052–60. doi: 10.1016/j.annonc.2022.06.008

9. Diagnosis, Treatment Guidelines For Colorectal Cancer Working Group C. Chinese society of clinical oncology (Csco) diagnosis and treatment guidelines for colorectal cancer 2018 (English version). *Chin J Cancer Res = Chung-kuo yen cheng yen chiu*. (2019) 31:117–34. doi: 10.21147/j.issn.1000-9604.2019.01.07

10. Diaz LA Jr., Shiu KK, Kim TW, Jensen BV, Jensen LH, Punt C, et al. Pembrolizumab versus chemotherapy for microsatellite instability-high or mismatch repair-deficient metastatic colorectal cancer (Keynote-177): final analysis of a randomised, open-label, phase 3 study. *Lancet Oncol*. (2022) 23:659–70. doi: 10.1016/s1470-2045(22)00197-8

11. Chalabi M, Verschoor YL, Tan PB, Balduzzi S, Van Lent AU, Grootscholten C, et al. Neoadjuvant immunotherapy in locally advanced mismatch repair-deficient colon cancer. *New Engl J Med*. (2024) 390:1949–58. doi: 10.1056/NEJMoa2400634

12. Cercek A, Sinopoli JC, Shia J, Weiss JA, Temple L, Smith JJ, et al. . doi: 10.1200/JCO.2024.42.17_suppl.LBA3512

13. Cuschieri S. The strobe guidelines. *Saudi J anaesthesia*. (2019) 13:S31–s4. doi: 10.4103/sja.SJA_543_18

14. Amin MB, Greene FL, Edge SB, Compton CC, Gershenwald JE, Brookland RK, et al. The eighth edition ajcc cancer staging manual: continuing to build a bridge from a population-based to a more "Personalized" Approach to cancer staging. *CA: Cancer J Clin*. (2017) 67:93–9. doi: 10.3322/caac.21388

15. Benson AB, Venook AP, Al-Hawary MM, Azad N, Chen YJ, Ciombor KK, et al. Rectal cancer, version 2.2023, nccn clinical practice guidelines in oncology. *J Natl Compr Cancer Network: JNCCN*. (2023) 20:1139–67. doi: 10.6004/jnccn.2022.0051

16. Freites-Martinez A, Santana N, Arias-Santiago S, Viera A. Using the common terminology criteria for adverse events (Ctcae - version 5.0) to evaluate the severity of adverse events of anticancer therapies. *Actas dermo-sifiliograficas*. (2021) 112:90–2. doi: 10.1016/j.ad.2019.05.009

17. Patel UB, Taylor F, Blomqvist L, George C, Evans H, Tekkis P, et al. Magnetic resonance imaging-detected tumor response for locally advanced rectal cancer predicts survival outcomes: mercury experience. *J Clin Oncol*. (2011) 29:3753–60. doi: 10.1200/jco.2011.34.9068

18. Conroy T, Bosset JF, Etienne PL, Rio E, François É, Mesgouez-Nebout N, et al. Neoadjuvant chemotherapy with folfirinox and preoperative chemoradiotherapy for patients with locally advanced rectal cancer (Unicancer-prodige 23): A multicentre, randomised, open-label, phase 3 trial. *Lancet Oncol*. (2021) 22:702–15. doi: 10.1016/s1470-2045(21)00079-6

19. Deng Y, Chi P, Lan P, Wang L, Chen W, Cui L, et al. Modified folfox6 with or without radiation versus fluorouracil and leucovorin with radiation in neoadjuvant treatment of locally advanced rectal cancer: initial results of the chinese fowarc multicenter, open-label, randomized three-arm phase iii trial. *J Clin Oncol*. (2016) 34:3300–7. doi: 10.1200/jco.2016.66.6198

20. Chalabi M, Verschoor YL, van den Berg J, Sikorska K, Beets G, Lent AV, et al. Lba7 neoadjuvant immune checkpoint inhibition in locally advanced mmr-deficient colon cancer: the niche-2 study. *Ann Oncol*. (2022) 33:S1389. doi: 10.1016/j.annonc.2022.08.016

21. Pan T, Yang H, Wang WY, Rui YY, Deng ZJ, Chen YC, et al. Neoadjuvant immunotherapy with ipilimumab plus nivolumab in mismatch repair deficient/microsatellite instability-high colorectal cancer: A preliminary report of case series. *Clin colorectal Cancer*. (2024) 23:104–10. doi: 10.1016/j.clcc.2024.01.002

22. Cercek A, Lumish M, Sinopoli J, Weiss J, Shia J, Lamendola-Essel M, et al. Pd-1 blockade in mismatch repair-deficient, locally advanced rectal cancer. *New Engl J Med*. (2022) 386:2363–76. doi: 10.1056/NEJMoa2201445

23. Hu H, Kang L, Zhang J, Wu Z, Wang H, Huang M, et al. Neoadjuvant pd-1 blockade with toripalimab, with or without celecoxib, in mismatch repair-deficient or microsatellite instability-high, locally advanced, colorectal cancer (Picc): A single-centre, parallel-group, non-comparative, randomised, phase 2 trial. *Lancet Gastroenterol Hepatol*. (2022) 7:38–48. doi: 10.1016/s2468-1253(21)00348-4

24. Chakrabarti S, Grewal US, Vora KB, Parikh AR, Almader-Douglas D, Mahipal A, et al. Outcome of patients with early-stage mismatch repair deficient colorectal cancer receiving neoadjuvant immunotherapy: A systematic review. *JCO Precis Oncol*. (2023) 7:e2300182. doi: 10.1200/po.23.00182

25. Andre T, Elez E, Cutsem EV, Jensen LH, Bennouna J, Mendez G, et al. Nivolumab (Nivo) plus ipilimumab (Ipi) vs chemotherapy (Chemo) as first-line (1l) treatment for microsatellite instability-high/mismatch repair-deficient (Msi-H/dmmr) metastatic colorectal cancer (Mcrc): first results of the checkmate 8hw study. *J Clin Oncol.*. (2024) 42(3_suppl):LBA768–LBA. doi: 10.1200/JCO.2024.42.3_suppl.LBA768

26. de Miguel M, Calvo E. Clinical challenges of immune checkpoint inhibitors. *Cancer Cell*. (2020) 38:326–33. doi: 10.1016/j.ccell.2020.07.004

27. André T, Shiu KK, Kim TW, Jensen BV, Jensen LH, Punt C, et al. Pembrolizumab in microsatellite-instability-high advanced colorectal cancer. *New Engl J Med*. (2020) 383:2207–18. doi: 10.1056/NEJMoa2017699

28. Peduzzi P, Concato J, Kemper E, Holford TR, Feinstein AR. A simulation study of the number of events per variable in logistic regression analysis. *J Clin Epidemiol*. (1996) 49:1373–9. doi: 10.1016/s0895-4356(96)00236-3

frontiers | Frontiers in Immunology

TYPE Original Research
PUBLISHED 24 October 2024
DOI 10.3389/fimmu.2024.1468342

OPEN ACCESS

EDITED BY
Elias Kouroumalis,
University of Crete, Greece

REVIEWED BY
Vasile Valeriu Lupu,
Grigore T. Popa University of Medicine and Pharmacy, Romania
Peng Jin,
Seventh Medical Center of PLA General Hospital, China

*CORRESPONDENCE
Feng Wang
zzuwangfeng@zzu.edu.cn

†These authors have contributed equally to this work and share first authorship

RECEIVED 21 July 2024
ACCEPTED 08 October 2024
PUBLISHED 24 October 2024

CITATION
Yang Y, Wang Z, Xin D, Guan L, Yue B, Zhang Q and Wang F (2024) Analysis of the treatment efficacy and prognostic factors of PD-1/PD-L1 inhibitors for advanced gastric or gastroesophageal junction cancer: a multicenter, retrospective clinical study. *Front. Immunol.* 15:1468342. doi: 10.3389/fimmu.2024.1468342

Analysis of the treatment efficacy and prognostic factors of PD-1/PD-L1 inhibitors for advanced gastric or gastroesophageal junction cancer: a multicenter, retrospective clinical study

Yuanyuan Yang[1†], Zhe Wang[2,3†], Dao Xin[2], Lulu Guan[2], Bingtong Yue[3], Qifan Zhang[2,3] and Feng Wang[2,4*]

[1]Department of Medical Oncology, National Cancer Center/National Clinical Research Center for Cancer/Cancer Hospital, Chinese Academy of Medical Sciences and Peking Union Medical College, Beijing, China, [2]Department of Oncology, The First Affiliated Hospital of Zhengzhou University, Zhengzhou, China, [3]Department of Clinical Medicine, The First Clinical Medical College, Zhengzhou University, Zhengzhou, China, [4]Henan Key Laboratory of Chronic Disease Prevention and Therapy & Intelligent Health Management, Zhengzhou, China

Introduction: Immune checkpoint inhibitors (ICIs) have transformed advanced gastric cancer treatment, yet patient responses vary, highlighting the need for effective biomarkers. Common markers, such as programmed cell death ligand-1 (PD-L1), microsatellite instability/mismatch repair (MSI/MMR), tumor mutational burden, tumor-infiltrating lymphocytes, and Epstein–Barr virus, face sampling challenges and high costs. This study seeks practical, minimally invasive biomarkers to enhance patient selection and improve outcomes.

Methods: This multicenter retrospective study analyzed 617 patients with advanced gastric or gastroesophageal junction cancer treated with programmed cell death protein-1 (PD-1)/PD-L1 inhibitors from January 2019 to March 2023. Clinical data and peripheral blood marker data were collected before and after treatment. The primary endpoints were overall survival (OS) and progression-free survival (PFS); the secondary endpoints included the objective response rate (ORR) and disease control rate (DCR). Least absolute shrinkage and selection operator (LASSO)-Cox and LASSO logistic regression analyses identified independent factors for OS, PFS, and ORR. Predictive nomograms were validated using receiver operating characteristic (ROC) curves, areas under the curve (AUCs), C-indices, and calibration curves, with clinical utility assessed via decision curve analysis (DCA), net reclassification improvement (NRI), and integrated discrimination improvement (IDI).

Results: OS-related factors included treatment line, T stage, ascites, pretreatment indirect bilirubin (pre-IBIL), posttreatment CA125, CA199, CA724, and the PLR. PFS-related factors included treatment lines, T stage, metastatic sites, pre-IBIL, posttreatment globulin (GLOB), CA125, and CA199 changes. ORR-related factors included treatment line, T stage, N stage, liver metastasis, pretreatment red cell distribution width-to-platelet ratio (RPR), CA125, and CA724 changes. The nomograms showed strong predictive performance and clinical utility.

Conclusions: Early treatment, lower T stage, the absence of ascites, and lower pre-IBIL, post-CA125, CA199, CA724, and PLR correlate with better OS. Factors for improved PFS include early treatment, lower T stage, fewer metastatic sites, and lower pre-IBIL, post-GLOB, and post-CA125 levels. Nomogram models can help identify patients who may benefit from immunotherapy, providing valuable clinical guidance.

KEYWORDS

PD-1/PD-L1 inhibitors, gastric or gastroesophageal junction cancer, predictive biomarkers, prognosis, efficacy

1 Introduction

Gastric cancer is one of the most common malignancies, ranking fifth in incidence and fourth in mortality globally in 2020 (1). It has a poor prognosis, with a global five-year survival rate between 20% and 40% (2). During the chemotherapy era, treatments for advanced gastric cancer include fluoropyrimidines and platinum or paclitaxel-based regimens, resulting in a survival time of approximately one year (3, 4). Immune checkpoint inhibitors (ICIs) have significantly improved survival in advanced gastric cancer patients, as shown in large phase III trials, such as the CheckMate 649, ATTRACTION-4, KEYNOTE-859, and KEYNOTE-811 studies. However, responses to ICIs vary, even among patients with programmed cell death ligand-1 (PD-L1) positivity or microsatellite instability (MSI-H) status. Some PD-L1-negative or microsatellite-stable patients may benefit from ICIs (5–7). Therefore, it is crucial to identify simple, accurate, and accessible biomarkers to predict which gastric cancer patients might benefit from immunotherapy.

Current clinical prognostic assessments, including assessments of tumor infiltration depth, lymph node metastasis, hematogenous metastasis, tumor location, histological grade, and lymphovascular invasion, are based on the American Joint Committee on Cancer (AJCC) staging system (8, 9). However, factors such as age, sex, tumor differentiation, and immunotherapy cycles, which may be significant for individual survival prediction, were not fully accounted for. Common biomarkers include PD-L1 expression, MSI/mismatch repair status, tumor mutational burden, and circulating tumor DNA, but some potential biomarkers, such as peripheral blood inflammation markers, tumor markers, and nutritional status, remain controversial.

The inflammatory response in the tumor microenvironment is closely related to tumor occurrence, progression, invasion, and metastasis (10). Peripheral blood inflammatory markers can not only predict gastric cancer prognosis (11–17) but are also linked to immunotherapy responses (18–21). Baseline serum tumor marker concentrations and their dynamic changes can also predict ICI outcomes (22–25). Huang J et al. reported that the serum levels of carcinoembryonic antigen (CEA) and CA125 predict progression-free survival (PFS) and overall survival (OS) in patients with non-small cell lung cancer (NSCLC) receiving first-line immunotherapy (26). Additionally, nutritional status is important for gastric cancer patients due to the anatomical features of the stomach (27–30). Albumin, prealbumin, and body mass index (BMI) are independent prognostic factors for gastric cancer (31). A low prognostic nutritional index (PNI) score before treatment was proven to be an independent risk factor for survival in advanced NSCLC patients receiving programmed cell death protein-1 (PD-1) inhibitors (32–34).

This study aimed to evaluate comprehensive clinical and pathological data, including peripheral blood inflammatory markers, tumor markers, and nutritional indices, to identify predictive biomarkers for advanced gastric cancer patients treated with PD-1/PD-L1 inhibitors. We hope to develop a robust prognostic model that enhances treatment precision and offers personalized clinical guidance. By integrating diverse biomarkers, we aim to improve patient outcomes and optimize the use of immunotherapy, ultimately refining therapeutic decision-making in advanced gastric cancer patients.

2 Methods

2.1 Study population

This retrospective study included 617 patients with advanced gastric or gastroesophageal junction cancer who received ICI treatment from January 2019 to March 2023 at The First Affiliated Hospital of Zhengzhou University, Henan Cancer Hospital, and Anyang Cancer Hospital.

The inclusion criteria for patients were as follows: (1) were over 18 years of age with histologically or cytologically confirmed gastric or gastroesophageal junction cancer; (2) had locally advanced unresectable, recurrent, or metastatic disease; (3) had undergone at least two cycles of systemic treatment based on PD-1/PD-L1 inhibitors; (4) had an Eastern Cooperative Oncology Group performance status of 0-2; (5) had at least one measurable target

lesion that could be monitored by computed tomography or magnetic resonance imaging; (6) had normal vital organ function; (7) had complete clinical data, including routine blood, liver and kidney function data and tumor marker data, one week before treatment and after two treatment cycles, before PD-1/PD-L1 inhibitor treatment; and (8) had regularly scheduled follow-up data available.

The exclusion criteria were as follows: (1) patients with other primary malignancies; (2) patients without assessable lesions or who did not undergo regular efficacy evaluations; (3) patients who experienced relapse within six months after neoadjuvant or adjuvant therapy; (4) patients with a history of surgery within the last month; (5) patients with severe infections or inflammatory diseases prior to immunotherapy; (6) patients with serious heart, cerebrovascular, lung, liver, or kidney diseases or other major illnesses that would prevent tolerance to treatment; (7) patients with autoimmune diseases or other immune system deficiencies; (8) patients who were using or had a long-term history of using hematopoietic factors, hormones, or immunosuppressive drugs; (9) patients allergic to PD-1/PD-L1 inhibitors or those with metabolic disorders; (10) patients with psychiatric disorders, a history of substance abuse, or who could not discontinue such substances; and (11) pregnant or breastfeeding women.

The primary endpoints were OS and PFS, while the secondary endpoints included the objective response rate (ORR) and disease control rate (DCR). OS was defined as the time from the start of PD-1/PD-L1 inhibitor treatment to death from any cause or the last follow-up, and PFS was defined as the time from the start of treatment to the first occurrence of disease progression, death, or last follow-up. The ORR was defined as the proportion of patients who achieved complete response (CR) or partial response (PR), and the DCR was defined as the proportion of patients who achieved CR, PR, or stable disease (SD). Patient efficacy was evaluated according to the Response Evaluation Criteria in Solid Tumors version 1.1. All patients were followed up regularly after the initiation of treatment to monitor disease recurrence or progression. The final follow-up date was August 31, 2023.

This study complied with the principles of the Helsinki Declaration and relevant ethical requirements and was approved by the Ethics Committee of Scientific Research and Clinical Trials of the First Affiliated Hospital of Zhengzhou University (Approval Identifier: 2023-KY-1308-002).

2.2 Study variables

We collected the pretreatment indicators of gastric cancer patients who met the inclusion criteria as follows. The patients' clinicopathological characteristics included sex, age, smoking history, alcohol consumption history, BMI, PD-L1 combined positive score (CPS), human epidermal growth factor receptor 2 (Her-2) expression, Ki-67 expression, pathological type, differentiation degree, and Lauren classification.

The tumor characteristics included the primary tumor location, TNM stage, sites of metastasis (e.g., liver, bone, lymph nodes, lung, peritoneum, malignant ascites), and number of metastatic sites. Treatment details included drug names, treatment regimens, treatment lines, presence of radical surgery, radiotherapy, start time of treatment, and progression time.

Hematological data included hemoglobin (Hb), platelet (PLT) count, neutrophil (Neut) count, lymphocyte (Lym) count, monocyte (Mono) count, red cell distribution width (RDW), total protein (TP), albumin (ALB), globulin (GLOB), total bilirubin (TBIL), direct bilirubin (DBIL), IBIL, CA125, CA199, CA724, and CEA. Moreover, hematological indicators were collected not only at baseline but also after two cycles of treatment.

Additionally, we calculated comprehensive indices before the first treatment and after two treatment cycles: PNI = ALB + 5 × Lym, the neutrophil-to-Lym ratio (NLR) = Neut/Lym, the platelet-to-lymphocyte ratio (PLR) = PLT/Lym, the monocyte-to-lymphocyte ratio (MLR) = Mono/Lym, the neutrophil-to-monocyte ratio (NMR) = Neut/Mono, the systemic immune-inflammation index (SII) = PLT× Neut/Lym, the neutrophil-to-lymphocyte ratio (NLPR) = Neut/Lym×PLT, the aggregate index of systemic inflammation (AISI) = Neut×PLT×Mono/Lym, the systemic inflammation response index (SIRI)= Neut×Mono/Lym, the red cell distribution width-to-albumin ratio (RAR)=RDW/ALB, the red cell distribution width-to-platelet ratio (RPR) = RDW/PLT, the red cell distribution width-to-lymphocyte ratio (RLR) = RDW/Lym, and the hemoglobin-to-platelet ratio (HPR) = Hb/PLT. Changes in tumor markers and comprehensive indices were calculated by subtracting pretreatment values from posttreatment values.

2.3 Study design and statistical analysis

The study design is shown in Figure 1. This study focused on patient survival status as the outcome variable. Receiver operating characteristic (ROC) curves were used to calculate the Youden index, and the corresponding level of each indicator at which the Youden index was maximized was taken as the optimal cutoff value. If the Youden index was not available or there was a significant difference in group size, the median was used as the cutoff. The upper limit of normal values was used as the cutoff of tumor markers. Patients were divided into high and low groups based on these values, and changes in indicators were categorized by whether values increased or decreased after immunotherapy.

All patients were randomly assigned to training and validation cohorts at a 7:3 ratio, and the $\chi 2$ test was applied to compare the intergroup differences. LASSO-Cox regression identified independent predictors for OS and PFS, while LASSO logistic regression identified predictors for ORR. These predictors were used to construct nomogram models for OS, PFS, and ORR. The model's discriminative ability was assessed using ROC curves and area under the curve (AUC), and the C-index and calibration ability were evaluated using calibration plots. The net benefit of the nomogram in a clinical setting was assessed by

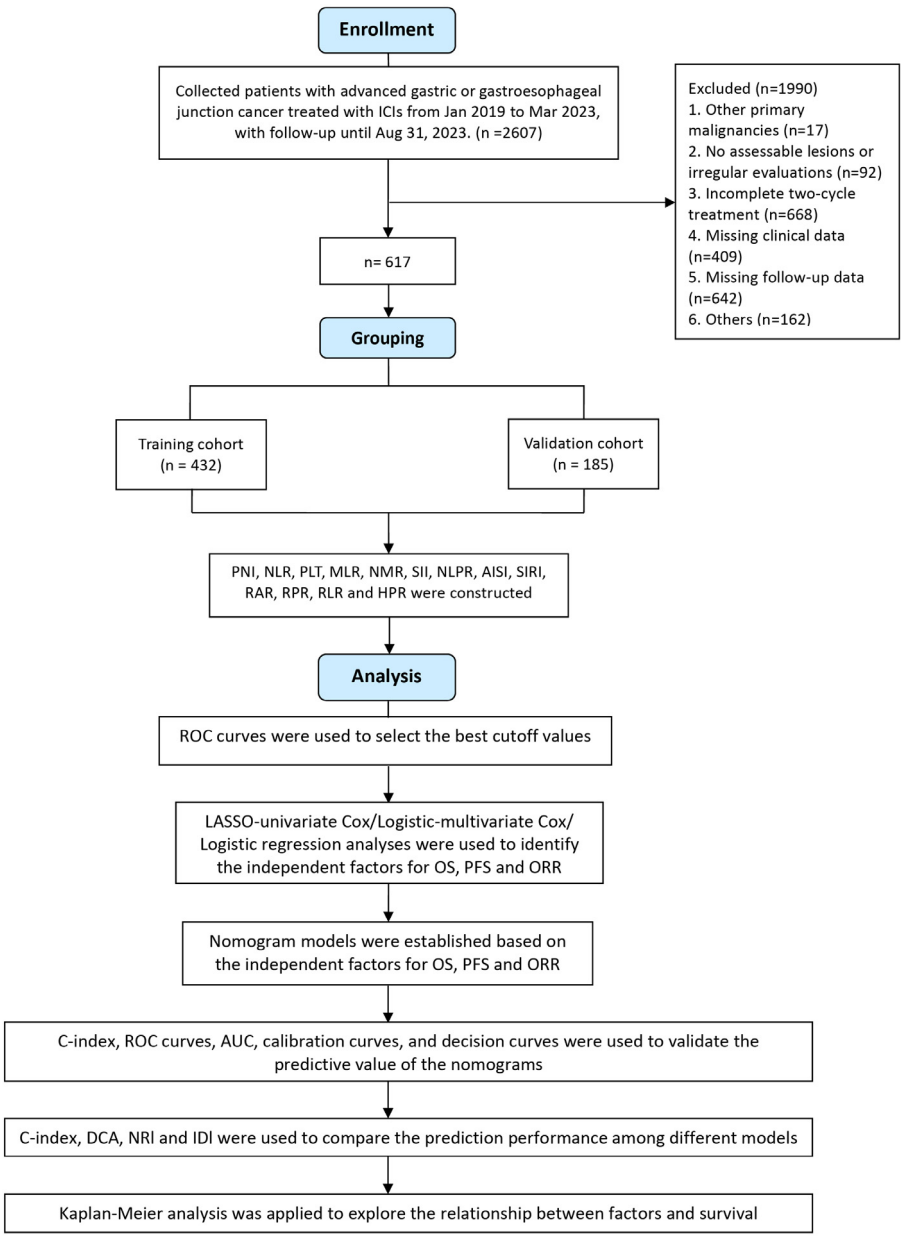

FIGURE 1
Flow chart of the study design.

decision curve analysis (DCA). To further evaluate the clinical benefit and utility of the nomogram model compared to the AJCC staging system, we applied the net reclassification improvement (NRI) and the integrated discrimination improvement (IDI). A positive NRI and IDI indicated improved predictive ability, while negative values indicated a decrease.

Kaplan-Meier (K-M) analysis was used for time-dependent variables to calculate median survival times and plot OS and PFS curves, with group differences compared using the log-rank test. Hazard ratios (HRs) and 95% confidence intervals (CIs) were used to quantify relative risks. All the statistical analyses were performed using R 4.3.2 software. *P* values less than 0.05 were considered to indicate statistical significance.

3 Results

3.1 Patient characteristics

A total of 91 variables were included in this study, and the primary patient characteristics are summarized in Table 1. The majority of patients were male; aged between 50 and 69 years; had advanced T3-4 and N2-3 stages; had M1 status; had not undergone radical surgery or radiotherapy; and had received first-line treatment. Tumor characteristics predominantly included Her-2-negative status, poor differentiation, adenocarcinoma type, and tumors located in the upper stomach. The majority of treatment drugs used were sintilimab and camrelizumab, with combination therapy mainly

10.3389/fimmu.2024.1468342

TABLE 1 Clinicopathological characteristics of the patients.

Characteristic	Training cohort [cases (%)] (n = 433)	Validation cohort [cases (%)] (n = 184)	Total population [cases (%)] (n = 617)	*P* value
Gender				0.272
Male	308 (71.1%)	122 (66.3%)	430 (69.7%)	
Female	125 (28.9%)	62 (33.7%)	187 (30.3%)	
Age (years)				0.258
<50	63 (14.5%)	23 (12.5%)	86 (13.9%)	
50-59	133 (30.7%)	71 (38.6%)	204 (33.1%)	
60-69	141 (32.6%)	50 (27.2%)	191 (31.0%)	
≥70	96 (22.2%)	40 (21.7%)	136 (22.0%)	
Smoking history				0.265
No	277 (64%)	127 (69%)	404 (65.5%)	
Yes	156 (36%)	57 (31%)	213 (34.5%)	
Alcohol history				1.000
No	330 (76.2%)	140 (76.1%)	470 (76.2%)	
Yes	103 (23.8%)	44 (23.9%)	147 (23.8%)	
Agent				0.901
Sintilimab	221 (51%)	88 (47.8%)	309 (50.1%)	
Camrelizumab	127 (29.3%)	57 (31%)	184 (29.8%)	
Tislelizumab	29 (6.7%)	15 (8.2%)	44 (7.1%)	
Toripalimab	15 (3.5%)	8 (4.3%)	23 (3.7%)	
Penpulimab	17 (3.9%)	5 (2.7%)	22 (3.6%)	
Nivolumab	12 (2.8%)	7 (3.8%)	19 (3.1%)	
Pembrolizumab	12 (2.8%)	4 (2.2%)	16 (2.6%)	
Combination				0.287
Chemotherapy	307 (70.9%)	133 (72.3%)	440 (71.3%)	
Targeted therapy	30 (6.9%)	18 (9.8%)	48 (7.8%)	
Chemotherapy + Targeted therapy	96 (22.2%)	33 (17.9%)	129 (20.9%)	
Treatment line				0.842
First line	313 (72.3%)	135 (73.4%)	448 (72.6%)	
Second line	95 (21.9%)	37 (20.1%)	132 (21.4%)	
Third or later	25 (5.8%)	12 (6.5%)	37 (6.0%)	
Radical surgery				0.776
No	338 (78.1%)	141 (76.6%)	479 (77.6%)	
Yes	95 (21.9%)	43 (23.4%)	138 (22.4%)	
Radiotherapy				0.051
No	425 (98.2%)	174 (94.6%)	599 (97.1%)	
Yes	8 (1.8%)	10 (5.4%)	18 (2.9%)	
BMI				0.088
Underweight (<18.5)	45 (10.4%)	27 (14.7%)	72 (11.7%)	

(Continued)

TABLE 1 Continued

Characteristic	Training cohort [cases (%)] (n = 433)	Validation cohort [cases (%)] (n = 184)	Total population [cases (%)] (n = 617)	*P* value
Normal (18.5-23.9)	259 (59.8%)	90 (48.9%)	349 (56.6%)	
Overweight (24-27.9)	99 (22.9%)	51 (27.7%)	150 (24.3%)	
Obese (≥28)	30 (6.9%)	16 (8.7%)	46 (7.5%)	
PD-L1 CPS				0.760
CPS < 1	96 (22.2%)	44 (23.9%)	140 (22.7%)	
CPS ≥ 1	154 (35.6%)	68 (37%)	222 (36.0%)	
Unknown	183 (42.3%)	72 (39.1%)	255 (41.3%)	
Her-2				0.068
Negative	291 (67.2%)	138 (75%)	429 (69.5%)	
Positive	69 (15.9%)	17 (9.2%)	86 (13.9%)	
Unknown	73 (16.9%)	29 (15.8%)	102 (16.5%)	
ki-67				0.853
<70%	108 (24.9%)	42 (22.8%)	150 (24.3%)	
≥70%	166 (38.3%)	73 (39.7%)	239 (38.7%)	
Unknown	159 (36.7%)	69 (37.5%)	228 (37.0%)	
Pathological type				1.000
Adenocarcinoma	406 (93.8%)	172 (93.5%)	578 (93.7%)	
Others	27 (6.2%)	12 (6.5%)	39 (6.3%)	
Differentiation degree				0.394
Poorly	262 (60.5%)	101 (54.9%)	363 (58.8%)	
Moderately and well	58 (13.4%)	26 (14.1%)	84 (13.6%)	
Unknown	113 (26.1%)	57 (31%)	170 (27.6%)	
Lauren classification				0.909
Intestinal type	57 (13.2%)	24 (13%)	81 (13.1%)	
Diffuse type	56 (12.9%)	24 (13%)	80 (13.0%)	
Mixed type	51 (11.8%)	18 (9.8%)	69 (11.2%)	
Unknown	269 (62.1%)	118 (64.1%)	387 (62.7%)	
Primary tumor site				0.446
Upper	235 (54.3%)	91 (49.5%)	326 (52.8%)	
Middle	96 (22.2%)	48 (26.1%)	144 (23.3%)	
Lower	89 (20.6%)	42 (22.8%)	131 (21.2%)	
Other	13 (3%)	3 (1.6%)	16 (2.6%)	
T stage				0.550
T1-T2	27 (6.2%)	11 (6%)	38 (6.2%)	
T3	141 (32.6%)	50 (27.2%)	191 (31.0%)	
T4	190 (43.9%)	91 (49.5%)	281 (45.5%)	
TX	75 (17.3%)	32 (17.4%)	107 (17.3%)	
N stage				0.219

(Continued)

TABLE 1 Continued

Characteristic	Training cohort [cases (%)] (n = 433)	Validation cohort [cases (%)] (n = 184)	Total population [cases (%)] (n = 617)	*P* value
N0	106 (24.5%)	52 (28.3%)	158 (25.6%)	
N1	34 (7.9%)	20 (10.9%)	54 (8.8%)	
N2	143 (33%)	47 (25.5%)	190 (30.8%)	
N3	150 (34.6%)	65 (35.3%)	215 (34.8%)	
M stage				0.816
M0	45 (10.4%)	21 (11.4%)	66 (10.7%)	
M1	388 (89.6%)	163 (88.6%)	551 (89.3%)	
Liver metastasis				0.171
No	281 (64.9%)	108 (58.7%)	389 (63.0%)	
Yes	152 (35.1%)	76 (41.3%)	228 (37.0%)	
Bone metastasis				0.416
No	405 (93.5%)	168 (91.3%)	573 (92.9%)	
Yes	28 (6.5%)	16 (8.7%)	44 (7.1%)	
Lymph node metastasis				0.475
No	66 (15.2%)	33 (17.9%)	99 (16.0%)	
Yes	367 (84.8%)	151 (82.1%)	518 (84.0%)	
Lung metastasis				0.851
No	394 (91%)	169 (91.8%)	563 (91.2%)	
Yes	39 (9%)	15 (8.2%)	54 (8.8%)	
Peritoneal metastasis				0.601
No	344 (79.4%)	142 (77.2%)	486 (78.8%)	
Yes	89 (20.6%)	42 (22.8%)	131 (21.2%)	
Ascites				0.327
No	364 (84.1%)	148 (80.4%)	512 (83.0%)	
Yes	69 (15.9%)	36 (19.6%)	105 (17.0%)	
Other metastases				0.855
No	355 (82%)	149 (81%)	504 (81.7%)	
Yes	78 (18%)	35 (19%)	113 (18.3%)	
Number of metastatic sites				0.584
0-1	167 (38.6%)	66 (35.9%)	233 (37.8%)	
2	165 (38.1%)	68 (37%)	233 (37.8%)	
≥3	101 (23.3%)	50 (27.2%)	151 (24.5%)	

involving immunotherapy combined with chemotherapy. There were no significant differences in any of the indices between the training and validation cohorts. Supplementary Figure 1 presents the correlation heatmap of clinicopathological features and peripheral blood indices before and after immunotherapy for the 617 patients with advanced gastric/gastroesophageal junction cancer. Notably, a strong positive correlation was observed between pre-CA199 and post-CA199, as well as between pre-SIRI and pre-NLR.

3.2 Survival outcomes and efficacy evaluation

In the total study population, the median overall survival (mOS) was 18.37 months (95% CI: 16.47 - 20.27) (Figure 2A), and the median progression-free survival (mPFS) was 7.20 months (95% CI: 6.58 - 7.83) (Figure 2B). The ORR was 31.12%, and the DCR was 90.1%. Among the patients, 1 achieved CR, 191 achieved PR, 364

had SD, and 61 experienced progressive disease (PD). The clinical and peripheral blood characteristics of the patients in the CR+PR, SD, and PD groups are detailed in Supplementary Table 1. Significant differences were observed among these groups in terms of combined treatment regimens, treatment lines, PD-L1 expression, Her-2 expression, TNM stage, metastasis status, tumor markers, nutritional indices, inflammation indices, and so on. Notably, a greater proportion of patients in the CR+PR group than in the SD and PD groups received first-line treatment.

Furthermore, we investigated the correlation between early treatment response and long-term survival. The CR+PR, SD, and PD groups showed significant differences in survival, with patients who achieved CR or PR having the best OS and PFS, while those with PD had the worst outcomes (Figures 2C, D). This indicated that patients with better early treatment responses were more likely to have improved long-term survival.

3.3 Subgroup analysis based on PD-L1 expression, Her-2 status, and treatment lines

Among the 362 patients with available PD-L1 expression data, the PD-L1 CPS ≥1 group exhibited a trend toward improved survival compared to the PD-L1 CPS <1 group, although no significant differences were observed in OS or PFS (Supplementary Table 2; Figures 3A, B).

Among the 515 patients with available Her-2 expression data, Her-2-positive patients had significantly better OS and PFS than Her-2-negative patients (Supplementary Table 3; Figures 3C, D).

When comparing first-line, second-line, and third-line or later treatments, first-line treatment was associated with significantly better OS and PFS than second-line and third-line treatments (Supplementary Table 4; Figures 3E, F).Given the widespread use of first-line anti-PD-1/PD-L1 treatment, we analyzed the first-line treatment group. Among the 448 patients, those in the PD-L1 CPS ≥1 group had significantly better OS than did those in the CPS <1 group, but there was no difference in PFS. Her-2-positive patients had better OS and PFS than Her-2-negative patients. No significant differences in OS or PFS were found among patients receiving different combinations of immunotherapy, chemotherapy, or targeted therapy. The detailed data are shown in Figures 3G-L and Supplementary Table 5.

For the 283 Her-2-negative patients who received first-line immunotherapy combined with chemotherapy, the mOS was 18.77 months (95% CI: 15.59–21.95) (Figure 3M), the mPFS was 7.77 months (95% CI: 6.79–8.75) (Figure 3N), the ORR was 34.63% (98/283), and the DCR was 95.76% (271/283). Further subgroup analysis based on the PD-L1 CPS is detailed in Supplementary Table 6 (Figures 3O-R). Among the 45 Her-2-positive patients who received first-line immunotherapy combined with chemotherapy and targeted therapy, the mOS was 28.13 months (95% CI: 22.60-NA) (Figure 3S), the mPFS was 12.17 months (95% CI: 10.25-14.10) (Figure 3T), the ORR was 62.22% (28/45), and the DCR was 100% (45/45).

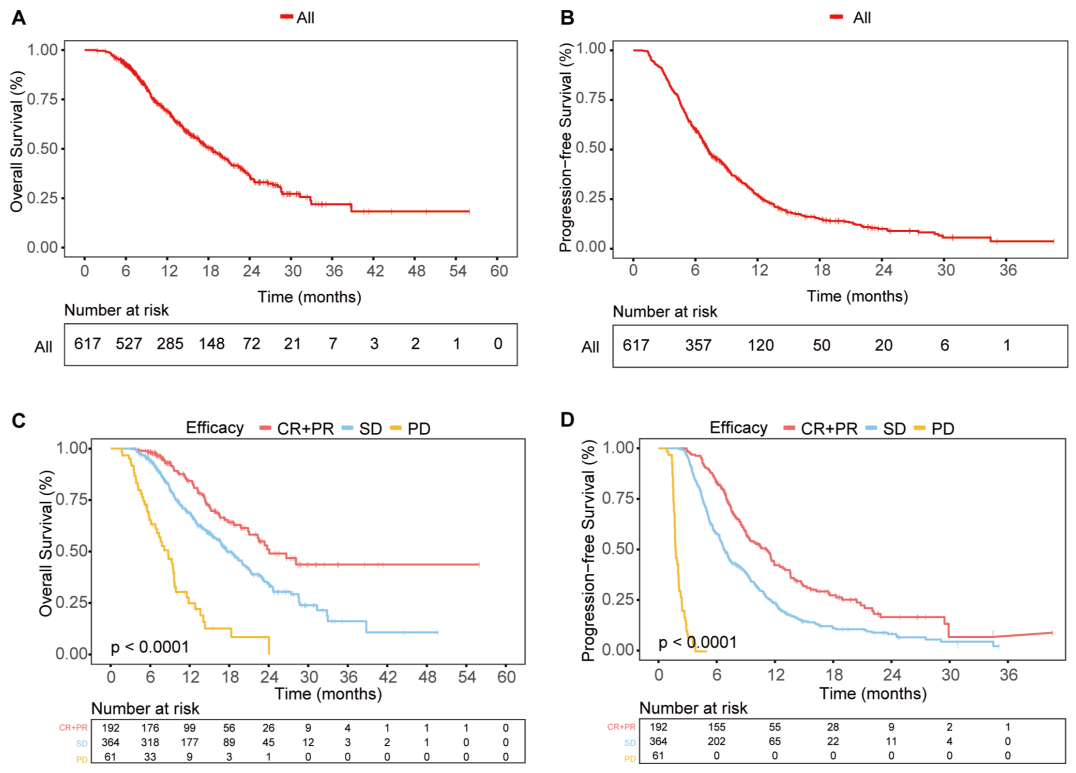

FIGURE 2
Survival outcomes in the total population **(A, B)** OS **(A)** and PFS **(B)** curves for the entire study population. **(C, D)** OS **(C)** and PFS **(D)** curves for different response groups: CR + PR, SD, and PD.

10.3389/fimmu.2024.1468342

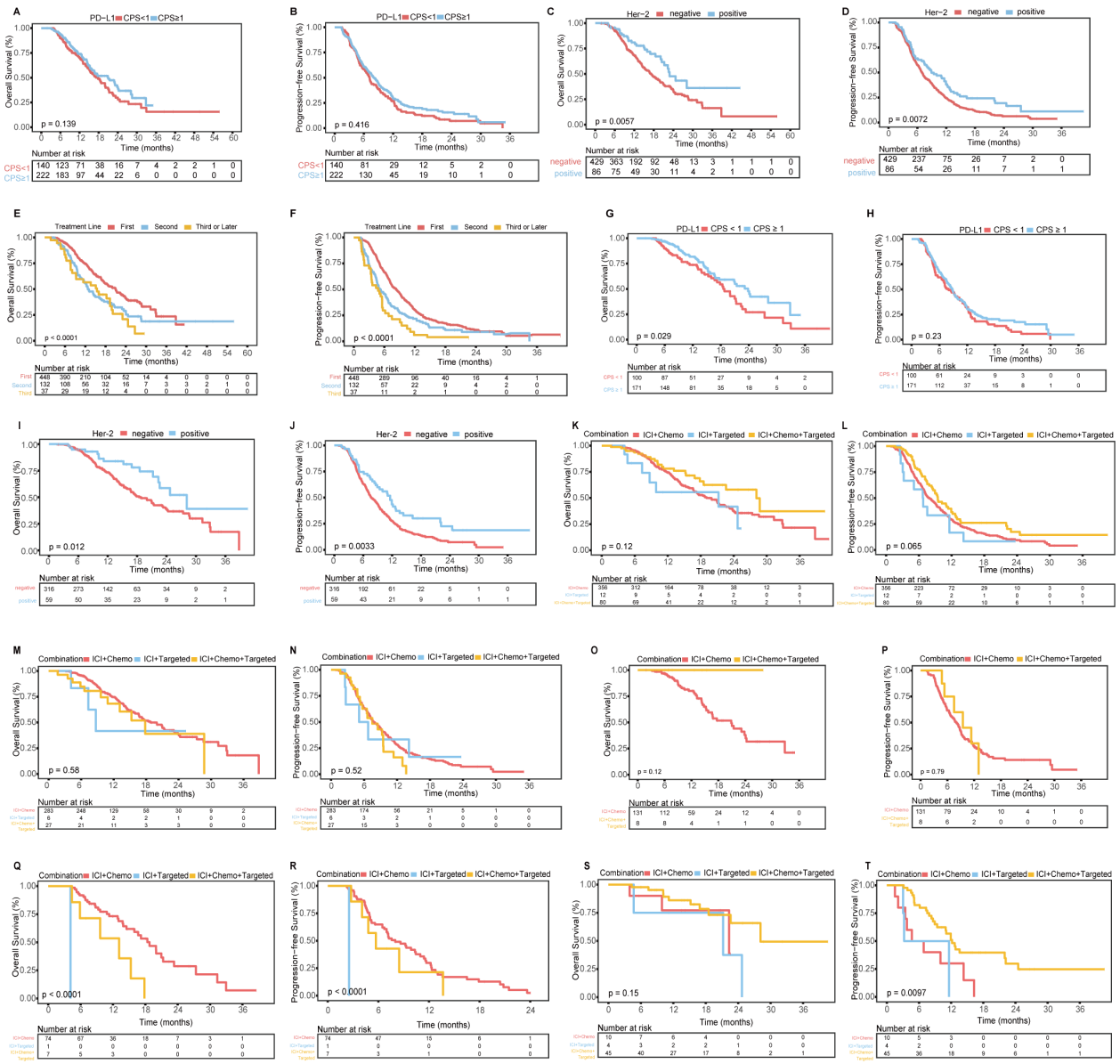

FIGURE 3
K-M curves related to PD-L1 expression, Her-2 expression, treatment lines, and treatment subgroups. **(A, B)** OS **(A)** and PFS **(B)** for patients with a PD-L1 CPS ≥1 vs. those with a CPS <1. **(C, D)** OS **(C)** and PFS **(D)** for Her-2-positive patients vs. Her-2-negative patients. **(E, F)** OS **(E)** and PFS **(F)** for patients receiving first-line vs. second-line vs. third-line or later treatments. **(G, H)** OS **(G)** and PFS **(H)** for first-line treatment subgroups of patients with a PD-L1 CPS ≥1 vs. those with a CPS <1. **(I, J)** OS **(I)** and PFS **(J)** for first-line treatment subgroups of Her-2-positive vs. Her-2-negative patients. **(K, L)** OS **(K)** and PFS **(L)** for first-line treatment subgroups receiving three different combined regimens. **(M, N)** OS **(M)** and PFS **(N)** for Her-2-negative patients receiving different first-line treatment regimens. **(O, P)** OS **(O)** and PFS **(P)** for Her-2-negative patients with a PD-L1 CPS ≥1 receiving different first-line treatment regimens. **(Q, R)** OS **(Q)** and PFS **(R)** for Her-2-negative patients with a PD-L1 CPS <1 receiving different first-line treatment regimens. **(S, T)** OS **(S)** and PFS **(T)** for Her-2-positive patients receiving different first-line treatment regimens.

3.4 OS nomogram construction and validation

Through LASSO-Cox regression analysis (Figures 4A, B), 8 independent factors associated with OS in patients receiving immunotherapy for advanced gastric cancer were identified, including treatment line, T stage, ascites, pretreatment indirect bilirubin (pre-IBIL), post-CA125, post-CA199, post-CA724, and post-PLR (Table 2). The multivariate Cox regression analysis results are presented in a forest plot (Figure 4C). Based on these eight factors, a nomogram was constructed to evaluate the 12-month, 18-month, and 24-month OS rates (Figure 4D). Each predictor has a corresponding risk score, and the total score estimates the patient's survival probability. T stage was the primary factor affecting OS.

To validate the model's predictive accuracy, ROC curves, calibration curves, and the C-index were used. ROC curves showed AUCs for 12-month, 18-month, and 24-month OS rates of 0.759, 0.752, and 0.750, respectively, in the training cohort (Supplementary Figure 2A) and 0.749, 0.703, and 0.795, respectively, in the validation cohort (Supplementary Figure 2B),

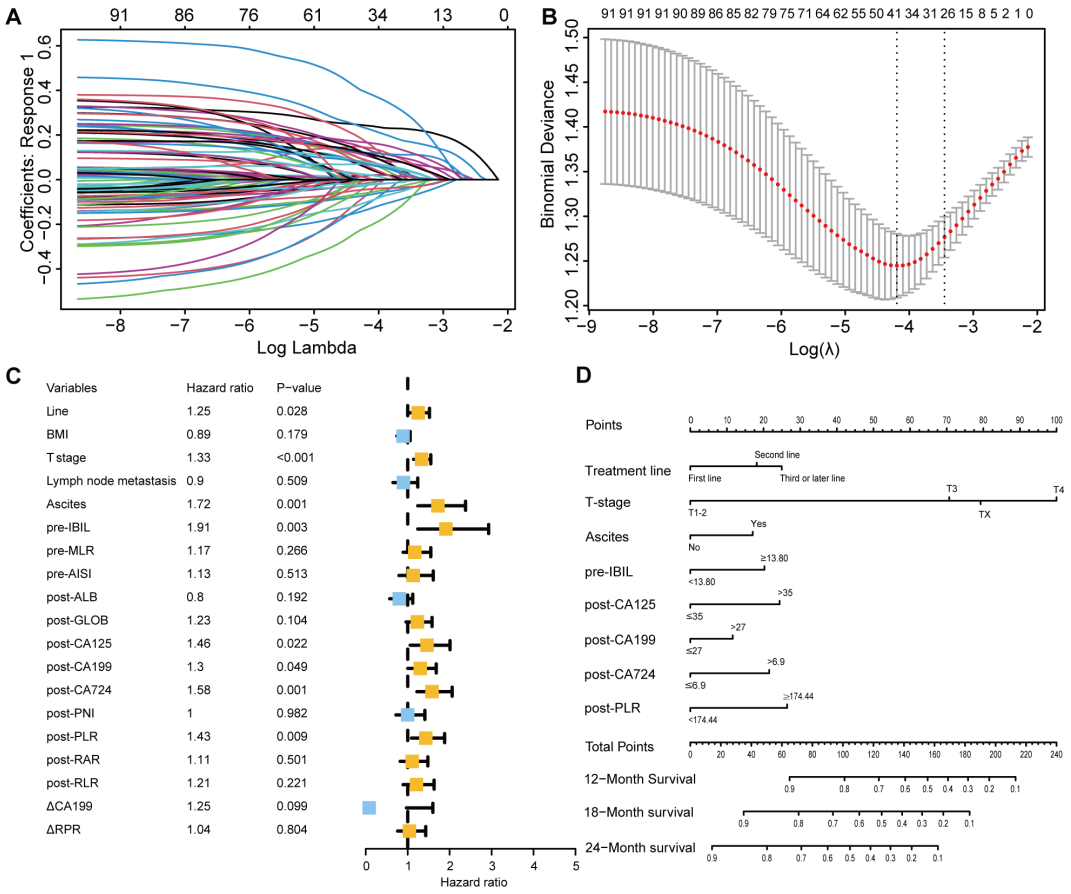

FIGURE 4
Selection of independent factors for OS and construction of the nomogram model **(A)** Overview of LASSO coefficients; **(B)** Selection of optimal parameters in the LASSO regression model; **(C)** Forest plot of multivariate Cox regression analysis results for OS; **(D)** Nomogram for predicting 12-month, 18-month, and 24-month OS rates.

indicating excellent discriminative ability. Calibration curves confirmed that the predicted OS rates at 12, 18, and 24 months were consistent with the actual outcomes in both cohorts (Supplementary Figures 2C-H). The C-indices for the training and validation cohorts were 0.728 and 0.742, respectively, suggesting good model accuracy and precision. When the model was compared with the AJCC tumor staging system, DCA showed greater net benefit for the nomogram in both cohorts (Supplementary Figure 3). The C-index, NRI, and IDI results indicated a statistically superior ability to predict OS compared to that of the AJCC staging system (Supplementary Table 7).

Based on the nomogram scores, the population was stratified into high-risk and low-risk groups. K-M curves for OS revealed significantly better survival in the low-risk group in both cohorts, further confirming the effectiveness of the OS predictive nomogram (Figures 5A-D).

3.5 PFS nomogram construction and validation

Using LASSO-Cox regression analysis (Figures 6A, B), seven independent factors associated with PFS in patients receiving immunotherapy for advanced gastric cancer, namely, treatment line, T stage, number of metastatic sites, pre-IBIL, post-GLOB, post-CA125, and △CA199, were identified (Table 3). The multivariate Cox regression analysis results are presented in a forest plot (Figure 6C). Based on these seven factors, a nomogram was constructed to evaluate the 6-month, 12-month, and 18-month PFS rates (Figure 6D). T stage was the primary factor affecting PFS, followed by treatment line.

ROC curves and calibration curves were used to evaluate the model's predictive ability. The ROC curves showed AUCs for 6-month, 12-month, and 18-month PFS rates of 0.764, 0.705, and 0.730, respectively, in the training cohort (Supplementary Figure 4A) and 0.730, 0.689, and 0.708, respectively, in the validation cohort (Supplementary Figure 4B). Calibration curves indicated that the predicted PFS rates at 6, 12, and 18 months were consistent with the actual outcomes in both cohorts (Supplementary Figures 4C-H). The DCA showed greater net benefit for the nomogram than for the AJCC staging system in both cohorts (Supplementary Figure 5). The C-index, NRI, and IDI results indicated that the nomogram had significantly superior clinical utility and effectiveness compared to the AJCC staging system (Supplementary Table 8).

Based on the nomogram scores, the population was stratified into high-risk and low-risk groups, with K-M curves for PFS

10.3389/fimmu.2024.1468342

TABLE 2 Univariate and multivariate Cox regression analyses for OS.

Variable	Univariate Analysis			Multivariate Analysis		
	HR	95% CI	*P* value	HR	95% CI	*P* value
Treatment line	1.45	(1.22 - 1.72)	<0.001	1.25	(1.02 - 1.52)	0.028
BMI	0.82	(0.69 - 0.98)	0.026	0.89	(0.74 - 1.06)	0.179
Differentiation degree	0.88	(0.77 - 1.02)	0.091			
Lauren classification	0.92	(0.83 - 1.02)	0.099			
T stage	1.43	(1.24 - 1.63)	<0.001	1.33	(1.14 - 1.55)	<0.001
Lymph node metastasis	0.65	(0.48 - 0.87)	0.004	0.90	(0.65 - 1.24)	0.509
Ascites	2.16	(1.62 - 2.89)	<0.001	1.72	(1.24 - 2.38)	0.001
Other metastases	0.98	(0.71 - 1.35)	0.895			
pre-GLOB	1.34	(0.95 - 1.90)	0.095			
pre-IBIL	1.91	(1.29 - 2.85)	0.001	1.91	(1.24 - 2.93)	0.003
pre-MLR	1.45	(1.14 - 1.84)	0.002	1.17	(0.89 - 1.55)	0.266
pre-AISI	1.59	(1.19 - 2.15)	0.002	1.13	(0.79 - 1.61)	0.513
pre-RAR	1.10	(0.86 - 1.39)	0.453			
post-ALB	0.74	(0.58 - 0.94)	0.014	0.80	(0.57 - 1.12)	0.192
post-GLOB	1.29	(1.02 - 1.64)	0.035	1.23	(0.96 - 1.58)	0.104
post-DBIL	1.23	(0.91 - 1.65)	0.178			
post-CA125	2.24	(1.70 - 2.94)	<0.001	1.46	(1.06 - 2.01)	0.022
post-CA199	1.79	(1.41 - 2.28)	<0.001	1.30	(1.00 - 1.68)	0.049
post-CA724	1.85	(1.45 - 2.36)	<0.001	1.58	(1.22 - 2.06)	0.001
post-PNI	0.73	(0.57 - 0.92)	0.009	1.00	(0.72 - 1.41)	0.982
post-PLR	1.85	(1.46 - 2.35)	<0.001	1.43	(1.09 - 1.88)	0.009
post-RAR	1.30	(1.03 - 1.66)	0.030	1.11	(0.82 - 1.48)	0.501
post-RLR	1.35	(1.05 - 1.73)	0.018	1.21	(0.89 - 1.63)	0.221
△CA199	1.44	(1.13 - 1.82)	0.003	1.25	(0.97 - 1.60)	0.080
△NMR	1.25	(0.97 - 1.60)	0.082			
△RPR	0.75	(0.57 - 0.97)	0.031	1.04	(0.76 - 1.43)	0.804

showing significantly better survival in the low-risk group in both cohorts (Figures 5E-H).

3.6 ORR predictive model construction and evaluation

Using LASSO logistic regression analysis (Figures 7A, B), 7 independent factors associated with the ORR in patients receiving immunotherapy for advanced gastric cancer were identified, including treatment line, T stage, N stage, liver metastasis, pre-RPR, post-CA125, and △CA724 (Table 4). The multivariate logistic regression analysis results are presented in a forest plot (Figure 7C). Based on these seven predictors, a nomogram was constructed to evaluate the probability of achieving CR or PR (Figure 7D). N stage, post-CA125, liver metastasis, and △CA724 were the primary factors affecting the ORR. Each variable in the nomogram has a corresponding score, and the total score, calculated by summing all predictor scores, indicates a greater probability of achieving CR or PR with a higher total score. Earlier treatment, earlier T stage, later N stage, the presence of liver metastasis, lower pre-RPR, lower post-CA125 and decreased CA724 were associated with a greater probability of achieving CR or PR.

To better evaluate the nomogram's predictive value, calibration curves, ROC curves, and decision curves were plotted. Calibration curves showed that the predicted probabilities were consistent with the actual outcomes in the training and validation cohorts (Figures 8A, B). The ROC curves showed AUCs of 0.804 in the training cohort and 0.722 in the validation cohort (Figures 8C, D), indicating excellent predictive accuracy. Decision curves

10.3389/fimmu.2024.1468342

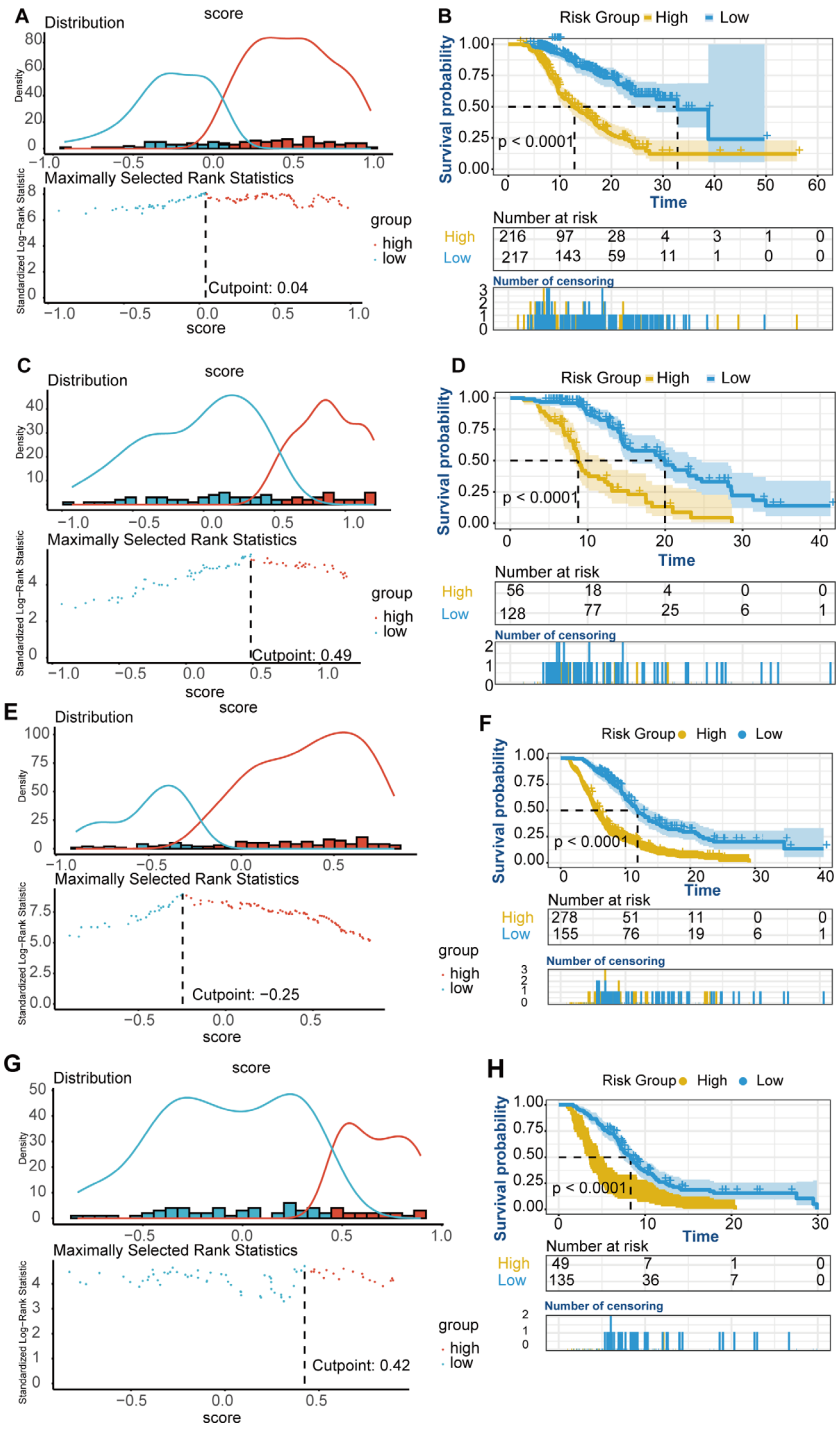

FIGURE 5
K-M curves for OS and PFS risk groups. **(A-D)** OS K-M curves for risk groups. **(A)** Risk stratification based on the OS nomogram score in the training cohort. **(B)** OS survival curves for high-risk and low-risk groups in the training cohort. **(C)** Risk stratification based on the OS nomogram score in the validation cohort. **(D)** OS survival curves for high-risk and low-risk groups in the validation cohort. **(E-H)** PFS K-M curves for risk groups. **(E)** Risk stratification based on the PFS nomogram score in the training cohort. **(F)** PFS survival curves for high-risk and low-risk groups in the training cohort. **(G)** Risk stratification based on the PFS nomogram score in the validation cohort. **(H)** PFS survival curves for high-risk and low-risk groups in the validation cohort.

indicated good clinical utility of the model (Figures 8E, F). These results confirmed that the nomogram is a simple yet effective model for predicting therapeutic response in advanced gastric cancer patients receiving immunotherapy.

According to the ORR predictive nomogram, a higher N stage and liver metastasis were paradoxically associated with a greater probability of achieving CR or PR. K-M analysis revealed no significant difference in OS among patients with different N

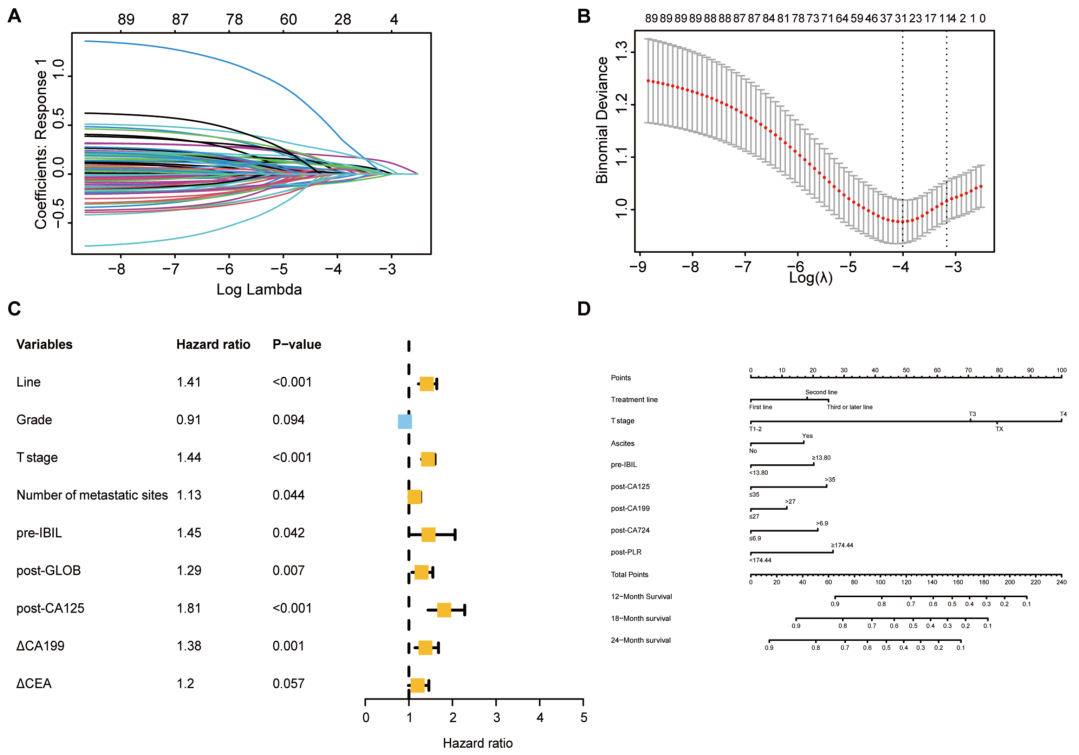

FIGURE 6
Selection of independent factors for PFS and construction of the nomogram model **(A)** Overview of LASSO coefficients; **(B)** Selection of the optimal parameters in the LASSO regression model; **(C)** Forest plot of multivariate Cox regression analysis for PFS; **(D)** Nomogram for predicting 6-month, 12-month, and 18-month PFS rates.

stages (Supplementary Figure 8E), but a significant difference in PFS was observed (Supplementary Figure 9E). No significant difference in OS was found between patients with and without liver metastasis (Supplementary Figure 8F), but those without liver metastasis had significantly better PFS (Supplementary Figure 9F). Further exploration of potential causes revealed differences in clinicopathological characteristics between patients with different N stages (Supplementary Table 9) and between patients with and without liver metastasis (Supplementary Table 10). The greater proportion of patients receiving combined chemotherapy and targeted therapy due to higher PD-L1 CPS≥1 and Her-2 positivity rates, along with the greater proportion of first-line treatment in N2-3 stage patients, might explain the greater probability of achieving CR or PR in these patients. In addition, N0 patients had a significantly lower BMI than patients in other N stages, indicating poorer nutritional status, which may have affected their treatment outcomes. A greater proportion of patients with liver metastasis without peritoneal metastasis or ascites than without

TABLE 3 Univariate and multivariate Cox regression analyses for PFS.

Variable	Univariate Analysis			Multivariate Analysis		
	HR	95% CI	*P* value	HR	95% CI	*P* value
Treatment line	1.53	(1.32 - 1.76)	<0.001	1.41	(1.22 - 1.64)	<0.001
Differentiation degree	0.88	(0.79 - 0.97)	0.015	0.91	(0.82 - 1.02)	0.094
T stage	1.47	(1.33 - 1.63)	<0.001	1.44	(1.29 - 1.60)	<0.001
Number of metastatic sites	1.19	(1.06 - 1.33)	0.004	1.13	(1.00 - 1.27)	0.044
pre-IBIL	1.89	(1.34 - 2.66)	<0.001	1.45	(1.01 - 2.06)	0.042
post-GLOB	1.34	(1.12 - 1.60)	0.001	1.29	(1.07 - 1.55)	0.007
post-CA125	1.83	(1.47 - 2.28)	<0.001	1.81	(1.44 - 2.28)	<0.001
△CA199	1.48	(1.24 - 1.77)	<0.001	1.38	(1.14 - 1.68)	0.001
△CEA	1.35	(1.13 - 1.62)	<0.001	1.20	(0.99 - 1.46)	0.057

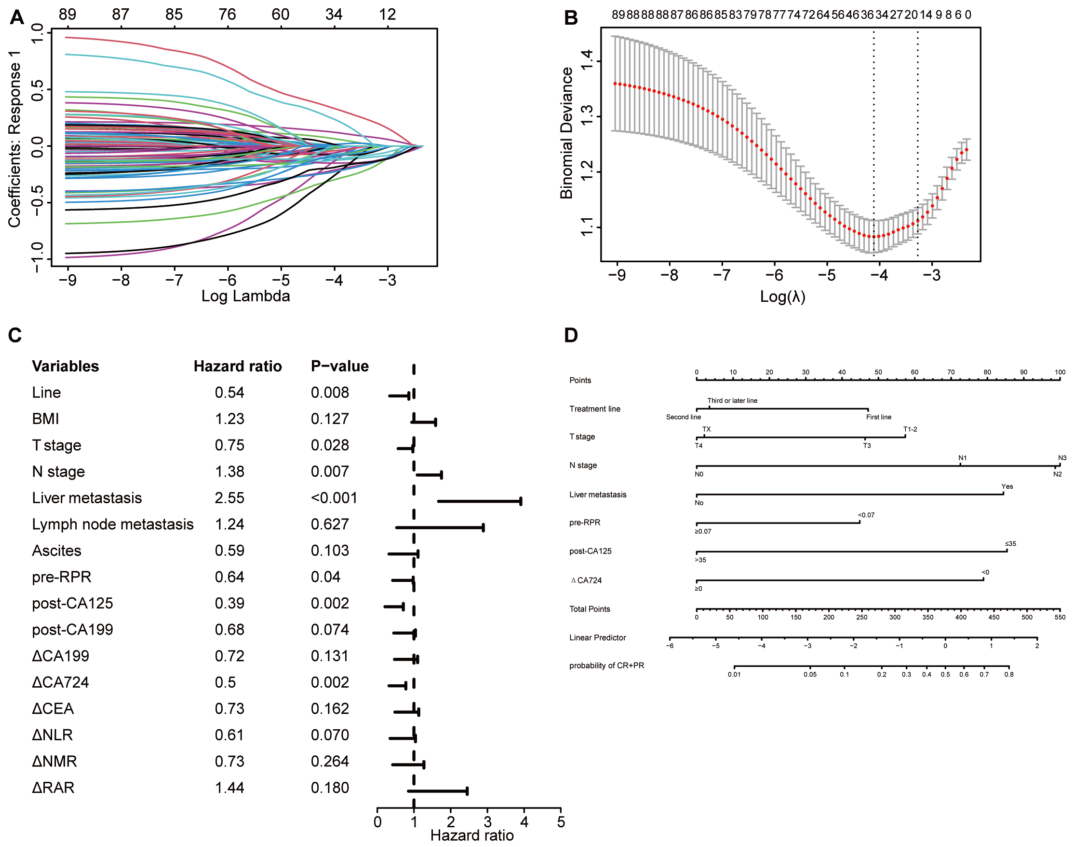

FIGURE 7
Selection of independent factors for ORR and construction of the nomogram model **(A)** Overview of LASSO coefficients; **(B)** Selection of optimal parameters in the LASSO regression model; **(C)** Forest plot of multivariate logistic regression analysis results for ORR; **(D)** Nomogram model predicting the probability of achieving CR or PR.

liver metastasis had liver metastasis, and their BMI was greater. Additionally, patients with liver metastasis had a greater prevalence of the intestinal type and a lower prevalence of the diffuse type, whereas those without liver metastasis had the opposite pattern. Previous studies have confirmed that the prognosis for diffuse-type gastric adenocarcinoma is generally worse than that for intestinal-type gastric adenocarcinoma (35).

3.7 Survival analysis

K-M analysis demonstrated survival differences for OS and PFS. OS predictors included treatment line (Figures 3E, F), T stage (Supplementary Figure 6A), ascites (Supplementary Figure 6B), pre-IBIL (Supplementary Figure 6C), post-CA125 (Supplementary Figure 6D), post-CA199 (Supplementary Figure 6E), post-CA724 (Supplementary Figure 6F), and post-PLR (Supplementary Figure 7A). Early treatment, early T stage, no ascites, and lower levels of pre-IBIL, post-CA125, post-CA199, post-CA724, and post-PLR were associated with longer OS. PFS predictors included treatment line (Figure 3), T stage (Supplementary Figure 8A), metastatic site (Supplementary Figure 9B), pre-IBIL (Supplementary Figure 9A), post-GLOB (Supplementary Figure 9C), post-CA125 (Supplementary Figure 8D), and △CA199 (Supplementary Figure 9D). Fewer metastatic sites, lower post-GLOB, and decreased △CA199 were associated with better PFS.

4 Discussion

Currently, for Her-2-negative, unresectable, advanced or recurrent gastric or gastroesophageal junction cancer patients, first-line treatment with a combination of anti-PD-1/PD-L1 therapy and chemotherapy is recommended. This recommendation is based on several large phase III clinical trials, including the ATTRACTION-4 study (36), CheckMate 649 study (37), KEYNOTE-859 study (38), ORIENT-16 study (39), and Rationale 305 study (68). In our study, for Her-2-negative patients receiving first-line immunotherapy combined with chemotherapy, the mOS and mPFS were 18.77 months and 7.77 months, respectively, with an ORR of 34.63% and a DCR of 95.76%. Although our study's OS and PFS results were comparable to or even better than those of large phase III trials, the ORR was not as high. Since this study reflected real-world clinical practice, a high proportion of patients had distant metastases, relatively poor baseline conditions, and significant tumor burden, which may have contributed to the poor ORR observed in this study. Additionally, the superior OS results in this study may be partly

10.3389/fimmu.2024.1468342

TABLE 4 Univariate and multivariate analysis of ORR.

Variable	Univariate Analysis			Multivariate Analysis		
	HR	95% CI	*P* value	HR	95% CI	*P* value
Treatment line	0.40	(0.27 - 0.59)	<0.001	0.54	(0.34 - 0.86)	0.008
BMI	1.44	(1.15 - 1.80)	0.002	1.23	(0.94 - 1.59)	0.127
T stage	0.57	(0.46 - 0.71)	<0.001	0.75	(0.57 - 0.97)	0.028
N stage	1.46	(1.25 - 1.71)	<0.001	1.38	(1.09 - 1.75)	0.007
Liver metastasis	2.15	(1.52 - 3.05)	<0.001	2.55	(1.67 - 3.91)	<0.001
Lymph node metastasis	3.86	(2.06 - 7.25)	<0.001	1.24	(0.53 - 2.89)	0.627
Lung metastasis	1.73	(0.98 - 3.05)	0.059			
Ascites	0.40	(0.23 - 0.69)	<0.001	0.59	(0.32 - 1.11)	0.103
pre-RPR	0.42	(0.30 - 0.59)	<0.001	0.64	(0.42 - 0.98)	0.040
post-CA125	0.42	(0.25 - 0.70)	<0.001	0.39	(0.21 - 0.71)	0.002
post-CA199	0.64	(0.44 - 0.91)	0.014	0.68	(0.45 - 1.04)	0.074
△CA199	0.54	(0.38 - 0.78)	<0.001	0.72	(0.47 - 1.10)	0.131
△CA724	0.45	(0.31 - 0.66)	<0.001	0.50	(0.32 - 0.78)	0.002
△CEA	0.48	(0.34 - 0.68)	<0.001	0.73	(0.48 - 1.13)	0.162
△NLR	0.37	(0.24 - 0.57)	<0.001	0.61	(0.35 - 1.04)	0.070
△NMR	0.43	(0.28 - 0.65)	<0.001	0.73	(0.42 - 1.27)	0.264
△RAR	2.04	(1.32 - 3.14)	0.001	1.44	(0.85 - 2.45)	0.180

explained by the fact that patients often adjust their treatment regimens and continue comprehensive therapy after the failure of first-line immunotherapy.

We also analyzed PD-L1 expression in Her-2-negative patients receiving first-line immunotherapy combined with chemotherapy. For patients with a PD-L1 CPS ≥1, the mOS was 20.87 months, the mPFS was 7.97 months, the ORR was 42.75%, and the DCR was 95.42%, outperforming the results from the CheckMate 649 and KEYNOTE-859 studies (37, 38). Currently, the role of PD-L1 expression in predicting the efficacy of immunotherapy is inconsistent. Although this study did not observe significant differences in OS or PFS between the PD-L1 CPS ≥1 and CPS <1 groups, the survival curves of the CPS ≥1 group showed a trend toward better outcomes than did those of the CPS <1 group. The CheckMate 649, KEYNOTE-859, ORIENT-16, and RATIONALE 305 studies demonstrated that nivolumab, pembrolizumab, sintilimab, and tislelizumab combined with chemotherapy provided survival benefits regardless of PD-L1 expression in the overall population. However, the ATTRACTION-4 study showed that patients with tumor cell PD-L1 expression ≥1% had shorter OS and PFS than did those with undefined or <1% PD-L1 expression. Therefore, it is still unclear whether the efficacy and survival advantage of gastric cancer immunotherapy increase with increasing PD-L1 expression levels, and the use of PD-L1 alone as a biomarker to predict immunotherapy efficacy is not accurate. A meta-analysis suggested that a PD-L1 CPS ≥1 was a critical threshold for survival benefit with immunotherapy alone, while immunotherapy combined with other therapies extended PFS and OS in all populations. In addition, the ORR was not affected by the PD-L1 CPS (40).

According to the analysis of Her-2 expression, Her-2-positive patients had significantly better OS and PFS than Her-2-negative patients, suggesting a potential benefit from combining immunotherapy with anti-Her-2 targeted therapy and chemotherapy. This hypothesis is supported by the KEYNOTE-811 study, which demonstrated that pembrolizumab combined with trastuzumab and chemotherapy significantly improved survival in advanced HER-2-positive gastric or gastroesophageal junction adenocarcinoma patients (41).

Additionally, we explored the relationship between recent treatment response and long-term survival. Patients who achieved CR or PR had significantly extended OS and PFS. The CheckMate 649 study explored the survival of patients with different response levels in the field of first-line immunotherapy for gastric cancer and revealed that Chinese patients (PD-L1 CPS ≥5) who achieved CR or PR at 18 weeks with nivolumab combined with chemotherapy had a 3-year OS rate of 37% and an mOS of 21.5 months (42). This indicated that achieving tumor shrinkage with immunotherapy likely led to longer survival. However, ORR and OS are not absolutely correlated. For example, several phase III studies in the field of gastric cancer immunotherapy have not achieved statistically significant OS benefits despite significant ORR benefits (41, 43). Additionally, the ability of different therapies to translate ORR benefits into long-term

10.3389/fimmu.2024.1468342

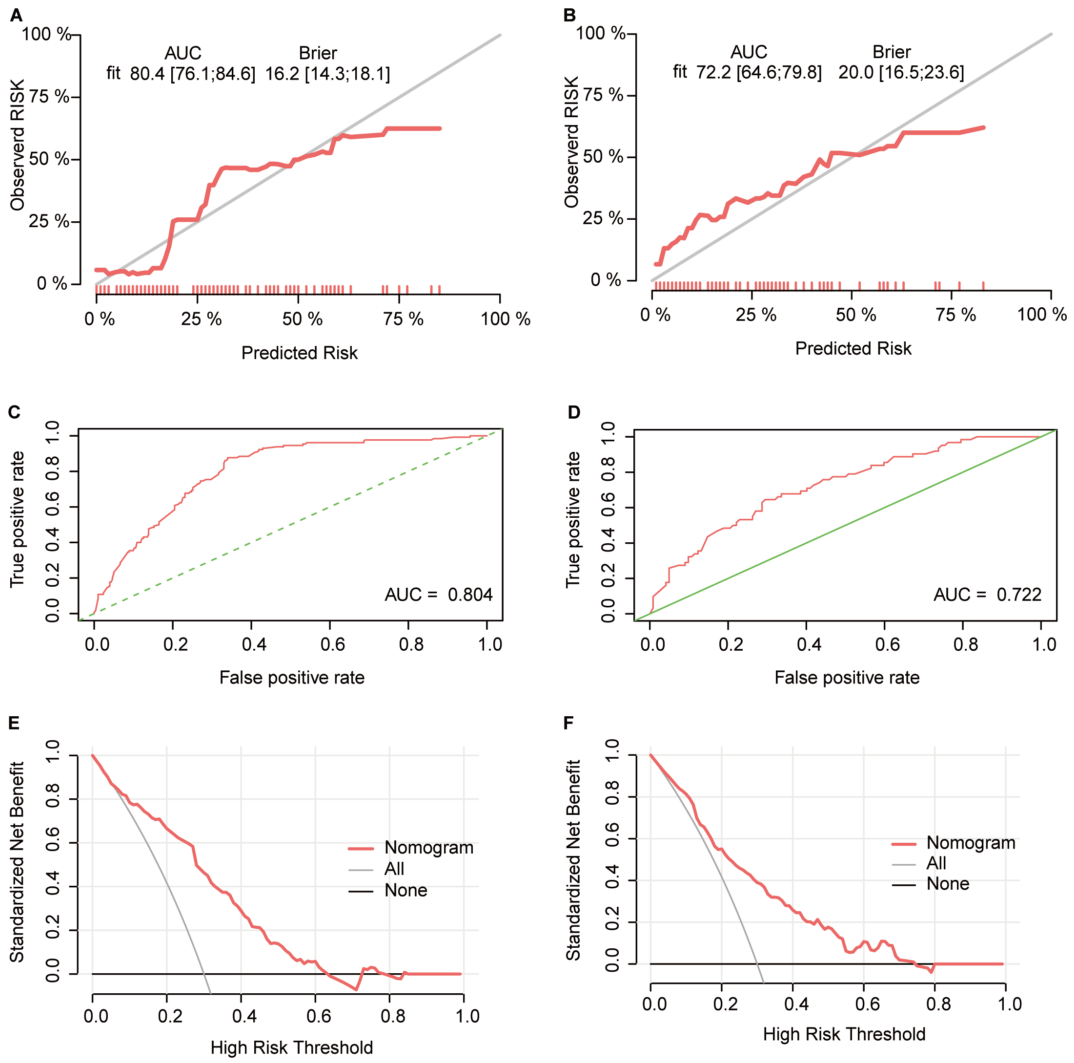

FIGURE 8
Validation of the ORR predictive nomogram model **(A, B)** Calibration curves for the CR+PR rate in the training **(A)** and validation **(B)** cohorts; **(C, D)** ROC curves of the treatment response nomogram in the training **(C)** and validation **(D)** cohorts; **(E, F)** DCA curve in the training **(E)** and validation **(F)** cohorts.

survival varies. For example, in the CheckMate 649 study, patients who achieved CR or PR in the chemotherapy group (PD-L1 CPS ≥5) had a 3-year OS rate of only 14% (44).

We observed that treatment line and T stage were independent predictors of OS, PFS, and ORR, which has been preliminarily confirmed in previous studies (45, 46). Since immunotherapy primarily enhances the antitumor immune response to kill tumor cells, theoretically, the earlier immunotherapy is applied, the better the effect. A meta-analysis of 25 clinical trials involving 20,013 patients with NSCLC also confirmed this hypothesis, showing that patients who received immunotherapy first and other treatments after failure had significantly longer OS than did those who received other treatments first and immunotherapy after failure, with a greater than 30% reduction in the risk of death (47). Our study also revealed that ascites and multiple organ metastases were associated with poor prognosis, consistent with previous studies (48). According to a Chinese subgroup analysis of the CheckMate 649 study, immunotherapy showed great therapeutic advantages for patients with peritoneal and liver metastases (42). Data from the PD-L1 CPS ≥5 subgroup showed that in the peritoneal metastasis group, nivolumab combined with chemotherapy achieved an mOS of 14.8 months, nearly three times that of the chemotherapy group; in the liver metastasis group, nivolumab combined with chemotherapy achieved an mOS of 14.3 months, nearly double that of the chemotherapy group.

In this study, several tumor markers exhibited strong predictive capabilities. Numerous studies have reported associations between baseline or dynamic serum tumor marker levels and immunotherapy efficacy (23–25, 49). Combining multiple tumor markers can increase the diagnostic sensitivity for gastric cancer and better predict its prognosis (50, 51). In a study of 146 patients with gastric cancer receiving chemotherapy or immunotherapy, CA724 was confirmed to be an independent prognostic factor for PFS and OS. The role of tumor markers in gastric cancer

immunotherapy may be underreported, possibly because most studies have focused on baseline tumor marker data. In our study, meaningful data included tumor marker indices after two cycles of immunotherapy and changes before and after treatment. We found that if tumor marker levels decrease from baseline after immunotherapy, patients might achieve better treatment efficacy and survival, providing new insights for subsequent research.

Our study revealed that pre-IBIL was an independent predictor of OS and PFS. The baseline IBIL concentration has been confirmed to be an independent prognostic factor for OS in gastric cancer patients receiving ICIs or chemotherapy but has not been studied in a cohort of patients exclusively receiving immunotherapy for gastric cancer (46). This finding fills that gap. Additionally, low levels of ALB or high levels of GLOB in many types of cancer are often associated with high mortality and recurrence rates (52–55). High levels of globulin are caused by an increase in acute phase proteins and immunoglobulins and are believed to be associated with tumor proliferation, immune evasion, and distant metastasis (56). Some studies have shown that baseline GLOB is a predictor of tumor-specific survival in gastric cancer patients, but multivariate analysis did not reveal an association between globulin levels and prognosis (57). In our study, post-GLOB was an independent predictor of PFS in advanced gastric cancer patients receiving immunotherapy.

Several retrospective studies and meta-analyses have suggested that a low pretreatment PLR may be a potential favorable prognostic biomarker for the survival of patients with various cancers, including gastric cancer (49, 58–61). In patients with advanced and metastatic gastric cancer receiving immunotherapy, pretreatment PLR was significantly associated with PFS and OS (62, 63). This study revealed that the posttreatment PLR might be an independent predictor of OS, providing new ideas for future research. We speculate that a high PLR is associated with poor OS because platelet activation is present at all stages of tumor development, spread, and metastasis (64). When tumor cells enter the bloodstream, platelets aggregate on their surface, protecting tumor cells from attack by immune cells. Platelets also promote tumor metastasis and angiogenesis by releasing various growth factors, such as vascular endothelial growth factor-A, and can promote immune evasion and chemoresistance in tumor cells (17). On the other hand, an increase in lymphocytes is also associated with increased sensitivity to ICIs (65). Therefore, an elevated PLR indicates a cellular environment highly conducive to tumor growth and a poor response to immunotherapy. Notably, other inflammatory composite indices, such as the NLR, MLR, NMR, SII, NLPR, AISI, and SIRI, did not show potential for predicting treatment efficacy or survival in this study. Therefore, the practical application of inflammatory markers in the clinic should still be approached with caution.

PLT and RDW have been confirmed to be associated with the prognosis of cancer patients, but both indicators are easily affected by diseases other than tumors (66). In contrast, the RPR may be a more reliable indicator of treatment efficacy and patient prognosis and has been confirmed to reflect the severity of tumors (67). In this study, the pre-RPR was found to be an independent predictor of the ORR in patients receiving advanced gastric cancer immunotherapy, demonstrating the potential of the RPR, which is distinct from the findings of previous studies.

By collecting a large sample of real-world patient data, which includes comprehensive clinicopathological characteristics and peripheral blood indicators, our study has constructed a robust and practical model for predicting the efficacy and survival of gastric cancer patients receiving immunotherapy. We integrated both baseline and post-treatment peripheral blood data, assessing changes after two treatment cycles. This dynamic analysis provides valuable insights into the potential of blood-based biomarkers for guiding immunotherapy in gastric cancer patients. Moreover, while prior studies have predominantly focused on PFS and OS, our research uniquely addresses the ORR, offering the first nomogram prediction models related to ORR in this context. This novel aspect of our study fills a crucial gap in the current literature, further enhancing its clinical relevance.

This study also has several limitations. First, although this was a multicenter clinical study, the uneven geographic distribution of hospitals may limit the generalizability of the findings. Second, due to inconsistent routine examinations in different hospitals, the completeness of the data is limited, and there are patients with unknown PD-L1 CPS, Her-2, and Ki-67 status, which may cause statistical bias. Third, the selection of ICIs in this study was not uniform. Therefore, to obtain higher-level medical evidence, larger sample prospective studies are needed. Fourth, the follow-up time for patients in this study was relatively short, and the nomogram can predict OS rates up to 2 years. Longer follow-up periods are needed to analyze the 3-year and 5-year survival rates and long-term prognosis of patients.

5 Conclusions

This study highlights several important findings regarding the clinical outcomes of advanced gastric or gastroesophageal junction cancer patients treated with PD-1/PD-L1 inhibitors. Earlier treatment, lower T stage, absence of ascites, and lower levels of pre-IBIL, post-CA125, post-CA199, post-CA724, and post-PLR were associated with better OS. PFS was improved in patients with earlier treatment, lower T stage, fewer metastatic sites, and lower levels of pre-IBIL, post-GLOB, and post-CA125. Additionally, patients with earlier treatment, lower T and N stages, absence of liver metastases, and lower pre-RPR and post-CA125 levels were more likely to achieve a favorable objective response. Our validated nomogram model based on these indicators offers a practical tool for identifying patients most likely to benefit from immunotherapy, providing valuable clinical guidance for personalized treatment strategies.

Data availability statement

The original contributions presented in the study are included in the article/Supplementary Material. Further inquiries can be directed to the corresponding author.

Ethics statement

The studies involving humans were approved by the Ethics Committee of Scientific Research and Clinical Trials of the First Affiliated Hospital of Zhengzhou University. The studies were conducted in accordance with the local legislation and institutional requirements. The participants provided their written informed consent to participate in this study.

Author contributions

YY: Conceptualization, Data curation, Software, Visualization, Writing – original draft, Writing – review & editing. ZW: Conceptualization, Data curation, Formal analysis, Funding acquisition, Software, Visualization, Writing – original draft, Writing – review & editing. DX: Methodology, Supervision, Visualization, Writing – original draft, Writing – review & editing. LG: Supervision, Writing – original draft, Writing – review & editing. BY: Formal analysis, Supervision, Writing – original draft, Writing – review & editing. QZ: Supervision, Writing – original draft, Writing – review & editing. FW: Conceptualization, Supervision, Visualization, Writing – original draft, Writing – review & editing.

Funding

The author(s) declare financial support was received for the research, authorship, and/or publication of this article. This study received funding from the Henan Zhongyuan Medical Science and Technology Innovation and Development Foundation.

Acknowledgments

We express our gratitude to Dr. Danyang Chen for aiding in the preparation of the manuscript. We also acknowledge the support from Henan Zhongyuan Medical Science and Technology Innovation and Development Foundation.

Conflict of interest

The authors declare that the research was conducted in the absence of any commercial or financial relationships that could be construed as a potential conflict of interest.

Publisher's note

Supplementary material

The Supplementary Material for this article can be found online at: https://www.frontiersin.org/articles/10.3389/fimmu.2024.1468342/full#supplementary-material

References

1. Sung H, Ferlay J, Siegel RL, Laversanne M, Soerjomataram I, Jemal A, et al. Global cancer statistics 2020: GLOBOCAN estimates of incidence and mortality worldwide for 36 cancers in 185 countries. *CA Cancer J Clin*. (2021) 71:209–49. doi: 10.3322/caac.21660

2. Allemani C, Matsuda T, Di Carlo V, Harewood R, Matz M, Nikšić M, et al. Global surveillance of trends in cancer survival 2000-14 (CONCORD-3): analysis of individual records for 37 513 025 patients diagnosed with one of 18 cancers from 322 population-based registries in 71 countries. *Lancet*. (2018) 391:1023–75. doi: 10.1016/s0140-6736(17)33326-3

3. Van Cutsem E, Moiseyenko VM, Tjulandin S, Majlis A, Constenla M, Boni C, et al. Phase III study of docetaxel and cisplatin plus fluorouracil compared with cisplatin and fluorouracil as first-line therapy for advanced gastric cancer: a report of the V325 Study Group. *J Clin Oncol*. (2006) 24:4991–7. doi: 10.1200/jco.2006.06.8429

4. Yamada Y, Higuchi K, Nishikawa K, Gotoh M, Fuse N, Sugimoto N, et al. Phase III study comparing oxaliplatin plus S-1 with cisplatin plus S-1 in chemotherapy-naïve patients with advanced gastric cancer. *Ann Oncol*. (2015) 26:141–8. doi: 10.1093/annonc/mdu472

5. Li K, Zhang A, Li X, Zhang H, Zhao L. Advances in clinical immunotherapy for gastric cancer. *Biochim Biophys Acta Rev Cancer*. (2021) 1876:188615. doi: 10.1016/j.bbcan.2021.188615

6. Formica V, Morelli C, Patrikidou A, Shiu KK, Nardecchia A, Lucchetti J, et al. A systematic review and meta-analysis of PD-1/PD-L1 inhibitors in specific patient subgroups with advanced gastro-oesophageal junction and gastric adenocarcinoma. *Crit Rev Oncol Hematol*. (2021) 157:103173. doi: 10.1016/j.critrevonc.2020.103173

7. Kim H, Hong JY, Lee J, Park SH, Park JO, Park YS, et al. Clinical sequencing to assess tumor mutational burden as a useful biomarker to immunotherapy in various solid tumors. *Ther Adv Med Oncol*. (2021) 13:1758835921992992. doi: 10.1177/1758835921992992

8. Kattan MW, Karpeh MS, Mazumdar M, Brennan MF. Postoperative nomogram for disease-specific survival after an R0 resection for gastric carcinoma. *J Clin Oncol*. (2003) 21:3647–50. doi: 10.1200/jco.2003.01.240

9. Song KY, Park YG, Jeon HM, Park CH. A nomogram for predicting individual survival of patients with gastric cancer who underwent radical surgery with extended lymph node dissection. *Gastric Cancer*. (2014) 17:287–93. doi: 10.1007/s10120-013-0270-x

10. Song M, Zhang Q, Song C, Liu T, Zhang X, Ruan G, et al. The advanced lung cancer inflammation index is the optimal inflammatory biomarker of overall survival in patients with lung cancer. *J Cachexia Sarcopenia Muscle*. (2022) 13:2504–14. doi: 10.1002/jcsm.13032

11. Namikawa T, Munekage E, Munekage M, Maeda H, Yatabe T, Kitagawa H, et al. Evaluation of systemic inflammatory response biomarkers in patients receiving chemotherapy for unresectable and recurrent advanced gastric cancer. *Oncology*. (2016) 90:321–6. doi: 10.1159/000446373

12. Miyamoto R, Inagawa S, Sano N, Tadano S, Adachi S, Yamamoto M. The neutrophil-to-lymphocyte ratio (NLR) predicts short-term and long-term outcomes in gastric cancer patients. *Eur J Surg Oncol*. (2018) 44:607–12. doi: 10.1016/j.ejso.2018.02.003

13. Lian L, Xia YY, Zhou C, Shen XM, Li XL, Han SG, et al. Application of platelet/lymphocyte and neutrophil/lymphocyte ratios in early diagnosis and prognostic prediction in patients with resectable gastric cancer. *Cancer biomark*. (2015) 15:899–907. doi: 10.3233/cbm-150534

14. Petrillo A, Laterza MM, Tirino G, Pompella L, Ventriglia J, Pappalardo A, et al. Systemic-inflammation-based score can predict prognosis in metastatic gastric cancer

patients before first-line chemotherapy. *Future Oncol*. (2018) 14:2493–505. doi: 10.2217/fon-2018-0167

15. Hirahara T, Arigami T, Yanagita S, Matsushita D, Uchikado Y, Kita Y, et al. Combined neutrophil-lymphocyte ratio and platelet-lymphocyte ratio predicts chemotherapy response and prognosis in patients with advanced gastric cancer. *BMC Cancer*. (2019) 19:672. doi: 10.1186/s12885-019-5903-y

16. Ota Y, Takahari D, Suzuki T, Osumi H, Nakayama I, Oki A, et al. Changes in the neutrophil-to-lymphocyte ratio during nivolumab monotherapy are associated with gastric cancer survival. *Cancer Chemother Pharmacol*. (2020) 85:265–72. doi: 10.1007/s00280-019-04023-w

17. Cao W, Yao X, Cen D, Zhi Y, Zhu N, Xu L. The prognostic role of platelet-to-lymphocyte ratio on overall survival in gastric cancer: a systematic review and meta-analysis. *BMC Gastroenterol*. (2020) 20:16. doi: 10.1186/s12876-020-1167-x

18. Stares M, Ding TE, Stratton C, Thomson F, Baxter M, Cagney H, et al. Biomarkers of systemic inflammation predict survival with first-line immune checkpoint inhibitors in non-small-cell lung cancer. *ESMO Open*. (2022) 7:100445. doi: 10.1016/j.esmoop.2022.100445

19. Ye K, Xiao M, Li Z, He K, Wang J, Zhu L, et al. Preoperative systemic inflammation response index is an independent prognostic marker for BCG immunotherapy in patients with non-muscle-invasive bladder cancer. *Cancer Med*. (2023) 12:4206–17. doi: 10.1002/cam4.5284

20. Gou M, Zhang Y, Liu T, Qu T, Si H, Wang Z, et al. The prognostic value of pre-treatment hemoglobin (Hb) in patients with advanced or metastatic gastric cancer treated with immunotherapy. *Front Oncol*. (2021) 11:655716. doi: 10.3389/fonc.2021.655716

21. Gou M, Qu T, Wang Z, Yan H, Si Y, Zhang Y, et al. Neutrophil-to-lymphocyte ratio (NLR) predicts PD-1 inhibitor survival in patients with metastatic gastric cancer. *J Immunol Res*. (2021) 2021:2549295. doi: 10.1155/2021/2549295

22. Kataoka Y, Hirano K, Narabayashi T, Hara S, Fujimoto D, Tanaka T, et al. Carcinoembryonic antigen as a predictive biomarker of response to nivolumab in non-small cell lung cancer. *Anticancer Res*. (2018) 38:559–63. doi: 10.21873/anticanres.12259

23. Dal Bello MG, Filiberti RA, Alama A, Orengo AM, Mussap M, Coco S, et al. The role of CEA, CYFRA21-1 and NSE in monitoring tumor response to Nivolumab in advanced non-small cell lung cancer (NSCLC) patients. *J Transl Med*. (2019) 17:74. doi: 10.1186/s12967-019-1828-0

24. Lang D, Horner A, Brehm E, Akbari K, Hergan B, Langer K, et al. Early serum tumor marker dynamics predict progression-free and overall survival in single PD-1/PD-L1 inhibitor treated advanced NSCLC-A retrospective cohort study. *Lung Cancer*. (2019) 134:59–65. doi: 10.1016/j.lungcan.2019.05.033

25. Zhang Z, Yuan F, Chen R, Li Y, Ma J, Yan X, et al. Dynamics of serum tumor markers can serve as a prognostic biomarker for chinese advanced non-small cell lung cancer patients treated with immune checkpoint inhibitors. *Front Immunol*. (2020) 11:1173. doi: 10.3389/fimmu.2020.01173

26. Huang J, Xiao Y, Zhou Y, Deng H, Yuan Z, Dong L, et al. Baseline serum tumor markers predict the survival of patients with advanced non-small cell lung cancer receiving first-line immunotherapy: a multicenter retrospective study. *BMC Cancer*. (2023) 23:812. doi: 10.1186/s12885-023-11312-4

27. Luo Z, Zhou L, Balde AI, Li Z, He L, ZhenWei C, et al. Prognostic impact of preoperative prognostic nutritional index in resected advanced gastric cancer: A multicenter propensity score analysis. *Eur J Surg Oncol*. (2019) 45:425–31. doi: 10.1016/j.ejso.2018.09.004

28. Kim JH, Bae YJ, Jun KH, Chin HM. Long-term trends in hematological and nutritional status after gastrectomy for gastric cancer. *J Gastrointest Surg*. (2017) 21:1212–9. doi: 10.1007/s11605-017-3445-7

29. Kim YN, Choi YY, An JY, Choi MG, Lee JH, Sohn TS, et al. Comparison of Postoperative Nutritional Status after Distal Gastrectomy for Gastric Cancer Using Three Reconstructive Methods: a Multicenter Study of over 1300 Patients. *J Gastrointest Surg*. (2020) 24:1482–8. doi: 10.1007/s11605-019-04301-1

30. Mizukami T, Piao Y. Role of nutritional care and general guidance for patients with advanced or metastatic gastric cancer. *Future Oncol*. (2021) 17:3101–9. doi: 10.2217/fon-2021-0186

31. Liu ZJ, Ge XL, Ai SC, Wang HK, Sun F, Chen L, et al. Postoperative decrease of serum albumin predicts short-term complications in patients undergoing gastric cancer resection. *World J Gastroenterol*. (2017) 23:4978–85. doi: 10.3748/wjg.v23.i27.4978

32. Liu N, Jiang A, Zheng X, Fu X, Zheng H, Gao H, et al. Prognostic Nutritional Index identifies risk of early progression and survival outcomes in Advanced Non-small Cell Lung Cancer patients treated with PD-1 inhibitors. *J Cancer*. (2021) 12:2960–7. doi: 10.7150/jca.55936

33. Matsubara T, Takamori S, Haratake N, Toyozawa R, Miura N, Shimokawa M, et al. The impact of immune-inflammation-nutritional parameters on the prognosis of non-small cell lung cancer patients treated with atezolizumab. *J Thorac Dis*. (2020) 12:1520–8. doi: 10.21037/jtd.2020.02.27

34. Li D, Yuan X, Liu J, Li C, Li W. Prognostic value of prognostic nutritional index in lung cancer: a meta-analysis. *J Thorac Dis*. (2018) 10:5298–307. doi: 10.21037/jtd.2018.08.51

35. Tang D, Ni M, Zhu H, Cao J, Zhou L, Shen S, et al. Differential prognostic implications of gastric adenocarcinoma based on Lauren's classification: a Surveillance, Epidemiology, and End Results (SEER)-based cohort study. *Ann Transl Med*. (2021) 9 (8):646. doi: 10.21037/atm-20-7953

36. Kang YK, Chen LT, Ryu MH, Oh DY, Oh SC, Chung HC, et al. Nivolumab plus chemotherapy versus placebo plus chemotherapy in patients with HER2-negative, untreated, unresectable advanced or recurrent gastric or gastro-oesophageal junction cancer (ATTRACTION-4): a randomised, multicentre, double-blind, placebo-controlled, phase 3 trial. *Lancet Oncol*. (2022) 23:234–47. doi: 10.1016/s1470-2045(21)00692-6

37. Janjigian YY, Shitara K, Moehler M, Garrido M, Salman P, Shen L, et al. First-line nivolumab plus chemotherapy versus chemotherapy alone for advanced gastric, gastro-oesophageal junction, and oesophageal adenocarcinoma (CheckMate 649): a randomised, open-label, phase 3 trial. *Lancet*. (2021) 398:27–40. doi: 10.1016/s0140-6736(21)00797-2

38. Rha SY, Oh DY, Yañez P, Bai Y, Ryu MH, Lee J, et al. Pembrolizumab plus chemotherapy versus placebo plus chemotherapy for HER2-negative advanced gastric cancer (KEYNOTE-859): a multicentre, randomised, double-blind, phase 3 trial. *Lancet Oncol*. (2023) 24:1181–95. doi: 10.1016/s1470-2045(23)00515-6

39. Xu J, Jiang H, Pan Y, Gu K, Cang S, Han L, et al. Sintilimab plus chemotherapy for unresectable gastric or gastroesophageal junction cancer: the ORIENT-16 randomized clinical trial. *Jama*. (2023) 330:2064–74. doi: 10.1001/jama.2023.19918

40. Xie T, Zhang Z, Zhang X, Qi C, Shen L, Peng Z. Appropriate PD-L1 cutoff value for gastric cancer immunotherapy: A systematic review and meta-analysis. *Front Oncol*. (2021) 11:646355. doi: 10.3389/fonc.2021.646355

41. Janjigian YY, Kawazoe A, Bai Y, Xu J, Lonardi S, Metges JP, et al. Pembrolizumab plus trastuzumab and chemotherapy for HER2-positive gastric or gastro-oesophageal junction adenocarcinoma: interim analyses from the phase 3 KEYNOTE-811 randomised placebo-controlled trial. *Lancet*. (2023) 402:2197–208. doi: 10.1016/s0140-6736(23)02033-0

42. Liu T, Bai Y, Lin X, Li W, Wang J, Zhang X, et al. First-line nivolumab plus chemotherapy vs chemotherapy in patients with advanced gastric, gastroesophageal junction and esophageal adenocarcinoma: CheckMate 649 Chinese subgroup analysis. *Int J Cancer*. (2023) 152:749–60. doi: 10.1002/ijc.34296

43. Shitara K, Van Cutsem E, Bang YJ, Fuchs C, Wyrwicz L, Lee KW, et al. Efficacy and safety of pembrolizumab or pembrolizumab plus chemotherapy vs chemotherapy alone for patients with first-line, advanced gastric cancer: the KEYNOTE-062 phase 3 randomized clinical trial. *JAMA Oncol*. (2020) 6:1571–80. doi: 10.1001/jamaoncol.2020.3370

44. Janjigian YY, Ajani JA, Moehler M, Shen L, Garrido M, Gallardo C, et al. First-line nivolumab plus chemotherapy for advanced gastric, gastroesophageal junction, and esophageal adenocarcinoma: 3-year follow-up of the phase III checkMate 649 trial. *J Clin Oncol*. (2024) 42:2012–20. doi: 10.1200/jco.23.01601

45. Gou M, Qian N, Zhang Y, Wei L, Fan Q, Wang Z, et al. Construction of a nomogram to predict the survival of metastatic gastric cancer patients that received immunotherapy. *Front Immunol*. (2022) 13:950868. doi: 10.3389/fimmu.2022.950868

46. Sun H, Chen L, Huang R, Pan H, Zuo Y, Zhao R, et al. Prognostic nutritional index for predicting the clinical outcomes of patients with gastric cancer who received immune checkpoint inhibitors. *Front Nutr*. (2022) 9:1038118. doi: 10.3389/fnut.2022.1038118

47. Blumenthal GM, Zhang L, Zhang H, Kazandjian D, Khozin S, Tang S, et al. Milestone analyses of immune checkpoint inhibitors, targeted therapy, and conventional therapy in metastatic non-small cell lung cancer trials: A meta-analysis. *JAMA Oncol*. (2017) 3:e171029. doi: 10.1001/jamaoncol.2017.1029

48. Men HT, Gou HF, Liu JY, Li Q, Luo DY, Bi F, et al. Prognostic factors of intraperitoneal chemotherapy for peritoneal carcinomatosis of gastric cancer: A retrospective study from a single center. *Oncol Lett*. (2016) 11:3501–7. doi: 10.3892/ol.2016.4403

49. Chen Y, Wen S, Xia J, Du X, Wu Y, Pan B, et al. Association of dynamic changes in peripheral blood indexes with response to PD-1 inhibitor-based combination therapy and survival among patients with advanced non-small cell lung cancer. *Front Immunol*. (2021) 12:672271. doi: 10.3389/fimmu.2021.672271

50. He CZ, Zhang KH, Li Q, Liu XH, Hong Y, Lv NH. Combined use of AFP, CEA, CA125 and CAl9-9 improves the sensitivity for the diagnosis of gastric cancer. *BMC Gastroenterol*. (2013) 13:87. doi: 10.1186/1471-230x-13-87

51. Feng F, Tian Y, Xu G, Liu Z, Liu S, Zheng G, et al. Diagnostic and prognostic value of CEA, CA19-9, AFP and CA125 for early gastric cancer. *BMC Cancer*. (2017) 17:737. doi: 10.1186/s12885-017-3738-y

52. Ikeda S, Yoshioka H, Ikeo S, Morita M, Sone N, Niwa T, et al. Serum albumin level as a potential marker for deciding chemotherapy or best supportive care in elderly, advanced non-small cell lung cancer patients with poor performance status. *BMC Cancer*. (2017) 17:797. doi: 10.1186/s12885-017-3814-3

53. Li Q, Meng X, Liang L, Xu Y, Cai G, Cai S. High preoperative serum globulin in rectal cancer treated with neoadjunctive chemoradiation therapy is a risk factor for poor outcome. *Am J Cancer Res*. (2015) 5:2856–64.

54. Liu X, Meng QH, Ye Y, Hildebrandt MA, Gu J, Wu X. Prognostic significance of pretreatment serum levels of albumin, LDH and total bilirubin in patients with non-metastatic breast cancer. *Carcinogenesis*. (2015) 36:243–8. doi: 10.1093/carcin/bgu247

55. Kang SC, Kim HI, Kim MG. Low serum albumin level, male sex, and total gastrectomy are risk factors of severe postoperative complications in elderly gastric cancer patients. *J Gastric Cancer*. (2016) 16:43–50. doi: 10.5230/jgc.2016.16.1.43

56. Du XJ, Tang LL, Mao YP, Sun Y, Zeng MS, Kang TB, et al. The pretreatment albumin to globulin ratio has predictive value for long-term mortality in nasopharyngeal carcinoma. *PloS One*. (2014) 9:e94473. doi: 10.1371/journal.pone.0094473

57. Chen J, Zhou Y, Xu Y, Zhu HY, Shi YQ. Low pretreatment serum globulin may predict favorable prognosis for gastric cancer patients. *Tumour Biol*. (2016) 37:3905–11. doi: 10.1007/s13277-015-3778-3

58. Wang Y, Li Y, Chen P, Xu W, Wu Y, Che G. Prognostic value of the pretreatment systemic immune-inflammation index (SII) in patients with non-small cell lung cancer: a meta-analysis. *Ann Transl Med*. (2019) 7:433. doi: 10.21037/atm.2019.08.116

59. Zhang N, Jiang J, Tang S, Sun G. Predictive value of neutrophil-lymphocyte ratio and platelet-lymphocyte ratio in non-small cell lung cancer patients treated with immune checkpoint inhibitors: A meta-analysis. *Int Immunopharmacol*. (2020) 85:106677. doi: 10.1016/j.intimp.2020.106677

60. Bilen MA, Martini DJ, Liu Y, Lewis C, Collins HH, Shabto JM, et al. The prognostic and predictive impact of inflammatory biomarkers in patients who have advanced-stage cancer treated with immunotherapy. *Cancer*. (2019) 125:127–34. doi: 10.1002/cncr.31778

61. Russo A, Russano M, FranChina T, Migliorino MR, Aprile G, Mansueto G, et al. Neutrophil-to-lymphocyte ratio (NLR), platelet-to-lymphocyte ratio (PLR), and outcomes with nivolumab in pretreated non-small cell lung cancer (NSCLC): A large retrospective multicenter study. *Adv Ther*. (2020) 37:1145–55. doi: 10.1007/s12325-020-01229-w

62. Gou M, Zhang Y. Pretreatment platelet-to-lymphocyte ratio (PLR) as a prognosticating indicator for gastric cancer patients receiving immunotherapy. *Discovery Oncol*. (2022) 13:118. doi: 10.1007/s12672-022-00571-5

63. Qu Z, Wang Q, Wang H, Jiao Y, Li M, Wei W, et al. The effect of inflammatory markers on the survival of advanced gastric cancer patients who underwent anti-programmed death 1 therapy. *Front Oncol*. (2022) 12:783197. doi: 10.3389/fonc.2022.783197

64. Schlesinger M. Role of platelets and platelet receptors in cancer metastasis. *J Hematol Oncol*. (2018) 11:125. doi: 10.1186/s13045-018-0669-2

65. Quigley DA, Kristensen V. Predicting prognosis and therapeutic response from interactions between lymphocytes and tumor cells. *Mol Oncol*. (2015) 9:2054–62. doi: 10.1016/j.molonc.2015.10.003

66. Zhang H, Liang K, Ke L, Tang S. Clinical application of red cell distribution width, mean platelet volume, and cancer antigen 125 detection in endometrial cancer. *J Clin Lab Anal*. (2020) 34:e23309. doi: 10.1002/jcla.23309

67. Takeuchi H, Abe M, Takumi Y, Hashimoto T, Miyawaki M, Okamoto T, et al. Elevated red cell distribution width to platelet count ratio predicts poor prognosis in patients with breast cancer. *Sci Rep*. (2019) 9:3033. doi: 10.1038/s41598-019-40024-8

68. Qiu MZ, Oh DY, Kato K, Arkenau T, Tabernero J, Correa MC, et al. Tislelizumab plus chemotherapy versus placebo plus chemotherapy as first line treatment for advanced gastric or gastro-oesophageal junction adenocarcinoma: RATIONALE-305 randomised, double blind, phase 3 trial. *Bmj*. (2024) 385:e078876. doi: 10.1136/bmj-2023-078876

frontiers | Frontiers in Immunology

TYPE Original Research
PUBLISHED 07 November 2024
DOI 10.3389/fimmu.2024.1463017

OPEN ACCESS

EDITED BY
Stavros P. Papadakos,
Laiko General Hospital of Athens, Greece

REVIEWED BY
Chao Yang,
Wuhan University, China
Xianli Jiang,
University of Texas MD Anderson Cancer Center, United States

*CORRESPONDENCE
Fanming Kong
kongfanming08@163.com
Yingjie Jia
1103197962@qq.com

†These authors have contributed equally to this work and share first authorship

RECEIVED 11 July 2024
ACCEPTED 21 October 2024
PUBLISHED 07 November 2024

CITATION
Xu Q, Yi D, Jia C, Kong F and Jia Y (2024) Immunotherapy plus chemotherapy versus chemotherapy alone in the first-line treatment for advanced gastric cancer/gastroesophageal junction cancer: a real-world retrospective study. *Front. Immunol.* 15:1463017. doi: 10.3389/fimmu.2024.1463017

Immunotherapy plus chemotherapy versus chemotherapy alone in the first-line treatment for advanced gastric cancer/gastroesophageal junction cancer: a real-world retrospective study

Qian Xu[1,2,3†], Dan Yi[1,2,3†], Caiyan Jia[1,2,3], Fanming Kong[1,2,3*] and Yingjie Jia[1,2,3*]

[1]Department of Oncology, First Teaching Hospital of Tianjin University of Traditional Chinese Medicine, Tianjin, China, [2]Department of Oncology, Tianjin Cancer Institute of Traditional Chinese Medicine, Tianjin, China, [3]Department of Oncology, National Clinical Research Center for Chinese Medicine Acupuncture and Moxibustion, Tianjin, China

Background: Immunotherapy offers new hope for improved survival in patients with advanced gastric cancer. Although large randomized controlled trials (RCTs) have been conducted to explore the efficacy and safety of first-line immunotherapy plus chemotherapy versus chemotherapy alone for advanced gastric cancer, the results are not completely consistent. And the strict inclusion criteria of RCTs lead to limited extrapolation. Therefore, it is of great significance to continue to conduct real-world studies comparing the clinical efficacy and safety of immunotherapy combined with chemotherapy versus chemotherapy alone in advanced gastric cancer.

Methods: This retrospective study included patients with HER-2 negative, unresectable advanced or recurrent gastric/gastroesophageal junction cancer (GC/GEJC) who received first-line immune checkpoint inhibitors (ICIs) in combination with chemotherapy or chemotherapy alone between January 1, 2018 to May 31, 2023. Progression-free survival (PFS), overall survival (OS), overall response rate (ORR), disease control rate (DCR) and adverse events (AEs) were compared between two groups.

Results: A total of 210 patients were enrolled in the combination treatment group (n=100) and chemotherapy alone group (n=110). After 12 months of follow-up, median PFS (mPFS) was 270 days (95%CI 177.510-362.490) in the chemotherapy alone group and 357 days (95%CI 250.103-463.897) in the combination treatment group (P<0.05). The median OS (mOS) was 14.9 months (95%CI 9.831-17.769) in the chemotherapy alone group and 15 months (95%CI 12.386-17.614) in the combination treatment group (P>0.05). There was no statistically significant difference in ORR between two groups (P=0.050). The DCR was 14.5% in the chemotherapy alone group and 38% in the combination treatment group (P<0.05). Subgroup analyses showed that primary tumor location of GEJC, ECOG PS of 1, without liver metastasis, and chemotherapy plus ICIs were associated with PFS benefit. Cox multivariate analysis showed that only surgery or not was correlated with patients' prognosis (P<0.05). Most of AEs were grade 1-2 and manageable.

Conclusions: Compared with chemotherapy alone, first-line ICIs combined with chemotherapy in patients with advanced GC/GEJC could greatly prolong PFS, but OS was not significantly improved, and the AEs were manageable.

KEYWORDS

gastric cancer, immune checkpoint inhibitors, chemotherapy, progression-free survival, overall survival

1 Introduction

Gastric cancer (GC) is responsible for over one million new cases in 2020 and estimated 769,000 deaths, ranking fifth for incidence and fourth for mortality globally (1). In China, approximately 358,700 new cases of GC and 260,400 deaths occurred in 2022, which is the third largest number of cancer deaths (2). Currently, systemic therapy for patients with HER-2 negative, unresectable advanced or recurrent gastric/gastroesophageal junction cancer (GC/GEJC) has been dominated by chemotherapy, and the common first-line agents include platinum, fluorouracil and taxane drugs worldwide (3–5). However, the efficacy of these treatments is not ideal, with the median overall survival (mOS) at approximately only 1 year (6).

Attraction 4, Checkmate 649, and Orient 16 have demonstrated a synergistic effect of immune checkpoint inhibitors (ICIs) in combination with chemotherapy in patients with HER-2 negative, unresectable advanced or recurrent GC/GEJC (7–9). Studies have found that chemotherapy can not only kill tumor cells through cytotoxic effects directly, but also promote anti-tumor immune responses by inducing immunogenic cell death (10–12). As of now, several guidelines, such as the Chinese Society of Clinical Oncology, the European Society for Medical Oncology, and the National Comprehensive Cancer Network, suggest that ICIs together with chemotherapy are used as the first-line treatment for patients with advanced GC especially who exhibit a high combined positive score (CPS) (5, 13, 14).

In China, ICIs are frequently applied to treat unresectable advanced or recurrent GC/GEJC. In order to explore the efficacy and safety of ICIs combined with chemotherapy in these patients, here we examined the short-term and long-term outcomes as well as the adverse events (AEs) of patients who received chemotherapy alone or chemotherapy combined with ICIs.

2 Materials and methods

2.1 Study design and participants

This retrospective study involved patients with HER-2 negative, unresectable advanced or recurrent GC/GEJC. All patients were fully aware of the purpose of this study and expressed informed consent. This study retrospectively analyzed clinical data of patients with advanced GC/GEJC from January 1, 2018 to May 31, 2023 at the First Teaching Hospital of Tianjin University of Traditional Chinese Medicine in China. Survival data were obtained through follow-up.

All patients had histologically or cytologically confirmed HER-2 negative, unresectable advanced or recurrent GC/GEJC; had received at least two cycles of chemotherapy or chemotherapy combined with ICIs; had received at least one efficacy assessment; had baseline Eastern Cooperative Oncology Group (ECOG) performance status (PS) of 0 or 1; and had normal hepatic and renal function. Patients were excluded if they could not tolerate immunotherapy or chemotherapy; or had severe systemic or autoimmune disease; or multiple primary tumors or unknown primary sites; or were HER-2 positive; or had incomplete clinical data.

2.2 Study procedures

All patients included in the final analysis received chemotherapy (XELOX or FOLFOX) and a subset of patients combined with ICIs (nivolumab, sintilimab, tislelizumab and camrelizumab) on this basis.

The baseline information below of each patient were collected: age, sex, family genetic history, history of smoking, history of drinking, ECOG PS, primary tumor location, surgery or not, metastatic site, organs with metastases, and chemotherapy regimen. The clinical efficacy was assessed by outcomes of CT or MRI, which was based on the Response Evaluation Criteria in Solid Tumors (RECIST) version 1.1 (15).

2.3 Outcomes

The primary endpoint of this study was progression-free survival (PFS), which was estimated from treatment initiation to progression or death. The secondary endpoints included overall survival (OS), which was defined as the duration from treatment initiation to death due to any reason; objective response rate (ORR), which was defined as the proportion of patients with the best overall

response of complete response (CR) or partial response (PR); and disease control rate (DCR), which was defined as the proportion of patients with CR, PR, or stable disease (SD). Safety endpoint included evaluation of AEs. AEs were monitored and classified according to the National Cancer Institute Common Terminology Criteria for Adverse Events (version 5.0).

2.4 Statistical analysis

In this study, SPSS 27.0 and GraphPad Prism 9.0 were used for statistical analysis and scientific mapping. Descriptive statistics were used for the basic characteristic data. Chi-square test or fisher's exact test was used to analyze the efficacy and incidence of adverse reactions. PFS and OS were estimated with Kaplan-Meier method, which was expressed with the two-sided 95% confidence intervals (CIs), and the differences between groups were compared by log-rank test, and the two-sided significance level was P=0.05. The ORR and DCR were analyzed with the Chi-square test. Univariate and multivariate analysis were performed using the Cox proportional hazards model, and hazard ratios (HRs) and 95% CIs were calculated. The difference of P<0.05 was statistically significant.

3 Results

3.1 Baseline characteristics

After screening 1745 patients according to the inclusion and exclusion criteria described above, we excluded 136 HER-2 positive patients, 169 patients who could not tolerate chemotherapy or immunotherapy, 179 patients who had severe systemic or autoimmune disease, 248 patients with multiple primary tumors or with unknown primary tumor sites, 123 patients without complete clinical data, and 118 patients without evaluable lesions for efficacy. A total of 210 patients were included in the final analysis (Figure 1).

The median age of the patients included in the chemotherapy alone group was 64 years old (interquartile range [IQR], 60-70), of which 83 (75.5%) were male, 26 (23.6%) had the family genetic history, 65 (59.1%) had the history of smoking, 52 (47.3%) had the history of alcohol, 101 (91.8%) had a primary tumor site of the stomach, 69 (62.7%) had undergone surgery, half (50%) had two or more sites of tumor metastasis, and the majority of patients (66.4%) received the FOLFOX chemotherapy regimen. The median age of the patients included in the immunotherapy together with chemotherapy group was 66 years old (IQR, 60-73), of whom 66 (66%) were male, 18 (18%) had the family genetic history, 67 (67%) had the history of smoking, 36 (36%) had the history of alcohol, 89 (89%) had a primary tumor site of the stomach, 55 (55%) had undergone surgery, more than half (51%) had two or more sites of metastases, and most (63%) received the FOLFOX chemotherapy regimen. ICIs included nivolumab (6%), sintilimab (70%), tislelizumab (10%), and camrelizumab (14%). All patients had an ECOG performance status of 0-1 (Table 1). Because precise PD-L1 CPS values were not available for more than 80% of enrolled patients (PD-L1 CPS ≤1 6 patients, CPS ≥1 10 patients, CPS ≥5 5 patients, and CPS ≥10 2 patients), this metric was not analyzed. Patients who completed first-line therapy without disease progression and tolerable AEs were eligible for maintenance therapy, which consisted of single-agent chemotherapy (S-1 or Capecitabine) with or without immunotherapy.

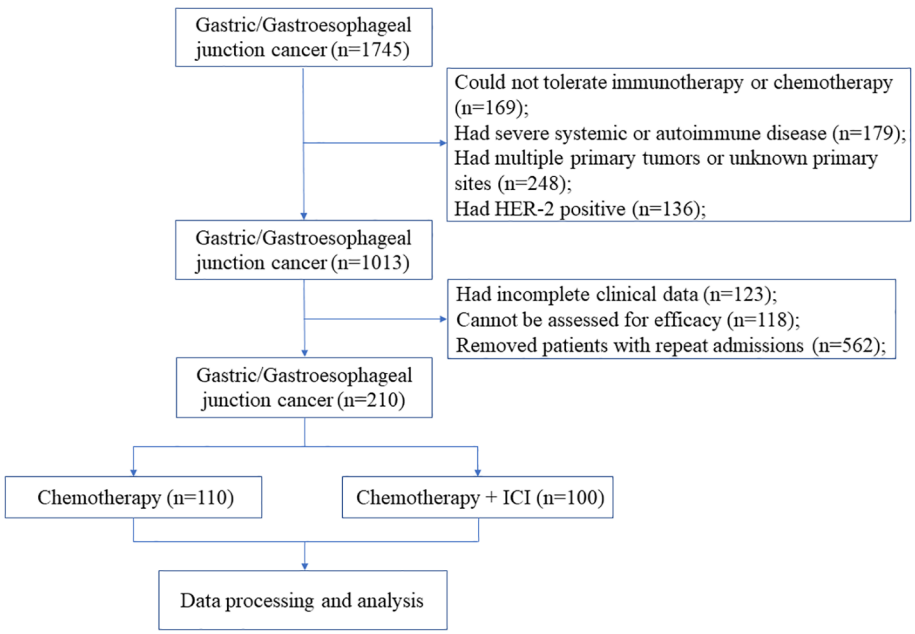

FIGURE 1
Flow diagram of the study.

10.3389/fimmu.2024.1463017

TABLE 1 Baseline clinical characteristics.

	Chemotherapy	Chemotherapy + ICI	*P* value
Years	64 (60,70)	66 (60,73)	0.725
Sex			**0.132**
Male	83 (75.5%)	66 (66%)	
Female	27 (24.5%)	34 (34%)	
Family genetic history			**0.316**
Yes	26 (23.6%)	18 (18%)	
NO	84 (76.4%)	82 (82%)	
Smoking			**0.236**
Yes	65 (59.1%)	67 (67%)	
NO	45 (40.9%)	33 (33%)	
Drinking			**0.098**
Yes	52 (47.3%)	36 (36%)	
NO	58 (52.7%)	64 (64%)	
ECOG performance status			**0.151**
0	54 (49.1%)	59 (59%)	
1	56 (50.9%)	41 (41%)	
Primary tumor location			**0.487**
GC	101 (91.8%)	89 (89%)	
GEJC	9 (8.2%)	11 (11%)	
Surgery			**0.255**
Yes	69 (62.7%)	55 (55%)	
NO	41 (37.3%)	45 (45%)	
Metastatic site			**0.231**
Lymph node	104 (94.5%)	89 (89%)	
Liver	26 (23.6%)	32 (32%)	
Peritoneum	30 (27.3%)	33 (33%)	
Organs with metastases			**0.885**
1	55 (50%)	49 (49%)	
≥2	55 (50%)	51 (51%)	
Chemotherapy regimen			**0.610**
FOLFOX	73 (66.4%)	63 (63%)	
XELOX	37 (33.6%)	37 (37%)	
ICIs	–		–
Nivolumab	–	6 (6%)	
Sintilimab	–	70 (70%)	
Tislelizumab	–	10 (10%)	
Camrelizumab	–	14 (14%)	

3.2 Efficacy

At the cutoff date, a total of 156 patients out of 210 patients had PD, including 94 in the chemotherapy alone group and 62 in the combination treatment group. Data analysis showed that the median PFS (mPFS) was 270 days (95%CI 177.510-362.490) in the chemotherapy group and 357 days (95%CI 250.103-463.897) in the combination treatment group, and the difference was statistically significant (P<0.05) (Figure 2). A total of 36 patients died in the chemotherapy alone group and 37 patients died in the combination treatment group. The median OS (mOS) was 14.9 months (95%CI 9.831-17.769) in the chemotherapy alone group, and 15 months (95%CI 12.386-17.614) in the combination treatment group, and the difference was not statistically significant (P>0.05) (Figure 3).

Based on RECIST1.1 criteria, no patients achieved CR and PR, 16 patients achieved SD in the chemotherapy alone group. In the combination treatment group, no patients achieved CR, 4 patients achieved PR, 34 patients achieved SD, and the ORR was 4%. There was no statistically significant difference in ORR between the two groups (P=0.050). The DCR was 14.5% in the chemotherapy alone group and 38% in the combination treatment group. The difference was statistically significant (P<0.05) (Table 2).

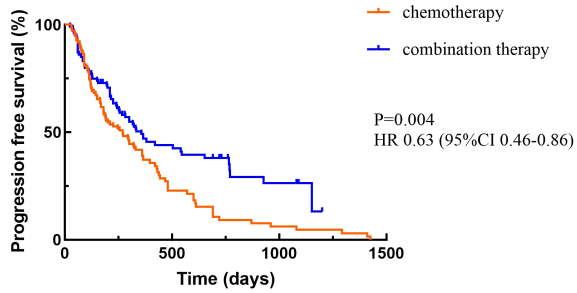

FIGURE 2
Progression-free survival.

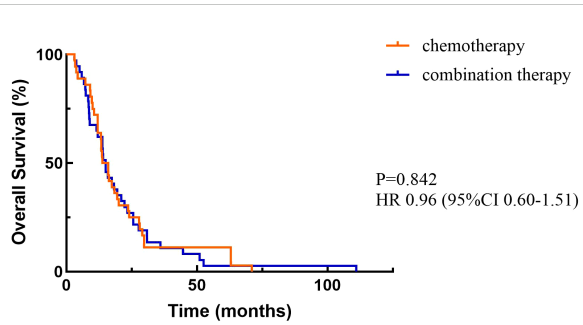

FIGURE 3
Overall survival.

TABLE 2 ORR and DCR for different treatment regimens.

	Chemotherapy	Chemotherapy + ICIs	*P*
CR	0	0	–
PR	0	4	–
PD	94	62	–
SD	16	34	–
ORR (%)	0%	4%	0.050
DCR (%)	14.5%	38%	0.000

ICI, immune checkpoint inhibitors; CR, complete response; PR, partial response; PD, progression disease; SD, stable disease; ORR, objective response rate; DCR, Disease control rate.

3.3 Subgroup analysis

Subgroup analyses showed that primary tumor location of GEJC, ECOG PS of 1, without liver metastasis, and chemotherapy plus ICIs were associated with PFS benefit. The results of univariate analysis of OS showed that age, family genetic history, surgery or not, and organs with metastases were influencing factors (P<0.05), while in further Cox multivariate analysis showed that only surgery or not was correlated with patients' prognosis (P<0.05). The results of the subgroup analyses of PFS and OS were shown in Tables 3, 4. In addition, we added the analysis of the effect of different ICIs on the efficacy of combination therapy (Table 5).

3.4 Safety

During the treatment, the most common AEs included: leucopenia, neutropenia, anemia, thrombocytopenia, alanine aminotransferase (ALT) increase, aspartate transaminase (AST) increase, creatinine increase, vomiting, peripheral neuropathy, and diarrhea, most of which were of grade 1-2 and manageable (Table 6). Any grade anemia was more common in the combination treatment group than in the chemotherapy alone group, but there was no significant difference in the incidence of grade 3 and above. Immunotherapy-related AEs included thyroid dysfunction (2 patients), myocarditis (3 patients), and pneumonitis (2 patients).

4 Discussion

Checkmate 649 established the importance of immunotherapy in advanced GC. Recent follow-up data showed (16) that nivolumab plus chemotherapy showed benefit in both OS and PFS compared with chemotherapy alone in both patients with PD-L1 CPS≥5 and all randomized patients. In patients with PD-L1 CPS≥5, mPFS was 8.3 versus 6.1 months (HR=0.71, 95%CI 0.61-0.82) and mOS was 14.4 versus 11.1 months (HR=0.70, 95%CI 0.61-0.81). In all randomized patients, mPFS was 7.7 versus 6.9 months (HR=0.80, 95%CI 0.71-0.89) and mOS was 13.7 versus 11.6 months (HR=0.79, 95%CI 0.71-0.88). Orient 16 (17) demonstrated the population-wide benefit of immunotherapy combined with chemotherapy as a first-line treatment for locally advanced/metastatic GC. The final results showed that in patients with PD-L1 CPS≥5 sintilimab combined with chemotherapy could significantly prolong mPFS (7.7 versus 5.8 months, HR=0.628, P=0.0002) and mOS (19.2 versus 12.9 months, HR=0.587, P<0.0001). In the whole population, mOS was 15.2 versus 12.3 months (HR=0.681, P<0.0001) and mPFS was 7.1 versus 5.7 months (HR=0.638, P<0.0001). Results of rationale

TABLE 3 Univariate and multivariate analyses of PFS.

Features	Univariate analysis		Multivariate analysis	
	HR (95%CI)	*P*	HR (95%CI)	*P*
Age	1.124(0.818,1.545)	0.470	1.201(0.844,1.708)	0.310
Sex	0.690(0.475,1.002)	0.051	0.665(0.423,1.045)	0.077
Primary tumor location	0.394(0.193,0.803)	0.010	0.464(0.220,0.981)	0.044
Family genetic history	0.800(0.538,1.190)	0.271	0.883(0.562,1.387)	0.589
Smoking	1.234(0.897,1.697)	0.197	1.403(0.874,2.254)	0.161
Drinking	0.943(0.685,1.298)	0.719	0.635(0.400,1.009)	0.055
Surgery	1.135(0.825,1.561)	0.437	1.105(0.743,1.645)	0.621
ECOG PS	1.513(1.194,1.917)	0.001	1.344(1.023,1.766)	0.034
Organs with metastases	1.134(0.969,1.328)	0.117	0.815(0.619,1.073)	0.145
Lymphatic metastases	1.016(0.584,1.768)	0.955	0.627(0.325,1.212)	0.165
Liver metastases	0.501(0.357,0.703)	0.000	0.415(0.257,0.669)	0.000
Peritoneal metastases	0.772(0.556,1.073)	0.123	0.699(0.426,1.148)	0.157
BMI	–	0.693	–	0.446
Treatment options	0.620(0.448,0.859)	0.004	0.666(0.466,0.950)	0.025

TABLE 4 Univariate and multivariate analyses of OS.

Features	Univariate analysis		Multivariate analysis	
	HR (95%CI)	*P*	HR (95%CI)	*P*
Age	0.594(0.363,0.970)	0.037	0.896(0.463,1.733)	0.744
Sex	0.870(0.495,1.531)	0.630	0.851(0.405,1.791)	0.672
Primary tumor location	1.210(0.437,3.346)	0.714	1.192(0.352,4.040)	0.778
Family genetic history	0.551(0.315,0.963)	0.036	0.562(0.271,1.165)	0.121
Smoking	1.044(0.652,1.670)	0.859	1.017(0.488,2.116)	0.965
Drinking	0.830(0.518,1.330)	0.440	1.019(0.464,2.241)	0.962
Surgery	1.913(1.177,3.108)	0.009	2.359(1.214,4.581)	0.011
ECOG PS	1.279(0.875,1.870)	0.204	1.415(0.862,2.324)	0.170
Organs with metastases	0.762(0.582,0.999)	0.049	0.604(0.350,1.040)	0.069
Lymphatic metastases	0.572(0.269,1.214)	0.146	0.616(0.239,1.583)	0.314
Liver metastases	0.998(0.619,1.610)	0.995	0.701(0.346,1.421)	0.325
Peritoneal metastases	1.329(0.815,2.167)	0.254	0.720(0.302,1.717)	0.459
BMI	–	0.579	–	0.734
Treatment options	1.048(0.657,1.671)	0.844	1.179(0.647,2.148)	0.591

305 (18) also showed that immunotherapy combined with chemotherapy as a first-line treatment can significantly prolong survival in patients with locally advanced unresectable or metastatic GC/GEJC.

Notably, keynote 062 (19) and attraction 4 (7) received partially negative results, which were also RCTs comparing the efficacy and safety of immunotherapy plus chemotherapy with chemotherapy alone, and the addition of immunotherapy did not result in a significant final OS benefit. In this retrospective study, we found that chemotherapy combined with ICIs was effective in improving PFS (mPFS 270 versus 357 days, P<0.05), which is consistent with previous studies. However, there was no significant difference in OS (mOS 14.9 versus 15 months, P>0.05), which we considered that it may be related to the level of CPS expression, mismatch repair status, subsequence lines of treatment and the length of follow-up. Although PD-L1 CPS≥5 has been shown to be a good independent prognostic factor for survival (16–18), interestingly a systematic review found that when ICI was combined with chemotherapy, the correlation between PD-L1 expression and ORR was not obvious. The pooled ORR in PD-L1 negative, PD-L1 CPS ≥1, PD-L1 CPS ≥5, and PD-L1 CPS ≥10 population was 57%, 48%, 60%, and 58%, respectively. It seems that the benefit brought about by the rise in PD-L1 expression was not obvious when ICI and chemotherapy were combined (20). This requires further exploration on the effect of CPS on the efficacy of immunotherapy combined with chemotherapy in advanced GC. In addition, OS was closely related to follow-up time. Because the follow-up of this study was only one year, there may be bias, and we will continue to follow up these patients in the future. None achieved CR or PR in the chemotherapy alone group, compared with only 4 patients of PR in the combination group. There was no statistically significant difference in ORR between two groups (P=0.050). The DCR was 14.5% in the chemotherapy alone group and 38% in the combination treatment group (P<0.05). ORR and DCR can be affected by a variety of factors, including the level of immunity, the type of ICIs used, PD-L1 CPS expression level, tumor characteristics, molecular phenotypes, and performance status of patients. The combination of these factors determined the efficacy of patients receiving immunotherapy in combination with chemotherapy. Subgroup analyses showed that primary tumor location of GEJC, ECOG PS of 1, without liver metastasis, and chemotherapy plus ICIs were associated with patient PFS benefit. Cox multivariate analysis showed that only surgery or not was correlated with patients' prognosis (P<0.05). Although there was no statistically significant difference in the effect of different ICIs on combination therapy in this study, it is still worth further exploring whether this is related to sample size and regional differences. Most AEs were grade 1-2 and manageable. In this study any grade of anemia was more common in the combination treatment group than in the chemotherapy alone group, but there was no significant difference in the incidence of grade 3 and above. Immunotherapy-related AEs included thyroid dysfunction (2 patients), myocarditis

TABLE 5 Efficacy of different ICIs.

	CR	PR	PD	SD	*P*
Nivolumab	0	0	4	2	0.587
Sintilimab	0	4	40	26	
Tislelizumab	0	0	6	4	
Camrelizumab	0	0	12	2	

TABLE 6 Summary of adverse events.

	Chemotherapy		Chemotherapy + ICI		*P*	
	Any (%)	≥3 grade (%)	Any (%)	≥3 grade (%)	Any	≥3 grade
Leucopenia	20 (18.2%)	0	17 (17%)	1 (1%)	0.822	0.476
Neutropenia	8 (7.3%)	5 (4.5%)	13 (13%)	2 (2%)	0.167	0.521
Anemia	75 (68.2%)	17 (15.5%)	82 (82%)	21 (21%)	0.021	0.297
Thrombocytopenia	17 (15.5%)	5 (4.5%)	18 (18%)	7 (7%)	0.621	0.444
ALT increase	11 (10.0%)	1 (0.9%)	14 (14%)	3 (3%)	0.371	0.547
AST increase	23 (20.9%)	10 (9.1%)	31 (31%)	14 (14%)	0.095	0.264
Creatinine increase	9 (8.2%)	3 (2.7%)	10 (10%)	1 (1%)	0.646	0.682
Vomiting	56 (50.9%)	4 (3.6%)	52 (52%)	5 (5%)	0.874	0.884
Peripheral neuropathy	78 (70.9%)	1 (0.9%)	82 (82%)	3 (3%)	0.059	0.547
Diarrhea	48 (43.6%)	0	43 (43%)	2 (2%)	0.926	0.226
Immunotherapy-related adverse events	–	–	7	0	–	–

ALT, alanine aminotransferase; AST, aspartate transaminase.

(3 patients), and pneumonitis (2 patients). Although the incidence of grade 3 and above AEs in chemotherapy combined with immunotherapy is low, close attention should be paid to prevent the occurrence of severe immune-related AEs and more in-depth analysis of it could follow to provide targeted remissions. At present, large real-world studies comparing the efficacy and safety of immunotherapy combined with chemotherapy are still needed, and there is an urgent need to study the dominant population and dominant stage of immunotherapy.

In this study, patients were collected according to strict inclusion criteria, and also multivariate analysis was used to control for the impact of confounding factors to minimize error. As this was a retrospective real-world study, clinical data collection was based on the extraction of electronic medical records and patient follow-up, and the data for safety analysis were mainly from medical records, laboratory indicators and imaging tests. The potential bias due to the retrospective, non-randomized design remains a limitation of this study. Many pathology centers, including ours, do not perform routine CPS detection, so the records of PD-L1 CPS expression level in patients were incomplete. And this study is only a single-center study, which has the problem of small sample size. In addition, HER-2 positive patients, who account for 20% of all GC patients (21), were not enrolled in the study, and there is also a clinical need to help these patients improve their survival, so we are conducting further prospective studies on different CPS levels, HER-2 expression levels, microsatellite status, and different ICIs.

5 Conclusion

In conclusion, the results of the study showed that in patients with HER-2 negative, unresectable advanced or recurrent GC/GEJC chemotherapy combined with ICIs could greatly prolong PFS, but OS was not significantly improved, and AEs were manageable. The outcomes confirmed the efficacy and safety of immunotherapy in combination with chemotherapy in the real-world setting, which could provide the basis for the standard first-line treatment of these patients.

Data availability statement

The original contributions presented in the study are included in the article/supplementary material. Further inquiries can be directed to the corresponding authors.

Ethics statement

Ethical approval was not required for the study involving humans in accordance with the local legislation and institutional requirements. Written informed consent to participate in this study was not required from the participants or the participants' legal guardians/next of kin in accordance with the national legislation and the institutional requirements.

Author contributions

QX: Conceptualization, Formal analysis, Investigation, Writing – original draft. DY: Conceptualization, Investigation, Writing – original draft. CJ: Investigation, Visualization, Writing – original draft. FK: Writing – review & editing. YJ: Writing – review & editing.

Funding

The author(s) declare financial support was received for the research, authorship, and/or publication of this article. This study

was funded by the National Clinical Research Center for Chinese Medicine Acupuncture and Moxibustion Open Funding Project (NCRCOP2023007), First Teaching Hospital of Tianjin University of Traditional Chinese Medicine TuoXin Project (2023008), and Special Fund for Clinical Research of Wu Jieping Medical Foundation (320.6750.2023-10-5).

Acknowledgments

Thanks to all the authors for their contributions to this article, and thanks to the institution for its support.

Conflict of interest

The authors declare that the research was conducted in the absence of any commercial or financial relationships that could be construed as a potential conflict of interest.

Publisher's note

All claims expressed in this article are solely those of the authors and do not necessarily represent those of their affiliated organizations, or those of the publisher, the editors and the reviewers. Any product that may be evaluated in this article, or claim that may be made by its manufacturer, is not guaranteed or endorsed by the publisher.

References

1. Sung H, Ferlay J, Siegel RL, Laversanne M, Soerjomataram I, Jemal A, et al. Global cancer statistics 2020: GLOBOCAN estimates of incidence and mortality worldwide for 36 cancers in 185 countries. *CA Cancer J Clin*. (2021) 71:209–49. doi: 10.3322/caac.21660

2. Zheng RS, Chen R, Han BF, Wang SM, Li L, Sun KX, et al. Cancer incidence and mortality in China, 2022. *Zhonghua Zhong Liu Za Zhi*. (2024) 46:221–31. doi: 10.3760/cma.j.cn112152-20240119-00035

3. Ajani JA, D'Amico TA, Bentrem DJ, Chao J, Cooke D, Corvera C, et al. Gastric Cancer, Version 2.2022, NCCN Clinical Practice Guidelines in Oncology. *J Natl Compr Canc Netw*. (2022) 20:167–92. doi: 10.6004/jnccn.2022.0008

4. Muro K, Van Cutsem E, Narita Y, Pentheroudakis G, Baba E, Li J, et al. Pan-Asian adapted ESMO Clinical Practice Guidelines for the management of patients with metastatic gastric cancer: a JSMO-ESMO initiative endorsed by CSCO, KSMO, MOS, SSO and TOS. *Ann Oncol*. (2019) 30:19–33. doi: 10.1093/annonc/mdy502

5. Wang FH, Zhang XT, Li YF, Tang L, Qu XJ, Ying JE, et al. The Chinese Society of Clinical Oncology (CSCO): Clinical guidelines for the diagnosis and treatment of gastric cancer, 2021. *Cancer Commun (Lond)*. (2021) 41:747–95. doi: 10.1002/cac2.12193

6. Zhu Y, Liu K, Zhu H, Wu H. Immune checkpoint inhibitors plus chemotherapy for HER2-negative advanced gastric/gastroesophageal junction cancer: a cost-effectiveness analysis. *Therap Adv Gastroenterol*. (2023) 16:17562848231207200. doi: 10.1177/17562848231207200

7. Kang YK, Chen LT, Ryu MH, Oh DY, Oh SC, Chung HC, et al. Nivolumab plus chemotherapy versus placebo plus chemotherapy in patients with HER2-negative, untreated, unresectable advanced or recurrent gastric or gastro-oesophageal junction cancer (ATTRACTION-4): a randomised, multicentre, double-blind, placebo-controlled, phase 3 trial. *Lancet Oncol*. (2022) 23:234–47. doi: 10.1016/S1470-2045(21)00692-6

8. Janjigian YY, Shitara K, Moehler M, Garrido M, Salman P, Shen L, et al. First-line nivolumab plus chemotherapy versus chemotherapy alone for advanced gastric, gastro-oesophageal junction, and oesophageal adenocarcinoma (CheckMate 649): a randomised, open-label, phase 3 trial. *Lancet*. (2021) 398:27–40. doi: 10.1016/S0140-6736(21)00797-2

9. Xu J, Jiang H, Pan Y, Gu K, Cang S, Han L, et al. Sintilimab plus chemotherapy for unresectable gastric or gastroesophageal junction cancer: the ORIENT-16 randomized clinical trial. *JAMA*. (2023) 330:2064–74. doi: 10.1001/jama.2023.19918

10. Hato SV, Khong A, de Vries IJ, Lesterhuis WJ. Molecular pathways: the immunogenic effects of platinum-based chemotherapeutics. *Clin Cancer Res*. (2014) 20:2831–7. doi: 10.1158/1078-0432.CCR-13-3141

11. Zitvogel L, Apetoh L, Ghiringhelli F, Kroemer G. Immunological aspects of cancer chemotherapy. *Nat Rev Immunol*. (2008) 8:59–73. doi: 10.1038/nri2216

12. Yoon J, Kim TY, Oh DY. Recent progress in immunotherapy for gastric cancer. *J Gastric Cancer*. (2023) 23:207–23. doi: 10.5230/jgc.2023.23.e10

13. Ajani JA, D'Amico TA, Bentrem DJ, Chao J, Cooke D, Corvera C, et al. Gastric cancer, version 2.2022, NCCN clinical practice guidelines in oncology. *J Natl Compr Canc Netw*. (2022) 20:167–92. doi: 10.6004/jnccn.2022.0008

14. Pavel M, Öberg K, Falconi M, Krenning EP, Sundin A, Perren A, et al. Gastroenteropancreatic neuroendocrine neoplasms: ESMO Clinical Practice Guidelines for diagnosis, treatment and follow-up. *Ann Oncol*. (2020) 31:844–60. doi: 10.1016/j.annonc.2020.03.304

15. Eisenhauer EA, Therasse P, Bogaerts J, Schwartz LH, Sargent D, Ford R, et al. New response evaluation criteria in solid tumours: revised RECIST guideline (version 1.1). *Eur J Cancer*. (2009) 45:228–47. doi: 10.1016/j.ejca.2008.10.026

16. Janjigian YY, Ajani JA, Moehler M, Shen L, Garrido M, Gallardo C, et al. First-line nivolumab plus chemotherapy for advanced gastric, gastroesophageal junction, and esophageal adenocarcinoma: 3-year follow-up of the phase III checkMate 649 trial. *J Clin Oncol*. (2024) 42:2012–20. doi: 10.1200/JCO.23.01601

17. Xu JM, Jiang HP, Pan YY, Gu KS, Cang SD, Han L, et al. Abstract CT078: First-line treatment with sintilimab (sin) vs placebo in combination with chemotherapy (chemo) in patients (pts) with unresectable gastric or gastroesophageal junction (G/GEJ) cancer: Final overall survival (OS) results from the randomized, phase III ORIENT-16 trial. *Cancer Res*. (2023) 83:CT078. doi: 10.1158/1538-7445.AM2023-CT078

18. Moehler M, Kato K, Arkenau T, Oh DY, Tabernero J, Correa M, et al. Rationale 305: Phase 3 study of tislelizumab plus chemotherapy vs placebo plus chemotherapy as first-line treatment (1L) of advanced gastric or gastroesophageal junction adenocarcinoma (GC/GEJC). *J Clin Oncol*. (2023) 41:abstr 286. doi: 10.1200/JCO.2023.41.4_suppl.286

19. Shitara K, Van Cutsem E, Bang YJ, Fuchs C, Wyrwicz L, Lee KW, et al. Efficacy and safety of pembrolizumab or pembrolizumab plus chemotherapy vs chemotherapy alone for patients with first-line, advanced gastric cancer: the KEYNOTE-062 phase 3 randomized clinical trial. *JAMA Oncol*. (2020) 6:1571–80. doi: 10.1001/jamaoncol.2020.3370

20. Xie T, Zhang Z, Zhang X, Qi C, Shen L, Peng Z. Appropriate PD-L1 cutoff value for gastric cancer immunotherapy: A systematic review and meta-analysis. *Front Oncol*. (2021) 11:646355. doi: 10.3389/fonc.2021.646355

21. Janjigian YY, Werner D, Pauligk C, Steinmetz K, Kelsen DP, Jäger E, et al. Prognosis of metastatic gastric and gastroesophageal junction cancer by HER2 status: a European and USA International collaborative analysis. *Ann Oncol*. (2012) 23:2656–62. doi: 10.1093/annonc/mds104

frontiers | Frontiers in Immunology

TYPE Brief Research Report
PUBLISHED 17 December 2024
DOI 10.3389/fimmu.2024.1456193

OPEN ACCESS

EDITED BY
Stavros P. Papadakos,
Laiko General Hospital of Athens, Greece

REVIEWED BY
Alessio Vagliasindi,
Oncological Center of Basilicata (IRCCS), Italy
Xiaofeng Duan,
Tianjin Medical University Cancer Institute and Hospital, China

*CORRESPONDENCE
Qixun Chen
Chenqix@yeah.net

RECEIVED 28 June 2024
ACCEPTED 25 November 2024
PUBLISHED 17 December 2024

CITATION
Feng J, Wang L, Yang X and Chen Q (2024) Adjuvant immunotherapy after neoadjuvant immunochemotherapy and esophagectomy for esophageal squamous cell carcinoma: a real-world study.
Front. Immunol. 15:1456193.
doi: 10.3389/fimmu.2024.1456193

Adjuvant immunotherapy after neoadjuvant immunochemotherapy and esophagectomy for esophageal squamous cell carcinoma: a real-world study

Jifeng Feng[1,2], Liang Wang[1], Xun Yang[1] and Qixun Chen[1,2]*

[1]Department of Thoracic Oncological Surgery, Zhejiang Cancer Hospital, Hangzhou Institute of Medicine (HIM), Chinese Academy of Sciences, Hangzhou, China, [2]Key Laboratory of Diagnosis and Treatment Technology on Thoracic Oncology (Lung and Esophagus) of Zhejiang Province, Zhejiang Cancer Hospital, Hangzhou, China

Background: The role of immunotherapy in the adjuvant setting seems promising in recent years. As per the findings of the CheckMate 577 trial, patients with esophageal cancer (EC) who had neoadjuvant chemoradiation with residual pathologic disease should be considered adjuvant immunotherapy (AIT). However, it is unknown if individuals with esophageal squamous cell carcinoma (ESCC) who have received neoadjuvant immunochemotherapy (NICT) followed by radical surgery also require AIT.

Methods: A retrospective analysis was performed on the data from patients who underwent NICT and radical surgery for ESCC between 2019 and 2020. To compare disease-free survival (DFS) and overall survival (OS), Kaplan-Meier survival curves were produced. To determine the parameters linked to DFS and OS, a Cox model using hazard ratios (HRs) was completed.

Results: Among the 292 eligible patients, 215 cases with a mean age of 63.3 $\pm$ 6.8 years, including 190 (88.4%) men and 25 (11.6%) women, were finally recruited. The percentage of R0 resection was 98.3%. After NICT, 65 (30.2%) patients achieved pathological complete response. AIT was given to 78 (36.3%) patients following radical resection. For all patients, the 3-year DFS and OS were 62.3% and 74.0%, respectively. In terms of 3-year DFS (61.5% vs. 62.8%, P=0.984) or OS (76.9% vs. 72.3%, P=0.384), no statistically significant difference was found between patients with and without AIT. AIT significantly improved survival in patients with ypT+N+ (DFS: 23.9% vs. 38.5%, P=0.036; OS: 37.0% vs. 61.5%, P=0.010), but not in those with ypT0N0 or ypT+N0. It was found that AIT was related to both DFS (HR: 0.297; P<0.001) and OS (HR: 0.321; P=0.001) in patients with ypT+N+.

Conclusion: In ypT+N+ ESCC patients, AIT after NICT followed by radical surgery reduces the recurrence and death, thereby improving the DFS and OS. Randomized controlled trials ought to be conducted to further assess the results of this retrospective investigation.

KEYWORDS

neoadjuvant immunochemotherapy, adjuvant immunotherapy, esophageal squamous cell carcinoma, disease-free survival, overall survival

Introduction

Ranking 7th and 6th in terms of cancer morbidity and mortality, respectively, esophageal cancer (EC), primarily esophageal adenocarcinoma (EAC) and esophageal squamous cell carcinoma (ESCC), is one of the most prevalent cancer types worldwide (1). The prognosis for EC is still unsatisfactory because of cancer metastasis and recurrence, even with significant efforts in multidisciplinary therapies (2). For individuals with locally advanced disease, neoadjuvant chemoradiotherapy (NCRT) or neoadjuvant chemotherapy (NCT) followed by radical surgery represents the standard treatment (3, 4). Post-surgery, for those with neoadjuvant therapy (NAT), the standard care strategy is observation. Patients confront a high risk of treatment failure, nevertheless, if they do not experience a pathological complete response (PCR) following surgery (5, 6). In order to improve the survival rate, researchers continue to explore more appropriate adjuvant therapies (ATs), such as adjuvant chemotherapy (ACT) or adjuvant chemoradiotherapy (ACRT) (7, 8).

Recently, the prognosis of advanced EC has significantly changed due to immunotherapy, an emerging treatment hotspot (9, 10). Additionally, studies have demonstrated the efficacy and safety of neoadjuvant immunochemotherapy (NICT) for locally advanced EC (11–13). However, further verification is necessary to fully understand the therapeutic response and clinical outcomes of NICT. Furthermore, the need for AT after NICT followed by radical resection has not yet been determined. In particular, a higher risk of recurrence is associated with patients who had pathologic residual disease following NICT and surgery. Therefore, a more appropriate AT should be administered to those patients. The phase III trial CheckMate 577 reported that nivolumab was most beneficial for patients with ESCC, with a disease-free survival (DFS) of 29.7 months. Additionally, following a median follow-up of 2 years, nivolumab was linked to a 31% lower risk of death or recurrence (14).

As NICT is a new treatment mode in recent years, although effective progress has been made in terms of safety and efficacy, there are still uncertainties about AT after surgery due to the lack of data and the fact that relevant studies have not reached the specified prognosis observation time. At present, NICT for EC can achieve good short-term clinical outcomes. There is a lack of evidence to support which AT should be given after NICT. The use of AIT following NICT and surgery is currently not well supported by the literature, raising questions about which patients to treat and how ultimate pathology may affect these clinical decisions. Accordingly, the purpose of this retrospective study was to assess the effectiveness of AIT in patients with ESCC following NICT plus surgery.

Abbreviations: EC, esophageal cancer; EAC, esophageal adenocarcinoma; ESCC, esophageal squamous cell carcinoma; NAT, neoadjuvant therapy; NCT, neoadjuvant chemotherapy; NCRT, neoadjuvant chemoradiotherapy; NICT, neoadjuvant immunochemotherapy; AT, adjuvant therapy; ACT, adjuvant chemotherapy; ACRT, adjuvant chemoradiotherapy; AIT, adjuvant immunotherapy; PCR, pathological complete response; TNM, tumor node metastasis; OS, overall survival; DFS, disease-free survival; LN, lymph node; HR, hazard ratio; CI, confidence interval.

Materials and methods

Patients

A retrospective analysis was performed on the data from patients who underwent NICT and surgery for ESCC between 2019 and 2020. Supplementary Figure S1 presents the inclusion criteria. All patients were enrolled in the investigator-initiated clinical trials (IITs). The following were the exclusion criteria: (1) pathological diagnosis of non-ESCC; (2) received non-radical resection; (3) in combination with NCRT; (4) surgical-related mortality; (5) accompanied or previously accompanied by cancers at other sites; (6) received ACRT after radical resection; and (7) incomplete clinical data or follow-up. Finally, 215 patients were included in the analysis. The 8th AJCC/UICC TNM classification system was used in this study (15). The Ethics Committee of Zhejiang Cancer Hospital gave its approval (IRB-2020-320) and the research was carried out in compliance with the Helsinki Declaration.

Treatment and follow-up

Two NICT cycles were administered to eligible patients in this investigation, with 200 mg of camrelizumab, tislelizumab, or sintilimab, 2mg/Kg of pembrolizumab, or 3mg/Kg of nivolumab,

administered on day 1, albumin-paclitaxel (120 mg/m^2) administered on days 1 and 8, and carboplatin [5 mg/ml/min on the basis of the area under the curve (AUC)] administered on day 1 of each 21-day cycle. McKeown or Ivor Lewis, as a classic surgical procedure, was typically carried out 4-6 weeks after the end of the last NICT cycle (16). In principle, two-field lymph node (LN) dissection is indicated when tumors are located at the middle to lower thoracic esophagus, while three-field LN dissection is applied for upper thoracic tumors. There is currently no agreement on AT in situations where radical surgery is needed after NICT. The CheckMate 577 trial suggests that AIT may be beneficial for patients following NCRT (14). Accordingly, AIT was advised for patients who did not obtain PCR, according to the EC expert agreement on perioperative immunotherapy (17). The duration time for patients to choose postoperative AIT was 1-2 years, but it is not mandatory, mainly based on the postoperative pathological results. The latest follow-up period was completed in December 2023.

Statistical analysis

The chi-square or Fisher's exact tests were used to compare categorical variables. The Student t-test was utilized for normally distributed continuous variables, whereas the Mann-Whitney U-test was employed for those variables with a non-normal distribution. Patient survival was compared according to AIT using the Kaplan-Meier method. To determine the parameters linked to DFS and overall survival (OS), a Cox proportional hazard model using hazard ratios (HRs) was completed. SPSS 20.0 was used to perform all two-sided statistical tests, with statistical significance indicated by P values <0.05.

Results

Patients characteristics

Table 1 summarizes patient characteristics. After all, 215 cases with a mean age of 63.3 ± 6.8 years, 190 men (88.4%), and 25 women (11.6%) were selected from the 292 eligible patients. Regarding NICT, there were 12 (5.6%), 27 (12.6%), 118 (54.8%), 43 (20.0%), and 15 (7.0%) patients who were treated with nivolumab, pembrolizumab, camrelizumab, tislelizumab, and sintilimab, respectively. The R0 resection rate was 98.3%. After NICT, 65 (30.2%) cases achieved PCR. A total of 78 (36.3%) cases received AIT, including 5 (6.4%) of nivolumab, 14 (18.0%) of pembrolizumab, 33 (42.3%) of camrelizumab, 21 (26.9%) of tislelizumab, and 5 (6.4%) of sintilimab, respectively. After NICT, 83 (83/137, 60.6%) patients in the non-AIT group and 67 (67/78, 85.9%) cases in the AIT group had any residual disease. Among all the patients, 39 (39/78, 50.0%) cases in the AIT group and 46 (46/137, 33.6%) cases in the non-AIT cohort had any residual nodal disease. Patients who did not get AIT had a greater rate of PCR (P<0.001), while those who got AIT had higher ypT (P<0.001), ypN (P=0.023), and ypTNM (P<0.001) stages.

Survival analyses for DFS and OS

In total, 82 (38.1%) cases had recurrence, and 56 (26.0%) cases died. Patients were classified as having a local recurrence or a distant recurrence based on their original presentation. Following treatment, 49 patients (59.8%) experienced distant recurrence, which included non-regional LN metastasis; in contrast, 33 patients (40.2%) experienced local recurrence, which included locoregional LN metastasis and anastomotic site recurrence. However, upon further analysis, the result revealed that AIT can effectively reduce distant recurrence (14.1% vs. 27.7%, P=0.022), but not for local recurrence (19.2% vs. 13.1%, P=0.233) (Supplementary Figure S2). The median follow-up period was 40 months. The 3-year DFS and OS were 62.3% (Figure 1A) and 74.0% (Figure 1B) in all patients, respectively. There was no statistically significant difference in the 3-year DFS (61.5% vs. 62.8%, P=0.984, Figure 1C) or 3-year OS (76.9% vs. 72.3%, P=0.384, Figure 1D) between patients with and without AIT.

Subgroup analysis in survival

Subgroup analysis of survival (DFS and OS) was carried out based on ypT0N0, ypT+N0, and ypT+N+ since AIT was typically carried out according to the pathologic status after surgery. For individuals with ypT0N0 (Figures 2A, B) and ypT+N0 (Figures 2C, D), the survival benefit of AIT was not statistically significant, but it was significant in those with ypT+N+ (3-year DFS: 23.9% vs. 38.5%, P=0.036, Figure 2E; 3-year OS: 37.0% vs. 61.5%, P=0.010, Figure 2F).

Patient characteristics in ypT+N+

Table 2 provides a summary of the features of ypT+N+ patients. Tumor length (P=0.012), positive LNs (P=0.007), and ypTNM stage (P=0.044) were different between the two groups, whereas other clinical characteristics were not significantly different between the two groups. Even though patients with AIT had longer tumor lengths, more metastatic LNs, and higher ypTNM stages, the results showed that these cases had a better prognosis than those without AIT, which further demonstrated the positive effect of AIT.

Prognostic factors for survival in ypT+N+

Supplementary Figures S3A, B presents the findings from multivariable analysis in ypT+N+ individuals. In patients with ypT+N+ ESCC, AIT was linked to survival following NICT plus radical surgery (DFS: HR=0.297, P<0.001; OS: HR=0.321, P=0.001). Consequently, AIT following NICT and surgery lowers the risk of death and recurrence in ypT+N+ ESCC patients, improving their prognosis. The Sankey diagrams regarding relations among AIT, ypTNM stages, and prognosis for all patients and ypT+N+ are shown in Supplementary Figures S3C, D.

10.3389/fimmu.2024.1456193

TABLE 1 Characteristics in all patients with ESCC receiving NICT.

	Total (n=215)	Non-AIT (n=137)	AIT (n=78)	P-value
Sex (n, %)				0.360
female	25 (11.6)	18 (13.1)	7 (9.0)	
male	190 (88.4)	119 (86.9)	71 (91.0)	
Age (median, Q1-3, years)	64 (57-69)	64 (57-68)	64.5 (58-69)	0.646
BMI (median, Q1-3, Kg/m^2)	21.7 (20.2-22.6)	21.5 (20.4-22.5)	21.7 (20.1-23.1)	0.632
Tumor location (n, %)				0.412
upper	20 (9.3)	15 (10.9)	5 (6.4)	
middle	124 (57.7)	80 (58.4)	44 (56.4)	
lower	71 (33.0)	42 (30.7)	29 (37.2)	
Differentiation (n, %)				0.002
well	49 (22.8)	39 (28.5)	10 (12.8)	
moderate	95 (44.2)	63 (46.0)	32 (41.0)	
poor	71 (33.0)	35 (25.5)	36 (46.2)	
Vessel invasion (n, %)	45 (20.9)	20 (14.6)	25 (32.1)	0.002
Perineural invasion (n, %)	47 (21.9)	24 (17.5)	23 (29.5)	0.041
Tumor length (median, Q1-3, cm)	1.90 (0.0-3.0)	1.20 (0.0-2.6)	2.75 (1.2-4.0)	<0.001
Immunotherapy (n, %)				0.052
nivolumab	12 (5.6)	7 (5.1)	5 (6.4)	
pembrolizumab	27 (12.6)	13 (9.5)	14 (17.9)	
camrelizumab	118 (54.8)	85 (62.0)	33 (42.3)	
tislelizumab	43 (20.0)	22 (16.1)	21 (26.9)	
sintilimab	15 (7.0)	10 (7.3)	5 (6.4)	
Surgical method (n, %)				0.386
McKeown	185 (86.0)	120 (87.6)	65 (83.3)	
Ivor-Lewis	30 (14.0)	17 (12.4)	13 (16.7)	
PCR (n, %)	65 (30.2)	54 (39.4)	11 (14.1)	<0.001
ypT stage (n, %)				<0.001
T0	65 (30.2)	54 (39.4)	11 (14.1)	
T1	35 (16.3)	24 (17.5)	11 (14.1)	
T2	38 (17.7)	27 (19.7)	11 (14.1)	
T3	57 (26.5)	25 (18.2)	32 (41.0)	
T4	20 (9.3)	7 (5.2)	13 (16.7)	
ypN stage (n, %)				0.023
N0	130 (60.5)	91 (66.4)	39 (50.0)	
N1	48 (22.3)	27 (19.7)	21 (26.9)	
N2	26 (12.1)	16 (11.7)	10 (12.8)	
N3	11 (5.1)	3 (2.2)	8 (10.3)	
ypTNM stage (n, %)				<0.001
stage 0	65 (30.2)	54 (39.4)	11 (14.1)	

(Continued)

TABLE 1 Continued

	Total (n=215)	Non-AIT (n=137)	AIT (n=78)	P-value
stage I	42 (19.5)	29 (21.2)	13 (16.7)	
stage II	20 (9.3)	7 (5.1)	13 (16.7)	
stage III	64 (29.8)	39 (28.5)	25 (32.1)	
stage IV	24 (11.2)	8 (5.8)	16 (20.5)	
Total LNs (median, Q1-3, n)	20 (16-26)	19 (15-25)	22 (18-29)	0.009
Positive LNs (median, Q1-3, n)	0 (0-1)	0 (0-1)	1 (0-2)	0.001
Negative LNs (median, Q1-3, n)	19 (15-26)	18 (14-25)	20 (16-26)	0.130

ESCC, esophageal squamous cell carcinoma; NICT, neoadjuvant immunochemotherapy; AIT, adjuvant immunotherapy; BMI, body mass index; SD, standard deviation; TNM, tumor node metastasis; PCR, pathological complete response; LN, lymph node.

Correlations between preoperative efficacy and prognosis

Further analysis was done on the correlation between prognosis following NICT and clinical stage decline. Any T and/or N decline in patients after NICT was regarded as a clinical stage decline in this study. A clinical stage decline was observed in 170 (79.1%) patients, while 57 (67.1%) of the ypT+N+ patients also showed a clinical stage decline. Clinical stage decline was strongly correlated with DFS and OS in both the total and ypT+N+ patients. The survival benefit was significant in those with clinical stage decline (Total: 3-year DFS: 66.5% vs. 46.7%, P=0.009, Supplementary Figure S4A; 3-year OS: 78.2% vs. 57.8%, P=0.008, Supplementary Figure S4B; ypT+N+: 3-year DFS: 38.6% vs. 14.3%, P=0.013, Supplementary Figure S4C; 3-year OS: 56.1% vs. 32.1%, P=0.016, Supplementary Figure S4D).

Discussion

For locally advanced EC, NAT is now the accepted therapeutic option in certain countries. For patients with localized EC, the National Comprehensive Cancer Network (NCCN) guidelines suggest NCRT (3). On the other hand, NCT is advised by Japanese recommendations for those with resectable stage II or III thoracic EC (4). Due to immunotherapy as an emerging treatment modality, there is currently a lack of information to enlighten clinicians of its potential benefits to the point of care and help guide clinical decision making. In our investigation, 30.2% of patients who had PCR after NICT demonstrated a respectable survival rate (3-year DFS: 86.2% and 3-year OS: 95.4%). Therefore, AIT did not significantly improve survival in patients with PCR (ypT0N0), and follow-up without further treatment was

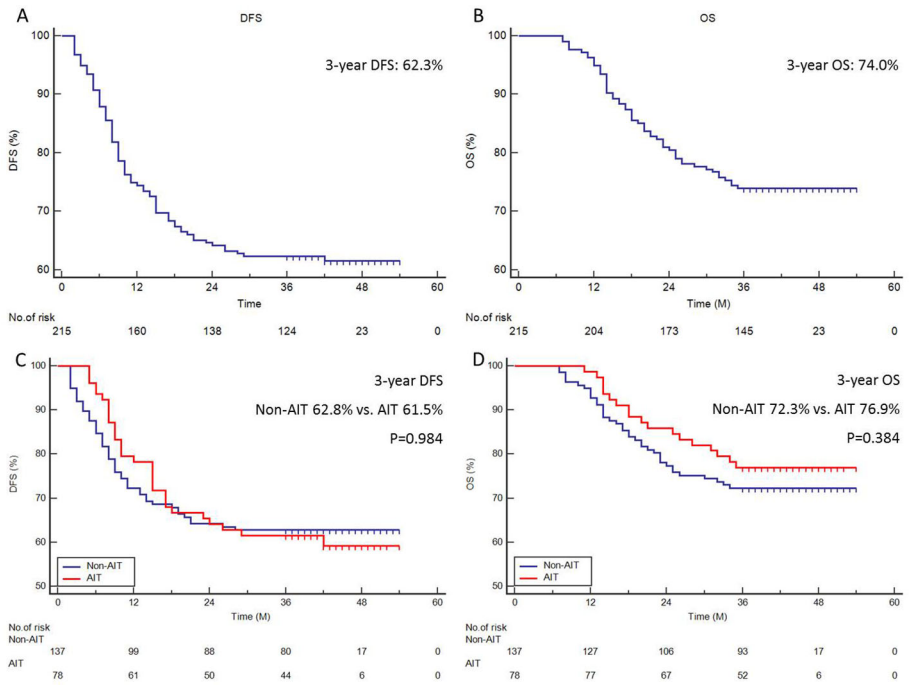

FIGURE 1
Survival analyses. The 3-year DFS **(A)** or 3-year OS **(B)** of all cohorts. The 3-year DFS **(C)** or 3-year OS **(D)** in patients with and without AIT.

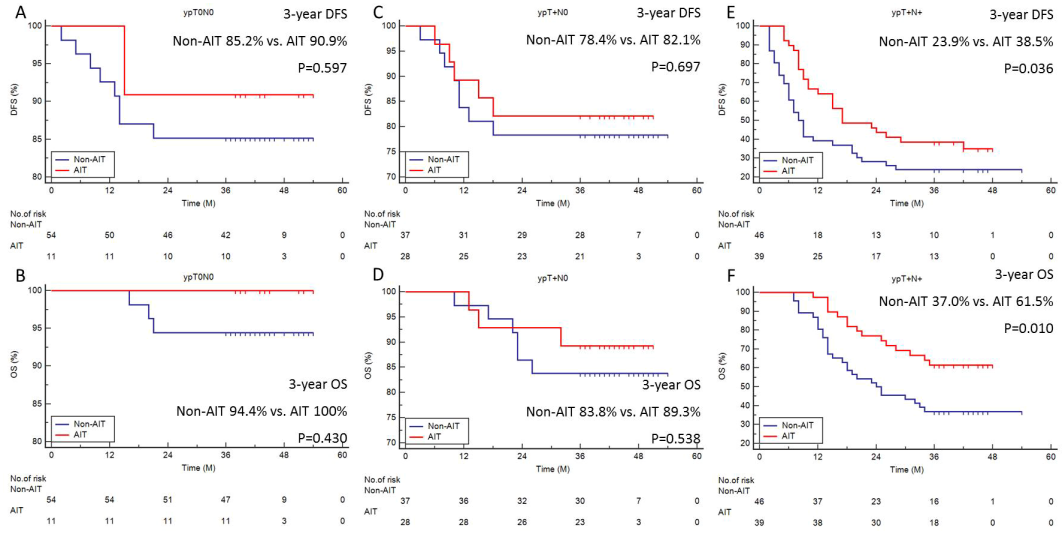

FIGURE 2
Subgroup analyses of survival. The 3-year DFS **(A)** or OS **(B)** in ypT0N0. The 3-year DFS **(C)** or OS **(D)** in ypT+N0. The 3-year DFS **(E)** or OS **(F)** in ypT+N+.

TABLE 2 Characteristics in ypT+N+ patients with ESCC receiving NICT.

	Total (n=85)	Non-AIT (n=46)	AIT (n=39)	P-value
Sex (n, %)				0.347
female	12 (14.1)	8 (17.4)	4 (10.3)	
male	73 (85.9)	38 (82.6)	35 (89.7)	
Age (median, Q1-3, years)	64 (57-69)	63 (57-68)	64 (57-69)	0.744
BMI (median, Q1-3, Kg/m^2)	21.8 (19.8-23.1)	21.6 (19.6-22.6)	21.8 (20.2-23.6)	0.359
Tumor location (n, %)				0.419
upper	10 (11.8)	5 (10.9)	5 (12.8)	
middle	37 (43.5)	23 (50.0)	14 (35.9)	
lower	38 (44.7)	18 (39.1)	20 (51.3)	
Differentiation (n, %)				0.204
well	15 (17.6)	9 (19.6)	6 (15.4)	
moderate	33 (38.8)	21 (45.7)	12 (30.8)	
poor	37 (43.6)	16 (34.7)	21 (53.8)	
Vessel invasion (n, %)	27 (20.9)	12 (26.1)	15 (38.5)	0.222
Perineural invasion (n, %)	27 (31.8)	14 (30.4)	13 (33.3)	0.775
Tumor length (median, Q1-3, cm)	3.00 (2.00-4.20)	2.80 (1.88-3.78)	3.20 (2.50-4.60)	0.012
Immunotherapy (n, %)				0.097
nivolumab	4 (4.7)	1 (2.2)	3 (7.7)	
pembrolizumab	14 (16.5)	6 (13.0)	8 (20.5)	
camrelizumab	44 (51.8)	30 (65.2)	14 (35.9)	
tislelizumab	16 (18.8)	6 (13.0)	10 (25.6)	
sintilimab	7 (8.2)	3 (6.6)	4 (10.3)	

(Continued)

TABLE 2 Continued

	Total (n=85)	Non-AIT (n=46)	AIT (n=39)	P-value
Surgical method (n, %)				0.082
McKeown	68 (80.0)	40 (87.0)	28 (71.8)	
Ivor-Lewis	17 (20.0)	6 (13.0)	11 (28.2)	
ypT stage (n, %)				0.055
T1	8 (9.4)	7 (15.2)	1 (2.6)	
T2	23 (27.1)	15 (32.6)	8 (20.5)	
T3	37 (43.5)	18 (39.1)	19 (48.7)	
T4	17 (20.0)	6 (13.0)	11 (28.2)	
ypN stage (n, %)				0.145
N1	48 (56.5)	27 (58.7)	21 (53.8)	
N2	26 (30.6)	16 (34.8)	10 (25.7)	
N3	11 (12.9)	3 (6.5)	8 (20.5)	
ypTNM stage (n, %)				0.044
stage IIIA	19 (22.4)	13 (28.3)	6 (15.4)	
stage IIIB	42 (49.4)	15 (54.3)	17 (43.6)	
stage IVA	24 (28.2)	8 (17.4)	16 (41.0)	
Total LNs (median, Q1-3, n)	21 (17-29)	20 (15-27)	22 (20-30)	0.064
Positive LNs (median, Q1-3, n)	2 (1-4)	1 (0-3)	2 (1-6)	0.007
Negative LNs (median, Q1-3, n)	19 (15-26)	18 (14-26)	20 (15-26)	0.466

ESCC, esophageal squamous cell carcinoma; NICT, neoadjuvant immunochemotherapy; AIT, adjuvant immunotherapy; BMI, body mass index; SD: standard deviation; TNM, tumor node metastasis; PCR, pathological complete response; LN, lymph node.

feasible. Regrettably, patients with a residual pathologic viable lesion have a poor prognosis, and PCR is frequently not obtained in most cases (5, 6). It needs more research to fully confirm how beneficial AIT is for individuals who have had surgery and NICT. In terms of 3-year DFS or 3-year OS, there was no statistically significant difference between those with and without AIT. Nonetheless, individuals with ypT+N+ showed a significant survival benefit from AIT (DFS: P=0.036; OS: P=0.010). It was also found that AIT was related to both DFS (HR: 0.297; P<0.001) and OS (HR: 0.321; P=0.001) in patients with ypT+N+.

It is generally acknowledged that NAT is useful for EC; nevertheless, the function of AT is still not really clear. AIT has been shown to enhance DFS in patients who had NCRT and surgical resection for EC, according to the recent Checkmate 577 trial (14). However, its use for those with NICT is limited. The administration of postoperative ACT to those with stage II or III ESCC who had NAT with surgery is not well-supported by available data, according to the Japan Esophageal Society's practice guidelines (18). Furthermore, the practice guidelines on multimodality treatment for EC published by the Society for Thoracic Surgeons also advise against providing the optimal treatment to node-positive patients who have already had multimodality therapy (19). In addition, a multiinstitutional study discovered that the rate of AT ranged from 3.2% to 50% in real clinical practice, indicating that AT is administered on a basis to numerous patients and varies greatly throughout clinicians and institutions (20).

The effects of AT following NAT and surgery have been investigated in a number of retrospective researches. Kim et al. (21) revealed that ACT after NCRT has been shown to be viable; however, the study's conclusions might have been impacted by the limited sample size. Mokda et al. (22) came to the same conclusion, with a small number of postoperative ACTs despite having up to 10,000 patients who underwent NCRT prior to surgery. According to studies published by Glatz et al. (23) and Kamarajah et al. (24), OS can be enhanced by ACT administered after NCT. Nonetheless, other research also presents differing findings. According to a multicenter cohort trial, patients with R1 resection were the only ones who benefited from ACT administered after NCT for EA, with no improvement in prognosis (25). Similar findings were also made by studies conducted by Bott et al. (26) and Li et al. (27). According to a recent meta-analysis, AT following NAT with negative resection margins improves 1- and 5-year OS with moderate to high confidence of evidence; however, because these outcomes are not widely reported, the benefit for DFS is still unknown (8). Patients contemplating AT should be advised on benefits versus morbidity because the benefit of AT is frequently minimal (7).

The primary NAT employed in these investigations was NCRT, while the primary pathogenic form of EC examined was EA. The

advantages of our study are demonstrated by the fact that, in contrast to earlier research, it examined a uniform pathology of ESCC and offered comprehensive information on the NICT. A further advantage of this research was that the follow-up period of three years and a specific sample size were chosen to provide a good predictive value for the prognosis analysis. According to earlier research, individuals with pathologic node-positive (ypN+) conditions greatly benefit from AT. Samson et al. (28) found that ACT led to a better median OS in patients with ypN+ from the National Cancer Database who had NAT plus surgery. Semenkovich et al. (20) indicated that patients with ypN+ who underwent NAT and surgery in a multicenter retrospective analysis who got ACT had a longer median OS compared to those who did not examine patients. In patients with ypT0N0 or ypT+N0, Burt and colleagues found that ACT did not significantly lower the probability of mortality. On the other hand, among individuals with ypTanyN+, ACT was linked to a 30% decrease in the risk of death in the whole cohort (29). According to Park et al.'s research, ACT following NAT and surgery improves the OS in those with ypT+N+ ESCC by reducing distant metastases (30). In our research, patients with ypT+N+ clearly benefit from AIT, but those with ypT+N0 or ypT0N+ did not demonstrate any benefit to survival. Compared to those with ypT+N0 or ypT0N+, the impact of additionally AIT may theoretically be more pronounced in those with ypT+N+ since they have a lower survival rate.

Although the primary finding of this study indicates that AIT improves DFS and OS in ypT+N+ patients following NICT and surgery, we believe that AIT cannot be consistently given to all ypT +N+ ESCC patients uniformly. Carefully assessing the patient's status following NICT and esophagectomy is necessary, as is weighing the advantages of AIT in terms of survival against the danger of recurrence. Furthermore, clinicians must find suitable patients with tolerance status so they can receive AIT, and further research is needed to determine the standards for candidate screening. In addition, efforts must be undertaken to lower postoperative complications and increase long-term survival because early postoperative morbidity and death are barriers to AIT.

There is currently no agreement on AIT in situations where R0 resection is required following NICT. Patients who achieved a PCR in the CheckMate 577 trial with the 5-year OS of 47-72% were excluded because they were thought to be at low risk of recurrence (14). Nonetheless, between 17% and 39% of these individuals later developed recurrences, with locoregional recurrence being the primary treatment failure pattern. In the current study, therefore, the purpose was to assess the effectiveness of AIT in patients with ESCC following NICT plus surgery as well as in those with PCR. The study indicated that AIT significantly improved both DFS and OS in patients with ypT+N+, but not in those with PCR.

Although there are no long-term follow-ups from trials, clinical evidence indicates that NICT with R0 resection may be an appealing therapeutic option for individuals with ESCC. Based on Checkmate 577 results, some national guidelines have changed their recommendations for adjuvant nivolumab for non-PCR patients after surgery following NCRT (14). Compared to historical data, Mamdani et al. (NCT02639065) demonstrated that adjuvant durvalumab significantly improved the 1-year recurrence-free survival for those with locally progressed EC and pathologically remaining disease after R0 resection following NCRT (31). However, the findings reported by Park et al. (NCT02520453) differ from the Checkmate 577 trial and Mamdani's. The results revealed that there was no significant difference in DFS or OS between the two groups (32). Furthermore, there are no guidelines to recommend how many courses of AIT are required. In another research (NCT04437212), Toripalimab was administered every three weeks for four cycles as adjuvant treatment (33). However, the authors stated that based on existing evidence and standards, four cycles of AIT may not be sufficient for those without PCR after NAT. Therefore, further research is needed to explore the optimal AT for patients who have undergone NICT and surgery.

This study has some limitations. Firstly, this is a retrospective cohort study from a single institution. However, the current study is of great significance in the absence of sufficient evidence-based medical evidence. A retrospective analysis was used to examine past cases in order to obtain evidence, as there haven't been any from these clinical studies to date. Secondly, there are a variety of immune drugs, and there may be differences in prognosis between different immune drugs. However, our findings showed that there was no statistical difference in the characteristics and prognosis of different immune agents. Finally, the decision for patients to receive AIT, with some selectivity, was largely determined by clinicians. However, in patients with ypT+N+, there was no significant difference between patients with or without AIT. Consequently, more randomized controlled clinical trials are necessary to determine the indications and treatment plan for AIT.

In summary, after NICT and surgery for ESCC, AIT increased DFS and OS in ypT+N+ patients. Since these individuals are able to tolerate the additional treatment, AIT may be a viable alternative for them. However, additional trials should be conducted to better examine the results of this retrospective investigation.

Data availability statement

The original contributions presented in the study are included in the article/Supplementary Material. Further inquiries can be directed to the corresponding author.

Ethics statement

The Ethics Committee of Zhejiang Cancer Hospital gave its approval (IRB-2020-320) and the research was carried out in compliance with the Helsinki Declaration. The studies were conducted in accordance with the local legislation and

institutional requirements. The participants provided their written informed consent to participate in this study.

Author contributions

JF: Conceptualization, Investigation, Writing – original draft, Writing – review & editing. LW: Data curation, Formal analysis, Methodology, Writing – review & editing. XY: Methodology, Resources, Software, Writing – review & editing. QC: Conceptualization, Project administration, Resources, Supervision, Writing – review & editing.

Funding

The author(s) declare that no financial support was received for the research, authorship, and/or publication of this article.

Conflict of interest

The authors declare that the research was conducted in the absence of any commercial or financial relationships that could be construed as a potential conflict of interest.

The author(s) declared that they were an editorial board member of Frontiers, at the time of submission. This had no impact on the peer review process and the final decision.

Publisher's note

Supplementary material

The Supplementary Material for this article can be found online at: https://www.frontiersin.org/articles/10.3389/fimmu.2024.1456193/full#supplementary-material

SUPPLEMENTARY FIGURE 1
The inclusion criteria of current study.

SUPPLEMENTARY FIGURE 2
Correlation between AIT and recurrence. AIT can effectively reduce distant recurrence (14.1% vs. 27.7%, P=0.022), but not for local recurrence (19.2% vs. 13.1%, P=0.233).

SUPPLEMENTARY FIGURE 3
Multivariable analysis in ypT+N+ individuals. Parameters linked to DFS **(A)** or OS **(B)** in patients with ypT+N+ ESCC. The Sankey diagrams regarding relations among AIT, ypTNM stages, and prognosis for all cohorts **(C)** or those with ypT+N+ **(D)**.

SUPPLEMENTARY FIGURE 4
Survival grouped by clinical stage decline. The 3-year DFS **(A)** or 3-year OS **(B)** of all cohorts with and without clinical stage decline. The 3-year DFS **(C)** or 3-year OS **(D)** in ypT+N+ patients with and without clinical stage decline.

References

1. Sung H, Ferlay J, Siegel RL, Laversanne M, Soerjomataram I, Jemal A, et al. Global cancer statistics 2020: GLOBOCAN estimates of incidence and mortality worldwide for 36 cancers in 185 countries. *CA Cancer J Clin*. (2021) 71:209–49. doi: 10.3322/caac.21660

2. Zhang Y, Gao J, Zheng A, Yang H, Li J, Wu S, et al. Definition and risk factors of early recurrence based on affecting prognosis of esophageal squamous cell carcinoma patients after radical resection. *Transl Oncol*. (2021) 14:101066. doi: 10.1016/j.tranon.2021.101066

3. Shapiro J, van Lanschot JJB, Hulshof MCCM, van Berge Henegouwen MI, Wijnhoven BPL, et al. Neoadjuvant chemoradiotherapy plus surgery versus surgery alone for oesophageal or junctional cancer (CROSS): long-term results of a randomised controlled trial. *Lancet Oncol*. (2015) 16:1090–8. doi: 10.1016/S1470-2045(15)00040-6

4. Ando N, Kato H, Igaki H, Shinoda M, Ozawa S, Shimizu H, et al. A randomized trial comparing postoperative adjuvant chemotherapy with cisplatin and 5-fluorouracil versus preoperative chemotherapy for localized advanced squamous cell carcinoma of the thoracic esophagus (JCOG9907). *Ann Surg Oncol*. (2012) 19:68–74. doi: 10.1245/s10434-011-2049-9

5. Hipp J, Kuvendjiska J, Hillebrecht HC, Herrmann S, Timme-Bronsert S, Fichtner-Feigl S, et al. Oncological recurrence following pathological complete response after neoadjuvant treatment in patients with esophageal cancer - a retrospective cohort study. *Langenbecks Arch Surg*. (2023) 408:363. doi: 10.1007/s00423-023-03100-2

6. Blum Murphy M, Xiao L, Patel VR, Maru DM, Correa AM, G Amlashi F, et al. Pathological complete response in patients with esophageal cancer after the trimodality approach: The association with baseline variables and survival-The University of Texas MD Anderson Cancer Center experience. *Cancer*. (2017) 123:4106–13. doi: 10.1002/cncr.v123.21

7. Rucker AJ, Raman V, Jawitz OK, Voigt SL, Harpole DH, D'Amico TA, et al. The impact of adjuvant therapy on survival after esophagectomy for node-negative esophageal adenocarcinoma. *Ann Surg*. (2022) 275:348–55. doi: 10.1097/SLA.0000000000003886

8. Lee Y, Samarasinghe Y, Lee MH, Thiru L, Shargall Y, Finley C, et al. Role of adjuvant therapy in esophageal cancer patients after neoadjuvant therapy and esophagectomy: A systematic review and meta-analysis. *Ann Surg*. (2022) 275:91–8. doi: 10.1097/SLA.0000000000005227

9. Kojima T, Shah MA, Muro K, Francois E, Adenis A, Hsu CH, et al. Randomized phase III KEYNOTE-181 study of pembrolizumab versus chemotherapy in advanced esophageal cancer. *J Clin Oncol*. (2020) 38:4138–48. doi: 10.1200/JCO.20.01888

10. Kato K, Cho BC, Takahashi M, Okada M, Lin CY, Chin K, et al. Nivolumab versus chemotherapy in patients with advanced oesophageal squamous cell carcinoma refractory or intolerant to previous chemotherapy (ATTRACTION-3): a multicentre, randomised, open-label, phase 3 trial. *Lancet Oncol*. (2019) 20:1506–17. doi: 10.1016/S1470-2045(19)30626-6

11. Yang W, Xing X, Yeung SJ, Wang S, Chen W, Bao Y, et al. Neoadjuvant programmed cell death 1 blockade combined with chemotherapy for resectable esophageal squamous cell carcinoma. *J Immunother Cancer*. (2022) 10:e003497. doi: 10.1136/jitc-2021-003497

12. Ge F, Huo Z, Cai X, Hu Q, Chen W, Lin G, et al. Evaluation of clinical and safety outcomes of neoadjuvant immunotherapy combined with chemotherapy for patients with resectable esophageal cancer: A systematic review and meta-analysis. *JAMA Netw Open*. (2022) 5:e2239778. doi: 10.1001/jamanetworkopen.2022.39778

13. Wang Z, Shao C, Wang Y, Duan H, Pan M, Zhao J, et al. Efficacy and safety of neoadjuvant immunotherapy in surgically resectable esophageal cancer: A systematic review and meta-analysis. *Int J Surg*. (2022) 104:106767. doi: 10.1016/j.ijsu.2022.106767

14. Kelly RJ, Ajani JA, Kuzdzal J, Zander T, Van Cutsem E, Piessen G, et al. Adjuvant nivolumab in resected esophageal or gastroesophageal junction cancer. *N Engl J Med*. (2021) 384:1191–203. doi: 10.1056/NEJMoa2032125

15. Rice TW, Ishwaran H, Hofstetter WL, Hofstetter WL, Apperson-Hansen C, Blackstone EH, et al. Recommendations for pathologic staging (pTNM) of cancer of the esophagus and esophagogastric junction for the 8th edition AJCC/UICC staging manuals. *Dis Esophagus*. (2016) 29:897–905. doi: 10.1111/dote.2016.29.issue-8

16. Jezerskyte E, Saadeh LM, Hagens ERC, Sprangers MAG, Noteboom L, van Laarhoven HWM, et al. Long-term health-related quality of life after McKeown and

Ivor Lewis esophagectomy for esophageal carcinoma. *Dis Esophagus*. (2020) 33: doaa022. doi: 10.1093/dote/doaa022

17. Kang X, Qin J, Zhang R, Wang Z, Zheng Q, Li Y, et al. 2021 NCC/CATS/CSTCVS/STM expert consensus on perioperative immunotherapy for esophageal cancer. *Ann Esophagus*. (2021) 4:33. doi: 10.21037/aoe-21-64

18. Kitagawa Y, Uno T, Oyama T, Kato K, Kato H, Kawakubo H, et al. Esophageal cancer practice guidelines 2017 edited by the Japan esophageal society: part 2. *Esophagus*. (2019) 16:25–43. doi: 10.1007/s10388-018-0642-8

19. Little AG, Lerut AE, Harpole DH, Hofstetter WL, Mitchell JD, Altorki NK, et al. The Society of Thoracic Surgeons practice guidelines on the role of multimodality treatment for cancer of the esophagus and gastroesophageal junction. *Ann Thorac Surg*. (2014) 98:1880–5. doi: 10.1016/j.athoracsur.2014.07.069

20. Semenkovich TR, Subramanian M, Yan Y, Hofstetter WL, Correa AM, Cassivi SD, et al. Adjuvant therapy for node-positive esophageal cancer after induction and surgery: A multisite study. *Ann Thorac Surg*. (2019) 108:828–36. doi: 10.1016/j.athoracsur.2019.04.099

21. Kim GJ, Koshy M, Hanlon AL, Horiba MN, Edelman MJ, Burrows WM, et al. The benefit of chemotherapy in esophageal cancer patients with residual disease after trimodality therapy. *Am J Clin Oncol*. (2016) 39:136–41. doi: 10.1097/COC.0000000000000036

22. Mokdad AA, Yopp AC, Polanco PM, Mansour JC, Reznik SI, Heitjan DF, et al. Adjuvant chemotherapy vs postoperative observation following preoperative chemoradiotherapy and resection in gastroesophageal cancer: A propensity score-matched analysis. *JAMA Oncol*. (2018) 4:31–8. doi: 10.1001/jamaoncol.2017.2805

23. Glatz T, Bronsert P, Schäfer M, Kulemann B, Marjanovic G, Sick O, et al. Perioperative platin-based chemotherapy for locally advanced esophagogastric adenocarcinoma: Postoperative chemotherapy has a substantial impact on outcome. *Eur J Surg Oncol*. (2015) 41:1300–7. doi: 10.1016/j.ejso.2015.07.010

24. Kamarajah SK, Markar SR, Phillips AW, Kunene V, Fackrell D, Salti GI, et al. Survival benefit of adjuvant chemotherapy following neoadjuvant therapy and oesophagectomy in oesophageal adenocarcinoma. *Eur J Surg Oncol*. (2022) 48:1980–7. doi: 10.1016/j.ejso.2022.05.014

25. Papaxoinis G, Kamposioras K, Weaver JMJ, Kordatou Z, Stamatopoulou S, Germetaki T, et al. The role of continuing perioperative chemotherapy postsurgery in patients with esophageal or gastroesophageal junction adenocarcinoma: a multicenter cohort study. *J Gastrointest Surg*. (2019) 23:1729–41. doi: 10.1007/s11605-018-04087-8

26. Bott RK, Beckmann K, Zylstra J, Wilkinson MJ, Knight WRC, Baker CR, et al. Adjuvant therapy following neoadjuvant chemotherapy and surgery for oesophageal adenocarcinoma in patients with clear resection margins. *Acta Oncol*. (2021) 60:672–80. doi: 10.1080/0284186X.2021.1885057

27. Li K, Hao W, Liu X, Li Y, Sun H, Liu S, et al. The role of adjuvant chemotherapy in the treatment of esophageal squamous cell carcinoma after neoadjuvant chemotherapy. *J Cancer*. (2023) 14:3130–8. doi: 10.7150/jca.84484

28. Samson P, Puri V, Lockhart AC, Robinson C, Broderick S, Patterson GA, et al. Adjuvant chemotherapy for patients with pathologic node-positive esophageal cancer after induction chemotherapy is associated with improved survival. *J Thorac Cardiovasc Surg*. (2018) 156:1725–35. doi: 10.1016/j.jtcvs.2018.05.100

29. Burt BM, Groth SS, Sada YH, Farjah F, Cornwell L, Sugarbaker DJ, et al. Utility of adjuvant chemotherapy after neoadjuvant chemoradiation and esophagectomy for esophageal cancer. *Ann Surg*. (2017) 266:297–304. doi: 10.1097/SLA.0000000000001954

30. Park SY, Kim HK, Jeon YJ, Lee J, Cho JH, Choi YS, et al. The role of adjuvant chemotherapy after neoadjuvant chemoradiotherapy followed by surgery in patients with esophageal squamous cell carcinoma. *Cancer Res Treat*. (2023) 55:1231–9. doi: 10.4143/crt.2022.1417

31. Mamdani H, Schneider B, Perkins SM, Burney HN, Kasi PM, Abushahin LI, et al. A phase II trial of adjuvant durvalumab following trimodality therapy for locally advanced esophageal and gastroesophageal junction adenocarcinoma: a big ten cancer research consortium study. *Front Oncol*. (2021) 17:736620. doi: 10.3389/fonc.2021.736620

32. Park S, Sun JM, Choi YL, Oh D, Kim HK, Lee T, et al. Adjuvant durvalumab for esophageal squamous cell carcinoma after neoadjuvant chemoradiotherapy: a placebo-controlled, randomized, double-blind, phase II study. *ESMO Open*. (2022) 7:100385. doi: 10.1016/j.esmoop.2022.100385

33. Xu X, Sun Z, Liu Q, Zhang Y, Shen L, Zhang C, et al. Neoadjuvant chemoradiotherapy combined with sequential perioperative toripalimab in locally advanced esophageal squamous cell cancer. *J Immunother Cancer*. (2024) 12: e008631. doi: 10.1136/jitc-2023-008631

frontiers | Frontiers in Immunology

TYPE Case Report
PUBLISHED 08 January 2025
DOI 10.3389/fimmu.2024.1496342

OPEN ACCESS

EDITED BY
Stavros P. Papadakos,
Laiko General Hospital of Athens, Greece

REVIEWED BY
Stamatina Vogli,
Metaxa Hospital, Greece
Ioannis Karniadakis,
NHS England, United Kingdom

*CORRESPONDENCE
Guangyong Zhang
guangyongzhang@hotmail.com

RECEIVED 14 September 2024
ACCEPTED 18 December 2024
PUBLISHED 08 January 2025

CITATION
Li L, Zhang D, Zhu J and Zhang G (2025) Hepatoid adenocarcinoma of the stomach with ideal response to neoadjuvant chemo-immunotherapy: a case report.
Front. Immunol. 15:1496342.
doi: 10.3389/fimmu.2024.1496342

Hepatoid adenocarcinoma of the stomach with ideal response to neoadjuvant chemo-immunotherapy: a case report

Linchuan Li[1,2], Dexu Zhang[3], Jiankang Zhu[1,2] and Guangyong Zhang[1,2]*

[1]Department of General Surgery, The First Affiliated Hospital of Shandong First Medical University & Shandong Provincial Qianfoshan Hospital, Shandong, China, [2]Department of General Surgery, Shandong Provincial Qianfoshan Hospital, The First Affiliated Hospital of Shandong First Medical University, Laboratory of Metabolism and Gastrointestinal Tumor, Shandong, China, [3]Shandong Provincial Qianfoshan Hospital, Shandong University, Shandong, China

Hepatoid adenocarcinoma of the stomach (HAS) is a rare subtype of gastric cancer characterized by histological features resembling hepatocellular carcinoma. Surgical intervention remains the preferred treatment modality for eligible patients. However, the efficacy of neoadjuvant therapy and alternative treatment regimens has been found to be suboptimal. Consequently, due to the high metastatic potential and unfavorable biological behavior of HAS, the prognosis for affected patients is exceedingly poor. We present a case involving a 64-year-old male diagnosed with advanced HAS, who demonstrated significant antitumor responses following a preoperative regimen of chemotherapy combined with immunotherapy, specifically utilizing oxaliplatin, S-1, and sintilimab. Over a 2-month period of neoadjuvant therapy, the patient's serum α-fetoprotein level significantly decreased from 52,951.56 ng/mL to 241.04 ng/mL. Computed tomography scans revealed substantial tumor regression. Subsequent radical surgical intervention confirmed significant tumor shrinkage, with no evidence of lymph node metastasis upon pathological examination. This is the first report of chemotherapy combined with sintilimab in the treatment of gastric hepatoid adenocarcinoma, which may provide novel insights into the therapeutic strategy for HAS.

KEYWORDS

hepatoid adenocarcinoma of stomach, immunotherapy, chemotherapy, programmed cell death-ligand 1, laparoscopic gastrectomy, gastric cancer

Introduction

Hepatoid adenocarcinoma of the stomach (HAS) is a rare subtype of gastric cancer featuring adenoid and hepatocyte differentiation, which is identical to hepatocellular carcinoma. HAS was first reported by Ishikura et al. in 1985, as a specificα-fetoprotein (AFP)-producing gastric cancer (1). HAS has been described in multiple organs, such as the stomach, pancreas, colon, and ovaries, of which the stomach is the most common site (2). HAS usually occurs in older males, with an average age at onset of approximately 60 years old (3). HAS accounts for only 0.3% to 1% of all kinds of gastric cancer (4, 5). The most common onset area of HAS is the gastric antrum, while it is rarely found in the cardia and gastric fundi (6).

Thus far, accurate diagnosis remains challenging due to the typically small proportion of the gastric region affected by HAS, which may complicate endoscopic biopsy procedures. With similar clinical features as common types of gastric cancer, HAS is typically latent and lacks specific clinical symptoms, which may make early diagnosis difficult (6).

Surgical intervention is commonly employed as the primary treatment strategy for HAS. Due to the high metastatic potential and adverse biobehavioral characteristics, the prognosis of HAS remains extremely poor. According to various studies, the 5-year survival rate ranges from 8.3% to 34.0% (7–10). Significant challenges persist in the development of appropriate and effective treatments for HAS. Despite many patients undergoing surgical treatment, the prognosis still appears poor (11). Although adjuvant chemotherapy and neoadjuvant chemotherapy have been employed for patients with HAS, it remains a challenge to determine a standard and effective treatment regimen, for either effective drugs or drug combinations (12, 13). However, herein, we report a case of a 64-year-old man who received preoperative chemotherapy and immunotherapy, followed by radical surgery, with satisfactory outcomes.

Case description

A 64-year-old male patient was admitted to the hospital with a 1-month history of fatigue and unspecified gastrointestinal discomfort. The patient claimed no symptoms of abdominal pain, nausea, vomiting, reflux, or dysphagia. The patient was treated with omeprazole tablets to suppress gastric acid secretion prior to admission, with no significant relief of symptoms. The patient claimed no family history of gastrointestinal tract cancer. Upon admission, laboratory tests revealed a hemoglobin level of 55.0 g/L, indicating anemia. Tumor markers for the digestive tract showed a significant elevation in serum AFP levels, measured at 52,951.56 ng/mL (reference range: 0-8.78 ng/mL), and a slight elevation in carcinoembryonic antigen, measured at 8.94 ng/mL (reference range:0-5.0 ng/mL). Additionally, stool analysis tested positive for occult blood. Gastroscopy indicated the presence of a large, irregular mass measuring approximately 4.5 cm in diameter located in the fundus of the cardia (Figure 1). The surface of the mass was uneven, brittle, and prone to bleeding. *Helicobacter pylori* testing was negative. Pathological analysis confirmed a diagnosis of poorly differentiated adenocarcinoma of the gastric cardia. Immunohistochemical results revealed positive expression of the carcinoembryonic protein alpha-fetoprotein (AFP), spalt-like transcription factor 4(SALL4), and hepatocyte-specific antigen. The expression of human epidermal growth factor receptor 2 (Her2) was negative. In conjunction with the aforementioned findings, the patient was ultimately diagnosed with gastric adenocarcinoma that produced AFP, with a subset identified as hepatoid adenocarcinoma. Contrast-enhanced computed

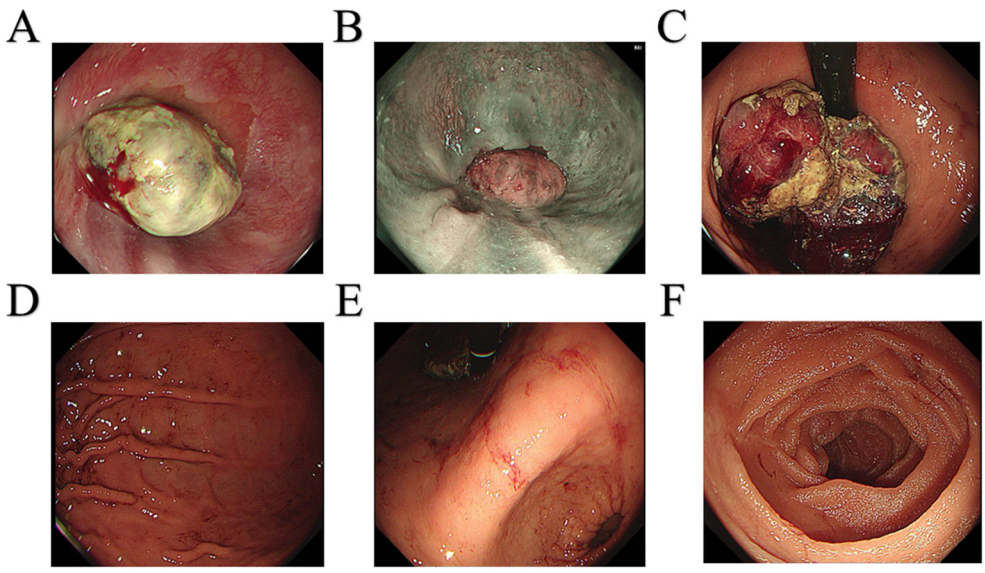

FIGURE 1
Gastroscopy images. **(A)** Dentate line. **(B)** Esophagus. **(C)** Fundus of the stomach. **(D)** Gastric body. **(E)** Gastric angle. **(F)** Duodenum.

tomography (CT) revealed an irregular lobulated mass with a diameter of approximately 6 cm, situated on the inferior curvature of the gastric fundus, exhibiting distinct heterogeneous enhancement. Additionally, multiple enlarged lymph nodes were observed surrounding the stomach and within the lesser omental sac, all demonstrating uniform enhancement (Figure 2A). Chest CT showed no signs of metastasis.

Following a multidisciplinary discussion involving the Imaging Department, Medical Oncology Department, and Gastrointestinal Surgery Department, the patient's TNM stage was determined to be T4N1-2Mx. Neoadjuvant therapy was initially recommended. An additional immunohistochemical test for programmed cell death-ligand 1(PD-L1) indicated that positive tumor cells and tumor-associated immune cells accounted for approximately 1%. A test for microsatellite instability showed no deficient mismatch repair. Therefore, the prescribed neoadjuvant therapy regimen comprised chemotherapy and immunotherapy and included oxaliplatin and S-1, in combination with sintilimab. The patient subsequently underwent three cycles of neoadjuvant therapy, resulting in significant tumor and lymph node regression as shown by enhanced CT (Figure 2B). After ruling out surgical contraindications, a laparoscopic total gastrectomy with lymph node dissection was successfully performed. Intraoperatively, it was observed that the tumor was located in the cardia and had not penetrated the serous membrane. Resected gastric and lymph node specimens were submitted for subsequent pathological examination.

Upon gross examination, a 3.8 x 1.5 cm infiltrating ulcerative mass was identified near the cardia, following an incision along the greater curvature. Sectioning of the tumor revealed a tough brown and gray mass that had invaded the muscle layer, lacking clear demarcation from the surrounding structures (Figure 3A). Mucosal erosion was observed around the tumor, with acute and chronic inflammation and hyperplasia of the fibro granulomatous tissue, which was consistent with chemotherapy changes. None of the perigastric lymph nodes exhibited metastatic involvement. Subsequent immunohistochemical analysis demonstrated positivity for Her2, while P63 and CK5/6 were negative (Figure 3B). The final diagnosis was AFP-producing gastric adenocarcinoma with partial hepatoid adenocarcinoma differentiation.

The patient experienced an uneventful postoperative recovery, with no short-term complications, and was discharged from the hospital on the ninth postoperative day. An iodine contrast study of the upper digestive tract indicated optimal recovery of the anastomotic site, with no evidence of leakage or stenosis. During the follow-up period, the patient's AFP levels exhibited a significant decline, decreasing from 52,951.56 ng/mL prior to surgery to 241.04 ng/mL following preoperative neoadjuvant therapy, and further reducing to 9.59 ng/mL 1 month after surgery. At the 6-month follow-up, the patient had excellent recovery and there was no evidence of recurrence in enhanced CT of the chest and abdomen. The serum AFP level was 5.63 ng/mL (Figure 4).

Discussion

Since hepatoid adenocarcinoma was first described in 1985, there have been multiple reports of cases affecting various organs, including gastrointestinal organs such as the esophagus, pancreas, and appendix; urogenital organs such as ovaries, the uterus, and adrenal glands; and other organs such as the lungs (14–20). Among these, the stomach is the most common site, and as such, hepatoid adenocarcinoma is classified as a rare type of gastric cancer. Recent studies from Asia have reported a HAS incidence of 0.17% to 0.36% (21, 22). The origin and pathogenesis of HAS remain uncertain. Previous research has suggested that HAS may originate from the endoderm, which develops from adenocarcinoma with an intestinal phenotype during embryonic development (23). A recent study investigating the origin of HAS demonstrated that both the adenocarcinomatous and hepatocellular-like components of HAS originate from a monoclonal pluripotent precursor cell (24).

The molecular characteristics of HAS remain poorly understood. However, a genetic analysis conducted on 42 patients with HAS identified TP53, CEBPA, RPTOR, WISP3, MARK1, and CD3EAP as genes with high-frequency mutations, exhibiting mutation rates ranging from 10% to 30% (25). These mutated genes may contribute to the enrichment of the HIF-1 signaling pathway and also signaling pathways regulating stem cell pluripotency in HAS.

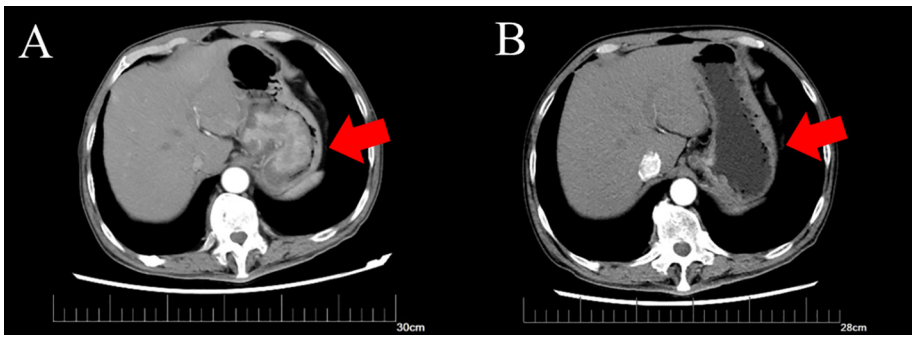

FIGURE 2
Computed tomography of gastric tumor before and after neoadjuvant therapy. **(A)** CT of the irregular mass with dimensions of 6.3*5.0 cm before neoadjuvant therapy. **(B)** CT of irregular thickening on the gastric fundus and the range is obviously regressed compared to before.

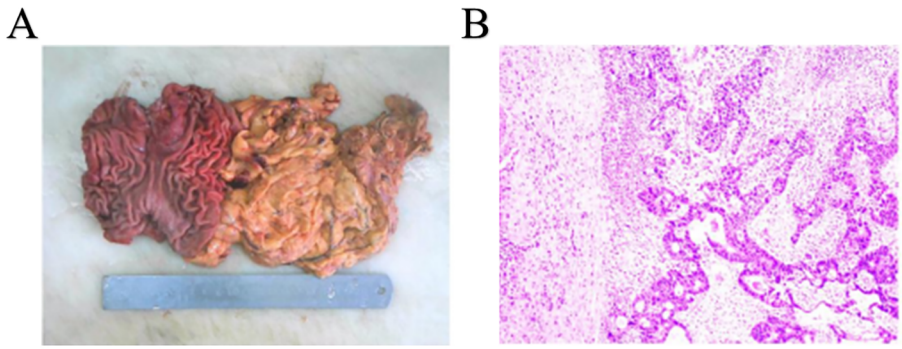

FIGURE 3
Completely resected tumor and histopathological findings. **(A)** Complete resected tumor. **(B)** histopathological findings of gastric tumor.

The manifestation of HAS is typically latent and lacks specific clinical symptoms, resembling common types of gastric cancer, thereby complicating early diagnosis. The initial clinical presentation often includes non-specific upper abdominal discomfort (26). Consequently, the accurate and reliable identification of HAS remains a significant challenge. CT is considered an optimal choice for the diagnosis of HAS, often revealing a thickened gastric wall and invasion of the peritumoral fatty space, accompanied by continuous enhancement (27, 28). However, some studies have suggested that the diagnostic value of CT for HAS may be limited, because it may not show significant anatomic abnormalities at the site of the primary tumor (29). Recently, some research studies have highlighted the significance of positron emission tomography (PET)/CT in diagnosing and differentiating HAS accurately, which needs confirmation for further application (30).

HAS exhibits similar histological features as hepatocellular carcinoma, which is characterized by the concurrent presence of adenocarcinoma and hepatoid components in pathological examinations (31). Furthermore, through immunohistochemical tests, HAS features the positive expression of AFP, GPC-3, and SALL4 (32). As the most prevalent subtype of AFP-producing gastric cancers, HAS is distinguished by its heightened invasive and metastatic potential, which is associated with an extremely poor prognosis (33). Furthermore, numerous studies have investigated the correlation between AFP expression levels and patient prognosis, though the findings remain contentious. A study conducted in China demonstrated that elevated serum AFP levels serve as an independent prognostic factor in gastric cancer, correlating with poorer outcomes, as evidenced by an analysis of 1,286 gastric cancer patients (34). Another study revealed that the 1-year survival rates for patients with AFP levels ≤20 ng/ml, ≤300

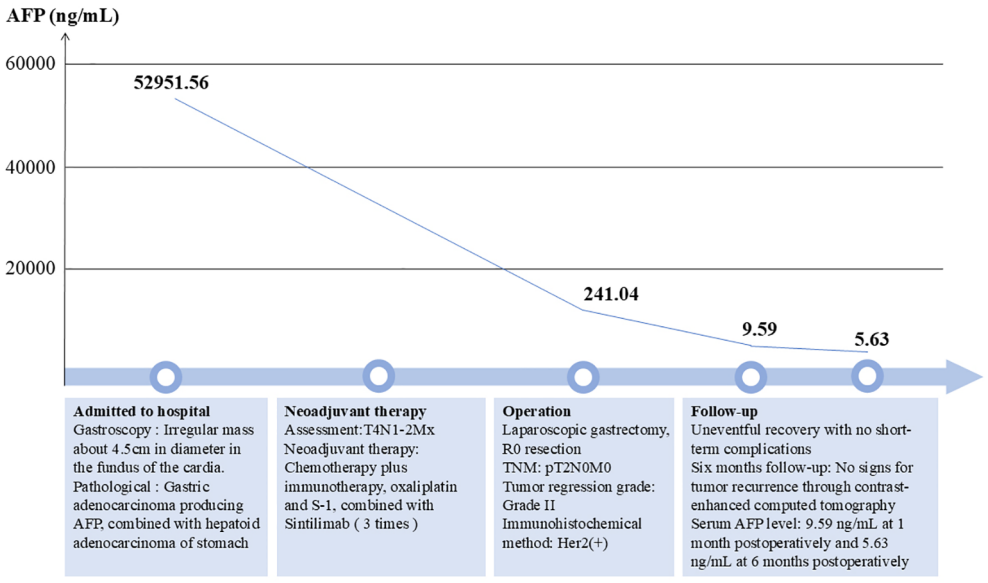

FIGURE 4
The whole treatment chart with the AFP trend.

ng/ml, and >300 ng/ml were 75.2%, 46.7%, and 15.4%, while the 5-year survival rates were 45.8%, 17.8%, and 0%, respectively (35). Furthermore, Yakun Wang and colleagues reported that a preoperative serum AFP level of ≥500 ng/mL was strongly associated with poor overall survival (25). In contrast, a Japanese study found no correlation between preoperative serum AFP levels and survival outcomes, although postoperative elevations in serum AFP were frequently indicative of tumor recurrence (10).

At present, there are no specialized treatments available for HAS, and the most common therapeutic approach remains radical surgery, which is also the conventional treatment for the more typical forms of gastric cancer. For patients with advanced-staged HAS that is not amenable to surgical resection, systemic chemotherapy, including neoadjuvant treatment, may represent a potential therapeutic option (3). Neoadjuvant therapy has the benefits of reducing the tumor burden and improving overall survival (36). However, there remains no established optimal and effective standard for such treatments. Genomic analysis of HAS has demonstrated elevated drug transport activity and increased expression of drug-resistance-related genes compared to more typical forms of gastric cancer, indicating that conventional chemotherapy may not be an ideal treatment approach (24). Although studies have demonstrated the clinical benefit of neoadjuvant chemotherapy for other forms of gastric cancer, its therapeutic efficacy for HAS still remains a subject of debate. Certain studies have suggested that FOLFOX could serve as a potential postoperative treatment for HAS, whereas other studies have reported less favorable outcomes (12, 37, 38). In our study, based on standard therapy for advanced gastric cancer, we applied the SOX protocol and found a remarkable curative effect on tumor reduction. Furthermore, due to the R0 resect of the tumor, with a TNM stage of T2N0M0, this patient received careful follow-up without postoperative chemotherapy. Through 6 months of follow-up, there was no evidence of tumor recurrence based on enhanced CT scans and serum tests for AFP level. Currently, immunotherapy is infrequently applied for HAS. A previous case report indicated that sintilimab exhibited a satisfactory therapeutic effect in a patient with advanced lung hepatoid adenocarcinoma (39). However, there have been no reports concerning its efficacy in the treatment of HAS. Our study represents the first report to demonstrate the significant efficacy of sintilimab in the treatment of HAS, which demonstrated promising therapeutic effects.

Our study suggests that the combination of chemotherapy and immunotherapy, such as sintilimab, may yield significant outcomes and could serve as a potential adjuvant treatment option for HAS. These findings may contribute valuable insights for the development of treatment strategies for patients with advanced HAS and underscore the importance of molecular diagnosis in informing treatment decisions.

Conclusion

HAS is an uncommon subtype of gastric cancer characterized by a poor prognosis. Metastasis to the lymph nodes and distant organs, especially the liver, is often present at diagnosis, which poses a huge challenge for treatment and less favorable therapeutic efficacy. The standard treatment protocol for HAS remains undefined. This case report suggests that a combination of SOX chemotherapy and immunotherapy, specifically sintilimab, may represent an effective therapeutic option for advanced HAS. Further in-depth investigations and prolonged follow-ups of related cases are necessary to provide more robust evidence for the treatment of HAS.

Data availability statement

The raw data supporting the conclusions of this article will be made available by the authors, without undue reservation.

Ethics statement

The studies involving humans were approved by Medical Ethics Committee of the First Affiliated Hospital of Shandong First Medical University &Shandong Qianfoshan Hospital. The studies were conducted in accordance with the local legislation and institutional requirements. The participants provided their written informed consent to participate in this study. Written informed consent was obtained from the individual(s) for the publication of any potentially identifiable images or data included in this article.

Author contributions

LL: Writing – original draft, Funding acquisition, Investigation. DZ: Data curation, Visualization, Writing – original draft. JZ: Supervision, Writing – review & editing. GZ: Supervision, Validation, Writing – review & editing, Writing – original draft.

Funding

The author(s) declare financial support was received for the research, authorship, and/or publication of this article. This research was funded by the Natural Science Foundation of Shandong Province (Grant No. ZR2022QH322).

Conflict of interest

The authors declare that the research was conducted in the absence of any commercial or financial relationships that could be construed as a potential conflict of interest.

Publisher's note

References

1. Ishikura H, Fukasawa Y, Ogasawara K, Natori T, Tsukada Y, Aizawa M. An AFP-producing gastric carcinoma with features of hepatic differentiation. *A Case Rep Cancer*. (1985) 56:840–8. doi: 10.1002/1097-0142(19850815)56:4<840::aid-cncr2820560423>3.0.co;2-e

2. Kashani A, Ellis JC, Kahn M, Jamil LH. Liver metastasis from hepatoid adenocarcinoma of the esophagus mimicking hepatocellular carcinoma. *Gastroenterol Rep (Oxf)*. (2017) 5:67–71. doi: 10.1093/gastro/gov021

3. Qu BG, Bi WM, Qu BT, Qu T, Han XH, Wang H, et al. PRISMA-compliant article: clinical characteristics and factors influencing prognosis of patients with hepatoid adenocarcinoma of the stomach in China. *Med (Baltimore)*. (2016) 95: e3399. doi: 10.1097/MD.0000000000003399

4. Lin JX, Wang ZK, Hong QQ, Zhang P, Zhang ZZ, He L, et al. Assessment of clinicopathological characteristics and development of an individualized prognostic model for patients with hepatoid adenocarcinoma of the stomach. *JAMA Netw Open*. (2021) 4:e2128217. doi: 10.1001/jamanetworkopen.2021.28217

5. Zhu M, Chen E, Yu S, Xu C, Yu Y, Cao X, et al. Genomic profiling and the impact of MUC19 mutation in hepatoid adenocarcinoma of the stomach. *Cancer Commun (Lond)*. (2022) 42:1032–5. doi: 10.1002/cac2.v42.10

6. Zeng XY, Yin YP, Xiao H, Zhang P, He J, Liu WZ, et al. Clinicopathological characteristics and prognosis of hepatoid adenocarcinoma of the stomach: evaluation of a pooled case series. *Curr Med Sci*. (2018) 38:1054–61. doi: 10.1007/s11596-018-1983-1

7. Chang YC, Nagasue N, Abe S, Taniura H, Kumar DD, Nakamura T. Comparison between the clinicopathologic features of AFP-positive and AFP-negative gastric cancers. *Am J Gastroenterol*. (1992) 87:321–5.

8. Kono K, Amemiya H, Sekikawa T, Iizuka H, Takahashi A, Fujii H, et al. Clinicopathologic features of gastric cancers producing alpha-fetoprotein. *Dig Surg*. (2002) 19:359–65. doi: 10.1159/000065838

9. Chang YC, Nagasue N, Kohno H, Taniura H, Uchida M, Yamanoi A, et al. Clinicopathologic features and long-term results of alpha-fetoprotein-producing gastric cancer. *Am J Gastroenterol*. (1990) 85:1480–5.

10. Inoue M, Sano T, Kuchiba A, Taniguchi H, Fukagawa T, Katai H. Long-term results of gastrectomy for alpha-fetoprotein-producing gastric cancer. *Br J Surg*. (2010) 97:1056–61. doi: 10.1002/bjs.7081

11. Liu X, Cheng Y, Sheng W, Lu H, Xu X, Xu Y, et al. Analysis of clinicopathologic features and prognostic factors in hepatoid adenocarcinoma of the stomach. *Am J Surg Pathol*. (2010) 34:1465–71. doi: 10.1097/PAS.0b013e3181f0a873

12. Velut G, Mary F, Wind P, Aparicio T. Adjuvant chemotherapy by FOLFOX for gastric hepatoid adenocarcinoma. *Dig Liver Dis*. (2014) 46:1135–6. doi: 10.1016/j.dld.2014.08.036

13. Nakao S, Nakata B, Tendo M, Kuroda K, Hori T, Inaba M, et al. Salvage surgery after chemotherapy with S-1 plus cisplatin for alpha-fetoprotein-producing gastric cancer with a portal vein tumor thrombus: a case report. *BMC Surg*. (2015) 15:5. doi: 10.1186/1471-2482-15-5

14. Chiba N, Yoshioka T, Sakayori M, Mikami Y, Miyazaki S, Akiyama S, et al. AFP-producing hepatoid adenocarcinoma in association with Barrett's esophagus with multiple liver metastasis responding to paclitaxel/CDDP: a case report. *Anticancer Res*. (2005) 25:2965–8.

15. Marchegiani G, Gareer H, Parisi A, Capelli P, Bassi C, Salvia R. Pancreatic hepatoid carcinoma: a review of the literature. *Dig Surg*. (2013) 30:425–33. doi: 10.1159/000355442

16. Wang XY, Bao WQ, Hua FC, Zuo CT, Guan YH, Zhao J. AFP-producing hepatoid adenocarcinoma of appendix: a case report of 18F-FDG PET/CT. *Clin Imaging*. (2014) 38:526–8. doi: 10.1016/j.clinimag.2014.02.019

17. Lazaro J, Rubio D, Repolles M, Capote L. Hepatoid carcinoma of the ovary and management. *Acta Obstet Gynecol Scand*. (2007) 86:498–9. doi: 10.1080/00016340600593117

18. Takahashi Y, Inoue T. Hepatoid carcinoma of the uterus that collided with carcinosarcoma. *Pathol Int*. (2003) 53:323–6. doi: 10.1046/j.1440-1827.2003.01467.x

19. Lin J, Cao Y, Yu L, Lin L. Non-alpha-fetoprotein-producing adrenal hepatoid adenocarcinoma: A case report and literature review. *Med (Baltimore)*. (2018) 97: e12336. doi: 10.1097/MD.0000000000012336

20. Chen Z, Ding C, Zhang T, He Y, Jiang G. Primary hepatoid adenocarcinoma of the lung: A systematic literature review. *Onco Targets Ther*. (2022) 15:609–27. doi: 10.2147/OTT.S364465

21. Baek SK, Han SW, Oh DY, Im SA, Kim TY, Bang YJ. Clinicopathologic characteristics and treatment outcomes of hepatoid adenocarcinoma of the stomach, a rare but unique subtype of gastric cancer. *BMC Gastroenterol*. (2011) 11:56. doi: 10.1186/1471-230X-11-56

22. Zhang JF, Shi SS, Shao YF, Zhang HZ. Clinicopathological and prognostic features of hepatoid adenocarcinoma of the stomach. *Chin Med J (Engl)*. (2011) 124:1470–6. doi: 10.3760/cma.j.issn.0366-6999.2011.10.006

23. Akiyama S, Tamura G, Endoh Y, Fukushima N, Ichihara Y, Aizawa K, et al. Histogenesis of hepatoid adenocarcinoma of the stomach: molecular evidence of identical origin with coexistent tubular adenocarcinoma. *Int J Cancer*. (2003) 106:510–5. doi: 10.1002/ijc.v106:4

24. Liu Z, Wang A, Pu Y, Li Z, Xue R, Zhang C, et al. Bai F et al: Genomic and transcriptomic profiling of hepatoid adenocarcinoma of the stomach. *Oncogene*. (2021) 40:5705–17. doi: 10.1038/s41388-021-01976-2

25. Wang Y, Sun L, Li Z, Gao J, Ge S, Zhang C, et al. Lu Z et al: Hepatoid adenocarcinoma of the stomach: a unique subgroup with distinct clinicopathological and molecular features. *Gastric Cancer*. (2019) 22:1183–92. doi: 10.1007/s10120-019-00965-5

26. Yoshizawa J, Ishizone S, Ikeyama M, Nakayama J. Gastric hepatoid adenocarcinoma resulting in a spontaneous gastric perforation: a case report and review of the literature. *BMC Cancer*. (2017) 17:368. doi: 10.1186/s12885-017-3357-7

27. Yan XY, Ju HY, Hou FJ, Li XT, Yang D, Tang L, et al. Analysis of enhanced CT imaging signs and clinicopathological prognostic factors in hepatoid adenocarcinoma of stomach patients with radical surgery: a retrospective study. *BMC Med Imaging*. (2023) 23:167. doi: 10.1186/s12880-023-01125-z

28. Yang Q, Liu Y, Zhang S. Hepatoid adenocarcinoma of the stomach: CT findings. *Front Oncol*. (2023) 13:1036763. doi: 10.3389/fonc.2023.1036763

29. Ren A, Cai F, Shang YN, Ma ES, Huang ZG, Wang W, et al. Gastric hepatoid adenocarcinoma: a computed tomography report of six cases. *World J Gastroenterol*. (2014) 20:15001–6. doi: 10.3748/wjg.v20.i40.15001

30. Seo HJ, Chung JK, Go H, Cheon GJ, Lee DS. A hepatoid adenocarcinoma of the stomach evaluated with (18)F-FDG PET/CT: intense (18)F-FDG uptake contrary to the previous report. *Clin Nucl Med*. (2014) 39:442–5. doi: 10.1097/RLU.0000000000000275

31. Plaza JA, Vitellas K, Frankel WL. Hepatoid adenocarcinoma of the stomach. *Ann Diagn Pathol*. (2004) 8:137–41. doi: 10.1016/j.anndiagpath.2004.03.005

32. Zhao M, Sun L, Lai JZ, Shi H, Mei K, He X, et al. Expression of RNA-binding protein LIN28 in classic gastric hepatoid carcinomas, gastric fetal type gastrointestinal adenocarcinomas, and hepatocellular carcinomas: An immunohistochemical study with comparison to SALL4, alpha-fetoprotein, glypican-3, and Hep Par1. *Pathol Res Pract*. (2018) 214:1707–12. doi: 10.1016/j.prp.2018.07.037

33. Liu X, Sheng W, Wang Y. An analysis of clinicopathological features and prognosis by comparing hepatoid adenocarcinoma of the stomach with AFP-producing gastric cancer. *J Surg Oncol*. (2012) 106:299–303. doi: 10.1002/jso.v106.3

34. Chen Y, Qu H, Jian M, Sun G, He Q. High level of serum AFP is an independent negative prognostic factor in gastric cancer. *Int J Biol Markers*. (2015) 30:e387–393. doi: 10.5301/jbm.5000167

35. Lin HJ, Hsieh YH, Fang WL, Huang KH, Li AF. Clinical manifestations in patients with alpha-fetoprotein-producing gastric cancer. *Curr Oncol*. (2014) 21:e394–399. doi: 10.3747/co.21.1768

36. Janjigian YY, Shitara K, Moehler M, Garrido M, Salman P, Shen L, et al. Campos Bragagnoli A et al: First-line nivolumab plus chemotherapy versus chemotherapy alone for advanced gastric, gastro-oesophageal junction, and oesophageal adenocarcinoma (CheckMate 649): a randomised, open-label, phase 3 trial. *Lancet*. (2021) 398:27–40. doi: 10.1016/S0140-6736(21)00797-2

37. Lucas ZD, Shah M, Trivedi A, Dailey ME. Hepatoid adenocarcinoma of the peritoneal cavity: Prolonged survival after debulking surgery and 5-fluorouracil, leucovorin and oxaliplatin (FOLFOX) therapy. *J Gastrointest Oncol*. (2012) 3:139–42. doi: 10.3978/j.issn.2078-6891.2011.052

38. Ye MF, Tao F, Liu F, Sun AJ. Hepatoid adenocarcinoma of the stomach: a report of three cases. *World J Gastroenterol*. (2013) 19:4437–42. doi: 10.3748/wjg.v19.i27.4437

39. Chen L, Han X, Gao Y, Zhao Q, Wang Y, Jiang Y, et al. Anti-PD-1 therapy achieved disease control after multiline chemotherapy in unresectable KRAS-positive hepatoid lung adenocarcinoma: A case report and literature review. *Onco Targets Ther*. (2020) 13:4359–64. doi: 10.2147/OTT.S248226

frontiers | Frontiers in Immunology

TYPE Systematic Review
PUBLISHED 27 January 2025
DOI 10.3389/fimmu.2025.1523455

OPEN ACCESS

EDITED BY
Stavros P. Papadakos,
Laiko General Hospital of Athens, Greece

REVIEWED BY
Ioanna Aggeletopoulou,
University Hospital of Patras, Greece
Ioannis Karniadakis,
NHS England, United Kingdom

*CORRESPONDENCE
Min Ren
renmin@wchscu.cn

†These authors have contributed equally to this work and share first authorship

RECEIVED 06 November 2024
ACCEPTED 06 January 2025
PUBLISHED 27 January 2025

CITATION
Zhang H, Huang J, Xu H, Yin N, Zhou L, Xue J and Ren M (2025) Neoadjuvant immunotherapy for DNA mismatch repair proficient/microsatellite stable non-metastatic rectal cancer: a systematic review and meta-analysis.
Front. Immunol. 16:1523455.
doi: 10.3389/fimmu.2025.1523455

Neoadjuvant immunotherapy for DNA mismatch repair proficient/microsatellite stable non-metastatic rectal cancer: a systematic review and meta-analysis

Huan Zhang[1†], Jing Huang[2†], Huanji Xu[3†], Nanhao Yin[1,4], Liyan Zhou[1,4], Jianxin Xue[1,4,5] and Min Ren[3*]

[1]Division of Thoracic Tumor Multimodality Treatment, Cancer Center, West China Hospital, Sichuan University, Chengdu, Sichuan, China, [2]Department of Ultrasound, West China Hospital, Sichuan University, Chengdu, Sichuan, China, [3]Abdominal Oncology Ward, Division of Radiation Oncology, Cancer Center, West China Hospital, Sichuan University, Chengdu, Sichuan, China, [4]Laboratory of Clinical Cell Therapy, West China Hospital, Sichuan University, Chengdu, Sichuan, China, [5]Department of Radiation Oncology, Cancer Center, West China Hospital, Sichuan University, Chengdu, Sichuan, China

Background: Neoadjuvant immunotherapy (NIT) has been endorsed by clinical guidelines for the management of DNA mismatch repair deficiency/microsatellite instability-high (dMMR/MSI-H) locally advanced rectal cancer (LARC). Nonetheless, the therapeutic efficacy of NIT in mismatch repair-proficient/microsatellite stable (pMMR/MSS) non-metastatic rectal cancer (RC) remain pending matters. Therefore, a meta-analysis was carried out to assess the efficacy and safety of NIT in patients with non-metastatic pMMR/MSS RC.

Methods: PubMed, Embase, Web of Science, the Cochrane Library, ClinicalTrials.gov, ASCO and ESMO were searched to obtain related studies up to July 2024. Two reviewers independently screened the included articles and extracted the pertinent data. The risk of publication bias was assessed by Begg or Egger tests and in cases of publication bias, the trim and fill method was applied. Heterogeneity was assessed using I^2 statistics.

Results: Thirteen articles including 582 eligible patients were analyzed. The pooled pCR, MPR, cCR and anus preservation rate were 37%, 57%, 26% and 77% separately and the incidence of irAEs≥3 grades and TRAEs≥3 grades were 3% and 29%, respectively. Non-metastatic pMMR/MSS RC receiving the short-course radiotherapy (SCRT) in neoadjuvant setting exhibited superior pooled pCR and MPR than long-course radiotherapy (LCRT) without upregulating the incidence of adverse effects. Furthermore, patients with MSS RC underwent neoadjuvant treatment with anti-PD-1 inhibitors demonstrated higher pooled pCR, MPR, cCR compared to those receiving PD-L1 inhibitors. Additionally, yielded improved pooled MPR and anal preservation rates compared to sequential immuno-radiotherapy (63.4% vs 51.2% and 88.5% vs 69.9%), without raising the incidence of irAEs≥3 grade. Interestingly, RC patients with lymph node metastasis showed a higher pooled pCR than those without lymph node metastasis (43% vs 35%).

Conclusion: NIT was linked to favorable response rates and anal preservation, alongside an acceptable safety profile. Non-metastatic pMMR/MSS RC patients receiving SCRT, PD-1 inhibitors, or concurrent immuno-radiotherapy in the neoadjuvant setting exhibited enhanced outcomes. This meta-analysis provides evidence for further exploration and application of NIT in non-metastatic pMMR/MSS RC and highlights the potential for organ preservation with this approach. The relatively small sample size and the uneven quality of included studies may have had some impact on the generality of the results. Therefore, further analysis with a higher number of high-quality studies is needed to verify the conclusions.

Systematic review registration: https://inplasy.com/, identifier: INPLASY202470110.

KEYWORDS

neoadjuvant immunotherapy, non-metastatic rectal cancer, mismatch repair-proficient/microsatellite stable, meta-analysis, efficacy

1 Introduction

Ranking second in cause of mortality and third in incidence of malignancy globally, colorectal cancer (CRC) brings a serious threat to human health with a persistent upward trend in incidence and fatalities, among which, rectal cancer (RC) accounts for approximately 33.3% of all the diagnosed cases (1). Although notable medical advancements had been achieved in the past few years, the locally advanced rectal cancer (LARC) was still a tricky disease to management with increased incidence, high propensity of local recurrence and distant metastasis (2) and prevalence in younger populations (3).

Total neoadjuvant therapy (TNT) refers to the perioperative treatment for LARC where the majority or entirety of postoperative adjuvant chemotherapy is administered prior to surgical intervention, in conjunction with concurrent chemoradiotherapy (CRT). In the Spanish phase II randomized GCR-3 trial, pathologic complete response (pCR) in the TNT group and neoadjuvant chemoradiotherapy (nCRT) group was not significantly different (13.5% vs 14.3%), yet the TNT cohort exhibited superior treatment adherence (91% vs 54%) (4). A retrospective analysis from Memorial Sloan Kettering Cancer Center (MSK) revealed that patients with LARC receiving TNT experienced higher pCR rates than those undergoing conventional chemoradiotherapy (5). Consequently, TNT is recommended as one of the standard treatments for LARC. Besides, for LARC patients achieving a complete clinical response (cCR) after neoadjuvant treatment, the conservative Watch and Wait (WW) strategy may offer comparable survival outcomes to surgical intervention (6). Nonetheless, despite the progress made with TNT for LARC, various limitations persist, including a distant metastasis rate exceeding 20% within three years, a postoperative pCR rate less than 30%, heightened toxicity from radiotherapy and chemotherapy, and poor long-term survival prospects, which somewhat restrict clinical application.

In the last decade, cancer immunotherapy—encompassing antibody therapy, cellular immunotherapy, and cytokine therapy—has transformed the oncology treatment landscape, yielding promising clinical results across a wide array of malignancies (7). However, only a minority of patients with specific molecular profiles derive substantial benefit from immunotherapy (8). Chromosome translocations and genomic instability are hallmarks in cancer development. The DNA mismatch repair (MMR) system is crucial for preserving DNA integrity, with DNA mismatch repair deficient/microsatellite instability-high (dMMR/MSI-H) defined by mutation status in microsatellite alleles. Characterized by high tumor mutational burden (TMB), abundant tumor infiltrating lymphocytes (TILs) and non-synonymous mutations, MSI-H/dMMR tumors often show greater response rate for immune checkpoint inhibitors (ICIs) treatment. Conversely, the vast majority of patients with mismatch repair proficient/microsatellite stable (pMMR/MSS), which feature low TMB and limited T cell infiltration, tend to show decreased sensitivity or resistance to ICIs (8, 9).

In addition to damaging cancer cells directly, irradiation also exerts immunostimulant properties by enhancing the cytotoxic activity of NK cells and fostering the accumulation of CD8+ cytotoxic T lymphocytes and tumor-associated M1 macrophages within the tumor microenvironment. The concomitantly used immunotherapy can potentiate the activity of immune cells, resulting in significant neoplastic cell destruction or exhibiting synergistic antitumor effects in combination with radiotherapy (10, 11), as evidenced in studies involving triple-negative breast cancer, small cell lung cancer, and other tumors (12).

Building on these principles, numerous studies have investigated the clinical advantages of neoadjuvant immunotherapy (NIT) in CRC. The KEYNOTE-016 trial found that metastatic CRC and other solid tumors exhibiting the dMMR/MSI-H phenotype significantly benefit from programmed death ligand-1 (PD-L1) monoclonal antibody immunotherapy (13). Therefore, guidelines recommended immunotherapy for the treatment of dMMR/MSI-H metastatic CRC. Although only a very small part (less than 10%) of RC can be classified as dMMR/MSI-H category, NIT could result in a higher complete response (CR) rate than nCRT with fewer adverse effects on sphincter, reproductive organs and sexual function in those group of population (14), and the latest ASCO guideline recommended the NIT and the first-line treatment option for dMMR/MSI-H LARC (15).

Despite advancements in the treatment of dMMR/MSI-H tumors, consensus on the clinical efficacy of NIT for pMMR/MSS non-metastatic RC remains elusive. Besides, there are only few published RCT studies reporting the clinical efficacy and safety of NIT in MSS RC, most of the on-going trials are single-arm prospective trials and the variations about intervention methods in these published and ongoing trials also impede the clinical application of NIT in MSS RC. Given the rising demand to achieve tumor regression, anus preservation and more satisfactory long-term survival outcomes through "increasing efficiency and decreasing toxicity" therapeutic strategy in RC patients recent years, the traditional nCRT or TNT treatment model reached an impasse. Therefore, we conducted this systematic review and meta-analysis to assess the effect and safety of immunotherapy-based neoadjuvant treatment in non-metastatic pMMR/MSS RC, aiming to offer novel management options for these patient populations and provide support for future study.

2 Methods

This systematic review with meta-analysis was executed in compliance with the Preferred Reporting Items for Systematic Reviews and Meta-Analyses (PRISMA) guidelines (16). The selection criteria were established based on the PICOS (population, intervention, comparison, outcome, and study design) framework.

2.1 Search strategy

We conducted comprehensive searches of several online databases for eligible trails from inception to July 2024, including PubMed, Embase, Web of Science and the Cochrane Library. Additionally, ClinicalTrials.gov, ASCO and ESMO also were searched for potential unpublished findings. Keywords used for the search included "rectal cancer" "neoadjuvant immunotherapy" "PD-1 inhibitors" "PD-L1 inhibitors" and "neoadjuvant therapy". To ensure comprehensive coverage, references from original studies and literature reviews were also examined. Details of the search methodology could be available in Supplementary File 1.

2.2 Inclusion and exclusion criteria

Inclusion criteria were as follows: 1) adults with primary cancer of pMMR/MSS RC; 2) non-metastatic disease; 3) immunotherapy (programmed cell death protein 1 (PD-1) inhibitor, programmed cell death 1 ligand 1 (PD-L1) inhibitor or cytotoxic T-lymphocyte–associated protein 4 (CTLA-4) inhibitor) used during neoadjuvant therapy period; 4) reporting 10 or more cases and 5) single-arm study, cohort or prospective study, retrospective study and RCTs.

Exclusion criteria included: 1) letters to the editor, and editorials, reviews, animal studies, case reports and study protocol; 2) articles lacking related data; 3) involving patients diagnosed with colorectal cancer (CRC) or other malignancies without distinct findings, 4) metastatic CRC or RC, 5) absence of immunotherapy in the neoadjuvant setting.

2.3 Efficacy indicators

The outcomes evaluated in these studies were the pathological complete response (pCR), major pathological response (MPR), clinical complete response (cCR) and the anal preservation rates.

2.4 Quality assessment

Most trials included in our analysis were single-arm studies, therefore, we evaluated the quality of the research using the methodological index for non-randomized studies (MINORS), which, was used for the quality assessment of non-randomize studies (17). Study qualities were classified as poor (0–12), or good (13–16) based on MINORS scores, and any discrepancies were resolved through consensus.

2.5 Data extraction

Two investigators (Huan Zhang and Jing Huang) independently extracted relevant data from the included studies, including characteristic data from the study (first author, publication year, country/region of the patient, study type, sample size, gender, patient age, Eastern Cooperative Oncology Group (ECOG) performance status, distance from primary tumor to anal verge, clinical stage, clinical T category, clinical N category, type of radiotherapy, intervention methods, type of checkpoint inhibitor) and statistical data (pCR, MPR, cCR, anus preservation rate, incidence of TRAEs and irAE≥3 grades). The details of TRAEs, irAEs and clinical stage were shown in the Supplementary Tables 1–3, respectively. Where necessary, corresponding authors were contacted for additional information.

2.6 Statistical analysis

The meta-analysis was performed using Stata/MP 14.0 software (StataCorp LP, College Station, TX). A p value<0.05 was considered statistically significant. Heterogeneity between studies was categorized as low (I^2<50%) or high (I^2>50%) using the Cochran Q chi-square test

and I^2 statistics. Random effects models and fixed effects model were used to analyze the data with huge heterogeneity (I^2≥50%) and little heterogeneity (I^2<50%), respectively. Subgroup analyses were conducted based on clinical factors to reduce heterogeneity. The identification of potential bias was accomplished by evaluating the asymmetry of the plot and Egger or Begg tests.

3 Results

3.1 Study selection and characteristics

After screening the title, abstract and full-text, a total of thirteen studies comprising 582 patients were ultimately included in this analysis (18–30). The selection process was conducted in accordance with the PRISMA flowchart guidelines (Figure 1). Of the studies included, seven were published as full papers and six were presented as conference abstracts. Among these studies included, four were randomized controlled trials (RCTs) and the remaining nine were prospective single-arm studies. The MINORS score system evaluated all studies as having good quality (Supplementary Table 4). The principal characteristics of studies included in this meta-analysis were summarized in Table 1.

3.2 Primary outcomes: pCR, MPR, cCR and anus preserving rate

Twelve studies reported results of pCR and the pooled pCR rate was 37% (95%CI: 0.31, 0.44) with small heterogeneity (I^2 = 35.93%, p=0.10) (Figure 2A). Seven studies reported the clinical data on MPR, and the pooled MPR was 57% [(95%CI: 0.43, 0.70), I^2 = 70.44%, p=0.00] (Figure 2B). Six studies reported cCR, resulting in a pooled cCR rate of 26% (95%CI: 0.18, 0.34, I^2 = 52.38%, p=0.06) (Figure 2C). As illustrated in Figure 2D, three studies reported anus preservation rate with a pooled rate of 77% (95%CI: 0.62, 0.88, I^2 = 45.30%, p=0.16).

3.3 Safety: TRAEs and irAEs

The incidence of irAEs≥3 grades was extracted from seven studies, yielding a pooled rate was 3% (95%CI: 0.00, 0.09; I^2 = 72.25%, p=0.00) (Figure 3A). Using a fixed-effects model with low heterogeneity (I^2 = 0.00%, p=0.61), the pooled incidence of TRAEs≥3 grades was found to be 29% (95%CI: 0.17, 0.41) (Figure 3B).

3.4 Publication bias and influence analysis

Funnel plots were employed to assess the potential for publication bias among the studies incorporated in the meta-analysis. As illustrated in Supplementary Figure 1, the funnel plots exhibited a certain degree of asymmetry, which may indicate possible publication bias stemming from a lack of RCT articles. Next, Egger's and Begg's tests were carried out to evaluate the publication bias. P value of Egger's and Begg's tests for pCR, MPR, cCR, anus preservation rate and TRAEs rates were all>0.05 (P>|t|=0.17, 0.26, 0.21, 0.24 and 0.97, respectively; Pr>|z|=1.70, 1.63, 0.26, 1.96 and 1.00, separately) and the symmetry of funnel plots from Egger`s publication bias analysis also suggested the stability of the results and the absence of bias and (Supplementary File 2, Figures 4A–D, F). Conversely, p value of Egger's and Begg's tests for

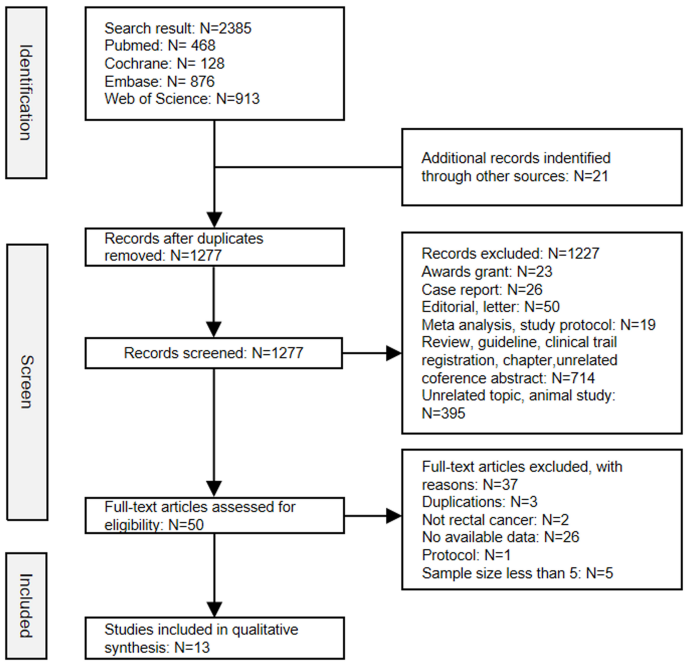

FIGURE 1
Flow diagram of the literature search in this meta-analysis.

TABLE 1 Characteristic of included studies.

First author, year	Region	Sample size	Male/ Female	Median age (year)	Type of study	Inhibitor	Neoadjuvant treatment
Bando et al., 2022 (18)	Non-China	44	29/15	59.5	Single-arm study	PD-1	Chemotherapy + LCRT + immunotherapy
Li et al., 2024 (19)	China	25	19/6	58	Single-arm study	PD-1	Chemoimmunotherapy + LCRT + chemotherapy
Lin et al., 2021 (20)	China	30	17/13	57	Single-arm study	PD-1	SCRT + Chemoimmunotherapy
Xiao et al., 2024 (21)	China	67	43/24	56	RCT	PD-1	Chemoimmunotherapy + LCRT
Shamseddine et al., 2020 (29)	Non-China	13	9/4	62	Single-arm study	PD-L1	SCRT+ Chemoimmunotherapy
Gao et al., 2023 (22)	China	26	14/12	60.5	Single-arm study	PD-1	LCRT + Chemoimmunotherapy
Lin et al., 2024 (23)	China	113	75/38	NA	RCT	PD-1	SCRT + Chemoimmunotherapy
George et al., 2022 (24)	Non-China	45	NA	NA	Single-arm study	PD-L1	Chemotherapy + LCRT + immunotherapy
Feng et al., 2024 (25)	China	22	NA	56	Single-arm study	PD-1	SCRT + Chemoimmunotherapy
Takahashi et al., 2023 (26)	Non-China	25	18/7	63	Single-arm study	PD-1	LCRT + Chemoimmunotherapy
Gooyer et al., 2024 (27)	Non-China	44	34/10	NA	Single-arm study	PD-L1	SCRT + Chemoimmunotherapy
Zhou et al., 2024 (28)	China	16	11/5	NA	RCT	PD-1	Chemoimmunotherapy
Xia et al., 2024 (30)	China	121	NA/NA	NA	RCT	PD-1	SCRT + Chemoimmunotherapy

irAEs ≥ 3 grades were both<0.05 (P>|t|=0.03, Pr>|z|=0.02) (Supplementary File 2) with associated funnel plots from Egger`s publication bias analysis exhibiting asymmetry (Figure 4E), indicating the publication bias existed in the study. Subsequently, the trim and fill method analysis was performed to evaluate the impact of publication bias. Based on the analysis results of the trim and fill method, there was almost minimal variation in the outcomes reinforcing the stability of the results (Supplementary File 3, Supplementary Figure 2). The significance remained consistent before and after the trim and fill method analysis, indicating that the combined effect size for the irAEs rate was not influenced by publication bias. Sensitivity analysis revealed that the exclusion of individual studies did not result in statistically significant changes in the combined analysis (Supplementary Figure 3), hereby suggesting that the overall conclusions drawn from this investigation can be regarded as valid and reliable.

3.5 Subgroup analysis

3.5.1 Subgroup based on type of radiotherapy

The pooled pCR and MPR in the short course radiation therapy (SCRT) subgroup was 45% (95%CI: 0.39, 0.52) and 65% (95%CI: 0.44, 0.83), whereas the pooled pCR and MPR in the LCRT subgroup was 34% (95%CI: 0.27, 0.41) and 57% (95%CI: 0.38, 0.74), respectively (Figures 5A, B), all lower than the long course radiation therapy (LCRT) subgroup, especially the pooled pCR. However, the pooled incidence of irAEs≥3 grades in the LCRT subgroup (4.2%, 95%CI: 0.00, 0.13) exceeded that in the SCRT subgroup (1%, 95%CI: 0.00, 0.07) (Figure 5C).

3.5.2 Subgroup based on PD-1/PD-L1 inhibitors

The PD-1 subgroup exhibited a pooled pCR of 40% (95%CI: 0.35, 0.46), which was significantly higher than that observed in the PD-L1 subgroup (22%, 95%CI: 0.11, 0.37) (Figure 6A). Similarly, the pooled MPR and cCR in the PD-1 subgroup (58%, 95%CI: 0.42, 0.72; 27%, 95%CI: 0.16, 0.40) was higher than these in the PD-L1 subgroup (50.0%, 95%CI: 0.21, 0.79; 24%, 95%CI: 0.15, 0.34) (Figures 6B, C), though there were no significant declines in heterogeneity.

3.5.3 Subgroup based on treatment sequence

Subsequent subgroup analyses were conducted to evaluate the sequence of immunotherapy and radiotherapy administration in the neoadjuvant context. The pMMR/MSS RC cohorts receiving concurrent immunotherapy and radiotherapy demonstrated a pooled MPR of 63% (95%CI: 0.38, 0.85) and an anal preservation rate of 88% (95%CI: 0.70, 0.99), respectively, both exceeding the outcomes observed in those undergoing sequential administration (Figures 7A, B). Furthermore, a notable reduction in heterogeneity for MPR was observed. Though there was only minimal declination in heterogeneity for the rate of irAEs, the pooled incidence of irAEs≥3 grades in the sequential radiotherapy group was significant higher compared to the concurrent group (6% vs 0.0%) (Figure 7C).

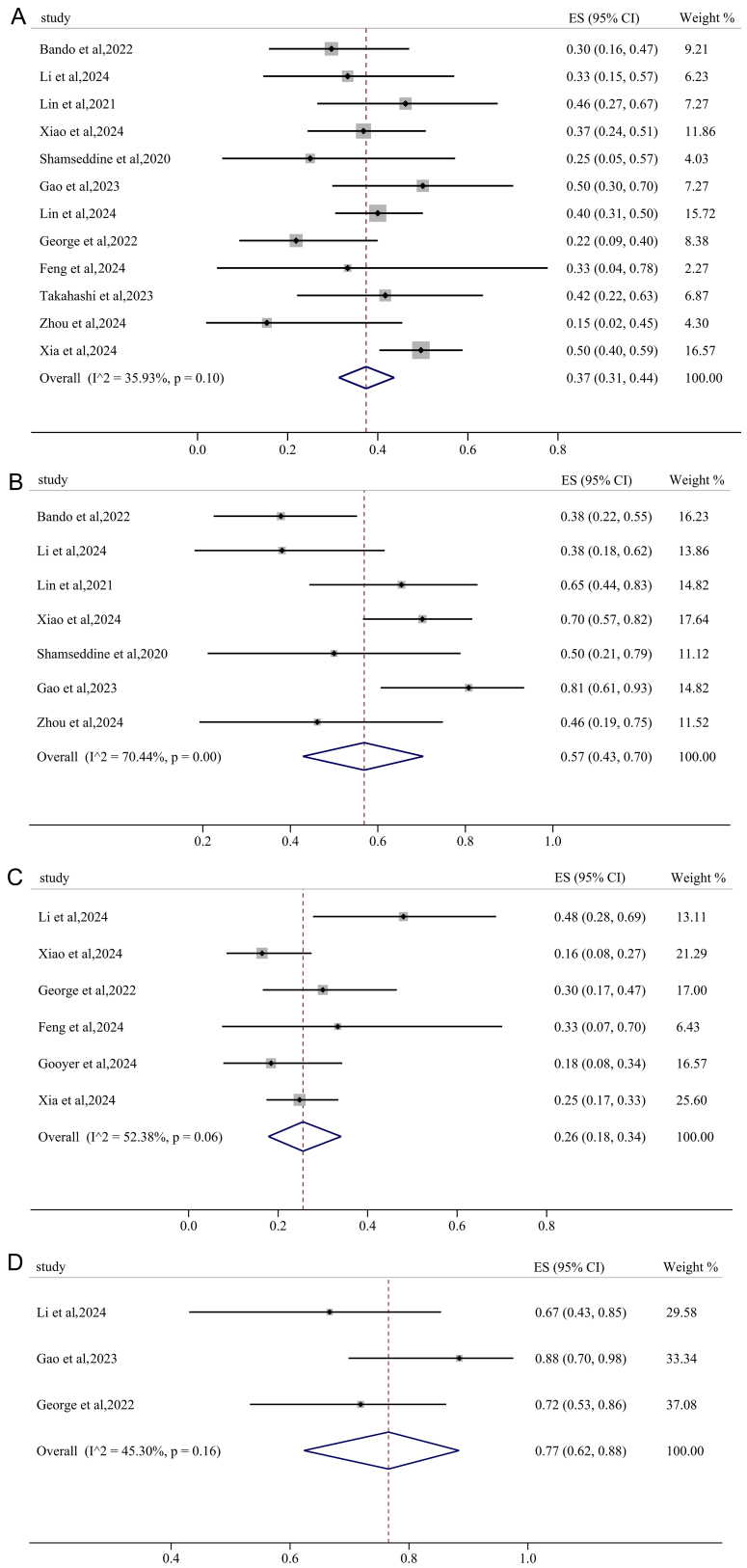

FIGURE 2
Primary outcomes of neoadjuvant immunotherapy for non-metastatic pMMR/MSS rectal cancer. **(A)** pathological complete response (pCR); **(B)** major pathological response (MPR); **(C)** clinical complete response (cCR); **(D)** anus preservation rate.

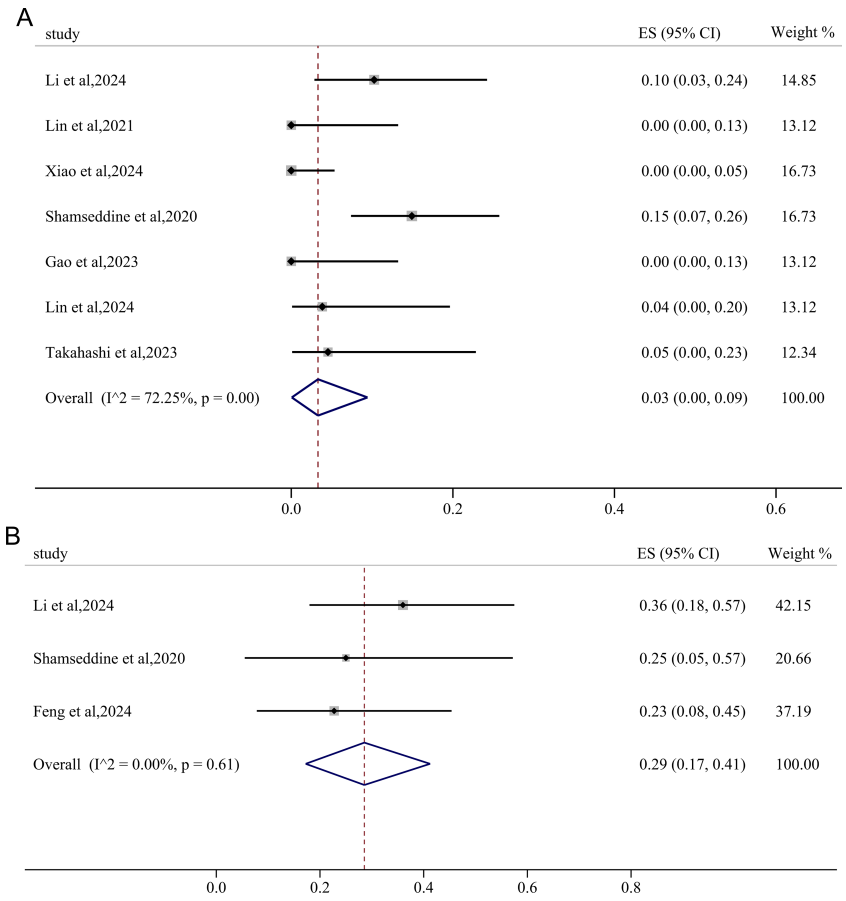

FIGURE 3
Forest plots showing the adverse effects of immunotherapy-based neoadjuvant therapy for RC. **(A)** immunotherapy -related adverse effects (irAEs)≥3 grades; **(B)** treatment-related adverse effects (TRAEs)≥3 grades.

3.5.4 Subgroup analysis based on clinical T and N category

In the subgroup analysis stratified by clinical T category, both the cT3 and cT4 subgroups exhibited a pooled pCR of 30% with negligible heterogeneity (Figure 8A). With negligible heterogeneity, the pooled MPR in cT3 and cT4 group was 37% (95%CI: 0.24, 0.51) and 30% (95%CI: 0.03, 0.64), respectively, demonstrating that the subgroup analysis based on clinical T category significantly diminished the heterogeneity in MPR (Figure 8B). Interestingly, for subgroup analysis stratified by clinical N category, pMMR/MSS non-metastatic RC patients with lymph node metastasis achieved a pooled pCR of 43% (95%CI: 0.23, 0.65) after receiving immunotherapy-based neoadjuvant treatment, higher than the pooled pCR of 35% (95%CI: 0.21, 0.51) in RC patients without lymph node metastasis (Figure 8C).

4 Discussion

In 2015, researchers from Johns Hopkins Hospital initially disclosed the KEYNOTE-016 study at the ASCO Annual Meeting, identifying MSI-H or dMMR as molecular markers indicative of immunotherapy responsiveness in metastatic CRC, thus heralding a transformative era in CRC immunotherapy (31). The NICHE study encompassing both dMMR and pMMR early-stage colon cancer patients first explores the efficacy and safety of NIT. In the primary results, MPR and pCR of the 20 dMMR patients are 95% and 60%, respectively, while the MPR rate is 20% in patients with pMMR colon cancer, which opens the door of NIT for CRC (32).

This systematic review comprehensively analyzed data from the 13 studies to assess the efficacy and safety of NIT in non-metastatic pMMR/MSS RC patients, revealing favorable outcomes with pooled pCR, MPR, cCR and anus preserving rate of 37%, 57%, 26% and 77%, respectively. Moreover, NIT did not significantly elevate the incidence of AEs, with the pooled rate of irAEs and TRAEs≥3 grades being 3% and 29% separately. Therefore, the implementation of immunotherapy in the neoadjuvant settings in patients with non-metastatic pMMR/MSS RC is a promising therapeutic strategy.

To evaluate the publication bias, Egger's and Begg's tests and funnel plots were employed. The asymmetry of funnel plots for irAEs indicated the possibility of publication bias, and the p value of the next Egger's and Begg's tests for irAEs ≥ 3 grades all<0.05 also suggested the potential of publication bias (Figure 4E, Supplementary File 2), which may be caused by lack of RCTs, small sample size, incomplete or selective reports due to the fact that the exploration of NIT for RC is still in its nascent stages. The

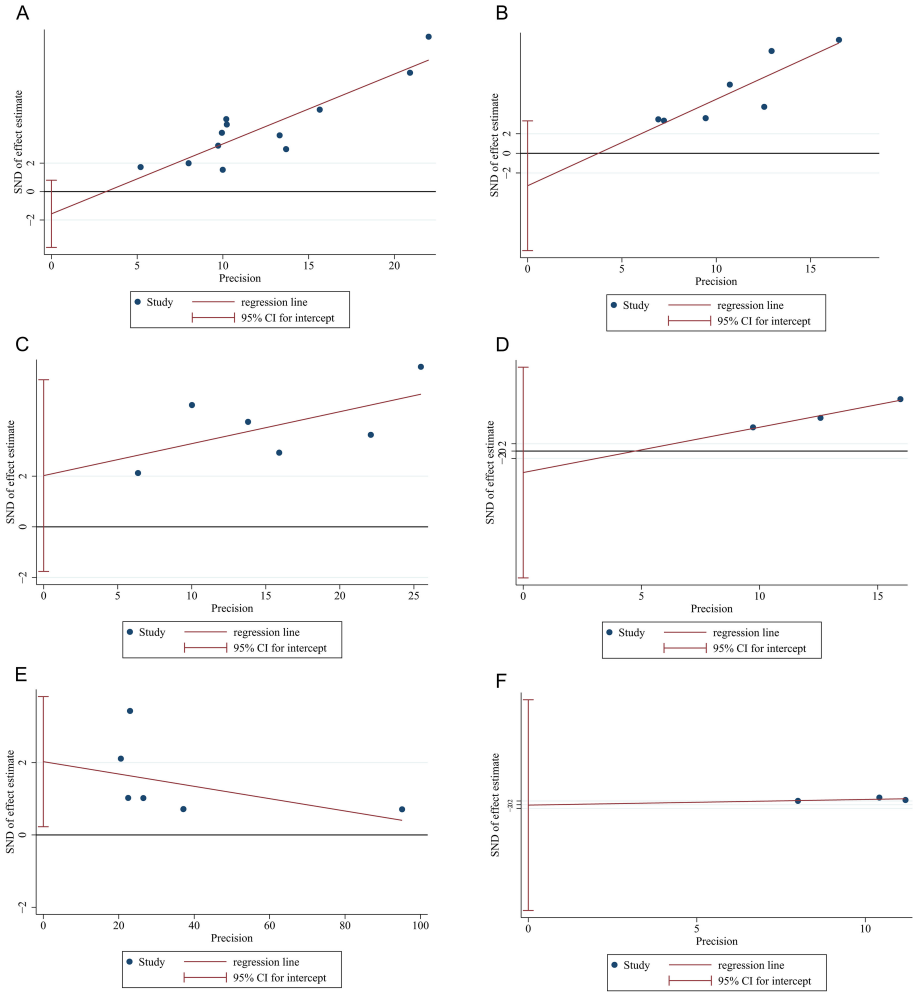

FIGURE 4
Funnel plots of Egger`s publication bias analysis for **(A)** pCR, **(B)** MPR, **(C)** cCR, **(D)** anus preservation rates, **(E)** incidence of irAE≥3 grades and **(F)** incidence of TRAEs ≥3 grades.

existing of publication bias may exaggerate treatment effects, mislead clinical practice and decision-making and affect the generality and reliability of results. However, the consistent significance before and after the trim and fill method analysis, indicating that the combined effect size for the irAEs rate in our study was not influenced by publication bias and the conclusions of our analysis (Supplementary File 3, Supplementary Figure 2).

Given the potential heterogeneity and publication bias, subgroup analyses were conducted. Significant reductions in heterogeneity were observed in the pooled pCR rates based on the type of radiotherapy and inhibitor subgroup analysis. Subsequent subgroup analysis based on the sequence of immunotherapy and radiotherapy application demonstrated a substantial decrease in heterogeneity in pooled pCR and MPR, suggesting that the treatment sequence of immunotherapy and radiotherapy in different studies may contribute to the heterogeneity in pCR and MPR outcomes. Similarly, subgroup analysis based on the clinical T category also revealed a reduction in heterogeneity of pCR and MPR, indicating another potential source of heterogeneity in the pooled pCR and MPR results. However, Egger's and Begg's tests yielded p values >0.05 for pCR, MPR, cCR, anus preservation rates and TRAEs, indicating the absence of publication bias. Sensitivity analysis further confirmed the stability of the pooled pCR. Although the p values of Egger's and Begg's tests for the incidence of irAEs of grade ≥3 were both <0.05, the consistent significance before and after the trim and fill method demonstrated that the combined effect size of irAEs rates was not influenced by the potential existed publication bias, ensuring the robustness of the findings.

Numerous studies indicated that a higher pCR is associated with favorable prognosis (30, 33). As one of the standard preoperative treatment for LARC, TNT showed superior rates of pCR compared with conventional CRT (29.9% versus 14.9%), as well as a reduction in distant relapse in meta-analysis of Anup Kasi, MD et al. (34). However, the relatively low pCR rates and high rates of distant metastasis and local disease recurrence following TNT and conventional CRT remain challenges in the management of LARC. In our meta-analysis, a pooled pCR rate of 37% was observed in patients with pMMR/MSS rectal cancer receiving NIT, surpassing the rates achieved with TNT and conventional CRT.

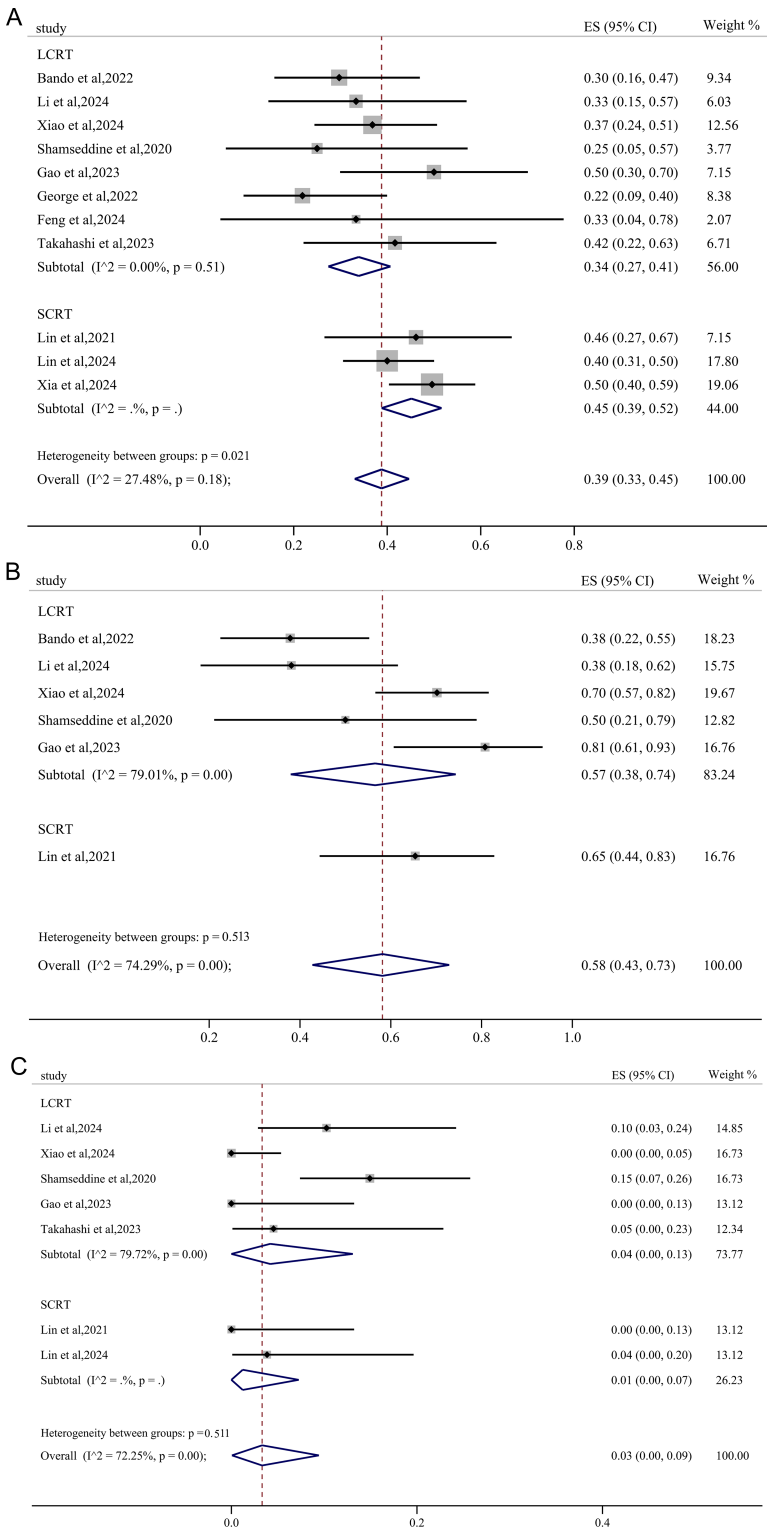

FIGURE 5
The forest figure of response rate (pCR, MPR and irAEs) based on radiotherapy strategies subgroup analysis. **(A)** pCR rate based on radiotherapy strategies subgroup analysis; **(B)** MPR rate based on radiotherapy strategies subgroup analysis; **(C)** irAEs rate based on radiotherapy strategies subgroup analysis.

For patients with early-stage and LARC, surgery still plays a critical role in the treatment course. However, older patients with multiple comorbidities may face a heightened risk of mortality and severe complications post-surgery, rendering them unsuitable candidates for operative intervention. Although advancements in medical technology have significantly enhanced anal preservation rates in RC patients, the rectum and anus preservation remain challenging for individuals with ultra-low rectal cancer (35). Therefore, in addition to tumor burden

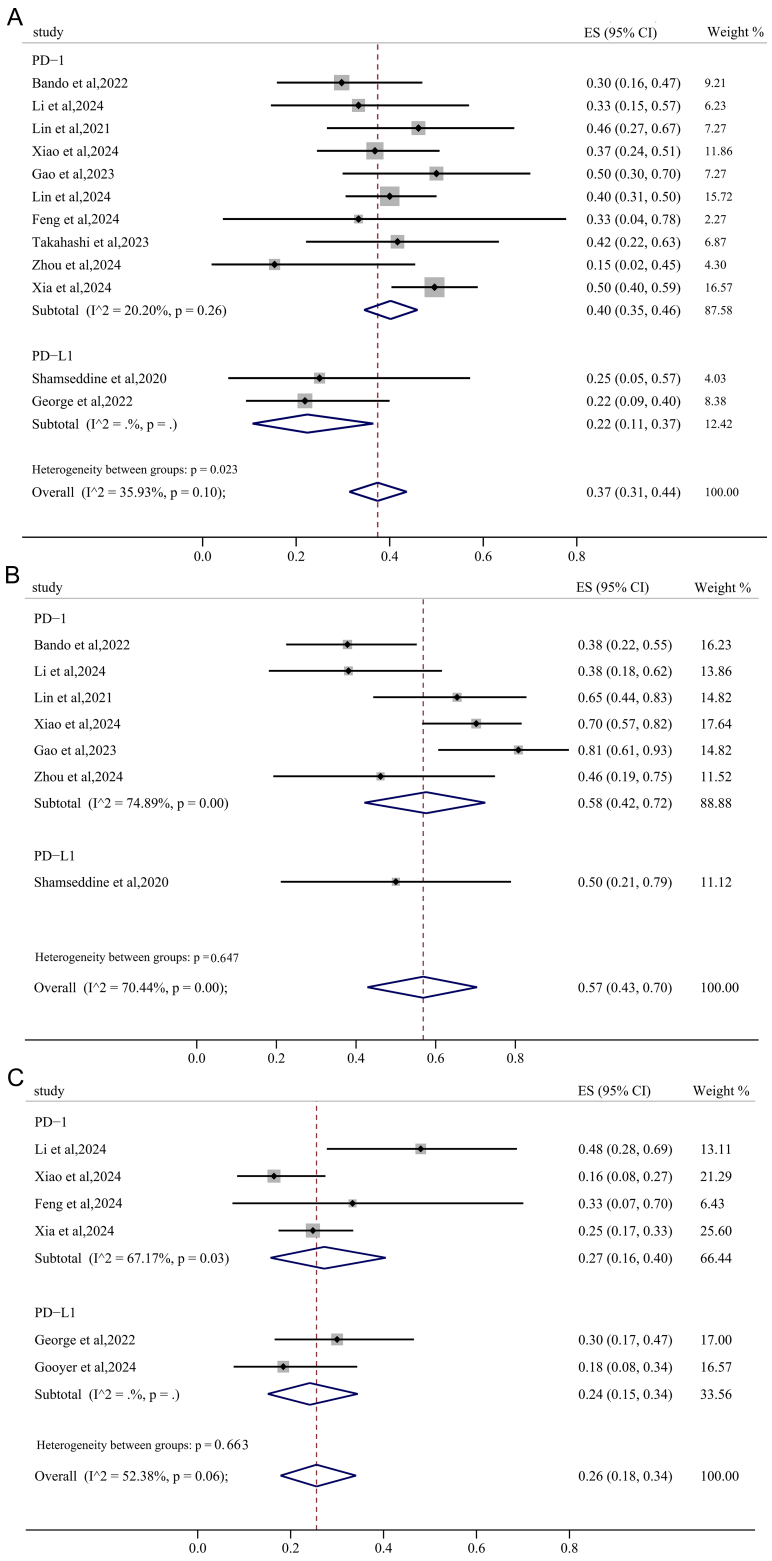

FIGURE 6
The forest figure of response rate (pCR, MPR, cCR) based on PD-1/PD-L1 inhibitors subgroup analysis. **(A)** pCR rate based on PD-1/PD-L1 inhibitors subgroup analysis; **(B)** MPR rate based on PD-1/PD-L1 inhibitors subgroup analysis; **(C)** cCR rate based on PD-1/PD-L1 inhibitors subgroup analysis.

reduction and survival improvement, organ preservation is a critical consideration in RC treatment.

The concept of the "wait-and-see" strategy for RC patients achieving cCR after neoadjuvant therapy, initially proposed by Prof. Habr-Gama from Brazil in 2004, has garnered increasing attention due to its positive impact on quality of life (QoL) and minimal effect on long-term survival outcomes (6). In 2016, Martens et al. reported a cCR rate of 17% among patients with RC who underwent

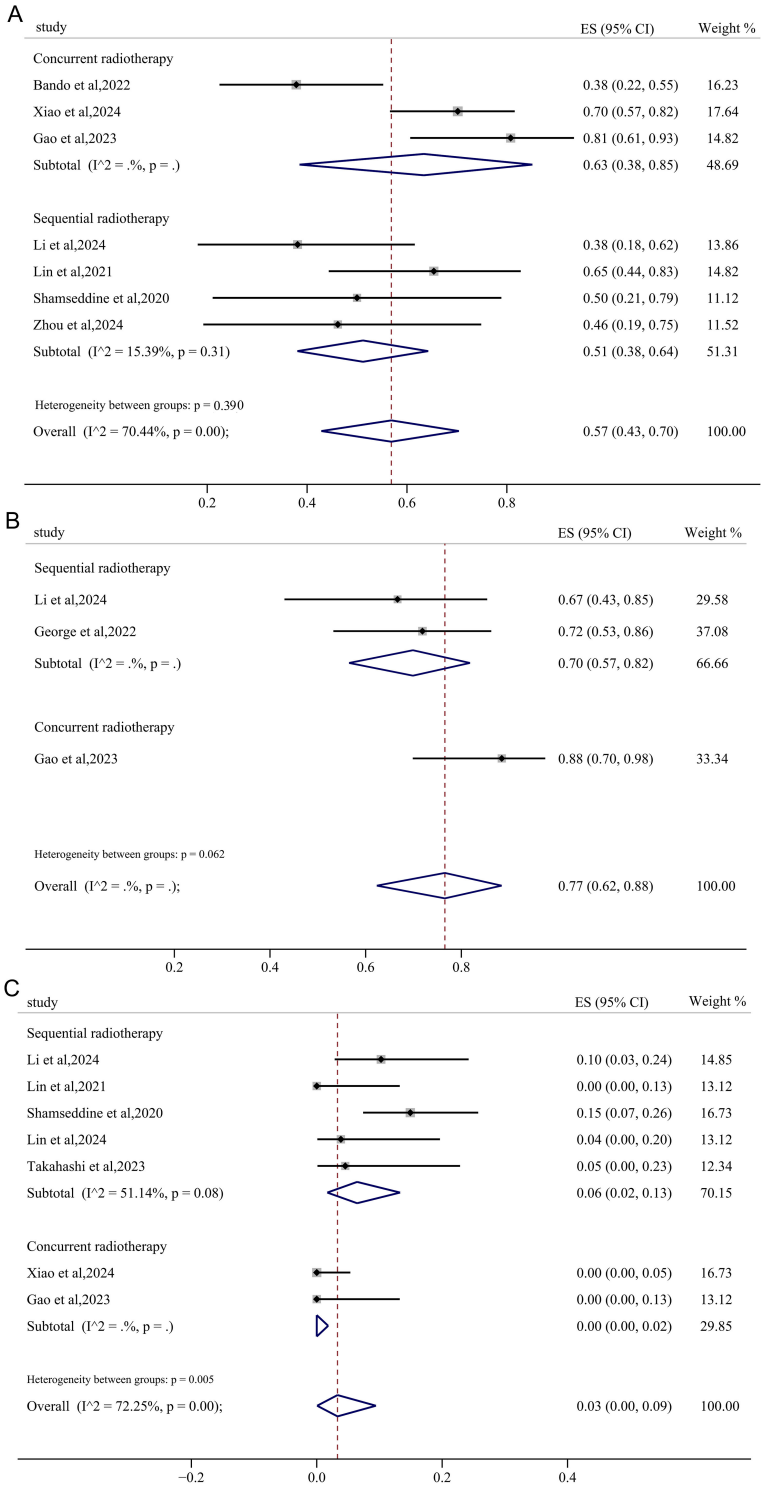

FIGURE 7
The forest figure based on treatment sequence subgroup analysis. The forest figure of MPR **(A)**, anus preservation rate **(B)** and incidence of irAEs ≥ 3 grades **(C)** based on sequence of immunotherapy and radiotherapy subgroup analysis.

neoadjuvant CRT (36). A meta-analysis evolving seventeen studies revealed a pooled cCR rate of 22.4% following conventional neoadjuvant chemoradiotherapy treatment (37). In our meta-analysis the pooled cCR rate of 26%, higher than the previous clinical study and meta-analysis, supported the utilization of NIT in patients with non-metastatic MSS RC and provided new options, particularly for older patients with comorbidities or those averse to surgery.

TRAEs or irAEs, which refers to a multitude of systems, are unignorable problems in immunotherapy-based neoadjuvant

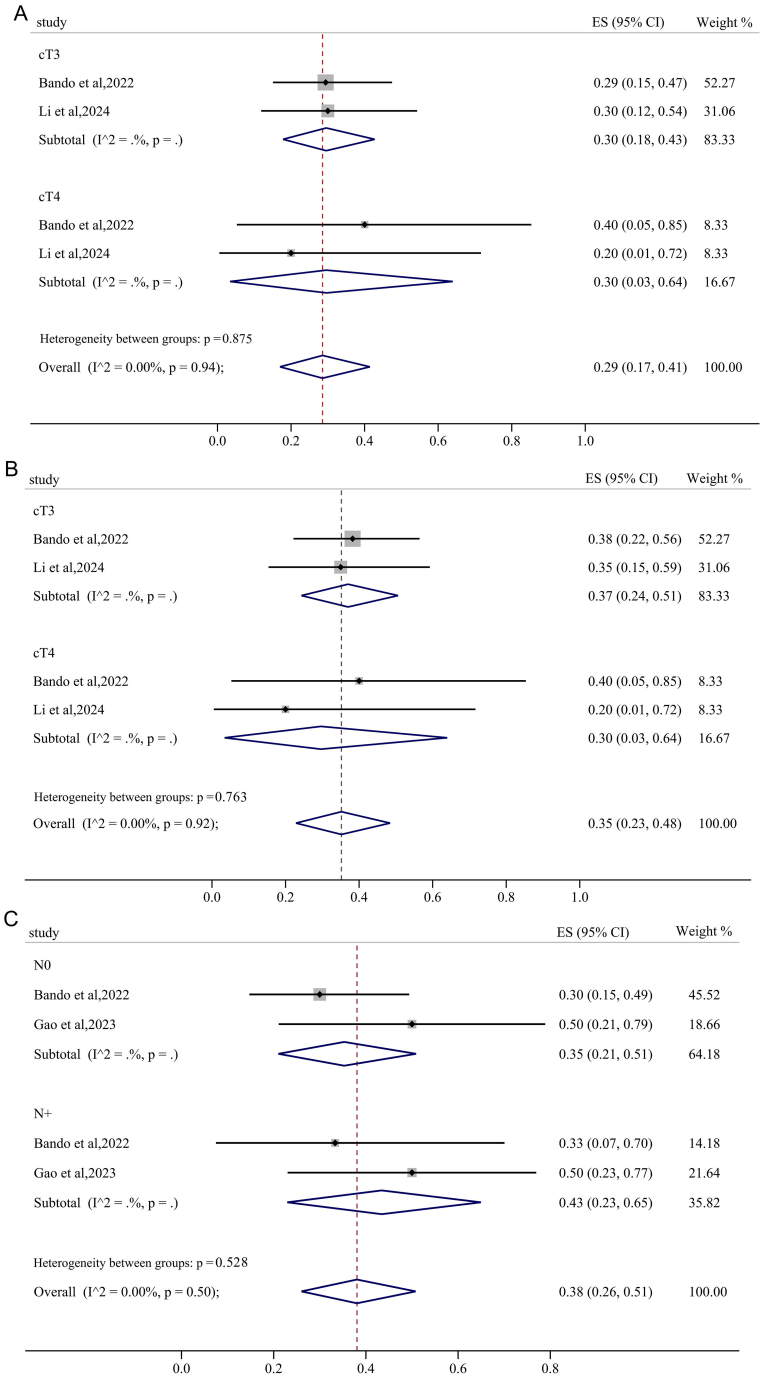

FIGURE 8
The forest figure based on clinical T category and N subgroup analysis. **(A)** pCR rate on clinical T category subgroup analysis; **(B)** MPR rate on clinical T category subgroup analysis; **(C)** pCR rate on clinical N category subgroup analysis.

treatment. Previous studies have reported that grades 3–5 TRAEs and irAEs were observed in 33% and 19% of advanced CRC patients receiving NIT, respectively (38). The pooled TRAEs rate of 29% and irAEs rate of 3% in our study demonstrated the favorable tolerability of NIT in non-metastatic pMMR/MSS RC. The satisfactory pooled pCR, MPR, cCR, anus preservation rate and low rate of AEs≥3 grades further support the use of NIT in non-metastatic pMMR/MSS RC patients. While the inconsistency in the identification of pCR and cCR warrants more future studies to solve the problem.

In the multicenter, open-label, randomized, controlled, phase III RAPIDO trial, patients in the experiment group receiving SCRT in neoadjuvant treatment period showed higher treatment compliance, reduced risk of disease recurrence and metastasis than the standard of care group receiving LCRT (39). Similarly, in the UNION trials, LARC patients received SCRT followed by chemoimmunotherapy in the neoadjuvant period achieved higher pCR rate with well-tolerated safety profile than those treated with LCRT in neoadjuvant period (23). Preclinical studies also indicated

that SCRT enhanced the infiltration of tumor-specific CD8+ T cells in draining lymph nodes, leading to improved local and distant anti-tumor effects compared to conventional fractionation (40). In concordance with the previous findings, the pooled pCR and MPR rates in the SCRT subgroup were 45.2% and 65.4%, respectively, both higher than the LCRT groups. The incidence of irAEs in the SCRT subgroup was 1%, significantly lower than the LCRT group. The favorable characteristics of SCRT treatment, including low toxicity, positive therapeutic effects, cost-effectiveness, and convenience, have garnered increasing interest in clinical practice.

PD-1 and PD-L1 inhibitors demonstrated comparable survival outcomes and safety profiles in patients with solid tumors (41, 42). However, non-metastatic pMMR/MSS RC patients receiving PD-1 inhibitors in the neoadjuvant treatment period in our subgroup analysis had a higher pCR rate and slightly higher or comparable MPR or cCR compared with patients receiving PD-L1 inhibitors. In addition, anus preservation rate in RC patients receiving PD-1 inhibitors in the neoadjuvant treatment period was also slightly higher than those received PD-L1 inhibitors (Supplementary Figure 4), further supporting the clinical utility of NIT for non-metastatic pMMR/MSS RC patients.

Discrepancies remain regarding the sequencing of radiotherapy and chemotherapy/immunotherapy in oncological treatment. In patients diagnosed with stage III non-small cell lung cancer, concurrent radiotherapy combined with chemotherapy demonstrated enhanced survival benefits but with increased toxicity compared to sequential radiotherapy (43). Conversely, another investigation revealed that concurrent radiotherapy paired with immunotherapy resulted in superior survival rates with reduced toxicity relative to sequential radiotherapy (44). In our analysis, RC patients undergoing concurrent radiotherapy alongside immunotherapy during the neoadjuvant phase achieved a MPR and anal preservation rates of 63% and 88%, respectively, and both of which surpassed the sequential radiotherapy group. Besides, the incidence of irAEs≥3 grades in the concurrent radiotherapy group was significantly lower than the sequential radiotherapy group. Prior studies indicated that concurrent radiotherapy plus camrelizumab elevated the expression levels of activation molecules CD38 and HLA-DR on CD8+ T cells, thereby enhancing the cytotoxicity and activation of PD-1+CD8+ T cells, which correlated with improved prognosis in patients with esophageal squamous cell carcinoma (45), potentially elucidating our findings. Nonetheless, additional research is warranted to further investigate these outcomes.

Clinical T4 stage, N2 stage, and EMVI positivity are recognized as high-risk factors for RC patients, typically associated with unfavorable prognoses. Nevertheless, the UNION trials (23) and numerous other clinical studies evolving RC patients with T3, T4 or N2 stage, demonstrate satisfactory survival outcomes and well tolerance when treated with specific strategies. Our subgroup analysis also revealed that patients with T4 RC exhibited a comparable pCR rate to those classified as clinical T3, while patients with lymph node metastasis demonstrated an even higher pCR rate compared to those without such metastasis. Therefore, for non-metastatic MSS RC patients with T4 category or other high-risk factors, the NIT may play a pivotal role.

In the KEYNOTE-966 study, patients with biliary tract cancers receiving pembrolizumab achieve a mOS of 14.1 (95%CI: 10.4-17.7) months, significantly exceeding the outcomes observed in the global cohort (46). The KEYNOTE-181 study also reveals that immunotherapy treatment brings significant OS benefit and better prognosis for Chinese population compared with the whole population (47). Currently, there is a dearth of studies assessing the efficacy and safety of NIT in both Chinese and non-Asian patients with MSS RC. Our subgroup analysis revealed that the pooled pCR, MPR and cCR rates in the Chinese cohort were 41%, 65% and 27% respectively, superior to those in non-Chinese populations (Supplementary Figure 5). Although approximately 61.5% of the trials included in our analysis were conducted within Chinese populations, publication bias assessments affirmed the robustness of the findings. Thus, our study offers valuable insights and support for future research and clinical applications when addressing patients from diverse ethnic backgrounds.

This systematic review acknowledges certain limitations. Firstly, while 4 RCTs were incorporated, the majority of the included studies were single-arm, phase II prospective trials or conference abstracts, leading to a limited patient cohort and incomplete clinical data. Secondly, the application of NIT for RC is still in its nascent stages, with most studies primarily reporting initial findings and lacking long-term survival data. Therefore, further multi-center, large-sample clinical trials were conducted to improve the reliability and universality of the study results and evaluate the long-term survival outcomes. Additionally, the small sample sizes and heterogeneity in treatment regimens and follow-up durations may also impact the results of the study, which need to be explored with more future studies. To optimize the treatment strategy for RC, the efficacy and safety of NIT combined with other therapeutic modalities need to be further investigated. Besides, by identifying molecular markers associated with the response of NIT, precise stratification of patients can be achieved to provide a basis for individualized treatment.

5 Conclusion

Our study has synthesized and examined the latest trials concerning neoadjuvant immunotherapy for non-metastatic pMMR/MSS RC patients, analyzing various outcomes. Due to relatively small sample size, heterogeneity between studies and uneven levels of included studies, there were no statistical significance for MPR in subgroup analysis based on radiotherapy type, PD-1/PD-L1 inhibitors and other factors, but statistically significant pCR rate based on radiotherapy strategies, PD-1/PD-L1 inhibitors subgroup analysis and other satisfactory outcomes in the subgroup analysis indicates that NIT is promising for the treatment of pMMR/MSS RC patients with an acceptable safety profile. Moreover, the high response rates among MSS patients, satisfactory anal preservation rates, and low incidences of TRAEs and irAEs provide a reference for future research and clinical practice. However, in light of these limitations, there is an urgent

need for large-scale, randomized controlled trials focusing on neoadjuvant approaches for non-metastatic MSS RC.

Data availability statement

The original contributions presented in the study are included in the article/Supplementary Material. Further inquiries can be directed to the corresponding author.

Author contributions

HZ: Data curation, Formal analysis, Methodology, Project administration, Resources, Software, Validation, Visualization, Writing – original draft, Writing – review & editing. JH: Formal analysis, Methodology, Project administration, Software, Validation, Visualization, Writing – original draft, Writing – review & editing. HX: Data curation, Validation, Writing – review & editing. NY: Writing – review & editing. LZ: Writing – review & editing. JX: Conceptualization, Supervision, Writing – review & editing. MR: Conceptualization, Funding acquisition, Supervision, Writing – review & editing.

Funding

The author(s) declare financial support was received for the research, authorship, and/or publication of this article. This work was supported by grants from Natural Science Foundation of Sichuan Province (2023YFS0319), National Natural Science Foundation of China (No. 82373021) and 1 • 3 • 5 Project for Disciplines of Excellence, West China Hospital, Sichuan University (ZYYC23010; ZYYC23008).

Acknowledgments

We thank all our authors listed in this manuscript.

Conflict of interest

The authors declare that the research was conducted in the absence of any commercial or financial relationships that could be construed as a potential conflict of interest.

Generative AI statement

The author(s) declare that no Generative AI was used in the creation of this manuscript.

Publisher's note

Supplementary material

The Supplementary Material for this article can be found online at: https://www.frontiersin.org/articles/10.3389/fimmu.2025.1523455/full#supplementary-material

References

1. Sung H, Ferlay J, Siegel RL, Laversanne M, Soerjomataram I, Jemal A, et al. Global cancer statistics 2020: globocan estimates of incidence and mortality worldwide for 36 cancers in 185 countries. *CA: Cancer J Clin.* (2021) 71:209–49. doi: 10.3322/caac.21660

2. Oronsky B, Reid T, Larson C, Knox SJ. Locally advanced rectal cancer: the past, present, and future. *Semin Oncol.* (2020) 47:85–92. doi: 10.1053/j.seminoncol.2020.02.001

3. Mauri G, Sartore-Bianchi A, Russo AG, Marsoni S, Bardelli A, Siena S. Early-onset colorectal cancer in young individuals. *Mol Oncol.* (2019) 13:109–31. doi: 10.1002/1878-0261.12417

4. Fernandez-Martos C, Garcia-Albeniz X, Pericay C, Maurel J, Aparicio J, Montagut C, et al. Chemoradiation, surgery and adjuvant chemotherapy versus induction chemotherapy followed by chemoradiation and surgery: long-term results of the spanish gcr-3 phase ii randomized trial†. *Ann oncology: Off J Eur Soc Med Oncol.* (2015) 26:1722–8. doi: 10.1093/annonc/mdv223

5. Cercek A, Roxburgh CSD, Strombom P, Smith JJ, Temple LKF, Nash GM, et al. Adoption of total neoadjuvant therapy for locally advanced rectal cancer. *JAMA Oncol.* (2018) 4:e180071. doi: 10.1001/jamaoncol.2018.0071

6. Habr-Gama A, Perez RO, Nadalin W, Sabbaga J, Ribeiro UJr., Silva e Sousa AHJr., et al. Operative versus nonoperative treatment for stage 0 distal rectal cancer following chemoradiation therapy: long-term results. *Ann Surg.* (2004) 240:711–7. doi: 10.1097/01.sla.0000141194.27992.32

7. Littman DR. Releasing the brakes on cancer immunotherapy. *Cell.* (2015) 162:1186–90. doi: 10.1016/j.cell.2015.08.038

8. Le DT, Uram JN, Wang H, Bartlett BR, Kemberling H, Eyring AD, et al. Pd-1 blockade in tumors with mismatch-repair deficiency. *New Engl J Med.* (2015) 372:2509–20. doi: 10.1056/NEJMoa1500596

9. Overman MJ, McDermott R, Leach JL, Lonardi S, Lenz HJ, Morse MA, et al. Nivolumab in patients with metastatic DNA mismatch repair-deficient or microsatellite instability-high colorectal cancer (Checkmate 142): an open-label, multicentre, phase 2 study. *Lancet Oncol.* (2017) 18:1182–91. doi: 10.1016/S1470-2045(17)30422-9

10. Bhalla N, Brooker R, Brada M. Combining immunotherapy and radiotherapy in lung cancer. *J Thorac Dis.* (2018) 10:S1447–s60. doi: 10.21037/jtd.2018.05.107

11. Wang Y, Shen L, Wan J, Zhang H, Wu R, Wang J, et al. Neoadjuvant chemoradiotherapy combined with immunotherapy for locally advanced rectal cancer: A new era for anal preservation. *Front Immunol.* (2022) 13:1067036. doi: 10.3389/fimmu.2022.1067036

12. Kang J, Demaria S, Formenti S. Current clinical trials testing the combination of immunotherapy with radiotherapy. *J immunotherapy Cancer.* (2016) 4:51. doi: 10.1186/s40425-016-0156-7

13. Franke AJ, Skelton WP, Starr JS, Parekh H, Lee JJ, Overman MJ, et al. Immunotherapy for colorectal cancer: A review of current and novel therapeutic approaches. *J Natl Cancer Institute.* (2019) 111:1131–41. doi: 10.1093/jnci/djz093

14. Cercek A, Lumish M, Sinopoli J, Weiss J, Shia J, Lamendola-Essel M, et al. Pd-1 blockade in mismatch repair-deficient, locally advanced rectal cancer. *New Engl J Med.* (2022) 386:2363–76. doi: 10.1056/NEJMoa2201445

15. Scott AJ, Kennedy EB, Berlin J, Brown G, Chalabi M, Cho MT, et al. Management of locally advanced rectal cancer: asco guideline. *J Clin oncology: Off J Am Soc Clin Oncol*. (2024) 42:3355–75. doi: 10.1200/jco.24.01160

16. Liberati A, Altman DG, Tetzlaff J, Mulrow C, Gøtzsche PC, Ioannidis JP, et al. The prisma statement for reporting systematic reviews and meta-analyses of studies that evaluate healthcare interventions: explanation and elaboration. *BMJ (Clinical Res ed)*. (2009) 339:b2700. doi: 10.1136/bmj.b2700

17. Slim K, Nini E, Forestier D, Kwiatkowski F, Panis Y, Chipponi J. Methodological index for non-randomized studies (Minors): development and validation of a new instrument. *ANZ J Surg*. (2003) 73:712–6. doi: 10.1046/j.1445-2197.2003.02748.x

18. Bando H, Tsukada Y, Inamori K, Togashi Y, Koyama S, Kotani D, et al. Preoperative chemoradiotherapy plus nivolumab before surgery in patients with microsatellite stable and microsatellite instability-high locally advanced rectal cancer. *Clin Cancer research: an Off J Am Assoc Cancer Res*. (2022) 28:1136–46. doi: 10.1158/1078-0432.Ccr-21-3213

19. Li Y, Pan C, Gao Y, Zhang L, Ji D, Cui X, et al. Total neoadjuvant therapy with pd-1 blockade for high-risk proficient mismatch repair rectal cancer. *JAMA Surg*. (2024) 159:529–37. doi: 10.1001/jamasurg.2023.7996

20. Lin Z, Cai M, Zhang P, Li G, Liu T, Li X, et al. Phase ii, single-arm trial of preoperative short-course radiotherapy followed by chemotherapy and camrelizumab in locally advanced rectal cancer. *J immunotherapy Cancer*. (2021) 9:457. doi: 10.1136/jitc-2021-003554

21. Xiao WW, Chen G, Gao YH, Lin JZ, Wu XJ, Luo HL, et al. Effect of neoadjuvant chemoradiotherapy with or without pd-1 antibody sintilimab in pmmr locally advanced rectal cancer: A randomized clinical trial. *Cancer Cell*. (2024) 42:1570–81.e4. doi: 10.1016/j.ccell.2024.07.004

22. Gao J, Zhang X, Yang Z, Zhang J, Bai Z, Deng W, et al. Interim result of phase ii, prospective, single-arm trial of long-course chemoradiotherapy combined with concurrent tislelizumab in locally advanced rectal cancer. *Front Oncol*. (2023) 13:1057947. doi: 10.3389/fonc.2023.1057947

23. Lin ZY, Zhang P, Chi P, Xiao Y, Xu XM, Zhang AM, et al. Neoadjuvant short-course radiotherapy followed by camrelizumab and chemotherapy in locally advanced rectal cancer (Union): early outcomes of a multicenter randomized phase iii trial. *Ann oncology: Off J Eur Soc Med Oncol*. (2024) 35:882–91. doi: 10.1016/j.annonc.2024.06.015

24. George TJ, Yothers G, Jacobs SA, Finley GG, Wade JL, Lima CMSPR, et al. Phase ii study of durvalumab following neoadjuvant chemort in operable rectal cancer: nsabp fr-2. *J Clin Oncol*. (2022) 40:99. doi: 10.1200/JCO.2022.40.4_suppl.099

25. Feng L, Tang Y, Zhang W, Xu T, Li H, Ma H, et al. 249p the efficacy and safety of short-course radiotherapy followed by sequential chemotherapy and cadonilimab for locally advanced rectal cancer: the preliminary findings of prospective, multicenter phase ii trial. *Ann Oncol*. (2024) 35:S107. doi: 10.1016/j.annonc.2024.05.256

26. Takahashi Y, Kato T, Bando H, Tsukada Y, Inamori K, Wakabayashi M, et al. P-172 voltage cohort D: preoperative chemoradiotherapy followed by consolidation nivolumab plus ipilimumab in patients with locally advanced rectal cancer. *Ann Oncol*. (2023) 34:S77. doi: 10.1016/j.annonc.2023.04.228

27. de Gooyer PGM, Verschoor YL, Aalbers AG, Lambregts DMJ, van Triest B, Peters F, et al. 247p radiotherapy (Rt), atezolizumab (Atezo) and bevacizumab (Bev) to increase organ preservation in rectal cancer: the tarzan study. *Ann Oncol*. (2024) 35:S106. doi: 10.1016/j.annonc.2024.05.254

28. Zhou H, Gong C, Zhang J, Zou S, Tang J, Liang J, et al. 243p neoadjuvant xelox chemotherapy with or without cadonilimab in locally advanced pmmr rectal cancer: preliminary results from a randomized, open-label phase ii trial. *Ann Oncol*. (2024) 35:S104. doi: 10.1016/j.annonc.2024.05.250

29. Shamseddine A, Zeidan YH, El Husseini Z, Kreidieh M, Al Darazi M, Turfa R, et al. Efficacy and safety-in analysis of short-course radiation followed by mfolfox-6 plus avelumab for locally advanced rectal adenocarcinoma. *Radiat Oncol (London England)*. (2020) 15:233. doi: 10.1186/s13014-020-01673-6

30. Xia F, Wang Y, Wang H, Shen L, Xiang Z, Zhao Y, et al. Randomized phase ii trial of immunotherapy-based total neoadjuvant therapy for proficient mismatch repair or microsatellite stable locally advanced rectal cancer (Torch). *J Clin oncology: Off J Am Soc Clin Oncol*. (2024) 42:3308–18. doi: 10.1200/jco.23.02261

31. Le DT, Durham JN, Smith KN, Wang H, Bartlett BR, Aulakh LK, et al. Mismatch repair deficiency predicts response of solid tumors to pd-1 blockade. *Sci (New York NY)*. (2017) 357:409–13. doi: 10.1126/science.aan6733

32. Chalabi M, Fanchi LF, Dijkstra KK, Van den Berg JG, Aalbers AG, Sikorska K, et al. Neoadjuvant immunotherapy leads to pathological responses in mmr-proficient and mmr-deficient early-stage colon cancers. *Nat Med*. (2020) 26:566–76. doi: 10.1038/s41591-020-0805-8

33. Fokas E, Glynne-Jones R, Appelt A, Beets-Tan R, Beets G, Haustermans K, et al. Outcome measures in multimodal rectal cancer trials. *Lancet Oncol*. (2020) 21:e252–e64. doi: 10.1016/s1470-2045(20)30024-3

34. Kasi A, Abbasi S, Handa S, Al-Rajabi R, Saeed A, Baranda J, et al. Total neoadjuvant therapy vs standard therapy in locally advanced rectal cancer: A systematic review and meta-analysis. *JAMA network Open*. (2020) 3:e2030097. doi: 10.1001/jamanetworkopen.2020.30097

35. Smith CA, Kachnic LA. Evolving treatment paradigm in the treatment of locally advanced rectal cancer. *J Natl Compr Cancer Network: JNCCN*. (2018) 16:909–15. doi: 10.6004/jnccn.2018.7032

36. Martens MH, Maas M, Heijnen LA, Lambregts DM, Leijtens JW, Stassen LP, et al. Long-term outcome of an organ preservation program after neoadjuvant treatment for rectal cancer. *J Natl Cancer Institute*. (2016) 108. doi: 10.1093/jnci/djw171

37. Dattani M, Heald RJ, Goussous G, Broadhurst J, São Julião GP, Habr-Gama A, et al. Oncological and survival outcomes in watch and wait patients with a clinical complete response after neoadjuvant chemoradiotherapy for rectal cancer: A systematic review and pooled analysis. *Ann Surg*. (2018) 268:955–67. doi: 10.1097/sla.0000000000002761

38. Li Y, Du Y, Xue C, Wu P, Du N, Zhu G, et al. Efficacy and safety of anti-pd-1/pd-L1 therapy in the treatment of advanced colorectal cancer: A meta-analysis. *BMC Gastroenterol*. (2022) 22:431. doi: 10.1186/s12876-022-02511-7

39. Bahadoer RR, Dijkstra EA, van Etten B, Marijnen CAM, Putter H, Kranenbarg EM, et al. Short-course radiotherapy followed by chemotherapy before total mesorectal excision (Tme) versus preoperative chemoradiotherapy, tme, and optional adjuvant chemotherapy in locally advanced rectal cancer (Rapido): A randomised, open-label, phase 3 trial. *Lancet Oncol*. (2021) 22:29–42. doi: 10.1016/s1470-2045(20)30555-6

40. Morisada M, Clavijo PE, Moore E, Sun L, Chamberlin M, Van Waes C, et al. Pd-1 blockade reverses adaptive immune resistance induced by high-dose hypofractionated but not low-dose daily fractionated radiation. *Oncoimmunology*. (2018) 7:e1395996. doi: 10.1080/2162402x.2017.1395996

41. Pillai RN, Behera M, Owonikoko TK, Kamphorst AO, Pakkala S, Belani CP, et al. Comparison of the toxicity profile of pd-1 versus pd-L1 inhibitors in non-small cell lung cancer: A systematic analysis of the literature. *Cancer*. (2018) 124:271–7. doi: 10.1002/cncr.31043

42. Duan J, Cui L, Zhao X, Bai H, Cai S, Wang G, et al. Use of immunotherapy with programmed cell death 1 vs programmed cell death ligand 1 inhibitors in patients with cancer: A systematic review and meta-analysis. *JAMA Oncol*. (2020) 6:375–84. doi: 10.1001/jamaoncol.2019.5367

43. Curran WJJr., Paulus R, Langer CJ, Komaki R, Lee JS, Hauser S, et al. Sequential vs. Concurrent chemoradiation for stage iii non-small cell lung cancer: randomized phase iii trial rtog 9410. *J Natl Cancer Institute*. (2011) 103:1452–60. doi: 10.1093/jnci/djr325

44. Bestvina CM, Pointer KB, Karrison T, Al-Hallaq H, Hoffman PC, Jelinek MJ, et al. A phase 1 trial of concurrent or sequential ipilimumab, nivolumab, and stereotactic body radiotherapy in patients with stage iv nsclc study. *J Thorac oncology: Off Publ Int Assoc Study Lung Cancer*. (2022) 17:130–40. doi: 10.1016/j.jtho.2021.08.019

45. Wei H, Li Y, Guo Z, Ma X, Li Y, Wei X, et al. Comparison of dynamic changes in the peripheral cd8(+) T cells function and differentiation in escc patients treated with radiotherapy combined with anti-pd-1 antibody or concurrent chemoradiotherapy. *Front Immunol*. (2022) 13:1060695. doi: 10.3389/fimmu.2022.1060695

46. Kelley RK, Ueno M, Yoo C, Finn RS, Furuse J, Ren Z, et al. Pembrolizumab in combination with gemcitabine and cisplatin compared with gemcitabine and cisplatin alone for patients with advanced biliary tract cancer (Keynote-966): A randomised, double-blind, placebo-controlled, phase 3 trial. *Lancet (London England)*. (2023) 401:1853–65. doi: 10.1016/s0140-6736(23)00727-4

47. Kojima T, Shah MA, Muro K, Francois E, Adenis A, Hsu CH, et al. Randomized phase iii keynote-181 study of pembrolizumab versus chemotherapy in advanced esophageal cancer. *J Clin oncology: Off J Am Soc Clin Oncol*. (2020) 38:4138–48. doi: 10.1200/jco.20.01888

frontiers | Frontiers in Immunology

TYPE Study Protocol
PUBLISHED 25 February 2025
DOI 10.3389/fimmu.2025.1519545

OPEN ACCESS

EDITED BY
Stavros P. Papadakos,
Laiko General Hospital of Athens, Greece

REVIEWED BY
Xing Xiao,
Sun Yat-sen University, China
Ioannis Katsaros,
National and Kapodistrian University of Athens, Greece

*CORRESPONDENCE
Ming Liu
liuming629@wchscu.cn

†These authors have contributed equally to this work and share first authorship

RECEIVED 30 October 2024
ACCEPTED 31 January 2025
PUBLISHED 25 February 2025

CITATION
Wei J, Zhang P, Hu Q, Cheng X, Shen C, Chen Z, Zhuang W, Yin Y, Zhang B, Gou H, Yang K, Bi F and Liu M (2025) Nab-paclitaxel combined with cadonilimab (AK104) as second-line treatment for advanced gastric cancer: protocol for a phase II prospective, multicenter, single-arm clinical trial. *Front. Immunol.* 16:1519545. doi: 10.3389/fimmu.2025.1519545

Nab-paclitaxel combined with cadonilimab (AK104) as second-line treatment for advanced gastric cancer: protocol for a phase II prospective, multicenter, single-arm clinical trial

Jing Wei[1†], Pengfei Zhang[1†], Qiancheng Hu[1], Xiaolong Cheng[2], Chaoyong Shen[2], Zhixin Chen[2], Wen Zhuang[2], Yuan Yin[2], Bo Zhang[2], Hongfeng Gou[1], Kun Yang[2], Feng Bi[3] and Ming Liu[1*]

[1]Gastric Cancer Center, Department of Medical Oncology, West China Hospital, Sichuan University, Chengdu, Sichuan, China, [2]Department of General Surgery/Gastric Cancer Center, West China Hospital, Sichuan University, Chengdu, Sichuan, China, [3]Division of Abdominal Cancer, Department of Medical Oncology, Cancer Center and Laboratory of Molecular Targeted Therapy in Oncology, West China Hospital, Sichuan University, Chengdu, China

Background: Gastric cancer (GC) is one of the most prevalent malignant tumors worldwide, often diagnosed at an advanced stage with a poor prognosis. Paclitaxel, nab-paclitaxel, and irinotecan, either as monotherapies or in combination with ramucirumab, are currently standard second-line treatments for GC. However, the efficacy of these therapies is limited, necessitating the development of new combination strategies to improve response rates. Immune checkpoint inhibitors (ICIs) have shown success in first-line treatment for advanced GC, leading to interest in immune rechallenge strategies for second-line treatment. Re-challenging patients with ICIs after progression on first-line treatment may restore immune responses and provide additional clinical benefit. Recently, cadonilimab (AK104), a bispecific antibody targeting PD-1 and CTLA-4, has demonstrated promising antitumor activity when combined with chemotherapy in advanced gastric and gastroesophageal junction (GEJ) adenocarcinoma. However, the efficacy and safety of nab-paclitaxel combined with AK104 for the treatment of advanced GC remain unclear. Furthermore, identifying predictive biomarkers of efficacy is essential to developing personalized treatment strategies. This study aims to explore the safety and efficacy of nab-paclitaxel combined with AK104 as a second-line treatment for patients who have progressed after first-line chemoimmunotherapy, focusing on evaluating the therapeutic effect of ICIs rechallenge in gastric cancer.

Methods: This is a prospective, multicenter, open-label, single-arm Phase II clinical study. Eligible patients were histologically or cytologically diagnosed with unresectable recurrent or metastatic GC, failed first-line chemotherapy in combination with immune checkpoint inhibitor, aged between 18-75 years old, expected survival ≥3 months, and with a physical status of 0 or 1 in the Eastern Cooperative Cancer Group (ECOG). Enrolled patients will receive intravenous cadonilimab (AK104) 6 mg/kg on days 1, and 15, and intravenous nab-paclitaxel 100 mg/m^2 every four weeks on days 1, 8, and 15. The primary endpoints were

objective response rate (ORR), and secondary endpoints were disease control rate (DCR), progression-free survival (PFS), and overall survival (OS). The exploratory objective was to identify biomarkers associated with efficacy, mechanism of action, and safety. A total of 59 participants were planned to be recruited using Simon's two-stage design. The trial was initiated in June 2024 in China.

Discussion: This study is the first prospective trial to evaluate the combination of nab-paclitaxel and cadonilimab as second-line treatment after first-line chemoimmunotherapy failure. By investigating immune rechallenge, it aims to reactivate anti-tumor immune responses and improve clinical outcomes in GC patients. The exploration of predictive biomarkers, such as ctDNA, TMB, MSI, PD-L1 expression, TIL profiles, and gut microbiota, will help personalize treatment and identify patients most likely to benefit from immune rechallenge. This trial could provide valuable insights into overcoming immune resistance and contribute to developing a promising second-line therapeutic strategy for advanced GC.

Clinical trial registration: ClinicalTrials.Gov, identifier NCT06349967

KEYWORDS

gastric cancer, cadonilimab (AK104), nab-paclitaxel, immunotherapy, phase II clinical trial

1 Introduction

Gastric cancer (GC) is the fifth most common cancer worldwide, with over 2 million new cases and over 611,720 deaths expected in 2024, ranking it as the fourth leading cause of cancer-related deaths (1). Most GC cases are diagnosed at an advanced stage, making radical surgical resection impossible. Currently, fluorouracil-based systemic chemotherapy is the primary treatment for advanced or metastatic GC. However, chemotherapy alone has limited efficacy, and treatment advancements have reached a bottleneck. Recently, immunotherapy has emerged as a promising treatment, showing effective progress in various tumor types (2–4). Immune checkpoint inhibitors (ICIs), such as PD-1 and CTLA-4 inhibitors, restore T cell function by alleviating the immunosuppressive effects of the tumor microenvironment, enabling T cells to effectively attack tumor cells. Studies, including CheckMate 649, ORIENT-16, KEYNOTE-859, GEMSTONE-303, and COMPASSION-15/AK104-302, have demonstrated that combining chemotherapy with ICIs (Nivolumab, Sintilimab, Pembrolizumab, Sugmilimab, and Cadonilimab) significantly improves overall survival (OS) and progression-free survival (PFS) compared to chemotherapy alone, facilitating the transition from first-line treatments to the broader adoption of chemoimmunotherapy in advanced GC (5–10). Despite these improvements, the 5-year survival rate for advanced or metastatic GC remains low (approximately 5-20%), and most patients experience disease progression during immunotherapy. After progression on first-line treatment, current second-line therapies include single-agent chemotherapy (paclitaxel, irinotecan, docetaxel, nab-paclitaxel) or paclitaxel combined with ramucirumab (11–14). However, response rates for these treatments are limited (approximately 10-30%), underscoring the need for new combination strategies to enhance second-line treatment efficacy for GC (15–18).

Tumor cells evade immune detection by upregulating immune checkpoint molecules such as CTLA-4 and PD-1 on T lymphocytes. In gastric adenocarcinoma, high expressions of PD-L1 (around 40%) and CTLA-4 (around 85%) are associated with poor prognosis (19–22). Dual-targeted immunotherapy, validated in both preclinical and clinical studies, has shown efficacy, with CTLA-4 and PD-1 inhibitors working synergistically to restore T cell function through distinct mechanisms (23–27). CTLA-4 upregulation during T cell activation suppresses T cell activity, particularly on tumor-infiltrating regulatory T cells (Tregs) and exhausted effector T cells (Teffs). Blockade of CTLA-4 enhances T cell activation and reduces Treg infiltration, alleviating the immunosuppressive tumor microenvironment. Similarly, PD-1 upregulation following T cell activation suppresses T cell responses by binding its ligand, and inhibiting PD-1/PD-L1 signaling can reinvigorate tumor-reactive T cells. However, recent studies suggest that PD-L1 blockade may paradoxically promote Treg activity, leading to therapeutic resistance, which can be reversed by depleting Tregs (28). Additionally, context-dependent PD-(L)1 checkpoint activation induced by CTLA4-Ig therapy may further suppress T cell activity (29). These findings highlight the potential synergy between checkpoint inhibitors and combination

therapies. Chemotherapy also enhances immune responses by inducing tumor apoptosis, upregulating MHC-I, promoting dendritic cell maturation, and inhibiting immunosuppressive cells like Tregs, MDSCs, and TAMs. Combining ICIs with chemotherapy has shown synergistic anti-tumor effects, supporting the rationale for combining chemotherapy with dual immune checkpoint blockade (anti-CTLA-4 and anti-PD-1) in solid tumors (30, 31).

Nab-paclitaxel, a novel formulation of paclitaxel, improves drug concentration and uptake in tumor tissues compared to traditional solvent-based paclitaxel. The ABSOLUTE study showed that nab-paclitaxel is non-inferior to weekly solvent-based paclitaxel and has been recommended as a standard second-line treatment for GC (32). However, its efficacy as a single-agent second-line treatment remains limited, highlighting the need for novel strategies to improve clinical outcomes.

Cadonilimab (AK104) is a bispecific antibody that targets both the PD-1 and CTLA-4 immune checkpoint pathways, utilizing a 4-valent IgG1-ScFv format. It reverses T-cell depletion by facilitating the endocytosis of cell-surface PD-1 and CTLA-4 receptors, which subsequently induces the secretion of IL-2 and IFN-γ. This mechanism not only reduces immune-related adverse events (irAEs) but also enhances the ability of T cells to kill tumor cells (33). Cadonilimab is currently approved in China for treating recurrent or metastatic cervical cancer that has progressed during or after platinum-based chemotherapy (34). In the multicenter, open-label Phase 1b/2 COMPASSION-03 trial, cadonilimab demonstrated significant antitumor activity and a manageable safety profile in patients with advanced solid tumors (9, 23, 35, 36). More recently, in the Phase 3 COMPASSION-15/AK104-302 trial, cadonilimab combined with chemotherapy as a first-line treatment for patients with HER2-negative unresectable advanced or metastatic gastric or gastroesophageal junction (GEJ) adenocarcinoma showed an objective remission rate (ORR) of up to 65.2% and an overall survival (OS) of up to 15 months (37). Additionally, this combination therapy reduced the risk of death by 44% in patients with high PD-L1 expression (CPS ≥ 5) and by 30% in those with low PD-L1 expression (CPS < 5).

This study aims to evaluate the efficacy and safety of nab-paclitaxel combined with cadonilimab as a second-line treatment for advanced GC following the failure of first-line chemoimmunotherapy (PD1 inhibitors). Additionally, emerging evidence highlights the critical role of gut microbiota and predictive biomarkers in shaping ICI responses, but their integration into GC treatment remains limited. This study will explore diagnostic biomarkers and gut microbiota as predictive and prognostic factors, providing deeper insights into the mechanisms of treatment resistance and therapeutic efficacy. By combining these exploratory analyses with efficacy assessments, the study represents a significant advancement toward personalized immunotherapy, addressing unmet clinical needs in the management of GC.

2 Methods and analysis

2.1 Study design

This prospective, multicenter, open-label, single-arm phase II clinical study aims to evaluate the efficacy and safety of nab-paclitaxel in combination with cadonilimab (AK104) as a second-line treatment for patients with gastric cancer (GC) who have failed first-line fluorouracil-based or platinum-based combination immunotherapy. The study design is illustrated in Figure 1.

Eligible patients are those with histologically or cytologically confirmed unresectable, recurrent, or metastatic GC who have experienced disease progression following first-line chemotherapy combined with immune checkpoint inhibitors (PD-1/PD-L1). Patients enrolled in the study will receive nab-paclitaxel in combination with cadonilimab until either disease progression (PD) or the onset of treatment intolerance.

The study will prospectively collect data on overall response rate (ORR), disease control rate (DCR), progression-free survival (PFS), overall survival (OS), and quality of life (QoL), alongside a comprehensive assessment of the medication's safety profile.

2.2 Inclusion and exclusion criteria

The inclusion and exclusion criteria are detailed in Table 1.

2.3 Treatment

Cadonilimab (AK104): Administered at a dose of 6 mg/kg via intravenous infusion over 30-60 minutes on Days 1 and 15 of each 28-day cycle (q28d).

Nab-paclitaxel: Administered at a dose of 100 mg/m^2 via intravenous infusion over 30-40 minutes, initiated 30 minutes after the completion of the cadonilimab (AK104) infusion, on Days 1, 8, and 15 of each 28-day cycle (q28d).

Eligible participants will receive nab-paclitaxel in combination with cadonilimab until one of the following occurs: PD, death, loss to follow-up, unacceptable toxicity, withdrawal of informed consent, or other treatment termination criteria as specified in the study protocol.

2.4 Objectives and endpoints

2.4.1 Objectives

2.4.1.1 Primary purpose

1. To evaluate the ORR of nab-paclitaxel in combination with cadonilimab (AK104) as a second-line treatment for GC patients who have failed first-line fluorouracil-based or platinum-based combination immunotherapy.

2.4.1.2 Secondary purpose

1. To assess the efficacy of nab-paclitaxel combined with cadonilimab (AK104) in the second-line treatment of GC patients who have failed first-line fluorouracil-based or platinum-based combination immunotherapy, including DCR, PFS, and OS.

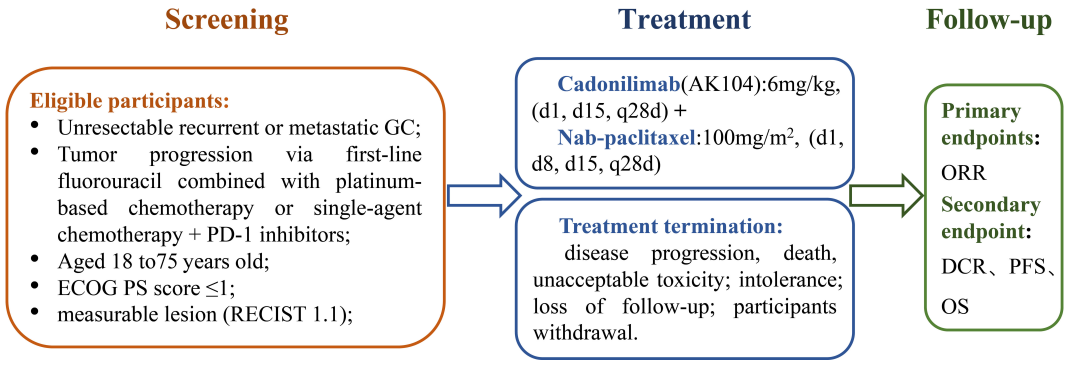

FIGURE 1
Study design of the clinical trial evaluating nab-paclitaxel combined with cadonilimab.

2. To evaluate the safety, tolerability, and impact on patient QoL of nab-paclitaxel in combination with cadonilimab (AK104).

2.4.1.3 Exploratory purpose

1. To investigate the antitumor efficacy, mechanism of action, and potential resistance mechanisms of nab-paclitaxel combined with cadonilimab (AK104).
2. To explore the role of tumor tissue PD-L1 expression, blood immune cell subpopulations, and serum cytokine levels as potential predictors of treatment efficacy.
3. To examine the role of liquid biopsy biomarkers, such as circulating tumor DNA (ctDNA), cell-free DNA (cf-DNA), and blood tumor mutational burden (bTMB), as predictors of efficacy, with a focus on their capacity to monitor minimal residual disease or treatment response.
4. To explore the association between gut microbiota composition and immunotherapy response using large-scale metagenomic analysis, aiming to identify microbial signatures that correlate with treatment outcomes.
5. To assess the impact of the treatment protocols on patient QoL using the QLQ-LC13 and EORTC QLQ-C30 questionnaires, with an emphasis on patient-reported outcomes related to physical and emotional well-being.

2.4.2 Endpoints

2.4.2.1 Primary endpoint

Objective response rate (ORR): defined as the proportion of subjects whose tumors achieved complete response (CR) or partial response (PR) after treatment. Evaluated by the Blinded Independent Image Review Committee (BIIRC). This serves as the primary indicator of treatment efficacy.

2.4.2.2 Secondary endpoints

Disease Control Rate (DCR): defined as the proportion of subjects whose tumors achieved CR, PR, or stable disease (SD) after treatment. This reflects broader disease stabilization benefits.

Progression-free survival (PFS): defined as the time from randomization to tumor progression or death due to any cause, providing insights into treatment durability.

Overall survival (OS): defined as the time from randomization to death due to any cause (last follow-up for patients lost to follow-up; end of follow-up date for patients alive at the end of the study). This serves as a critical measure of long-term efficacy.

2.4.2.3 Exploratory endpoint

Accompanying diagnostic biomarkers and gut flora characterization: This exploratory analysis aims to identify predictive and prognostic biomarkers, with a particular focus on gut microbiota and its interaction with immunotherapy. These findings may provide novel insights into the mechanisms underlying treatment responses and immune-related adverse events (irAEs).

2.5 Efficacy and safety assessment

2.5.1 Efficacy assessment

Laboratory tests, including hematology, liver and kidney function, electrolytes, cardiac markers, thyroid function, coagulation, and transmission nine tests, were performed on the first day of each treatment cycle. Tumor biomarker assessments, including carbohydrate antigen 19-9 (CA19-9), CA125, carcinoembryonic antigen (CEA), and alpha-fetoprotein (AFP), were also conducted. Additionally, 12-lead electrocardiograms and echocardiograms were performed at the same time. These tests were performed according to the protocol, with additional assessments performed if clinically indicated.

Antitumor efficacy was evaluated every 8 weeks (approximately at the end of every two dosing cycles) via CT or MRI examinations (chest, abdomen, pelvis, and any other site suspected of having tumor lesions). Tumor imaging response was assessed according to RECIST version 1.1. Tumor assessments may be conducted more frequently if clinically necessary, based on the investigator's judgment.

All procedures were conducted in accordance with the study protocol and with informed consent from the participants.

TABLE 1 Inclusion and exclusion criteria.

Primary Inclusion Criteria	Primary Exclusion Criteria
(1) Patients with unresectable gastric or gastroesophageal junction adenocarcinoma confirmed by laparoscopic exploration and pathological/cytological examination;	(1) Participation in any clinical trials of a drug, or ongoing clinical trials of other drugs within 1 month prior to enrollment;
(2) Aged 18 to 75 years;	(2) Hyper-progression occurred during first-line immunotherapy: • An increase in tumor load of more than 50% compared to the baseline period when first assessed after 2 to 4 cycles of first-line therapy; • The tumor growth rate after immunotherapy is more than twice the previous rate;
(3) Tumor progression after first-line treatment with a fluoropyrimidine (5-FU, S-1, or capecitabine) combined with a platinum-based agent (oxaliplatin or cisplatin), or single-agent chemotherapy plus a PD-1/PD-L1 inhibitor	(3) Presence of any active autoimmune disease or history of autoimmune disease (including but not limited to: interstitial pneumonia, uveitis, enteritis, hepatitis, nephritis, hyperthyroidism, hypothyroidism);
(4) Expected survival of at least 3 months;	(4) First-line immunotherapy-related Grade 3-4 immune hepatitis, immune pneumonia, and immune myocarditis, etc.;
(5) Eastern Cooperative Oncology Group (ECOG) Performance Status ≤1	(5) Currently receiving immunosuppressive agents or hormone therapy (administered systemically or locally) for the purpose of immunosuppression and having continued such treatment within two weeks prior to enrollment;
(6) Presence of at least one measurable lesion as defined by the RECIST 1.1 criteria;	(6) ≥ grade 3 bleeding event within 4 weeks prior to enrollment; thromboembolic or arteriovenous event such as cerebrovascular event (including transient ischemic attack), deep vein thrombosis, or pulmonary embolism within 6 months prior to enrollment, etc.;
(7) Patients must have adequate liver, kidney, and bone marrow function, as demonstrated by the following laboratory test criteria: • Total bilirubin ≤ 1.5 times the upper limit of normal (ULN) • Serum alanine aminotransferase (ALT) and aspartate aminotransferase (AST) levels ≤ 3 times the ULN; • Alkaline phosphatase ≤ 2.5 times the ULN (≤ 3 times the ULN if the tumor has intrahepatic invasion); • Blood creatinine ≤ 1.5 times the ULN and creatinine clearance (Ccr) ≥ 60 mL/min; • Serum amylase and lipase levels ≤ 1.5 times the ULN; • International Normalized Ratio (INR) and/or Partial Thromboplastin Time (PTT) ≤ 1.5 times the ULN; • Have not received a blood cell-boosting intervention, such as a transfusion or stimulating factor, for at least 2 weeks prior to administration, with a platelet count ≥ 75,000/mm^3, hemoglobin ≥ 9 g/dL, and neutrophil count ≥ 1,500/mm^3;	(7) Active or clinically significant cardiovascular disease: • Congestive heart failure: New York Heart Association (NYHA) Class > II; • Active coronary artery disease; • Arrhythmias requiring treatment other than β-blockers or digoxin; • Unstable angina (angina symptoms at rest), new angina within 3 months prior to enrollment, or new myocardial infarction within 6 months prior to enrollment;
(8) Strict contraception;	(8) Symptomatic brain metastases or meningioma;
(9) Voluntary participation and signed informed consent;	(9) Patients with other significant medical or surgical conditions that, in the investigator's judgment, render them unsuitable for participation in this clinical trial: • Active, symptomatic interstitial lung disease, pleural effusion, or ascites causing dyspnea (grade ≥ 2); • Patients with renal failure who require hemodialysis or peritoneal dialysis; • Presence of gastrointestinal perforation, gastrointestinal obstruction, or uncontrolled diarrhea within 6 months prior to enrollment; • Presence of unhealed wounds, ulcers, or fractures;
	(10) • Must not have untreated or concurrent other tumors, except for treated cervical carcinoma in situ, basal cell carcinoma, or superficial bladder tumors; • Enrollment is allowed if the tumor has been eradicated and there is no evidence of disease for more than 3 years; • Treatment of all other tumors must have been completed at least 3 years prior to enrollment;
	(11) Patients with a history of HIV infection or active hepatitis B or C;
	(12) Ongoing infection with severity greater than grade 2;
	(13) Pregnant or breastfeeding females;
	(14) Substance abuse, along with medical, psychological, or social conditions, may impact patient enrollment and the evaluation of experimental results;

(Continued)

TABLE 1 Continued

Primary Inclusion Criteria	Primary Exclusion Criteria
	(15) • During the treatment period, no additional antineoplastic therapies (chemotherapy, radiotherapy, surgery, immunotherapy, biological therapy, or chemoembolization) beyond the investigational drug are permitted; • Palliative external-beam radiotherapy to non-target lesions is allowed;
	(16) Has previously received the same class of chemotherapeutic agents or immune checkpoint inhibitors;
	(17) • Allergy or suspected allergy to the study drug or any drug of the same class; • Major surgery, open biopsy, or major traumatic surgery within 4 weeks prior to enrollment; • History of organ transplantation (including corneal transplantation); History of allogeneic blood transfusion within the past 6 months; • Vaccination history within 4 weeks prior to enrollment;
	(18) Patients deemed unsuitable for inclusion in this study at the discretion of the investigator.

2.5.2 Safety evaluation

Safety assessments will be conducted throughout the study, with participants closely monitored for adverse events (AEs) until resolution, stabilization, or confirmation of non-clinical significance.

AE Definition: defined as any untoward medical occurrence in a participant receiving the investigational product, irrespective of its causal relationship to the treatment. AEs will be evaluated for severity (graded per NCI-CTCAE v5.0), duration, and relationship to the study treatment.

Serious Adverse Event (SAE) Definition: defined as any event that results in death, is life-threatening, causes significant disability, requires hospitalization or prolongs an existing hospitalization, leads to congenital anomalies, or constitutes other medically significant conditions. SAEs must be reported to the regulatory authority, ethics committee, and sponsor within 24 hours, with follow-up reports submitted as needed. All AEs/SAEs must be thoroughly documented in the case report form (CRF), including details on onset, duration, resolution, and any interventions taken.

The study team will follow the study protocol and standard operating procedures (SOPs) for AE/SAE management, implementing necessary measures such as dose adjustments or treatment discontinuation when required.

2.6 Management plan for adverse events

2.6.1 Management of adverse events related to AK104

For low-grade adverse events (Grade 1 or 2), symptomatic and topical treatments are recommended. Persistent low-grade events or severe events (Grade ≥3) should be managed with systemic corticosteroids, such as prednisone or intravenous equivalents.

Discontinuation of AK104 therapy is not mandatory for Grade 3 or 4 inflammatory responses (e.g., inflammation at metastatic sites or lymph nodes) attributable to a localized tumor response. In cases of multiple concurrent low-grade AEs that individually would not necessitate therapy termination, the decision to discontinue AK104 treatment will be at the investigator's discretion.

The investigator will evaluate the severity of immune-related adverse events (irAEs) using the NCI CTCAE version 5.0 grading criteria and adjust AK104 therapy as necessary. General management recommendations for irAEs are outlined in Table 2.

2.7 Study follow-up

Overall survival (OS) analysis will be conducted throughout the trial period. During the follow-up phase, subjects will be assessed every three months to document their survival status, including PD, AEs, and QoL where applicable. Follow-up visits may be conducted through in-person consultations, phone calls, or electronic surveys, depending on patient circumstances.

Follow-up will continue until the subject's death, loss to follow-up, or the end of the study period. All data collected during follow-up will be systematically recorded in the study database. Measures will be implemented to ensure adherence to follow-up schedules, including regular reminders and patient support initiatives.

2.8 Exploratory endpoint analysis

This study focuses on biomarker analysis and gut microbiota characterization to explore the predictive value of peripheral biomarkers in assessing disease activity and survival benefits associated with AK104 treatment, leveraging advancements in liquid biopsy technologies and their therapeutic potential.

Peripheral blood samples were collected before the first dose (Day 1, Cycle 1) and at disease progression. Fresh whole blood was processed within 2 hours to extract plasma, which was stored at -80° C for next-generation sequencing (NGS) analysis. NGS was used to evaluate cancer-related genes, including ctDNA, cfDNA somatic mutations, and bTMB. Changes in immune cell subsets, cytokines, and tumor immunotherapy biomarkers were also assessed.

TABLE 2 General principles for dose adjustment.

Grade of irAE	Treatment plan adjustments
Grade 1 irAE	No adjustments to the treatment plan are required
Grade 2 irAE	Suspend AK104 therapy until grade 2 adverse events subside to ≤ grade 1 or baseline level: a) If toxicity worsens, it is recommended to manage as grade 3 or 4; b) If toxicity improves, consider resuming AK104 therapy at the appropriate scheduled treatment visit; c) Permanent discontinuation of AK104 should be considered if grade 2 irAE does not subside to ≤ grade 1 or baseline level within 12 weeks after symptomatic treatment;
Grade 3 irAE	Suspend AK104 therapy until grade 3 adverse events (irAE) regress to ≤ grade 1 or baseline level: a) If toxicity improves, the investigator may consider whether to permanently terminate AK104 treatment based on the type of individual toxicity, its occurrence, and the course of regression; b) Permanent termination of AK104 therapy is recommended if grade 3 irAE does not regress to ≤ grade 1 or baseline level within 12 weeks with symptomatic treatment;
Grade 4 irAE	The treatment with AK104 must be discontinued permanently;

Fecal samples, collected before treatment initiation, were analyzed using large-scale metagenomic sequencing. This approach provided comprehensive taxonomic and functional profiling to assess associations between gut microbiota composition and immunotherapy response.

Data from biomarker and microbiota analyses were evaluated using multivariate regression and survival models, with adjustments for confounding factors. All patients provided informed consent, and the study protocol received approval from the institutional review board (IRB).

2.9 Sample size calculation and statistical analysis

Sample size calculations were performed using Simon's optimal two-stage design to balance ethical considerations and resource efficiency. This design minimizes the expected sample size under the null hypothesis while ensuring adequate power to detect a meaningful treatment effect if the alternative hypothesis is true. Simon's two-stage design was chosen due to its widespread use in early-phase clinical trials to assess efficacy and safety efficiently.

The minimax design parameters were set as follows: an alpha error of 5% and a power (1-β) of 80% were used for calculations. The minimax two-stage design resulted in parameters (6/31, 15/53). Stage 1: Enroll 31 patients. If ≤6 patients achieve ORR, the trial is terminated due to futility. Stage 2: If >6 responses are observed, an additional 22 patients are enrolled, resulting in a total of 53 patients. Success Criteria: The treatment regimen is considered successful if ≥15 patients achieve ORR. To account for potential patient dropout, the sample size was increased by 10%, resulting in a final planned enrollment of 59 patients. PFS and OS will be analyzed using the Kaplan-Meier method. Median survival times and 95% confidence intervals (CI) will be reported. Differences between groups will be assessed using the log-rank test. If applicable, Cox proportional hazards regression analysis will be performed to evaluate the impact of baseline covariates on survival outcomes. ORR, DCR, and AEs will be analyzed using descriptive statistics. The Clopper-Pearson method will be used to calculate 95% confidence intervals for proportions. Subgroup analyses may be conducted based on predefined stratification factors. Sample size calculations were performed using PASS 2024 software (version 24.0.2, NCSS).

Exploratory analyses will be conducted to identify predictive and prognostic biomarkers using advanced immunoassays and bioinformatics tools. Adverse events will be graded according to CTCAE v5.0, and comparisons between different severity grades will be performed using chi-square or Fisher's exact tests. This statistical approach ensures rigorous evaluation of efficacy and safety while accommodating the exploratory nature of biomarker identification.

3 Discussion

Although first-line chemotherapy regimens for advanced gastric cancer (GC) have improved, the survival times remains below 12 months, highlighting the need for further efficacy advancements. Immunotherapy has made significant strides in treating advanced GC, overcoming the long-standing survival limitations associated with traditional chemotherapy (38–40). Notably, the CheckMate-649 trial, a randomized, open-label, multicenter Phase III study, evaluated nivolumab combined with chemotherapy, nivolumab plus ipilimumab, and single-agent chemotherapy in HER2-negative advanced GC patients. Results showed that nivolumab plus chemotherapy significantly improved OS and PFS compared to chemotherapy alone, with an acceptable safety profile (41). Importantly, in patients with PD-L1 CPS ≥ 5, nivolumab in combination with chemotherapy reduced the risk of death by 29% compared to chemotherapy alone. As a result, nivolumab combined with chemotherapy has become a recommended first-line treatment option in clinical guidelines from CSCO, NCCN, and ESMO. Similarly, the ATTRACTION-04 trial, a randomized multicenter Phase II/III study, demonstrated that first-line nivolumab with chemotherapy significantly improved PFS in Asian patients with HER2-negative advanced or recurrent GC (PFS: 10-45 months vs. 8-34 months; HR 0.68; 98.51% CI: 0.51-0.90; P=0.0007), suggesting it may become the new standard of care (42). Additional studies, including ORIENT-16, RATIONALE-305, KEYNOTE-859, GEMSTONE-303, and COMPASSION-15/AK104-302, showed that combining chemotherapy with PD-1/PD-L1 monoclonal antibodies such as sindilizumab, tirilizumab, pabolizumab, sugemalimab, and cadonilimab improved median overall survival (mOS) to 13-15 months. In patients with high

PD-L1 expression, mOS reached 15-18 months, with an ORR of approximately 60%.

The combination of ICIs and chemotherapy has now become the standard first-line treatment for advanced GC without driver gene mutations, including in unresectable locally advanced GC and perioperative settings (43–45). Despite these significant improvements in prognosis, around 40% of patients still experience PD, and OS often falls short of expectations. Re-challenge with ICIs, which involves reintroducing these agents after PD or serious irAEs, has been extensively studied in melanoma and urologic cancers (46–48). ICI rechallenge works by either reactivating the normal immune cycle or bypassing immune dysfunction to resensitize tumor cells to ICIs (49–51). Tumor cells that initially responded to ICIs may still harbor susceptible populations, and the interactions between the immune system and the tumor microenvironment may provide new opportunities for anti-tumor responses. Additionally, immunotherapy can alter the tumor neoantigen profile, enabling tumors to evade recognition by memory T cells, but ICI rechallenge can restore T cells' ability to recognize these neoantigens (4, 52). Studies such as CheckMate 066/067 and KEYNOTE-010 have demonstrated that rechallenge with nivolumab and pembrolizumab resulted in lesion shrinkage and significant OS improvements in patients with advanced melanoma and PD-L1-positive advanced non-small-cell lung cancer (NSCLC), with no additional AEs reported (53–56).

Although chemotherapy combined with immunotherapy demonstrates synergistic effects through the promotion of immunogenic cell death (ICD) and the release of neoantigens, the rechallenge of ICIs in advanced GC remains underexplored due to limited clinical evidence and the lack of large-scale prospective studies. Furthermore, identifying biomarkers for ICI rechallenge in advanced GC is crucial for facilitating precise, individualized immunotherapy and improving the effectiveness of combination therapies. Significant progress has been made in identifying biomarkers for gastrointestinal cancers, with PD-L1 expression, microsatellite instability (MSI), and mismatch repair deficiency (dMMR) emerging as key indicators (57). Ongoing research is also focusing on other biomarkers, including tumor mutational burden (TMB), circulating tumor DNA (ctDNA), Epstein-Barr virus (EBV), and the gut microbiome. Advanced immunoassays, multi-omics approaches, and bioinformatics tools offer additional potential for identifying biomarkers predictive of positive responses to ICI rechallenge. By integrating these biomarkers with clinicopathological features, we can more effectively stratify advanced GC patients undergoing ICI treatment, explore mechanisms of ICI drug resistance, identify potential strategies for sensitization, and ultimately improving overall prognosis (58–62).

Managing irAEs is a critical aspect of immunotherapy. As a bispecific antibody targeting both PD-1 and CTLA-4, cadonilimab may have a unique irAE profile. Common irAEs include dermatologic, gastrointestinal, hepatic, and endocrine disorders, all of which require timely diagnosis and management. Strategies such as early corticosteroid intervention, immune-modulating agents, and careful monitoring are essential to mitigate irAEs. Our study emphasizes the need for standardized irAE management protocols, especially for novel agents like cadonilimab.

This study has several strengths, including the investigation of a novel combination therapy, exploration of predictive biomarkers, and well-defined patient stratification. However, it also has limitations, as it was conducted within a single geographic region and focused primarily on an Asian population. While the findings offer valuable insights into the efficacy of cadonilimab in this group, their generalizability to other populations remains uncertain. Gastric cancer epidemiology, genetic diversity, and healthcare access vary globally, which may influence treatment responses and outcomes. Additionally, potential confounding from prior immunotherapy treatment could impact the interpretation of results. Future multicenter and global studies are needed to validate these results and ensure the broader applicability of cadonilimab-based regimens.

This Phase II clinical trial is the first to evaluate nab-paclitaxel combined with cadonilimab (AK104) as a second-line treatment for advanced GC. The study aims to investigate the efficacy and safety of ICI rechallenge in patients who have progressed after first-line chemoimmunotherapy, focusing on immune resistance mechanisms and predictive biomarkers of susceptibility. By exploring real-world rechallenge strategies, this research provides evidence-based insights to optimize immunotherapy outcomes and paves the way for future studies, highlighting cadonilimab's potential to transform treatment for advanced gastric cancer.

Ethics statement

The studies involving humans were approved by Biomedical Ethics Review Committee, West China Hospital, Sichuan University. The studies were conducted in accordance with the local legislation and institutional requirements. The participants provided their written informed consent to participate in this study.

Author contributions

JW: Data curation, Software, Writing – original draft. QH: Methodology, Supervision, Writing – review & editing. XC: Supervision, Writing – review & editing. CS: Supervision, Writing – review & editing. ZC: Supervision, Writing – review & editing. WZ: Supervision, Writing – review & editing. YY: Supervision, Writing – review & editing. BZ: Supervision, Writing – review & editing. HG: Supervision, Writing – review & editing. KY: Supervision, Writing – review & editing. FB: Conceptualization, Supervision, Writing – review & editing. PZ: Methodology, Validation, Writing – review & editing. ML: Conceptualization, Methodology, Project administration, Writing – review & editing.

Funding

The author(s) declare that financial support was received for the research, authorship, and/or publication of this article. This work

was supported by 1.3.5 Project for Disciplines of Excellence, West China Hospital, Si-chuan University (Grant No. ZYJC21043). Science and technology innovation talent project of Sichuan Science and Technology Department (2020JDRC0025). Sichuan Provincial Science and Technology Department 2023 key research and development project in the field of social development science and technology (2023YFS0111).

Conflict of interest

The authors declare that the research was conducted in the absence of any commercial or financial relationships that could be construed as a potential conflict of interest.

Generative AI statement

The author(s) declare that no Generative AI was used in the creation of this manuscript.

Publisher's note

All claims expressed in this article are solely those of the authors and do not necessarily represent those of their affiliated organizations, or those of the publisher, the editors and the reviewers. Any product that may be evaluated in this article, or claim that may be made by its manufacturer, is not guaranteed or endorsed by the publisher.

References

1. Siegel RL, Giaquinto AN, Jemal A. Cancer statistics, 2024. *CA: Cancer J Clin*. (2024) 74:12–49. doi: 10.3322/caac.21820

2. Alsina M, Arrazubi V, Diez M, Tabernero J. Current developments in gastric cancer: from molecular profiling to treatment strategy. *Nat Rev Gastroenterol hepatology*. (2023) 20:155–70. doi: 10.1038/s41575-022-00703-w

3. Svrcek M, Voron T, André T, Smyth EC, de la Fouchardière C. Improving individualised therapies in localised gastro-oesophageal adenocarcinoma. *Lancet Oncol*. (2024) 25:e452–e63. doi: 10.1016/s1470-2045(24)00180-3

4. Patel MA, Kratz JD, Lubner SJ, Loconte NK, Uboha NV. Esophagogastric cancers: integrating immunotherapy therapy into current practice. *J Clin oncology: Off J Am Soc Clin Oncol*. (2022) 40:2751–62. doi: 10.1200/jco.21.02500

5. Janjigian YY, Ajani JA, Moehler M, Shen L, Garrido M, Gallardo C, et al. First-line nivolumab plus chemotherapy for advanced gastric, gastroesophageal junction, and esophageal adenocarcinoma: 3-year follow-up of the phase iii checkmate 649 trial. *J Clin oncology: Off J Am Soc Clin Oncol*. (2024) 42:2012–20. doi: 10.1200/jco.23.01601

6. Xu J, Jiang H, Pan Y, Gu K, Cang S, Han L, et al. Sintilimab plus chemotherapy for unresectable gastric or gastroesophageal junction cancer: the orient-16 randomized clinical trial. *Jama*. (2023) 330:2064–74. doi: 10.1001/jama.2023.19918

7. Rha SY, Oh DY, Yañez P, Bai Y, Ryu MH, Lee J, et al. Pembrolizumab plus chemotherapy versus placebo plus chemotherapy for her2-negative advanced gastric cancer (Keynote-859): A multicentre, randomised, double-blind, phase 3 trial. *Lancet Oncol*. (2023) 24:1181–95. doi: 10.1016/s1470-2045(23)00515-6

8. Zhang X, Wang J, Wang G, Zhang Y, Fan Q, Chuangxin L, et al. Lba79 gemstone-303: prespecified progression-free survival (Pfs) and overall survival (Os) final analyses of a phase iii study of sugemalimab plus chemotherapy vs placebo plus chemotherapy in treatment-na&Xef;Ve advanced gastric or gastroesophageal junction (G/gej) adenocarcinoma. *Ann Oncol*. (2023) 34:S1319. doi: 10.1016/j.annonc.2023.10.080

9. Gao X, Ji K, Jia Y, Shan F, Chen Y, Xu N, et al. Cadonilimab with chemotherapy in her2-negative gastric or gastroesophageal junction adenocarcinoma: the phase 1b/2 compassion-04 trial. *Nat Med*. (2024) 30:1943–51. doi: 10.1038/s41591-024-03007-5

10. *A Randomized, Double-Blind, Multicenter, Phase Iii Study Comparing the Efficacy and Safety of Ak104 Plus Oxaliplatin and Capecitabine (Xelox) Versus Placebo Plus Xelox as First-Line Treatment for Locally Advanced Unresectable or G/Gej Adenocarcinoma* (2021). Available online at: https://clinicaltrials.gov/study/NCT05008783.

11. Ward ZJ, Gaba Q, Atun R. Cancer incidence and survival for 11 cancers in the commonwealth: A simulation-based modelling study. *Lancet Oncol*. (2024) 25:1127–34. doi: 10.1016/s1470-2045(24)00336-x

12. Pavlakis N, Shitara K, Sjoquist K, Martin A, Jaworski A, Tebbutt N, et al. Integrate iia phase iii study: regorafenib for refractory advanced gastric cancer. *J Clin oncology: Off J Am Soc Clin Oncol*. (2024) 43(4):453-63. doi: 10.1200/jco.24.00055

13. Kang YK, Kim HD, Yook JH, Park YK, Lee JS, Kim YW, et al. Neoadjuvant docetaxel, oxaliplatin, and S-1 plus surgery and adjuvant S-1 for resectable advanced gastric cancer: updated overall survival outcomes from phase iii prodigy. *J Clin oncology: Off J Am Soc Clin Oncol*. (2024) 42:2961–65. doi: 10.1200/jco.23.02167

14. Hegewisch-Becker S, Mendez G, Chao J, Nemecek R, Feeney K, Van Cutsem E, et al. First-line nivolumab and relatlimab plus chemotherapy for gastric or gastroesophageal junction adenocarcinoma: the phase ii relativity-060 study. *J Clin oncology: Off J Am Soc Clin Oncol*. (2024) 42:2080–93. doi: 10.1200/jco.23.01636

15. Tougeron D, Dahan L, Evesque L, Le Malicot K, El Hajbi F, Aparicio T, et al. Folfiri plus durvalumab with or without tremelimumab in second-line treatment of advanced gastric or gastroesophageal junction adenocarcinoma: the prodige 59-ffcd 1707-durigast randomized clinical trial. *JAMA Oncol*. (2024) 10:709–17. doi: 10.1001/jamaoncol.2024.0207

16. Kim CG, Jung M, Kim HS, Lee CK, Jeung HC, Koo DH, et al. Trastuzumab combined with ramucirumab and paclitaxel in patients with previously treated human epidermal growth factor receptor 2-positive advanced gastric or gastroesophageal junction cancer. *J Clin oncology: Off J Am Soc Clin Oncol*. (2023) 41:4394–405. doi: 10.1200/jco.22.02122

17. Wang F, Shen L, Guo W, Liu T, Li J, Qin S, et al. Fruquintinib plus paclitaxel versus placebo plus paclitaxel for gastric or gastroesophageal junction adenocarcinoma: the randomized phase 3 frutiga trial. *Nat Med*. (2024) 30:2189–98. doi: 10.1038/s41591-024-02989-6

18. Xu RH, Zhang Y, Pan H, Feng J, Zhang T, Liu T, et al. Efficacy and safety of weekly paclitaxel with or without ramucirumab as second-line therapy for the treatment of advanced gastric or gastroesophageal junction adenocarcinoma (Rainbow-asia): A randomised, multicentre, double-blind, phase 3 trial. *Lancet Gastroenterol hepatology*. (2021) 6:1015–24. doi: 10.1016/s2468-1253(21)00313-7

19. Chen Y, Jia K, Chong X, Xie Y, Jiang L, Peng H, et al. Implications of pd-L1 expression on the immune microenvironment in her2-positive gastric cancer. *Mol cancer*. (2024) 23:169. doi: 10.1186/s12943-024-02085-w

20. Cousin S, Guégan JP, Shitara K, Palmieri LJ, Metges JP, Pernot S, et al. Identification of microenvironment features associated with primary resistance to anti-pd-1/pd-L1 + Antiangiogenesis in gastric cancer through spatial transcriptomics and plasma proteomics. *Mol cancer*. (2024) 23:197. doi: 10.1186/s12943-024-02092-x

21. Weng N, Zhou C, Zhou Y, Zhong Y, Jia Z, Rao X, et al. Ikzf4/nono-rab11fip3 axis promotes immune evasion in gastric cancer via facilitating pd-L1 endosome recycling. *Cancer letters*. (2024) 584:216618. doi: 10.1016/j.canlet.2024.216618

22. Dovedi SJ, Elder MJ, Yang C, Sitnikova SI, Irving L, Hansen A, et al. Design and efficacy of a monovalent bispecific pd-1/ctla4 antibody that enhances ctla4 blockade on pd-1(+) activated T cells. *Cancer Discovery*. (2021) 11:1100–17. doi: 10.1158/2159-8290.Cd-20-1445

23. Keam SJ. Cadonilimab: first approval. *Drugs*. (2022) 82:1333–39. doi: 10.1007/s40265-022-01761-9

24. Principe N, Phung AL, Stevens KLP, Elaskalani O, Wylie B, Tilsed CM, et al. Anti-metabolite chemotherapy increases lag-3 expressing tumor-infiltrating lymphocytes which can be targeted by combination immune checkpoint blockade. *J Immunother Cancer*. (2024) 12. doi: 10.1136/jitc-2023-008568

25. Jiang Y, Bei W, Li W, Huang Y, He S, Zhu X, et al. Single-cell transcriptome analysis reveals evolving tumour microenvironment induced by immunochemotherapy in nasopharyngeal carcinoma. *Clin Trans Med*. (2024) 14:e70061. doi: 10.1002/ctm2.70061

26. Skoulidis F, Araujo HA, Do MT, Qian Y, Sun X, Cobo AG, et al. Ctla4 blockade abrogates keap1/stk11-related resistance to pd-(L)1 inhibitors. *Nature*. (2024) 635 (8038):462-71. doi: 10.1038/s41586-024-07943-7

27. Wang K, Coutifaris P, Brocks D, Wang G, Azar T, Solis S, et al. Combination anti-pd-1 and anti-ctla-4 therapy generates waves of clonal responses that include progenitor-exhausted cd8(+) T cells. *Cancer Cell*. (2024) 42:1582–97.e10. doi: 10.1016/j.ccell.2024.08.007

28. van Gulijk M, van Krimpen A, Schetters S, Eterman M, van Elsas M, Mankor J, et al. Pd-L1 checkpoint blockade promotes regulatory T cell activity that underlies therapy resistance. *Sci Immunol*. (2023) 8:eabn6173. doi: 10.1126/sciimmunol.abn6173

29. Oxley EP, Kershaw NJ, Louis C, Goodall KJ, Garwood MM, Jee Ho SM, et al. Context-restricted pd-(L)1 checkpoint agonism by ctla4-ig therapies inhibits T cell activity. *Cell Rep*. (2024) 43:114834. doi: 10.1016/j.celrep.2024.114834

30. Chen YY, Zeng XT, Gong ZC, Zhang MM, Wang KQ, Tang YP, et al. Euphorbia pekinensis rupr. Sensitizes colorectal cancer to pd-1 blockade by remodeling the tumor microenvironment and enhancing peripheral immunity. *Phytomedicine: Int J phytotherapy phytopharmacology*. (2024) 135:156107. doi: 10.1016/j.phymed.2024.156107

31. Skubleny D, Purich K, McLean DR, Martins-Filho SN, Buttenschoen K, Haase E, et al. The tumour immune microenvironment drives survival outcomes and therapeutic response in an integrated molecular analysis of gastric adenocarcinoma. *Clin Cancer research: an Off J Am Assoc Cancer Res*. (2024) 30(23):5385-98. doi: 10.1158/1078-0432.Ccr-23-3523

32. Shitara K, Takashima A, Fujitani K, Koeda K, Hara H, Nakayama N, et al. Nab-paclitaxel versus solvent-based paclitaxel in patients with previously treated advanced gastric cancer (Absolute): an open-label, randomised, non-inferiority, phase 3 trial. *Lancet Gastroenterol hepatology*. (2017) 2:277–87. doi: 10.1016/s2468-1253(16)30219-9

33. Pang X, Huang Z, Zhong T, Zhang P, Wang ZM, Xia M, et al. Cadonilimab, a tetravalent pd-1/ctla-4 bispecific antibody with trans-binding and enhanced target binding avidity. *mAbs*. (2023) 15:2180794. doi: 10.1080/19420862.2023.2180794

34. Lou H, Cai H, Huang X, Li G, Wang L, Liu F, et al. Cadonilimab combined with chemotherapy with or without bevacizumab as first-line treatment in recurrent or metastatic cervical cancer (Compassion-13): A phase 2 study. *Clin Cancer research: an Off J Am Assoc Cancer Res*. (2024) 30:1501–08. doi: 10.1158/1078-0432.Ccr-23-3162

35. Frentzas S, Gan HK, Cosman R, Coward J, Tran B, Millward M, et al. A phase 1a/1b first-in-human study (Compassion-01) evaluating cadonilimab in patients with advanced solid tumors. *Cell Rep Med*. (2023) 4:101242. doi: 10.1016/j.xcrm.2023.101242

36. Gao X, Xu N, Li Z, Shen L, Ji K, Zheng Z, et al. Safety and antitumour activity of cadonilimab, an anti-pd-1/ctla-4 bispecific antibody, for patients with advanced solid tumours (Compassion-03): A multicentre, open-label, phase 1b/2 trial. *Lancet Oncol*. (2023) 24:1134–46. doi: 10.1016/s1470-2045(23)00411-4

37. . <Aacr2024_Ak104-302_Final.Pdf>.

38. Rached L, Laparra A, Sakkal M, Danlos FX, Barlesi F, Carbonnel F, et al. Toxicity of immunotherapy combinations with chemotherapy across tumor indications: current knowledge and practical recommendations. *Cancer Treat Rev*. (2024) 127:102751. doi: 10.1016/j.ctrv.2024.102751

39. Shah MA, Kennedy EB, Alarcon-Rozas AE, Alcindor T, Bartley AN, Malowany AB, et al. Immunotherapy and targeted therapy for advanced gastroesophageal cancer: asco guideline. *J Clin oncology: Off J Am Soc Clin Oncol*. (2023) 41:1470–91. doi: 10.1200/jco.22.02331

40. Liang H, Yan X, Li Z, Chen X, Qiu Y, Li F, et al. Clinical outcomes of conversion surgery following immune checkpoint inhibitors and chemotherapy in stage iv gastric cancer. *Int J Surg (London England)*. (2023) 109:4162–72. doi: 10.1097/js9.0000000000000738

41. Janjigian YY, Shitara K, Moehler M, Garrido M, Salman P, Shen L, et al. First-line nivolumab plus chemotherapy versus chemotherapy alone for advanced gastric, gastro-oesophageal junction, and oesophageal adenocarcinoma (Checkmate 649): A randomised, open-label, phase 3 trial. *Lancet (London England)*. (2021) 398:27–40. doi: 10.1016/s0140-6736(21)00797-2

42. Kang YK, Chen LT, Ryu MH, Oh DY, Oh SC, Chung HC, et al. Nivolumab plus chemotherapy versus placebo plus chemotherapy in patients with her2-negative, untreated, unresectable advanced or recurrent gastric or gastro-oesophageal junction cancer (Attraction-4): A randomised, multicentre, double-blind, placebo-controlled, phase 3 trial. *Lancet Oncol*. (2022) 23:234–47. doi: 10.1016/s1470-2045(21)00692-6

43. Schutte T, Derks S, van Laarhoven HWM. Pembrolizumab plus chemotherapy for advanced gastric cancer. *Lancet Oncol*. (2024) 25:e51. doi: 10.1016/s1470-2045(23)00621-6

44. Kang YK, Terashima M, Kim YW, Boku N, Chung HC, Chen JS, et al. Adjuvant nivolumab plus chemotherapy versus placebo plus chemotherapy for stage iii gastric or gastro-oesophageal junction cancer after gastrectomy with D2 or more extensive lymph-node dissection (Attraction-5): A randomised, multicentre, double-blind, placebo-controlled, phase 3 trial. *Lancet Gastroenterol hepatology*. (2024) 9:705–17. doi: 10.1016/s2468-1253(24)00156-0

45. An M, Mehta A, Min BH, Heo YJ, Wright SJ, Parikh M, et al. Early immune remodeling steers clinical response to first-line chemoimmunotherapy in advanced gastric cancer. *Cancer Discovery*. (2024) 14:766–85. doi: 10.1158/2159-8290.Cd-23-0857

46. Topp BG, Channavazzala M, Mayawala K, De Alwis DP, Rubin E, Snyder A, et al. Tumor dynamics in patients with solid tumors treated with pembrolizumab beyond disease progression. *Cancer Cell*. (2023) 41:1680–88.e2. doi: 10.1016/j.ccell.2023.08.004

47. Yochum ZA, Braun DA. Rechallenging with anti-pd-1 therapy in advanced renal cell carcinoma. *Lancet (London England)*. (2024) 404:1280–82. doi: 10.1016/s0140-6736(24)01866-x

48. Sun L, Cohen RB, D'Avella CA, Singh AP, Schoenfeld JD, Hanna GJ. Overall survival, treatment duration, and rechallenge outcomes with ici therapy for recurrent or metastatic hnscc. *JAMA network Open*. (2024) 7:e2428526. doi: 10.1001/jamanetworkopen.2024.28526

49. Baessler A, Fuchs B, Perkins B, Richens AW, Novis CL, Harrison-Chau M, et al. Tet2 deletion in cd4+ T cells disrupts th1 lineage commitment in memory cells and enhances T follicular helper cell recall responses to viral rechallenge. *Proc Natl Acad Sci United States America*. (2023) 120:e2218324120. doi: 10.1073/pnas.2218324120

50. Gang X, Yan J, Li X, Shi S, Xu L, Liu R, et al. Immune checkpoint inhibitors rechallenge in non-small cell lung cancer: current evidence and future directions. *Cancer letters*. (2024) 604:217241. doi: 10.1016/j.canlet.2024.217241

51. Virassamy B, Caramia F, Savas P, Sant S, Wang J, Christo SN, et al. Intratumoral cd8(+) T cells with a tissue-resident memory phenotype mediate local immunity and immune checkpoint responses in breast cancer. *Cancer Cell*. (2023) 41:585–601.e8. doi: 10.1016/j.ccell.2023.01.004

52. Kuhn NF, Lopez AV, Li X, Cai W, Daniyan AF, Brentjens RJ. Cd103(+) cdc1 and endogenous cd8(+) T cells are necessary for improved cd40l-overexpressing car T cell antitumor function. *Nat Commun*. (2020) 11:6171. doi: 10.1038/s41467-020-19833-3

53. Robert C, Long GV, Brady B, Dutriaux C, Di Giacomo AM, Mortier L, et al. Five-year outcomes with nivolumab in patients with wild-type braf advanced melanoma. *J Clin oncology: Off J Am Soc Clin Oncol*. (2020) 38:3937–46. doi: 10.1200/jco.20.00995

54. Wolchok JD, Chiarion-Sileni V, Gonzalez R, Grob JJ, Rutkowski P, Lao CD, et al. Long-term outcomes with nivolumab plus ipilimumab or nivolumab alone versus ipilimumab in patients with advanced melanoma. *J Clin oncology: Off J Am Soc Clin Oncol*. (2022) 40:127–37. doi: 10.1200/jco.21.02229

55. Wolchok JD, Chiarion-Sileni V, Rutkowski P, Cowey CL, SChadendorf D, Wagstaff J, et al. Final, 10-year outcomes with nivolumab plus ipilimumab in advanced melanoma. *New Engl J Med*. (2024) 392(1):11-22. doi: 10.1056/NEJMoa2407417

56. Herbst RS, Garon EB, Kim DW, Cho BC, Perez-Gracia JL, Han JY, et al. Long-term outcomes and retreatment among patients with previously treated, programmed death-ligand 1–Positive, advanced non–Small-cell lung cancer in the keynote-010 study. *J Clin oncology: Off J Am Soc Clin Oncol*. (2020) 38:1580–90. doi: 10.1200/jco.19.02446

57. Lee CK, Kim HS, Jung M, Kim H, Bae WK, Koo DH, et al. Open-label, multicenter, randomized, biomarker-integrated umbrella trial for second-line treatment of advanced gastric cancer: K-umbrella gastric cancer study. *J Clin oncology: Off J Am Soc Clin Oncol*. (2024) 42:348–57. doi: 10.1200/jco.23.00971

58. Singh H, Lowder KE, Kapner K, Kelly RJ, Zheng H, McCleary NJ, et al. Clinical outcomes and ctdna correlates for capox betr: A phase ii trial of capecitabine, oxaliplatin, bevacizumab, trastuzumab in previously untreated advanced her2+ Gastroesophageal adenocarcinoma. *Nat Commun*. (2024) 15:6833. doi: 10.1038/s41467-024-51271-3

59. Shi M, Zeng D, Luo H, Xiao J, Li Y, Yuan X, et al. Tumor microenvironment rna test to predict immunotherapy outcomes in advanced gastric cancer: the times001 trial. *Med (New York NY)*. (2024) 5(11):1378-92. doi: 10.1016/j.medj.2024.07.006

60. Yagisawa M, Taniguchi H, Satoh T, Kadowaki S, Sunakawa Y, Nishina T, et al. Trastuzumab deruxtecan in advanced solid tumors with human epidermal growth factor receptor 2 amplification identified by plasma cell-free DNA testing: A multicenter, single-arm, phase ii basket trial. *J Clin oncology: Off J Am Soc Clin Oncol*. (2024) 42(32):3817-25. doi: 10.1200/jco.23.02626

61. Bos J, Groen-van Schooten TS, Brugman CP, Jamaludin FS, van Laarhoven HWM, Derks S. The tumor immune composition of mismatch repair deficient and epstein-barr virus-positive gastric cancer: A systematic review. *Cancer Treat Rev*. (2024) 127:102737. doi: 10.1016/j.ctrv.2024.102737

62. Kim CG, Koh JY, Shin SJ, Shin JH, Hong M, Chung HC, et al. Prior antibiotic administration disrupts anti-pd-1 responses in advanced gastric cancer by altering the gut microbiome and systemic immune response. *Cell Rep Med*. (2023) 4:101251. doi: 10.1016/j.xcrm.2023.101251

frontiers | Frontiers in Immunology

TYPE Original Research
PUBLISHED 31 March 2025
DOI 10.3389/fimmu.2025.1493234

OPEN ACCESS

EDITED BY
Elias Kouroumalis,
University of Crete, Greece

REVIEWED BY
Mithun Rudrapal,
Vignan's Foundation for Science, Technology and Research, India
Netzahualcóyotl Castañeda-Leyva,
Autonomous University of Aguascalientes, Mexico

*CORRESPONDENCE
Ji Ma
maji@wchscu.cn
Dan Cao
caodan@scu.edu.cn

†These authors have contributed equally to this work and share first authorship

RECEIVED 08 September 2024
ACCEPTED 14 March 2025
PUBLISHED 31 March 2025

CITATION
Zheng Y, Guo J, Ren T, Ma J and Cao D (2025) Efficacy and safety of immune checkpoint inhibitors in advanced biliary tract cancer: a real-world study. *Front. Immunol.* 16:1493234. doi: 10.3389/fimmu.2025.1493234

Efficacy and safety of immune checkpoint inhibitors in advanced biliary tract cancer: a real-world study

Yichen Zheng†, Jiamin Guo†, Tonghui Ren, Ji Ma* and Dan Cao*

Department of Medical Oncology, Cancer Center and Laboratory of Molecular Targeted Therapy in Oncology, West China Hospital, Sichuan University, Chengdu, Sichuan, China

Background: Immune checkpoint inhibitors (ICIs) combined with gemcitabine and cisplatin chemotherapy have become the standard first-line treatment for advanced biliary tract cancer (BTC). However, real-world evidence on domestic ICIs widely used in China and the therapeutic outcomes across treatment lines remains limited. This study aimed to assess the real-world effectiveness and safety profiles of ICIs in advanced BTC patients, while concurrently elucidating potential efficacy variations among distinct ICI subtypes.

Methods: We analyzed patients with unresectable, locally advanced, or metastatic BTC treated with ICIs at West China Hospital (January 2019–October 2023). Primary endpoint was overall survival (OS), while secondary endpoints included progression-free survival (PFS), objective response rate (ORR), disease control rate (DCR), and safety. Kaplan-Meier survival curves, propensity score matching (PSM), and Cox proportional hazards regression analyzed treatment efficacy.

Results: A total of 221 advanced BTC patients were enrolled. Among them, 137 patients received ICIs treatment in the first line, while 84 patients in the second or later lines. For patients treated with ICIs as first-line therapy, the median OS was 15.7 months (95% CI: 13.1-19.8) and PFS was 8.4 months (95% CI: 7.6-10.3). In contrast, patients treated in second or later lines had shorter median OS of 9.8 months (95% CI: 8.1–12.3) and median PFS of 5.6 months (95% CI: 4.2–6.8). The reduced efficacy in later-line treatments may reflect prior therapeutic resistance and generally poorer patient conditions compared to first-line recipients. 211 (95.5%) patients experienced at least one adverse event (AE), and 93 (42.1%) of them experienced grade 3 or higher AEs. The incidence of immune-related adverse events (irAEs) was 35.8%, with 8.6% of patients experiencing grade 3-4 irAEs. The most common ICI treatments are with Durvalumab or Sintilimab, which we are interested in comparing. Durvalumab showed numerically superior OS vs Sintilimab (19.3 vs 10.2 months, $p<0.001$) in unmatched analysis, though significance attenuated after PSM (16.1 vs 13.1 months, $p=0.299$).

Conclusion: ICIs demonstrate robust efficacy and manageable toxicity in real-world settings, supporting their use in both first- and later-line treatments for advanced BTC. However, whether domestic ICI alternatives remain viable options warranting further validation.

KEYWORDS

biliary tract cancer, immune checkpoint inhibitors, real-world study, efficacy, safety, first-line, second or later lines

1 Introduction

Biliary tract cancer (BTC) includes intrahepatic cholangiocarcinoma (ICC), perihilar cholangiocarcinoma, distal cholangiocarcinoma, and gallbladder cancer (1). Compared to other gastrointestinal tumors, BTC is relatively rare. However, its incidence is increasing globally (1). Due to late diagnosis, high tumor aggressiveness, and limited effective treatment options, the prognosis of BTC is generally poor (2). For localized disease, surgical resection remains the only potentially curative method, but the postoperative recurrence rate is as high as 70%-75% (3). Additionally, many patients are diagnosed at an advanced stage, limiting surgical treatment options. According to the ABC-02 trial results, gemcitabine combined with cisplatin chemotherapy was the main treatment for locally advanced or metastatic BTC, but the efficacy was not ideal (4). Over the following decade, many attempts were made to improve efficacy, such as using novel drugs or adding a third chemotherapeutic agent to the cisplatin-gemcitabine (CisGem) regimen, but unfortunately, clinical improvements were not significant (5).

In recent years, immune checkpoint inhibitors (ICIs) have been rapidly changing the treatment paradigm across various cancer types. However, BTC is typically considered an immunologically "cold" tumor (6–8), and thus the clinical efficacy of ICIs in BTC has generally been disappointing. With the exception of select patient subgroups exhibiting high microsatellite instability (MSI-H)/mismatch repair deficiency (dMMR) or high PD-L1 expression (9), the effectiveness of ICIs remains limited. Data from various small single-arm studies indicate that, for the broader BTC patient population, ICIs yield ORR ranging from 3% to 13% and median OS ranging from 5.2 to 8.1 months (10, 11). Only with the recent publication of the TOPAZ-1 and KEYNOTE-966 trials have ICIs been formally incorporated into first-line treatment for advanced BTC. Specifically, the TOPAZ-1 trial demonstrated that durvalumab combined with CisGem significantly improved median OS (12.8 vs. 11.5 months) and PFS (7.2 vs. 5.7 months) compared to chemotherapy alone (12). Similarly, the KEYNOTE-966 study indicated that pembrolizumab combined with CisGem significantly extended median OS (12.7 vs. 10.9 months) and PFS (6.5 vs. 5.6 months) (13). Nevertheless, these survival gains have been modest. Therefore, the overall efficacy of ICIs in advanced BTC warrants further exploration in real-world settings.

However, treatment options remain very limited for advanced BTC that has failed first-line treatment. Although the ABC-06 study evaluated FOLFOX (folinic acid, fluorouracil, and oxaliplatin) as a second-line treatment after CisGem progression, the efficacy was low, and chemotherapy alone could not meet clinical needs (14). Furthermore, several promising targets have been identified in BTC, including fibroblast growth factor receptor 2 (FGFR-2) fusions/rearrangements, isocitrate dehydrogenase 1/2 (IDH-1/2) mutations, human epidermal growth factor receptor 2 (HER-2) amplification, B-Raf proto-oncogene serine/threonine kinase (BRAF) V600E mutation, and neurotrophic tyrosine receptor kinase (NTRK) fusions. Targeted therapies against these targets have shown promising results in some phase II studies (15). Accumulated clinical evidence has suggested that systemic treatment with tyrosine kinase inhibitors (TKIs) combined with immunotherapy may improve clinical outcomes in advanced BTC patients who have failed first-line treatment (16, 17). Nevertheless, the value of immunotherapy in the later lines for advanced BTC still lacks high-quality evidence and remains in the clinical exploration stage.

Although pembrolizumab and Durvalumab are recommended as the standard first-line immunotherapeutic agents for advanced BTC, their high cost and lack of health insurance coverage make them difficult choices for many patients in China. Some domestic PD-1 or PD-L1, due to their lower cost and higher accessibility, are more widely used among Chinese patients, but their specific efficacy has not been evaluated. Although several real-world studies have assessed the efficacy of these ICIs in advanced BTC (18, 19), the limited sample size and different research focus indicated the need for more evidence. In summary, there is currently a lack of data on the efficacy and safety of ICIs treatment for advanced BTC patients (including first-line or ≥2 lines), as well as an analysis of the differences among various ICIs drugs.

Therefore, we conducted this single-center real-world study with a large sample size and detailed subgroup analysis to reflect the safety and efficacy of ICIs in different treatment stages of advanced BTC.

2 Methods

2.1 Study design

This study is a retrospective single-center analysis of real-world data. The study population included patients with unresectable, locally advanced, or metastatic BTC who received ICIs treatment at West China hospital between January 2019 and October 2023. Inclusion criteria were as follows: histologically confirmed advanced, unresectable, or metastatic BTC; age ≥18 years; any gender; ECOG performance status of 0-1; and at least two cycles of immunotherapy, whether as monotherapy or in combination with chemotherapy. Patients with incomplete clinical information or without pathological evidence of BTC were excluded (Figure 1). We collected clinical characteristics, laboratory and imaging reports, treatment history, survival status, treatment-related adverse events (AEs), and immune-related adverse events (irAEs) through electronic medical records and telephone follow-ups. The follow-up cutoff date was April 30, 2024.

2.2 Treatment protocol

The treatment regimens and dosages of ICIs, chemotherapeutic drugs, and targeted therapy drugs in this study were determined by oncologists. The initial doses were based on the guidelines of the National Comprehensive Cancer Network (NCCN) or the Chinese Society of Clinical Oncology (CSCO). The most common ICIs included Durvalumab 1500 mg every three weeks, Sintilimab, pembrolizumab, and camrelizumab 200 mg every three weeks, and toripalimab 240 mg every three weeks. Only a minority of patients received alternative ICIs such as Nivolumab and Tislelizumab. The doses of chemotherapeutic and targeted drugs were adjusted during treatment based on patient tolerance and general condition.

2.3 Evaluation

Baseline CT or MRI scans were performed before starting ICIs treatment, followed by imaging assessments every 2-3 cycles. Tumor efficacy was evaluated according to the Response Evaluation Criteria in Solid Tumors (RECIST 1.1) (20). The primary endpoint of this study was overall survival (OS), and secondary endpoints included progression-free survival (PFS), objective response rate (ORR), disease control rate (DCR), and safety. OS was defined as the time from initiation of ICIs treatment to death caused by cancer. PFS was defined as the time from initiation of ICIs treatment to disease progression, death, or the last follow-up date (whichever occurred first). Patients lost to follow-up were right censored at the last contact date. ORR was defined as the proportion of patients achieving complete response (CR) or partial response (PR) according to RECIST 1.1 criteria. DCR was defined as the proportion of patients achieving CR, PR, and stable disease (SD). Safety assessment included the occurrence of AEs from the start of ICIs treatment to the last follow-up. This included irAEs (mainly rash, thyroid-related events, immune-related pneumonitis, immune-related myocarditis, etc.) and other adverse events. The severity of AEs was graded according to the Common Terminology Criteria for Adverse Events (CTCAE) version 5.0 (21), and the incidence of irAEs was calculated separately.

2.4 Statistical analysis

Quantitative data were analyzed using t-tests or Mann-Whitney U tests (for non-normally distributed data), and qualitative data were analyzed using chi-square test or Fisher's exact probability method. In survival analysis, hazard ratios (HRs) and their corresponding p-values were calculated using both univariate and multivariate Cox proportional hazards regression models (22). Multivariate cox regression covariates were selected based on univariate analysis ($p<0.1$). Kaplan-Meier (KM) method was used

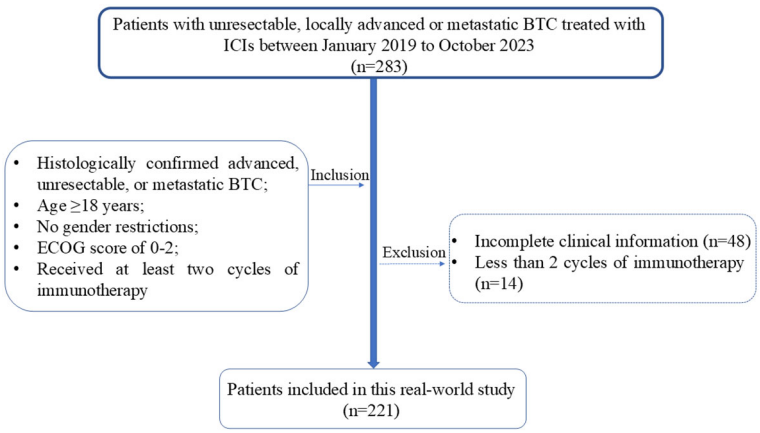

FIGURE 1
Patients inclusion and exclusion flowchart. BTC. BTC, Biliary Tract Cancer; ECOG, Eastern Cooperative Oncology Group; ICIs, Immune Checkpoint Inhibitors.

to plot survival curves (23). The fundamental formula of the Cox proportional hazards regression model is as follows:

$$h(t \mid X) = h_0(t)\exp(\beta_1 X_1 + \beta_2 X_2 + \cdots + \beta_p X_p)$$

In this equation, $h(t|X)$ represents the instantaneous hazard at time t, given the covariates X. The term $h_0(t)$ is the baseline hazard function, which indicates the hazard when all covariates are zero. The expression $\exp(\beta_1 X_1 + \beta_2 X_2 + \cdots + \beta_p X_p)$ is the linear combination of covariates, reflecting the influence of these covariates on the hazard. Here, $\beta_1,\beta_2,\ldots\beta_p$ are the regression coefficients, quantifying the effect of each covariate on the hazard. Finally, $X_1,X_2,\ldots X_p$ are the covariates, which can be either continuous or categorical variables.

Due to the retrospective nature of this study and the observed baseline differences between patients receiving Durvalumab and Sintilimab treatments, propensity score matching (PSM) was employed (24, 25) to address the limitations of using regression analysis to adjust for potential confounders, particularly when the effective sample size (number of outcome events) is small (26, 27). This approach aimed to minimize confounding factors and enhance comparability between treatment groups, facilitating a more robust evaluation of the efficacy and safety of the two regimens. Propensity scores were calculated using logistic regression, incorporating potential confounders that could influence OS as matching variables. These confounders were identified as factors with a p-value< 0.1 in the univariate Cox proportional hazards regression analysis of OS in the pre-matched sample. The formula for estimating propensity scores using the logistic regression model is as follows:

$$logit[P(G = 1 \mid X)] = \alpha + \beta_1 x_1 + \cdots + \beta_m x_m$$

In this formula, G represents the group or exposure factor, where $G = 1$ indicates the individual is in the exposed group and $G = 0$ indicates the individual is in the control group. X is the vector of covariates, $X = (x_1,x_2,\ldots,x_m)$, while $P(G = 1X)$ represents the estimated probability of an individual receiving the treatment ($G = 1$) given the covariates X, which corresponds to the individual's propensity score. A 1:2 nearest neighbor matching method with a caliper width of 0.1(the maximum allowable difference in propensity scores) was applied to match individuals based on their propensity scores (24, 25, 28). Although equal ratio matching is sometimes considered more persuasive, the disparity in group sizes justified using a 1:2 matching ratio to better utilize available data. Nevertheless, we conducted a 1:1 matching as a sensitivity analysis. A p-value<0.05 was considered statistically significant. Data analysis and survival curve plotting were performed using R software.

3 Results

3.1 Patient baseline characteristics

A total of 221 patients with advanced BTC who met the study criteria were included. This cohort comprised 142 cases of intrahepatic cholangiocarcinoma (64.3%), 41 cases of extrahepatic cholangiocarcinoma (18.6%), and 38 cases of gallbladder cancer (17.2%). Among them, there were 117 male patients (52.9%) and 104 female patients (47.1%). Chronic hepatitis B virus infection was present in 152 patients (68.8%). 110 patients (49.8%) had primary unresectable tumors, and 111 patients (50.2%) had postoperative recurrence. Metastatic BTC was present in 80.1% of the patients, while 19.9% had locally advanced BTC. More than half of the patients (62.0%) had poorly differentiated tumors. In the entire cohort, 137 patients (62.0%) received ICIs as first-line treatment, while 84 patients (38.0%) received ICIs as second or later-lines treatment. 148 patients (67.0%) were treated with PD-1 inhibitors, and 73 patients (33.0%) were treated with PD-L1 inhibitors. The most commonly used ICIs included Durvalumab (59 patients, 26.7%), Sintilimab (50 patients, 22.6%), Camrelizumab (25 patients, 11.3%), Pembrolizumab (20 patients, 9.0%) and Toripalimab (20 patients, 9.0%). In addition, 192 patients (86.9%) received chemotherapy combined with immunotherapy, 41 patients (18.6%) received anti-angiogenic therapy, 53 patients (24.0%) received radiotherapy, and 56 patients (25.3%) received local interventional therapy. Baseline sociodemographic and clinical characteristics of all patients are shown in Table 1.

3.2 Efficacy

The median follow-up duration for the entire cohort was 10.1 months (95% CI: 9.6-10.7). Among the 221 patients, 2 achieved CR (0.9%), 50 achieved PR (22.6%), 112 achieved SD (50.7%), and 57 did not achieve either response or disease control, experiencing progressive disease (PD) at the time of the first efficacy assessment (25.8%). The ORR and DCR were 23.5% and 74.2%, respectively. In the first-line treatment group, 2 patients achieved CR (1.5%), 40 achieved PR (29.2%), 73 achieved SD (53.3%), and 22 experienced PD (16.1%). The ORR and DCR for first-line patients were 30.7% and 83.9%, respectively. In the second or later-lines treatment group, no patients achieved CR, 10 achieved PR (11.9%), 39 achieved SD (46.4%), and 35 experienced PD (41.7%). The ORR and DCR were 11.9% and 58.3%, respectively (Table 2).

By the follow-up cutoff date (April 30, 2024), 174 patients experienced disease progression, and 126 of them died. The median OS and PFS for the entire cohort were 12.9 months (95% CI: 11.7-14.9) and 7.2 months (95% CI: 6.3-8.2), respectively. For patients receiving first-line ICIs treatment, the median OS was 15.7 months (95% CI: 13.1-19.8) and PFS was 8.4 months (95% CI: 7.6-10.3). For patients receiving second or later-lines ICIs treatment, the median OS was 9.8 months (95% CI: 8.1-12.3) and PFS was 5.6 months (95% CI: 4.2-6.8). The OS and PFS for first-line and second or later-lines are shown in Figure 2. Univariate and multivariate Cox regression analysis (Table 3) indicated that tumor differentiation, pre-treatment CA-199 levels<500 U/ml, pre-treatment CA-125 levels<28.65 U/ml, and the number of ICIs treatment lines were independent risk factors for OS (p<0.05). All these factors, together with received subsequent treatments, were the independent predictive factors for PFS (p<0.05) (Supplementary Table S1).

10.3389/fimmu.2025.1493234

TABLE 1 Patients' characteristics in the entire cohort.

Characteristic	Overall, N = 221[1]	First line, N = 137[1]	≥2 lines, N = 84[1]
Age, years	58.0 (10.3)	57.7 (10.8)	58.4 (9.4)
Sex			
Male	117 (52.9%)	74 (54.0%)	43 (51.2%)
Female	104 (47.1%)	63 (46.0%)	41 (48.8%)
Virology_status			
No viral hepatitis	68 (30.8%)	38 (27.7%)	30 (35.7%)
Any viral hepatitis B	152 (68.8%)	98 (71.5%)	54 (64.3%)
Prior hepatitis C	1 (0.5%)	1 (0.7%)	0 (0%)
Disease_status			
Initially unresectable	110 (49.8%)	85 (62.0%)	25 (29.8%)
Recurrent	111 (50.2%)	52 (38.0%)	59 (70.2%)
Disease_classification			
Locally advanced	44 (19.9%)	30 (21.9%)	14 (16.7%)
Metastatic	177 (80.1%)	107 (78.1%)	70 (83.3%)
Site_of_origin			
Intrahepatic	142 (64.3%)	96 (70.1%)	46 (54.8%)
Extrahepatic	41 (18.6%)	23 (16.8%)	18 (21.4%)
Gallbladder	38 (17.2%)	18 (13.1%)	20 (23.8%)
Degree_of_differentiation			
Poorly	137 (62.0%)	92 (67.2%)	45 (53.6%)
moderately-to-well	84 (38.0%)	45 (32.8%)	39 (46.4%)
Type_of_ICIs			
Anti-PD-1	148 (67.0%)	74 (54.0%)	74 (88.1%)
Anti-PD-L1 = 1	73 (33.0%)	63 (46.0%)	10 (11.9%)
ICIs			
Durvalumab	59 (26.7%)	52 (38.0%)	7 (8.3%)
Sintilimab	50 (22.6%)	21 (15.3%)	29 (34.5%)
Camrelizumab	25 (11.3%)	12 (8.8%)	13 (15.5%)
Pembrolizumab	20 (9.0%)	13 (9.5%)	7 (8.3%)
Toripalimab	20 (9.0%)	6 (4.4%)	14 (16.7%)
others	47 (21.3%)	33 (24.1%)	14 (16.7%)
Combination_with_chemotherapy			
No	29 (13.1%)	4 (2.9%)	25 (29.8%)
Yes	192 (86.9%)	133 (97.1%)	59 (70.2%)
Combination_with_anti_angiogenic_drugs			
No	180 (81.4%)	124 (90.5%)	56 (66.7%)
Yes	41 (18.6%)	13 (9.5%)	28 (33.3%)

(Continued)

TABLE 1 Continued

Characteristic	Overall, N = 221[1]	First line, N = 137[1]	≥2 lines, N = 84[1]
ECOG_performance_status			
0	165 (74.7%)	105 (76.6%)	60 (71.4%)
1	55 (24.9%)	32 (23.4%)	23 (27.4%)
2	1 (0.5%)	0 (0%)	1 (1.2%)
Have_received_radiotherapy			
No	168 (76.0%)	110 (80.3%)	58 (69.0%)
Yes	53 (24.0%)	27 (19.7%)	26 (31.0%)
Have_undergone_interventional_therapy			
No	165 (74.7%)	102 (74.5%)	63 (75.0%)
Yes	56 (25.3%)	35 (25.5%)	21 (25.0%)
Pre_treatment_CA199_level_less_than_500 U/mL			
No	65 (29.4%)	38 (27.7%)	27 (32.1%)
Yes	156 (70.6%)	99 (72.3%)	57 (67.9%)
Pre_treatment_CEA_level_less_than_5 ng/mL			
No	82 (37.1%)	49 (35.8%)	33 (39.3%)
Yes	139 (62.9%)	88 (64.2%)	51 (60.7%)
Pre_treatment_CA125_less_than_28.65 U/mL			
No	115 (52.0%)	68 (49.6%)	47 (56.0%)
Yes	106 (48.0%)	69 (50.4%)	37 (44.0%)
NLR_less_than_3			
No	110 (49.8%)	65 (47.4%)	45 (53.6%)
Yes	111 (50.2%)	72 (52.6%)	39 (46.4%)

CA125, Cancer Antigen 125; CA199, Carbohydrate Antigen 19-9; CEA, Carcinoembryonic Antigen; ECOG, Eastern Cooperative Oncology Group; ICI, Immune Checkpoint Inhibitor; NLR, Neutrophil-to-Lymphocyte Ratio.
[1] Sample mean (SD), for age characteristic; Sample size n (percent %), for others.

This suggests a consistent relationship between the two outcome indicators, OS and PFS.

Among 221 patients, Durvalumab (59 patients, 26.7%) and Sintilimab (50 patients, 22.6%) were the most commonly used ICIs. Significant baseline differences existed between these groups before PSM, including age, disease status, chemotherapy, anti-angiogenic therapy, treatment lines, and CA125 levels (Supplementary Table S2). PSM balanced potential confounders that could influence OS (Supplementary Table S3), but differences in age, disease status, and anti-angiogenic therapy persisted (Supplementary Table S4). In the unmatched cohort, Durvalumab showed superior OS (median: 19.3 months, 95% CI: 14.1–not estimable) vs. Sintilimab (10.2 months, 95% CI: 8.6–13.1; HR: 2.47, 95% CI: 1.46–4.20, p< 0.001; Figure 3A).

TABLE 2 Tumor response in patients treated with ICIs therapy, for overall sample, first-line, and ≥2-lines.

Tumor response	All patients (n=221)	First line (n=137)	≥2 lines (n=84)
CR	2 (0.9%)	2 (1.5%)	0
PR	50 (22.6%)	40 (29.2%)	10 (11.9%)
SD	112 (50.7%)	73 (53.3%)	39 (46.4%)
PD	57 (25.8%)	22 (16.1%)	35 (41.7%)
ORR (CR+PR)	52 (23.5%)	42 (30.7%)	10 (11.9%)
DCR (CR+PR+SD)	164 (74.2%)	115 (83.9%)	49 (58.3%)

CR, Complete Response; PR, Partial Response; SD, Stable Disease; PD, Progressive Disease.

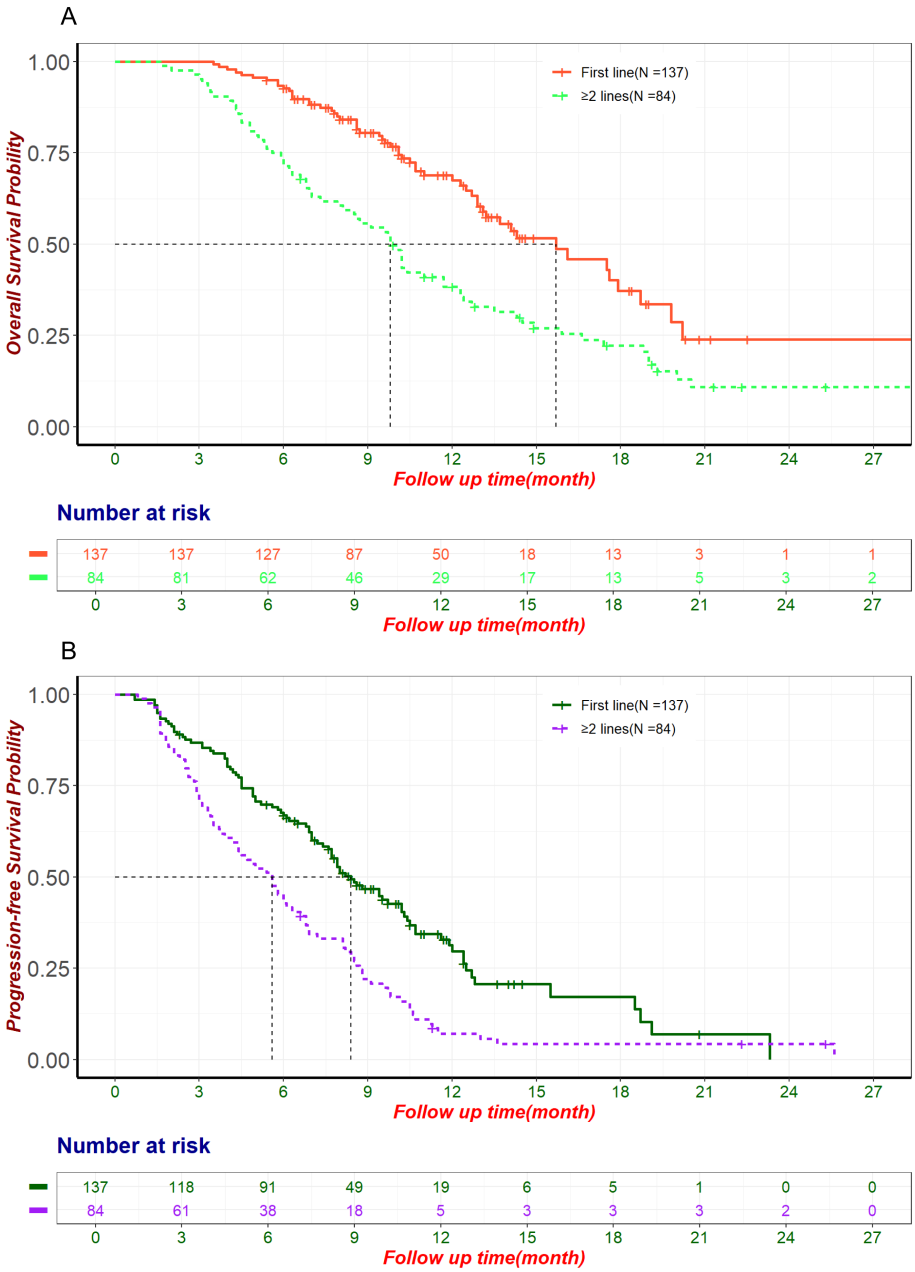

FIGURE 2
The OS and PFS for first-line and second or later-lines. **(A)** Kaplan-Meier curve of OS in patients treated with ICIs in the first line and second or later-lines. **(B)** Kaplan-Meier curve of PFS in patients treated with ICIs in the first line and second or later-lines. ICIs, Immune Checkpoint Inhibitors; OS, Overall Survival; PFS, Progression-Free Survival.

PFS was also longer for Durvalumab (median: 7.9 months, 95% CI: 6.0–10.4) vs. Sintilimab (5.0 months, 95% CI: 3.9–8.6; HR: 1.66, 95% CI: 1.08–2.55, p = 0.021; Figure 3B). However, patients in the Durvalumab group had more favorable prognostic factors such as predominantly first-line treatment, necessitating further adjustment for potential biases. After multivariate Cox regression, OS differences remained significant (HR: 2.16, 95% CI: 1.07–4.36, p = 0.031; Figure 3A), while PFS differences did not (HR: 1.43, 95% CI: 0.85–2.40, p = 0.177; Figure 3B). Given the limitations of regression analysis in small samples, we conducted an exploratory PSM analysis to further control for confounding factors. After PSM (67 matched patients), no significant OS difference was observed (Durvalumab: 16.1 months, 95% CI: 12.5–not estimable; Sintilimab: 13.1 months, 95% CI: 11.0–not estimable; HR: 1.50, 95% CI: 0.70–3.20, p = 0.299; Supplementary Figure S1). Multivariate Cox proportional hazards regression in the matched cohort (adjusted HR: 2.08, 95% CI: 0.81–5.37, p = 0.129; Supplementary Figure S1) and sensitivity analysis using 1:1 matching ratio (Supplementary Figure S2) confirmed this. ORR was higher with Durvalumab (27%) than Sintilimab (14%) in the unmatched cohort, although this difference was not statistically significant (p = 0.094). The observed trend suggests a potential

10.3389/fimmu.2025.1493234

TABLE 3 Univariate and multivariate cox proportional hazards regression for OS in the overall population.

Covariate	All patients (n=221)	HR (univariable)	HR (multivariable)
Sex			
Male	117 (52.9%)		
Female	104 (47.1%)	0.93 (0.65-1.33, p=.698)	
Age (Mean ± SD)	58.0 ± 10.3	1.01 (0.99-1.03, p=.326)	
Virology_status			
No viral hepatitis	68 (30.8%)		
Any viral hepatitis B	152 (68.8%)	0.94 (0.65-1.37, p=.754)	
Prior hepatitis C	1 (0.5%)	3.54 (0.48-26.0, p=.215)	
Disease_status			
Initially unresectable	110 (49.8%)		
Recurrent	111 (50.2%)	1.02 (0.71-1.46, p=.920)	
Disease_classification			
Locally advanced	44 (19.9%)		
Metastatic	177 (80.1%)	1.47 (0.92-2.36, p=.110)	
Site_of_origin			
Intrahepatic	142 (64.3%)		
Extrahepatic	41 (18.6%)	1.63 (1.03-2.57, p=.035) *	1.40 (0.88-2.21, p=.155)
Gallbladder	38 (17.2%)	1.72 (1.13-2.63, p=.012) *	1.02 (0.64-1.63, p=.936)
Degree_of_differentiation			
Poorly	137 (62.0%)		
moderately-to-well	84 (38.0%)	0.65 (0.45-0.94, p=.022) *	0.58 (0.39-0.85, p=.006) *
Type_of_ICIs			
Anti-PD-1	148 (67.0%)		
Anti-PD-L1	73 (33.0%)	0.52 (0.34-0.78, p=.002) *	0.66 (0.41-1.04, p=.075)
Combination_with_chemotherapy			
No	29 (13.1%)		
Yes	192 (86.9%)	0.85 (0.53-1.38, p=.517)	
Combination_with_anti_angiogenic_drugs			
No	180 (81.4%)		
Yes	41 (18.6%)	1.15 (0.75-1.76, p=.528)	
ECOG_performance_status			
0	165 (74.7%)		
≥1	56 (25.3%)	1.23 (0.84-1.81, p=.287)	
Have_received_radiotherapy			
No	168 (76.0%)		
Yes	53 (24.0%)	0.86 (0.57-1.29, p=.467)	
Have_undergone_interventional_therapy			
No	165 (74.7%)		

(Continued)

TABLE 3 Continued

Covariate	All patients (n=221)	HR (univariable)	HR (multivariable)
Have_undergone_interventional_therapy			
Yes	56 (25.3%)	0.73 (0.48-1.10, p=.134)	
Occurrence_of_irAE			
No	142 (64.3%)		
Yes	79 (35.7%)	0.88 (0.61-1.27, p=.493)	
Pre_treatment_CA199_level_less_than_500 U/mL			
No	65 (29.4%)		
Yes	156 (70.6%)	0.42 (0.29-0.61, p<.001) *	0.35 (0.23-0.53, p<.001) *
Pre_treatment_CEA_level_less_than_5 ng/mL			
No	82 (37.1%)		
Yes	139 (62.9%)	0.52 (0.37-0.75, p<.001) *	0.75 (0.51-1.11, p=.153)
Pre_treatment_CA125_less_than_28.65 U/mL			
No	115 (52.0%)		
Yes	106 (48.0%)	0.47 (0.32-0.68, p<.001) *	0.57 (0.38-0.85, p=.006) *
NLR_less_than_3			
No	110 (49.8%)		
Yes	111 (50.2%)	0.76 (0.53-1.08, p=.125)	
Received_subsequent_treatment			
No	124 (56.1%)		
Yes	97 (43.9%)	0.89 (0.63-1.28, p=.539)	
Use_of_antibiotics_within_one_month_after_immunotherapy			
No	211 (95.5%)		
Yes	10 (4.5%)	1.69 (0.74-3.86, p=.211)	
Smoking_status			
Never	170 (76.9%)		
Former/Current	51 (23.1%)	0.66 (0.42-1.05, p=.076)	0.85 (0.51-1.39, p=.508)
Line_of_treatment_for_ICIs			
First line	137 (62.0%)		
≥2 lines	84 (38.0%)	2.12 (1.48-3.03, p<.001) *	2.22 (1.47-3.33, p<.001) *

n=221, events=126 (for OS, events refer to the number of deaths caused by cancer).
CA125, Cancer Antigen 125; CA199, Carbohydrate Antigen 19-9; CEA, Carcinoembryonic Antigen; ECOG, Eastern Cooperative Oncology Group; ICIs, Immune Checkpoint Inhibitors; irAE, immune-related Adverse Event; NLR, Neutrophil-to-Lymphocyte Ratio; OS, Overall Survival; PD-1, Programmed Death-1; PD-L1, Programmed Death-Ligand 1.
*P < 0.05.

clinical benefit of Durvalumab. This is particularly noteworthy considering that statistical significance (p< 0.05) is relatively difficult to achieve in small-sample comparisons and should be interpreted as a reference tool rather than a definitive measure. Relying solely on p-values may underestimate the actual clinical significance of the observed difference.

The efficacy of other commonly used ICIs is as follows: Camrelizumab (used in 25 patients) demonstrated a median OS of 14.5 months (95% CI: 11.7-not estimable), a median PFS of 7.7 months (95% CI: 6.3-not estimable), and an ORR of 32%. Pembrolizumab (used in 20 patients) had a median OS of 10.2 months (95% CI: 9.6-not estimable), a median PFS of 7.55 months (95% CI: 5.9-18.7), and an ORR of 20%. Toripalimab (used in 20 patients) showed a median OS of 12.3 months (95% CI: 6.3-not estimable), a median PFS of 5.85 months (95% CI: 4.2-9.1), and an ORR of 15%. However, we did not conduct direct comparisons of the efficacy among these ICIs, and the reasons for this will be elaborated in the Discussion section.

3.3 Safety

Among the 221 patients receiving ICIs treatment for advanced BTC, 211(95.5%) patients experienced at least one AEs. A total of 93 patients (42.1%) experienced grade 3 or higher AEs. The most common AEs included anemia (40.3%), neutropenia (33.0%), thrombocytopenia (29.0%), and hypoproteinemia (19.9%) (Table 4). The most frequent grade 3-4 AEs were neutropenia (13.6%), thrombocytopenia (12.2%), hypoproteinemia (9.5%) and anemia (8.6%). Most patients improved with symptomatic supportive care and/or dose reduction, but 24 patients (10.9%) discontinued treatment due to intolerable AEs. There were no AE-related deaths in the entire cohort.

A total of 79 patients (35.8%) experienced irAEs, with the most common being hypothyroidism (17.2%), rash (6.3%), and cardiac events (including elevated troponin levels and myocarditis) (5.0%) (Table 5). 19 patients (8.6%) experienced grade 3/4 irAEs, including hypothyroidism (13 cases, 5.9%), rash (4 cases, 1.8%), and cardiac events (6 cases, 2.7%). Symptoms of irAEs improved or stabilized with systemic or local corticosteroid therapy and symptomatic

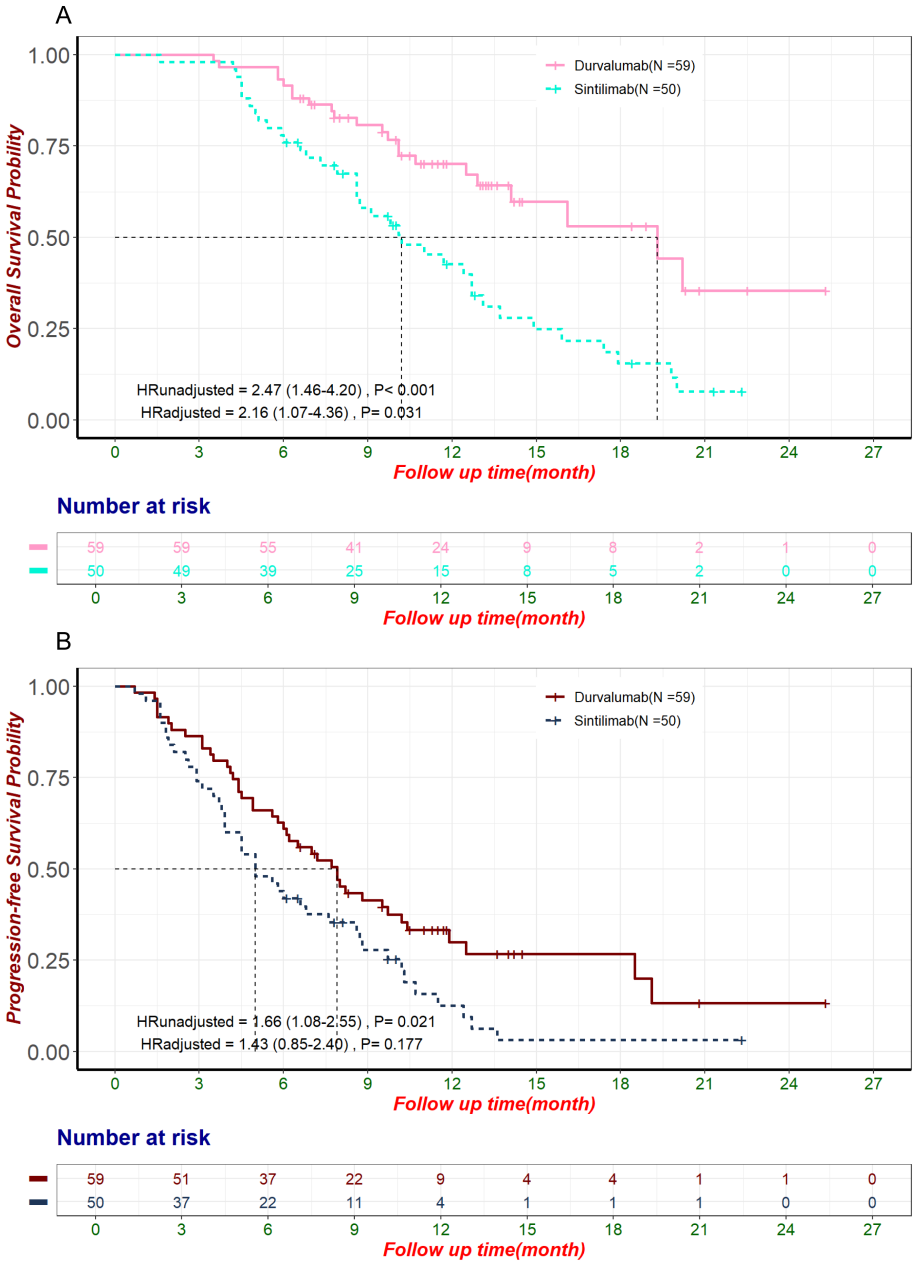

FIGURE 3
OS and PFS in the pre-matched sample of patients treated with Durvalumab and Sintilimab. HRunadjusted and HRadjusted represent the hazard ratios for Sintilimab compared to Durvalumab, derived from univariate and multivariate Cox proportional hazards regression analyses, respectively. **(A)** Kaplan-Meier curve of OS in the pre-matched sample of patients using Durvalumab and Sintilimab. **(B)** Kaplan-Meier curve of PFS in the pre-matched sample of patients using Durvalumab and Sintilimab. HR, Hazard Ratio; OS, Overall Survival; PFS, Progression-Free Survival.

supportive care, but 7 patients (3.2%) discontinued treatment due to intolerable irAEs. Among the 12 patients who experienced grade 3/4 irAEs but did not discontinue ICI therapy, all achieved resolution of irAEs after receiving interventions such as corticosteroids. Of these, four patients were identified as having PD during imaging evaluations conducted before the resumption of ICI therapy and therefore did not continue treatment. One patient experienced an allergic reaction upon resuming ICI therapy, which necessitated discontinuation. Another patient voluntarily discontinued treatment due to severe myelosuppression and a poor general condition. One patient developed intolerable rashes after restarting the original ICI regimen and did not proceed with maintenance therapy. Additionally, one patient stopped ICI treatment due to financial constraints. The remaining four patients successfully resumed the original ICI regimen under medical supervision and did not encounter further intolerable irAEs, enabling them to continue treatment. Of the 79 patients with irAEs, 18 received Durvalumab, 10 received Pembrolizumab, 20 received Sintilimab, 10 received Camrelizumab, 4 received Toripalimab, and 17 received other ICIs. Subgroup analysis of patients treated with Durvalumab and Sintilimab showed no significant differences in the incidence of AEs and irAEs between the two groups ($p>0.05$).

4 Discussion

The treatment options for advanced BTC are limited, and the prognosis is very poor. In recent years, positive results from numerous clinical studies have significantly changed the treatment paradigm for advanced BTC, making ICIs an important therapeutic option for this complex disease (12, 13). However, a substantial amount of real-world research is still needed to provide efficacy and safety data for ICIs in a broader patient population outside of clinical trials. Our study cohort was larger than previous, and the results showed that among the 221 advanced BTC patients treated with ICIs, the ORR and DCR were 23.5% and 74.2%, respectively, with a median PFS and OS of 7.2 months and 12.9 months. 42.1% of patients experienced grade 3/4 AEs, primarily hematological toxicities caused by myelosuppression; 8.6% of patients experienced grade ≥3 irAEs, mainly hypothyroidism and immune-related cardiac events. Our study results demonstrate that ICIs are an effective and safe option for treating advanced BTCs.

We set a minimum criterion of two cycles for ICI infusion, primarily because in China, imaging and efficacy evaluations are typically conducted after two to three cycles of systemic treatment. If tumor progression is observed at this stage, treatment plans are often adjusted, and ICI therapy may be discontinued. Excluding patients who received fewer than four infusions might inadvertently omit a significant subset of individuals who discontinued ICI due to an apparent poor response, potentially leading to a biased representation of the therapy's impact on advanced BTC. In the entire cohort, 137 patients (62.0%) received ICIs as first-line treatment, with a median OS and PFS of 15.7 months and 8.4 months, respectively, and ORR and DCR of 30.7% and 83.9%. The TOPAZ-1 trial reported that the median OS and PFS in the CisGem combined with Durvalumab group were significantly longer than those in the CisGem combined with the placebo group (median OS

TABLE 4 Treatment-related adverse events.

Adverse events	All patients (n=221)		First line (n=137)		≥2 lines (n=84)	
	Any grade	Grade 3 or 4	Any grade	Grade 3 or 4	Any grade	Grade 3 or 4
Total	211 (95.5%)	93 (42.1%)	129 (94.2%)	59 (43.1%)	82 (97.6%)	34 (40.5%)
Anemia	89 (40.3%)	19 (8.6%)	48 (35.0%)	8 (5.8%)	41 (48.8%)	11 (13.1%)
Neutropenia	73 (33.0%)	30 (13.6%)	34 (24.8%)	13 (9.5%)	39 (46.4%)	17 (20.2%)
Thrombocytopenia	64 (29.0%)	27 (12.2%)	33 (24.1%)	14 (10.2%)	31 (36.9%)	13 (15.5%)
Hypoproteinemia	44 (19.9%)	21 (9.5%)	19 (13.9%)	11 (8.0%)	25 (29.8%)	10 (11.9%)
Hypothyroidism	38 (17.2%)	13 (5.9%)	20 (14.6%)	7 (5.1%)	18 (21.4%)	6 (7.1%)
Elevated ALT or AST	34 (15.4%)	7 (3.2%)	21 (15.3%)	4 (2.9%)	13 (15.5%)	3 (3.6%)
Elevated bilirubin	20 (9.0%)	4 (1.8%)	8 (5.8%)	2 (1.5%)	12 (14.3%)	2 (2.4%)
Nausea and vomiting	17 (7.7%)	3 (1.4%)	12 (8.8%)	2 (1.5%)	5 (5.9%)	1 (1.2%)
Rash	14 (6.3%)	4 (1.8%)	6 (4.4%)	1 (0.7%)	8 (9.5%)	3 (3.6%)
Electrolyte disturbance	9 (4.1%)	1 (0.5%)	3 (2.2%)	0	6 (7.1%)	1 (1.2%)
Diarrhea	6 (2.7%)	0	4 (2.9%)	0	2 (2.4%)	0
Fever	5 (2.3%)	0	3 (2.2%)	0	2 (2.4%)	0
Fatigue	4 (1.8%)	1 (0.5%)	3 (2.2%)	0	1 (1.2%)	1 (1.2%)
Allergy	3 (1.4%)	1 (0.5%)	2 (1.4%)	1 (0.7%)	1 (1.2%)	0

ALT, Alanine Aminotransferase; AST, Aspartate Aminotransferase.

11.5 months vs. 12.8 months, median PFS 5.7 months vs. 7.2 months), with ORR and DCR of 26.7% and 85.3% in the Durvalumab combined treatment group (12). Similarly, the KEYNOTE-966 trial showed that the median OS and PFS for BTC patients treated with pembrolizumab combined with chemotherapy were 12.7 months and 6.5 months, respectively (13). Notably, our first-line cohort achieved superior OS and PFS compared to the TOPAZ-1 and KEYNOTE-966 trials, while the ORR and DCR remained comparable to those observed in TOPAZ-1. The following reasons may explain these longer survival data. Firstly, our study population consisted entirely of Chinese patients, whereas the TOPAZ-1 study observed that the survival period of Asian patients was higher than that of non-Asian patients, with a median OS of up to 13.6 months. The risk of death and progression decreased by 28% and 33%, respectively, and the discontinuation rate due to AEs was lower in the Asian population (29, 30). The specificity of the study population may be one of the important reasons for the long survival observed in our study. Secondly, the TOPAZ-1 study proved that patients with ICC benefited most significantly from Durvalumab combined with CisGem treatment (30). Compared to the TOPAZ-1 study, our first-line treatment included a higher proportion of ICC patients (70.1%) versus 55.3% in TOPAZ-1. Different anatomical sites of tumors in BTC patients respond differently to drugs, and the different proportions of anatomical sites in the study population may be another reason for the better survival data in our study. Thirdly, compared to the fixed treatment protocols in clinical trials, real-world treatment may include a wider variety of treatment combinations, such as intensified chemotherapy regimens, with or without anti-angiogenic therapy, or the addition of radiotherapy or interventional therapy to chemotherapy and immunotherapy. These local treatments not only exert a direct killing effect on tumor cells but may also trigger immunogenic cell death of tumor cells, release tumor-associated antigens, damage-associated molecular patterns (DAMPs), and cytokines that stimulate the host's immune response while reducing immunosuppressive factors within the tumor (such as regulatory T cells), thereby enhancing the efficacy of ICIs (31). In our first-line ICIs-treated patients, 19.7% received radiotherapy, 25.5% received interventional therapy, and 9.5% received anti-angiogenic therapy. Lastly, in the TOPAZ-1 study, the incidence of AEs was 99.4%, with grade 3/4 AEs at 75.7%. Compared to TOPAZ-1, the incidence of AEs and grade 3/4 AEs in our first-line treatment was lower, at 94.2% and 43.1%, respectively. Therefore, these patient characteristics, heterogeneity in treatment protocols, and the lower incidence of AEs may be the main reasons why our results differ from those of previous clinical studies.

In prior research, Rimini et al. first validated the results of the TOPAZ-1 trial in a real-world setting (18). Their study included 145 patients with advanced BTC receiving Durvalumab in combination with CisGem chemotherapy as first-line treatment, showing a median PFS of 8.9 months and median OS of 12.9 months. Their latest global multicenter real-world study reaffirmed the results of TOPAZ-1. The 666 patients had a median OS of 15.1 months and a median PFS of 8.2 months, which was generally consistent with the survival outcomes of our patients treated with ICIs in the first line (32). However, these studies only explored the performance of single-treatment regimens in real-world scenarios. Another study indicated that PD-1 inhibitor combination therapy in first-line treatment for advanced BTC resulted in a median PFS and OS of 6.6 months and 13.9 months, respectively (33). However, this real-world study had a sample size of only 54 patients, did not include gallbladder cancer patients, and included only PD-1 inhibitors as ICIs. In contrast, 46% of our first-line patients used PD-L1 inhibitors, with higher proportions receiving radiotherapy (19.7% vs. 5.6%) and anti-angiogenic therapy (9.5% vs. 5.6%), potentially contributing to the longer median OS and PFS observed in our study compared to theirs.

The ABC-06 trial investigated the efficacy of FOLFOX regimen as second-line chemotherapy for advanced BTC patients who progressed after first-line treatment (14). Results showed a median OS of only 6.2

TABLE 5 Immune-Related adverse events.

Immune-related adverse events	All patients (n=221)			First line (n=137)			≥2 lines (n=84)		
	Any grade	Grade 1 or 2	Grade 3 or 4	Any grade	Grade 1 or 2	Grade 3 or 4	Any grade	Grade 1 or 2	Grade 3 or 4
Total	79 (35.8%)	60 (27.1%)	19 (8.6%)	46 (33.6%)	35 (25.5%)	11 (8.0%)	33 (39.3%)	25 (29.8%)	8 (9.5%)
Hypothyroidism	38 (17.2%)	25 (11.3%)	13 (5.9%)	20 (14.6%)	13 (9.5%)	7 (5.1%)	18 (21.4%)	12 (14.3%)	6 (7.1%)
Rash	14 (6.3%)	10 (4.5%)	4 (1.8%)	6 (4.4%)	5 (3.6%)	1 (0.7%)	8 (9.5%)	5 (6.0%)	3 (3.6%)
Cardiac events	11 (5.0%)	5 (2.3%)	6 (2.7%)	5 (3.6%)	2 (1.5%)	3 (2.2%)	6 (7.1%)	3 (3.6%)	3 (3.6%)
Pneumonia	4 (1.8%)	1 (0.5%)	3 (1.4%)	3 (2.2%)	1 (0.7%)	2 (1.5%)	1 (1.2%)	0	1 (1.2%)
Colitis	1 (0.5%)	1 (0.5%)	0	0	0	0	1 (1.2%)	0	0
hepatitis	2 (0.9%)	1(0.5%)	1(0.5%)	1 (0.7%)	1 (0.7%)	0	1 (1.2%)	0	1(1.2%)
Type 1 diabetes	0	0	0	0	0	0	0	0	0
Hypophysitis	0	0	0	0	0	0	0	0	0
Pancreatic events	0	0	0	0	0	0	0	0	0

months, an ORR of 5.1%, and a 52% incidence of grade 3-5 adverse events. Given its limited survival benefits and high toxicity, there is a need to explore more effective second-line treatment options for advanced BTC. Immune therapy remains investigational in the second-line treatment of advanced BTC. A phase II single-arm clinical trial evaluated 20 advanced BTC patients receiving Sintilimab in combination with anlotinib as second-line therapy, reporting a median OS of 12.3 months, median PFS of 6.5 months, ORR of 30%, and DCR of 95% (34). Another multicenter phase II clinical study demonstrated that nivolumab as salvage therapy for advanced BTC resulted in an ORR of 11%, DCR of 50%, median PFS of 3.68 months, and median OS of 14.24 months (11). Lin et al. explored pembrolizumab in combination with lenvatinib as non-first-line therapy, showing an ORR of 25%, DCR of 78.1%, median PFS of 4.9 months, and median OS of 11.0 months (16). In addition, a real-world study in China included 74 patients who failed gemcitabine-based chemotherapy and received lenvatinib plus PD-1 antibodies as salvage therapy, reporting a median PFS of 4.0 months and median OS of 9.50 months (19). In our study, 84 patients received ICIs as second-line treatment, with a median OS of 9.8 months, median PFS of 5.6 months, ORR of 11.9%, and DCR of 58.3%. Our results show better median OS and ORR compared to ABC-06, likely due to the use of combined local treatment strategies in our salvage therapy patients.

Despite pembrolizumab and Durvalumab being first-line recommended ICIs by CSCO and NCCN guidelines, their high cost and lack of reimbursement in China lead many patients to opt for domestically produced ICIs that are more affordable and accessible. However, there is currently insufficient clinical evidence to establish the efficacy of these domestically produced ICIs in BTC. Unlike pembrolizumab and Durvalumab, which have large phase III Randomized controlled trials (RCTs) like TOPAZ-1 and KEYNOTE-966 supporting their use, domestically produced ICIs have only small single-arm studies as clinical evidence (35–38). For example, a phase II single-arm clinical trial studied Sintilimab in combination with gemcitabine and cisplatin as first-line therapy in 30 patients with advanced BTC, reporting a median OS of 15.9 months, median PFS of 5.1 months, and ORR of 36.7% (37). Another phase II single-arm clinical trial evaluated the efficacy of teraplizumab, lenvatinib in combination with gemcitabine and oxaliplatin (GEMOX) in ICC, showing an ORR of 80% and DCR of 93.3%, though median PFS and OS were not reached (38). A study of camrelizumab in 38 patients with BTC showed an ORR of 54%, median PFS of 6.1 months, and median OS of 11.8 months (35), whereas another study of 47 BTC patients reported an ORR of 7.0% and DCR of 67.4% for camrelizumab plus GEMOX as first-line therapy (36). Due to their small sample sizes, lack of randomization, blinding, control, and maturity of some study indicators, these single-arm studies have limited reliability and low evidence grade. In our study, we compared Durvalumab, a guideline-recommended ICI, with Sintilimab, a domestically produced alternative, in an exploratory analysis of clinical efficacy. Durvalumab showed longer OS and PFS, with no significant differences in ORR or safety profiles. However, Durvalumab patients had better prognostic factors, such as more first-line treatment cases. To address these potential biases, multivariate Cox regression analysis adjusted for these confounders and confirmed Durvalumab's OS advantage. Nonetheless, previous research suggests that for each covariate included in a regression model, at least 10 events (e.g., deaths) should be observed (26, 27). In our subgroups of Durvalumab and Sintilimab users, the number of patients with outcome events (i.e., deaths) was only 59, and the number of covariates exceeded one-tenth of the effective sample size. To further validate our conclusions, we employed PSM to control for confounding factors. Propensity score methods, first introduced by Rosenbaum and Rubin (25), has become increasingly popular in observational studies for mitigating confounding effects. Among these methods, PSM provides relatively better control over confounders. However, it also has drawbacks, such as excluding unmatched patients, which reduces sample size (24). In our PSM analysis, no significant OS difference was observed, diverging from regression results. This discrepancy likely stems from the exclusion of half of the Sintilimab patients and 17 Durvalumab patients during matching, further diminishing the already limited sample size and reducing statistical power. Moreover, regression analysis results, while statistically significant, carry a heightened risk of Type I errors due to multiple hypothesis testing (e.g., OS, PFS, and ORR comparisons). Adjustments like Bonferroni correction would nullify significance. With a limited sample size and baseline heterogeneity, our findings do not definitively establish Durvalumab's superiority. However, It is worth noting that achieving statistical significance in small-sample comparisons is challenging, and p-values should be viewed as a reference rather than a conclusive metric. Sole reliance on p-values may underestimate the true clinical significance of the observed difference. Our results suggest a potential advantage of Durvalumab over Sintilimab, highlighting the need for more robust clinical evidence to validate domestically produced ICIs, which are favored in China due to lower cost.

We did not compare other ICIs directly for the following reasons: Both pembrolizumab and Durvalumab are the only ICIs recommended in current guidelines, with robust evidence from large-scale randomized controlled trials supporting their efficacy (13, 30). While no head-to-head comparison exists between the two, our study was not aimed at determining the relative ranking of these ICIs. Instead, our exploratory analysis focused on evaluating the efficacy of domestically produced ICIs, which are more affordable and popular among Chinese patients, and demonstrating the need for further evidence of their efficacy in advanced BTC. As for other domestically produced ICIs, such as camrelizumab, they share similar pricing and accessibility with Sintilimab but also lack sufficient clinical evidence for efficacy in advanced BTC. In our cohort, the number of patients using these ICIs was less than half of those using Sintilimab. Given the sample size limitations already encountered in comparing Sintilimab and Durvalumab, further comparisons involving these other ICIs would inevitably suffer from patient heterogeneity and insufficient sample sizes, precluding meaningful conclusions from regression analyses or PSM. Additionally, conducting multiple pairwise comparisons among these ICIs would further increase the risk of Type I errors under a fixed significance threshold. Our primary aim was to highlight the need for more clinical evidence to validate the efficacy of domestically produced ICIs favored by Chinese

patients, rather than ranking these ICIs against guideline-recommended treatments. The comparison between Durvalumab and Sintilimab suffices to meet this objective, and further comparisons with other ICIs are unnecessary at this stage.

With the widespread application of ICIs in the real world, there is an urgent need to identify biomarkers that predict tumor response. Our study identified tumor differentiation, pretreatment CA-199 level<500 U/ml, pretreatment CA-125 level<28.65U/ml, and the number of prior ICIs treatment lines as independent risk factors influencing OS. Factors independently predicting PFS included tumor differentiation, number of ICIs treatment lines, pretreatment CA-199 level, pretreatment CA-125 level and whether subsequent treatments were received. These results aligned with traditional understanding, where poor differentiation and elevated tumor markers were often associated with a worse prognosis. In our multifactorial analysis, NLR did not demonstrate a prognostic effect, despite prior studies showing an association between elevated pretreatment NLR and adverse outcomes in BTC patients (39, 40). This discrepancy may be due to our inclusion of 84 patients who received second-line treatment, often experiencing bone marrow suppression and other adverse effects from prior treatments, which may not reflect the host's systemic inflammatory status through NLR.

Regarding safety, our study showed that 129 patients (94.2%) experienced any grade of AEs during first-line treatment, with 59 patients (43.1%) experiencing ≥ grade 3 AEs, primarily attributed to chemotherapy-induced neutropenia, anemia, and thrombocytopenia. The incidence rates of overall AEs and grade ≥3 AEs in our study were comparable to other real-world studies (18, 33) but lower than those reported in the TOPAZ-1 trial (99.4% and 75.7%, respectively) (30) and the KEYNOTE-966 trial (99% and 79%, respectively) (13), potentially due to enhanced monitoring practices in RCTs compared to real-world settings. Forty-six patients (33.6%) experienced irAEs, with a rate of grade 3-4 irAEs at 8.0%. These results are similar to some real-world findings (33) but higher than those reported in TOPAZ-1 (12.7% and 2.4%, respectively) (30) and KEYNOTE-966 (22% and 7%, respectively) (13). Several reasons might explain these discrepancies. First, our study included patients receiving later-line treatments, who might have experienced cumulative toxicity. Second, our analysis involved multiple types of ICIs, and prior studies have indicated that PD-1 inhibitors are associated with higher irAE rates than PD-L1 inhibitors (41), potentially explaining why our data align more closely with KEYNOTE-966 and are higher than TOPAZ-1. Additionally, patients with autoimmune diseases are typically excluded from RCTs, yet previous studies have indicated that these patients may have a higher incidence of irAEs (42, 43). In second-line treatment, the incidence rates of AEs and ≥ grade 3 AEs were 97.6% and 40.5%, respectively, consistent with previous real-world study data (19).

Our study has several limitations. Firstly, its retrospective design may introduce selection bias, particularly concerning treatment allocation. Secondly, as the study was conducted at a single medical center, the generalizability of the findings may be limited, highlighting the need for multicenter validation. Thirdly, the relatively small sample size in subgroup analyses could limit statistical power. Additionally, the inclusion of different treatment regimens, such as chemotherapy or anti-angiogenic therapy, may affect the interpretation of ICI-related outcomes. Lastly, the lack of biomarker data (e.g., PD-L1 expression, MSI status) in our study precluded the analysis of predictive factors.

5 Conclusion

This real-world study demonstrates that ICIs provide clinically meaningful survival benefits in both first-line (median OS 15.7 months) and ≥2nd-line settings (median OS 9.8 months) for advanced BTC. Notably, in addition to the first-line treatment commonly investigated by most studies, our data represent a large real-world cohort validating ICIs in later-line settings, where outcomes have historically been dismal (e.g., ABC-06 OS 6.2 months with chemotherapy alone). While domestically produced ICIs are widely used in clinical practice in China, observed differences in efficacy (unadjusted HR 2.47 for OS comparing Sintilimab with Durvalumab) and the lack of robust clinical trial evidence underscore the need for further validation. These findings underscore the importance of real-world data in complementing trial evidence for BTC treatment optimization.

Data availability statement

The datasets presented in this article are not readily available because data supporting the results of this research can be reasonably requested from the corresponding authors. Requests to access the datasets should be directed to maji@wchscu.cn.

Ethics statement

The studies involving humans were approved by Ethics Committee of West China Hospital (No. 2023699). The studies were conducted in accordance with the local legislation and institutional requirements. The ethics committee/institutional review board waived the requirement of written informed consent for participation from the participants or the participants' legal guardians/next of kin because due to the retrospective nature of the study and the minimal risk to the subjects, our Ethics Committee waived the requirement for informed consent.

Author contributions

YZ: Data curation, Investigation, Methodology, Validation, Writing – original draft. JG: Data curation, Investigation, Methodology, Validation, Writing – original draft. TR: Data curation, Investigation, Writing – original draft. JM: Conceptualization, Funding acquisition, Methodology, Resources, Writing – review & editing. DC: Conceptualization, Funding acquisition, Methodology, Project administration, Resources, Supervision, Writing – review & editing.

Funding

The author(s) declare that financial support was received for the research and/or publication of this article. This research was supported by Key Research and Development Project of Sichuan Province (2020YFS0273 and 2023YFS0171 to JM) and Key Research and Development Project of Chengdu City (2024-YF0500546-SN to JM).

Conflict of interest

The authors declare that the research was conducted in the absence of any commercial or financial relationships that could be construed as a potential conflict of interest.

Publisher's note

All claims expressed in this article are solely those of the authors and do not necessarily represent those of their affiliated organizations, or those of the publisher, the editors and the reviewers. Any product that may be evaluated in this article, or claim that may be made by its manufacturer, is not guaranteed or endorsed by the publisher.

Supplementary material

The Supplementary Material for this article can be found online at: https://www.frontiersin.org/articles/10.3389/fimmu.2025.1493234/full#supplementary-material

References

1. Valle JW, Kelley RK, Nervi B, Oh DY, Zhu AX. Biliary tract cancer. *Lancet (London England)*. (2021) 397:428–44. doi: 10.1016/s0140-6736(21)00153-7

2. Vogel A, Bridgewater J, Edeline J, Kelley RK, Klümpen HJ, Malka D, et al. Biliary tract cancer: ESMO Clinical Practice Guideline for diagnosis, treatment and follow-up. *Ann Oncol: Off J Eur Soc Med Oncol*. (2023) 34:127–40. doi: 10.1016/j.annonc.2022.10.506

3. Lamarca A, Edeline J, Goyal L. How I treat biliary tract cancer. *ESMO Open*. (2022) 7:100378. doi: 10.1016/j.esmoop.2021.100378

4. Valle J, Wasan H, Palmer DH, Cunningham D, Anthoney A, Maraveyas A, et al. Cisplatin plus gemcitabine versus gemcitabine for biliary tract cancer. *N Engl J Med*. (2010) 362:1273–81. doi: 10.1056/NEJMoa0908721

5. Rizzo A, Brandi G. First-line chemotherapy in advanced biliary tract cancer ten years after the ABC-02 trial: "And yet it moves! *Cancer Treat Res Commun*. (2021) 27:100335. doi: 10.1016/j.ctarc.2021.100335

6. Harding JJ, Khalil DN, Fabris L, Abou-Alfa GK. Rational development of combination therapies for biliary tract cancers. *J Hepatol*. (2023) 78:217–28. doi: 10.1016/j.jhep.2022.09.004

7. Job S, Rapoud D, Dos Santos A, Gonzalez P, Desterke C, Pascal G, et al. Identification of four immune subtypes characterized by distinct composition and functions of tumor microenvironment in intrahepatic cholangiocarcinoma. *Hepatol (Baltimore Md)*. (2020) 72:965–81. doi: 10.1002/hep.31092

8. Martin-Serrano MA, Kepecs B, Torres-Martin M, Bramel ER, Haber PK, Merritt E, et al. Novel microenvironment-based classification of intrahepatic cholangiocarcinoma with therapeutic implications. *Gut*. (2023) 72:736–48. doi: 10.1136/gutjnl-2021-326514

9. Marabelle A, Le DT, Ascierto PA, Di Giacomo AM, De Jesus-Acosta A, Delord JP, et al. Efficacy of pembrolizumab in patients with noncolorectal high microsatellite instability/mismatch repair-deficient cancer: results from the phase II KEYNOTE-158 study. *J Clin Oncol: Off J Am Soc Clin Oncol*. (2020) 38:1–10. doi: 10.1200/jco.19.02105

10. Piha-Paul SA, Oh DY, Ueno M, Malka D, Chung HC, Nagrial A, et al. Efficacy and safety of pembrolizumab for the treatment of advanced biliary cancer: Results from the KEYNOTE-158 and KEYNOTE-028 studies. *Int J Cancer*. (2020) 147:2190–8. doi: 10.1002/ijc.33013

11. Kim RD, Chung V, Alese OB, El-Rayes BF, Li D, Al-Toubah TE, et al. A phase 2 multi-institutional study of nivolumab for patients with advanced refractory biliary tract cancer. *JAMA Oncol*. (2020) 6:888–94. doi: 10.1001/jamaoncol.2020.0930

12. Burris HA 3rd, Okusaka T, Vogel A, Lee MA, Takahashi H, Breder V, et al. Durvalumab plus gemcitabine and cisplatin in advanced biliary tract cancer (TOPAZ-1): patient-reported outcomes from a randomised, double-blind, placebo-controlled, phase 3 trial. *Lancet Oncol*. (2024) 25:626–35. doi: 10.1016/s1470-2045(24)00082-2

13. Kelley RK, Ueno M, Yoo C, Finn RS, Furuse J, Ren Z, et al. Pembrolizumab in combination with gemcitabine and cisplatin compared with gemcitabine and cisplatin alone for patients with advanced biliary tract cancer (KEYNOTE-966): a randomised, double-blind, placebo-controlled, phase 3 trial. *Lancet (London England)*. (2023) 401:1853–65. doi: 10.1016/s0140-6736(23)00727-4

14. Lamarca A, Palmer DH, Wasan HS, Ross PJ, Ma YT, Arora A, et al. Second-line FOLFOX chemotherapy versus active symptom control for advanced biliary tract cancer (ABC-06): a phase 3, open-label, randomised, controlled trial. *Lancet Oncol*. (2021) 22:690–701. doi: 10.1016/s1470-2045(21)00027-9

15. Berchuck JE, Facchinetti F, DiToro DF, Baiev I, Majeed U, Reyes S, et al. The clinical landscape of cell-free DNA alterations in 1671 patients with advanced biliary tract cancer. *Ann Oncol: Off J Eur Soc Med Oncol*. (2022) 33:1269–83. doi: 10.1016/j.annonc.2022.09.150

16. Lin J, Yang X, Long J, Zhao S, Mao J, Wang D, et al. Pembrolizumab combined with lenvatinib as non-first-line therapy in patients with refractory biliary tract carcinoma. *Hepatobiliary Surg Nutr*. (2020) 9:414–24. doi: 10.21037/hbsn-20-338

17. Dreikhausen L, Kusnik A, Schulte N, Eckardt M, Teufel A, Gaiser T, et al. Durable response with lenvatinib and pembrolizumab combination therapy in a patient with pre-treated metastatic cholangiocarcinoma. *J Gastrointestinal Liver Diseases: JGLD*. (2021) 30:409–10. doi: 10.15403/jgld-3730

18. Rimini M, Fornaro L, Lonardi S, Niger M, Lavacchi D, Pressiani T, et al. Durvalumab plus gemcitabine and cisplatin in advanced biliary tract cancer: An early exploratory analysis of real-world data. *Liver International: Off J Int Assoc Study Liver*. (2023) 43:1803–12. doi: 10.1111/liv.15641

19. Shi C, Li Y, Yang C, Qiao L, Tang L, Zheng Y, et al. Lenvatinib plus programmed cell death protein-1 inhibitor beyond first-line systemic therapy in refractory advanced biliary tract cancer: A real-world retrospective study in China. *Front Immunol*. (2022) 13:946861. doi: 10.3389/fimmu.2022.946861

20. Schwartz LH, Litière S, de Vries E, Ford R, Gwyther S, Mandrekar S, et al. RECIST 1.1-Update and clarification: From the RECIST committee. *Eur J Cancer (Oxford England: 1990)*. (2016) 62:132–7. doi: 10.1016/j.ejca.2016.03.081

21. Freites-Martinez A, Santana N, Arias-Santiago S, Viera A. Using the common terminology criteria for adverse events (CTCAE - version 5.0) to evaluate the severity of adverse events of anticancer therapies. *Actas Dermo-sifiliograficas*. (2021) 112:90–2. doi: 10.1016/j.ad.2019.05.009

22. Cox DR. *Breakthroughs in Statistics: Methodology and Distribution*. Kotz S, Johnson NL, editors. New York: Springer (1992) p. 527–41.

23. Kaplan EL, Meier P. Non-parametric estimation from incomplete observation. *J Am Stat Assoc*. (1965) 53:203–24. doi: 10.1007/978-1-4612-4380-9_25

24. Austin PC. An introduction to propensity score methods for reducing the effects of confounding in observational studies. *Multivariate Behav Res*. (2011) 46:399–424. doi: 10.1080/00273171.2011.568786

25. Rosenbaum PR, Rubin DB. The central role of the propensity score in observational studies for causal effects. *Biometrika*. (1983) 70:41–55. doi: 10.1093/biomet/70.1.41

26. Peduzzi P, Concato J, Feinstein AR, Holford TR. Importance of events per independent variable in proportional hazards regression analysis. II. Accuracy and precision of regression estimates. *J Clin Epidemiol*. (1995) 48:1503–10. doi: 10.1016/0895-4356(95)00048-8

27. Peduzzi P, Concato J, Kemper E, Holford TR, Feinstein AR. A simulation study of the number of events per variable in logistic regression analysis. *J Clin Epidemiol*. (1996) 49:1373–9. doi: 10.1016/s0895-4356(96)00236-3

28. Chen JW, Maldonado DR, Kowalski BL, Miecznikowski KB, Kyin C, Gornbein JA, et al. Best practice guidelines for propensity score methods in medical research: consideration on theory, implementation, and reporting. A review. *Arthroscopy: J Arthroscopic Related Surgery: Off Publ Arthroscopy Assoc North America Int Arthroscopy Assoc*. (2022) 38:632–42. doi: 10.1016/j.arthro.2021.06.037

29. Mauro E, Forner A. Immunotherapy in biliary tract cancer: The race has begun! *Liver International: Off J Int Assoc Study Liver*. (2023) 43:1620–2. doi: 10.1111/liv.15651

30. Oh D-Y, He AR, Qin S, Chen L-T, Okusaka T, Vogel A, et al. Durvalumab plus gemcitabine and cisplatin in advanced biliary tract cancer. *NEJM Evid*. (2022) 1: EVIDoa2200015. doi: 10.1056/EVIDoa2200015

31. Greten TF, Schwabe R, Bardeesy N, Ma L, Goyal L, Kelley RK, et al. Immunology and immunotherapy of cholangiocarcinoma. *Nat Rev Gastroenterol Hepatol*. (2023) 20:349–65. doi: 10.1038/s41575-022-00741-4

32. Rimini M, Fornaro L, Rizzato MD, Antonuzzo L, Rossari F, Satake T, et al. Durvalumab plus gemcitabine and cisplatin in advanced biliary tract cancer: A large real-life worldwide population. *Eur J Cancer (Oxford England: 1990)*. (2024) 208:114199. doi: 10.1016/j.ejca.2024.114199

33. Ye Z, Zhang Y, Chen J, Wang X, Hong Y, Zhao Q. First-line PD-1 inhibitors combination therapy for patients with advanced cholangiocarcinoma: A retrospective real-world study. *Int Immunopharmacol*. (2023) 120:110344. doi: 10.1016/j.intimp.2023.110344

34. Jin S, Zhao R, Zhou C, Zhong Q, Shi J, Su C, et al. Feasibility and tolerability of sintilimab plus anlotinib as the second-line therapy for patients with advanced biliary tract cancers: An open-label, single-arm, phase II clinical trial. *Int J Cancer*. (2023) 152:1648–58. doi: 10.1002/ijc.34372

35. Chen X, Wu X, Wu H, Gu Y, Shao Y, Shao Q, et al. Camrelizumab plus gemcitabine and oxaliplatin (GEMOX) in patients with advanced biliary tract cancer: a single-arm, open-label, phase II trial. *J Immunother Cancer*. (2020) 8:e001240. doi: 10.1136/jitc-2020-001240

36. Qin S, Chen Z, Liu Y, Xiong J, Ren Z, Meng Z, et al. A phase II study of anti–PD-1 antibody camrelizumab plus FOLFOX4 or GEMOX systemic chemotherapy as first-line therapy for advanced hepatocellular carcinoma or biliary tract cancer. *J Clin Oncol*. (2019) 37:4074–4. doi: 10.1200/JCO.2019.37.15_suppl.4074

37. Zeng TM, Yang G, Lou C, Wei W, Tao CJ, Chen XY, et al. Clinical and biomarker analyses of sintilimab plus gemcitabine and cisplatin as first-line treatment for patients with advanced biliary tract cancer. *Nat Commun*. (2023) 14:1340. doi: 10.1038/s41467-023-37030-w

38. Jian Z, Jia F, Shi GM, Xianliang H, Dong W, Gang Y, et al. Anti-PD1 antibody toripalimab, lenvatinib and gemox chemotherapy as first-line treatment of advanced and unresectable intrahepatic cholangiocarcinoma: A phase II clinical trial. *Ann Oncol*. (2020) 31:S262–3. doi: 10.1016/j.annonc.2020.08.034

39. Tang H, Lu W, Li B, Li C, Xu Y, Dong J. Prognostic significance of neutrophil-to-lymphocyte ratio in biliary tract cancers: a systematic review and meta-analysis. *Oncotarget*. (2017) 8:36857–68. doi: 10.18632/oncotarget.16143

40. McNamara MG, Templeton AJ, Maganti M, Walter T, Horgan AM, McKeever L, et al. Neutrophil/lymphocyte ratio as a prognostic factor in biliary tract cancer. *Eur J Cancer (Oxford England: 1990)*. (2014) 50:1581–9. doi: 10.1016/j.ejca.2014.02.015

41. Wang Y, Zhou S, Yang F, Qi X, Wang X, Guan X, et al. Treatment-related adverse events of PD-1 and PD-L1 inhibitors in clinical trials: A systematic review and meta-analysis. *JAMA Oncol*. (2019) 5:1008–19. doi: 10.1001/jamaoncol.2019.0393

42. Abdel-Wahab N, Shah M, Lopez-Olivo MA, Suarez-Almazor ME. Use of immune checkpoint inhibitors in the treatment of patients with cancer and preexisting autoimmune disease: A systematic review. *Ann Intern Med*. (2018) 168:121–30. doi: 10.7326/m17-2073

43. Meserve J, Facciorusso A, Holmer AK, Annese V, Sandborn WJ, Singh S. Systematic review with meta-analysis: safety and tolerability of immune checkpoint inhibitors in patients with pre-existing inflammatory bowel diseases. *Alimentary Pharmacol Ther*. (2021) 53:374–82. doi: 10.1111/apt.16217

frontiers | Frontiers in Immunology

TYPE Original Research
PUBLISHED 25 April 2025
DOI 10.3389/fimmu.2025.1549229

OPEN ACCESS

EDITED BY
Stavros P. Papadakos,
Laiko General Hospital of Athens, Greece

REVIEWED BY
Ym Tsui,
The University of Hong Kong, Hong Kong SAR, China
Muhammad Farooq,
King Saud University, Saudi Arabia

*CORRESPONDENCE
Tetyana Yevsa
Yevsa.Tetyana@mh-hannover.de

†PRESENT ADDRESS
Nina Bondarenko,
Institute of Pathology, MHH, Hannover, Germany

‡These authors have contributed equally to this work

RECEIVED 20 December 2024
ACCEPTED 21 March 2025
PUBLISHED 25 April 2025

CITATION
Hochnadel I, Hoenicke L, Petriv N, Suo H, Groebe L, Olijnik C, Bondarenko N, Alfonso JC, Jarek M, Shi R, Jeron A, Timrott K, Hirsch T, Jedicke N, Bruder D, Klawonn F, Lichtinghagen R, Geffers R, Lenzen H, Manns MP and Yevsa T (2025) *In vivo* RNAi screen and validation reveals Ngp, Hba-a1, and S100a8 as novel inhibitory targets on T lymphocytes in liver cancer. *Front. Immunol.* 16:1549229. doi: 10.3389/fimmu.2025.1549229

In vivo RNAi screen and validation reveals Ngp, Hba-a1, and S100a8 as novel inhibitory targets on T lymphocytes in liver cancer

Inga Hochnadel[1‡], Lisa Hoenicke[1‡], Nataliia Petriv[1‡], Huizhen Suo[1], Lothar Groebe[2], Chantal Olijnik[1], Nina Bondarenko[1,3†], Juan C. Alfonso[4], Michael Jarek[5], Ruibing Shi[6], Andreas Jeron[7,8], Kai Timrott[9], Tatjana Hirsch[7], Nils Jedicke[1], Dunja Bruder[7,8], Frank Klawonn[6,10,11], Ralf Lichtinghagen[12], Robert Geffers[5], Henrike Lenzen[1,13], Michael P. Manns[1] and Tetyana Yevsa[1*]

[1]Department of Gastroenterology, Hepatology, Infectious Diseases and Endocrinology, Hannover Medical School (MHH), Hannover, Germany, [2]Experimental Immunology, Helmholtz Centre for Infection Research (HZI), Braunschweig, Germany, [3]Department of Pathological Anatomy, Forensic Medicine and Pathological Physiology, Dnipro State Medical University, Dnipro, Ukraine, [4]Department of Systems Immunology, Technical University Braunschweig and HZI, Braunschweig, Germany, [5]Genome Analytics, HZI, Braunschweig, Germany, [6]Biostatistics Research Group, HZI, Braunschweig, Germany, [7]Immune Regulation Group, HZI, Braunschweig, Germany, [8]Infection Immunology Group, Institute of Medical Microbiology and Hospital Hygiene, Otto-von-Guericke University Magdeburg, Magdeburg, Germany, [9]Department of General, Visceral and Transplant Surgery, MHH, Hannover, Germany, [10]Munich Biomarker Research Center, Institute of Laboratory Medicine, German Heart Center, Technical University of Munich, Munich, Germany, [11]Department of Computer Science, Ostfalia University, Wolfenbüttel, Germany, [12]Department of Clinical Chemistry, MHH, Hannover, Germany, [13]Department of Gastroenterology, Hepatology, Interventional Endoscopy and Diabetology, Academic Teaching Hospital Braunschweig, Braunschweig, Germany

Background: Hepatocellular carcinoma (HCC) represents the third deadliest cancer worldwide with limited treatment options. Immune checkpoint inhibitors (ICIs) have revolutionized HCC therapy, but immune suppression within the tumor microenvironment remains a major challenge. Therefore, in this study, we aimed to define novel ICI molecules arising on T cells during aggressive HCC development.

Methods: Using autochthonous HCC models, we performed microarray analyses followed by *in vivo* RNA interference screen and identified several new ICI molecules on CD4 and CD8 T lymphocytes in HCC-bearing mice. Short hairpin RNA (shRNA)-mediated knockdown of the ICI molecules was performed to validate their functional role in T cell activity and survival of HCC-bearing mice. Finally, we searched for the presence of the defined ICI molecules in HCC patients.

Results: We identified neutrophilic granule protein (*Ngp*), hemoglobin subunit alpha-1 (*Hba-a1*), and S100 calcium-binding protein a8 (*S100a8*) as novel inhibitory molecules of T cells in HCC. The specific shRNA-based knockdown of these inhibitory targets was safe, led to a downregulation of classical ICI molecules

(PD-1, PD-L1, 4-1BBL, CD160), and kept liver parameters under control in murine HCC. Besides, we detected upregulation of *S100A8* and *S100A9* in blood and liver tissues in HCC patients, supporting their clinical relevance.

Conclusion: The obtained results pave the way for the use of the newly defined ICI molecules *Ngp*, *Hba-a1*, and *S100a8* as novel immunotherapeutic targets in further preclinical and clinical studies in HCC patients.

KEYWORDS

RNA interference screen, T lymphocytes, hepatocellular carcinoma, immunotherapy, immune checkpoint inhibitors

1 Introduction

Hepatocellular carcinoma (HCC) is a highly lethal cancer that represents the third most common cause of cancer-related deaths worldwide, with about 830,000 patients dying from the disease annually (1, 2). The primary risk factors for HCC include cirrhosis and chronic infection with hepatitis B or C viruses (3). HCC incidence continues to rise globally, and most HCC cases are estimated to occur in Asia (72%) followed by Europe (10%), Africa (7.8%), and least cases in Oceanic (0.5%) (4). Current treatment options for HCC, like surgical liver resection, liver transplantation, and locoregional therapies, including radiofrequency ablation (5) and transarterial chemoembolization, are limited to very early stages of the malignant disease and cannot prevent recurrence (6). In addition, in the majority of patients (>80%), HCC is diagnosed in unresectable tumor stages, thereby limiting the treatment options to systemic therapies (7). Sorafenib, a multikinase kinase inhibitor, used to be a standard therapy for HCC since 2007 (8). Immunotherapy recently replaced sorafenib, as the first-line therapy in unresectable HCC (9), as described below.

Abbreviations: ALP, Alkaline phosphatase; ALT, Alanine aminotransferase; AST, Aspartate aminotransferase; CAMP, Cathelicidin; CAR-T cell, Chimeric antigen receptor T cell; CTLA-4, Cytotoxic T-lymphocyte-associated protein; DCs, Dendritic cells; GDH, Glutamatdehydrogenase; GFP, Green fluorescent protein; Hba-a1, Hemoglobin subunit alpha-1; HCC, Hepatocellular carcinoma; HDI, Hydrodynamic tail vein injection; ICIs, Immune checkpoint inhibitors; IHC, Immunohistochemistry; IrrelLN, Irrelevant lymph node; LAG3, Lymphocyte-activation gene 3; LCN2, Lipocalin 2; LDH, Lactate dehydrogenase;LN, Lymph node; Ngp, Neutrophil granule protein; PBMCs, Peripheral blood mononuclear cells; PD-1, Programmed cell death protein 1; PD-L1, Programmed cell death ligand 1; qPCR, Quantitative polymerase chain reaction; RelLN, Relevant lymph node; RFP, Red fluorescent protein; RNAi, RNA interference; SB13, Sleeping Beauty 13 transposase; shRNA, Short hairpin RNA; TILs, Tumor-infiltrating lymphocytes; TIM3, T cell immunoglobulin and mucin-domain containing-3; TME, Tumor microenvironment; Tregs, Regulatory T cells; VEGF, Vascular endothelial growth factor; VISTA, V-domain Ig suppressor of T cell activation.

Considering the permanently growing incidence of HCC and the limited efficacy of current therapies, there is an urgent need for new innovative treatment strategies. Since HCC is modulating the tumor microenvironment (TME) (10) to evade the immune system, immunotherapy represents an attractive alternative to target and re-activate immune cells, which became dysfunctional due to suppression by HCC. Importantly, since HCC has been shown to be immunogenic and several HCC-specific tumor-associated antigens that are targeted by T cells have been identified (11–13), T cell-based immunotherapy is considered as a promising treatment. It has been shown that T lymphocytes are highly infiltrating HCC, which is also correlating with better survival prognosis (14–16). Nevertheless, tumor-infiltrating T lymphocytes or tumor-specific T lymphocytes in close proximity to tumor, are found to be exhausted and display an over-expression of several immune checkpoint inhibitors (ICIs) in which programmed cell death protein 1 (PD-1), cytotoxic T-lymphocyte-associated protein-4 (CTLA-4), T-cell immunoglobulin and mucin-domain containing-3 (TIM-3), V-domain Ig suppressor of T cell activation (VISTA) and lymphocyte activating 3 (LAG3) are frequently studied (17, 18). In line with above mentioned, recently approved therapies for unresectable HCC comprising atezolizumab and bevacizumab, inhibitors of PD-L1 and vascular endothelial growth factor (VEGF), showed better prognosis in HCC patients and were approved as the first-line therapy for unresectable HCC (9). In addition, many ongoing clinical trials are evaluating antibodies targeting specific ICIs as a single-agent therapy. However, combination strategies have been shown to be more effective in treating this complex malignant disease (18–20).

The discovery of ICIs has revolutionized cancer treatment, but it still needs to be further investigated, and new inhibitory targets need to be explored. Therefore, we performed microarray analysis on $CD4^+$ and $CD8^+$ T lymphocytes isolated from HCC-bearing mice to identify further immune inhibitory molecules associated with HCC development. Additionally, we approved our findings by performing an RNA interference (RNAi) screen *in vivo*. Among several upregulated genes, we found neutrophilic granule protein (*Ngp*), hemoglobin subunit beta-1 (*Hbb-b1*), hemoglobin subunit

alpha-1 *(Hba-a1)*, S100 calcium-binding protein a8 (*S100a8*), and others highly expressed on T lymphocytes in HCC-bearing mice. We performed *in vivo* validation experiments and investigated the functional role of *Ngp*, *Hbb-b1*, *Hba-a1*, and *S100a8* on T lymphocytes during HCC development. Using a short hairpin RNA (shRNA)-based specific knockdown of these targets in donor-derived T lymphocytes, we tested the impact of adoptive T cell transfer therapy on survival and ICIs repertoire in HCC-bearing animals and thereby identified the most promising targets. Furthermore, we confirmed our data obtained in a preclinical mouse model in samples obtained from HCC patients.

2 Materials and methods

The section "Materials and Methods" can be found in Supplementary Materials.

3 Results

3.1 HCC development and isolation of T lymphocytes for microarray analysis

In the first part of our study, we aimed to identify to date unknown inhibitory molecules on CD4 and CD8 T lymphocytes, which are upregulated during HCC development using microarray analysis (see "Experimental setup" in Supplementary Figure S1).

3.1.1 HCC Model

To induce HCC development, we delivered transposons expressing two oncogenes, $NRAS^{G12V}$ and *c-Myc*, together with a Sleeping Beauty transposase (*SB13*) into C57BL/6-Foxp3^{tm1Flv}/J mice expressing red fluorescent protein (RFP) regulatory T cells (Tregs) using the hydrodynamic tail vein injection (HDI) technique (Supplementary Figure S1A). Control tumor-free mice received either $NRAS^{G12V}$ or *c-Myc* with *SB13* (Supplementary Figure S1A). After 5-8 weeks post-HDI, mice with overexpression of both oncogenes ($NRAS^{G12V}$ and *c-Myc*) developed tumors and were sampled together with the corresponding tumor-free controls ($NRAS^{G12V}$ or *c-Myc*) (Supplementary Figure S2A).

3.1.2 Isolation of CD4 and CD8 memory T cells

Several organs (liver, liver-draining lymph nodes (later designated as: relevant lymph nodes (relLN)), not liver-draining lymph nodes (later designated as: irrelevant lymph nodes (irrelLN)), and spleen) were isolated and single-cell suspensions thereof were prepared (Supplementary Figure S1B). Cell suspensions were stained using the established protocols (21–24) and sorted for memory CD4 and CD8 T cells (Supplementary Figure S1B): CD3$^+$ NK1.1$^-$ CD4$^+$ CD8$^-$ Foxp3$^-$ CD44$^+$ (designated as CD4$^+$ CD44$^+$ T cells) and CD3$^+$ NK1.1$^-$ CD4$^-$ CD8$^+$ CD44$^+$ T cell populations (designated as CD8$^+$ CD44$^+$ T cells), respectively. Supplementary Figure S2B demonstrates a gating strategy used at sorting to define both populations of memory CD4 and CD8 T cells.

3.1.3 RNA isolation and microarray analysis

In the next step, total RNA from CD4$^+$ CD44$^+$ and CD8$^+$ CD44$^+$ T cells was isolated and processed for microarray analysis (Supplementary Figure S1C).

We performed in total two independent experiments giving rise to two independent replicates for each organ (liver, relLN, irrelLN, spleen) and cell type (CD4$^+$ CD44$^+$ and CD8$^+$ CD44$^+$ T cells).

3.2 Microarray analysis reveals 72 upregulated genes in CD4$^+$ CD44$^+$ and CD8$^+$ CD44$^+$ T lymphocytes during HCC development

To identify genes that are upregulated in T lymphocytes during HCC development, we conducted a microarray analysis comparing CD4$^+$ CD44$^+$ and CD8$^+$ CD44$^+$ T cells isolated from HCC-bearing (genotype HCC: $NRAS^{G12V}$/*c-Myc*) mice with those isolated from HCC-free control animals (genotype C1: *c-Myc*; genotype C2: $NRAS^{G12V}$, Supplementary Figure S1A, Supplementary Figure S2A). To identify target genes for validation studies, the log2 values in T lymphocytes originating from HCC-bearing mice were analyzed. Importantly, log2 values obtained in HCC-free controls were subtracted from log2 values of the tumor-bearing group. This allowed us to define genes that were consistently upregulated (enriched) in the TME of HCC-bearing animals. The term "enriched genes" in this context refers to those genes that were significantly upregulated in T cells from HCC-bearing mice compared to HCC-free controls.

In CD4$^+$ CD44$^+$ T cells, we identified a total of 615 upregulated genes with log2≥0.5, distributed among the liver (261 genes), relLN (84 genes), spleen (191 genes), and irrelLN (79 genes) (Figure 1A). Among these, 17 genes were commonly upregulated in both liver and relLN, 26 genes in liver and spleen, 7 genes in HCC liver and irrelLN, and 5 genes in HCC liver, relLN, and spleen (Figure 1A). Intersections among spleen, relLN, and irrelLN ranged from 2 to 6 genes (Figure 1A).

Similarly, in CD8$^+$ CD44$^+$ T cells, we found 736 upregulated genes, with the liver showing the highest number (382 genes), followed by relLNs (90 genes), irrelLNs (77 genes), and spleen (187 genes) (Figure 1B). In comparison to CD4$^+$ CD44$^+$ T cells, CD8$^+$ CD44$^+$ T cells showed 121 additional genes that originated from the liver. Gene intersections among organs showed 18 genes shared between liver and relLN, 45 between liver and spleen, and 15 between liver and irrelLN (Figure 1B). Notably, 9 genes were identified in the intersection of liver, spleen, and relLN in CD8$^+$ CD44$^+$ T cells in comparison to CD4$^+$ CD44$^+$ T cells.

To narrow down our analysis, we next focused on genes with log2≥1, selecting 99 highly upregulated genes in CD4$^+$ CD44$^+$ T cells and 72 genes in CD8$^+$ CD44$^+$ T cells (Figure 1C for CD4$^+$ CD44$^+$ T cells and Figure 1D for CD8$^+$ CD44$^+$ T cells). These genes were distributed across different tissues: 23 genes in liver, 11 genes in relLN, 44 genes in spleen, 21 genes in irrelLN in CD4$^+$ CD44$^+$ T cells (Figure 1C). In CD8$^+$ CD44$^+$ T cells, 6 genes were shared from liver and spleen, 1 gene between liver and relLN, and 1 gene

10.3389/fimmu.2025.1549229

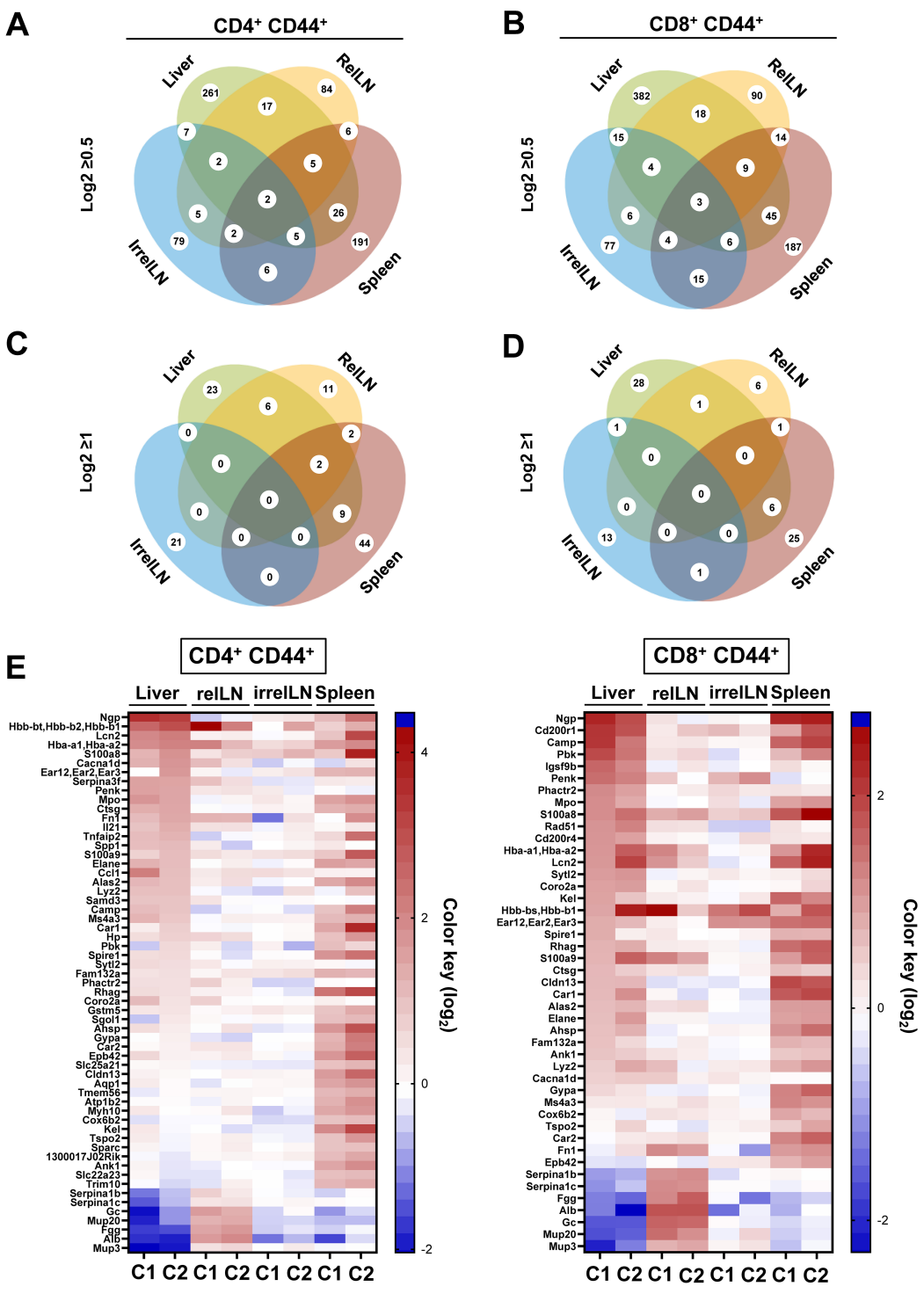

FIGURE 1
Microarray analysis on CD4$^+$ CD44$^+$ and CD8$^+$ CD44$^+$ T cells isolated from the liver, relLN, spleen, and irrelLN of HCC-bearing and HCC-free control mice. **(A-D)** Venn diagrams depicting the distribution of upregulated genes in **(A)** CD4$^+$ CD44$^+$ T cells with log2>0.5, **(B)** CD8$^+$ CD44$^+$ T cells with log2>0.5, **(C)** CD4$^+$ CD44$^+$ T cells with log2≥1, **(D)** CD8$^+$ CD44$^+$ T cells with log2>0.5. **(E)** Heatmap showing highly upregulated genes in CD4$^+$ CD44$^+$ and CD8$^+$ CD44$^+$ T cells isolated from liver, relLN, irrelN, and spleen of HCC-bearing mice, compared to HCC-free controls (C1: *c-Myc*/C2: *NRAS*^{G12V}). Genes selected based on the microarray analysis were included as targets in the shRNA library for the *in vivo* RNAi screen. Data represents a pool of two independent experiments, with n=6 for each replicate (6 HCC-bearing mice vs. 6 HCC-free mice). HCC, hepatocellular carcinoma; relLN, relevant lymph nodes; irrelLN, irrelevant lymph nodes.

between liver and irrelLN (Figure 1D). No genes met the log2≥1 threshold across liver, relLN, and spleen in CD8 T cells (Figure 1D).

Finally, to visualize and prioritize the most biologically relevant targets, we used a heatmap highlighting 72 of the most upregulated (enriched) genes in HCC liver, relLN, and spleen (Figure 1E). These genes were selected for the *in vivo* RNAi screen to uncover new targets on CD4 and CD8 T cells in HCC.

3.3 *In vivo* RNAi screen and identification of key players in T cell inhibition during HCC development

To identify key players in T cell inhibition, we performed the RNAi screen targeting 72 of the most upregulated genes identified in the microarray analysis.

3.3.1 RNAi screen setup

We first induced HCC development using the HDI technique and isolated CD4 and CD8 T cells from HCC-bearing donor mice (Figure 2). These T cells were stimulated and transduced with a pooled shRNA library which contained 4-5 shRNAs per selected target gene. An shRNA targeting *Renilla* (shRen), a non-coding gene in mice, served as a negative control. The shRNA constructs were cloned into a third-generation pGIPZ lentiviral vector system expressing green fluorescent protein (GFP) allowing for a tracking of the transduction efficiency, as previously described (25). The lentiviral packaging was performed using a system consisting of pMD2.G, pMDLg/pRRE, and pRSV-Rev vectors, expressing envelope and transport proteins (VSV-G, Gag/Pol, Rev) (Figure 2). CD4 and CD8 T cells were transduced with the virus harboring the shRNA library. Following viral transduction, GFP^+ CD4 and CD8 T cells were sorted (a gating strategy is shown in Supplementary Figure S3) and labeled with a proliferation dye (eFluor450). Thereafter, the transduced GFP^+ $eFluor450^+$ T cells were adoptively transferred into HCC-bearing recipient mice (Figure 2). For the adoptive transfer, GFP^+ $eFluor450^+$ CD4 and GFP^+ $eFluor450^+$ CD8 T cells were pooled and approximately $2x10^5$ cells were transferred intravenously (*i.v.*) (Figure 2). Five days post-transfer, the recipient mice were sacrificed, and liver, spleen, relLN, irrelLN, and blood were collected for further analysis. T cells were isolated and sorted according to $CD3^+$ $CD4^+$ GFP^+ $eFluor450^{-/}$ $CD3^+$ $CD8^+$ GFP^+ $eFluor450^-$ and $CD3^+$ $CD4^+$ GFP^+ $eFluor450^{+/}$ $CD3^+$ $CD8^+$ GFP^+ $eFluor450^+$ profiles (a gating strategy is shown in Supplementary Figure S4). Sorted CD4 and CD8 T cell populations were subjected to DNA isolation followed by Illumina sequencing to determine the shRNA representation/abundance (Figure 2). We searched for shRNA enrichment (log2-fold changes) detected in isolated T cells of HCC-bearing recipient mice (out-probes) compared to T cells prior to the adoptive transfer (original pool, in-probes). Enriched shRNAs (which we used to refer to overrepresented in out-probes, compared to the original pool (in-probes)) mean, that these shRNAs target inhibitory genes whose knockdown is beneficial for the proliferation of the corresponding T cell.

3.3.2 RNAi screen data analysis

To ensure reproducibility, four individual mice received shRNA-transduced CD4 and CD8 T cells. The sequencing results were pooled, and the 20 most enriched shRNAs targeting inhibitory

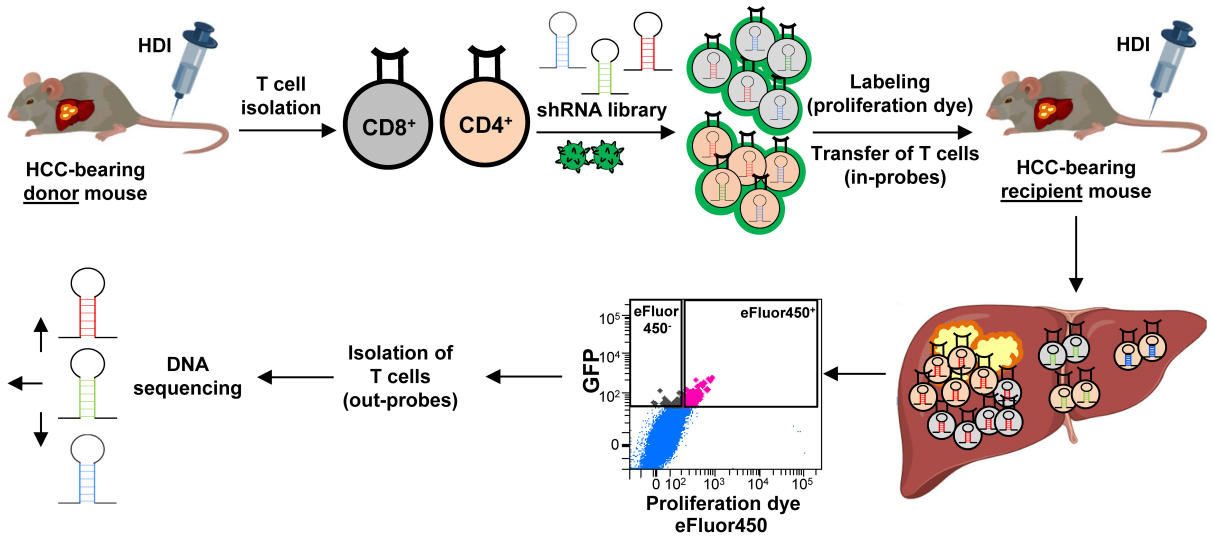

FIGURE 2
Experimental setup of the *in vivo* RNAi screen. CD4 and CD8 T cells were isolated from HCC-bearing mice ($NRAS^{G12V}$/*c-Myc* genotype) and transduced with the shRNA library using a GFP-expressing lentivirus (pGIPZ). Successfully transduced GFP^+ CD4 and CD8 T cells were sorted and labeled with a proliferation dye eFluor450 (in-probes). Thereafter, the cells were adoptively transferred into HCC-bearing recipient mice. Five days post-transfer, recipient mice were sacrificed, and the liver along with other organs were collected. Adoptively transferred T cells were isolated from the explanted organs, sorted for $eFluor450^+$ and for $eFluor450^-$ populations (out-probes), and subsequently subjected to DNA sequencing for shRNA representation/abundance analysis. HCC, hepatocellular carcinoma; HDI, hydrodynamic tail vein injection; GFP, green fluorescent protein; shRNA, short hairpin RNA.

genes for both CD4 and CD8 T cell subsets were identified (Figures 3 and 4). Data from individual mice are presented in Supplementary Figure S5-12.

In general, only a limited number of enriched shRNAs were identified in CD4 T cells, primarily originating from spleen (3 shRNAs), relLN (6 shRNAs), and blood (4 shRNAs) (Figure 3). Interestingly, these shRNAs were found in eFluor450$^-$ CD4 T cells (Figure 3). In contrast to the pooled data on CD4 T cells (Figure 3), individual mouse analysis revealed a presence of many more enriched shRNAs on CD4 T cells in each of the explanted organs. Those shRNAs were detected in both eFluor450$^-$ and eFluor450$^+$ CD4 T cells (Supplementary Figure S5, Supplementary Figure S7, Supplementary Figure S9, Supplementary Figure S11).

In contrast to pooled data from CD4 T cells, a shRNA enrichment was observed in all analyzed organs in CD8 T cells (Figure 4), especially in CD8 T cells isolated from relLN with different shRNAs enriched in eFluor450$^-$ and eFluor450$^+$ CD8 T cells (Figure 4). Enriched shRNAs in CD8 T cells were also present in all organs of the individual mice showing a constant strong enrichment in relLN (Supplementary Figure S6, Supplementary Figure S8, Supplementary Figure S10, Supplementary Figure S12).

Importantly, among the enriched shRNAs in the pooled analysis of both, CD4 and CD8 T cell populations, several shRNAs were present and targeted prominent genes, such as: CD200 receptor 1 (*CD200r1*), calcium channel, voltage-dependent, L type, alpha 1D subunit (*Cacnad1*), and translocator

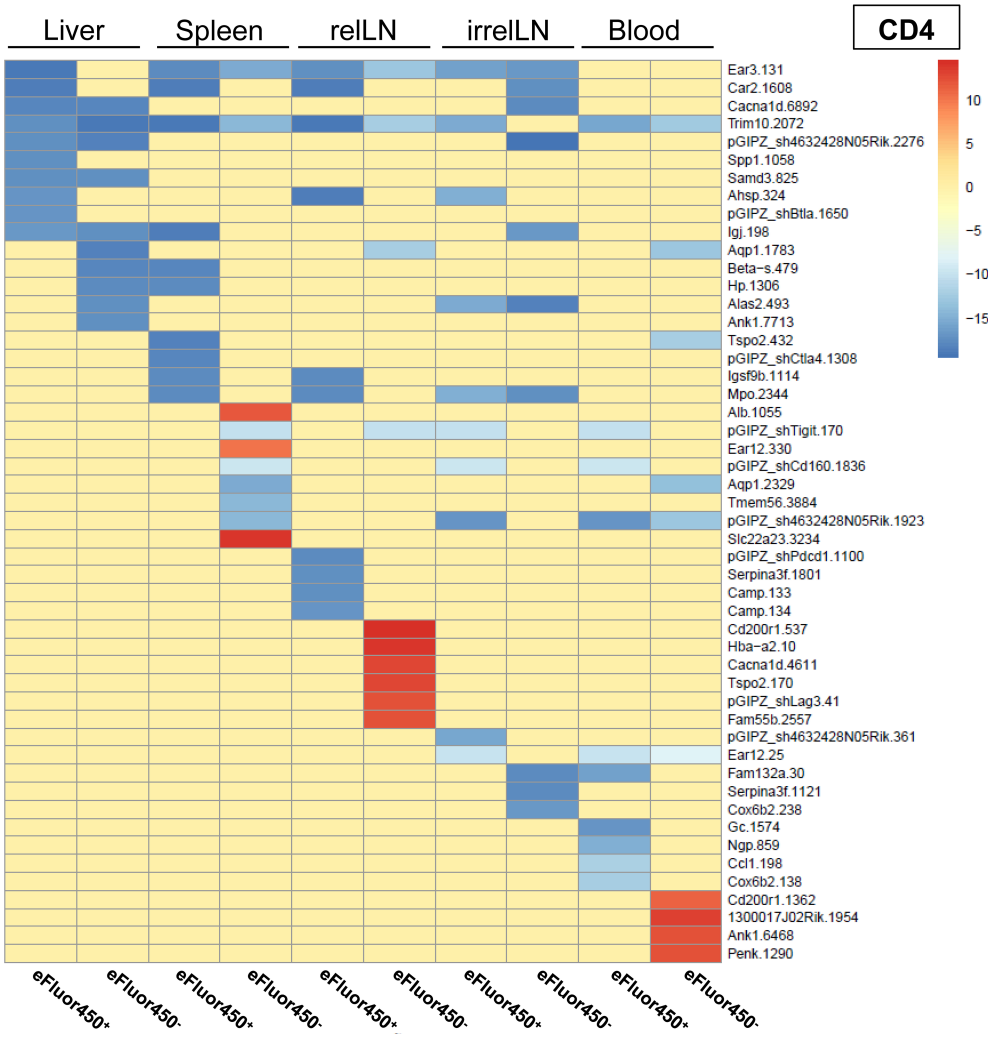

FIGURE 3
In vivo RNAi screen revealed several enriched shRNAs in CD4 T cells during HCC development. RNAi screen analysis was performed on eFluor450$^-$ and eFluor450$^+$ CD4 T cells isolated five days post-adoptive transfer from liver, spleen, relLN, irrelLN, and blood (out-probes) of HCC-bearing mice (*NRAS*^{G12V}*/c-Myc* genotype). The CD4 T cells in out-probes were compared to the CD4 T cells before the adoptive transfer (in-probes). ShRNA enrichment (log2 fold-changes) detected in isolated CD4 T cells of HCC-bearing recipient mice (out-probes) compared to CD4 T cells before the adoptive transfer (in-probes) are presented in a heatmap. Upregulated shRNAs (>0) are marked in red and downregulated shRNAs (<0) are marked in blue. Data represent a pooled analysis from four recipient mice. relLN, relevant lymph nodes; irrelLN, irrelevant lymph nodes.

10.3389/fimmu.2025.1549229

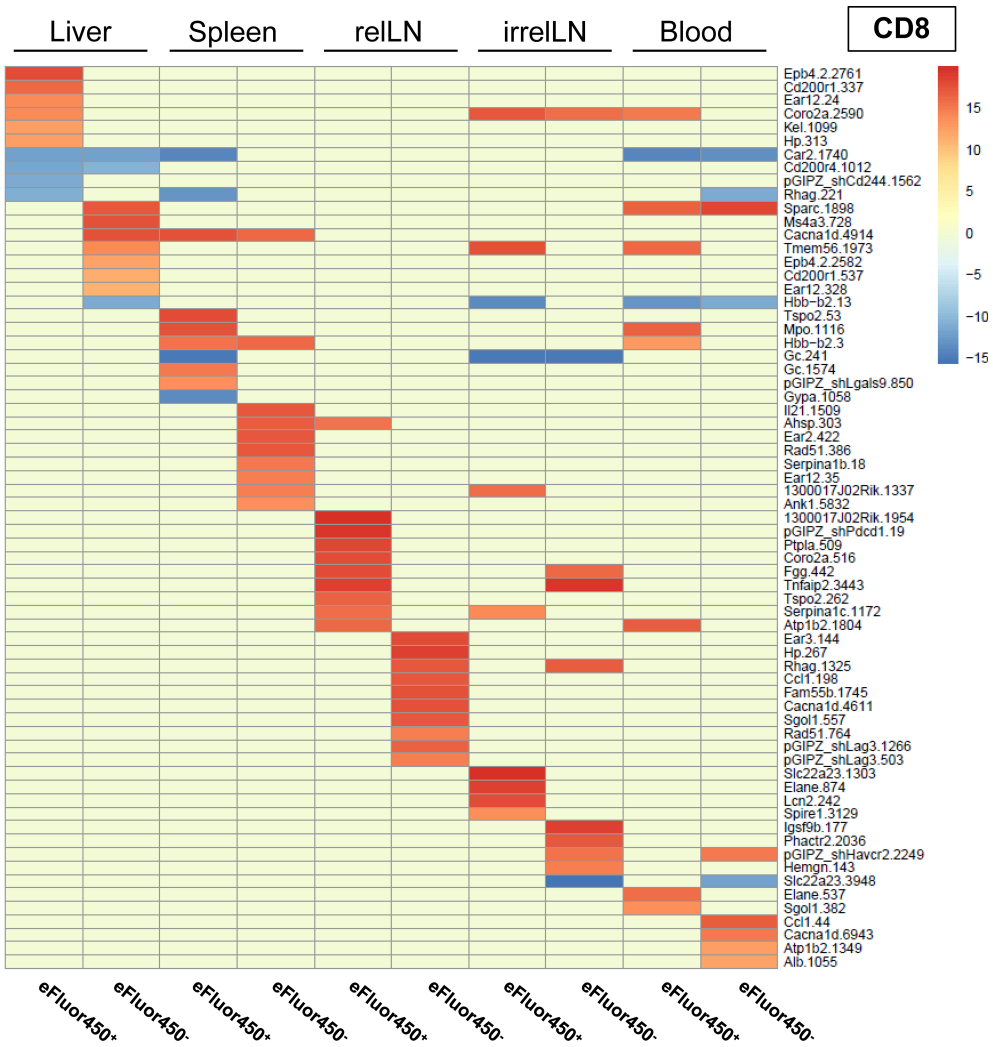

FIGURE 4
In vivo RNAi screen revealed several enriched shRNAs in CD8 T cells during HCC development. RNAi screen analysis was performed on eFluor450^{-} and eFluor450^{+} CD8 T cells isolated five days post-adoptive transfer from liver, spleen, relLN, irrelLN, and blood (out-probes) of HCC-bearing mice (*NRAS*^{G12V}/*c-Myc* genotype). The CD8 T cells in out-probes were compared to the CD8 T cells before the adoptive transfer (in-probes). ShRNA enrichment (log2-fold changes) detected in isolated CD8 T cells of HCC-bearing recipient mice (out-probes) compared to CD8 T cells before the adoptive transfer (in-probes) are depicted in a heatmap with upregulated (>0, marked in red) and downregulated shRNAs (<0, marked in blue). Data represent a pooled analysis from four recipient mice. relLN, relevant lymph nodes; irrelLN, irrelevant lymph nodes.

protein (*Tspo*), which were found in T cells isolated from liver and/or relLN, the local organs of HCC development (Figures 3, 4).

When comparing the RNAi screen data with the microarray results (comparing enriched genes from the microarray with enriched shRNAs targeting the same genes), we found that several genes previously identified as highly upregulated, including *Ngp*, *Hbb-b1*, *Hba-a1*, and *S100a8*, were consistently detected in individual mice in the RNAi screen via enriched shRNAs targeting these genes (Figure 1 and Supplementary Figure S5-12, respectively). Based on these findings, we selected these four target genes for *in vivo* validation studies to further investigate their role as potential inhibitory regulators of T cell function in HCC.

3.4 Validation of potential targets *in vitro* using a specific shRNA-based knockdown of endogenous mRNA expression

To perform validation studies, we first defined the most potent shRNAs to efficiently knockdown the selected target genes (*Ngp*, *Hbb-b1*, *Hba-a1*, *S100a8*). The knockdown efficiency of each shRNA was tested in T cells isolated from HCC-bearing mice. To achieve this, we first induced HCC (genotype: *NRAS*^{G12V}/*c-Myc*). Upon HCC development, mice were sacrificed, and CD4 and CD8 T cells were sorted from the liver, relLN, irrelLN, and spleen. T cells were then stimulated *in vitro* for three days with anti-CD3, anti-CD28, and IL-2. In parallel, HEK293T packaging cells, which were used as lentivirus-

producer cells, were transfected with pGIPZ lentiviral vector system expressing a shRNA of interest. ShRen served as a control. Freshly produced lentiviral particles expressing a shRNA of interest and a GFP reporter were harvested after two days. CD4 and CD8 T cells were transduced with GFP-expressing lentiviral particles and on day three post-transduction, alive and GFP^+ were isolated using cell sorting. The gating strategy used for sorting is depicted in Supplementary Figure S3A, B. Isolated GFP^+ CD4 and GFP^+ CD8 T cells were subjected to RNA isolation. The efficiency of shRNA-mediated knockdown was assessed using quantitative polymerase chain reaction (qPCR). Two representative *in vitro* knockdown examples are shown in Supplementary Figure S13A-B. The qPCR results showed that in comparison to control shRen, shNgp.140, and shNgp.452 demonstrated the highest knockdown in CD4 and CD8 T cells (Supplementary Figure S13A). Similarly, the most potent shRNA was defined in CD4, and CD8 T cells for *Hba-a1* (Supplementary Figure S13B), for *Hbb-b1* (data not shown), and *S100a8* (data not shown).

Based on the obtained data, the most efficient shRNA was selected for each of the target genes *Ngp* (shNgp.140), *Hbb-b1* (shHbb-b1.541), Hba-a1 (shHba-a1.122), and S100a8 (shS100a8), accordingly. The selected shRNAs were further tested in *in vivo* validation experiments, as described in the next section.

3.5 Experimental design for the *in vivo* validation of shRNA-mediated knockdown

In the next step of our study, we performed *in vivo* validation experiments to investigate the efficacy of shRNA-mediated knockdown of the selected target genes (*Ngp, Hbb-b1, Hba-a1, S100a8*) on CD4 and CD8 T cells function using several therapeutic regimes and different readouts. The experimental layout is described in Supplementary Figure S13C.

3.5.1 T cell isolation, transduction, and sorting

CD4 and CD8 T cells were first isolated from HCC-bearing donor mice, and transduced with shRNA-expressing lentiviral particles, followed by sorting of GFP^+ transduced T cells, as described previously (Figure 2).

3.5.2 Adoptive transfer and therapeutic intervention

To evaluate the therapeutic effect of shRNA-mediated knockdown of a target gene, we used C57BL/6J recipient mice harboring HCCs (genotype: $NRAS^{G12V}$/*c-Myc*, Supplementary Figure S13C). According to previous survival studies (data not shown), we defined the optimal time for the therapeutic intervention (adoptive transfer of modified shRNA-transduced CD4 and CD8 T cells) at two weeks post-HDI (Supplementary Figure S13C). Importantly, to achieve a comparable HCC stage in recipient animals, we selected those age- and gender-matched HCC-harboring animals which showed similar values in the classical diagnostic parameters for HCC and other liver diseases used in the clinic (26): aspartate aminotransferase (AST), alanine aminotransferase (ALT) and lactate dehydrogenase (LDH).

The therapy, comprising adoptively transferred T cells with shRNA-mediated knockdown of a target gene was applied once or twice in a weekly interval. For the adoptive transfer, transduced and previously pooled CD4 and CD8 T cells (approximately $2x10^5$ cells each) expressing shRNA of interest were administered to mice *i.v.* (Supplementary Figure S13C). Mice receiving T cells transduced with shRen served as a control (Supplementary Figure S13C).

To evaluate the impact of shRNA-mediated knockdown on the HCC progression, we systematically monitored several parameters in recipient mice: survival, body weight changes, liver inflammation using biochemical parameters, and expression of ICIs on CD4 and CD8 T cells.

3.6 *In vivo* knockdown of Ngp on CD4 and CD8 T cells significantly prolonged the survival of HCC-bearing mice while decreasing liver biochemical parameters

First, we aimed to validate *Ngp* as a potent T cell inhibitor, by using shNgp.140 (designated as shNgp) for *in vivo* knockdown. Prior to the adoptive transfer of shNgp-transduced T cells into C57BL/6J mice harboring HCC (genotype: $NRAS^{G12V}$/*c-Myc*), we assessed the levels of the diagnostic parameters AST, ALT, and LDH in plasma of HCC-bearing recipient mice (genotype: $NRAS^{G12V}$/*c-Myc*) (Supplementary Figure S13D) and selected comparable individuals as described above. On day 13 and 20 post-HDI, shNgp-transduced CD4 and CD8 T cells or shRen-transduced controls were adoptively transferred to the recipients. ShNgp-mediated knockdown in CD4 and CD8 T cells significantly prolonged the survival of HCC-bearing mice by 41 days compared to the shRen group (Figure 5A). We neither observed any impact on the body weight upon T cell transfer in both recipient groups (Figure 5B), nor did we detect any differences in liver tumor burden between shRen and shNgp groups at sampling, when reaching the termination criteria due to HCC development (Supplementary Figure S13E).

Over the course of the survival study, several biochemical parameters in the plasma of recipient mice were monitored to exclude toxic effects on liver metabolism caused by T cell therapy (Figure 5C, 2 representative mice are depicted). On day 34 post-HDI, we observed a six-fold increase of AST in the shNgp group which decreased by day 42 post-HDI (Figure 5C). At all other time points tested, including sampling, the AST level was lower in the shNgp group than in the shRen control group (Figure 5C). The ALT level showed to be constantly low in both groups, shNgp, and shRen, until day 54 post-HDI, when a dramatic increase was detected in the shRen group, which correlated with the advanced HCC development (Figure 5C). The kinetic of LDH was similar to AST (Figure 5C). Except for a threefold increase in shNgp group on day 42 post-HDI, LDH levels were lower in the shNgp recipient throughout the entire duration of the experiment, compared to the shRen control group (Figure 5C). Additional metabolic parameters

10.3389/fimmu.2025.1549229

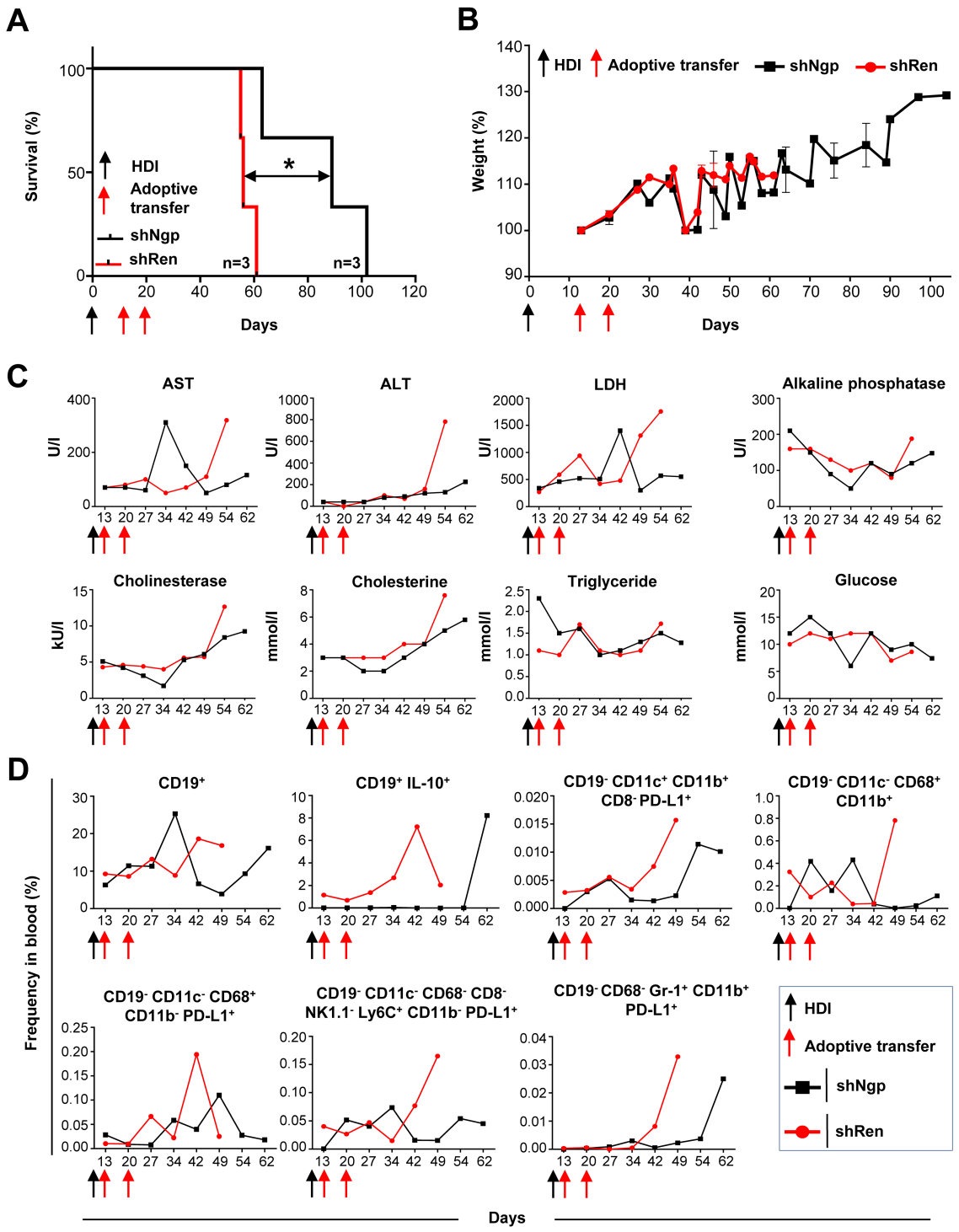

FIGURE 5
Ngp knockdown prolonged the survival of HCC-bearing recipient mice by decreasing biochemical parameters, $CD19^+$ $IL\text{-}10^+$ B cells, PD-L1-expressing monocytes, macrophages, and DCs in blood. **(A)** Kaplan-Meier survival curve (n=3 in each group). **(B)** Weight development (n=3 in each group). **(C)** Biochemical parameters in plasma (depicted are the data obtained in individual mice, as representative examples of the group). **(D)** Flow cytometry data on innate immune cells and B lymphocytes in blood (depicted are the data obtained in individual mice, as representative examples of the group). HDI, hydrodynamic tail vein injection; AST, alanine aminotransferase; ALT, aspartate aminotransferase; LDH, lactate dehydrogenase.

including alkaline phosphatase, cholinesterase, cholesterine, triglyceride, and glucose also tended to be lower in the shNgp group compared to the shRen control (Figure 5C).

In summary, our results demonstrated a significant extension of survival in HCC-bearing mice, along with improvements in liver biochemical markers, suggesting a beneficial impact of targeting *Ngp* in T cell therapy.

3.7 *In vivo* knockdown of *Ngp* resulted in the reduction of PD-L1$^+$ dendritic cells (DCs), macrophages, and IL-10$^+$ B cells in HCC-bearing mice

To assess the efficacy of *Ngp* knockdown on immune cell dynamics, we collected blood samples from the retro-orbital plexus of recipient mice and checked for potential changes in the frequency of innate immune cells and B cells over time (Figure 5D, gating strategy in Supplementary Figure S14).

The frequency of CD19$^+$ B cells remained similar between the shNgp and shRen groups until day 27 post-HDI (Figure 5D). However, in the shNgp group, CD19$^+$ B cells dramatically increased on day 34, followed by a decline on day 42 post-HDI (Figure 5D). In contrast, in the shRen group, CD19$^+$ B cells continued increasing on days 42 and 49 post-HDI, correlating with the aggressive HCC progression and recipien´s death (Figure 5D). Furthermore, shNgp-mediated knockdown led to a decreased level of immunosuppressive CD19$^+$ IL-10$^+$ B cells in comparison to the shRen control group (Figure 5D).

The *Ngp* knockdown also influenced DCs and macrophages. The proportion of PD-L1-expressing DCs (CD19$^-$ CD11c$^+$ CD11b$^+$ CD8$^-$ PD-L1$^+$) was consistently lower in the shNgp group compaired to shRen group (Figure 5D). The macrophage (CD19$^-$ CD11c$^-$ CD68$^+$ CD11b$^+$) population showed fluctuations between the shNgp and shRen groups in the first 34 days post-HDI with a dramatic increase in shRen group and a moderate decrease in shNgp group when HCC developed and animals had to be sampled (Figure 5D). The counts for macrophages expressing PD-L1$^+$ (CD19$^-$ CD11c$^-$ CD68$^+$ CD11b$^-$ PD-L1$^+$) were, in general, lower in the shNgp group (Figure 5D). Similar counts of monocytes (CD19$^-$ CD11c$^-$ CD68$^-$ CD8$^-$ NK1.1$^-$ Ly6C$^+$ CD11b$^-$ PD-L1$^+$) were observed in both groups until day 27 post-HDI with a dramatic increase from day 42 post-HDI in the shRen and a decrease in the shNgp group (Figure 5D). The frequency of neutrophils (CD19$^-$ CD68$^-$ Gr-1$^+$ CD11b$^+$ PD-L1$^+$) was comparable low and started to increase due to HCC development on day 42 and 62 in the shRen and shNgp groups, respectively (Figure 5D).

In summary, *Ngp* knockdown reduced immunosuppressive PD-L1$^+$ DCs, macrophages, and IL-10$^+$ B cells in HCC-bearing mice.

3.8 *In vivo* knockdown of *Ngp* controlled the expression of classical ICI molecules and reduced Tregs in HCC-bearing mice

To assess the impact of *Ngp* knockdown on T cell activation and classical ICIs repertoire expression, we analyzed both endogenous (GFP$^-$) and adoptively transferred (exogenous, GFP$^+$) CD4 and CD8 T cells while tracking their proliferation using eFluor450 labeling (Figure 6, Supplementary Figure S15).

We found that the PD-1 expression on endogenous GFP$^-$ CD4 T cells was similar between both groups until day 34 post-HDI followed by a strong increase from day 49 post-HDI in the shRen group and day 64 post-HDI in the shNgp group (Figure 6A). Surprisingly, exogenous GFP$^+$ CD4 T cells in the shNgp group showed a controlled, low level of PD-1 expression until the day of sampling, where a dramatic PD-1 peak was detected (Figure 6A).

Contrary results were observed between both groups regarding the expression of 4-1BBL on exogenous CD4 T cells (CD4$^+$ GFP$^+$ 4-1BBL$^+$) (Figure 6A). While the 4-1BBL expression on exogenous CD4 T cells in the shRen group dramatically dropped on the day of sampling, a strong increase of 4-1BBL was found on exogenous CD4 T cells in the shNgp group at the time of HCC development (Figure 6A). The latter effect was observed *vice versa* on CD4$^+$ GFP$^+$ eFluor450$^+$ 4-1BBL$^+$ cells (Figure 6A).

We tested a further ICI molecule CD160 in our analysis: the treatment with shNgp and shRen had only a minor effect on CD160 expression level between both groups as shown by comparable curve pattern and frequency counts (Figure 6A). The expression of CD160 on exogenous CD4 T cells (CD4$^+$ GFP$^+$ CD160$^+$) was more controlled in the shNgp group (Figure 6A).

Further analysis showed that exogenous CD4 T cells in the shNgp group showed lower IL-10 expression (CD4$^+$ GFP$^+$ eFluor450$^+$ IL-10$^+$) and a higher CD25 expression (CD4$^+$ GFP$^+$ eFluor450$^+$ CD25$^+$) compared to the shRen group (Figure 6A).

In addition, Tregs counts (CD4$^+$ GFP$^+$ Foxp3$^+$/CD4$^+$ GFP$^+$ eFluor450$^+$ Foxp3$^+$) were lower in the shNgp group compared to the shRen group, indicating reduced immunosuppression (Figure 6A).

Similar to the PD-1 expression on endogenous CD4 T cells, CD8$^+$ PD1$^+$ T cells in both treatment groups showed until day 42 post-HDI comparable counts but were in contrast to data in CD4 T cells dramatically increasing in the shNgp treatment group 54 days post-HDI (Figure 6B). The frequency of exogenous CD8$^+$ GFP$^+$ PD-1$^+$ cells in both groups was similar until day 54 post-HDI: here a strong increase of PD-1 in the shNgp group was detected and was similar to the finding on CD4$^+$ GFP$^+$ PD-1$^+$ (Figure 6B and 6A, respectively). Also, a stronger expression of PD-1 in the CD8$^+$ GFP$^+$ eFluor450$^+$ population was observed in the shNgp compared to the shRen group upon HCC development (Figure 6B). The expression pattern of 4-1BBL on endogenous CD8 T cells (CD8$^+$ 4-1BBL$^+$) resembled that on exogenous CD8 T cells (CD8$^+$ GFP$^+$ 4-1BBL$^+$) showing both a strong increase of 4-1BBL on the day of sampling in the shNgp group but not in the shRen recipient (Figure 6B). Similar observations were made for CD160 on endogenous CD8 T cells (CD8$^+$ GFP$^-$ CD160$^+$) and on exogenous CD8 T cells (CD8$^+$ GFP$^+$ CD160$^+$) (Figure 6B).

Similar to CD4 T cells, the expression of CD25 on exogenous CD8 T cells (CD8$^+$ GFP$^+$ eFluor450$^+$ CD25$^+$) was higher in the shNgp group than in the shRen recipient (Figure 6B).

In summary, the *in vivo* knockdown of *Ngp* in CD4 and CD8 T cells controlled classical ICI molecules, including PD-1, 4-1BBL, and CD160, reduced Tregs and increased CD25 expression on the transduced T cells, suggesting an enhanced T cell activation and reduced immunosuppression in HCC-bearing mice.

10.3389/fimmu.2025.1549229

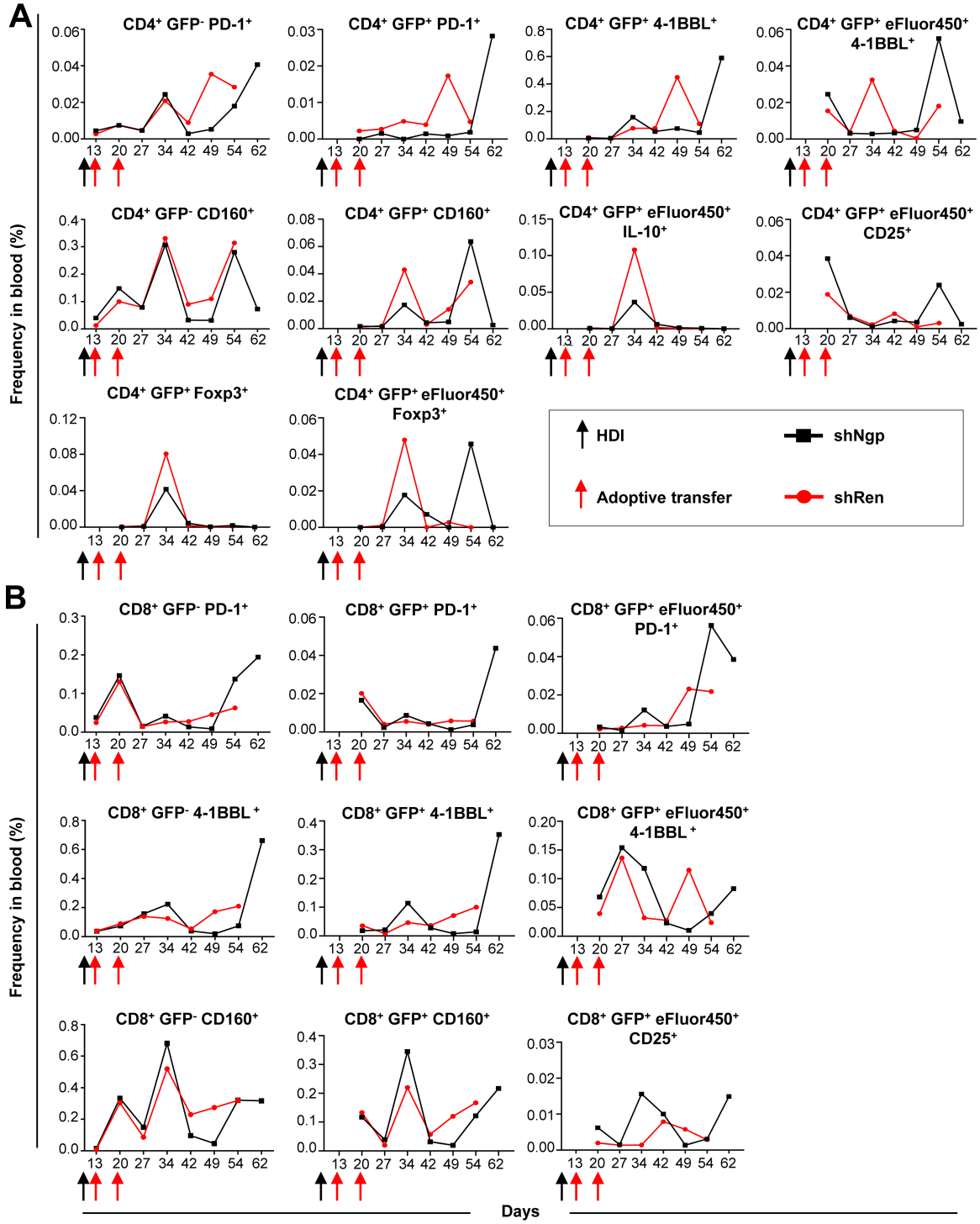

FIGURE 6
Ngp knockdown decreased the expression of PD-1, 4-1BBL, and CD160 ICIs on endogenous and exogenous CD4 T cells and increased CD25 expression on CD4 and CD8 T cells in blood. **(A, B)** Flow cytometry kinetic data of endogenous and exogenous **(A)** CD4 and **(B)** CD8 T cells in the blood of shNgp and shRen recipient mice, monitoring the expression of activation and inhibition markers upon adoptive transfer (depicted are the data obtained in individual mice, as representative examples of the group). HDI, hydrodynamic tail vein injection; GFP, green fluorescent protein.

3.9 *In vivo* knockdown of *Hbb-b1* moderately prolonged the survival of HCC-bearing mice

In a further validation study, we investigated the effect of *Hbb-b1* knockdown on HCC development (Figures 7A, B). Recipient groups were gender- and age-matched and selected according to similar AST, ALT, and LDH levels, as described in previous sections (data not shown). After the induction of HCC development in these mice, T cells were transferred on days 13 and 20 post-HDI (Figure 7A).

Upon *Hbb-b1* knockdown, we detected a moderate survival benefit of 11 days (Figure 7A). Upon T cell transfer, no toxicity was observed, as confirmed by a stable body weight in both experimental groups (Figure 7B). This was in line with previous experiments using shNgp (see section above and Figure 5B). No influence on the tumor burden was observed between the experimental and control group (data not shown).

In summary, *Hbb-b1* knockdown resulted in a moderate survival extension in HCC-bearing mice, with no observed toxicity or impact on tumor burden.

3.10 *In vivo* knockdown of *Hba-a1* and *S100a8* prolonged the survival of HCC-bearing mice, decreased liver biochemical parameters, PD-L1-expressing immune cells, and kept under control Tregs and several classical ICIs on T cells

We further tested an *in vivo* knockdown of *Hba-ba1* and *S100a8* using this time only a single transfer of T cells on day 13 post-HDI (Figure 7C). A single dose of shS100a8- and shHba-a1-transduced T cells led to a survival benefit of 19 and 25 days, respectively, in comparison to the shRen control group (Figure 7C). Next, we monitored the biochemical parameters in these mice. On day 27 post-HDI, we observed a decreased level of AST in the shS100a8- and shHba-a1 groups in comparison to shRen control mice, whereas ALT levels varied among the groups (Supplementary Figure S16A). The LDH level was highest in the shRen control group, moderately increased in the sh1008a8, and constantly low in the shHba-a1 group (Supplementary Figure S16A). The level of alkaline phosphatase was constantly low in the shS100a8- and shHba-a1 groups in comparison to the shRen control with a peak of this parameter on day 27 post-HDI (Supplementary Figure S16A). The levels of cholinesterase and cholesterine were similar among the groups, however, both parameters massively increased in mice with *S100a8* knockdown on day 68 post-HDI upon HCC development (Supplementary Figure S16A). The kinetic of triglyceride and glucose did not change in comparison to the shRen group (Supplementary Figure S16A).

Besides the survival study, we also monitored immune cells in the blood of recipient mice (Supplementary Figure S16B). Similar to the Ngp data, we observed lower numbers of $CD19^+$ and $CD19^+$ $IL\text{-}10^+$ B cells in shHba-a1 and shS100a8 recipient mice, in comparison to the shRen control group (Supplementary Figure S16B). Furthermore, the *Hba-a1* and *S100a8* knockdown led to a constant lower level of PD-L1-expressing DCs and macrophages ($CD19^-$ $CD11c^+$ $CD11b^+$ $CD8^-$ $PD\text{-}L1^+$ and $CD19^-$ $CD11c^-$ $CD68^+$ $CD11b^-$ $PD\text{-}L1^+$, respectively) (Supplementary Figure S16B). The frequency of $CD11b^+$ macrophages ($CD19^-$ $CD11c^-$ $CD68^+$ $CD11b^+$) was in general increased in the shHba-a1 and shS100a8 groups, similar to the shNgp group (Supplementary Figure S16B and Figure 5D). Similarly to the Ngp data, the counts for macrophages expressing $PD\text{-}L1^+$ ($CD19^-$ $CD11c^-$ $CD68^+$ $CD11b^-$ $PD\text{-}L1^+$) were in general lower in the shHba-a1 and shS100a8 groups (Supplementary Figure S16B and Figure 5D). A comparable pattern was observed in the monocyte population ($CD19^-$ $CD11c^-$ $CD68^-$ $CD8^-$ $NK1.1^-$ $Ly6C^+$ $CD11b^-$ $PD\text{-}L1^+$) in all groups (Supplementary Figure S16B). Despite a peak in the frequency of $PD\text{-}L1^+$ neutrophils ($CD19^-$ $CD68^-$ $Gr\text{-}1^+$ $CD11b^+$ $PD\text{-}L1^+$) on day 41 post-HDI, the shS100a8 group kept those cells in controlled lower levels in comparison to shRen and shHba-a1 groups (Supplementary Figure S16B).

Further analysis of CD4 T cells showed the constantly low PD-1 expression in endogenous $CD4^+$ $PD\text{-}1^+$ and exogenous GFP^+ $CD4^+$ $PD\text{-}1^+$ T cells in the shHba-a1 and shS100a8 groups, in comparison to shRen control (Supplementary Figure S17A). As observed in the Ngp data, we detected an increase of exogenous $CD4^+$ GFP^+ $4\text{-}1BBL^+$ and $CD4^+$ GFP^+ $eFluor450^+$ $4\text{-}1BBL^+$ T cells in shS100a8 and shRen groups (Supplementary Figure S17A). Interestingly, the *in vivo* knockdown of *Hba-a1* kept at the stable level not only PD-1 but also 4-1BBL expression despite the HCC development (Supplementary Figure S17A). Further analysis of CD4 T cells showed similar fluctuations in the expression of the CD160 molecule as detected in Ngp data set. Still, the expression of CD160 on endogenous $CD4^+$ $CD160^+$ as well as exogenous CD4 T cells ($CD4^+$ GFP^+ $CD160^+$) was more controlled in shHba-a1 and shS100a8 groups when compared to the shRen control (Supplementary Figure S17A).

Exogenous CD4 T cells in the shHba-a1 and shS100a8 groups also showed a lower IL-10 ($CD4^+$ GFP^+ $eFluor450^+$ $IL\text{-}10^+$) and CD25 ($CD4^+$ GFP^+ $eFluor450^+$ $CD25^+$) expression compared to the shRen control group (Supplementary Figure S17A). Importantly, Tregs counts ($CD4^+$ GFP^+ $Foxp3^+$/$CD4^+$ GFP^+ $eFluor450^+$ $Foxp3^+$) remained low and well controlled in the shHba-a1 and shS100a8 groups, starting from day 44 until HCC development, in contrast to the shRen control group (Supplementary Figure S17A).

We further analyzed CD8 T cells and detected that the shS100a8 group showed a similar pattern of control of PD-1 and 4-1BBL expression, as detected in the shNgp group, whereas the shHba-a1 group fully controlled the expression of both molecules on CD8 T cells (Supplementary Figure S17B and Supplementary Figure S8B). Similar to CD4 T cells, the expression of CD160 on endogenous CD8 T cells ($CD8^+$ $CD160^+$) and on exogenous CD8 T cells ($CD8^+$ GFP^+ $CD160^+$) was more controlled in shHba-a1 and shS100a8 groups in comparison to shRen control (Supplementary Figure S17B). Interestingly, CD25 expression in the shHba-a1 and shS100a8 groups was not as pronounced as in the shNgp group (Supplementary Figure S17B and Figure 6B).

10.3389/fimmu.2025.1549229

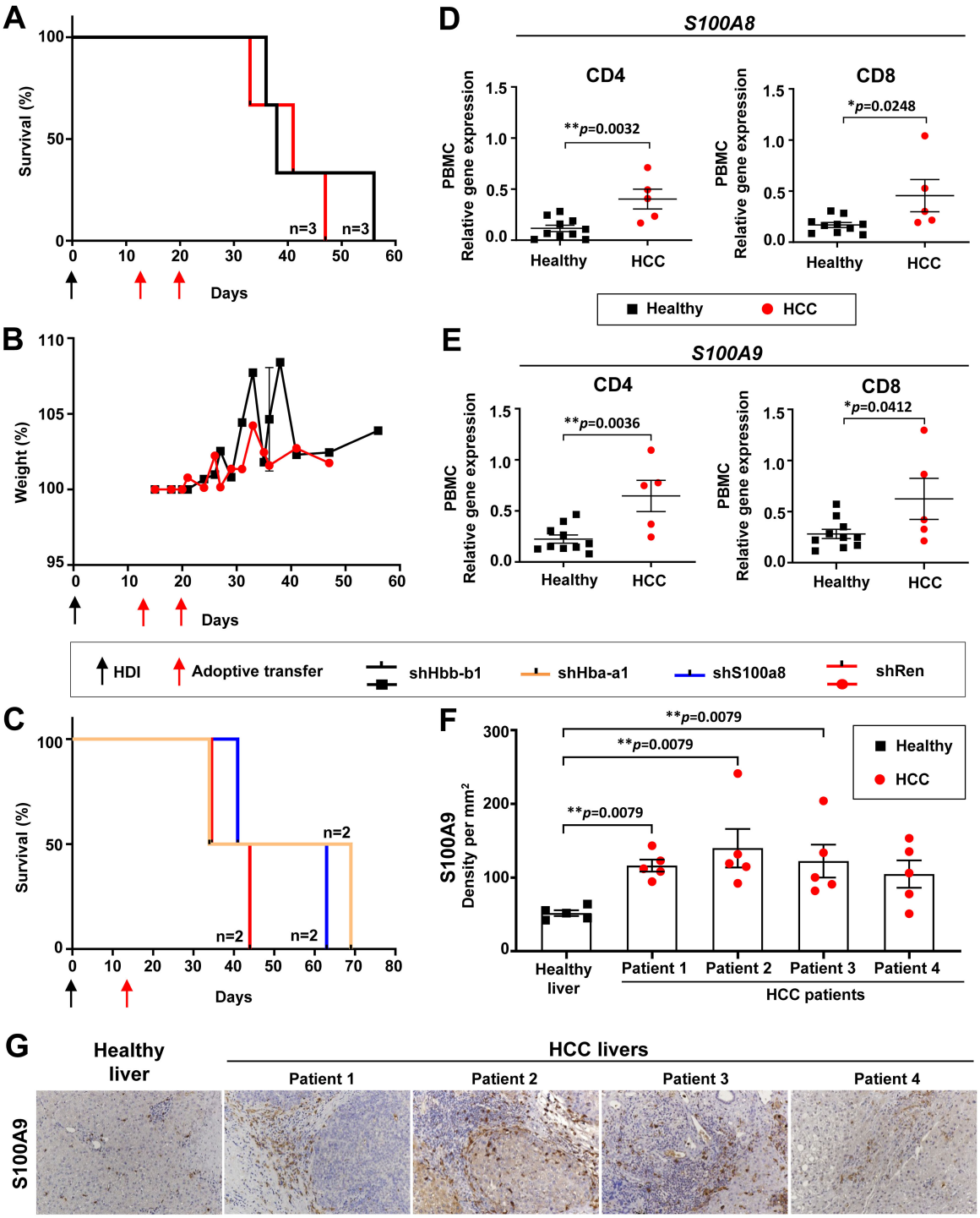

FIGURE 7
Hba-a1 and *S100a8* knockdown prolonged the survival of HCC-bearing recipient mice and *S100A8* & *S100A9* were found upregulated in HCC patients. **(A)** Kaplan-Meier survival curve of mice that received two transfers of shHbb-b1-transduced CD4 and CD8 T cells or control (shRen) (n=3 in each group). **(B)** Weight development of mice that received two transfers of shHbb-b1-transduced CD4 and CD8 T cells or control (shRen) (n=3 in each group). **(C)** Kaplan-Meier survival curve of mice that received one transfer of shHba-a1- or shS100a8-transduced CD4 and CD8 T cells or control (shRen) (n=2 in each group). **(D, E)** CD4 T cells and CD8 T cells were isolated from PBMCs and liver tissues of HCC patients and healthy donors and analyzed for the expression of **(D)** *S100A8* and **(E)** *S100A9* using qPCR. **(G)** Representative images of IHC using anti-S100A9 staining in human HCCs (n=4) and healthy donor (n=1). Scale bar, 100 μm. **(F)** Cellular density of S100A9 positive cells in human HCCs (n=4) and healthy donor (n=1). HCC, hepatocellular carcinoma; HDI, hydrodynamic tail vein injection; *S100A8*, S100 calcium-binding protein A8; *S100A9*, S100 calcium-binding protein A9.

In summary, the *in vivo* knockdown of *Hba-a1* and *S100a8* prolonged the survival of HCC-bearing mice already after one T cell transfer, thereby decreasing liver biochemical parameters, $CD19^+$ $IL\text{-}10^+$ B cells, PD-L1-expressing DCs, and macrophages as well as Tregs and inhibitory markers, like PD-1, CD160 and 4-1BBL, on T cells. *In vivo* knockdown of *Hba-a1* was especially efficient while leading to a constantly low expression of inhibitory markers on both, CD4 and CD8 T cells.

3.11 T cell therapy and *in vivo* knockdown of *Ngp*, *Hbb-b1*, *Hba-a1*, and *S100a8* was safe as confirmed by histopathological analyses of different murine organs

To exclude organ pathology upon T cell therapy, we isolated different organs from all mice in validation studies. Importantly, we could not detect any significant histopathological changes in any of tested groups after T cell transfer (Supplementary Figure S18). The brain, heart, lungs, kidneys, pancreas, spleen preserved their histoarchitecture and cellular structure as confirmed by an experienced pathologist (Supplementary Figure S18). As expected, microscopical examination of liver tissues revealed the presence of multiple neoplastic nodules composed of pleomorphic cells in all experimental groups, consistent with HCC development (Supplementary Figure S18). However, no additional pathological alterations were detected in liver tissues beyond those associated with tumor progression, further supporting the safety of the administered T cell therapy and gene knockdown approaches.

3.12 Upregulation of neutrophil-associated proteins and significant increase in expression of *S100A8* and *S100A9* genes in CD4 and CD8 T cells in PBMCs of HCC patients

To extrapolate the data obtained in mice to humans, we analyzed patients-derived material for the expression of the newly identified target genes. For these purposes, CD4 and CD8 T lymphocytes were isolated and sorted from HCC tumor tissue, HCC-free tissue areas, and healthy liver tissue, as well as from the peripheral blood mononuclear cells (PBMCs) of HCC patients and healthy donors. qPCR analysis was performed to define the expression of target genes in human CD4 and CD8 T cells (Figures 7D, E, Supplementary Figure S19). As *Ngp* encodes a mouse-specific neutrophil-associated protein (27) not present in humans, we analyzed cathelicidin (*CAMP*), the closest orthologue of mouse *Ngp* (28). Surprisingly, we could not confirm an upregulation of CAMP on PBMCs isolated from HCC patients in comparison to healthy controls (Supplementary Figure S19A).

Next, we investigated the expression of *HBB*, the human orthologue to mouse-specific *Hbb-b1*, in the PBMCs of HCC patients. We could not identify any differences in *HBB* expression between PBMCs from HCC patients and healthy donors (Supplementary Figure S19B). We compared further prominent and highly upregulated neutrophil-associated genes, *lipocalin2* (*Lcn2*), *S100a8*, and *S100a9*, identified as potential new targets in the microarray data (27). Interestingly, we detected lower expression levels of *LCN2* in CD4 and CD8 T cells in PBMCs from HCC patients (Supplementary Figure S19C). However, in T cells isolated from HCC liver tissues (HCC-free and HCC tissue areas), the opposite effect (not significant) was observed as *LCN2* expression was increased compared to healthy controls (Supplementary Figure S19D).

Finally, we analyzed the expression of *S100A8* and *S100A9* and found a significant increase of both genes in CD4 and CD8 T cells in PBMCs of HCC patients compared to healthy controls (Figures 7D–F).

Importantly, too low numbers of CD4 and CD8 T cells were obtained from resected HCC and healthy liver tissues, and thus, RNA thereof was a limiting factor in these experiments. Due to the limited amount of material, we could not perform further qPCR analysis on T lymphocytes isolated from liver tissue for other targets. We, therefore, continued checking *S100A8/S100A9* molecule in human paraffin liver sections (see next section).

3.13 Immunohistochemistry analysis revealed increased S100A9-expressing immune cell infiltration in human HCC

IHC analysis of selected HCC patients revealed a strong infiltration of tumor stroma and parenchyma with S100A9-expressing immune cells in comparison to healthy control (Figures 7F, G), as defined by an experienced pathologist. The cellular density of S100A9-expressing immune cells in the HCC tumor core in four tested HCC patients was significantly increased compared to healthy control samples (Figure 7F).

4 Discussion

In the present study, we aimed to identify new inhibitory targets, novel ICIs, on T lymphocytes that are triggered by the HCC TME and are subsequently leading to the inactivation of T cell function in patients with HCC.

We first worked in mice and performed a microarray analysis on T lymphocytes isolated from autochthonous HCC murine models, which highly reflect human disease (21–23, 25, 29, 30). Based on our results, we identified several upregulated genes (72 genes) in memory ($CD44^+$) (31) CD4 and CD8 T lymphocytes in HCC-bearing mice, which were further validated using the shRNA library and the RNAi screen.

The RNAi screen study was performed in four individually treated mice and for the analysis we used pooled data from all four mice and data obtained from individual animals were additionally considered. Surprisingly, only a few shRNAs enrichments were found on CD4 T cells (liver, relLN, blood), whereas shRNAs in CD8 T cells were found enriched in all the analyzed organs. Among the

obtained data, we found that shRNAs were targeting prominent target genes such as: *CD200r1, Tspo*, and *Cacna1d*, which were detected in the liver and relLN of HCC-bearing mice. In humans, *CD200R1* is mainly expressed on myeloid-derived and lymphoid-derived immune competent cells (32) and the interaction with its ligand *CD200R1* was reported to promote relapse of rectal cancer (33), to be involved in HCC progression (34) and high expression of *CD200R1* was associated with poor prognosis in non-small cell lung cancer (35). In humans, *TSPO* was reported to be involved in the regulation of cellular proliferation, apoptosis, and mitochondrial functions (36). Further, *TSPO* was found up-regulated in colorectal and breast cancer, where it promotes the malignancy of aberrant cells (37, 38). *CACNA1D* belongs to the family of Voltage-gated calcium channels, which play a role in cellular functions including mitogenesis, proliferation, differentiation, apoptosis, and metastasis (39). High expression of *CACNA1D* correlated with various types of cancer (40).

For the validation studies, we focused on *Ngp*, *Hbb-b1*, *Hba-a1*, and *S100a8*, which were highly upregulated in the microarray analysis and T cells, harboring shRNAs which targeted these genes, were present at higher frequencies in RNAi screen data of individual mice.

The closest human orthologue to *Ngp* is the anti-microbial peptide *CAMP* (28). Neutrophils contain several abundant anti-microbial proteins and some of those proteins are shared between mice and humans, such as LCN2, cathepsin G (CTSG), myeloperoxidase, and S100A8/A9 (27, 41). Importantly, *Lcn2, S100a8, and S100a9* were also found to be highly upregulated in HCC liver, relLN, and spleen in the microarray and screen studies (individual mouse analysis). Interestingly, no expression of *Ngp* on T lymphocytes could be detected to date and it seems that our data demonstrated the involvement of *Ngp* (its upregulation) in T cells in murine HCC for the first time. However, the overexpression of *Ngp´* s orthologues in human CD4 and CD8 T cells in HCC remains to be investigated using patient-derived HCC tissues, as discussed below.

The *Hbb-b1* gene is one out of four subunits of hemoglobin, a protein in red blood cells, which is mediating the oxygen transport (42). The human orthologue *HBB* (42, 43), mainly present in erythrocytes, is also expressed in macrophages, epithelial cells, neurons, and hepatocytes (44). In liver cancer, low oxygen levels lead to hypoxic conditions, which in turn augment an increased availability of hemoglobin and other factors to provide tumor angiogenesis (42, 45). To the best of our knowledge, we are the first to show upregulation of *Hbb-b1* in T cells in HCC. However, its expression in the human HCC context remains to be elucidated, as discussed below.

The *Hba-a1* gene, which encodes the alpha 1 subunit of hemoglobin, is crucial for the oxygen transport (46). Hba-a1 is located in the myelin sheath and is expressed in different structures, including blood vessels, early conceptus, the hematopoietic system, liver, and visceral pericardium (47). Its human orthologue *HBA1* (48) is associated with different hemoglobin disorders (Heinz body anemia, alpha thalassemia, familial erythrocytosis 7, and hemoglobin H disease) (49). Interestingly, the knockdown of *Hba-a1* was more efficient and led to a better survival in our validation studies than knockdown of *Hbb-b1*. However, this is reported for the first time and requires follow-up studies with a deeper analysis of data with an increased group size and a direct comparison of both molecules.

S100A8 and S100A9 are two closely related proteins that belong to the S100 family of calcium-binding proteins (50). Both S100A8 and S100A9 play important roles in various cellular processes, including inflammation and immune response (51, 52). S100A8 and S100A9 are frequently expressed in neutrophils, macrophages, monocytes, and other immune cells (51, 53, 54). Among them, calprotectin is abundantly expressed in neutrophils, accounting for approximately 50% of cytoplasmic proteins (55, 56). In an inflammatory environment, S100A8 and S100A9 can be expressed in activated keratinocytes, epithelial cells, and osteoclasts (50, 52, 57). Most S100 family members, such as S100A8 and S100A9, have already been reported to be involved in liver cancer (50). Extracellular S100A9 enhanced the activation of the mitogen-activated protein kinase (MAPK) signaling pathway via combination with the receptor advanced glycation end-product (58, 59). Besides, both S100A8 and S100A9 were previously reported to be associated with HCC by promoting cell proliferation (60, 61).

In our study, the knockdown of *Ngp* in T cells resulted in a significant prolongation of survival of HCC-bearing mice upon two therapeutic T cell transfers (41 days). Whereas *Hbb-b1* (10 days) was not as effective. Furthermore, a single therapeutic transfer of shHba-a1 and shS100a8-transduced T cells showed a prolongation of survival (26 and 20 days, respectively).

Importantly, the adoptive T cell therapy comprising CD4 and CD8 T cells with either *Ngp, Hbb-b1*, *Hba-a1* or *S100a8* knockdown was well tolerated and showed no toxicity, weight loss or any other side effects. Currently, many clinical trials on HCC are investigating the safety of T cell receptor and chimeric antigen receptor T cell (CAR-T) therapy. Two studies reported an objective response (62, 63). Until today, four approved CAR-T cell therapies for the treatment of hematologic cancer are available and two further CAR-T cell therapies for multiple myeloma are on the way to approval as standard use (62, 63). Key limitation factors for the approval of T cell therapies in solid tumors are the accessibility of T cells in the complex tumor structure, high heterogeneity and the immunosuppressive TME, inducing up-regulation of ICIs and subsequent dysfunction of T cells. A limited expansion and persistence of transferred CAR-T cells were also reported and are considered as critical parameters to prevent from tumor recurrence (62, 63). In our study, a survival benefit upon *Ngp*, *Hba-a1*, and *S1008* knockdown in T cells in HCC was achieved and was accomplished by a reduction of PD-1 on CD4 T cells in the blood. This highlights the efficacy of T cell therapy to influence PD-1 expression without additional intervention, such as anti-PD-1 blocking antibodies, like e.g. Nivolumab which are approved by the U.S. Food and Drug Administration and are currently used for HCC treatment (64). Another benefit of *Ngp*, *Hba-a1*, and *S1008* knockdown was the reduction of Foxp3 T cells (Tregs), which are associated with poor survival prognosis in HCC patients (65). Interestingly, we observed similar patterns among

shNgp and shS1008 groups regarding the control of expression of PD-1, 4-1BBL, and CD160 inhibitory molecules with a final increase of those on T cells upon HCC development. In contrast, in the shHba-a1 group, the expression of all three inhibitory molecules was kept mostly at constantly low levels. However, its efficacy needs to be further studied in follow-up studies.

The knockdown of *Ngp*, *Hba-a1*, and *S1008* also positively impacted innate immune cell populations by reducing PD-L1-expressing monocytes, DCs, and macrophages. In our previous studies, B cells were shown to be increased in HCC, suggesting a tumor-promoting role (24, 66). In line with this, we found IL-10$^+$-expressing B cells to be decreased in groups treated with shNgp, shHba-a1, and shS1008-transduced T cells.

Another beneficial effect of T cell therapy could be observed on biochemical parameters in plasma such as AST, ALT, LDH, ALP, GDH, cholesterine, triglyceride, and glucose. These parameters belong to a standard clinical biochemical analysis of plasma which is used to detect hepatotoxicity in patients (67). In our study, the biochemical parameters AST, ALT, and LDH were kept at lower levels upon T cell therapy with the knockdown of *Ngp*, *Hba-a1*, and *S1008* in comparison to the control (shRen).

To extrapolate our observations into human/clinic, we identified human orthologues for the defined murine inhibitory target genes. Thereby, we could partially confirm our microarray data by showing upregulation of *S100A8* and *S100A9* in T cells and also in human samples using qPCR - both *S100A8* and *S100A9* were found significantly upregulated on CD4 and CD8 T cells isolated from blood PBMCs of HCC patients. Importantly, S100A9-positive cells were also upregulated in human HCC tissues derived from four patients.

In contrast to our expectation, *LCN2*, *CAMP*, and *HBB*, did not confirm our data obtained in mice and were not found upregulated in blood PBMCs isolated from HCC patients. Although *LCN2*, *CAMP*, and *HBB* are orthologues of mouse *Lcn2, Ngp*, and *Hbb-b1*, it was reported that there are divergences in the expression and the splicing of genes between human and mouse which might explain the observed discrepancies (68, 69).

It is also important to mention that T cells in our mouse study were isolated from tissues and predominantly compared to human T cells isolated from PBMCs. Different cell localization contains different composition of activation/inhibitory receptors in the surrounding compartment which shapes the phenotype of immune cells (70). In studies of Tada et al. on patients with advanced gastric cancer and VEGF-blocking antibody treatment, tumor-infiltrating lymphocytes (TILs) and PBMCs were compared regarding their expression of ICIs (PD-1, LAG3, CTLA-4, ICOS) and demonstrated a higher presence of ICIs on TILs than on PBMCs, highlighting the influence of T cell localization on the T cell phenotype (71). Performing single-cell sequencing of TILs from different tumors revealed that even within the same tumor different subtypes of T cells are present which differ from T cells in normal tissue (72). Also, it was mentioned that TILs found in one type of cancer, differ from those found in another type of cancer (72), which might be also influenced by the stage of the disease (72, 73). Therefore, to establish tools for phenotyping T cells as prognostic markers, sufficient characterizations are necessary and for treatments with immunomodulatory agents, the stages of disease and the T cell source have to be considered. Importantly and in line with the above mentioned, upregulation of *LCN2* which was not detected in PBMCs, although not significant, was shown in our study in human HCC tissues in CD4 and CD8 T cells. Therefore, it remains to be elucidated using patients-derived HCC tissues, whether *Ngp*, *Hbb-b1*, *Hba-a1*, and *S1008* orthologues are upregulated on T cells during HCC development. Also, further prominent genes identified in the screen (*CD200r1, Tspo, Cacna1d*) need to be validated in human material. While planning validation experiments, it is highly important to perform kinetic studies and to follow-up the changes in counts as well as ICIs phenotype in adoptively transferred as well as endogenous T cells. Our kinetic studies showed that T cell therapy influences also endogenous CD4 and CD8 T cells and that the expression pattern on transferred (exogenous) T cells mostly resembled the expression pattern of endogenous CD4 and CD8 T cells.

We performed validation studies for only four (*Ngp, Hbb-b1, Hba-a1, S100a8*) genes. Further studies on genes identified in the screen need to be performed and confirmed in human material, including a thorough mechanistic characterization. Also, CD4 and CD8 T cells should be applied *in vivo* separately to unravel the potential of shRNA for each T cell type individually. Further, a combination therapy, comprising i) "therapeutic" T cells with ii) antibodies targeting classical ICIs such as α-PD-1 and/or cancer vaccines based e.g. on attenuated *Listeria monocytogenes* as recently developed in our study (66), could be further considered, especially at advanced stages of this highly aggressive malignant liver disease.

5 Conclusions

In conclusion, in our study, we defined new inhibitory markers (ICI molecules) arising on memory T cells during aggressive HCC development. Employing a murine model that closely mimics human disease, we identified a repertoire of upregulated genes in CD4 and CD8 T lymphocytes, unveiling potential targets for therapeutic intervention.

The adoptive T cell therapy was safe and targeting *Ngp*, *Hba-a1*, and *S100a8* genes demonstrated a substantial survival benefit in aggressive murine HCC models. Moreover, this therapeutic approach exhibited efficacy in modulating immune checkpoints, such as PD-1, 4-1BBL, and CD160 on endogenous and exogenous (transferred) CD4 and CD8 T cells.

Beyond survival outcomes, our T cell therapy exerted positive effects on innate immune cell populations while reducing PD-L1 molecules on DCs, monocytes, and macrophages, decreasing IL-10$^+$ B cells and controlling liver biochemical parameters, altogether offering a comprehensive perspective on its potential clinical applications. In addition, we identified the presence of at least one target (*S100A8/S100A9*) in human samples using qPCR analysis in PBMCs and via IHC on HCC liver tissues. The obtained results

pave the way for the use of the defined molecules as important immunotherapeutic targets in further preclinical and clinical studies in HCC patients.

Data availability statement

The data presented in the study are deposited in the Gene Expression Omnibus (GEO) repository, under the link GEO Accession viewer, the accession number GSE144811.

Ethics statement

The studies involving humans were approved by the Helsinki Declaration and was approved by the Ethics Committee of the MHH (ethical codes: 8742_BO_K_2019). The studies were conducted in accordance with the local legislation and institutional requirements. The participants provided their written informed consent to participate in this study. The animal study was approved by LAVES, Niedersächsisches Landesamt für Verbraucherschutz und Lebensmittelsicherheit; AZ 18/2808, 15/1766, 13/1342. The study was conducted in accordance with the local legislation and institutional requirements.

Author contributions

IH: Formal analysis, Investigation, Methodology, Validation, Visualization, Writing – original draft. LH: Formal analysis, Investigation, Methodology, Validation, Visualization, Writing – original draft. NP: Formal analysis, Investigation, Methodology, Validation, Writing – original draft, Visualization. HS: Investigation, Methodology, Data curation, Formal analysis, Validation, Writing – original draft. LG: Formal analysis, Investigation, Methodology, Data curation, Software, Validation, Visualization, Resources, Writing – original draft. CO: Formal analysis, Investigation, Data curation, Methodology, Validation, Visualization, Writing – original draft. NB: Formal analysis, Investigation, Methodology, Validation, Visualization, Data curation, Software, Writing – original draft. JA: Data curation, Formal analysis, Investigation, Methodology, Software, Validation, Visualization, Writing – original draft. MJ: Data curation, Formal analysis, Investigation, Methodology, Software, Validation, Visualization, Writing – original draft. RS: Data curation, Formal analysis, Software, Investigation, Methodology, Validation, Visualization, Writing – original draft. AJ: Data curation, Formal analysis, Investigation, Methodology, Software, Validation, Visualization, Writing – original draft. KT: Investigation, Validation, Visualization, Data curation, Formal analysis, Methodology, Resources, Writing – original draft. TH: Investigation, Methodology, Data curation, Formal analysis, Validation, Visualization, Writing – original draft. NJ: Investigation, Methodology, Formal analysis, Validation, Visualization, Writing – original draft. DB: Conceptualization, Project administration, Resources, Supervision, Data curation, Formal analysis, Validation, Writing – original draft. FK: Data curation, Formal analysis, Investigation, Resources, Supervision, Validation, Methodology, Project administration, Visualization, Writing – original draft. RL: Formal analysis, Investigation, Methodology, Resources, Supervision, Data curation, Project administration, Validation, Writing – original draft. RG: Formal analysis, Investigation, Methodology, Software, Supervision, Validation, Data curation, Project administration, Writing – original draft. HL: Funding acquisition, Investigation, Project administration, Supervision, Validation, Resources, Writing – original draft. MM: Conceptualization, Project administration, Resources, Supervision, Writing – original draft. TY: Conceptualization, Data curation, Formal analysis, Funding acquisition, Investigation, Methodology, Project administration, Resources, Software, Supervision, Validation, Visualization, Writing – original draft, Writing – review & editing.

Funding

The author(s) declare that financial support was received for the research and/or publication of this article. TY acknowledges the support by the German Research Foundation (DFG) (grant YE 151/2-1, AOBJ: 618426), Young Academy MHH, HiLFII MHH, Ellen Schmidt Program MHH. This work was also supported in part by the Fritz Thyssen Foundation (grant REF.10.16.1.031MN), Wilhelm-Sander Foundation (grant 2013.107.1), Gilead Sciences International Research Scholars Program in Liver Disease (Research Award to TY), Niedersächsische Krebsgesellschaft e.V., Foundation MHH PLUS (grant to TY and HL). This work was supported in part by the German Academic Exchange Service (DAAD) in the scope of the Doctoral Program in Germany 2019/2024 under Grant (Project-ID 91736778 to NP).

Acknowledgments

We thank Frank Dsiosa for excellent technical support (Department of Clinical Chemistry, MHH, Hannover). We are thankful to Qingluan Hu, Kateryna Potapenko, Anastasiia Semenets, Sofiya Kotsyuda, Oladimeji Paul Duduyemi, Jennifer Schmidt (Department of Gastroenterology, Hepatology, Infectious Diseases and Endocrinology, MHH, Hannover), Maria Höxter, and Petra Hagendorff (Experimental Immunology, HZI, Braunschweig) for excellent technical support.

Conflict of interest

The authors declare that the research was conducted in the absence of any commercial or financial relationships that could be construed as a potential conflict of interest.

Generative AI statement

The author(s) declare that no Generative AI was used in the creation of this manuscript.

Publisher's note

Supplementary material

The Supplementary Material for this article can be found online at: https://www.frontiersin.org/articles/10.3389/fimmu.2025.1549229/full#supplementary-material

References

1. Sung H, Ferlay J, Siegel RL, Laversanne M, Soerjomataram I, Jemal A, et al. Global cancer statistics 2020: globocan estimates of incidence and mortality worldwide for 36 cancers in 185 countries. *CA: Cancer J Clin*. (2021) 71:209–49. doi: 10.3322/caac.21660

2. World Health Organization. *Cancer* (2021). Available online at: https://www.who.int/news-room/fact-sheets/detail/cancer (Accessed March 3, 2021). https://www.who.Int/News-Room/Fact-Sheets/Detail/Cancer.

3. Llovet JM, Kelley RK, Villanueva A, Singal AG, Pikarsky E, Roayaie S, et al. Hepatocellular carcinoma. *Nat Rev Dis Primers*. (2021) 7:6. doi: 10.1038/s41572-020-00240-3

4. Singal AG, Lampertico P, Nahon P. Epidemiology and surveillance for hepatocellular carcinoma: new trends. *J Hepatol*. (2020) 72:250–61. doi: 10.1016/j.jhep.2019.08.025

5. Schwartz H, Blacher E, Amer M, Livneh N, Abramovitz L, Klein A, et al. Incipient melanoma brain metastases instigate astrogliosis and neuroinflammation. *Cancer Res*. (2016) 76:4359–71. doi: 10.1158/0008-5472.CAN-16-0485

6. Kumari R, Sahu MK, Tripathy A, Uthansingh K, Behera M. Hepatocellular carcinoma treatment: hurdles, advances and prospects. *Hepat Oncol*. (2018) 5: HEP08. doi: 10.2217/hep-2018-0002

7. Celsa C, Giuffrida P, Stornello C, Grova M, Spatola F, Rizzo GEM, et al. Systemic therapies for hepatocellular carcinoma: the present and the future. *Recenti Prog Med*. (2021) 112:110–6. doi: 10.1701/3559.35371

8. Llovet JM, Ricci S, Mazzaferro V, Hilgard P, Gane E, Blanc JF, et al. Sorafenib in advanced hepatocellular carcinoma. *N Engl J Med*. (2008) 359:378–90. doi: 10.1056/NEJMoa0708857

9. Finn RS, Qin S, Ikeda M, Galle PR, Ducreux M, Kim TY, et al. Atezolizumab plus bevacizumab in unresectabl e hepatocellular carcinoma. *New Engl J Med*. (2020) 382:1894–905. doi: 10.1056/NEJMoa1915745

10. Cassetta L, Bruderek K, Skrzeczynska-Moncznik J, Osiecka O, Hu X, Rundgren IM, et al. Differential expansion of circulating human mdsc subsets in patients with cancer, infection and inflammation. *J Immunother Cancer*. (2020) 8:e001223. doi: 10.1136/jitc-2020-001223

11. Greten TF, Manns MP, Korangy F. Immunotherapy of hcc. *Rev Recent Clin Trials*. (2008) 3:31–9. doi: 10.2174/157488708783330549

12. Korangy F, Hochst B, Manns MP, Greten TF. Immunotherapy of hepatocellular carcinoma. *Expert Rev Gastroenterol Hepatol*. (2010) 4:345–53. doi: 10.1586/egh.10.18

13. Breous E, Thimme R. Potential of immunotherapy for hepatocellular carcinoma. *J Hepatol*. (2011) 54:830–4. doi: 10.1016/j.jhep.2010.10.013

14. Ding W, Xu X, Qian Y, Xue W, Wang Y, Du J, et al. Prognostic value of tumor-infiltrating lymphocytes in hepatocellular carcinoma: A meta-analysis. *Med (Baltimore)*. (2018) 97:e13301. doi: 10.1097/MD.0000000000013301

15. Wada Y, Nakashima O, Kutami R, Yamamoto O, Kojiro M. Clinicopathological study on hepatocellular carcinoma with lymphocytic infiltration. *Hepatology*. (1998) 27:407–14. doi: 10.1002/hep.510270214

16. Chew V, Tow C, Teo M, Wong HL, Chan J, Gehring A, et al. Inflammatory tumour microenvironment is associated with superior survival in hepatocellular carcinoma patients. *J Hepatol*. (2010) 52:370–9. doi: 10.1016/j.jhep.2009.07.013

17. Marin-Acevedo JA, Dholaria B, Soyano AE, Knutson KL, Chumsri S, Lou Y. Next generation of immune checkpoint therapy in cancer: new developments and challenges. *J Hematol Oncol*. (2018) 11:39. doi: 10.1186/s13045-018-0582-8

18. Qin W, Cao Z-Y, Liu S-Y, Xu X-D. Recent advances regarding tumor microenvironment and immunotherapy in hepatocellular carcinoma. *Hepatoma Res*. (2020) 6:24. doi: 10.20517/2394-5079.2020.04

19. Mohr R, Jost-Brinkmann F, Ozdirik B, Lambrecht J, Hammerich L, Loosen SH, et al. Lessons from immune checkpoint inhibitor trials in hepatocellular carcinoma. *Front Immunol*. (2021) 12:652172. doi: 10.3389/fimmu.2021.652172

20. Federico P, Petrillo A, Giordano P, Bosso D, Fabbrocini A, Ottaviano M, et al. Immune checkpoint inhibitors in hepatocellular carcinoma: current status and novel perspectives. *Cancers (Basel)*. (2020) 12:3025. doi: 10.3390/cancers12103025

21. Kang TW, Yevsa T, Woller N, Hoenicke L, Wuestefeld T, Dauch D, et al. Senescence surveillance of pre-malignant hepatocytes limits liver cancer development. *Nature*. (2011) 479:547–51. doi: 10.1038/nature10599

22. Eggert T, Wolter K, Ji J, Ma C, Yevsa T, Klotz S, et al. Distinct functions of senescence-associated immune responses in liver tumor surveillance and tumor progression. *Cancer Cell*. (2016) 30:533–47. doi: 10.1016/j.ccell.2016.09.003

23. Petriv N, Neubert L, Vatashchuk M, Timrott K, Suo H, Hochnadel I, et al. Increase of alpha-dicarbonyls in liver and receptor for advanced glycation end products on immune cells are linked to nonalcoholic fatty liver disease and liver cancer. *Oncoimmunology*. (2021) 10:1874159. doi: 10.1080/2162402X.2021.1874159

24. Petriv N, Suo H, Hochnadel I, Timrott K, Bondarenko N, Neubert L, et al. Essential roles of B-cell subsets in the progression of MASLD and HCC. *JHEP Rep*. (2024) 11:101189. doi: 10.1016/j.jhepr.2024.101189

25. Dauch D, Rudalska R, Cossa G, Nault JC, Kang TW, Wuestefeld T, et al. A myc-aurora kinase a protein complex represents an actionable drug target in P53-altered liver cancer. *Nat Med*. (2016) 22:744–53. doi: 10.1038/nm.4107

26. Anstee QM, Reeves HL, Kotsiliti E, Govaere O, Heikenwalder M. From nash to hcc: current concepts and future challenges. *Nat Rev Gastroenterol Hepatol*. (2019) 16:411–28. doi: 10.1038/s41575-019-0145-7

27. Cassatella MA, Ostberg NK, Tamassia N, Soehnlein O. Biological roles of neutrophil-derived granule proteins and cytokines. *Trends Immunol*. (2019) 40:648–64. doi: 10.1016/j.it.2019.05.003

28. Hong J, Qu P, Wuest TR, Huang H, Huang C, Lin PC. Neutrophilic granule protein is a novel murine lps antagonist. *Immune network*. (2019) 19:e34. doi: 10.4110/in.2019.19.e34

29. Rudalska R, Dauch D, Longerich T, McJunkin K, Wuestefeld T, Kang TW, et al. *In vivo* rnai screening identifies a mechanism of sorafenib resistance in liver cancer. *Nat Med*. (2014) 20:1138–46. doi: 10.1038/nm.3679

30. Seehawer M, Heinzmann F, D'Artista L, Harbig J, Roux PF, Hoenicke L, et al. Necroptosis microenvironment directs lineage commitment in liver cancer. *Nature*. (2018) 562:69–75. doi: 10.1038/s41586-018-0519-y

31. Schumann J, Stanko K, Schliesser U, Appelt C, Sawitzki B. Differences in cd44 surface expression levels and function discriminates il-17 and ifn-gamma producing helper T cells. *PloS One*. (2015) 10:e0132479. doi: 10.1371/journal.pone.0132479

32. Sun H, Xu J, Huang M, Huang Q, Sun R, Xiao W, et al. Cd200r, a co-inhibitory receptor on immune cells, predicts the prognosis of human hepatocellular carcinoma. *Immunol Lett*. (2016) 178:105–13. doi: 10.1016/j.imlet.2016.08.009

33. Bisgin A, Meng WJ, Adell G, Sun XF. Interaction of cd200 overexpression on tumor cells with cd200r1 overexpression on stromal cells: an escape from the host immune response in rectal cancer patients. *J Oncol*. (2019) 2019:5689464. doi: 10.1155/2019/5689464

34. Huang S, Pan Y, Zhang Q, Sun W. Role of cd200/cd200r signaling pathway in regulation of cd4+T cell subsets during thermal ablation of hepatocellular carcinoma. *Med Sci Monit*. (2019) 25:1718–28. doi: 10.12659/MSM.913094

35. Yoshimura K, Suzuki Y, Inoue Y, Tsuchiya K, Karayama M, Iwashita Y, et al. Cd200 and cd200r1 are differentially expressed and have differential prognostic roles in non-small cell lung cancer. *Oncoimmunology*. (2020) 9:1746554. doi: 10.1080/2162402X.2020.1746554

36. Bhoola NH, Mbita Z, Hull R, Dlamini Z. Translocator protein (Tspo) as a potential biomarker in human cancers. *Int J Mol Sci*. (2018) 19:2176. doi: 10.3390/ijms19082176

37. Jia JB, Ling X, Xing M, Ludwig JM, Bai M, Kim HS. Novel tspo-targeted doxorubicin prodrug for colorectal carcinoma cells. *Anticancer Res*. (2020) 40:5371–8. doi: 10.21873/anticanres.14545

38. Wu X, Gallo KA. The 18-kda translocator protein (Tspo) disrupts mammary epithelial morphogenesis and promotes breast cancer cell migration. *PloS One*. (2013) 8:e71258. doi: 10.1371/journal.pone.0071258

39. Phan NN, Wang CY, Chen CF, Sun Z, Lai MD, Lin YC. Voltage-gated calcium channels: novel targets for cancer therapy. *Oncol Lett*. (2017) 14:2059–74. doi: 10.3892/ol.2017.6457

40. Wang CY, Lai MD, Phan NN, Sun Z, Lin YC. Meta-analysis of public microarray datasets reveals voltage-gated calcium gene signatures in clinical cancer patients. *PloS One*. (2015) 10:e0125766. doi: 10.1371/journal.pone.0125766

41. Rorvig S, Ostergaard O, Heegaard NH, Borregaard N. Proteome profiling of human neutrophil granule subsets, secretory vesicles, and cell membrane: correlation with transcriptome profiling of neutrophil precursors. *J Leukoc Biol*. (2013) 94:711–21. doi: 10.1189/jlb.1212619

42. Lin D, Wu J. Hypoxia inducible factor in hepatocellular carcinoma: A therapeutic target. *World J Gastroenterol*. (2015) 21:12171–8. doi: 10.3748/wjg.v21.i42.12171

43. Zeng S, Lei S, Qu C, Wang Y, Teng S, Huang P. Crispr/cas-based gene editing in therapeutic strategies for beta-thalassemia. *Hum Genet*. (2023) 142:1677–703. doi: 10.1007/s00439-023-02610-9

44. Saha D, Patgaonkar M, Shroff A, Ayyar K, Bashir T, Reddy KV. Hemoglobin expression in nonerythroid cells: novel or ubiquitous? *Int J Inflammation*. (2014) 2014:803237. doi: 10.1155/2014/803237

45. Lin C-A, Chang L-L, Zhu H, He Q-J, Yang B. Hypoxic microenvironment and hepatocellular carcinoma treatment. *Hepatoma Res*. (2018) 4:26. doi: 10.20517/2394-5079.2018.27

46. Stankiewicz AM, Goscik J, Swiergiel AH, Majewska A, Wieczorek M, Juszczak GR, et al. Social stress increases expression of hemoglobin genes in mouse prefrontal cortex. *BMC Neurosci*. (2014) 15:130. doi: 10.1186/s12868-014-0130-6

47. Kambe J, Miyata S, Li C, Yamamoto Y, Nagaoka K. Xanthine-induced deficits in hippocampal behavior and abnormal expression of hemoglobin genes. *Behav Brain Res*. (2023) 449:114476. doi: 10.1016/j.bbr.2023.114476

48. Brown HM, Anastasi MR, Frank LA, Kind KL, Richani D, Robker RL, et al. Hemoglobin: A gas transport molecule that is hormonally regulated in the ovarian follicle in mice and humans. *Biol Reprod*. (2015) 92:26. doi: 10.1095/biolreprod.114.124594

49. Patrinos GP, Kollia P, Papadakis MN. Molecular diagnosis of inherited disorders: lessons from hemoglobinopathies. *Hum Mutat*. (2005) 26:399–412. doi: 10.1002/humu.20225

50. Chen Y, Ouyang Y, Li Z, Wang X, Ma J. S100a8 and S100a9 in cancer. *Biochim Biophys Acta Rev Cancer*. (2023) 1878:188891. doi: 10.1016/j.bbcan.2023.188891

51. Wang S, Song R, Wang Z, Jing Z, Wang S, Ma J. S100a8/A9 in inflammation. *Front Immunol*. (2018) 9:1298. doi: 10.3389/fimmu.2018.01298

52. Gebhardt C, Nemeth J, Angel P, Hess J. S100a8 and S100a9 in inflammation and cancer. *Biochem Pharmacol*. (2006) 72:1622–31. doi: 10.1016/j.bcp.2006.05.017

53. Xia C, Braunstein Z, Toomey AC, Zhong J, Rao X. S100 proteins as an important regulator of macrophage inflammation. *Front Immunol*. (2017) 8:1908. doi: 10.3389/fimmu.2017.01908

54. Ryckman C, Vandal K, Rouleau P, Talbot M, Tessier PA. Proinflammatory activities of S100: proteins S100a8, S100a9, and S100a8/A9 induce neutrophil chemotaxis and adhesion. *J Immunol*. (2003) 170:3233–42. doi: 10.4049/jimmunol.170.6.3233

55. Shabani F, Farasat A, Mahdavi M, Gheibi N. Calprotectin (S100a8/S100a9): A key protein between inflammation and cancer. *Inflammation research: Off J Eur Histamine Res Soc [et al]*. (2018) 67:801–12. doi: 10.1007/s00011-018-1173-4

56. Jukic A, Bakiri L, Wagner EF, Tilg H, Adolph TE. Calprotectin: from biomarker to biological function. *Gut*. (2021) 70:1978–88. doi: 10.1136/gutjnl-2021-324855

57. Xia P, Ji X, Yan L, Lian S, Chen Z, Luo Y. Roles of S100a8, S100a9 and S100a12 in infection, inflammation and immunity. *Immunology*. (2023) 171:365–76. doi: 10.1111/imm.13722

58. Turovskaya O, Foell D, Sinha P, Vogl T, Newlin R, Nayak J, et al. Rage, carboxylated glycans and S100a8/A9 play essential roles in colitis-associated carcinogenesis. *Carcinogenesis*. (2008) 29:2035–43. doi: 10.1093/carcin/bgn188

59. Zhang C, Yao R, Chen J, Zou Q, Zeng L. S100 family members: potential therapeutic target in patients with hepatocellular carcinoma: A strobe study. *Medicine*. (2021) 100:e24135. doi: 10.1097/MD.0000000000024135

60. Liu K, Zhang Y, Zhang C, Zhang Q, Li J, Xiao F, et al. Methylation of S100a8 is a promising diagnosis and prognostic marker in hepatocellular carcinoma. *Oncotarget*. (2016) 7:56798–810. doi: 10.18632/oncotarget.10792

61. De Ponti A, Wiechert L, Schneller D, Pusterla T, Longerich T, Hogg N, et al. A pro-tumorigenic function of S100a8/A9 in carcinogen-induced hepatocellular carcinoma. *Cancer Lett*. (2015) 369:396–404. doi: 10.1016/j.canlet.2015.09.005

62. Guedan S, Madar A, Casado-Medrano V, Shaw C, Wing A, Liu F, et al. Single residue in cd28-costimulated car-T cells limits long-term persistence and antitumor durability. *J Clin Invest*. (2020) 130:3087–97. doi: 10.1172/JCI133215

63. Rochigneux P, Chanez B, De Rauglaudre B, Mitry E, Chabannon C, Gilabert M. Adoptive cell therapy in hepatocellular carcinoma: biological rationale and first results in early phase clinical trials. *Cancers*. (2021) 13:271. doi: 10.3390/cancers13020271

64. Twomey JD, Zhang B. Cancer immunotherapy update: fda-approved checkpoint inhibitors and companion diagnostics. *AAPS J*. (2021) 23:39. doi: 10.1208/s12248-021-00574-0

65. Wang F, Jing X, Li G, Wang T, Yang B, Zhu Z, et al. Foxp3+ Regulatory T cells are associated with the natural history of chronic hepatitis B and poor prognosis of hepatocellular carcinoma. *Liver Int*. (2012) 32:644–55. doi: 10.1111/j.1478-3231.2011.02675.x

66. Hochnadel I, Hoenicke L, Petriv N, Neubert L, Reinhard E, Hirsch T, et al. Safety and efficacy of prophylactic and therapeutic vaccine based on live-attenuated listeria monocytogenes in hepatobiliary cancers. *Oncogene*. (2022) 41:2039–53. doi: 10.1038/s41388-022-02222-z

67. Meunier L, Larrey D. Drug-induced liver injury: biomarkers, requirements, candidates, and validation. *Front Pharmacol*. (2019) 10:1482. doi: 10.3389/fphar.2019.01482

68. Schroder SK, Gasterich N, Weiskirchen S, Weiskirchen R. Lipocalin 2 receptors: facts, fictions, and myths. *Front Immunol*. (2023) 14:1229885. doi: 10.3389/fimmu.2023.1229885

69. Grieshaber-Bouyer R, Radtke FA, Cunin P, Stifano G, Levescot A, Vijaykumar B, et al. The neutrotime transcriptional signature defines a single continuum of neutrophils across biological compartments. *Nat Commun*. (2021) 12:2856. doi: 10.1038/s41467-021-22973-9

70. Kim R, Emi M, Tanabe K. Cancer immunoediting from immune surveillance to immune escape. *Immunology*. (2007) 121:1–14. doi: 10.1111/j.1365-2567.2007.02587.x

71. Tada Y, Togashi Y, Kotani D, Kuwata T, Sato E, Kawazoe A, et al. Targeting vegfr2 with ramucirumab strongly impacts effector/activated regulatory T cells and cd8 (+) T cells in the tumor microenvironment. *J Immunother Cancer*. (2018) 6:106. doi: 10.1186/s40425-018-0403-1

72. Zhang L, Zhang Z. Recharacterizing tumor-infiltrating lymphocytes by single-cell rna sequencing. *Cancer Immunol Res*. (2019) 7:1040–6. doi: 10.1158/2326-6066.CIR-18-0658

73. Brummel K, Eerkens AL, de Bruyn M, Nijman HW. Tumour-infiltrating lymphocytes: from prognosis to treatment selection. *Br J Cancer*. (2023) 128:451–8. doi: 10.1038/s41416-022-02119-4

frontiers | Frontiers in Immunology

TYPE Original Research
PUBLISHED 13 May 2025
DOI 10.3389/fimmu.2025.1575627

OPEN ACCESS

EDITED BY
Stavros P. Papadakos,
Laiko General Hospital of Athens, Greece

REVIEWED BY
Xuwei Shao,
Pace Analytical labs, United States
Ioannis Katsaros,
National and Kapodistrian University of Athens, Greece

*CORRESPONDENCE
Maojin You
youmaojin@163.com
Yanqing Yang
yangyanqing2025@163.com

†These authors have contributed equally to this work

RECEIVED 12 February 2025
ACCEPTED 24 April 2025
PUBLISHED 13 May 2025

CITATION
Zhou Z, Yang Y, Chen S and You M (2025) Cost-effectiveness analysis of first-line cadonilimab plus chemotherapy in HER2-negative advanced gastric or gastroesophageal junction adenocarcinoma. *Front. Immunol.* 16:1575627. doi: 10.3389/fimmu.2025.1575627

Cost-effectiveness analysis of first-line cadonilimab plus chemotherapy in HER2-negative advanced gastric or gastroesophageal junction adenocarcinoma

Zhifeng Zhou[1], Yanqing Yang[2*†], Shaofang Chen[3] and Maojin You[3*†]

[1]Department of Pharmacy, Fuzhou University Affiliated Provincial Hospital, Fuzhou, Fujian, China, [2]Department of Clinical Nutrition, Zhangzhou Affiliated Hospital of Fujian Medical University, Zhangzhou, Fujian, China, [3]Department of Pharmacy, Mindong Hospital Affiliated to Fujian Medical University, Ningde, Fujian, China

Background: The COMPASSION-15 trial demonstrated that cadonilimab plus chemotherapy (CAD-CHM) confers clinical benefits over placebo plus chemotherapy (PLA-CHM) as a first-line treatment for human epidermal growth factor receptor 2 (HER2)-negative advanced gastric or gastroesophageal junction (G/GEJ) adenocarcinoma. However, the introduction of cadonilimab substantially elevates treatment costs, and its cost-effectiveness relative to PLA-CHM remains undetermined. This study evaluates the cost-effectiveness of CAD-CHM compared with PLA-CHM from the perspective of the Chinese healthcare system.

Methods: A Markov model with three health states was developed to assess the cost-effectiveness of CAD-CHM in HER2-negative advanced G/GEJ adenocarcinoma. Clinical efficacy data were sourced from the COMPASSION-15 trial, while drug costs were calculated based on national tender prices, and additional costs and utility values were extracted from published literature. The analysis encompassed the overall population, as well as subgroups stratified by programmed death ligand 1 (PD-L1) combined positive score (CPS) $\geq$ 5 and CPS < 5. Outcomes included total costs, quality-adjusted life-years (QALYs), and incremental cost-effectiveness ratios (ICERs). Sensitivity analyses were conducted to evaluate model robustness.

Results: The ICER of CAD-CHM was $67,378.09 per QALY in the overall population, $48,433.34 per QALY in the PD-L1 CPS $\geq$ 5 subgroup, and $78,463.86 per QALY in the PD-L1 CPS < 5 subgroup. Key determinants influencing model outcomes included patient weight, cadonilimab cost, and the utility value of progression-free survival. Across all groups, CAD-CHM resulted in an ICER exceeding the willingness-to-pay threshold of $41,511 per QALY, with a 0% probability of cost-effectiveness compared with PLA-CHM.

10.3389/fimmu.2025.1575627

Conclusion: From the perspective of the Chinese healthcare system, CAD-CHM is not cost-effective as a first-line treatment for HER2-negative advanced G/GEJ adenocarcinoma, either in the overall population or in subgroups stratified by PD-L1 CPS status, compared with chemotherapy alone.

KEYWORDS

cadonilimab, chemotherapy, cost-effectiveness, first-line treatment, HER2-negative, gastric or gastroesophageal junction adenocarcinoma

1 Introduction

Gastric cancer, including gastroesophageal junction (GEJ) cancer, remains a major global health challenge, ranking fifth in both incidence and mortality among malignant tumors. In 2022, over 968,000 new cases and nearly 660,000 deaths were reported worldwide (1, 2). China bears a disproportionately high gastric or GEJ (G/GEJ) burden, accounting for 42% of global new cases and 45% of gastric cancer-related deaths (3). Due to the lack of specific clinical symptoms, nearly 90% of patients with G/GEJ cancer are diagnosed at an advanced stage (4), resulting in a dismal prognosis, with a five-year survival rate below 5% (5). Adenocarcinoma is the predominant histological subtype, representing over 90% of G/GEJ cancers, and the majority of these tumors are human epidermal growth factor receptor 2 (HER2)-negative (6, 7). For decades, platinum- and fluorouracil-based combination chemotherapy has remained the standard first-line treatment for HER2-negative advanced G/GEJ adenocarcinoma (8). However, therapeutic outcomes remain suboptimal, with a median survival of less than one year (9).

Recent clinical trials have demonstrated that combining programmed cell death protein 1 (PD-1) inhibitors with chemotherapy improves survival in patients with HER2-negative G/GEJ adenocarcinoma (10–14). Moreover, evidence suggests that dual blockade of PD-1 and cytotoxic T-lymphocyte-associated protein 4 (CTLA-4) enhances antitumor responses across multiple solid tumors (15–17). Cadonilimab, a tetravalent bispecific human antibody targeting PD-1 and CTLA-4, exhibits enhanced binding activity in tumor tissues (18–20). The COMPASSION-15 phase III trial recently evaluated the efficacy and safety of cadonilimab plus chemotherapy (CAD-CHM) as a first-line treatment for HER2-negative advanced G/GEJ adenocarcinoma (21). The results demonstrated a significant improvement in median overall survival (OS) (14.1 vs. 11.1 months) and median progression-free survival (PFS) (7.0 vs. 5.3 months) compared with placebo plus chemotherapy (PLA-CHM), with manageable safety. These findings suggest CAD-CHM as a potential first-line treatment option for HER2-negative advanced G/GEJ adenocarcinoma.

Despite its promising clinical efficacy, the incorporation of cadonilimab into combination therapy substantially increases treatment costs, particularly drug-related expenses, imposing a significant financial burden. In resource-limited settings such as China, the cost-effectiveness of CAD-CHM remains a critical consideration for clinicians and policymakers. To date, no comprehensive economic evaluation has assessed CAD-CHM as a first-line treatment for HER2-negative advanced G/GEJ adenocarcinoma. The absence of such analyses may hinder its adoption in healthcare systems with constrained resources. Therefore, this study aims to evaluate the cost-effectiveness of CAD-CHM compared with PLA-CHM as a first-line treatment for HER2-negative advanced G/GEJ adenocarcinoma from the perspective of the Chinese healthcare system.

2 Methodology

This study was conducted following the Consolidated Health Economic Evaluation Reporting Standards 2022 (Supplementary Table 1) (22).

2.1 Model development

A Markov model was developed using TreeAge 2022 software to assess the cost-effectiveness of CAD-CHM versus PLA-CHM as first-line treatments for HER2-negative advanced G/GEJ adenocarcinoma (Figure 1). The model comprised three health states: PFS, progressive disease (PD), and death. All patients entered the model in the PFS state, with death as the absorbing state (23). During each cycle, patients could either remain in their current state or transition to the next state, with no possibility of reversal. The cycle length was set at 21 days to align with the treatment cycle, and the model was run for 160 cycles (approximately 9.2 years), by which point 99% of patients were expected to have died. The primary model outcomes included total costs, quality-adjusted life-years (QALYs), and the incremental cost-effectiveness ratios (ICERs). In accordance with the Chinese Guidelines for Pharmacoeconomic Evaluation, the willingness-to-pay (WTP) threshold was set at three times the per capita GDP of China in 2024 ($41,511 per QALY) (24), with an ICER below this threshold considered cost-effective.

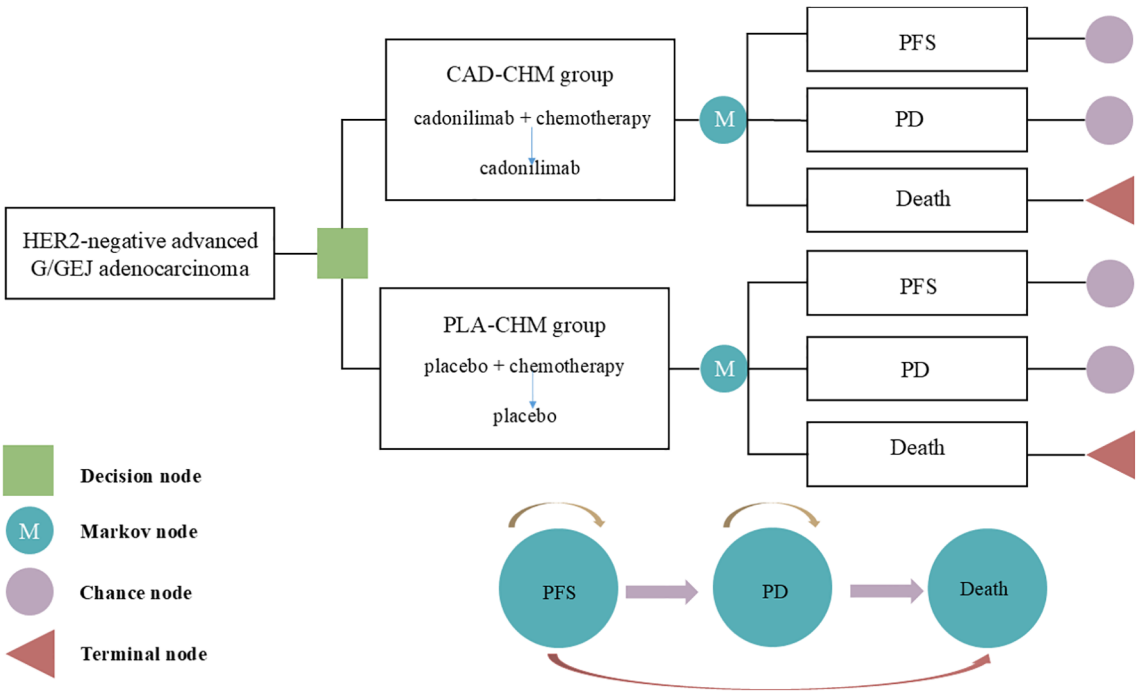

FIGURE 1
The Markov model simulating outcomes for the COMPASSION-15 trial. All patients started with PFS state and received treatment with CAD-CHM or PLA-CHM. CAD-CHM, cadonilimab plus chemotherapy; G/GEJ, gastric or gastroesophageal junction; HER2, human epidermal growth factor receptor 2; PD, progressive disease; PFS, progression-free survival; PLA-CHM, placebo plus chemotherapy.

2.2 Patient clinical treatment data

Clinical treatment data were derived from the COMPASSION-15 trial (21), a multicenter, randomized, phase III trial conducted across 75 hospitals in China. Eligible patients were aged 18–75 years, had histologically confirmed unresectable, locally advanced, or metastatic HER2-negative G/GEJ adenocarcinoma, and had not received prior systemic anticancer therapy. A total of 610 patients were enrolled in the COMPASSION-15 trial, including 256 patients with a PD-L1 Combined Positive Score (CPS) ≥ 5 and 304 patients with a PD-L1 CPS < 5. Patients were randomized to receive either cadonilimab or placebo in combination with chemotherapy (oxaliplatin and capecitabine) (CAD-CHM or PLA-CHM). Specifically, cadonilimab (10 mg/kg) or placebo was administered *via* intravenous infusion on Day 1 of each cycle, oxaliplatin (130 mg/m^2) *via* intravenous injection on Day 1 of each cycle, and capecitabine (1,000 mg/m^2) orally twice daily on Days 1–14 of each cycle, with each cycle lasting 3 weeks for up to 6 cycles. Thereafter, patients continued maintenance therapy with cadonilimab or placebo until disease progression or intolerable toxicity. According to the COMPASSION-15 trial (21), the median treatment duration for cadonilimab in the CAD-CHM group was 5.62 months, while oxaliplatin and capecitabine were administered for a median of 4.14 months and 4.17 months, respectively. In the PLA-CHM group, oxaliplatin and capecitabine were administered for a median of 4.14 months. As post-progression treatment details were not provided in the COMPASSION-15 trial, it was assumed that all patients received the best supportive care following disease progression. The study population included the overall population as well as subgroups stratified by PD-L1 CPS (≥ 5 and < 5).

2.3 Survival transition probabilities

GetData Graph Digitizer (version 2.26) was used to digitize the PFS and OS curves from the COMPASSION-15 trial. Patient survival data were reconstructed in R software following the method outlined by Guyot et al. (25), and various survival distributions were fitted to extrapolate survival curves beyond the clinical trial follow-up period. The evaluated distributions included exponential, gamma, generalized F, generalized gamma, Gompertz, Weibull, log-logistic, and log-normal models (26, 27). The optimal survival distribution was selected based on Akaike and Bayesian information criteria (28, 29) and subsequently used to estimate transition probabilities between health states (Supplementary Table 2). The best-fitting survival distributions and their parameters are detailed in Table 1.

2.4 Costs and utilities

This study exclusively considered direct medical costs, including drug expenses, diagnostic tests, routine follow-up, best supportive

10.3389/fimmu.2025.1575627

TABLE 1 Relevant parameters of survival distribution.

Variable	Value	Source
Survival model for the overall population		
Log-logistic survival model of PFS		
CAD-CHM group	Scale = 0.1263066, Shape = 1.744355	(21)
PLA-CHM group	Scale = 0.2011074, Shape = 2.190154	(21)
Log-logistic survival model of OS		
CAD-CHM group	Scale = 0.06831391, Shape = 1.691376	(21)
PLA-CHM group	Scale = 0.09292127, Shape = 1.952410	(21)
Survival model for the PD-L1 CPS ≥ 5 subgroup		
Log-logistic survival model of PFS		
CAD-CHM group	Scale = 0.1233483, Shape = 1.668463	(21)
PLA-CHM group	Scale = 0.1973213, Shape = 2.321586	(21)
Log-logistic survival model of OS		
CAD-CHM group	Scale = 0.05837011, Shape = 1.482514	(21)
PLA-CHM group	Scale = 0.09334744, Shape = 1.898245	(21)
Survival model for the PD-L1 CPS < 5 subgroup		
Log-logistic survival model of PFS		
CAD-CHM group	Scale = 0.1318699, Shape = 1.857267	(21)
PLA-CHM group	Scale = 0.1999651, Shape = 2.147308	(21)
Log-logistic survival model of OS		
CAD-CHM group	Scale = 0.07192116, Shape = 1.754681	(21)

CAD-CHM, cadonilimab plus chemotherapy; CPS, combined positive score; OS, overall survival; PD-L1, programmed death ligand 1; PFS, progression-free survival; PLA-CHM, placebo plus chemotherapy.

care, management of grade 3 or higher adverse events with an incidence exceeding 5%, and end-of-life care (Table 2). Drug costs were sourced from national tender prices, while other expenditures were obtained from published literature and adjusted to 2024 values using the medical price index from the National Bureau of Statistics of China (30). All costs were reported in US dollars and converted at the 2024 average exchange rate (1 USD = 7.12 CNY). As the COMPASSION-15 trial did not provide quality-of-life data, utility values for PFS and PD were derived from published studies in China (31). To address the potential bias arising from the use of identical utility values for the CAD-CHM and PLA-CHM groups, we considered the disutility of grade 3 or higher adverse events with an incidence exceeding 5% in each treatment group, to improve the accuracy of the health utility values for each treatment group. All costs and utility values were discounted at an annual rate of 5%, in line with pharmacoeconomic guidelines (24). Drug dosages were calculated based on an assumed patient weight of 65 kg and a body surface area of 1.72 m^2 (32).

2.5 Sensitivity analysis

A one-way sensitivity analysis was performed to evaluate the impact of parameter variations on model outcomes. Each parameter was adjusted within its reported 95% confidence interval, and where unavailable, a ±20% range around the baseline value was applied. The discount rate was varied from 0% to 8% (Table 2). The results were visualized using a tornado diagram. To assess the combined effect of parameter uncertainty, a probabilistic sensitivity analysis was conducted using 1,000 Monte Carlo simulations, with each parameter assigned a specific probability distribution (Table 2). The results were illustrated in a scatter plot. Additionally, the ICER of CAD-CHM compared with PLA-CHM was iteratively recalculated while progressively reducing the price of cadonilimab to determine the threshold at which CAD-CHM becomes cost-effective.

2.6 Scenario analysis

Two scenario analyses were performed for the overall population. In Scenario 1, the model duration was adjusted to 2, 4, and 6 years to assess its influence on model outcomes. In Scenario 2, it was assumed that only 30% or 50% of patients received the best supportive care after disease progression, simulating real-world scenarios where some patients discontinue treatment for various reasons.

3 Results

3.1 Results of the base case analysis

In the overall population, CAD-CHM incurred a total cost of $36,207.12 and yielded 1.25 QALYs, while PLA-CHM had a total cost of $10,248.88 and provided 0.86 QALYs, resulting in an ICER of $67,378.09 per QALY. In the PD-L1 CPS ≥ 5 subgroup, CAD-CHM cost $39,098.19 and achieved 1.46 QALYs, whereas PLA-CHM cost $10,301.32 and yielded 0.87 QALYs, with an ICER of $48,433.34 per QALY. In the PD-L1 CPS < 5 subgroup, CAD-CHM incurred a total cost of $33,824.19 and provided 1.17 QALYs, while PLA-CHM cost $10,334.52 and generated 0.87 QALYs, resulting in an ICER of $78,463.86 per QALY (Table 3). All ICERs exceeded the WTP threshold of $41,511 per QALY, indicating that CAD-CHM is not cost-effective compared with chemotherapy alone for HER2-negative advanced G/GEJ adenocarcinoma from the perspective of the Chinese healthcare system.

3.2 Sensitivity analysis

One-way sensitivity analysis results, visualized in a tornado diagram (Figures 2–4), indicated that patient weight, cadonilimab cost, and PFS utility value were the most influential parameters in the overall population and the PD-L1 CPS < 5 subgroup. However, even under parameter variations, the ICER remained above the WTP threshold, suggesting minimal impact on model conclusions.

10.3389/fimmu.2025.1575627

TABLE 2 The basic parameters of the input model and the range of sensitivity analyses.

Variable	Base Value	Range		Distribution	Source
		Min	Max		
PLA-CHM group: Incidence of AEs					
Decreased platelet count	0.285	0.228	0.342	Beta	(21)
Decreased neutrophil count	0.151	0.121	0.181	Beta	(21)
Decreased white blood cell count	0.072	0.058	0.086	Beta	(21)
Anemia	0.102	0.082	0.122	Beta	(21)
Hypokalemia	0.059	0.047	0.071	Beta	(21)
PLA-CHM group: Incidence of AEs					
Decreased platelet count	0.250	0.200	0.300	Beta	(21)
Decreased neutrophil count	0.148	0.118	0.178	Beta	(21)
Decreased white blood cell count	0.063	0.050	0.076	Beta	(21)
Anemia	0.125	0.100	0.150	Beta	(21)
Hypokalemia	0.010	0.008	0.012	Beta	(21)
Cost ($)					
Cadonilimab (125mg)	235.96	188.77	283.15	Gamma	(33)
Oxaliplatin (100mg)	32.88	26.30	39.46	Gamma	(33)
Capecitabine (500mg)	0.75	0.60	0.90	Gamma	(33)
Decreased platelet count	1157.50	926.00	1389.00	Gamma	(31)
Decreased neutrophil count	454.71	363.77	545.65	Gamma	(34)
Decreased white blood cell count	211.06	168.85	253.27	Gamma	(35)
Anemia	336.97	269.58	404.36	Gamma	(36)
Hypokalemia	3003.00	2402.40	3603.60	Gamma	(37)
Best supportive care per cycle	182.41	145.93	218.89	Gamma	(38)
Routine follow-up per cycle	73.79	59.03	88.55	Gamma	(38)
Diagnostic tests per cycle	357.70	286.16	429.24	Gamma	(34)
End-of-life care	1491.00	1192.80	1789.19	Gamma	(27)
Utility value					
PFS	0.797	0.638	0.956	Beta	(31)
PD	0.577	0.462	0.692	Beta	(31)
Disutility due to AEs					
Decreased platelet count	0.02	0.016	0.024	Beta	(39)
Decreased neutrophil count	0.20	0.160	0.240	Beta	(40)
Decreased white blood cell count	0.20	0.160	0.240	Beta	(40)
Anemia	0.07	0.056	0.084	Beta	(41)
Hypokalemia	0.03	0.024	0.036	Beta	(37)
Discount rate	0.05	0.08	0.00	Fixed	(24)
Weight (kg)	65	52	78	Normal	(31)

AE, adverse event; CAD-CHM, cadonilimab plus chemotherapy; OS, overall survival; PD, progressive disease; PFS, progression-free survival; PLA-CHM, placebo plus chemotherapy.

TABLE 3 The cost and outcome results of the base-case analysis.

Parameters	Overall population		PD-L1 CPS ≥ 5 subgroup		PD-L1 CPS < 5 subgroup	
	CAD-CHM group	PLA-CHM group	CAD-CHM group	PLA-CHM group	CAD-CHM group	PLA-CHM group
Total cost ($)	36,207.12	10,248.88	39,098.19	10,301.32	33,824.19	10,334.52
Incremental costs ($)	25,958.24	–	28,793.87	–	23,489.67	–
Total effectiveness (QALYs)	1.25	0.86	1.46	0.87	1.17	0.87
Incremental effectiveness (QALYs)	0.39	–	0.59	–	0.30	–
ICER ($/QALY)	67,378.09	–	48,433.34	–	78,463.86	–

CAD-CHM, cadonilimab plus chemotherapy; CPS, combined positive score; ICER, incremental cost-effectiveness ratio; OS, overall survival; PD, progressive disease; PD-L1, programmed death ligand 1; PFS, progression-free survival; PLA-CHM, placebo plus chemotherapy; QALY, quality-adjusted life year.

In contrast, in the PD-L1 CPS ≥ 5 subgroup, CAD-CHM became cost-effective when patient weight and cadonilimab cost approached their lower limits. Probabilistic sensitivity analysis results, illustrated in a scatter plot (Figures 5–7), showed that the probability of CAD-CHM being cost-effective at a WTP threshold of $41,511 per QALY was 6.4% in the overall population, 31.0% in the PD-L1 CPS ≥ 5 subgroup, and 2.4% in the PD-L1 CPS < 5 subgroup. Additionally, cost-reduction analysis revealed that CAD-CHM would only become a cost-effective first-line option for HER2-negative advanced G/GEJ adenocarcinoma in the overall population if the cost of cadonilimab (150 mg) dropped below $129.5.

3.3 Scenario analysis

Scenario analysis results are presented in Table 4. In Scenario 1, when the model duration was adjusted to 2, 4, and 6 years, the ICERs of CAD-CHM compared with PLA-CHM were $115,126.94/QALY, $81,383.15/QALY, and $72,632.12/QALY, respectively. This indicates a progressive decline in ICER with increasing model duration. In Scenario 2, when the proportion of patients receiving the best supportive care was set at 30% and 50%, the ICERs of CAD-CHM compared with PLA-CHM were $66,971/QALY and $67,087.94/QALY, respectively. This indicates that the model results are relatively insensitive to assumptions regarding changes in the proportion of patients receiving the best supportive care.

4 Discussion

Co-inhibition of PD-1 and CTLA-4 induces a synergistic anti-tumor response by reshaping the tumor immune microenvironment into a more immunogenic phenotype (42). The complementary effects of CTLA-4 and PD-1 inhibitors have been well established (43). Cadonilimab, the first bispecific immune checkpoint inhibitor

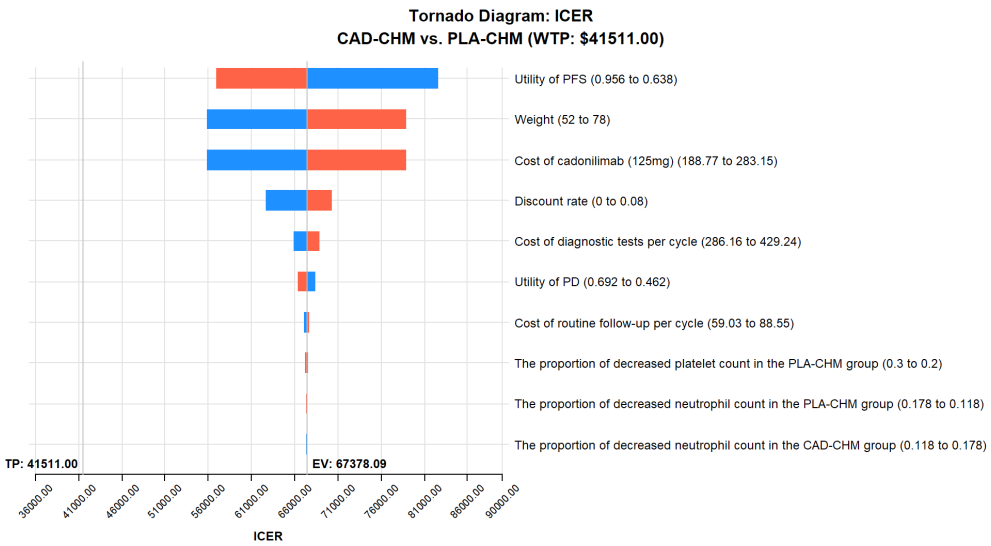

FIGURE 2
One-way sensitivity analyses in the overall population. CAD-CHM, cadonilimab plus chemotherapy; ICER, incremental cost-effectiveness ratio; PD, progressive disease; PFS, progression-free survival; PLA-CHM, placebo plus chemotherapy.

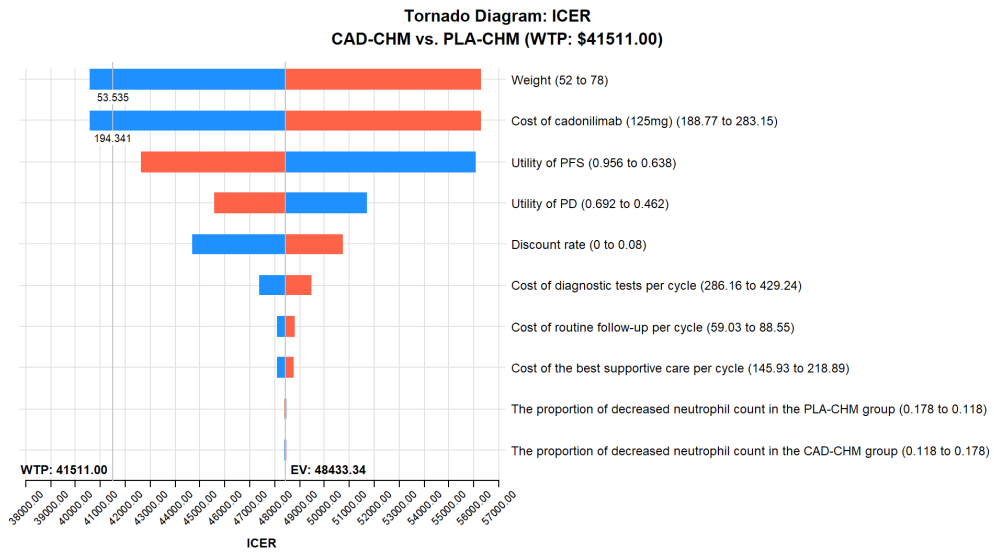

FIGURE 3
One-way sensitivity analyses in PD-L1 CPS ≥ 5 subgroup. CAD-CHM, cadonilimab plus chemotherapy; ICER, incremental cost-effectiveness ratio; PD, progressive disease; PFS, progression-free survival; PLA-CHM, placebo plus chemotherapy.

approved globally, simultaneously targets PD-1 and CTLA-4, enhancing anti-tumor efficacy through dual-pathway blockade (18). The COMPASSION-15 trial (21) demonstrated that CAD-CHM significantly improves survival in patients with HER2-negative advanced G/GEJ adenocarcinoma, underscoring its clinical potential. However, the escalating costs of novel cancer therapies pose a substantial challenge to healthcare system sustainability. As previously reported (23, 44), comprehensive cost-effectiveness evaluations are crucial for guiding policy decisions and optimizing healthcare resource allocation. Given the high cost of CAD-CHM, a thorough assessment of its cost-effectiveness as a first-line treatment for HER2-negative advanced G/GEJ adenocarcinoma is imperative to ensure both economic feasibility and equitable access within resource-constrained healthcare systems.

This study represents the first cost-effectiveness analysis of CAD-CHM as a first-line treatment for HER2-negative advanced G/GEJ adenocarcinoma within the Chinese healthcare system. Beyond its domestic significance, the findings offer valuable

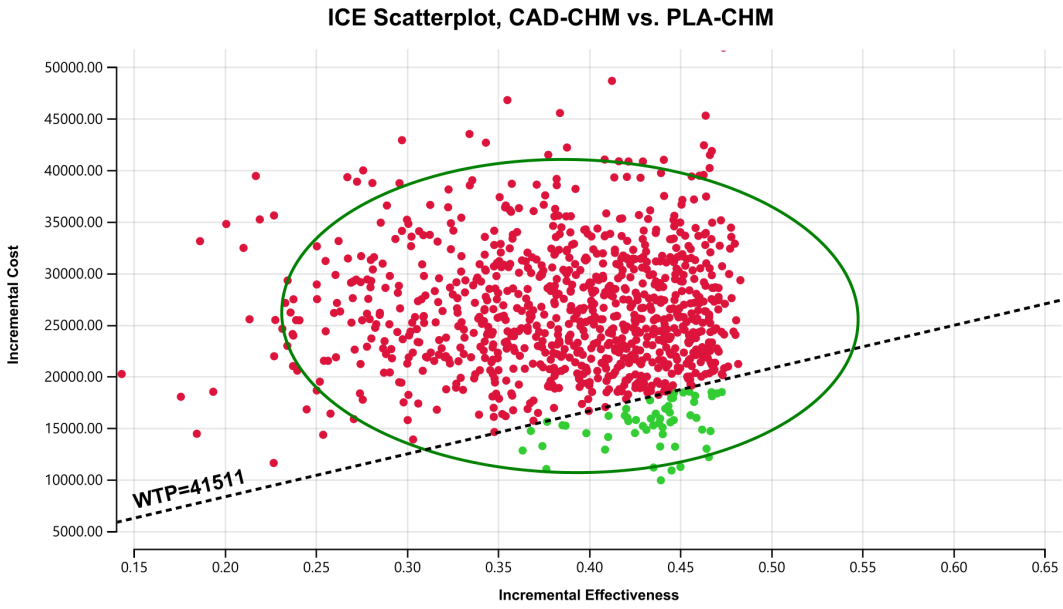

FIGURE 4
One-way sensitivity analyses in the PD-L1 CPS < 5 subgroup. CAD-CHM, cadonilimab plus chemotherapy; ICER, incremental cost-effectiveness ratio; PD, progressive disease; PFS, progression-free survival; PLA-CHM, placebo plus chemotherapy.

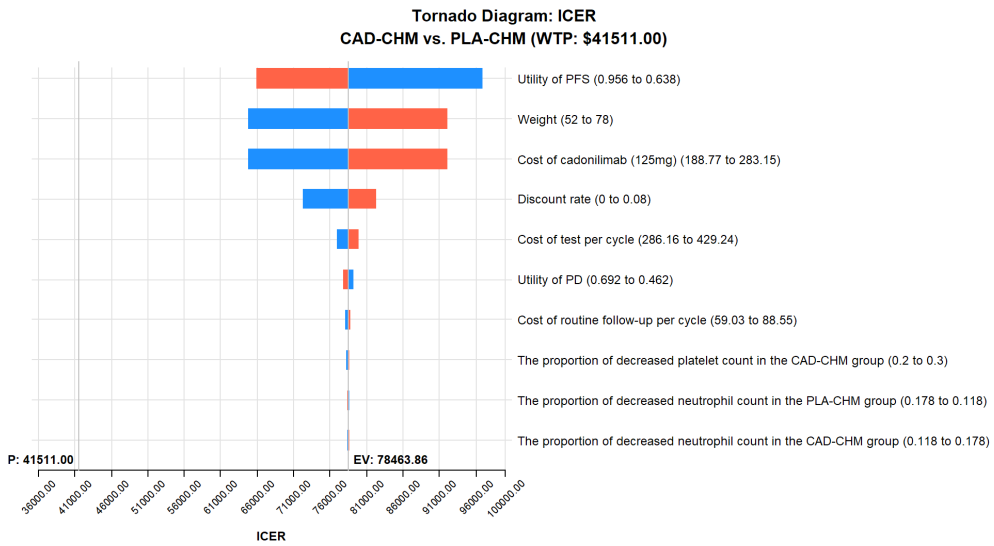

FIGURE 5
Probabilistic sensitivity analysis in the overall population. CAD-CHM, cadonilimab plus chemotherapy; ICE, incremental cost-effectiveness; PLA-CHM, placebo plus chemotherapy; WTP, willingness-to-pay.

insights for the global medical community, marking a core innovation of this research. Compared with PLA-CHM, the incremental cost per additional QALY gained with CAD-CHM amounts to $67,378.09 in the overall population, $48,433.34 in the PD-L1 CPS ≥ 5 subgroup, and $78,463.86 in the PD-L1 CPS < 5 subgroup—substantially exceeding the predefined WTP threshold of $41,511 per QALY. Consequently, CAD-CHM does not demonstrate cost-effectiveness as a first-line therapy for HER2-negative advanced G/GEJ adenocarcinoma, irrespective of PD-L1 CPS status, from the perspective of the Chinese healthcare system. This outcome likely stems from the prolonged maintenance therapy required for cadonilimab and its substantially higher cost relative to oxaliplatin and capecitabine, leading to significantly elevated drug expenditures without providing sufficient incremental survival benefits. One-way sensitivity analysis identified patient weight (which determines cadonilimab dosing) and drug cost as the most influential factors in the cost-effectiveness of CAD-CHM, further supporting this conclusion. These findings highlight an urgent need to reduce the cost of cadonilimab to improve the affordability of the CAD-CHM regimen. Policy interventions should be implemented

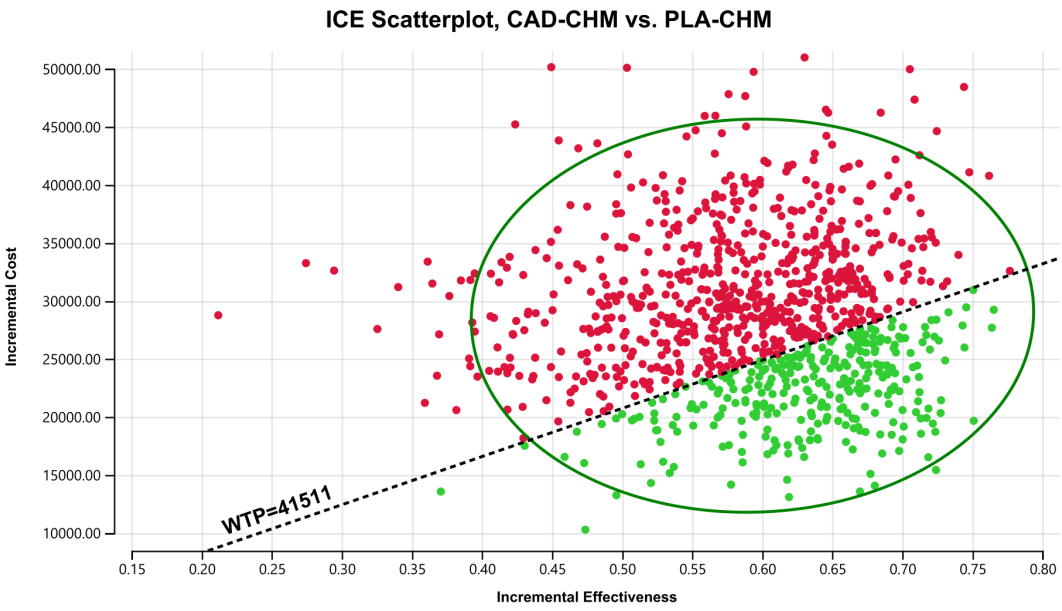

FIGURE 6
Probabilistic sensitivity analysis in PD-L1 CPS ≥ 5 subgroup. CAD-CHM, cadonilimab plus chemotherapy; ICE, incremental cost-effectiveness; PLA-CHM, placebo plus chemotherapy; WTP, willingness-to-pay.

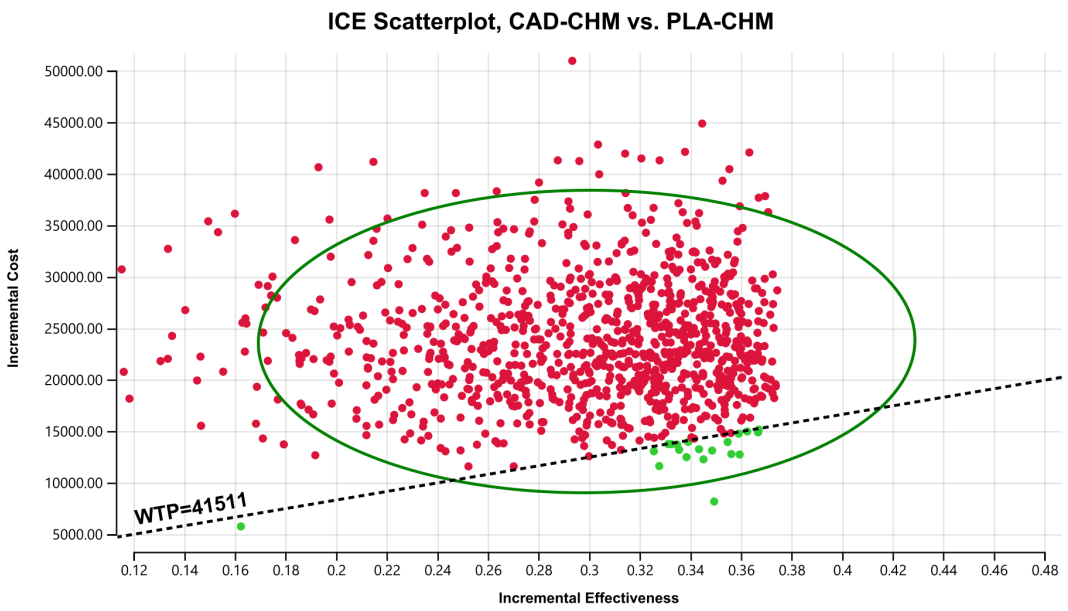

FIGURE 7
Probabilistic sensitivity analysis in PD-L1 CPS < 5 subgroup. CAD-CHM, cadonilimab plus chemotherapy; ICE, incremental cost-effectiveness; PLA-CHM, placebo plus chemotherapy; WTP, willingness-to-pay.

to enhance the cost-effectiveness of these promising treatments, ensuring broader patient access. Pharmaceutical companies can mitigate costs by optimizing manufacturing processes, improving supply chain efficiency, and refining pricing strategies, thereby enhancing the economic viability of this regimen and facilitating the widespread adoption of innovative therapies. Additionally, the analysis suggests that the cost of cadonilimab (125 mg) must be reduced to below 54.89% of its current price—specifically, under $129.50—for CAD-CHM to become a cost-effective first-line option for HER2-negative advanced G/GEJ adenocarcinoma in the overall population. This threshold provides a critical pricing benchmark for both healthcare policymakers and pharmaceutical manufacturers.

Subgroup analysis revealed that the ICER in the PD-L1 CPS ≥ 5 subgroup was substantially lower than that in the overall population, whereas the ICER in the PD-L1 CPS < 5 subgroup exceeded that of the overall population. Although neither subgroup achieved cost-effectiveness, the CAD-CHM regimen demonstrated greater economic viability in the PD-L1 CPS ≥ 5 subgroup. This underscores the critical role of PD-L1 expression level detection, which may serve as a strategy to enhance the cost-effectiveness of CAD-CHM in treating HER2-negative advanced G/GEJ adenocarcinoma. These findings provide valuable guidance for Chinese medical insurance policymakers in defining appropriate reimbursement criteria for cadonilimab.

Scenario analysis has proven instrumental in evaluating drug cost-effectiveness by accounting for varying assumptions and uncertainties, thereby better approximating real-world complexities. Accordingly, two scenario analyses were conducted. Scenario 1 demonstrated that prolonged treatment duration improves the cost-effectiveness of CAD-CHM. Scenario 2 indicated that following disease progression, an increased

TABLE 4 Scenario analyses in the overall population.

Scenarios	Cost ($)		QALY		ICER ($/QALY)
	CAD-CHM group	PLA-CHM group	CAD-CHM group	PLA-CHM group	
Scenario 1					
Model runtime (year) =2	28,851.56	9,018.77	0.88	0.71	115,126.94
Model runtime (year) =4	33,334.83	9,824.75	1.10	0.81	81,383.15
Model runtime (year) =6	35,029.39	10,085.97	1.18	0.84	72,632.12
Scenario 2					
30% of patients receive BSC	33,935.08	8,133.34	1.25	0.86	66,971.88
50% of patients receive BSC	34,584.24	8,737.78	1.25	0.86	67,087.94

BSC, best supportive care; CAD-CHM, cadonilimab plus chemotherapy; CPS, combined positive score; ICER, incremental cost-effectiveness ratio; PLA-CHM, placebo plus chemotherapy; QALY, quality-adjusted life year.

proportion of patients receiving the best supportive care does not substantially impact the ICER of CAD-CHM, suggesting that continued supportive care does not significantly diminish the cost-effectiveness of CAD-CHM. These analyses suggest that extended treatment adherence may optimize therapeutic value, aligning with the interests of clinicians, patients, and their families, as well as broader ethical and societal considerations.

To date, only two cost-effectiveness studies have assessed the use of immune checkpoint inhibitors as first-line treatments for HER2-negative advanced G/GEJ adenocarcinoma within the Chinese healthcare system. Lang et al. (45) and Zhang et al. (46) concluded that pembrolizumab plus chemotherapy is not cost-effective as a first-line option for treating HER2-negative advanced G/GEJ adenocarcinoma. These findings are consistent with the present study, which similarly identified no economic advantage of CAD-CHM over chemotherapy alone.

This study possesses several notable strengths. First, it leverages the most recent data from the COMPASSION-15 trial, incorporating nearly two years of survival analysis to compare the efficacy of cadonilimab plus chemotherapy with chemotherapy alone, thereby providing the latest clinical evidence. Second, as all participants in the COMPASSION-15 trial were Chinese patients, the findings exhibit strong population-specific applicability, offering a more accurate reflection of treatment outcomes and economic benefits within the Chinese healthcare system. Lastly, through comprehensive subgroup and scenario analyses, the study evaluates economic impacts across diverse patient cohorts and treatment conditions, furnishing critical insights for clinicians, patients, and policymakers in making personalized treatment decisions.

However, certain limitations should be acknowledged. First, given that the COMPASSION-15 trial remains ongoing, long-term survival data are currently unavailable. This study extrapolated survival beyond the follow-up period using survival models, which may introduce some deviation from actual outcomes. For instance, the tail of the survival curve for patients receiving immunotherapy may exhibit a plateau (47). Our model does not account for the possibility of long-term survival and may therefore underestimate the efficacy of immunotherapy. Future studies should validate these findings using real-world data for cost-effectiveness analysis. Second, post-progression treatment details were not reported in the COMPASSION-15 trial, necessitating the assumption that all patients received the best supportive care after first-line treatment failure, which may not fully align with real-world clinical practice. In reality, the selection of subsequent treatment regimens is individualized based on each patient's specific circumstances. Fortunately, the results of the one-way sensitivity analysis provided reassurance, as they consistently indicated that altering the estimated range of subsequent treatments would not change the model's outcomes. Third, due to the absence of quality-of-life data in the trial, health utility values were sourced from Chinese literature, potentially introducing bias into the model; however, sensitivity analysis confirmed that this does not alter the study's overall conclusions. However, it must be acknowledged that obtaining more accurate health utility values is crucial for enhancing the accuracy of our model outcomes. Should future clinical studies report health-related quality-of-life outcomes specific to the Chinese population, incorporating these reliable data would optimize our model results. Lastly, this analysis focused solely on the cost-effectiveness of CAD-CHM relative to chemotherapy alone, without considering alternative treatment regimens such as pembrolizumab plus chemotherapy, owing to the lack of direct comparative data. However, the studies by Lang et al. (45) and Zhang et al. (46) suggest that pembrolizumab combined with chemotherapy is not cost-effective compared to chemotherapy alone. Therefore, we believe that selecting chemotherapy as the comparator in the cost-effectiveness analysis of CAD-CHM is reasonable. Despite these limitations, the findings remain highly informative for healthcare policymakers, clinicians, and patients.

5 Conclusion

The study results indicate that, from the perspective of the Chinese healthcare system, CAD-CHM as a first-line treatment for HER2-negative advanced G/GEJ adenocarcinoma lacks cost-effectiveness compared with chemotherapy alone, irrespective of PD-L1 CPS subgroup stratification.

Data availability statement

The original contributions presented in the study are included in the article/Supplementary Material. Further inquiries can be directed to the corresponding author.

Author contributions

ZZ: Writing – original draft, Writing – review & editing. YY: Writing – original draft, Writing – review & editing. SC: Writing – original draft, Writing – review & editing. MY: Writing – original draft, Writing – review & editing.

Funding

The author(s) declare that financial support was received for the research and/or publication of this article. This study was supported in part by grants from the Natural Science Foundation of Fujian Province (Grant number: 2023J011188); the Natural Science Foundation of Ningde (Grant number: 2022J29). This study was not supported by any pharmaceutical company.

Conflict of interest

The authors declare that the research was conducted in the absence of any commercial or financial relationships that could be construed as a potential conflict of interest.

Generative AI statement

The author(s) declare that no Generative AI was used in the creation of this manuscript.

Publisher's note

Supplementary material

The Supplementary Material for this article can be found online at: https://www.frontiersin.org/articles/10.3389/fimmu.2025.1575627/full#supplementary-material

References

1. Bray F, Laversanne M, Sung H, Ferlay J, Siegel RL, Soerjomataram I, et al. Global cancer statistics 2022: GLOBOCAN estimates of incidence and mortality worldwide for 36 cancers in 185 countries. *CA Cancer J Clin*. (2024) 74:229–63. doi: 10.3322/caac.21834

2. Smyth EC, Nilsson M, Grabsch HI, van Grieken NC, Lordick F. Gastric cancer. *Lancet*. (2020) 396:635–48. doi: 10.1016/S0140-6736(20)31288-5

3. Chen W, Zheng R, Baade PD, Zhang S, Zeng H, Bray F, et al. Cancer statistics in China, 2015. *CA Cancer J Clin*. (2016) 66:115–32. doi: 10.3322/caac.21338

4. Zeng H, Chen W, Zheng R, Zhang S, Ji JS, Zou X, et al. Changing cancer survival in China during 2003-15: a pooled analysis of 17 population-based cancer registries. *Lancet Glob Health*. (2018) 6:e555–555e567. doi: 10.1016/S2214-109X(18)30127-X

5. Ajani JA, Lee J, Sano T, Janjigian YY, Fan D, Song S. Gastric adenocarcinoma. *Nat Rev Dis Primers*. (2017) 3:17036. doi: 10.1038/nrdp.2017.36

6. Van Cutsem E, Bang YJ, Feng-Yi F, Xu JM, Lee KW, Jiao SC, et al. HER2 screening data from ToGA: targeting HER2 in gastric and gastroesophageal junction cancer. *Gastric Cancer*. (2015) 18:476–84. doi: 10.1007/s10120-014-0402-y

7. Abrahao-MaChado LF, Scapulatempo-Neto C. HER2 testing in gastric cancer: An update. *World J Gastroenterol*. (2016) 22:4619–25. doi: 10.3748/wjg.v22.i19.4619

8. Wang FH, Zhang XT, Tang L, Wu Q, Cai MY, Li YF, et al. The Chinese Society of Clinical Oncology (CSCO): Clinical guidelines for the diagnosis and treatment of gastric cancer, 2023. *Cancer Commun (Lond)*. (2024) 44:127–72. doi: 10.1002/cac2.12516

9. Shitara K, Lordick F, Bang YJ, Enzinger P, Ilson D, Shah MA, et al. Zolbetuximab plus mFOLFOX6 in patients with CLDN18.2-positive, HER2-negative, untreated, locally advanced unresectable or metastatic gastric or gastro-oesophageal junction adenocarcinoma (SPOTLIGHT): a multicentre, randomised, double-blind, phase 3 trial. *Lancet*. (2023) 401:1655–68. doi: 10.1016/S0140-6736(23)00620-7

10. Janjigian YY, Shitara K, Moehler M, Garrido M, Salman P, Shen L, et al. First-line nivolumab plus chemotherapy versus chemotherapy alone for advanced gastric, gastro-oesophageal junction, and oesophageal adenocarcinoma (CheckMate 649): a randomised, open-label, phase 3 trial. *Lancet*. (2021) 398:27–40. doi: 10.1016/S0140-6736(21)00797-2

11. Xu J, Jiang H, Pan Y, Gu K, Cang S, Han L, et al. Sintilimab plus chemotherapy for unresectable gastric or gastroesophageal junction cancer: the ORIENT-16 randomized clinical trial. *JAMA*. (2023) 330:2064–74. doi: 10.1001/jama.2023.19918

12. Qiu MZ, Oh DY, Kato K, Arkenau T, Tabernero J, Correa MC, et al. Tislelizumab plus chemotherapy versus placebo plus chemotherapy as first line treatment for advanced gastric or gastro-oesophageal junction adenocarcinoma: RATIONALE-305 randomised, double blind, phase 3 trial. *BMJ*. (2024) 385:e078876. doi: 10.1136/bmj-2023-078876

13. Shitara K, Ajani JA, Moehler M, Garrido M, Gallardo C, Shen L, et al. Nivolumab plus chemotherapy or ipilimumab in gastro-oesophageal cancer. *Nature*. (2022) 603:942–8. doi: 10.1038/s41586-022-04508-4

14. Rha SY, Oh DY, Yañez P, Bai Y, Ryu MH, Lee J, et al. Pembrolizumab plus chemotherapy versus placebo plus chemotherapy for HER2-negative advanced gastric cancer (KEYNOTE-859): a multicentre, randomised, double-blind, phase 3 trial. *Lancet Oncol*. (2023) 24:1181–95. doi: 10.1016/S1470-2045(23)00515-6

15. Larkin J, Chiarion-Sileni V, Gonzalez R, Grob JJ, Cowey CL, Lao CD, et al. Combined nivolumab and ipilimumab or monotherapy in untreated melanoma. *N Engl J Med*. (2015) 373:23–34. doi: 10.1056/NEJMoa1504030

16. Antonia SJ, López-Martin JA, Bendell J, Ott PA, Taylor M, Eder JP, et al. Nivolumab alone and nivolumab plus ipilimumab in recurrent small-cell lung cancer (CheckMate 032): a multicentre, open-label, phase 1/2 trial. *Lancet Oncol*. (2016) 17:883–95. doi: 10.1016/S1470-2045(16)30098-5

17. Overman MJ, Lonardi S, Wong K, Lenz HJ, Gelsomino F, Aglietta M, et al. Durable clinical benefit with nivolumab plus ipilimumab in DNA mismatch repair-deficient/microsatellite instability-high metastatic colorectal cancer. *J Clin Oncol*. (2018) 36:773–9. doi: 10.1200/JCO.2017.76.9901

18. Pang X, Huang Z, Zhong T, Zhang P, Wang ZM, Xia M, et al. Cadonilimab, a tetravalent PD-1/CTLA-4 bispecific antibody with trans-binding and enhanced target binding avidity. *MAbs*. (2023) 15:2180794. doi: 10.1080/19420862.2023.2180794

19. Hou X, Liu S, Zeng Z, Wang Z, Ding J, Chen Y, et al. Preclinical imaging evaluation of a bispecific antibody targeting hPD1/CTLA4 using humanized mice. *BioMed Pharmacother*. (2024) 175:116669. doi: 10.1016/j.biopha.2024.116669

20. Caushi JX, Zhang J, Ji Z, Vaghasia A, Zhang B, Hsiue EH, et al. Transcriptional programs of neoantigen-specific TIL in anti-PD-1-treated lung cancers. *Nature*. (2021) 596:126–32. doi: 10.1038/s41586-021-03752-4

21. Shen L, Zhang Y, Li Z, Zhang X, Gao X, Liu B, et al. First-line cadonilimab plus chemotherapy in HER2-negative advanced gastric or gastroesophageal junction adenocarcinoma: a randomized, double-blind, phase 3 trial. *Nat Med*. (2025) 31(4):1163–70. doi: 10.1038/s41591-024-03450-4

22. Husereau D, Drummond M, Augustovski F, de Bekker-Grob E, Briggs AH, Carswell C, et al. Consolidated health economic evaluation reporting standards 2022 (CHEERS 2022) statement: updated reporting guidance for health economic evaluations. *Value Health*. (2022) 25:3–9. doi: 10.1016/j.jval.2021.11.1351

23. Zhang J, Lei J, You C, Fu W, Zheng B, Cai H, et al. Cost-effectiveness analysis of durvalumab with chemotherapy and maintenance durvalumab with or without olaparib for advanced endometrial cancer. *Sci Rep*. (2025) 15:2497. doi: 10.1038/s41598-025-86021-y

24. Yue X, Li Y, Wu J, Guo JJ. Current development and practice of pharmacoeconomic evaluation guidelines for universal health coverage in China. *Value Health Reg Issues*. (2021) 24:1–5. doi: 10.1016/j.vhri.2020.07.580

25. Guyot P, Ades AE, Ouwens MJ, Welton NJ. Enhanced secondary analysis of survival data: reconstructing the data from published Kaplan-Meier survival curves. *BMC Med Res Methodol*. (2012) 12:9. doi: 10.1186/1471-2288-12-9

26. Su D, Wu B, Shi L. Cost-effectiveness of atezolizumab plus bevacizumab vs sorafenib as first-line treatment of unresectable hepatocellular carcinoma. *JAMA Netw Open*. (2021) 4:e210037. doi: 10.1001/jamanetworkopen.2021.0037

27. Liu L, Wang L, Chen L, Ding Y, Zhang Q, Shu Y. Cost-effectiveness of sintilimab plus chemotherapy versus chemotherapy alone as first-line treatment of locally advanced or metastatic oesophageal squamous cell carcinoma. *Front Immunol*. (2023) 14:1092385. doi: 10.3389/fimmu.2023.1092385

28. Ishak KJ, Kreif N, Benedict A, Muszbek N. Overview of parametric survival analysis for health-economic applications. *Pharmacoeconomics*. (2013) 31:663–75. doi: 10.1007/s40273-013-0064-3

29. Williams C, Lewsey JD, Mackay DF, Briggs AH. Estimation of survival probabilities for use in cost-effectiveness analyses: A comparison of a multi-state modeling survival analysis approach with partitioned survival and Markov decision-analytic modeling. *Med Decis Making*. (2017) 37:427–39. doi: 10.1177/0272989X16670617

30. Compiled by national bureau of statistics of China. Available online at: https://www.stats.gov.cn/sj/ndsj/2024/indexch.htm (Accessed February 1, 2024).

31. Xu L, Long Y, Yao L, Wang H, Ge W. Updated cost-effectiveness analysis of tislelizumab in combination with chemotherapy for the first-line treatment of advanced gastric cancer or gastroesophageal junction adenocarcinoma. *Front Oncol*. (2024) 14:1477722. doi: 10.3389/fonc.2024.1477722

32. Zhang PF, Xie D, Li Q. Cost-effectiveness analysis of nivolumab in the second-line treatment for advanced esophageal squamous cell carcinoma. *Future Oncol*. (2020) 16:1189–98. doi: 10.2217/fon-2019-0821

33. Yao ZH. *The big data service platform for China's health industry: Information Query of Drug Bid Winning* . Available online at: https://data.yaozh.com/ (Accessed February 1, 2024).

34. Liu S, Dou L, Wang K, Shi Z, Wang R, Zhu X, et al. Cost-effectiveness analysis of nivolumab combination therapy in the first-line treatment for advanced esophageal squamous-cell carcinoma. *Front Oncol.* (2022) 12:899966. doi: 10.3389/fonc.2022.899966

35. Shen J, Du Y, Shao R, Jiang R. First-line sintilimab plus chemotherapy in locally advanced or metastatic esophageal squamous cell carcinoma: A cost-effectiveness analysis from China. *Front Pharmacol.* (2022) 13:967182. doi: 10.3389/fphar.2022.967182

36. Zhan M, Xu T, Zheng H, He Z. Cost-effectiveness analysis of pembrolizumab in patients with advanced esophageal cancer based on the KEYNOTE-181 study. *Front Public Health.* (2022) 10:790225. doi: 10.3389/fpubh.2022.790225

37. Liu S, Dou L, Li S. Cost-effectiveness analysis of PD-1 inhibitors combined with chemotherapy as first-line therapy for advanced esophageal squamous-cell carcinoma in China. *Front Pharmacol.* (2023) 14:1055727. doi: 10.3389/fphar.2023.1055727

38. Zhang Q, Wu P, He X, Ding Y, Shu Y. Cost-effectiveness analysis of camrelizumab vs. Placebo added to chemotherapy as first-line therapy for advanced or metastatic esophageal squamous cell carcinoma in China. *Front Oncol.* (2021) 11:790373. doi: 10.3389/fonc.2021.790373

39. Ionova Y, Vuong W, Sandoval O, Fong J, Vu V, Zhong L, et al. Cost-effectiveness analysis of atezolizumab versus durvalumab as first-line treatment of extensive-stage small-cell lung cancer in the USA. *Clin Drug Investig.* (2022) 42:491–500. doi: 10.1007/s40261-022-01157-3

40. Nafees B, Lloyd AJ, Dewilde S, Rajan N, Lorenzo M. Health state utilities in non-small cell lung cancer: An international study. *Asia Pac J Clin Oncol.* (2017) 13:e195–195e203. doi: 10.1111/ajco.12477

41. Cai H, Xu B, Li N, Zheng B, Zheng Z, Liu M. Cost-effectiveness analysis of camrelizumab versus chemotherapy as second-line treatment of advanced or metastatic esophageal squamous cell carcinoma. *Front Pharmacol.* (2021) 12:732912. doi: 10.3389/fphar.2021.732912

42. Rotte A. Combination of CTLA-4 and PD-1 blockers for treatment of cancer. *J Exp Clin Cancer Res.* (2019) 38:255. doi: 10.1186/s13046-019-1259-z

43. Motzer RJ, Tannir NM, McDermott DF, Arén Frontera O, Melichar B, Choueiri TK, et al. Nivolumab plus Ipilimumab versus Sunitinib in Advanced Renal-Cell Carcinoma. *N Engl J Med.* (2018) 378:1277–90. doi: 10.1056/NEJMoa1712126

44. Lang W, He Y, Hou C, Li H, Jiang Q, Mei L. Cost-effectiveness analysis of pembrolizumab plus chemotherapy versus chemotherapy in untreated advanced pleural mesothelioma in the Chinese healthcare system. *Front Pharmacol.* (2024) 15:1402423. doi: 10.3389/fphar.2024.1402423

45. Lang W, Deng L, Lu M, Ouyang M. Cost-effectiveness analysis of pembrolizumab plus chemotherapy versus placebo plus chemotherapy for HER2-negative advanced gastric/gastroesophageal junction cancer in the Chinese healthcare system. *Expert Rev Pharmacoecon Outcomes Res.* (2024) 24:1027–42. doi: 10.1080/14737167.2024.2378983

46. Zheng Z, Song X, Cai H, Zhu H. Pembrolizumab combined with chemotherapy versus placebo combined with chemotherapy for HER2-negative advanced gastric cancer in China: a cost-effectiveness analysis. *Expert Rev Pharmacoecon Outcomes Res.* (2024) 24:1017–25. doi: 10.1080/14737167.2024.2378986

47. Allemani C, Matsuda T, Di Carlo V, Harewood R, Matz M, Nikšić M, et al. Global surveillance of trends in cancer survival 2000-14 (CONCORD-3): analysis of individual records for 37 513 025 patients diagnosed with one of 18 cancers from 322 population-based registries in 71 countries. *Lancet.* (2018) 391:1023–75. doi: 10.1016/S0140-6736(17)33326-3

frontiers | Frontiers in Immunology

TYPE Case Report
PUBLISHED 27 June 2025
DOI 10.3389/fimmu.2025.1625273

OPEN ACCESS

EDITED BY
Stavros P. Papadakos,
Laiko General Hospital of Athens, Greece

REVIEWED BY
Spyridon Zouridis,
Saint Louis University, United States
Eleni Myrto Maria Trifylli,
National and Kapodistrian University of Athens, Greece

*CORRESPONDENCE
Lin Zhu
13880262860@163.com
Ming Liu
liuming629@wchscu.cn

RECEIVED 08 May 2025
ACCEPTED 11 June 2025
PUBLISHED 27 June 2025

CITATION
Li W, Wei J, Zhang P, Cheng M, Xu M, Zhu L and Liu M (2025) Hyperbaric oxygen therapy as an immunosensitizing strategy in advanced gastric hepatoid adenocarcinoma: a case report. *Front. Immunol.* 16:1625273. doi: 10.3389/fimmu.2025.1625273

Hyperbaric oxygen therapy as an immunosensitizing strategy in advanced gastric hepatoid adenocarcinoma: a case report

Wenke Li[1], Jing Wei[1], Pengfei Zhang[1], Mo Cheng[1], Menghui Xu[1], Lin Zhu[2*] and Ming Liu[1*]

[1]Gastric Cancer Center/Cancer Center, West China Hospital, Sichuan University, Chengdu, Sichuan, China, [2]Department of Integrated Traditional and Western Medicine, West China Hospital, Sichuan University, Chengdu, China

Background: Hepatoid adenocarcinoma of the stomach (HAS) is a rare but highly aggressive subtype of gastric cancer (GC) associated with an unfavorable prognosis, particularly in advanced or metastatic stages. While the standard first-line treatment for advanced GC involves immune checkpoint inhibitors (ICIs) combined with chemotherapy, HAS often shows a poor therapeutic response to this regimen. The hypoxia in the tumor microenvironment is considered a key factor limiting ICI efficacy, and combining hyperbaric oxygen therapy (HBOT) with immunotherapy may offer a synergistic sensitizing effect.

Methods: We report a case of advanced HAS with peritoneal metastasis who received standard first-line immunochemotherapy (CAPOX plus sintilimab). After four cycles, the patient achieved only stable disease (SD) per RECIST 1.1 criteria. Consequently, HBOT was introduced as a sensitizing agent after the fifth cycle, and the patient subsequently completed the sixth cycle. This report was prepared using the CARE reporting guideline and checklist (Supplement A).

Results: Following the addition of HBOT, the patient's tumor markers normalized. Subsequent imaging and endoscopic evaluations revealed a complete resolution of all lesions, meeting the criteria for a clinical complete response (cCR) under RECIST 1.1.

Conclusions: This case suggests that adding HBOT may enhance the efficacy of immunotherapy and overcome resistance to ICIs in advanced HAS. These promising findings warrant further investigation through prospective clinical studies to confirm this observation.

KEYWORDS

gastric cancer, hepatoid adenocarcinoma of the stomach, hyperbaric oxygen therapy, immune checkpoint inhibitors, immunosensitization, clinical complete response

Introduction

Hepatoid adenocarcinoma of the stomach (HAS), a rare subtype of gastric cancer (GC), accounts for only 0.3%-15% of all GC cases (1). Histologically, HAS resembles hepatocellular carcinoma, characterized by abundant eosinophilic cytoplasm, centrally located nuclei, and frequent elevation of serum alpha-fetoprotein (AFP). Clinically, HAS exhibits a high propensity for vascular invasion and distant metastasis, particularly to the liver and peritoneum, a prognosis that is even worse than that of conventional gastric adenocarcinomas (2).

The peritoneum is one of the most common metastatic sites in GC, occurring in approximately 4%–14% of patients (3). Treatment of gastric cancer with peritoneal metastasis (GCPM) remains challenging and primarily relies on systemic therapy. While the combination of chemotherapy and immune checkpoint inhibitors (ICIs) has improved survival outcomes in advanced GC, achieving a complete clinical response (cCR) in unresectable cases with peritoneal dissemination is exceedingly rare. Moreover, primary or acquired resistance to ICIs is common, significantly limiting their therapeutic efficacy. Recent preclinical studies have highlighted the potential of hyperbaric oxygen therapy (HBOT) to favorably modulate the tumor microenvironment (TME), alleviate tumor hypoxia, and enhance the efficacy of ICIs (4). Therefore, combining HBOT with standard chemotherapy and ICIs offers a promising strategy for immunosensitization or overcoming ICI resistance.

This report describes the case of a 62-year-old male patient with advanced stage IVB (rT2N2M1) HAS with peritoneal metastasis. Initial systemic therapy with CAPOX chemotherapy combined with sintilimab yielded limited efficacy. Remarkably, after the incorporation of HBOT into his regimen, the patient achieved a cCR. To our knowledge, this is the first reported case of advanced HAS with peritoneal metastasis achieving cCR with this combination, highlighting the potential of HBOT as a novel immunosensitizing therapeutic strategy in advanced GC.

Case description

A timeline summarizing the key clinical events, from initial diagnosis to the last follow-up, is presented in Figure 1A.

Patient background and initial diagnosis

In March 2022, a 62-year-old male with no history of smoking, alcohol use, or other chronic diseases presented with epigastric pain. Psychosocially, the patient was a retired civil servant, married with strong family support, and had no history of significant psychological distress. His family history was notable for gastric cancer in his father, and subsequent genetic testing revealed a pathogenic RAD51D germline mutation alongside a TP53 somatic mutation of uncertain significance. Physical examination identified left upper quadrant tenderness, though laboratory results, including tumor markers and organ function tests, were within normal limits. An initial computed tomography (CT) scan demonstrated thickening of the gastric wall and enlarged perigastric lymph nodes (Figure 2A). Gastroscopy revealed ulcers at the gastric angle, and biopsy confirmed moderately to poorly differentiated adenocarcinoma. Based on these findings, the patient was clinically staged as cT2N1M0 (Stage IIA) according to the AJCC 8th Edition Cancer Staging Manual.

Surgical treatment and pathological findings

On March 16, 2022, the patient underwent laparoscopic radical distal gastrectomy with D2 lymphadenectomy, achieving a complete (R0) resection. Postoperative pathological examination of the resected specimen revealed a 4.8 × 4.0 cm, Borrmann type II tumor with a rough surface, which had focally infiltrated the muscularis propria. Histologically, the tumor was classified as an intestinal-type adenocarcinoma, that was predominantly tubular and graded as G2-G3 (moderately to poorly differentiated). Metastatic carcinoma was identified in three lymph nodes, one each from stations 3a, 7, and 11P.

Immunohistochemistry (IHC) analysis yielded the following results: HER2 (1+), CLDN18.2 (0), PD-L1 (CPS=2), and proficient mismatch repair (pMMR). PD-1 was positive in a minority of lymphocytes, while CDX2 and CK20 were positive, and Desmin was positive in smooth muscle. Epstein-Barr virus-encoded small RNA (EBER) *in situ* hybridization was negative. Additional IHC markers revealed positivity for SALL4 and GPC3, and negativity for CD34, AFP, and SOX10. These findings led to a final diagnosis of adenocarcinoma with features of both enteroblastic differentiation and hepatoid adenocarcinoma (Figures 2B, C). Based on the AJCC 8th Edition TNM staging system, the pathological stage was confirmed as pT2N2M0, Stage IIA.

Postoperative adjuvant chemotherapy and recurrence

Following surgery, the patient completed six cycles of adjuvant SOX chemotherapy and entered a period of surveillance. However, in December 2023, approximately one year after his initial surgery, he presented with abdominal distension. Laboratory tests revealed markedly elevated levels of serum AFP (>1210 ng/ml) and CA724 (16.10 U/ml). An abdominal CT scan subsequently confirmed the presence of peritoneal metastasis (Figure 1B). To establish a definitive diagnosis of recurrence, a therapeutic and diagnostic paracentesis was performed on December 8, 2023, which yielded approximately 700 mL of hemorrhagic ascitic fluid. Cytological analysis of this fluid confirmed recurrent adenocarcinoma. Consequently, the patient's diagnosis was updated to recurrent hepatoid adenocarcinoma of the gastric angle with peritoneal metastasis, and he was restaged as rT2N2M1 (Stage IV) according to the AJCC staging system.

10.3389/fimmu.2025.1625273

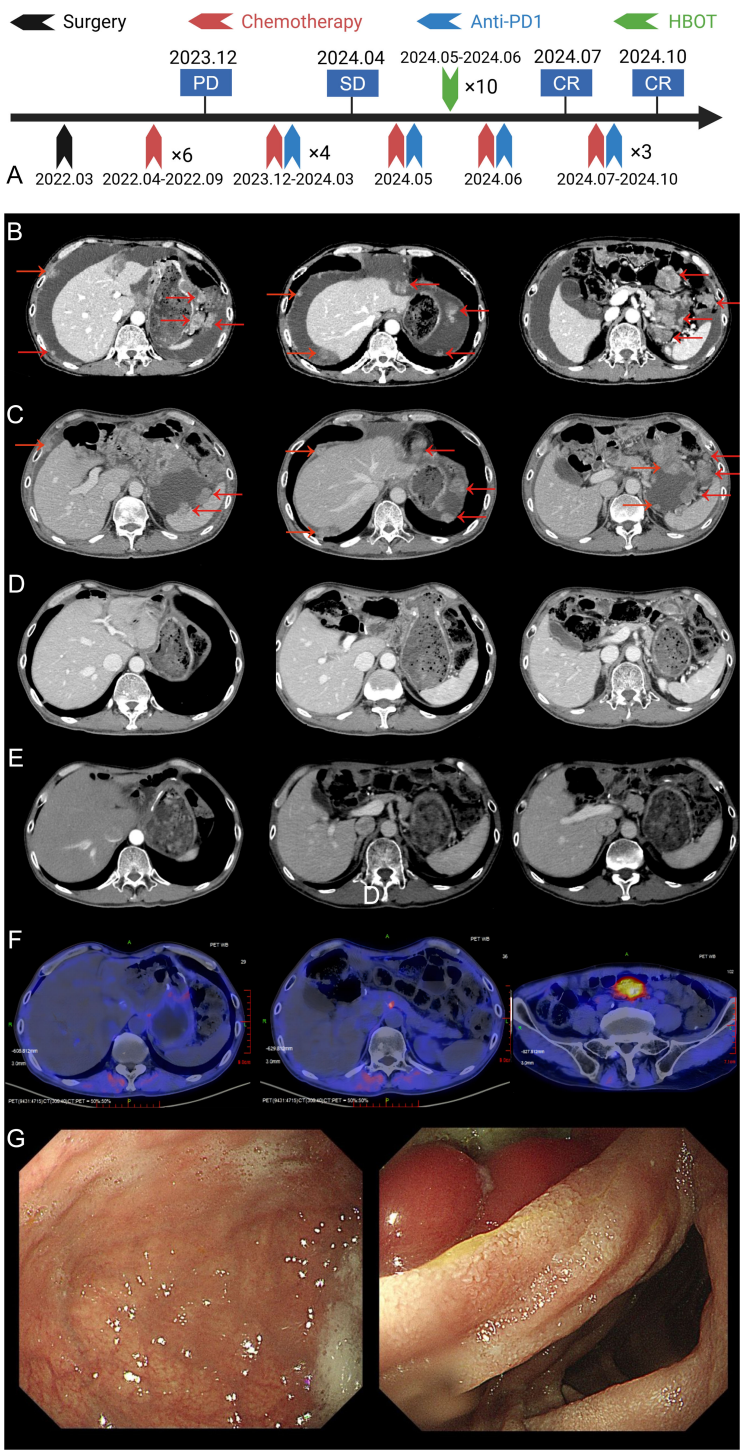

FIGURE 1
Imaging and treatment timeline of the patient. **(A)** The overall treatment timeline of the patient, including surgery, chemotherapy, anti-PD-1 therapy, and HBOT. **(B)** Abdominal enhanced CT at the time of recurrence showing tumor recurrence in the liver and surrounding tissues (tumor marked by red arrows). **(C)** Abdominal enhanced CT after 4 cycles of chemotherapy combined with ICIs treatment, showing partial tumor response (tumor marked by red arrows). **(D)** Abdominal enhanced CT after HBOT and an additional cycle of chemotherapy combined with ICIs, showing further tumor regression (tumor marked by red arrows). **(E)** Abdominal enhanced CT after 7–9 cycles of chemotherapy combined with ICIs, showing near-complete tumor resolution (tumor marked by red arrows). **(F)** FAPI PET/CT performed on January 3, 2025, revealing no evidence of tumor recurrence throughout the body. **(G)** Upper gastrointestinal endoscopy findings after 7–9 cycles of treatment. The gastric mucosa appeared smooth, and no active lesions were observed.

10.3389/fimmu.2025.1625273

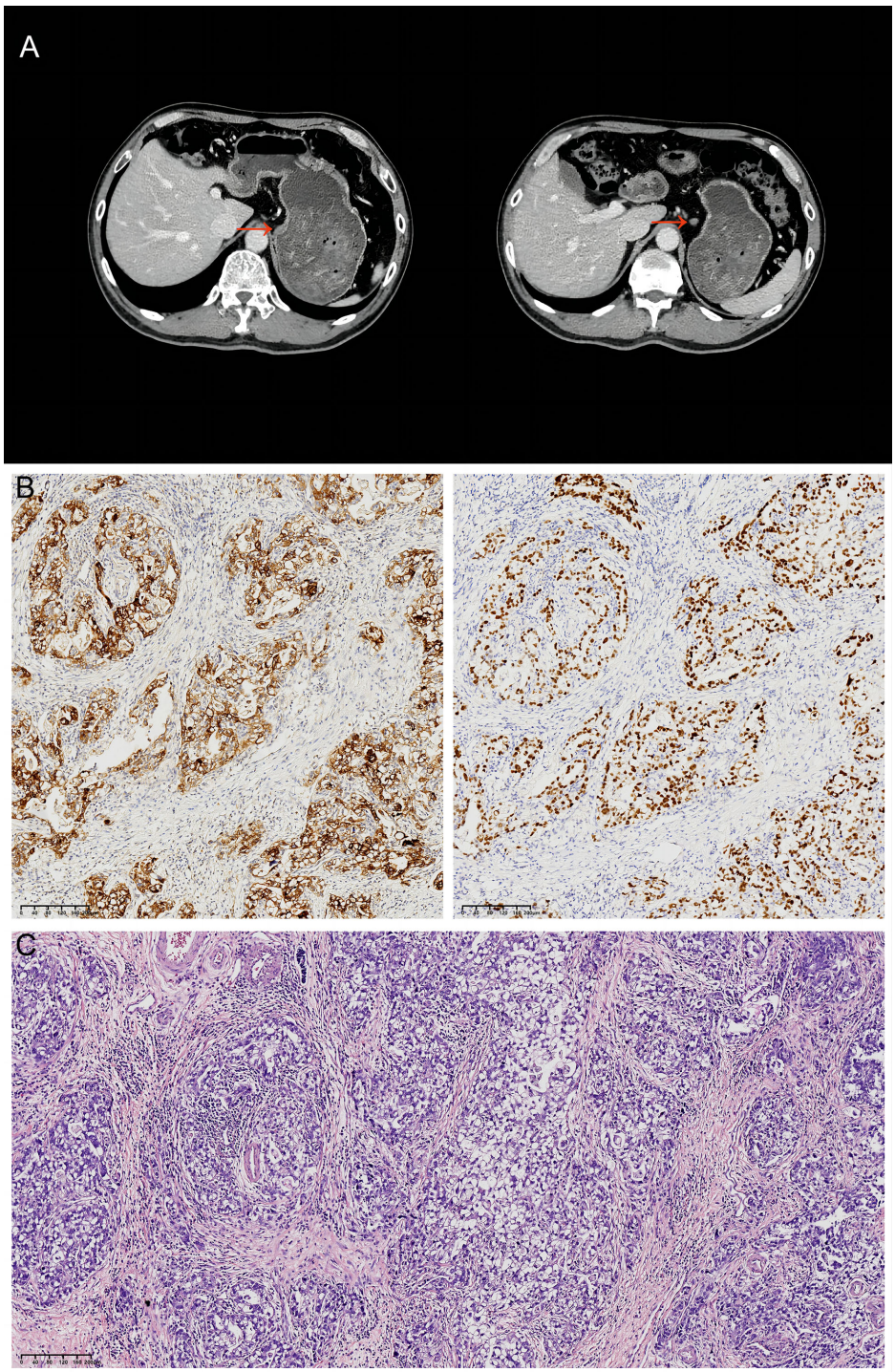

FIGURE 2
Initial CT findings and subsequent histopathology. **(A)** Abdominal CT from March 2022 showing thickening of the gastric lesser curvature (red arrows) and enlargement of the adjacent lymph nodes. **(B)** GPC3 (left) and SALL4 (right) immunohistochemical staining of the resected specimen. *Original magnification:×100; scale bar = 100 μm.* **(C)** Hematoxylin and eosin (H&E) staining of the resected specimen. *Original magnification:×100; scale bar = 100 μm.*

Systemic therapy

Following the diagnosis of recurrence, the patient received a single dose of intraperitoneal paclitaxel (60 mg) on December 9, 2023. Subsequently, from December 10, 2023, to March 12, 2024, he was treated with four cycles of first-line systemic immunochemotherapy. This regimen, administered every three weeks, consisted of CAPOX (capecitabine: 1.5 g orally, twice daily on days 1–14; oxaliplatin: 200 mg by intravenous infusion on day 1) combined with sintilimab (200 mg by intravenous infusion on day 1). An initial treatment response

evaluation was performed in March 2024. An enhanced abdominal CT scan (Figure 1C) revealed stable disease (SD) according to the RECIST 1.1 criteria.

Effective combination therapy

The decision to add HBOT was prompted by the limited clinical benefit observed after the initial four cycles: imaging evaluation revealed stable disease (SD), and the patient's abdominal distension had not significantly improved. To overcome potential resistance and prevent disease progression, and because the evaluation coincided with the scheduled start of the fifth cycle, the clinical team decided to introduce HBOT as a sensitizing strategy immediately after administering the next planned cycle of immunochemotherapy to maintain treatment continuity. Accordingly, on April 30, 2024, the patient received the 5th cycle of CAPOX and sintilimab with all drug doses maintained as in previous cycles. This was immediately followed by 10 sessions of HBOT (1-hour oxygen inhalation at 2 atmospheres absolute [ATA] per session). After completing the sixth cycle of the combined therapy on June 22, 2024, a follow-up evaluation in July 2024 showed a remarkable response. An enhanced abdominal CT scan revealed a complete resolution of the recurrent lesion at the gastric anastomosis and the peritoneal metastases (Figure 1D). Concurrently, tumor markers normalized, with AFP decreasing to 3.06 ng/mL (normal range: 0–7 ng/mL) and CA724 to 2.81 U/mL (normal range: 0–6.9 U/mL). The changes in AFP during treatment are illustrated in the Table 1. Based on RECIST 1.1 criteria, the patient had achieved complete response (CR).

The patient then proceeded to maintenance therapy with capecitabine and sintilimab. The maintenance regimen included the following: capecitabine: 1.5 g orally, twice daily, from day 1 to day 14; sintilimab: 200 mg by intravenous infusion, day 1. Each cycle was administered every three weeks. Follow-up imaging, including an enhanced chest and abdominal CT scan on October 15, 2024, confirmed a sustained cCR (Figure 1E). A fibroblast activation protein inhibitor (FAPI) PET/CT scan on January 3, 2025, showed a focal area of high tracer uptake in the peritoneum without a corresponding mass on CT, a finding suggestive of post-treatment inflammation rather than tumor recurrence (Figure 1F). Finally, a painless endoscopy on November 18, 2024, revealed no abnormalities in the remnant stomach (Figure 1G), further corroborating the complete response.

TABLE 1 Changes in AFP levels during treatment.

Date	AFP (ng/ml)
2022-03-03	2.57
2023-12-08	>1210.00
2024-01-03	>1210.00
2024-02-06	>1210.00
2024-03-12	>1210.00
2024-04-30	>1210.00
2024-07-17	3.06
2024-10-14	1.72
2024-11-14	1.88

Patient perspective

The patient reported no increase in adverse effects after the addition of hyperbaric oxygen therapy and demonstrated good treatment compliance throughout the course.

Follow-up

The patient is currently undergoing follow-up, including hematological tests, imaging evaluations, and quality of life assessments. Compliance with the treatment plan is excellent, and the patient maintains a good quality of life, with no signs of recurrence or significant adverse effects observed. As of the last follow-up on March 29, 2025, the patient remained progression-free. The progression-free survival (PFS) since the confirmation of recurrence on December 8, 2023, has been ongoing for over 15 months.

Discussion

The management of HAS, a rare but highly aggressive subtype of GC, presents a significant clinical challenge due to its poor prognosis and limited response to standard therapies. Characterized by histological features resembling hepatocellular carcinoma, HAS is frequently associated with elevated serum AFP levels (2, 5). Despite its rarity, the high global burden of GC, one of the top five most common malignancies worldwide, means that a substantial number of patients are still diagnosed with HAS each year (6). Currently, the therapeutic strategies for HAS do not differ from those for conventional gastric adenocarcinoma. For patients with unresectable advanced or metastatic HAS, systemic therapy remains the primary treatment modality. Pivotal Phase III trials, such as KEYNOTE-859 (7), CheckMate-649 (8), and ORIENT-16 (9), have established the combination of chemotherapy and a PD-1 inhibitor as the standard of care for first-line treatment of HER2-negative advanced GC (with mPFS of 6.9–7.7 months), a recommendation endorsed by major clinical guidelines including NCCN, CSCO, and ESMO. Indeed, subsequent meta-analyses have confirmed that this combination provides a significant survival benefit compared to chemotherapy alone (10). However, HAS is associated with a poorer prognosis than conventional GC, which is attributed to its higher propensity for distant metastasis and limited responsiveness to immunotherapy (11). Consequently, developing strategies to overcome this resistance and sensitize HAS to immunotherapy represents a critical clinical challenge.

The present case offers evidence for the potential of HBOT. The patient, diagnosed with advanced HAS and peritoneal metastasis, initially showed a suboptimal response to four cycles of standard immunochemotherapy (CAPOX plus sintilimab), achieving only SD. However, a dramatic clinical turnaround was observed following the introduction of HBOT after the fifth cycle. Subsequent evaluations revealed a cCR, evidenced by the normalization of tumor markers and the disappearance of all lesions on imaging and endoscopic examinations. Notably, the patient's progression-free survival has already exceeded 15 months. This remarkable improvement strongly suggests that HBOT acted as a potent immunosensitizing agent, overcoming the initial resistance and unlocking the therapeutic potential of the existing immunotherapy regimen.

The poor responsiveness of HAS to immunotherapy is largely attributed to its unique TME. HAS is typically characterized as an immunologically "cold" tumor, featuring diminished infiltration of CD8+ T cells, an abundance of regulatory T cells (Tregs) and M2-type macrophages, low PD-L1 expression, and a low tumor mutational burden (TMB). The majority of HAS cases are also microsatellite stable (MSS), all of which are hallmarks of poor responsiveness to immunotherapy (12). A salient feature of HAS is the elevation of serum AFP (11), a biomarker strongly associated with poor prognosis in GC. Elevated AFP not only indicates a poor outcome but also actively promotes tumor progression by enhancing proliferation, invasion, and migration (13). Furthermore, a distinctive feature of HAS is its extensive and abnormal tumor vasculature, which has been linked to the overexpression of vascular endothelial growth factor C (VEGF-C) and angiopoietin-like proteins (ANGPTLs) (14, 15). AFP itself can exacerbate this by upregulating VEGF expression and increasing microvessel density (14). However, this dysregulated angiogenesis results in dysfunctional vessels that are irregular, tortuous, and poorly branched. The consequent inefficient blood perfusion leads to extensive hypoxic regions within the tumor, creating a profoundly hypoxic and immunosuppressive TME (16). This tumor-induced hypoxia is a pivotal factor undermining the efficacy of ICIs. It triggers a cascade of immunosuppressive events, primarily through the activation of the hypoxia-inducible factor-1α (HIF-1α) signaling pathway. Activation of HIF-1α promotes the recruitment of inhibitory cells, including myeloid-derived suppressor cells (MDSCs), Tregs, and M2-type tumor-associated macrophages. It also upregulates PD-L1 expression on both cancer and dendritic cells, which directly inhibits cytotoxic T lymphocyte function and reinforces the immunosuppressive landscape (17–21). Additionally, hypoxic conditions are known to promote cancer stem cell maintenance, thereby increasing tumor invasiveness and therapeutic resistance (22, 23). Collectively, these features likely explain the limited efficacy of the initial immunochemotherapy regimen observed in our patient.

HBOT may enhance the efficacy of ICIs through multiple synergistic mechanisms. Foremost, HBOT directly counteracts the hypoxic tumor microenvironment. By increasing oxygen tension, it downregulates the expression of HIF-1α, thereby mitigating the recruitment of immunosuppressive cells such as Tregs and M2-macrophages (24–26). Concurrently, the hyperoxic state promotes the normalization of tumor vasculature, partly by upregulating the expression of platelet endothelial cell adhesion molecule-1 (PECAM-1/CD31), which facilitates increased infiltration of immune cells into the tumor site (27). Beyond remodeling the TME, HBOT has been shown to directly augment the effector functions of immune cells. It can enhance the cytotoxic activity of both effector T cells and natural killer (NK) cells, boosting their antitumor capabilities (27). Furthermore, emerging evidence suggests that HBOT can amplify the efficacy of PD-1 blockade by activating the cGAS-STING signaling pathway, a key innate immune sensing mechanism (27). Another proposed mechanism involves the degradation of the extracellular matrix (ECM) by HBOT, which may improve the physical delivery and penetration of large-molecule therapeutics like anti-PD-1/PD-L1 monoclonal antibodies into the TME (28). Collectively, these multifaceted mechanisms provide a strong theoretical basis for the role of HBOT as an effective immunosensitizing strategy in cancer therapy.

Indeed, the "abnormal vasculature-hypoxia-immunosuppression axis" is not exclusive to HAS but is a common pathological feature of gastric adenocarcinoma, particularly in advanced stages (16, 29). This hypoxia-driven, immunosuppressive microenvironment is thought to be a key mechanism underlying the limited efficacy of ICIs in a significant proportion of GC patients. Consequently, this highlights the therapeutic potential of HBOT in the broader population of patients with advanced or metastatic gastric adenocarcinoma. Upon reviewing the existing clinical literature, we found that studies on HBOT in cancer treatment are limited, with most focusing on its role as an adjunct to radiotherapy or chemotherapy, primarily aimed at improving quality of life, and demonstrating good tolerability in most cases. To further investigate the immunosensitizing mechanisms of HBOT and to validate the efficacy of this combination therapy, our team has initiated a Phase Ib/II clinical trial. This study will evaluate CAPOX chemotherapy combined with the PD-1 inhibitor sintilimab and HBOT as a first-line treatment for advanced or metastatic gastric or gastroesophageal junction cancer (GC/GEJC) (NCT06742411).

To our knowledge, this is the first reported case of a patient with advanced, HER2-negative HAS and peritoneal metastasis achieving a cCR through the combination of HBOT with chemotherapy and immunotherapy. This outcome highlights the potential of HBOT as an effective immunosensitizing strategy in GC. The primary strengths of this report lie in its novelty, as well as the favorable safety profile and low cost of HBOT, which would facilitate its widespread adoption if proven effective in large-scale clinical trials. However, this case report has several limitations. Firstly, as a single case, it lacks a control group for comparison, and the influence of the patient's specific, albeit of uncertain significance, genetic mutations on the observed efficacy of HBOT and ICIs remains unknown. Secondly, because no residual tumor was found during the follow-up endoscopy, we were unable to perform a comparative analysis of the TME before and after HBOT to elucidate the underlying mechanisms. Furthermore, predictive biomarkers to identify patients who would most benefit from the HBOT-immunochemotherapy combination are currently lacking. Although imaging techniques to assess tumor hypoxia in GC

exist, their accuracy and correlation with treatment outcomes need to be validated in larger-scale clinical trials. Therefore, despite the promising results of this case, further prospective studies are essential to confirm these findings, explore the mechanisms of action, and define the optimal patient population for this novel therapeutic approach.

Conclusion

This case report details the successful treatment of a patient with advanced HAS who achieved a remarkable clinical CR. The addition of HBOT to a standard immunochemotherapy regimen appeared to overcome initial treatment resistance. These findings suggest that HBOT may serve as an effective immunosensitizing strategy, enhancing the efficacy of ICIs in the treatment of GC. Future clinical studies are warranted to further verify the efficacy and safety of HBOT combined with immunotherapy, explore its mechanisms of action, and provide new insights for the comprehensive treatment of advanced GC.

Data availability statement

The original contributions presented in the study are included in the article/supplementary material. Further inquiries can be directed to the corresponding authors.

Ethics statement

The studies involving humans were approved by Ethics Committee of West China Hospital, Sichuan University. The studies were conducted in accordance with the local legislation and institutional requirements. The participants provided their written informed consent to participate in this study. Written informed consent was obtained from the individual(s) for the publication of any potentially identifiable images or data included in this article.

Author contributions

WL: Conceptualization, Data curation, Formal Analysis, Investigation, Methodology, Software, Writing – original draft, Writing – review & editing. JW: Investigation, Writing – review & editing. PZ: Writing – review & editing. MC: Investigation, Software, Writing – review & editing. MX: Writing – review & editing. LZ: Investigation, Project administration, Software, Writing – review & editing. ML: Conceptualization, Formal Analysis, Funding acquisition, Investigation, Project administration, Software, Writing – original draft, Writing – review & editing.

Funding

The author(s) declare that no financial support was received for the research and/or publication of this article.

Conflict of interest

The authors declare that the research was conducted in the absence of any commercial or financial relationships that could be construed as a potential conflict of interest.

Generative AI statement

The author(s) declare that no Generative AI was used in the creation of this manuscript.

Publisher's note

References

1. Zhu M, Chen E, Yu S, Xu C, Yu Y, Cao X, et al. Genomic profiling and the impact of MUC19 mutation in hepatoid adenocarcinoma of the stomach. *Cancer Commun (Lond).* (2022) 42:1032–5. doi: 10.1002/cac2.12336

2. Xia R, Zhou Y, Wang Y, Yuan J, Ma X. Hepatoid adenocarcinoma of the stomach: current perspectives and new developments. *Front Oncol.* (2021) 11:633916. doi: 10.3389/fonc.2021.633916

3. Sirody J, Kaji AH, Hari DM, Chen KT. Patterns of gastric cancer metastasis in the United States. *Am J Surg.* (2022) 224:445–8. doi: 10.1016/j.amjsurg.2022.01.024

4. Liu X, Ye N, Liu S, Guan J, Deng Q, Zhang Z, et al. Hyperbaric oxygen boosts PD-1 antibody delivery and T cell infiltration for augmented immune responses against solid tumors. *Adv Sci (Weinh).* (2021) 8:e2100233. doi: 10.1002/advs.202100233

5. Li M, Mei YX, Wen JH, Jiao YR, Pan QR, Kong XX, et al. Hepatoid adenocarcinoma-Clinicopathological features and molecular characteristics. *Cancer Lett.* (2023) 559:216104. doi: 10.1016/j.canlet.2023.216104

6. Bray F, Laversanne M, Sung H, Ferlay J, Siegel RL, Soerjomataram I, et al. Global cancer statistics 2022: GLOBOCAN estimates of incidence and mortality worldwide for 36 cancers in 185 countries. *CA Cancer J Clin.* (2024) 74:229–63. doi: 10.3322/caac.21834

7. Rha SY, Oh D-Y, Yañez P, Bai Y, Ryu M-H, Lee J, et al. Pembrolizumab plus chemotherapy versus placebo plus chemotherapy for HER2-negative advanced gastric cancer (KEYNOTE-859): a multicentre, randomised, double-blind, phase 3 trial. *Lancet Oncol.* (2023) 24:1181–95. doi: 10.1016/S1470-2045(23)00515-6

8. Janjigian YY, Shitara K, Moehler M, Garrido M, Salman P, Shen L, et al. First-line nivolumab plus chemotherapy versus chemotherapy alone for advanced gastric, gastro-oesophageal junction, and oesophageal adenocarcinoma (CheckMate 649): a randomised, open-label, phase 3 trial. *Lancet*. (2021) 398:27–40. doi: 10.1016/S0140-6736(21)00797-2

9. Xu J, Jiang H, Pan Y, Gu K, Cang S, Han L, et al. Sintilimab plus chemotherapy for unresectable gastric or gastroesophageal junction cancer: the ORIENT-16 randomized clinical trial. *Jama*. (2023) 330:2064–74. doi: 10.1001/jama.2023.19918

10. Pu W, Li S, Zhang J, Huang J, Li J, Jiang Y, et al. The efficacy and safety of PD-1/PD-L1 inhibitors in combination with chemotherapy as a first-line treatment for unresectable, locally advanced, HER2-negative gastric or gastroesophageal junction cancer: a meta-analysis of randomized controlled trials. *Front Immunol*. (2025) 16:1566939. doi: 10.3389/fimmu.2025.1566939

11. Jiang J, Ding Y, Lu J, Chen Y, Chen Y, Zhao W, et al. Integrative analysis reveals a clinicogenomic landscape associated with liver metastasis and poor prognosis in hepatoid adenocarcinoma of the stomach. *Int J Biol Sci*. (2022) 18:5554. doi: 10.7150/ijbs.71449

12. Taniguchi Y, Kiyozawa D, Kohashi K, Kawatoko S, Yamamoto T, Torisu T, et al. Volume of hepatoid component and intratumor M2 macrophages predict prognosis in patients with hepatoid adenocarcinoma of the stomach. *Gastric Cancer*. (2025) 28:41–50. doi: 10.1007/s10120-024-01562-x

13. Zhan Z, Chen B, Yu J, Zheng J, Zeng Y, Sun M, et al. Elevated serum alpha-fetoprotein is a significant prognostic factor for patients with gastric cancer: Results based on a large-scale retrospective study. *Front Oncol*. (2022) 12:901061. doi: 10.3389/fonc.2022.901061

14. Kamei S, Kono K, Amemiya H, Takahashi A, Sugai H, Ichihara F, et al. Evaluation of VEGF and VEGF-C expression in gastric cancer cells producing α-fetoprotein. *J Gastroenterol*. (2003) 38:540–7. doi: 10.1007/s00535-002-1099-y

15. Chen E, Tang C, Peng K, Cheng X, Wei Y, Liu T. ANGPTL6-mediated angiogenesis promotes alpha fetoprotein-producing gastric cancer progression. *Pathol-Res Pract*. (2019) 215:152454. doi: 10.1016/j.prp.2019.152454

16. Chen Z, Han F, Du Y, Shi H, Zhou W. Hypoxic microenvironment in cancer: molecular mechanisms and therapeutic interventions. *Signal Transduction Targeted Ther*. (2023) 8:70. doi: 10.1038/s41392-023-01332-8

17. Greijer A, van der Wall E. The role of hypoxia inducible factor 1 (HIF-1) in hypoxia induced apoptosis. *J Clin Pathol*. (2004) 57:1009–14. doi: 10.1136/jcp.2003.015032

18. Semenza GL. Targeting HIF-1 for cancer therapy. *Nat Rev Cancer*. (2003) 3:721–32. doi: 10.1038/nrc1187

19. Luo F, Lu F-T, Cao J-X, Ma W-J, Xia Z-F, Zhan J-H, et al. HIF-1α inhibition promotes the efficacy of immune checkpoint blockade in the treatment of non-small cell lung cancer. *Cancer Lett*. (2022) 531:39–56. doi: 10.1016/j.canlet.2022.01.027

20. Ding X-C, Wang L-L, Zhang X-D, Xu J-L, Li P-F, Liang H, et al. The relationship between expression of PD-L1 and HIF-1α in glioma cells under hypoxia. *J Hematol Oncol*. (2021) 14:92. doi: 10.1186/s13045-021-01102-5

21. Shurin MR, Umansky V. Cross-talk between HIF and PD-1/PD-L1 pathways in carcinogenesis and therapy. *J Clin Invest*. (2022) 132:e159473. doi: 10.1172/JCI159473

22. Bar EE, Lin A, Mahairaki V, Matsui W, Eberhart CG. Hypoxia increases the expression of stem-cell markers and promotes clonogenicity in glioblastoma neurospheres. *Am J Pathol*. (2010) 177:1491–502. doi: 10.2353/ajpath.2010.091021

23. Li P, Zhou C, Xu L, Xiao H. Hypoxia enhances stemness of cancer stem cells in glioblastoma: an *in vitro* study. *Int J Med Sci*. (2013) 10:399. doi: 10.7150/ijms.5407

24. Zhang L, Ke J, Min S, Wu N, Liu F, Qu Z, et al. Hyperbaric oxygen therapy represses the Warburg effect and epithelial–mesenchymal transition in hypoxic NSCLC cells via the HIF-1α/PFKP axis. *Front Oncol*. (2021) 11:691762. doi: 10.3389/fonc.2021.691762

25. Wang P, Gong S, Pan J, Wang J, Zou D, Xiong S, et al. Hyperbaric oxygen promotes not only glioblastoma proliferation but also chemosensitization by inhibiting HIF1α/HIF2α-Sox2. *Cell Death Discov*. (2021) 7:103. doi: 10.1038/s41420-021-00486-0

26. Wu X, Zhu Y, Huang W, Li J, Zhang B, Li Z, et al. Hyperbaric oxygen potentiates doxil antitumor efficacy by promoting tumor penetration and sensitizing cancer cells. *Adv Sci*. (2018) 5:1700859. doi: 10.1002/advs.201700859

27. Chen S-Y, Tsuneyama K, Yen M-H, Lee J-T, Chen J-L, Huang S-M. Hyperbaric oxygen suppressed tumor progression through the improvement of tumor hypoxia and induction of tumor apoptosis in A549-cell-transferred lung cancer. *Sci Rep*. (2021) 11:12033. doi: 10.1038/s41598-021-91454-2

28. Li K, Gong Y, Qiu D, Tang H, Zhang J, Yuan Z, et al. Hyperbaric oxygen facilitates teniposide-induced cGAS-STING activation to enhance the antitumor efficacy of PD-1 antibody in HCC. *J ImmunoTher Cancer*. (2022) 10:e004006. doi: 10.1136/jitc-2021-004006

29. Ozcan G. The hypoxia-inducible factor-1α in stemness and resistance to chemotherapy in gastric cancer: Future directions for therapeutic targeting. *Front Cell Dev Biol*. (2023) 11:1082057. doi: 10.3389/fcell.2023.1082057

frontiers | Frontiers in Immunology

TYPE Original Research
PUBLISHED 18 July 2025
DOI 10.3389/fimmu.2025.1624943

OPEN ACCESS

EDITED BY
Stavros P. Papadakos,
Laiko General Hospital of Athens, Greece

REVIEWED BY
Tao Li,
People's Liberation Army General Hospital, China
Bingyu Li,
Tongji University, China

*CORRESPONDENCE
Helei Hou
houhelei@qdu.edu.cn;
houheleihhl@163.com
Haitao Jiang
jianght67122@sina.com

†These authors have contributed equally to this work

RECEIVED 08 May 2025
ACCEPTED 30 June 2025
PUBLISHED 18 July 2025

CITATION
Zhang X, Tian Y, Wang H, Song S, Chen Y, Liu N, Zhang C, Huang X, Jiang H and Hou H (2025) Additions of trastuzumab to preoperative chemotherapy or chemoimmunotherapy for patients with potentially resectable stage III to IV_B HER2-positive gastric cancer. *Front. Immunol.* 16:1624943. doi: 10.3389/fimmu.2025.1624943

Additions of trastuzumab to preoperative chemotherapy or chemoimmunotherapy for patients with potentially resectable stage III to IV_B HER2-positive gastric cancer

Xuchen Zhang[1], Yulong Tian[2], Huiyun Wang[1], Shanai Song[1], Yunqing Chen[3], Ning Liu[1], Chuantao Zhang[1], Xiao Huang[1], Haitao Jiang[2*†] and Helei Hou[1*†]

[1]Department of Oncology, The Affiliated Hospital of Qingdao University, Qingdao, China, [2]Department of Gastrointestinal Surgery, The Affiliated Hospital of Qingdao University, Qingdao, China, [3]Department of Pathology, The Affiliated Hospital of Qingdao University, Qingdao, China

Background: Whether the addition of trastuzumab to chemo(immuno)therapy for the preoperative treatment of patients with potentially resectable HER2-positive gastric cancer has clinical benefits remains to be explored. This real-world observational study was designed to evaluate the efficacy and safety of trastuzumab plus chemo(immuno)therapy for neoadjuvant or conversion therapy in patients with potentially resectable HER2-positive gastric cancer.

Methods: We retrospectively collected the clinical data of treatment-naïve patients with potentially resectable stage III to IV_B HER2-positive gastric cancer who received preoperative therapy prior to D2 gastrectomy. The main outcomes of interest included tumour regression grade (TRG), treatment-related adverse events (TRAEs), and event-free survival (EFS).

Results: A total of 40 patients were included in the analysis, specifically, 27 patients (67.5%, 95% CI 0.520-0.799) received preoperative trastuzumab plus chemo(immuno)therapy, and 13 patients (32.5%, 95% CI 0.201-0.480) received chemo(immuno)therapy. All these patients subsequently underwent D2 gastrectomy. Regarding surgical outcomes, TRG0/1 rates were 33.3% (95% CI 0.186-0.522) in the trastuzumab-containing treatment group and 15.4% (95% CI 0.043-0.422) in the chemotherapy/chemoimmunotherapy group. Regarding safety, 66.7% (95% CI 0.478-0.814) of patients in the trastuzumab-containing treatment group and 61.5% (95% CI 0.355-0.823) of patients in the chemotherapy/chemoimmunotherapy group experienced preoperative TRAEs. The probabilities of EFS were not statistically significant between the two groups by the last follow-up.

Conclusion: Additions of trastuzumab to preoperative chemotherapy or chemoimmunotherapy resulted in a TRG0/1 rate of 33.3% among patients with potentially resectable HER2-positive gastric cancer, and the combined regimen exhibited a favourable safety profile.

KEYWORDS

HER2-positive gastric cancer, preoperative therapy, trastuzumab, immune checkpoint blockade, tumour regression grade

Introduction

Gastric cancer (GC) remains a severe medical burden with high morbidity and mortality worldwide (1), and human epidermal growth factor receptor-2 (HER2)-positive GC is a distinct subtype with high invasiveness. HER2-positive GC accounts for approximately 10% to 20% of all GC cases, and the prognosis of patients with HER2-positive GC is dismal (2). For patients with potentially resectable HER2-positive GC, the malignant biological behaviours of the tumour worsen surgical outcomes and prognoses; thus, exploring the optimal preoperative treatment options for patients with potentially resectable HER2-positive GC is important.

Based on the results of the milestone phase III MAGIC trial (3), perioperative chemotherapy and D2 radical gastrectomy has become the standard treatment regimen for patients with locally advanced GC. In recent years, the combination of neoadjuvant programmed cell-death receptor (ligand)-1 (PD-1/PD-L1) blockade and chemotherapy has resulted in higher pathological complete response (pCR) rates than neoadjuvant chemotherapy alone, according to the phase III KEYNOTE-585 study (4) and the MATTERHORN study (5). However, previous studies have not specifically reported outcomes in HER2-positive cohorts, and whether the addition of HER2 blockade and/or immune checkpoint blockade to chemotherapy would have clinical benefits for patients with potentially resectable HER2-positive GC remains unclear.

For patients with unresectable or metastatic HER2-positive GC, trastuzumab plus chemotherapy is the standard first-line treatment regimen, according to the phase III ToGA trial (6). Recently, with the rapid development of immune checkpoint blockade therapies for solid tumours, the combination of pembrolizumab, trastuzumab and chemotherapy has been shown to result in promising clinical outcomes as a first-line treatment for patients with unresectable or metastatic HER2-positive GC, with significantly increased objective response rates (ORRs) and prolonged progression-free survival (PFS), as demonstrated by the phase III KEYNOTE-811 trial (7). In the preoperative neoadjuvant or conversion setting for patients with partially resectable HER2-positive GC, several studies, albeit only phase II, have investigated the efficacy and safety of preoperative trastuzumab with or without PD-1 blockade plus chemotherapy in patients with potentially resectable HER2-positive GC (8–14). According to the phase II NEOHX study (8) and HER-FLOT study (9), the pCR rates of neoadjuvant trastuzumab plus chemotherapy ranged from 8% to 22%. Additionally, the combination of PD-(L)1 blockade, trastuzumab and chemotherapy resulted in pCR rates ranging from 31% to 43% (10, 11, 14). However, the efficacy and safety of this combined regimen in patients with potentially resectable HER2-positive GC warrant further exploration in larger cohorts.

In this observational study, we retrospectively evaluated the efficacy and safety profile of the additions of trastuzumab to preoperative chemo(immuno)therapy in patients with potentially resectable HER2-positive GC.

Methods

Study design

We retrospectively collected clinical data from treatment-naïve, clinical stage $T_{3\text{-}4a}N_{+}M_0$ (stage III) or stage $T_{any}N_{any}M_1$ (stage IV_B) HER2-positive gastric cancer patients who were treated at our centre between November 2018 and August 2024. Patients with stage IV_B disease in this study were considered to have partially resectable GC after multidisciplinary discussions. All procedures were approved by the Ethics Committee of the Affiliated Hospital of Qingdao University (QYFYWZLL28829, Qingdao, China). All investigations were carried out according to the principles of the Declaration of Helsinki.

The major inclusion criteria for the patients were as follows: a) a diagnosis of clinical stage $T_{3\text{-}4a}N_{+}M_0$ (stage III) or stage $T_{any}N_{any}M_1$ (stage IV_B) gastric cancer with HER2 positivity; b) a lack of previous antitumour treatment; c) an Eastern Cooperative Oncology Group performance status (ECOG PS) score of 0 to 1; and d) sufficient vital organ function. The exclusion criteria for patients were as follows: a) inadequate vital organ function or systemic autoimmune disease; or b) other primary malignancies in addition to gastric cancer.

Treatment

The included patients received trastuzumab plus chemo(immuno) therapy (trastuzumab-containing treatment group), or chemo

(immuno)therapy alone (chemotherapy/chemoimmunotherapy group) as preoperative treatment. Following the final dose of preoperative treatment, tumour response was assessed, and multidisciplinary discussions were conducted to determine the feasibility of surgical resection. Subsequently, all patients underwent standardized D2 gastrectomy.

Trastuzumab was administered at the dosage of 8 mg/kg for the first cycle and subsequent 6 mg/kg, iv drip, and every three weeks. The PD-1 blockade used included one of the following regimens: sintilimab (200 mg iv drip, every three weeks), camrelizumab (200 mg iv drip, every three weeks), tislelizumab (200 mg iv drip, every three weeks) and pembrolizumab (200 mg iv drip, every three weeks). The chemotherapy regimen included standardized FLOT, SOX, XELOX, TP, TS, FOLFOX, and DCF regimens. Post-operative treatment would be continued based on the surgical outcomes and the results of multi-disciplinary treatment discussions.

Assessments

Contrast-enhanced computed tomography (CT) and endoscopic ultrasound (EUS) were used to assess the primary tumour at baseline and the response to preoperative treatment according to Response Evaluation Criteria in Solid Tumors (RECIST) version 1.1 (15). Tumour tissue biopsies were collected both at baseline and during surgery. Surgical samples from primary tumours and lymph nodes were staged based on the gastric cancer staging system in the eighth edition of the American Joint Committee on Cancer staging manual (16).

The pathological response of the primary lesion after surgery was evaluated in accordance with the tumour regression grade (TRG) criteria (17). TRG0, TRG1, TRG2, and TRG3 were defined as no residual viable tumour cells (pCR), no more than 2% residual viable tumour cells, more than 2% but no more than 50% residual viable tumour cells, and more than 50% residual viable tumour cells, respectively. The pathological images were scanned using Nano Zoomer S210 (Hamamatsu).

Next-generation sequencing (NGS), immunohistochemical (IHC) staining with an anti-HER2 antibody, and HER2 *in situ* hybridization (ISH) were used to evaluate the expression of HER2. HER2 positivity was defined as HER2 amplification shown by NGS, an IHC staining score of 3+, or an IHC staining score of 2+ in combination with HER2 amplification confirmed by ISH (18).

The expression of programmed death ligand-1 (PD-L1) was evaluated using IHC staining with the anti-PD-L1 antibody 22C3 (Dako, Glostrup, Denmark). The combined positive score (CPS) was calculated to evaluate the number of PD-L1-positive cells, including tumour cells, macrophages and lymphocytes. Briefly, a CPS<1 indicated PD-L1 negativity, and a CPS≥1 indicated PD-L1 positivity.

The mismatch repair (MMR) status was evaluated using immunohistochemical staining with primary antibodies against MSH2, MSH6, MLH1, and PMS2. As for the microsatellite instability (MSI) status, real-time quantitative polymerase chain reaction was used to detect the amplification of five microsatellite loci: BAT25, BAT26, D5S346, D17S250, and D2S123. If two or more unstable markers were observed at these five loci, MSI-H status was defined; otherwise, the microsatellite status was defined as MSI-low (MSI-L) or MSS (19).

The observed treatment-related adverse events (TRAEs) during the preoperative treatment period were evaluated according to National Cancer Institute Common Terminology Criteria for Adverse Events (CTCAE) version 5.0.

Outcome evaluation

The outcomes of interest were pathological tumour response and radiographic tumour response (complete response, CR; partial response, PR; stable disease, SD; progressive disease, PD). Other outcomes included the event-free survival (EFS) time (defined as the time from diagnosis to any one of the following three events: inability to undergo surgery due to disease progression, local or distant disease relapse, or death due to any cause) and observed TRAEs.

Statistical analysis

Descriptive statistics for continuous variables were presented as either medians (interquartile ranges) or means (standard deviations), depending on data distribution. Categorical variables were summarized using frequencies and percentages with 95% confidential intervals (CIs). To assess differences between two groups, Student's *t*-test was employed for continuous variables, while the chi-square test or Fisher's exact test was used for categorical variables, as appropriate. A two-tailed P value<0.05 was considered indicative of statistical significance. All analyses were performed using SPSS 25.0 (IBM Corp., Armonk, NY, USA) and GraphPad Prism 9.5 (GraphPad Software, Inc., San Diego, CA, USA).

Results

Enrolled patients and treatment

A total of 40 patients were included in the analysis, among whom 27 patients (67.5%, 95% CI 0.520-0.799) received trastuzumab plus chemotherapy/chemoimmunotherapy (trastuzumab-containing treatment group), and 13 patients (32.5%, 95% CI 0.201-0.480) were treated with chemotherapy/chemoimmunotherapy alone (chemotherapy/chemoimmunotherapy group). Most patients in the two groups had stage III diseases, and the tumours in all the patients were considered potentially resectable after multidisciplinary discussions. Following the final dose of neoadjuvant or conversion treatment, all patients underwent standardized D2 radical gastrectomy, and the patients with stage IV_B disease received additional local therapy for metastatic lesions. Postoperative adjuvant treatment was administered based on the surgical outcomes such as HER2 and PD-L1 expression levels, and statuses of TMB and MSI/MMR.

11 patients (11/27, 40.7%, 95% CI 0.245-0.593) in the trastuzumab-containing treatment group were treated with the combined regimen of trastuzumab, PD-1 blockade and

chemotherapy; and 4 patients (4/9, 44.4%, 95% CI 0.189-0.733) in the chemotherapy/chemoimmunotherapy group received PD-1 blockade plus chemotherapy. Trastuzumab was administered at the dosage of 8 mg/kg for the first cycle and subsequent 6 mg/kg, iv drip, and every three weeks. The details of PD-1 blockade used in these patients were: eight cases of sintilimab (200 mg iv drip, every three weeks), four cases of camrelizumab (200 mg iv drip, every three weeks), two cases of pembrolizumab (200 mg iv drip, every three weeks), and one case of tislelizumab (200 mg iv drip, every three weeks). The chemotherapy regimens used included standardized FLOT, SOX, XELOX, TP, TS, FOLFOX, and DCF regimens. Table 1 shows the baseline characteristics and details of the treatment regimens of the patients.

In addition, a total of 10 patients completed next-generation sequencing testing, and *TP53* missense alterations were the most common co-occurred mutations.

TABLE 1 Demographics and baseline characteristics of the included patients.

Characteristics	Trastuzumab-containing treatment group (N=27)	Chemotherapy or chemoimmunotherapy group (N=13)	*P* value
Age (years)			0.280
Mean (Standard Deviation)	60.6 (8.77)	63.8 (8.86)	
Gender, n (%)			>0.999
Male	25 (92.6)	12 (92.3)	
Female	2 (7.4)	1 (7.7)	
Preoperative treatment, n (%)			0.730
Chemotherapy-based	16 (59.3)	9 (69.2)	
Chemoimmunotherapy-based	11 (40.7)	4 (30.8)	
Primary tumour location, n (%)			0.437
Gastro-oesophageal junction	5 (18.5)	4 (30.8)	
Non-gastro-oesophageal junction	22 (81.5)	9 (69.2)	
Tumour differentiation, n (%)			0.446
Well	0	1 (7.6)	
Moderately	10 (37.1)	4 (30.8)	
Moderately-poorly	6 (22.2)	4 (30.8)	
Poorly	11 (40.8)	4 (30.8)	
Baseline T staging, n (%)			0.400
T_{2-3}	4 (14.8)	4 (30.8)	
T_{4a-4b}	23 (85.2)	9 (69.2)	
Baseline N staging, n (%)			0.393
N_{1-2}	21 (77.8)	12 (92.3)	
N_3	6 (22.2)	1 (7.7)	
Baseline PD-L1 expression, n (%)			0.710
CPS<1	1 (3.7)	1 (7.7)	
1≤CPS<5	6 (22.2)	3 (23.1)	
CPS≥5	5 (18.5)	4 (30.8)	
Unknown	15 (55.6)	5 (38.4)	

Clinical activity and tumour response

According to the radiographical tumour response to preoperative treatment, all the patients in the trastuzumab-containing treatment group and most patients (12/13, 92.3%, 95% CI 0.667-0.986) in the chemotherapy/chemoimmunotherapy group had PR or SD, while one patient (1/13, 7.7%, 95% CI 0.014-0.333) in the chemotherapy/chemoimmunotherapy group exhibited PD. The ORRs were 74.1% (20/27, 95% CI 0.553-0.868) in the trastuzumab-containing treatment group, and 53.8% (7/13, 95% CI 0.292-0.768) in the chemotherapy/chemoimmunotherapy group (Figure 1 and Table 2).

R0 resection was achieved in all the patients. Three patients (11.1%, 95% CI 0.039-0.281) in the trastuzumab-containing treatment group achieved TRG0, including two baseline stage IV_B patients with oligometastatic lesions in the liver; while none of the patients in the chemotherapy/chemoimmunotherapy group achieved TRG0. The overall TRG0/1 rates were 33.3% (9/27, 95% CI 0.186-0.522) in the trastuzumab-containing treatment group and 15.4% (2/13, 95% CI 0.043-0.422) in the chemotherapy/chemoimmunotherapy group (P=0.286). Figure 2 illustrates the tumour response in a patient who received preoperative treatment with trastuzumab, pembrolizumab, and XELOX chemotherapy, and subsequently achieved a pathological TRG0.

By the last follow-up, the median follow-up time was 24.5 months in the trastuzumab-containing treatment group and 27.1 months in the chemotherapy/chemoimmunotherapy group. Ten patients (37.0%, 95% CI 0.215-0.558) in the trastuzumab-containing treatment group and six patients (46.2%, 95% CI 0.232-0.709) in the chemotherapy/chemoimmunotherapy group had reached EFS endpoints (Figure 3A). The median EFS time was 30.5 months in the trastuzumab-containing treatment group and 33.4 months in the chemotherapy/chemoimmunotherapy group, respectively (P=0.487), as shown in Figures 3B–D.

One patient with a surgical outcome of TRG1 underwent post-operative dynamic monitoring of minimal residual disease (MRD). The results indicated a relatively high risk of recurrence; however, after a follow-up period of 9.6 months, no evidence of recurrence was observed. A longer follow-up period is required to further assess this patient's survival outcome.

Safety and feasibility

Generally, preoperative treatment regimens containing trastuzumab plus chemotherapy or chemoimmunotherapy have shown a favourable safety profile. 18 patients (66.7%, 95% CI 0.478-0.814) in the trastuzumab-containing treatment group and eight patients (61.5%, 95% CI 0.355-0.823) in the chemotherapy/chemoimmunotherapy group experienced TRAEs of any grade, with anaemia and decreased neutrophil count being the most common. Other TRAEs observed in the patients were well tolerated and could be managed by symptomatic treatment. Table 3 shows the details of the preoperative TRAEs.

Discussion

The optimal treatment options for patients with potentially resectable HER2-positive GC have been under explorations. In patients with locally advanced HER2-positive breast cancer, the efficacy and safety of preoperative trastuzumab-based therapy have been confirmed in several randomized controlled trials (20–22). However, for patients with potentially resectable HER2-positive GC, whether the addition of trastuzumab with/without PD-1 blockade to preoperative chemotherapy has clinical benefits is not clear. In our current study, we observed that preoperative trastuzumab plus chemo(immuno)therapy as neoadjuvant or conversion therapy resulted in a TRG0/1 rate of 33.3% in patients with potentially resectable stage III-IV_B, HER2-positive GC, and this combination approach was well tolerated. Encouragingly, this combined regimen also showed promising outcomes in patients with baseline IV_B disease, with two patients achieving TRG0. Although the limited sample sizes made it difficult to show statistically significances, these results still indicated that preoperative trastuzumab-containing therapy can potentially benefit patients with potentially resectable HER2-positive GC.

According to the phase II NEOHX study (8) and HER-FLOT study (9), trastuzumab can be safely added to neoadjuvant chemotherapy, and this combination approach resulted in pCR rates ranging from 8.3% to 22.2% in patients with locally advanced

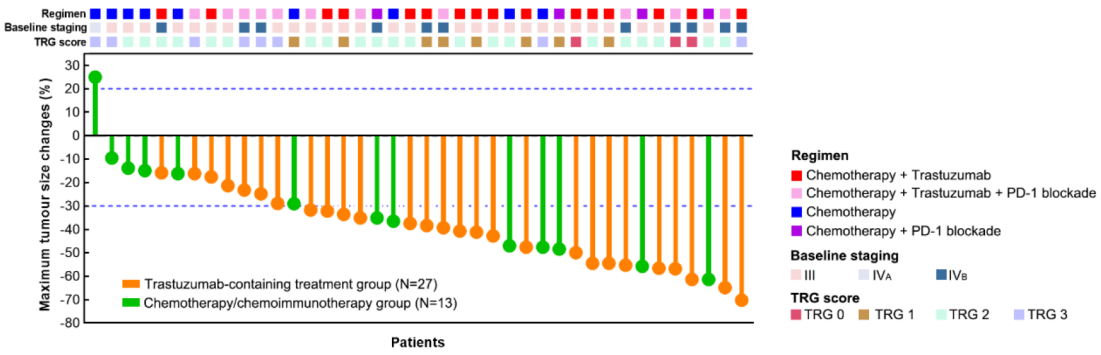

FIGURE 1
Assessments of best tumour responses to preoperative treatment based on RECIST and surgical outcomes of the patients.

10.3389/fimmu.2025.1624943

TABLE 2 Tumour responses and surgical outcomes.

Characteristics	Trastuzumab-containing treatment group (N=27)	Chemotherapy or chemoimmunotherapy group (N=13)	*P* value
Tumour responses (RECIST), n (%)			0.216
Partial response (PR)	20 (74.1)	7 (53.8)	
Stable disease (SD)	7 (25.9)	5 (38.5)	
Progressive disease (PD)	0	1 (7.7)	
Tumour regression grade (TRG), n (%)			0.564
TRG0	3 (11.1)	0	
TRG1	6 (22.2)	2 (15.4)	
TRG2	13 (48.2)	8 (61.5)	
TRG3	5 (18.5)	3 (23.1)	
Type of gastrectomy, n (%)			0.216
Proximal partial	2 (7.4)	2 (15.4)	
Distal partial	14 (51.9)	3 (23.1)	
Total	11 (40.7)	8 (61.5)	
Extent of resection, n (%)			-
R_0	27 (100.0)	13 (100.0)	
Lymph nodes, mean (range)			
Harvested	23.0 (5-44)	27.9 (13-43)	0.168
Involved	1.9 (0-15)	1.5 (0-9)	0.711
Lauren's classification, n (%)			0.627
Intestinal	5 (18.5)	4 (30.8)	
Diffused	3 (11.1)	2 (15.4)	
Mixed	10 (37.0)	5 (38.4)	
Unknown	9 (33.4)	2 (15.4)	
Post-operative PD-L1 expression, n (%)			0.858
CPS<1	1 (3.7)	0	
1≤CPS<5	6 (22.2)	3 (23.1)	
CPS≥5	10 (37.0)	6 (46.1)	
Unknown	10 (37.0)	4 (30.8)	

HER2-positive GC. In the randomized phase II JCOG1301C study, grade 1a/1b surgical efficacy was achieved in 50% of patients in the trastuzumab plus S-1/CDDP cohort (12) (Table 4). In our study, among the patients treated with preoperative trastuzumab plus chemotherapy, 12.5% (2/16) achieved TRG0 and 31.3% (5/16) achieved TRG1, with an overall TRG0/1 rate of 43.8% (7/16), consistent with the results in the above trials. In addition, the efficacy and safety of perioperative trastuzumab, PD-(L)1 blockade, and chemotherapy in patients with potentially resectable HER2-positive GC are being investigated in several ongoing phase II trials (10, 11, 23), and the pCR rates range from 31.3% to 42.9% according to the preliminary results, as shown in Table 4. In our study, the TRG0 rate was 9.1% (1/11) in patients receiving preoperative trastuzumab, PD-1 blockade, and chemotherapy, and the overall TRG0/1 rate of this cohort was 18.2% (2/11), which was inferior to that in the abovementioned studies, possibly owing to the relatively late stage and the limited sample size.

Given the heterogeneity in PD-L1 expression and MSI/MMR status among GC patients, it is crucial to consider these biomarkers when selecting optimal treatment strategies. In HER2-positive GC, the phase III KEYNOTE-811 trial demonstrated that patients in the CPS≥1 subgroup had significantly higher benefits of overall survival after treatment with pembrolizumab, trastuzumab and chemotherapy, while those in the CPS<1 subgroup hardly gained

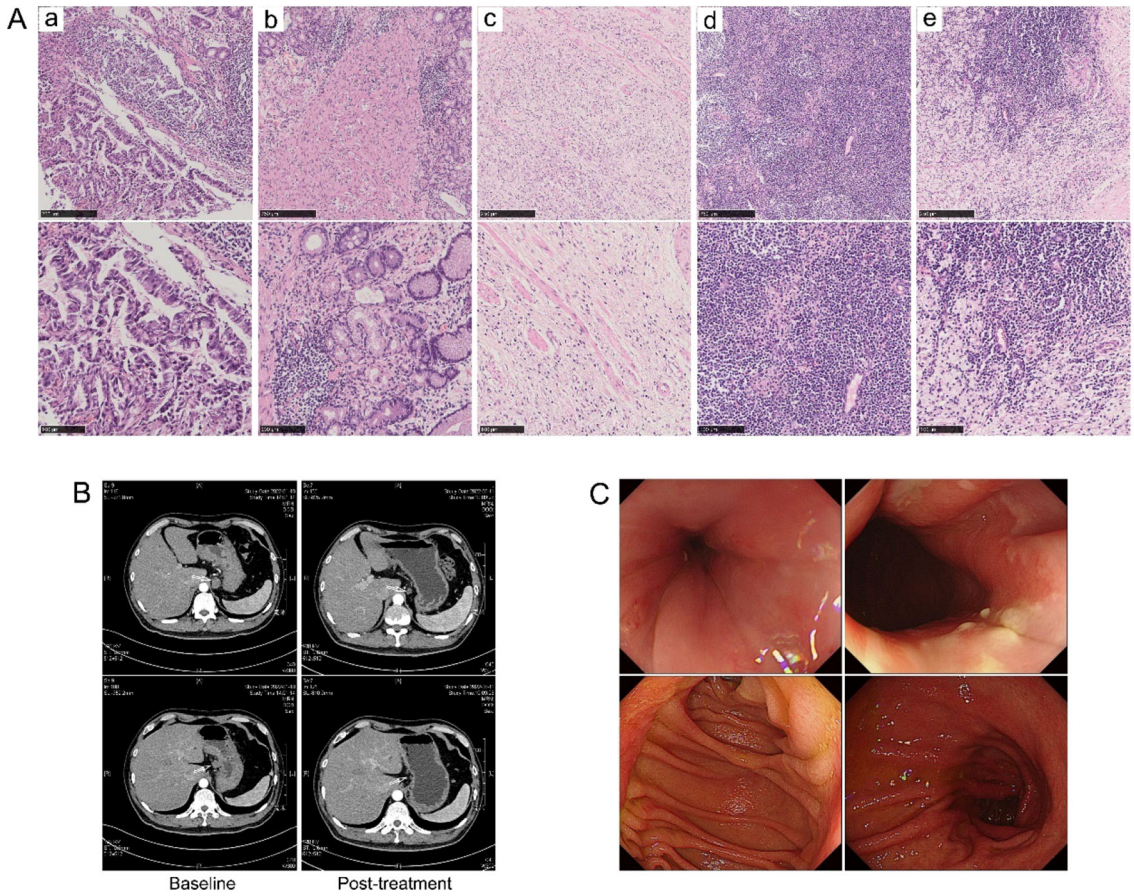

FIGURE 2
Tumour response in a patient who received preoperative treatment with trastuzumab, pembrolizumab, and XELOX chemotherapy, and subsequently achieved a pathological TRG0. **(A)** H&E staining images (a) at baseline and (b–e) post-operative. **(B)** Radiographical images at baseline and after preoperative treatment. **(C)** Gastroscopy images at 32 months post-surgery, with no evidence of recurrence observed.

clinical benefits (24), highlighting the differences in tumour immune microenvironment features between PD-L1 positive and negative patients. However, evidence regarding perioperative treatment for HER2-positive GC patients remains limited. Additionally, for GC patients with MSI-high or MMR deficiency, neoadjuvant treatment with ipilimumab plus nivolumab has been recommended (25); while the percentage of MSI-high or MMR deficiency status in HER2-positive GC is relatively low. In our study, among the 11 patients who received preoperative trastuzumab, PD-1 blockade and chemotherapy, both of the patients who achieved TRG0/1 had a CPS of 1. None of the patients were MSI-H or MMR deficiency status. The predictive role of the PD-L1 CPS and MSI/MMR in patients with potentially resectable HER2-positive GC still warrants further investigation.

In the neoadjuvant setting for patients with locally advanced HER2-positive breast cancer, postneoadjuvant treatment HER2 status conversion might predict the risk of relapse (26). However, the role of the loss of HER2 expression after preoperative treatment in HER2-positive GC patients remains unclear. In our study, four patients in the trastuzumab-containing treatment group exhibited loss of HER2 positivity after preoperative treatment. Their TRG scores were one case of TRG1 and TRG3, respectively, and two cases of TRG2; while none of them had experienced relapse by the last follow-up. Further studies are required to explore the roles and mechanisms of HER2 conversion after preoperative treatment in patients with HER2-positive GC.

HER2 amplification occurs in 23-38% of patients with hepatoid adenocarcinoma of the stomach (HAS) (27, 28). Mechanistic evidence indicates that PD-1 blockade-based immunotherapy might also be effective in patients with HAS (29). However, the optimal treatment options for patients with locally advanced HAS with concurrent HER2 amplification remain under debate. In our study, the patient with HAS developed immune-related hepatitis and myositis after one cycle of neoadjuvant PD-1 blockade plus chemotherapy, and consequently, he had to discontinue PD-1 blockade treatment. The TRG score of the patient was TRG2 after subsequent neoadjuvant treatment with trastuzumab and chemotherapy. This further indicates the importance of exploring the underlying mechanisms and optimizing treatment regimens for patients with locally advanced HAS and concurrent HER2 positivity.

RECIST has been widely applied in the evaluation of preoperative treatment efficacy in several solid tumours (15), but it seems inadequate for the evaluation of patients with potentially

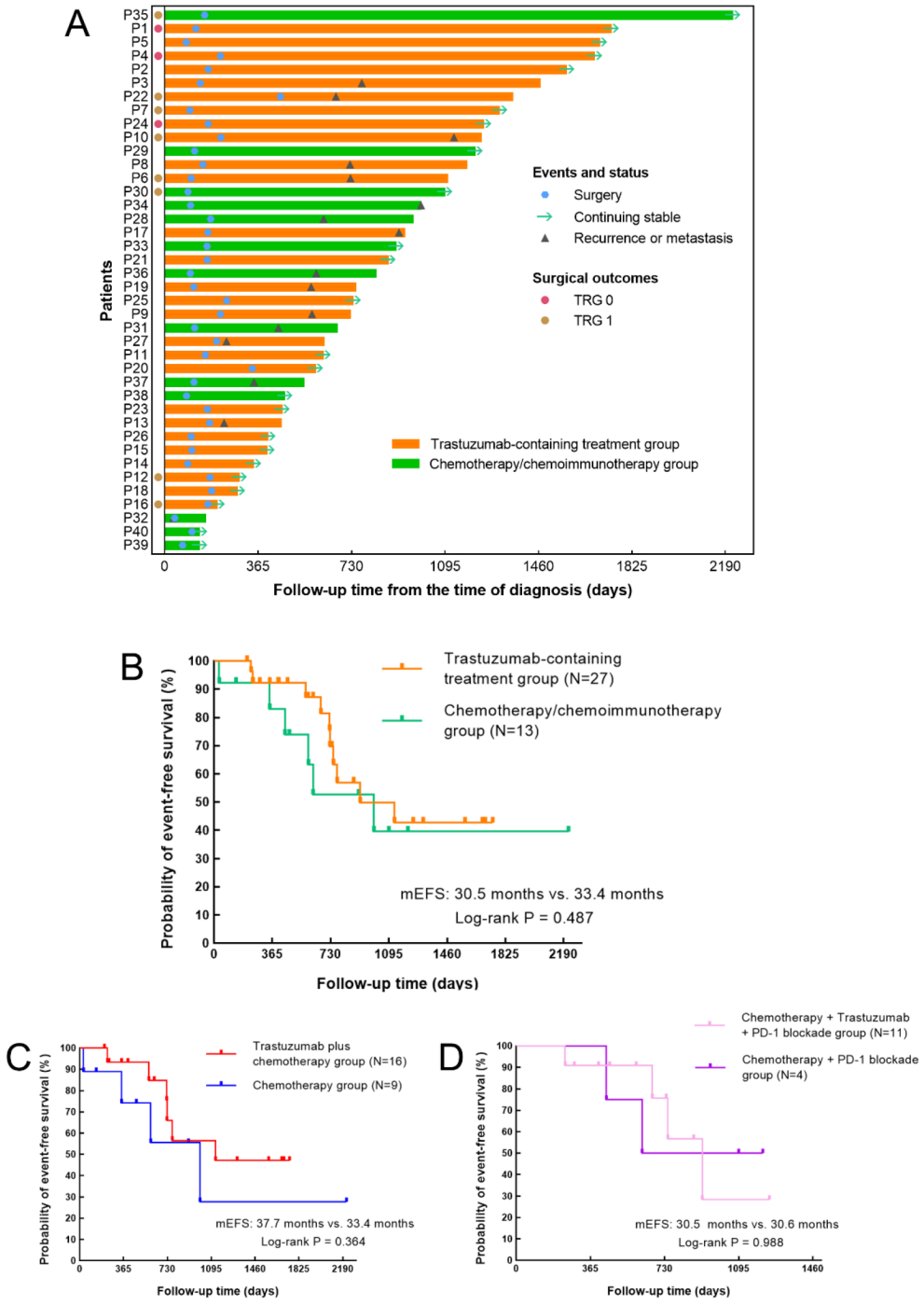

FIGURE 3
Treatment process and Kaplan–Meier curves for event-free survival (EFS). **(A)** Swimmer plot of the treatment process and follow-up of the patients from the time of diagnosis. **(B–D)** Kaplan–Meier curves for EFS **(B)** in patients receiving trastuzumab-containing treatment versus patients receiving chemo(immuno)therapy (*P*=0.487), **(C)** in patients receiving trastuzumab plus chemotherapy versus patients receiving chemotherapy alone (*P*=0.364), and **(D)** in patients receiving trastuzumab, PD-1 blockade and chemotherapy versus patients receiving PD-1 blockade plus chemotherapy (*P*=0.988).

resectable GC. The dissimilar assessments of RECIST and TRG (17) might lead to inconsistencies in radiological and pathological evaluations. In the current study, the results of radiographical tumour responses evaluated by RECIST and pathological tumour responses evaluated by TRG in some patients were inconsistent. With the emergence of Positron Emission Tomography (PET) Response Criteria in Solid Tumours (PERCIST) (30) and its applications in several recent studies of neoadjuvant immunotherapy (31, 32), the detection of tiny lesions and quantification of metabolic activity are gradually maturing. In

10.3389/fimmu.2025.1624943

TABLE 3 Preoperative treatment-related adverse events in the included patients.

TRAEs, n (%)	Trastuzumab-containing treatment group (N=27)		Chemotherapy or chemoimmunotherapy group (N=13)	
	Grade 1-2	Grade 3-4	Grade 1-2	Grade 3-4
Haematological system				
Neutrophil count decreased	6 (22.2)	7 (25.9)	3 (23.1)	1 (7.7)
Anaemia	9 (33.3)	2 (7.4)	2 (15.4)	2 (15.4)
Platelet count decreased	1 (3.7)	1 (3.7)	0	1 (7.7)
Digestive system				
Anorexia	1 (3.7)	0	1 (7.7)	0
Vomiting	3 (11.1)	0	1 (7.7)	0
Diarrhoea	1 (3.7)	0	0	0
Increased aminotransferase level	2 (7.4)	2 (7.4)	1 (7.7)	0
Skin				
Rash	1 (3.7)	0	0	0
Immune-related AEs				
Hepatitis	0	1 (3.7)	0	0
Myositis	0	1 (3.7)	0	0

TABLE 4 Summary of clinical trials focusing on perioperative treatment of trastuzumab plus chemotherapy with/without PD-1 blockade in patients with partially resectable, HER2-positive gastric cancer.

Clinical trial	Phase of trial	Regimen	Number of patients	R0 resection rates	pCR rates[†]	Incidences of grades 3 4 TRAEs
NEOHX study (8, 33)	Phase II	XELOX+ trastuzumab	36	77.8%	8.3%	33.3%
HER-FLOT study (9)	Phase II	FLOT+ trastuzumab	58	93.3%	22.2%	27.6%
JCOG1301C study (12)	Randomized, Phase II	Arm A: S-1/CDDP; Arm B: S-1/CDDP with trastuzumab	A: 22; B: 24	A: 91%; B: 92%	A: 23%; B: 50%[†] (P=0.072)	Unknown
NCT03950271 (2022 ASCO) (10)	Single-arm, Phase II	CAPOX+ SHR1210+ trastuzumab	22	100%	31.3%	22.7%
NCT04819971 (2023 ESMO) (11)	Single-arm, Phase II	DOS+ trastuzumab+ tislelizumab	12	100%	42.9%	8.3%
NCT04661150 (14)	Randomized, Phase II	Arm A: CAPOX+ trastuzumab with atezolizumab; Arm B: CAPOX + trastuzumab	A: 21; B: 21	Unknown	A: 38.1%; B: 14.3% (P=0.079)	A: 57.1%; B: 66.7%
AIO STO 0321 study (13)[‡]	Single-arm, Phase II	FLOT+ pembrolizumab+ trastuzumab	30 (estimated)	/	/	/
NCT05218148[‡]	Single-arm, Phase II	SOX+ trastuzumab+ sintilimab	44 (estimated)	/	/	/
NCT05715931[‡]	Single-arm, Phase II	FLOT+ trastuzumab+ toripalimab	30 (estimated)	/	/	/

CAPOX/XELOX, capecitabine and oxaliplatin; FLOT, 5-FU, leucovorin, oxaliplatin and docetaxel; DOS, Docetaxel, S-1 and oxaliplatin; SOX, S-1 and oxaliplatin; CDDP, cisplatin.
[†]In JCOG1301C trial, the results of pathological response were displayed as grade 1a/1b in accordance with Japanese classification.
[‡]These trials are still ongoing and have not disclosed related results.

addition, the detection of serum biomarkers may provide insights. Robust methods for evaluating the efficacy of these preoperative treatments in patients with potentially resectable GC are needed.

There are several limitations of this study. First, the nonrandomized design might lead to inevitable bias, and the relatively limited sample size could result in a lack of power. In addition, the follow-up time was not sufficient to obtain exhaustive survival outcomes. Finally, various agents were used for PD-1 blockade and for chemotherapy; thus, conclusions on the effectiveness of a certain regimen could not be drawn. More researches are needed to explore the optimal preoperative treatment strategies for patients with potentially resectable HER2-positive GC.

Conclusion

This study implied that trastuzumab could be safely added to preoperative chemo(immuno)therapy, and this regimen induced a TRG0/1 rate of 33.3% in patients with potentially resectable stage III to IV_B HER2-positive GC. Our findings should be further validated by the ongoing clinical trials.

Data availability statement

The raw data supporting the conclusions of this article will be made available by the authors, without undue reservation.

Ethics statement

The studies involving humans were approved by The Institutional Review Board of the Affiliated Hospital of Qingdao University (Approval No. QYFYWZLL28829). The studies were conducted in accordance with the Declaration of Helsinki, local legislation and institutional requirements. All subjects gave their informed consent for inclusion before they participated in the study.

Author contributions

XZ: Data curation, Formal Analysis, Writing – original draft. YT: Data curation, Formal Analysis, Writing – original draft. HW: Data curation, Formal Analysis, Writing – original draft. SS: Data curation, Formal Analysis, Writing – original draft. YC: Data curation, Writing – original draft. NL: Data curation, Funding acquisition, Writing – original draft. CZ: Data curation, Writing – original draft. XH: Data curation, Writing – original draft. HJ: Conceptualization, Data curation, Writing – review & editing. HH: Conceptualization, Data curation, Funding acquisition, Validation, Writing – review & editing.

Funding

The author(s) declare that financial support was received for the research and/or publication of this article. This study was supported by Special Funding for Qilu Sanitation and Health Leading Talents Cultivation Project (to Helei Hou) and Natural Science, Foundation of Shandong (ZR2020MH225 to NL).

Acknowledgments

We would love to show our sincere gratitude to the patients and their families for their kind support and cooperation.

Conflict of interest

The authors declare that the research was conducted in the absence of any commercial or financial relationships that could be construed as a potential conflict of interest.

Generative AI statement

The author(s) declare that no Generative AI was used in the creation of this manuscript.

Publisher's note

References

1. Bray F, Laversanne M, Sung H, Ferlay J, Siegel RL, Soerjomataram I, et al. Global cancer statistics 2022: GLOBOCAN estimates of incidence and mortality worldwide for 36 cancers in 185 countries. *CA Cancer J Clin*. (2024) 74:229–63. doi: 10.3322/caac.21834

2. Boku N. HER2-positive gastric cancer. *Gastric Cancer*. (2014) 17:1–12. doi: 10.1007/s10120-013-0252-z

3. Cunningham D, Allum WH, Stenning SP, Thompson JN, Van de Velde CJ, Nicolson M, et al. Perioperative chemotherapy versus surgery alone for resectable gastroesophageal cancer. *N Engl J Med*. (2006) 355:11–20. doi: 10.1056/NEJMoa055531

4. Shitara K, Rha SY, Wyrwicz LS, Oshima T, Karaseva N, Osipov M, et al. Neoadjuvant and adjuvant pembrolizumab plus chemotherapy in locally advanced gastric or gastro-oesophageal cancer (KEYNOTE-585): an interim analysis of the

multicentre, double-blind, randomised phase 3 study. *Lancet Oncol*. (2023) 25:212–24. doi: 10.1016/S1470-2045(23)00541-7

5. Janjigian YY, Al-Batran S-E, Wainberg ZA, Cutsem EV, Molena D, Muro K, et al. Pathological complete response (pCR) to 5-fluorouracil, leucovorin, oxaliplatin and docetaxel (FLOT) with or without durvalumab (D) in resectable gastric and gastroesophageal junction cancer (GC/GEJC): Subgroup analysis by region from the phase 3, randomized, double-blind MATTERHORN study. *J Clin Oncol*. (2024) 42: LBA246–6. doi: 10.1200/JCO.2024.42.3_suppl.LBA246

6. Bang YJ, Van Cutsem E, Feyereislova A, Chung HC, Shen L, Sawaki A, et al. Trastuzumab in combination with chemotherapy versus chemotherapy alone for treatment of HER2-positive advanced gastric or gastro-oesophageal junction cancer (ToGA): a phase 3, open-label, randomised controlled trial. *Lancet*. (2010) 376:687–97. doi: 10.1016/S0140-6736(10)61121-X

7. Janjigian YY, Kawazoe A, Bai Y, Xu J, Lonardi S, Metges JP, et al. Pembrolizumab plus trastuzumab and chemotherapy for HER2-positive gastric or gastro-oesophageal junction adenocarcinoma: interim analyses from the phase 3 KEYNOTE-811 randomised placebo-controlled trial. *Lancet*. (2023) 402:2197–208. doi: 10.1016/S0140-6736(23)02033-0

8. Rivera F, Izquierdo-Manuel M, Garcia-Alfonso P, Martinez de Castro E, Gallego J, Limon ML, et al. Perioperative trastuzumab, capecitabine and oxaliplatin in patients with HER2-positive resectable gastric or gastro-oesophageal junction adenocarcinoma: NEOHX phase II trial. *Eur J Cancer*. (2021) 145:158–67. doi: 10.1016/j.ejca.2020.12.005

9. Hofheinz R, Hegewisch-Becker S, Thuss-Patience PC, Kunzmann V, Fuchs M, Graeven U, et al. HER-FLOT: Trastuzumab in combination with FLOT as perioperative treatment for patients with HER2-positive locally advanced esophagogastric adenocarcinoma: A phase II trial of the AIO Gastric Cancer Study Group. *J Clin Oncol*. (2014) 32:4073–3. doi: 10.1200/jco.2014.32.15_suppl.4073

10. Li N, Li Z, Fu Q, Zhang B, Zhang J, Wan X, et al. Phase II study of SHR1210 and trastuzumab in combination with CAPOX for neoadjuvant treatment of HER2-positive gastric or gastroesophageal junction (GEJ) adenocarcinoma. *J Clin Oncol*. (2022) 40:296–6. doi: 10.1200/JCO.2022.40.4_suppl.296

11. Zhao C, Meng X, Shan Z, Jiang J, Liu X, Li H, et al. Efficacy and safety of perioperative chemotherapy combined with tislelizumab and trastuzumab for HER2-positive resectable gastric/gastroesophageal junction cancer (GC/EGJC): Preliminary results of a phase 2, single-arm trial. *J Clin Oncol*. (2023) 41:e16084–4. doi: 10.1200/JCO.2023.41.16_suppl.e16084

12. Tokunaga M, Machida N, Mizusawa J, Ito S, Yabusaki H, Hirao M, et al. Early endpoints of a randomized phase II trial of preoperative chemotherapy with S-1/CDDP with or without trastuzumab followed by surgery for HER2-positive resectable gastric or esophagogastric junction adenocarcinoma with extensive lymph node metastasis: Japan Clinical Oncology Group study JCOG1301C (Trigger Study). *Gastric Cancer*. (2024) 27:580–9. doi: 10.1007/s10120-024-01467-9

13. Tintelnot J, Stein A, Al-Batran SE, Ettrich T, Gotze T, Grun B, et al. Pembrolizumab and trastuzumab in combination with FLOT in the perioperative treatment of HER2-positive, localized esophagogastric adenocarcinoma-a phase II trial of the AIO study group (AIO STO 0321). *Front Oncol*. (2023) 13:1272175. doi: 10.3389/fonc.2023.1272175

14. Peng Z, Zhang X, Liang H, Zheng Z, Wang Z, Liu H, et al. Atezolizumab and trastuzumab plus chemotherapy for ERBB2-positive locally advanced resectable gastric cancer: A randomized clinical trial. *JAMA Oncol*. (2025) 11:619–24. doi: 10.1001/jamaoncol.2025.0522

15. Eisenhauer EA, Therasse P, Bogaerts J, Schwartz LH, Sargent D, Ford R, et al. New response evaluation criteria in solid tumours: revised RECIST guideline (version 1.1). *Eur J Cancer*. (2009) 45:228–47. doi: 10.1016/j.ejca.2008.10.026

16. Ikoma N, Blum M, Estrella JS, Das P, Hofstetter WL, Fournier KF, et al. Evaluation of the American Joint Committee on Cancer 8th edition staging system for gastric cancer patients after preoperative therapy. *Gastric Cancer*. (2018) 21:74–83. doi: 10.1007/s10120-017-0743-4

17. Ikoma N, Estrella JS, Blum Murphy M, Das P, Minsky BD, Mansfield P, et al. Tumor regression grade in gastric cancer after preoperative therapy. *J Gastrointest Surg*. (2021) 25:1380–7. doi: 10.1007/s11605-020-04688-2

18. Wolff AC, Hammond MEH, Allison KH, Harvey BE, Mangu PB, Bartlett JMS, et al. Human epidermal growth factor receptor 2 testing in breast cancer: American society of clinical oncology/college of American pathologists clinical practice guideline focused update. *J Clin Oncol*. (2018) 36:2105–22. doi: 10.1200/JCO.2018.77.8738

19. Cancer Genome Atlas Research N. Comprehensive molecular characterization of gastric adenocarcinoma. *Nature*. (2014) 513:202–9. doi: 10.1038/nature13480

20. Shao Z, Pang D, Yang H, Li W, Wang S, Cui S, et al. Efficacy, safety, and tolerability of pertuzumab, trastuzumab, and docetaxel for patients with early or locally advanced ERBB2-positive breast cancer in Asia: the PEONY phase 3 randomized clinical trial. *JAMA Oncol*. (2020) 6:e193692. doi: 10.1001/jamaoncol.2019.3692

21. Gianni L, Pienkowski T, Im YH, Roman L, Tseng LM, Liu MC, et al. Efficacy and safety of neoadjuvant pertuzumab and trastuzumab in women with locally advanced, inflammatory, or early HER2-positive breast cancer (NeoSphere): a randomised multicentre, open-label, phase 2 trial. *Lancet Oncol*. (2012) 13:25–32. doi: 10.1016/S1470-2045(11)70336-9

22. Gianni L, Eiermann W, Semiglazov V, Manikhas A, Lluch A, Tjulandin S, et al. Neoadjuvant chemotherapy with trastuzumab followed by adjuvant trastuzumab versus neoadjuvant chemotherapy alone, in patients with HER2-positive locally advanced breast cancer (the NOAH trial): a randomised controlled superiority trial with a parallel HER2-negative cohort. *Lancet*. (2010) 375:377–84. doi: 10.1016/S0140-6736(09)61964-4

23. Peng Z, Zhang X, Liang H, Zheng Z, Wang Z, Liu H, et al. Atezolizumab and trastuzumab plus chemotherapy in patients with HER2+ locally advanced resectable gastric cancer or adenocarcinoma of the gastroesophageal junction: A multicenter, randomized, open-label phase II study. *J Clin Oncol*. (2024) 42:312–2. doi: 10.1200/JCO.2024.42.3_suppl.312

24. Janjigian YY, Kawazoe A, Bai Y, Xu J, Lonardi S, Metges JP, et al. 1400O Final overall survival for the phase III, KEYNOTE-811 study of pembrolizumab plus trastuzumab and chemotherapy for HER2+ advanced, unresectable or metastatic G/GEJ adenocarcinoma. *Ann Oncol*. (2024) 35:S877–8. doi: 10.1016/j.annonc.2024.08.1466

25. Andre T, Tougeron D, Piessen G, de la Fouchardiere C, Louvet C, Adenis A, et al. Neoadjuvant nivolumab plus ipilimumab and adjuvant nivolumab in localized deficient mismatch repair/microsatellite instability-high gastric or esophagogastric junction adenocarcinoma: the GERCOR NEONIPIGA phase II study. *J Clin Oncol*. (2023) 41:255–65. doi: 10.1200/JCO.22.00686

26. Guarneri V, Dieci MV, Barbieri E, Piacentini F, Omarini C, Ficarra G, et al. Loss of HER2 positivity and prognosis after neoadjuvant therapy in HER2-positive breast cancer patients. *Ann Oncol*. (2013) 24:2990–4. doi: 10.1093/annonc/mdt364

27. Zhou K, Wang A, Wei J, Ji K, Li Z, Ji X, et al. The value of perioperative chemotherapy for patients with hepatoid adenocarcinoma of the stomach undergoing radical gastrectomy. *Front Oncol*. (2021) 11:789104. doi: 10.3389/fonc.2021.789104

28. Akazawa Y, Saito T, Hayashi T, Yanai Y, Tsuyama S, Akaike K, et al. Next-generation sequencing analysis for gastric adenocarcinoma with enteroblastic differentiation: emphasis on the relationship with hepatoid adenocarcinoma. *Hum Pathol*. (2018) 78:79–88. doi: 10.1016/j.humpath.2018.04.022

29. Liu Z, Wang A, Pu Y, Li Z, Xue R, Zhang C, et al. Genomic and transcriptomic profiling of hepatoid adenocarcinoma of the stomach. *Oncogene*. (2021) 40:5705–17. doi: 10.1038/s41388-021-01976-2

30. Wahl RL, Jacene H, Kasamon Y, Lodge MA. From RECIST to PERCIST: Evolving Considerations for PET response criteria in solid tumors. *J Nucl Med*. (2009) 50 Suppl 1:122S–50S. doi: 10.2967/jnumed.108.057307

31. Gao S, Li N, Gao S, Xue Q, Ying J, Wang S, et al. Neoadjuvant PD-1 inhibitor (Sintilimab) in NSCLC. *J Thorac Oncol*. (2020) 15:816–26. doi: 10.1016/j.jtho.2020.01.017

32. Jiang H, Yu X, Li N, Kong M, Ma Z, Zhou D, et al. Efficacy and safety of neoadjuvant sintilimab, oxaliplatin and capecitabine in patients with locally advanced, resectable gastric or gastroesophageal junction adenocarcinoma: early results of a phase 2 study. *J Immunother Cancer*. (2022) 10:e003635. doi: 10.1136/jitc-2021-003635

33. Rivera F, Jiménez-Fonseca P, Alfonso PG, Gallego J, Limon ML, Alsina M, et al. NEOHX study: Perioperative treatment with trastuzumab in combination with capecitabine and oxaliplatin (XELOX-T) in patients with HER-2 resectable stomach or esophagogastric junction (EGJ) adenocarcinoma—18 m DFS analysis. *J Clin Oncol*. (2015) 33:107–7. doi: 10.1200/jco.2015.33.3_suppl.107

frontiers | Frontiers in Immunology

TYPE Case Report
PUBLISHED 18 July 2025
DOI 10.3389/fimmu.2025.1611281

OPEN ACCESS

EDITED BY
Stavros P. Papadakos,
Laiko General Hospital of Athens, Greece

REVIEWED BY
Yuan Tian,
Affiliated Hospital of Shandong University of Traditional Chinese Medicine, China
Tao Li,
People's Liberation Army General Hospital, China
Hesong Wang,
Fourth Hospital of Hebei Medical University, China

*CORRESPONDENCE
Xian-Wen Liang
lxwzndx@163.com
Xiong-hui He
hxh7582@163.com
Ke-jian Zou
zoukejian188@163.com

†These authors share first authorship

RECEIVED 14 April 2025
ACCEPTED 30 June 2025
PUBLISHED 18 July 2025

CITATION
Sun Y-h, Ma Y, Chen L, Li H-r, Liang X-W, He X-h and Zou K-j (2025) Case Report: Pathological complete response achieved with neoadjuvant immunochemotherapy in synchronous multiple gastric adenocarcinoma. *Front. Immunol.* 16:1611281. doi: 10.3389/fimmu.2025.1611281

Case Report: Pathological complete response achieved with neoadjuvant immunochemotherapy in synchronous multiple gastric adenocarcinoma

Ya-hui Sun[1†], Yan Ma[1†], Liang Chen[2], Hai-rong Li[3], Xian-Wen Liang[1*], Xiong-hui He[1*] and Ke-jian Zou[1*]

[1]Department of Gastrointestinal Surgery, Hainan General Hospital (Hainan Affiliated Hospital of Hainan Medical University), Haikou, China, [2]Department of Hepatobiliary and Pancreatic Surgery, Hainan General Hospital (Hainan Affiliated Hospital of Hainan Medical University), Haikou, China, [3]Department of Pathology, Hainan General Hospital (Hainan Affiliated Hospital of Hainan Medical University), Haikou, China

Synchronous multiple gastric cancers (SMGC) represent a rare clinical entity with no established treatment guidelines. We report a 76-year-old female with two synchronous poorly differentiated adenocarcinomas (dMMR/MSI-H phenotype) in the gastric lesser curvature, clinically staged as cT4bN2M0. Following three cycles of neoadjuvant immunochemotherapy, the patient demonstrated remarkable tumor regression (RECIST 1.1 partial response) and subsequently underwent R0 distal gastrectomy. Histopathological examination confirmed a pathological complete response (ypT0N0, TRG 0).To our knowledge, this represents the first documented case of SMGC achieving pCR with neoadjuvant immunochemotherapy. Our findings suggest that PD-1 inhibition combined with chemotherapy may induce profound tumor regression in SMGC, even in cases with high tumor burden, potentially converting unresectable to resectable disease. This case provides compelling evidence for incorporating immunotherapy in SMGC management and warrants further investigation through clinical trials.

KEYWORDS

SMGC, neoadjuvant immunochemotherapy, pathological complete response, immune checkpoint inhibitors, microsatellite instability

Background

Synchronous multiple gastric cancer (SMGC), defined as ≥2 distinct primary gastric malignancies occurring simultaneously (1), accounting for 6%–14% of all gastric cancer cases (2). The pathogenesis involves complex interactions between field cancerization, tumor microenvironment heterogeneity, and genetic predisposition (3–5). Current treatment paradigms extrapolate from solitary gastric cancer protocols, despite evidence suggesting SMGC exhibits more aggressive biology and poorer chemotherapy responses (6, 7).

The advent of immune checkpoint inhibitors (ICIs) has revolutionized management of microsatellite instability-high (MSI-H) gastrointestinal malignancies. While recent trials demonstrate promising efficacy of neoadjuvant immunochemotherapy in gastric cancer (8), SMGC-specific data remains absent due to routine exclusion from clinical studies. This knowledge gap is particularly significant given potential inter-lesional heterogeneity in treatment response.

We present the first documented case of SMGC achieving pathological complete response (pCR) following neoadjuvant PD-1 inhibition combined with chemotherapy, providing critical insights into the management of this challenging clinical scenario.

Case presentation

A 76-year-old female with 12 months of intermittent epigastric pain with well-controlled type 2 diabetes presented and 10 kg unintentional weight loss. No family history of malignancy was reported.

Diagnostic evaluation

Endoscopy

Extensive mucosal ulceration was observed in the lesser curvature to the antrum, with two irregularly elevated ulcerative lesions (Figure 1).

Histopathology

Both lesions demonstrated poorly differentiated adenocarcinoma (Lauren's diffuse type) with identical immunohistochemical profiles: MSH2(+), MSH6(+), MLH1(-), PMS2(-), HER2 (1+), Claudin18.2(-) (Figure 2).

Radiological staging (CT)

Gastric wall thickening in the lesser curvature with pancreatic invasion, multiple enlarged lymph nodes (maximum: 4.1 cm × 2.7 cm) and no distant metastases. Final clinical stage: cT4bN2M0 (AJCC 8th ed. stage IVA) (Figures 3A-C).

Multidisciplinary decision-making

A multidisciplinary team (MDT) determined that R0 resection was unlikely due to pancreatic involvement and confluent lymph node metastases. The patient received neoadjuvant therapy with SOX (Oxaliplatin + tegafur/gimeracil/octeracil (S-1)) combined with tislelizumab (200 mg on day 1), every 3 weeks, for three cycles, with no significant adverse effects.

Therapeutic response

Post-treatment CT demonstrated significantly reduction in primary lesions and lymph node (Figures 3D-F).

Surgical intervention

Laparoscopic distal gastrectomy with D2 lymphadenectomy (R0) was performed. Intraoperative findings revealed Two fibrotic ulcer beds (1.7cm×2.4 cm; 3.8cm×2.1 cm) with significant post-treatment scarring (Figure 4).

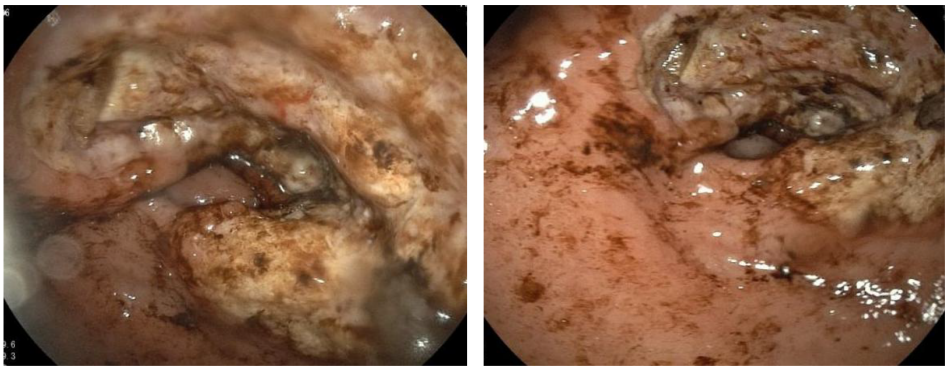

FIGURE 1
Extensive mucosal ulceration from the lesser curvature of the fundus to the gastric antrum was observed by gastroscopy.

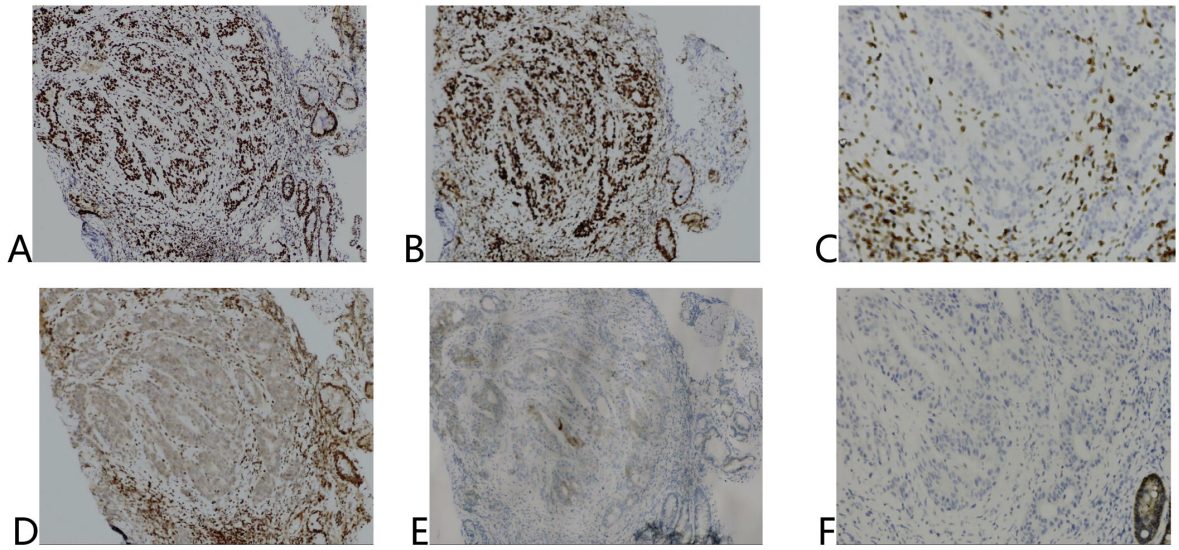

FIGURE 2
Immunohistochemical results of tumor tissue before treatment. **(A)** MSH2 (+), **(B)** MSH6 (+), **(C)** MLH1 (-), **(D)** PMS2 (-), **(E)** HER2 (1+), **(F)** Claudin18.2 (-).

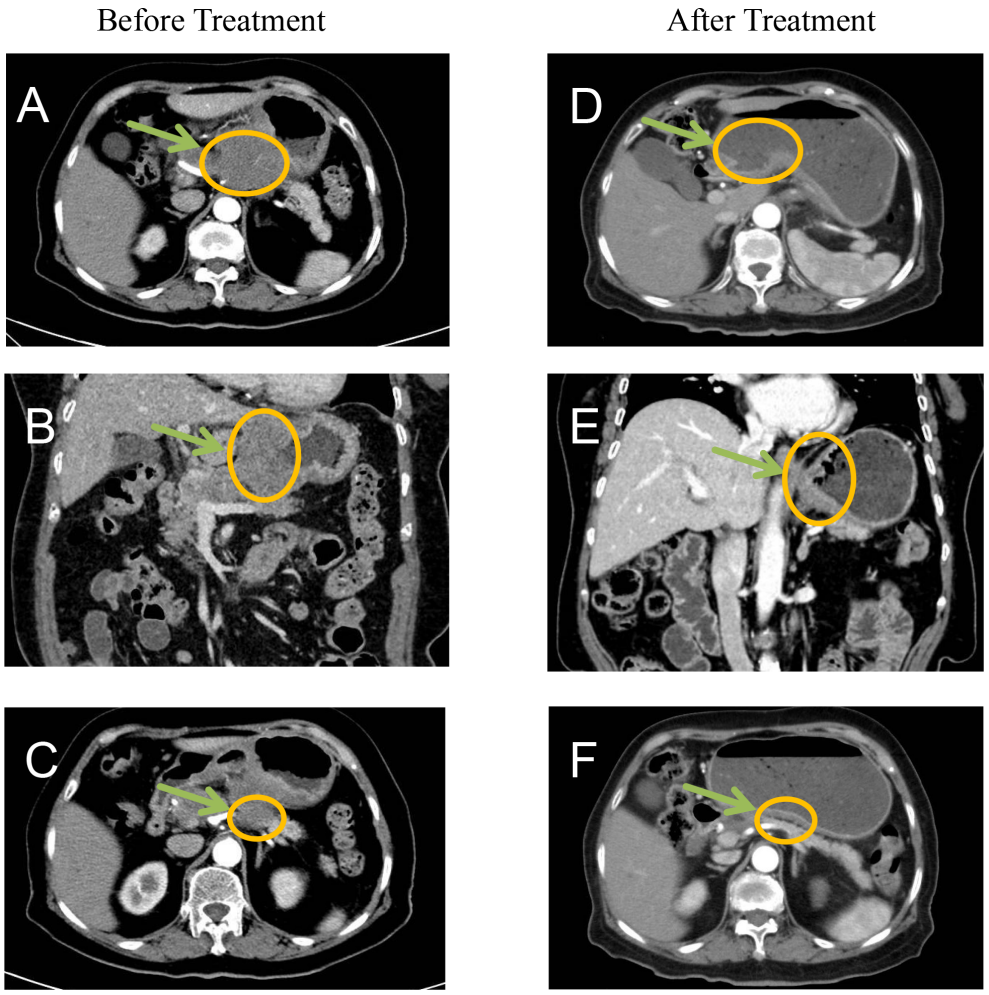

FIGURE 3
Before treatment CT imaging demonstrated: **(A, B)** Marked thickening and nodularity along the gastric curvature with contrast enhancement, showing poorly defined margins between the stomach and pancreas. **(C)** Significant enlargement of lesser curvature lymph nodes. After treatment imaging revealed: **(D-F)** Substantial reduction in both the primary tumor mass and associated lymphadenopathy, indicating favorable treatment response.

Pathological evaluation

No residual cancer cells were detected in the ulcers or lymph nodes (ypT0N0). Tumor regression grade (TRG): 0 (Ryan criteria) (Figure 5).

Discussion

Comprehensive genomic profiling has established gastric cancer as a molecularly heterogeneous disease comprising distinct subtypes, each exhibiting unique molecular characteristics and clinical behaviors. Per the Cancer Genome Atlas (TCGA) classification system, gastric cancer can be categorized into four molecular subtypes: microsatellite instability (MSI), chromosomal instability (CIN), Epstein-Barr virus (EBV)-positive, and genomically stable (GS) tumors (9, 10). Of these, the MSI subtype has emerged as a particularly noteworthy entity.

Microsatellites (MS), defined as short, repetitive DNA sequences ubiquitously distributed throughout the human genome, are highly prone to replication errors (11). The DNA mismatch repair (MMR) system serves as the primary mechanism for detecting and correcting such errors. Consequently, genetic or epigenetic alterations in MMR genes may compromise MMR function (dMMR), thereby inducing a high microsatellite instability (MSI-H) phenotype. This molecular signature is associated with genomic instability and an increased tumor mutational burden (12–14).

The advent of immune checkpoint inhibitors (ICIs) targeting programmed death-1 (PD-1) and programmed cell death ligand 1 (PD-L1) has revolutionized cancer treatment paradigms (9). Accumulating evidence has demonstrated a strong association between MSI status and ICI efficacy, and more and more studies have begun to pay attention to the effect of ICIs in neoadjuvant therapy for gastric cancer (15, 16).

Notably, the recently published NEOSUMMIT-01 trial reported a pathological complete response (pCR) rate of 22.2% in locally advanced gastric cancer patients receiving neoadjuvant immunochemotherapy (the PD-1 inhibitor tislelizumab plus SOX regimen), representing a significant improvement over chemotherapy alone (7.4%) (8). However, this study specifically excluded patients with SMGC, leaving the efficacy of immunotherapy in this population unexplored.

To our knowledge, this represents the first documented case of SMGC achieving pCR following neoadjuvant immunochemotherapy. Notably, despite presenting with extensive lymph node metastasis at diagnosis, postoperative pathological examination revealed complete tumor regression, suggesting that immunotherapy may eradicate micrometastases through systemic immune activation. Intraoperative findings demonstrated significant fibrosis along the lesser curvature, potentially attributable to immunotherapy-induced fibroblast activation and collagen deposition. While these changes may obscure surgical planes and increase procedural complexity, they are

FIGURE 4
Surgically removed specimens showed two ulcers in the lesser curvature of the stomach and significant receding scars after neoadjuvant therapy.

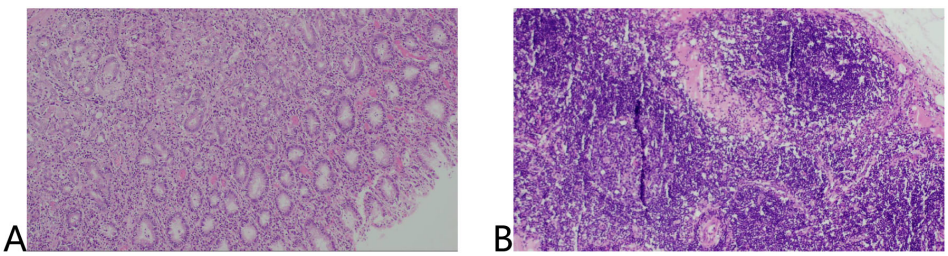

FIGURE 5
HE staining of surgical specimens including tumor tissue **(A)** and lymph nodes **(B)**.

considered favorable prognostic indicators. Furthermore, current evidence indicates that cancer stage, rather than lesion multiplicity, serves as the primary determinant of SMGC prognosis (17).

In the present case, the achieved pathological pCR following immunotherapy may be associated with multiple factors including systemic immune activation, elevated tumor mutational burden (TMB), MSI-H status, and dynamic tumor microenvironment remodeling. Moreover, the establishment of immunological memory might facilitate eradication of minimal residual disease and potentially mitigate recurrence risk.

Extensive research has been conducted on laparoscopic gastrectomy following neoadjuvant chemotherapy for gastric cancer. Although neoadjuvant chemotherapy induces significant tissue edema and fibrosis, increasing surgical complexity, advancements in surgical instrumentation (e.g., ultrasonic dissectors) and refined operative techniques have substantially minimized iatrogenic damage to normal tissues (18). The safety and feasibility of this approach have been robustly validated in multiple clinical studies.

Data availability statement

The original contributions presented in the study are included in the article/Supplementary Material. Further inquiries can be directed to the corresponding authors.

Ethics statement

The studies involving humans were approved by Ethics Committee of Hainan General Hospital. The studies were conducted in accordance with the local legislation and institutional requirements. The human samples used in this study were acquired from primarily isolated as part of your previous study for which ethical approval was obtained. Written informed consent for participation was not required from the participants or the participants' legal guardians/next of kin in accordance with the national legislation and institutional requirements. Written informed consent was obtained from the individual(s) for the publication of any potentially identifiable images or data included in this article.

Author contributions

Y-HS: Writing – original draft, Writing – review & editing. LC: Writing – original draft. H-RL: Data curation, Writing – review & editing. YM: Data curation, Writing – review & editing. X-WL: Data curation, Writing – review & editing. X-HH: Supervision, Writing – review & editing. K-JZ: Supervision, Writing – review & editing.

Funding

The author(s) declare that financial support was received for the research and/or publication of this article. This study was Supported by Joint Program on Health Science & Technology Innovation of Hainan Province, No. WSJK2024MS236.

Conflict of interest

The authors declare that the research was conducted in the absence of any commercial or financial relationships that could be construed as a potential conflict of interest.

Generative AI statement

The author(s) declare that no Generative AI was used in the creation of this manuscript.

Publisher's note

Supplementary material

The Supplementary Material for this article can be found online at: https://www.frontiersin.org/articles/10.3389/fimmu.2025.1611281/full#supplementary-material

References

1. Kanaya N, van Schaik TA, Aoki H, Sato Y, Taniguchi F, Shigeyasu K, et al. High risk of multiple gastric cancers in Japanese individuals with Lynch syndrome. *Ann Gastroenterol Surg.* (2024) 8:1008–16. doi: 10.1002/ags3.12809

2. Lee HJ, Lee YJ, Lee JY, Kim ES, Chung WJ, Jang BK, et al. Characteristics of synchronous and metachronous multiple gastric tumors after endoscopic submucosal dissection of early gastric neoplasm. *Clin Endosc.* (2018) 51:266–73. doi: 10.5946/ce.2017.109

3. Yoon JH, Choi BJ, Nam SW, Park WS. Gastric cancer exosomes contribute to the field cancerization of gastric epithelial cells surrounding gastric cancer. *Gastric Cancer.* (2022) 25:490–502. doi: 10.1007/s10120-021-01269-3

4. Balkwill FR, Capasso M, Hagemann T. The tumor microenvironment at a glance. *J Cell Sci.* (2012) 125:5591–6. doi: 10.1242/jcs.116392

5. Baghban R, Roshangar L, Jahanban-Esfahlan R, Seidi K, Ebrahimi-Kalan A, Jaymand M, et al. Tumor microenvironment complexity and therapeutic implications at a glance. *Cell Commun Signal.* (2020) 18:59. doi: 10.1186/s12964-020-0530-4

6. Isobe T, Hashimoto K, Kizaki J, Murakami N, Aoyagi K, Koufuji K, et al. Characteristics and prognosis of synchronous multiple early gastric cancer. *World J Gastroenterol.* (2013) 19:7154–9. doi: 10.3748/wjg.v19.i41.7154

7. Kim JH, Jeong SH, Yeo J, Lee WK, Chung DH, Kim KO, et al. Clinicopathologic similarities of the main and minor lesions of synchronous multiple early gastric cancer. *J Korean Med Sci*. (2016) 31:873–8. doi: 10.3346/jkms.2016.31.6.873

8. Yuan SQ, Nie RC, Jin Y, Liang CC, Li YF, Jian R, et al. Perioperative toripalimab and chemotherapy in locally advanced gastric or gastro-esophageal junction cancer: a randomized phase 2 trial. *Nat Med*. (2024) 30:552–9. doi: 10.1038/s41591-023-02721-w

9. Ooki A, Shinozaki E, Yamaguchi K. Immunotherapy in colorectal cancer: current and future strategies. *J Anus Rectum Colon*. (2021) 5:11–24. doi: 10.23922/jarc.2020-064

10. Ooki A, Osumi H, Yoshino K, Yamaguchi. Potent therapeutic strategy in gastric cancer with microsatellite instability-high and/or deficient mismatch repair. *Gastric Cancer*. (2024) 27:907–31. doi: 10.1007/s10120-024-01523-4

11. Liu B, Shen C, Yin X, Jiang T, Han Y, Yuan R, et al. Perioperative chemotherapy for gastric cancer patients with microsatellite instability or deficient mismatch repair: A systematic review and meta-analysis. *Cancer*. (2025) 131:e35831. doi: 10.1002/cncr.v131.7

12. Wang CW, Muzakky H, Lee YC, Chung YP, Wang YC, Yu MH, et al. Interpretable multi-stage attention network to predict cancer subtype, microsatellite instability, TP53 mutation and TMB of endometrial and colorectal cancer. *Comput Med Imaging Graph*. (2025) 121:102499. doi: 10.1016/j.compmedimag.2025.102499

13. Liao Y, Yang R, Wang B, Ruan Y, Cui L, Yang J, et al. Mevalonate kinase inhibits anti-tumor immunity by impairing the tumor cell-intrinsic interferon response in microsatellite instability colorectal cancer. *Oncogene*. (2025) 44:944–57. doi: 10.1038/s41388-024-03255-2

14. Tsilimigras DI, Kurzrock R, Pawlik TM. Molecular testing and targeted therapies in hepatobiliary cancers: A review. *JAMA Surg*. (2025) 160:576–585. doi: 10.1001/jamasurg.2025.0242

15. Le DT, Diaz LJ, Kim TW, Van Cutsem E, Geva R, Jager D, et al. Pembrolizumab for previously treated, microsatellite instability-high/mismatch repair-deficient advanced colorectal cancer: final analysis of KEYNOTE-164. *Eur J Cancer*. (2023) 186:185–95. doi: 10.1016/j.ejca.2023.02.016

16. Lordick F, Rha SY, Muro K, Yong WP, Lordick OR. Systemic therapy of gastric cancer-state of the art and future perspectives. *Cancers (Basel)*. (2024) 16:3337. doi: 10.3390/cancers16193337

17. Song DH, Kim N, Jo HH, Kim S, Choi Y, Oh HJ, et al. Analysis of characteristics and risk factors of patients with single gastric cancer and synchronous multiple gastric cancer among 14,603 patients. *Gut Liver*. (2024) 18:231–44. doi: 10.5009/gnl220491

18. Liao XL, Liang XW, Pang HY, Yang K, Chen XZ, Chen XL, et al. Safety and efficacy of laparoscopic versus open gastrectomy in patients with advanced gastric cancer following neoadjuvant chemotherapy: A meta-analysis. *Front Oncol*. (2021) 11:704244. doi: 10.3389/fonc.2021.704244

frontiers | Frontiers in Immunology

TYPE Original Research
PUBLISHED 27 August 2025
DOI 10.3389/fimmu.2025.1609352

OPEN ACCESS

EDITED BY
Qiang Cao,
Kunming University of Science and Technology, China

REVIEWED BY
André Mauricio De Oliveira,
Federal Center for Technological Education of Minas Gerais, Brazil
Dr. Kratika Singh,
Centre of Bio-Medical Research (CBMR), India
Liangjing Xia,
Panzhihua Central Hospital, China

*CORRESPONDENCE
Zhengwei Leng
lengzhengwei@scszlyy.org.cn
Xiaolun Huang
huangxiaolun@med.uestc.edu.cn

†These authors have contributed equally to this work

RECEIVED 10 April 2025
ACCEPTED 11 August 2025
PUBLISHED 27 August 2025

CITATION
Liang Y, Wang M, Zhong D, Yan H, Su Y, Chen X, Huang X and Leng Z (2025) Efficacy and safety of postoperative adjuvant HAIC combining lenvatinib with or without PD-1 inhibitors in solitary large HCC: A multicenter retrospective study. *Front. Immunol.* 16:1609352. doi: 10.3389/fimmu.2025.1609352

Efficacy and safety of postoperative adjuvant HAIC combining lenvatinib with or without PD-1 inhibitors in solitary large HCC: A multicenter retrospective study

Yuxin Liang[1,2†], Ming Wang[1†], Deyuan Zhong[1,2], Hongtao Yan[1], Yuhao Su[1], Xing Chen[3], Xiaolun Huang[1*] and Zhengwei Leng[1,4*]

[1]Department of Liver Transplantation Center and HBP Surgery, Sichuan Clinical Research Center for Cancer, Sichuan Cancer Hospital and Institute, Sichuan Cancer Center, School of Medicine, University of Electronic Science and Technology of China, Chengdu, China, [2]Department of Hepatobiliary-Pancreatic Surgery, Cell Transplantation Center, Sichuan Provincial People's Hospital, University of Electronic Science and Technology of China, Chengdu, China, [3]State Key Laboratory of Quality Research in Chinese Medicine, Macau Institute for Applied Research in Medicine and Health, Macau University of Science and Technology, Taipa, Macao, Macao SAR, China, [4]Department of Hepatobiliary Surgery II, Affiliated Hospital of North Sichuan Medical College, Nanchong, China

Purpose: To evaluate the efficacy and safety of postoperative adjuvant hepatic arterial infusion chemotherapy (PA-HAIC) combined with lenvatinib and PD-1 inhibitors versus PA-HAIC with lenvatinib alone in patients with solitary large hepatocellular carcinoma (HCC, >5 cm).

Methods: A total of 183 patients who underwent curative resection and subsequent PA-HAIC plus lenvatinib (HAIC-L, n = 108) or PA-HAIC combined with lenvatinib and PD-1 inhibitors (HAIC-L-P, n = 75) were enrolled from three centers between April 2021 and April 2023. Propensity score matching (PSM) was applied to balance baseline characteristics. Disease-free survival (DFS) and overall survival (OS) were analyzed using the Kaplan–Meier method and Cox proportional hazards models, while treatment-related adverse events (TRAEs) were compared between groups.

Results: The HAIC-L-P group demonstrated significantly improved DFS compared to the HAIC-L group both before (HR: 0.570; P = 0.007) and after PSM (HR: 0.518; P = 0.018). In contrast, no statistically significant difference was observed in OS between the two groups. Multivariate analysis identified elevated AFP (≥400 ng/mL), microvascular invasion, and treatment strategy (HAIC-L *vs.* and HAIC-L-P) as independent predictors of DFS. Additionally, the overall safety profiles were comparable, with similar incidences of TRAEs and no significant increase in hepatic toxicity with PD-1 inhibitor addition.

Conclusion: PA-HAIC combined with lenvatinib and PD-1 inhibitors significantly enhances DFS in patients with solitary large HCC, offering a promising adjuvant approach with acceptable safety. Further prospective, biomarker-driven trials are warranted to validate these findings and optimize patient selection.

KEYWORDS

solitary large hepatocellular carcinoma, postoperative adjuvant therapy, hepatic arterial infusion chemotherapy, PD-1 inhibitors, combined therapy

1 Introduction

Hepatocellular carcinoma (HCC) remains a significant global health burden, ranking as the fourth leading cause of cancer-related mortality worldwide (1). While surgical resection, ablation, and liver transplantation could offer curative potential for early-stage HCC (2, 3), solitary large HCC (tumor diameter >5 cm) remains a therapeutic challenge due to its aggressive biology and high postoperative recurrence rates, even after curative resection (4–7). Tumor size often serves as an independent prognostic factor in HCC, with larger tumors correlating with increased vascular invasion, rapid progression, and diminished survival (8, 9).

Nowadays, postoperative adjuvant hepatic arterial infusion chemotherapy (PA-HAIC) has emerged as a viable option for HCC patients with high-risk features, including microvascular invasion (MVI), and huge single HCC (10–12). By delivering high-dose chemotherapeutic agents directly to the liver, PA-HAIC targets residual micrometastases and circulating tumor cells, potentially delaying recurrence (13). Emerging evidence have also indicated that combining HAIC with tyrosine kinase inhibitors (TKIs) such as lenvatinib (a multi-targeted antiangiogenic agent) may enhance therapeutic efficacy by suppressing angiogenesis and tumor regrowth (14, 15). Furthermore, immune checkpoint inhibitors, particularly programmed death-1 (PD-1) inhibitors, have shown synergistic antitumor effects when combined with TKIs and HAIC in advanced HCC, presumably by modulating the immunosuppressive tumor microenvironment and extending patient survival (16, 17).

Despite these promising advances, the triple-modality regimen of PA-HAIC, lenvatinib, and PD-1 inhibitors remains unexplored in the adjuvant management of solitary large HCC. Moreover, overlapping toxicities from chemotherapy (HAIC), antiangiogenic agents (lenvatinib), and immunotherapy (PD-1 inhibitors) necessitate rigorous safety evaluations, particularly in postoperative patients with compromised liver function. Addressing these gaps is imperative, as solitary large HCC represents a high-risk subgroup with limited therapeutic options and disproportionately poor outcomes.

This multicenter retrospective study aimed to evaluate the efficacy and safety of PA-HAIC combined with lenvatinib and PD-1 inhibitors versus PA-HAIC plus lenvatinib alone in patients with solitary large HCC after curative resection. By comparing disease-free survival (DFS), overall survival (OS), and adverse events between the two groups, this study seeks to provide evidence for optimizing adjuvant strategies in this high-risk population.

2 Materials and methods

2.1 Patient cohort and study design

This retrospective study enrolled patients with solitary large HCC (>5cm) who underwent PA-HAIC combined with lenvatinib or PA-HAIC combined with lenvatinib and PD-1 inhibitors at Sichuan Cancer Hospital, Sichuan Provincial People's Hospital, and the Affiliated Hospital of North Sichuan Medical College from April 2021 to April 2023. The inclusion criteria were as follows: (1) histologically confirmation of HCC; (2) Eastern Cooperative Oncology Group performance status of 0 or 1; (3) no prior or concomitant anticancer therapy; (3) R0 surgical resection with curative intent; (4) solitary tumor >5 cm in diameter; (5) adjuvant PA-HAIC with lenvatinib ± PD-1 inhibitor as the only postoperative therapy. The exclusion criteria included: (1) having history of non-HCC malignancies; (2) preoperative evidence of HCC recurrence or distant metastasis; (3) multiple tumors or a solitary tumor ≤5 cm; (4) drug allergy or intolerance to HAIC; (5) postoperative death within 30 days; (6) incomplete clinicopathological or follow-up data. A total of 183 eligible patients were included into the study. The study design is illustrated in Figure 1.

The study protocol was approved by the Human Ethics Committee of Sichuan Cancer Hospital. All procedures complied with the principles of the Helsinki Declaration. At the time of treatment, all patients provided written informed consent for their clinical data to be used in scientific researches (including retrospective studies).

2.2 Follow up

Patients were followed up every 1–2 months during the first postoperative year and every 3 months thereafter if no recurrence or metastasis was detected. Follow-up evaluations included laboratory tests and imaging via computed tomography (CT) or magnetic resonance imaging (MRI). The primary endpoint was disease-free

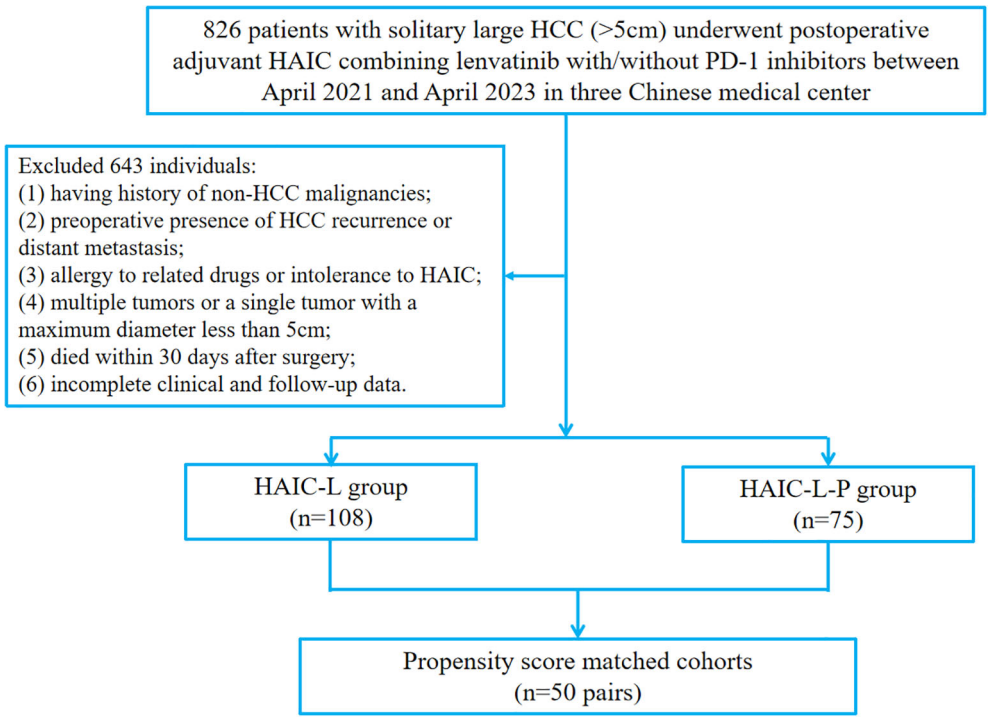

FIGURE 1
The flowchart of patient enrollment. HCC, hepatocellular carcinoma; HAIC, hepatic arterial infusion chemotherapy; PD-1, programmed cell death protein 1.

survival (DFS), defined as the time from surgery to recurrence, metastasis, or death from any cause. The secondary endpoint was overall survival (OS), defined as the time from surgery to death from any cause. Patients without recurrence, metastasis, or death by the end of follow-up (April 2024) were censored as alive and event-free.

2.3 Clinicopathological data collection

Clinicopathological data potentially related to prognosis were collected within 7 days prior to surgery, including demographic characteristics (age, sex, body mass index [BMI]), laboratory parameters (serum biomarkers, liver function tests, coagulation profile, and hepatitis B virus markers), and tumor-related features. Tumor characteristics included histopathological type, presence of cirrhosis, tumor diameter, number of nodules, and MVI. MVI was defined as the presence of cancer cell clusters within a vascular lumen lined by endothelial cells, observable only under microscopy (18).

2.4 Treatment

All patients initiated adjuvant therapy 4–6 weeks after surgery. Treatment consisted of either PA-HAIC with lenvatinib or in combination with PD-1 inhibitors. HAIC was performed based on established protocols (10, 19). Each patient received 1–3 cycles of HAIC with 4-week intervals. Treatment efficacy and toxicity were monitored regularly via imaging and clinical assessments. Therapy was discontinued in the event of unacceptable adverse effects, patient withdrawal, or disease progression. PD-1 inhibitors (Sintilimab) were administered intravenously at a fixed dose of 200 mg every three weeks, with dose modifications as per toxicity management guidelines provided by the manufacturer.

2.5 Statistical analysis

Continuous variables were expressed as medians with interquartile ranges (IQRs) or mean ± standard deviation (SD), while categorical variables were reported as counts and percentages. Categorical variables were compared using the Chi-square or Fisher's exact test, and continuous variables were compared using the Student's *t* test or Mann–Whitney *U* test, as appropriate. To adjust for baseline confounding between groups, propensity score matching (PSM) was conducted using a 1:1 nearest-neighbor algorithm with a caliper width of 0.05. Variables included in the propensity score model were age, gender, and albumin (ALB). DFS and OS were analyzed using the Kaplan–Meier method, and survival curves were compared using the log-rank test. Univariate and multivariate Cox proportional hazards models were employed to identify independent prognostic factors. Variables with $P < 0.05$ in univariate analysis were included in the multivariate model. All statistical analyses were performed using SPSS software version 22.0 (IBM Corp., Armonk, NY, USA). A two-sided P value < 0.05 was considered statistically significant.

3 Results

3.1 Patient characteristics

A total of 183 patients with solitary large HCC (>5cm) were included, including 108 patients in the HAIC-L group and 75 in the HAIC-L-P group. The clinicopathological characteristics before and after PSM are summarized in Table 1. Of the entire cohort, 156 patients (85.2%) were male, with a median age of 52 years. Hepatitis B virus (HBV) infection was present in 136 patients (74.3%), and 144 patients (78.7%) were classified as Barcelona Clinic Liver Cancer (BCLC) stage A. Before PSM, significant differences were observed between the two groups in age (P = 0.022), gender (P = 0.036), and ALB levels (P = 0.041). After PSM, no significant differences remained, indicating that baseline characteristics were well-balanced between the two groups.

TABLE 1 Baseline characteristics of the HCC patients before and after PSM.

Characteristics	Before PSM			After PSM		
	HAIC-L (n=108)	HAIC-L-P (n=75)	P value	HAIC-L (n=50)	HAIC-L-P (n=50)	P value
Age, years	57 (47-66)	59 (54-67)	**0.022**	59 ± 10	59 ± 9	0.943
Gender			**0.036**			1.000
Male	97 (53%)	59 (32.2%)		46 (46%)	46 (46%)	
Female	11 (6%)	16 (8.7%)		4 (4%)	4 (4%)	
BMI, kg/m^2	22.09 (20.58-23.66)	22.31 (20.26-24.64)	0.334	22.49 (20.83-23.97)	22.34 (20.10, 24.88)	0.850
Etiology of HCC			0.436			0.349
HBV	78 (42.6%)	58 (31.7%)		36 (36%)	40 (40%)	
Others	30 (16.4%)	17 (9.3%)		14 (14%)	10 (10%)	
BCLC stage			0.467			0.461
A	83 (45.4%)	61 (33.3%)		38 (38%)	41 (41%)	
C	25 (13.7%)	14 (7.7%)		12 (12%)	9 (9%)	
Child-Pugh class			0.191			0.640
A	74 (40.4%)	58 (31.7%)		37 (37%)	39 (39%)	
B	34 (18.6%)	17 (9.3%)		13 (13%)	11 (11%)	
ALT, U/L	29 (18-49)	33 (19-46)	0.663	33 (19-53)	34 (18-46)	1.000
ALB, g/L	37.4 (33.7-40.3)	39.1 (35.4-41.0)	**0.041**	38.7 (35.2-40.9)	39.1 (35.4-41.4)	0.639
Bilirubin, μmol/L	15.8 (11.5-22.23)	15.0 (9.9, 21.5)	0.391	17.9 (10.9-23.1)	14.1 (9.9-22.4)	0.221
Leukocyte count, 10^9/L	5.80 (4.46-6.79)	5.18 (4.17-6.77)	0.226	5.57 (4.44-6.46)	5.36 (4.72-6.58)	0.524
Neutrophil count, 10^9/L	3.62 (2.64-4.56)	3.45 (2.35-4.25)	0.160	3.35 (2.55-4.03)	3.52 (2.78-4.20)	0.542
Lymphocyte count, 10^9/L	1.27 (1.00-1.60)	1.2 (0.94-1.70)	0.889	1.33 ± 0.53	1.40 ± 0.48	0.510
Platelet count, 10^9/L	166 (114-218)	141 (95-199)	0.083	159 (107-203)	155 (98-199)	0.689
Prothrombin time, s	11.9 (11.1-12.7)	11.9 (11.4-12.9)	0.274	11.9 (11.2-12.6)	12.1 (11.4-12.9)	0.368
AFP, ng/mL	145.32 (6.54-1000)	129.02 (8.55-964.14)	0.897	103.11 (7.50-1000)	169.20 (8.82-982.07)	0.923
Tumor size (cm)	8.3 (6.5-11.1)	8.0 (6.5-11.0)	0.626	8.5 (6.6-10.4)	8.0 (6.5-10.5)	0.513
Histopathological type			0.331			0.656
Poorly differentiated	33 (18%)	18 (9.8%)		15 (15%)	13 (13%)	
Medium-high differentiated	75 (41%)	57 (31.1%)		35 (35%)	37 (37%)	
MVI			0.210			0.317
No	46 (25.1%)	39 (21.3%)		22 (22%)	27 (27%)	
Yes	62 (33.9%)	36 (19.7%)		28 (28%)	23 (23%)	

(Continued)

TABLE 1 Continued

Characteristics	Before PSM			After PSM		
	HAIC-L (n=108)	HAIC-L-P (n=75)	P value	HAIC-L (n=50)	HAIC-L-P (n=50)	P value
Cirrhosis			0.669			0.221
No	37 (23%)	28 (15.3%)		23 (23%)	17 (17%)	
Yes	71 (36.1%)	47 (25.7%)		27 (27%)	33 (33%)	

HCC, hepatocellular carcinoma; PSM, propensity score matching; HAIC, hepatic arterial infusion chemotherapy; BMI, body mass index; HBV, hepatitis B virus; BCLC, Barcelona Clinic Liver Cancer; ALT, alanine transaminase; ALB, albumin; AFP, alpha-fetoprotein; MVI, microvascular invasion.
Bold values indicate statistically significant P values.

3.2 Survival analysis

The median follow-up duration was 21 months (interquartile range, 14–31 months). At the end of the follow-up, tumor progression was observed in 69 patients (63.9%) and 32 patients (29.6%) had died in the HAIC-L group. Moreover, 31 patients (41.3%) in the HAIC-L-P group experienced tumor progression, and 16 patients (21.3%) died.

Before PSM, DFS was significantly better in the HAIC-L-P group than in the HAIC-L group (hazard ratio [HR]: 0.570; 95% confidence interval [CI]: 0.384–0.846; P = 0.007; Figure 2A). After PSM, the HAIC-L-P group also demonstrate superior DFS (HR: 0.518; 95% CI: 0.297–0.903; P = 0.018; Figure 3A). However, no significant difference in OS was observed between the groups, both before and after PSM (P = 0.322; Figure 2B; P = 0.232; Figure 3B).

3.3 Analysis of independent prognostic factors

In the matched cohort, all variables were categorized and analyzed using univariate and multivariate Cox regression (Table 2). Univariate analysis revealed that alpha-fetoprotein (AFP, <400 ng/mL *vs.* ≥400 ng/mL, P = 0.001), microvascular invasion (MVI, no *vs.* yes, P = 0.013), and treatment strategy (HAIC-L *vs.* HAIC-L-P, P = 0.021) were significantly associated with DFS. For OS, significant predictors included alanine aminotransferase (ALT, <35 U/L *vs.* ≥35 U/L, P = 0.004) and AFP (<400 ng/mL *vs.* ≥400 ng/mL, P = 0.017). Multivariate analysis identified AFP (HR: 2.466; 95% CI: 1.405–4.326; P = 0.002), MVI (HR: 1.825; 95% CI: 1.022–3.259; P = 0.042), and treatment strategy (HR: 0.530; 95% CI: 0.297–0.946; P = 0.032) as independent prognostic factors for DFS. AFP (HR: 2.759; 95% CI: 1.216–6.261; P = 0.015) and ALT (HR: 3.873; 95% CI: 1.538–9.755; P = 0.004) were identified as independent predictors of OS.

3.4 Safety

To compare safety profiles between groups post-PSM, treatment-related adverse events (TRAEs) were presented in Table 3. The overall incidence of TRAEs was similar between the HAIC-L and HAIC-L-P groups (any grade: 90% *vs.* 92%, P > 0.999; grade 1/2: 90% *vs.* 90%, P > 0.999; grade 3/4: 14% *vs.* 18%, P = 0.585).

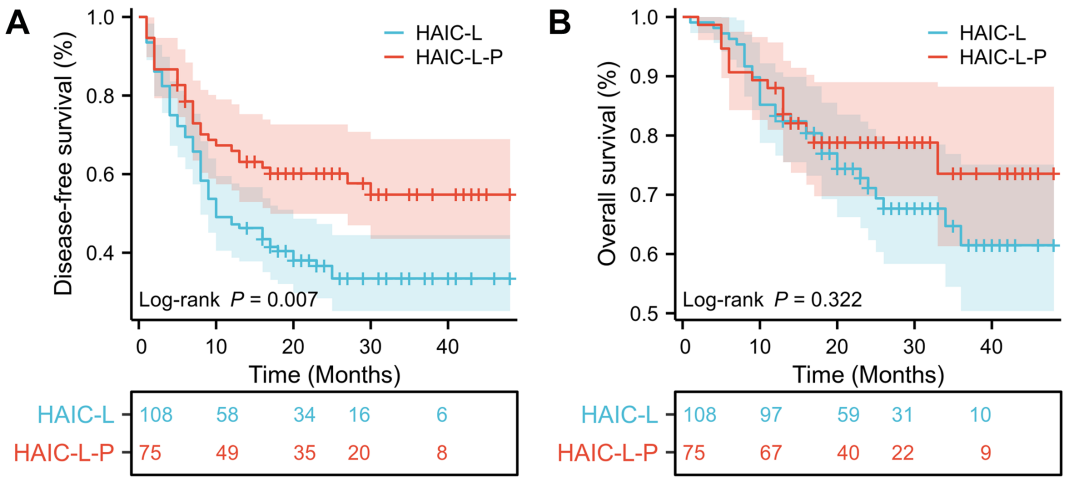

FIGURE 2
Kaplan-Meier survival curves of disease-free survival **(A)** and overall survival **(B)** for the patients with solitary large HCC in the two groups before PSM. HCC, hepatocellular carcinoma; PSM, propensity score matching; HAIC, hepatic arterial infusion chemotherapy.

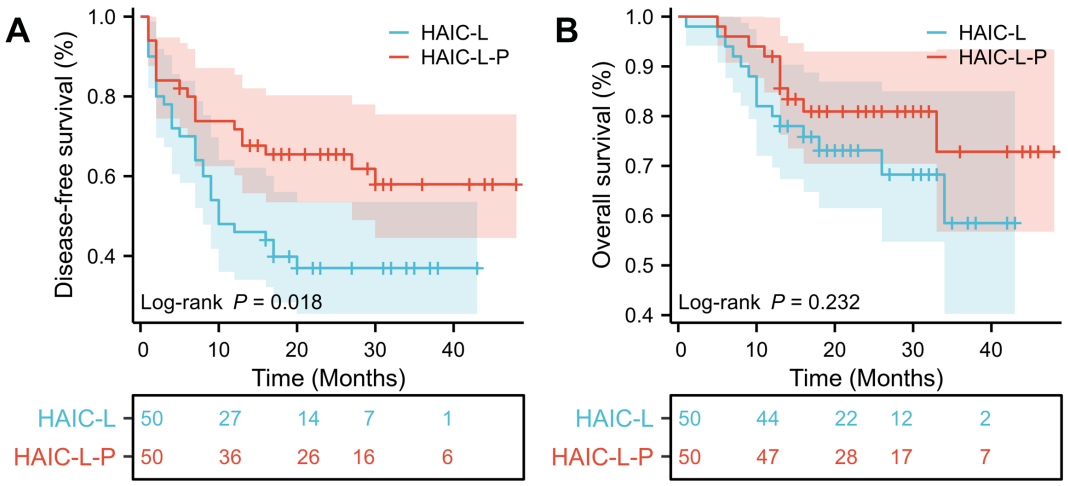

FIGURE 3
Kaplan-Meier survival curves of disease-free survival **(A)** and overall survival **(B)** for the patients with solitary large HCC in the two groups after PSM. HCC, hepatocellular carcinoma; PSM, propensity score matching; HAIC, hepatic arterial infusion chemotherapy.

Most TRAEs were mild to moderate (grades 1-2), and no significant differences were observed in individual adverse events (P > 0.05). Notably, no treatment-related deaths or adverse events above grade 4 occurred in either group up to 12 months post-treatment. All adverse events resolved following symptomatic management or treatment discontinuation.

4 Discussion

To date, no universally accepted postoperative adjuvant therapy exists for HCC patients with high-risk features, and optimal strategies for solitary large HCC (>5 cm) remain underexplored. In this multicenter retrospective study, we demonstrated that postoperative adjuvant HAIC combined with lenvatinib and PD-1 inhibitors (HAIC-L-P) significantly improved DFS compared to HAIC plus lenvatinib alone (HAIC-L) in patients with solitary large HCC (>5 cm), both before and after PSM (HR: 0.570; P = 0.007; Figure 2A; HR: 0.518; P = 0.018; Figure 3A). Notably, the addition of PD-1 inhibitors led to a 48.2% reduction in progression risk after PSM, underscoring the potential of PD-1 inhibitors to augment the antitumor efficacy of combined locoregional and targeted therapy in this high-risk population. However, no significant OS benefit was observed between the two groups (P < 0.05). Multivariate analysis identified the treatment strategy (HAIC-L *vs.* HAIC-L-P; HR: 0.530; P = 0.032) as an independent predictor of DFS, reinforcing the clinical relevance of multimodal therapy in this setting.

The observed DFS benefit may arise from synergistic mechanisms between HAIC, lenvatinib, and PD-1 inhibitors. HAIC delivers high-dose chemotherapy directly to the liver, eliminating residual micrometastases and circulating tumor cells (11, 13). Recent studies have demonstrated the therapeutic efficacy and potential mechanisms of combining HAIC with PD-1 inhibitors (20, 21). Lenvatinib, a potent antiangiogenic agent, has been shown to promote vascular normalization and immune cell infiltration, thereby enhancing the efficacy of PD-1 inhibitors (22, 23). Furthermore, PD-1 inhibitors could reverse T-cell exhaustion and enhance immune surveillance against residual neoplastic clones. When combined with HAIC or anti-angiogenic therapy, these effects are further amplified, resulting in improved immune cell recruitment and function within the tumor milieu (20, 24, 25). This tri-modality approach aligns with emerging evidence in unresectable HCC, where HAIC/TACE combined with lenvatinib and PD-1 inhibitors has demonstrated superior tumor control (14, 26). Our findings extend these observations to the postoperative adjuvant setting, suggesting that combining locoregional chemotherapy, targeted therapy, and immunotherapy may disrupt the "seed-and-soil" interplay driving early recurrence in solitary large HCC.

A key observation in our study is the absence of an OS benefit despite the significant DFS advantage. This discrepancy, when contrasted with studies in advanced HCC where HAIC has frequently translated into prolonged OS (14, 27), may reflect inherent differences in tumor biology and treatment objectives. In the adjuvant setting, the aim is to eliminate micrometastatic disease. However, long-term survival after resection is also influenced by the availability and efficacy of salvage therapies following recurrence. Moreover, variations in patient characteristics and the underlying molecular and immunological heterogeneity of early-stage versus advanced HCC may contribute to these divergent outcomes. Recent comprehensive genomic analyses have identified distinct molecular subtypes of HCC with varying prognoses and therapeutic sensitivities (28). In our study cohort, it is plausible that PD-1 inhibitors effectively delayed recurrence in tumors with immunologically active microenvironments, thereby improving DFS. However, subsequent recurrences may have involved resistant clones or occurred in tumors with immunosuppressive features, leading to limited impact on OS. This hypothesis is supported by single-cell RNA sequencing studies revealing the

TABLE 2 Univariate and multivariate Cox regression analyses of the predictors for disease-free survival and overall survival of the HCC patients after PSM.

Characteristics	DFS				OS			
	Univariate analysis		Multivariate analysis		Univariate analysis		Multivariate analysis	
	HR (95% CI)	P value	HR (95% CI)	P value	HR (95% CI)	P value	HR (95% CI)	P value
Age, years (<60 *vs.* ≥60)	0.569 (0.310 - 1.043)	0.068			0.866 (0.382 - 1.964)	0.731		
Bilirubin, μmol/L (<20 *vs.* ≥20)	0.690 (0.372 - 1.279)	0.239			0.836 (0.360 - 1.940)	0.677		
ALT, U/L (<35 *vs.* ≥35)	1.012 (0.581 - 1.762)	0.966			3.801 (1.515 - 9.536)	**0.004**	3.873 (1.538 - 9.755)	**0.004**
Histopathological type (Poorly *vs.* Medium-high)	0.602 (0.335 - 1.083)	0.090			0.555 (0.244 - 1.262)	0.160		
Cirrhosis (No *vs.* Yes)	1.062 (0.600 - 1.881)	0.837			1.495 (0.645 - 3.466)	0.349		
AFP, ng/mL (<400 *vs.* ≥400)	2.521 (1.442 - 4.408)	**0.001**	2.466 (1.405 - 4.326)	**0.002**	2.677 (1.196 - 5.989)	**0.017**	2.759 (1.216 - 6.261)	**0.015**
MVI (No *vs.* Yes)	2.076 (1.169 - 3.687)	**0.013**	1.825 (1.022 - 3.259)	**0.042**	0.663 (0.299 - 1.472)	0.313		
ALB, g/L (<35 *vs.* ≥35)	0.819 (0.435 - 1.542)	0.536			0.477 (0.210 - 1.081)	0.076		
Treatment (HAIC-L *vs.* HAIC-L-P)	0.509 (0.287 - 0.904)	**0.021**	0.530 (0.297 - 0.946)	**0.032**	0.618 (0.278 - 1.377)	0.239		

HCC, hepatocellular carcinoma; PSM, propensity score matching; DFS, disease-free survival; OS, overall survival; HR, hazard ratio; ALT, alanine transaminase; AFP, alpha-fetoprotein; MVI, microvascular invasion; ALB, albumin; HAIC, hepatic arterial infusion chemotherapy.
Bold values indicate statistically significant P values.

10.3389/fimmu.2025.1609352

10.3389/fimmu.2025.1609352

TABLE 3 Treatment-related adverse events of the patients with solitary large HCC after PSM.

Events, n (%)	HAIC-L (n=50)			HAIC-L-P (n=50)			P value		
	Any Grade	Grade 1/2	Grade 3/4	Any Grade	Grade 1/2	Grade 3/4	Any Grade	Grade 1/2	Grade 3/4
Any TRAE	45	45	7	46	45	9	>0.999	>0.999	0.585
Hematologic toxic effects									
Leukopenia	9	7	2	11	8	3	0.617	0.779	>0.999
Thrombocytopenia	4	4	0	7	7	0	0.338	0.338	>0.999
Hepatic function abnormalities									
Increased ALT	8	6	2	7	5	2	0.779	0.749	>0.999
Increased AST	6	5	1	6	4	2	>0.999	>0.999	>0.999
Hyperbilirubinemia	5	5	0	9	9	0	0.249	0.249	>0.999
Nonhematologic toxic effects									
Nausea	9	8	1	12	10	2	0.461	0.603	>0.999
Fatigue	11	9	2	13	11	2	0.640	0.617	>0.999
Fever	5	5	0	9	9	0	0.249	0.249	>0.999
Hypertension	7	7	0	4	4	0	0.338	0.338	>0.999
Pain	18	18	0	22	21	1	0.414	0.539	>0.999
Diarrhea	6	6	0	5	5	0	0.749	0.749	>0.999
Hypothyroidism	1	1	0	4	4	0	0.359	0.359	>0.999
Gastrointestinal hemorrhage	4	4	0	2	2	0	0.674	0.674	>0.999
RCCEP	0	0	0	3	3	0	0.241	0.241	>0.999

HCC, hepatocellular carcinoma; PSM, propensity score matching; HAIC, hepatic arterial infusion chemotherapy; ALT, alanine transaminase; AST, aspartate aminotransferase; RCCEP, reactive cutaneous capillary endothelial proliferation.

dynamic evolution of immune cell states in HCC, including transitions toward exhausted or immunosuppressive phenotypes (29). Together, these factors highlight the complexities associated with translating DFS gains into OS benefits in the context of postoperative adjuvant therapy.

Multivariate analysis identified AFP ≥400 ng/mL and MVI as independent predictors of poor DFS, consistent with their established roles as biomarkers of aggressive biology and intrahepatic dissemination (30–32). The HAIC-L-P regimen appeared to mitigate the adverse prognostic impact of these factors, paralleling findings by Deng et al. (12), who reported that HAIC-based therapy reduced AFP levels more effectively than TACE in large HCC. The immunomodulatory effects of PD-1 inhibitors may further suppress AFP-secreting tumor subclones, warranting further investigation.

In our findings, safety profiles were comparable between the two groups, with no significant differences in all grade of TRAEs ($P > 0.05$). These findings demonstrated that both treatment approaches were generally well-tolerated, which consistent with previous studies (10, 33). The most common TRAEs were leukopenia, nausea, fatigue, and pain, which were consistent with known toxicities of HAIC, lenvatinib, and PD-1 inhibitors (15, 34). Notably, the addition of PD-1 inhibitors did not exacerbate hepatic toxicity, which is of particular concern in postoperative patients with compromised liver function.

Despite these promising findings, several limitations warrant consideration. First, the retrospective design of our study introduces inherent selection bias and unmeasured factors in treatment allocation, despite the use of PSM to minimize confounding. Second, the lack of biomarker data limits our mechanistic understanding of the immunotherapeutic response. Lastly, the relatively short follow-up period and small sample size may restrict the interpretation of OS outcomes. Future large-scale, randomized controlled trials are essential to validate these preliminary observations and to refine adjuvant therapeutic strategies for patients with solitary large HCC.

5 Conclusion

In conclusion, PA-HAIC combined with lenvatinib and PD-1 inhibitors represents a promising strategy for improving the DFS benefits in solitary large HCC, with a favorable safety profile. Future prospective trials with biomarker-driven designs and extended

follow-up are warranted to validate these findings and optimize patient selection.

Data availability statement

The original contributions presented in the study are included in the article/supplementary material. Further inquiries can be directed to the corresponding authors.

Ethics statement

The studies involving humans were approved by the Human Ethics Committee of Sichuan Cancer Hospital. The studies were conducted in accordance with the local legislation and institutional requirements. At the time of treatment, all patients provided written informed consent for their clinical data to be used in scientific research (including in retrospective studies such as this one).

Author contributions

YL: Conceptualization, Formal Analysis, Writing – original draft, Writing – review & editing. MW: Conceptualization, Formal Analysis, Writing – original draft, Writing – review & editing. DZ: Validation, Writing – review & editing. HY: Validation, Writing – review & editing. YS: Validation, Writing – review & editing. XC: Validation, Writing – review & editing. XH: Conceptualization, Validation, Writing – review & editing. ZL: Conceptualization, Validation, Writing – review & editing.

Funding

The author(s) declare financial support was received for the research and/or publication of this article. This study was supported by Sichuan Province Science and Technology Support Program (No. 2021YFH0187), and Sichuan Medical Science and Technology Innovation Research Institute Fund (YCH-KY-YCZD2024-163).

Conflict of interest

The authors declare that the research was conducted in the absence of any commercial or financial relationships that could be construed as a potential conflict of interest.

Generative AI statement

The author(s) declare that no Generative AI was used in the creation of this manuscript.

Any alternative text (alt text) provided alongside figures in this article has been generated by Frontiers with the support of artificial intelligence and reasonable efforts have been made to ensure accuracy, including review by the authors wherever possible. If you identify any issues, please contact us.

Publisher's note

Supplementary material

The Supplementary Material for this article can be found online at: https://www.frontiersin.org/articles/10.3389/fimmu.2025.1609352/full#supplementary-material

References

1. Sung H, Ferlay J, Siegel RL, Laversanne M, Soerjomataram I, Jemal A, et al. Global cancer statistics 2020: GLOBOCAN estimates of incidence and mortality worldwide for 36 cancers in 185 countries. *CA: Cancer J Clin.* (2021) 71:209–49. doi: 10.3322/caac.21660

2. Govalan R, Lauzon M, Luu M, Ahn JC, Kosari K, Todo T, et al. Comparison of surgical resection and systemic treatment for hepatocellular carcinoma with vascular invasion: national cancer database analysis. *Liver Cancer.* (2021) 10:407–18. doi: 10.1159/000515554

3. Lin S, Hoffmann K, Schemmer P. Treatment of hepatocellular carcinoma: a systematic review. *Liver Cancer.* (2012) 1:144–58. doi: 10.1159/000343828

4. Reig M, Forner A, Rimola J, Ferrer-Fàbrega J, Burrel M, Garcia-Criado Á, et al. BCLC strategy for prognosis prediction and treatment recommendation: The 2022 update. *J Hepatol.* (2022) 76:681–93. doi: 10.1016/j.jhep.2021.11.018

5. European Association for the Study of the Liver. EASL Clinical Practice Guidelines: Management of hepatocellular carcinoma. *J Hepatol.* (2018) 69:182–236. doi: 10.1016/j.jhep.2018.03.019

6. Yau T, Tang VY, Yao TJ, Fan ST, Lo CM, Poon RT. Development of Hong Kong Liver Cancer staging system with treatment stratification for patients with hepatocellular carcinoma. *Gastroenterology.* (2014) 146:1691–1700.e1693. doi: 10.1053/j.gastro.2014.02.032

7. Zhou J, Sun H, Wang Z, Cong W, Wang J, Zeng M, et al. Guidelines for the diagnosis and treatment of hepatocellular carcinoma (2019 edition). *Liver Cancer.* (2020) 9:682–720. doi: 10.1159/000509424

8. Zhang W, Wang X, Jiang R, Hou J, Mu X, Li G, et al. Effect of tumor size on cancer-Specific survival in small hepatocellular carcinoma. *Mayo Clinic Proc.* (2015) 90:1187–95. doi: 10.1016/j.mayocp.2015.06.018

9. Lee MW, Han S, Gu K, Rhim H. Local ablation therapy for hepatocellular carcinoma: clinical significance of tumor size, location, and biology. *Invest Radiol.* (2025) 60:53–9. doi: 10.1097/RLI.0000000000001100

10. Liang Y, Zhong D, Shang J, Yan H, Su Y, Chen Y, et al. Efficacy and safety of postoperative adjuvant HAIC with FOLFOX combining PD-1 inhibitors in HCC patients with microvascular invasion: a propensity score matching analysis. *BMC Cancer.* (2025) 25:418. doi: 10.1186/s12885-025-13793-x

11. Li SH, Mei J, Cheng Y, Li Q, Wang QX, Fang CK, et al. Postoperative adjuvant hepatic arterial infusion chemotherapy with FOLFOX in hepatocellular carcinoma with

microvascular invasion: A multicenter, phase III, randomized study. *J Clin oncol: Off J Am Soc Clin Oncol*. (2023) 41:1898–908. doi: 10.1200/JCO.22.01142

12. Deng M, Cai H, He B, Guan R, Lee C, Guo R. Hepatic arterial infusion chemotherapy versus transarterial chemoembolization, potential conversion therapies for single huge hepatocellular carcinoma: a retrospective comparison study. *Int J Surg (London England)*. (2023) 109:3303–11. doi: 10.1097/JS9.0000000000000654

13. Emens LA, Middleton G. The interplay of immunotherapy and chemotherapy: harnessing potential synergies. *Cancer Immunol Res*. (2015) 3:436–43. doi: 10.1158/2326-6066.CIR-15-0064

14. Chang X, Li X, Sun P, Li Z, Sun P, Ning S. HAIC Combined with lenvatinib plus PD-1 versus lenvatinib Plus PD-1 in patients with high-risk advanced HCC: a real-world study. *BMC Cancer*. (2024) 24:480. doi: 10.1186/s12885-024-12233-6

15. Sun R, Gou Y, Pan L, He Q, Zhou Y, Luo Y, et al. Hepatic arterial infusion chemotherapy (HAIC) combined with Tislelizumab and Lenvatinib for unresectable hepatocellular carcinoma: a retrospective single-arm study. *Cell Oncol (Dordrecht Netherlands)*. (2024) 47:2265–76. doi: 10.1007/s13402-024-01031-8

16. Cheu JW, Wong CC. Mechanistic rationales guiding combination hepatocellular carcinoma therapies involving immune checkpoint inhibitors. *Hepatol (Baltimore Md)*. (2021) 74:2264–76. doi: 10.1002/hep.31840

17. Montagner A, Arleo A, Suzzi F, D'Assoro AB, Piscaglia F, Gramantieri L, et al. Notch signaling and PD-1/PD-L1 interaction in hepatocellular carcinoma: potentialities of combined therapies. *Biomolecules*. (2024) 14(12):1581. doi: 10.3390/biom14121581

18. Rodríguez-Perálvarez M, Luong TV, Andreana L, Meyer T, Dhillon AP, Burroughs AK. A systematic review of microvascular invasion in hepatocellular carcinoma: diagnostic and prognostic variability. *Ann Surg Oncol*. (2013) 20:325–39. doi: 10.1245/s10434-012-2513-1

19. Li S, Mei J, Wang Q, Guo Z, Lu L, Ling Y, et al. Postoperative adjuvant transarterial infusion chemotherapy with FOLFOX could improve outcomes of hepatocellular carcinoma patients with microvascular invasion: A preliminary report of a phase III, randomized controlled clinical trial. *Ann Surg Oncol*. (2020) 27:5183–90. doi: 10.1245/s10434-020-08601-8

20. Huang Y, Du Z, Lai Z, Wen D, Huang L, He M, et al. Single-Nucleus and spatial transcriptome profiling delineates the multicellular ecosystem in hepatocellular carcinoma after hepatic arterial infusion chemotherapy. *Advanced Sci (Weinheim Baden-Wurttemberg Germany)*. (2025) 12:e2405749. doi: 10.1002/advs.202405749

21. Li QJ, He MK, Chen HW, Fang WQ, Zhou YM, Xu L, et al. Hepatic arterial infusion of oxaliplatin, fluorouracil, and leucovorin versus transarterial chemoembolization for large hepatocellular carcinoma: A randomized phase III trial. *J Clin oncol: Off J Am Soc Clin Oncol*. (2022) 40:150–60. doi: 10.1200/JCO.21.00608

22. Yang J, Guo Z, Song M, Pan Q, Zhao J, Huang Y, et al. Lenvatinib improves anti-PD-1 therapeutic efficacy by promoting vascular normalization via the NRP-1-PDGFRβ complex in hepatocellular carcinoma. *Front Immunol*. (2023) 14:1212577. doi: 10.3389/fimmu.2023.1212577

23. Chen Y, Dai S, Cheng CS, Chen L. Lenvatinib and immune-checkpoint inhibitors in hepatocellular carcinoma: mechanistic insights, clinical efficacy, and future perspectives. *J Hematol Oncol*. (2024) 17:130. doi: 10.1186/s13045-024-01647-1

24. Allen E, Jabouille A, Rivera LB, Lodewijckx I, Missiaen R, Steri V, et al. Combined antiangiogenic and anti-PD-L1 therapy stimulates tumor immunity through HEV formation. *Sci Trans Med*. (2017) 9(385):eaak9679. doi: 10.1126/scitranslmed.aak9679

25. Cao Q, Wang Q, Wu X, Zhang Q, Huang J, Chen Y, et al. A literature review: mechanisms of antitumor pharmacological action of leonurine alkaloid. *Front Pharmacol*. (2023) 14:1272546. doi: 10.3389/fphar.2023.1272546

26. Wang WJ, Liu ZH, Wang K, Yu HM, Cheng YQ, Xiang YJ, et al. Efficacy and safety of TACE combined with lenvatinib and PD-1 inhibitors for unresectable recurrent HCC: A multicenter, retrospective study. *Cancer Med*. (2023) 12:11513–24. doi: 10.1002/cam4.5880

27. Wei M, Zhang P, Yang C, Li Y. Hepatic arterial infusion chemotherapy combined with lenvatinib and PD-1 inhibitors versus lenvatinib and PD-1 inhibitors for unresectable HCC: a meta-analysis. *Front Oncol*. (2024) 14:1500496. doi: 10.3389/fonc.2024.1500496

28. Chen L, Zhang C, Xue R, Liu M, Bai J, Bao J, et al. Deep whole-genome analysis of 494 hepatocellular carcinomas. *Nature*. (2024) 627:586–93. doi: 10.1038/s41586-024-07054-3

29. Yin Z, Song Y, Wang L. Single-cell RNA sequencing reveals the landscape of the cellular ecosystem of primary hepatocellular carcinoma. *Cancer Cell Int*. (2024) 24:379. doi: 10.1186/s12935-024-03574-0

30. Si YQ, Wang XQ, Fan G, Wang CY, Zheng YW, Song X, et al. Value of AFP and PIVKA-II in diagnosis of HBV-related hepatocellular carcinoma and prediction of vascular invasion and tumor differentiation. *Infect Agents Cancer*. (2020) 15:70. doi: 10.1186/s13027-020-00337-0

31. Xing H, Sun LY, Yan WT, Quan B, Liang L, Li C, et al. Repeat hepatectomy for patients with early and late recurrence of hepatocellular carcinoma: A multicenter propensity score matching analysis. *Surgery*. (2021) 169:911–20. doi: 10.1016/j.surg.2019.11.005

32. Wang J, He XD, Yao N, Liang WJ, Zhang YC. A meta-analysis of adjuvant therapy after potentially curative treatment for hepatocellular carcinoma. *Can J Gastroenterol*. (2013) 27:351–63. doi: 10.1155/2013/417894

33. Yu J, Li Y, Yu J, Yang Y, Chen Y, Yi P. Hepatic arterial infusion chemotherapy enhances the efficacy of lenvatinib and PD-1 inhibitors for advanced hepatocellular carcinoma: A meta-analysis and trial sequential analysis. *Eur J Surg oncol: J Eur Soc Surg Oncol Br Assoc Surg Oncol*. (2025) 51:109573. doi: 10.1016/j.ejso.2025.109573

34. Li H, Wang J, Zhang G, Kuang D, Li Y, He X, et al. Transarterial chemoembolization combined donafenib with/without PD-1 for unresectable HCC in a multicenter retrospective study. *Front Immunol*. (2023) 14:1277329. doi: 10.3389/fimmu.2023.1277329

frontiers | Frontiers in Immunology

TYPE Original Research
PUBLISHED 01 September 2025
DOI 10.3389/fimmu.2025.1620390

OPEN ACCESS

EDITED BY
Georgios Germanidis,
University General Hospital of Thessaloniki AHEPA, Greece

REVIEWED BY
Junmeng Li,
Henan Provincial People's Hospital, China
Yifan Li,
Shanxi Provincial Cancer Hospital, China

*CORRESPONDENCE
Hai Huang
huanghai828@gmc.edu.cn

RECEIVED 29 April 2025
ACCEPTED 14 August 2025
PUBLISHED 01 September 2025

CITATION
Wen X, Cui M, Zhang J and Huang H (2025) Liquid-liquid phase separation in gastric cancer: identifying novel biomarkers and therapeutic targets through gene signature analysis. *Front. Immunol.* 16:1620390. doi: 10.3389/fimmu.2025.1620390

Liquid-liquid phase separation in gastric cancer: identifying novel biomarkers and therapeutic targets through gene signature analysis

Xianhui Wen [1,2], Miaomiao Cui [3], Junhua Zhang [4] and Hai Huang [1,2]*

[1]Center for Clinical Laboratories, The Affiliated Hospital of Guizhou Medical University, Guiyang, China, [2]School of Clinical Laboratory Science, Guizhou Medical University, Guiyang, China, [3]Department of Clinical Laboratory, The Second People's Hospital of Guiyang, Guiyang, China, [4]Department of Blood Transfusion, The Third Xiangya Hospital Central South University, Changsha, China

Background and objective: Liquid-liquid phase separation (LLPS) plays an important role in the development of many tumors, including gastric cancer, but its prognostic value is unclear. The aim of this study was to explore the prognostic significance of LLPS-related genes in gastric cancer to provide a basis for improving the accuracy of prognostic prediction and finding potential therapeutic targets in gastric cancer.

Methods: Clinical and transcriptomic data of gastric cancer were downloaded from TCGA and GEO databases, and LLPS-related genes were extracted from PhaSepDB. Unsupervised clustering was used to identify molecular subtypes based on LLPS gene expression. LLPS gene features were constructed and validated by LASSO Cox regression, and their staging prediction value was also evaluated by machine learning methods. Key genes were validated by qRT-PCR, Western blot, immunofluorescence, and functional experiments (shRNA knockdown, CCK-8, clone formation, and scratch assay).

Results: Twenty LLPS-associated genes showed significant mRNA expression, copy number variation, somatic mutation, and interaction network alterations in gastric cancer tissues. Two LLPS molecular isoforms with different survival outcomes and immune microenvironment characteristics were identified. A four-gene LLPS prognostic signature consisting of *DACT1, EZH2, PAK2,* and *PSPC1* was constructed, and the high-risk group had a poorer prognosis and was prone to drug resistance. Machine learning analysis further confirmed the predictive value of this gene signature. Functional experiments showed that knockdown of PSPC1 significantly inhibited the proliferation (inhibition rate >50%, P <0.001) and migration ability (P<0.0001) of gastric cancer cells. Immunofluorescence confirmed the localization and aggregation characteristics of DACT1 and PSPC1.

Conclusion: This study revealed the important role of LLPS in gastric cancer, and the constructed four-gene LLPS signature is expected to be a novel biomarker for prognostic assessment and treatment of gastric cancer. PSPC1 plays a key role in gastric cancer progression, and has the value of a potential therapeutic target.

KEYWORDS

gastric cancer, liquid-liquid phase separation, tumor immune microenvironment, prognosis, nomogram

1 Introduction

GC ranks as the fifth most common malignancy and is the fourth leading cause of cancer-related death worldwide (1). Despite its high occurrence, a large proportion of patients are unfortunately diagnosed at more advanced stages, resulting in poor clinical outcomes due to the lack of clear clinical markers (2). Among patients with locoregionally confined GC, the 5-year relative overall survival rate is 77.7%, but for those with advanced cancer, it drops to just 10.2% (3). Therefore, discovering new prognostic biomarkers and potential therapeutic targets is essential for better patient outcomes.

LLPS is a physicochemical process within cells that has gained significant attention in recent years (4). LLPS results in the formation of membraneless, droplet-like structures in the cytoplasm or nucleoplasm, creating dynamic microenvironments that regulate various biological processes (5, 6). LLPS is driven by multivalent interactions among macromolecules, with one key mechanism involving the intrinsically disordered regions (IDRs) of proteins (7). Increasing evidence indicates that LLPS plays a crucial role in cancer initiation (8, 9), progression (10), immune escape (11, 12), vascularization (13, 14), metabolism, phenotypic plasticity (15), and metastasis (16, 17). However, the role of LLPS in GC remains insufficiently understood and requires further in-depth investigation.

Based on this background, this study aimed to systematically identify and assess the importance of LLPS-associated genes in GC through comprehensive bioinformatics analysis. We developed an innovative molecular signature centered on LLPS-related genes, offering clinically actionable tools for personalized treatment and prognosis assessment of GC, and laying the groundwork for a deeper understanding of LLPS's role in GC development and progression.

2 Materials and methods

2.1 Ethical approval

All data usage complied strictly with the relevant data use policies and ethical governance frameworks of the TCGA and GEO databases. All analyses were conducted using anonymized public data.

2.2 Data acquisition and preliminary processing

Figure 1 provided a schematic overview of the study's design and methodological flowchart. Transcriptomic data and clinically annotated patient information were sourced from the TCGA-STAD project and the GSE84437 dataset available in the GEO database. In August 2024, we obtained the TCGA-STAD data from the official TCGA portal (https://portal.gdc.cancer.gov/), which comprises RNA sequencing and clinical information for 412 gastric adenocarcinoma patients and 36 normal tissues on August 15, 2024. The GSE84437 dataset, consisting of data from 433 GC patients, was retrieved from the GEO database (https://www.ncbi.nlm.nih.gov/geo/query/acc.cgi?acc=GSE84437). Survival records for 448 patients were extracted from the TCGA dataset, and the analysis included only those patients with complete gene expression and survival data. The 561 LLPS-related genes were sourced from PhaSepDB (http://db.phasep.pro/) (18). GSE19826 and GSE79973 datasets as validation sets.

Before merging the TCGA and GEO datasets, batch effect correction was performed using the ComBat function from the "sva" R package to minimize technical variation between different data sources. The corrected data were then used for subsequent differential expression analysis and model construction.

2.3 Determination of molecular subtypes

We utilized the "ConsensusClusterPlus" R package to perform unsupervised consensus clustering for patient classification. Subsequently, patient clusters were discerned and verified through Principal Component Analysis (PCA).

2.4 Investigating pathological profiles and prognostic patterns across LLPS clusters

We utilized the "survival" and "survminer" packages in R to conduct Kaplan-Meier (K-M) survival analyses, examining the prognostic relevance of GC patients grouped by distinct LLPS-

10.3389/fimmu.2025.1620390

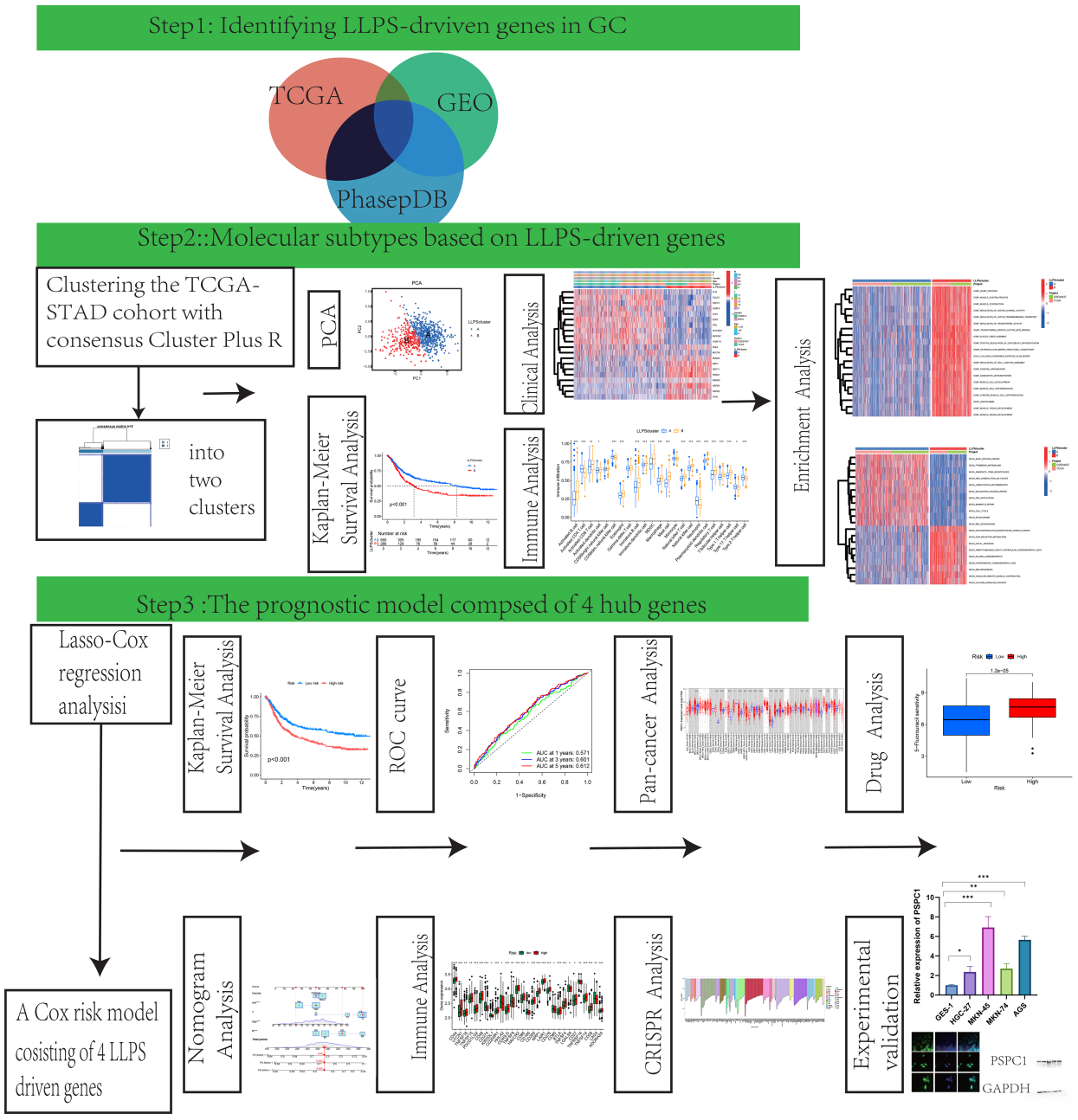

FIGURE 1
The flow diagram of our study.

based clusters. Moreover, we assessed clinical variables such as age, tumor stage (T stage), and lymph node stage (N stage) across these clusters to identify any statistically significant associations.

2.5 Molecular signature characterization through gene set variation analysis of LLPS clusters

To investigate the underpinning mechanisms of the distinctive LLPS-derived clusters identified in this research, we applied the R package "GSVA". This method enabled us to assess pathway activity differences associated with the unique LLPS patterns, providing insights into the functional implications of LLPS in GC.

2.6 Estimation of the tumor microenvironment in different LLPS clusters

By applying single-sample Gene Set Enrichment Analysis (ssGSEA), we quantified the relative representation of 23 human

immune cell populations within the tumor microenvironment (TME) across multiple LLPS clusters. Furthermore, we assessed the transcript abundance of 33 key immune–checkpoint regulators across these clusters to investigate differences in immune profile.

2.7 Establishment of a prognostic index derived from a differentially expressed gene model

The study utilized a dataset of 871 GC samples, consisting of 433 samples from the GEO database (GSE84437), noted for its large size and detailed clinical follow-up, and 438 gastric adenocarcinoma samples with survival information from the TCGA database. Utilizing the R–based toolkit "caret" (19), we splited the combined dataset evenly into a training and testing subsets, each comprising 436 patients. The training set underwent univariate Cox regression analysis to find LLPS-related differentially expressed genes (DEGs) correlated with overall survival (OS) (20). We then employed the Least Absolute Shrinkage and Selection Operator (LASSO) algorithm with the R package "glmnet" to choose the DEGs with the highest prognostic potential. Subsequently, multivariate Cox regression analysis was employed to identify independent prognostic DEGs associated with GC, which were then utilized to construct the prognostic model. In conclusion, aligning with findings from previous oncological research (21), the risk–prediction score was determined based on the following equation involving the selected genes:

Prognostic Score = (Gene A expression × Coefficient A) + (Gene B expression × Coefficient B) + …

2.8 Independent prognostic analysis of the risk model

To evaluate the independent prognostic significance of the risk signature, univariate and multivariate Cox proportional-hazards regression analyses were carried out utilizing the R package "survival". These analyses assessed the impact of the risk score and other clinicopathological variables on overall survival. The K-M method was employed to analyze survival outcomes, and survival curves between different prognostic groups were compared using the log-rank test to assess statistical significance.

Furthermore, we constructed a nomogram integrating both clinicopathological characteristics and the prognostic risk score using the"rms"R package. The concordance index (c-index) was computed to evaluate the model's predictive performance and the agreement between projected survival probabilities and observed outcomes. Furthermore, calibration plots and receiver operating characteristic (ROC) curves were constructed to examine the model's reliability and predictive accuracy.

2.9 TIDE analysis

We applied the TIDE (Tumor Immune Dysfunction and Exclusion) tool to assess tumor immune evasion mechanisms and analyzed the discrepancies in TIDE scores between different risk groups.

2.10 Mutation data analysis

We used the R package "maftools" to preprocess and visualize mutation data from TCGA stomach adenocarcinoma samples, including mutation frequency analysis, distribution of mutation types, and waterfall plots of mutated genes.

2.11 Investigation of the immunological microenvironment characteristics and pharmacological response profiles

We utilized the ESTIMATE computational framework to quantify stromal and immune cell infiltration levels in gastric carcinoma specimens. Through the R package "estimate", we systematically generated three quantitative metrics: stromal scores reflecting extracellular matrix components, immune scores representing leukocyte infiltration, and composite ESTIMATE scores. To examine therapeutic response patterns, pharmacological sensitivity data were acquired from the publicly accessible Genomics of Drug Sensitivity in Cancer repository(https://www.cancerrxgene.org/) (22). Spearman rank correla- tion was applied to explore the association between drug–response patterns and the prognostic index. Furthermore, the R computational toolkit "pRRophetic" was implemented to predict half-maximal inhibitory concentrations (IC50), enabling comparative analysis of chemotherapeutic efficacy between prognostic subgroups.

2.12 The whole-gene CRISPR-Cas9 screens via the computational estimation of CRISPR effects by relative screen signal

Genome-wide screening CRISPR were downloaded from DepMap database (https://depmap.org/portal/download/). Approximately 17000 candidate genes were calculated by using CERES algorithm the dependence of the score (23). A negative score indicates cell growth inhibition or death following gene knockout, with scores of 0 and -1 representing the median effects of non-essential genes and common core essential genes, respectively. The top 200 negatively scoring genes were visualized in a bar char.

2.13 Pan-cancer analysis of gene expression

Gene expression data was derived from the normalized TCGA dataset, with RNA-seq data obtained from the EBPlusPlusAdjust PANCAN_IlluminaHiSeq_RNASeqV2.geneExp.tsv file provided by PanCanAtlas. The data was transformed into dimensionless Z-Score values by tumor using $(x-\mu)/\sigma$. Z-score values less than -3 or greater than 3 were considered outliers and were removed. After outlier removal, tumors were included in the analysis when there were at least three normal samples. Wilcoxon Rank Sum Tests were used to compare the statistical differences in expression levels between tumor and normal tissues in the digestive system tumor dataset.

2.14 Cell culture

The gastric epithelial cell line GES and gastric cancer cell lines HGC-27, MKN-45, MKN-74, and AGS were acquired from the Chinese Academy of Sciences Cell Bank (Shanghai, China). Cells were cultured in RPMI-1640 medium (Gibco, NY, USA) enriched with 10% fetal bovine serum (FBS) (Biological Industries, KBH, IL) and 1% penicillin-streptomycin solution (Gibco, NY, USA). All cell cultures were maintained in incubation vessels at 37 °C in a humidified atmosphere containing 5% CO₂.

2.15 Quantitative reverse-transcription polymerase chain reaction validate RNA expression of key genes

GC cells were collected for RNA extraction using TRIzol reagent (Invitrogen, CA, USA). Total RNA was reverse transcribed to cDNA using PrimeScriptTM RT reagent Kit (TaKaRa, Shiga, Japan). Quantitative real-time PCR was performed using ChamQ SYBR qPCR Master Mix (Vazyme, Nanjing, China) according to the manufacturer's instructions. The relative expression levels were normalized to HPRT and calculated using the $2^{-\triangle\triangle Ct}$ method. All primer sequences used for RT-qPCR analysis are listed in Supplementary Table S1.

2.16 Immunofluorescence

Following culture, cells underwent fixation with 4% paraformaldehyde solution (10 min) and membrane permeabilization using 1% Triton X-100 (5 min) at ambient temperature. To prevent non-specific interactions, cells were immersed in a 5% BSA solution for 1 h at ambient temperature. The samples were then exposed to specific primary antibodies and maintained at 4°C for 12 hours to ensure complete reaction equilibrium. After thorough PBS washing steps, samples were treated with goat anti-mouse secondary antibodies conjugated to Alexa Fluor 488 (Thermo Fisher Scientific) for one hour under ambient conditions. Nuclear visualization was achieved through DAPI counterstaining. Immunofluorescence(IF) images were acquired using a DMi8 LEICA fluorescence microscope system. Supplementary Table S2 presents the full set of primary antibodies utilized in this study.

2.17 Western blot analysis

Protein samples were isolated through RIPA buffer-mediated lysis (Solarbio, Beijing, China). Following protein separation through SDS-PAGE electrophoresis, the samples were transferred to PVDF membranes (Millipore, MA, USA). Subsequently, the membranes underwent blocking with 5% non-fat dry milk solution in TBST buffer at ambient temperature for 2 h. After blocking, membranes were incubated overnight at 4 °C with the designated primary antibodies, then exposed for 1h at room temperature to the matching HRP–conjugated secondary antibodies. Immunoreactive bands were detected using an enhanced chemiluminescence substrate (MeilunBio, Dalian, China) and documented using a ChemiDoc XRS+ system (Bio-Rad, CA, USA). Detailed information regarding the primary antibodies utilized is available in Supplementary Table S2.

2.18 Lentivirus production and generation of stable cell lines

Short hairpin RNAs (shRNAs) targeting human PSPC1 were purchased from Zhenjiang Huamao Biotechnology Co., Ltd. (Zhenjiang, China) and supplied in the lentiviral vector pLenti-U6-shRNA-CMV- GFP-2A-Puro. Silencing were generated in HEK293T cells co-transfected with the PSPAX2 plasmid and PMD2G plasmid via Polyethylenimine(PEI) transfection reagent (Solarbio,China). Viral supernatants were collected at 48h and 72h post-transfection, filtered using a 0.45μm pore-size membrane, and enriched with 10% PEG-6000. Target cells were transduced with the lentiviral preparations in the presence of 8 mg/mL polybrene. At 48h later, puromycin (Solarbio,China) was added to a final concentration of 2 μg/mL for selection, alongside a negative-selection control group at the same density. Selection was discontinued once all cells in the control dish had died, and the surviving population was expanded as a stably transduced line.

2.19 CCK8 assay

HGC-27 and AGS cells were seeded at a density of 3×10^3 cells per well. Each well received 10μL of CCK-8 solution (MCE, Shanghai, China). Following an additional 2-hour incubation period, the optical density at 450 nm was determined using a microplate reader (Thermo Fisher Scientific, MA, USA).

2.20 Colony formation assay

For colony formation analysis, HGC-27 and AGS cells were plated in 6-well plates at 1×10^3 cells per well. After 10 days, colonies

were fixed with 4% paraformaldehyde and stained using 0.1% crystal violet solution. The number of colonies formed was counted using Image J software.

2.21 Wound healing assay

AGS cells were transferred to 6-well plates. Following 24 hours of incubation to allow cell attachment, a scratch wound was generated in the cell monolayer using a sterile 200μL pipette tip. The culture medium was then replaced with medium containing 1% FBS instead of 10% FBS. Cell migration was monitored by capturing images at various time points, and the wound area was quantified using Image J software.

2.22 Statistical analysis

Comprehensive data assessments were performed through the R environment (version 4.4.0) and validated using GraphPad Prism (version 9.0) for all statistical computations. For continuous variables, the Student's t-test was applied; for categorical variables, the Chi-square test or Fisher's exact test was used. By applying the "limma" R package for differential expression analysis, significant differences were identified using criteria of FDR<0.05 combined with |log₂–fold change|>1. Survival analysis was conducted using the "survival" and "survminer" R packages, with the K-M method employed to calculate survival functions and the log-rank test used to compare survival curves between different prognostic groups. In cases involving multiple comparisons, the Benjamini-Hochberg correction was employed to maintain the false discovery rate (FDR) at an acceptable level. All p-values were founded on two-sided tests, and results with p-values below 0.05 were considered statistically significant.

3 Results

3.1 Panoramic profiling of LLPS-linked genetic features in GC

The diagram of research was demonstrated in Figure 1. Using TCGA data and the "limma" package, we analyzed LLPS-related gene expression and found significant differences between two groups (Supplementary Figure 1A). Among them, 68 genes were upregulated and 5 were downregulated (Supplementary Figure 1B). Functional enrichment indicated that these genes are involved in DNA replication initiation, cell division, RNA metabolism, nuclear structure, chromosome regulation, transcription regulation, and epigenetic modifications (Figure 2A). Pathway analysis further highlighted enrichment in the Polycomb Repressive Complex, cell cycle, and lysine metabolism pathways (Figure 2B).

Univariate Cox regression analysis demonstrated the roles of different genes in survival outcomes (Figure 2C).To further understand the genomic alterations and interactions of these differentially expressed LLPS-related genes, we examined CNVs of 22 differentially expressed LLPS-related genes in GC, identifying chromosomal alterations and their locations. SURF6 showed the highest CNV gain (~15%), while EZH2 exhibited the highest CNV loss (~15%) (Figure 2D). The chromosomal distribution of CNV alterations for these genes was delineated (Figure 2E). A correlation network revealed positive (red lines) and negative (blue lines) correlations among the LLPS genes (Figure 2F).

3.2 Identification of LLPS clusters in GC and prognostic significance

To further explore the transcriptional profiles of LLPS-related genes involved in gastric cancer tumorigenesis, we combined GC datasets from both the TCGA database and GSE84437, creating a merged TCGA-GSE cohort (N = 845). Using the "ConsensusClusterPlus" package in R, we performed an unsupervised clustering analysis, with k = 2 as the optimal number of clusters based on empirical CDF plots. This selection showed the highest intra-cluster similarity and the greatest inter-cluster separation (Figures 3A, B). The resulting clusters displayed two distinct expression patterns of LLPS-related genes. Additionally, cases of GC in the TCGA-GEO cohort were effectively stratified into separate groups (Figure 3C). Kaplan-Meier survival curves were generated to assess the prognostic value of these clusters, revealing significantly worse OS in patients within cluster B (Figure 3D). Univariate analysis also identified differences in gene expression between the two clusters (Figure 3E). Finally, we examined the clinical and pathological features of the two groups to evaluate their association with LLPS-linked gene levels (Figure 3F).

Next, we systematically evaluated a gastric cancer staging prediction model based on LLPS-related genes by multiple machine learning and deep learning methods. Four independent gastric cancer gene expression datasets (GSE26253, GSE27342, GSE84433, GSE26899) were integrated in this study, containing a total of 985 gastric cancer samples. To ensure the consistency and comparability of the analysis, we uniformly classified all samples into three groups of early, intermediate and advanced stages according to the AJCC/UICC TNM staging system. The specific classification criteria were as follows: both the GSE26253 dataset (n=360) and the GSE27342 dataset (n=160) directly provided the AJCC clinical staging information, and we categorized stages IB and II as the early group, stages IIIA and IIIB as the intermediate group, and stage IV as the advanced group. Some of the stage III samples in the GSE27342 dataset that were not subdivided into substages were also uniformly categorized into the intermediate group.For the GSE84433 dataset (n=357), which provides detailed TNM staging information, we grouped samples according to the combination of depth of primary tumor invasion (T), lymph node metastasis (N), and distant metastasis (M): samples that were T1-T2 and N0-N1 were categorized as the early stage group, samples that were T3-T4 or N2-N3 (without distant metastasis) were categorized as the

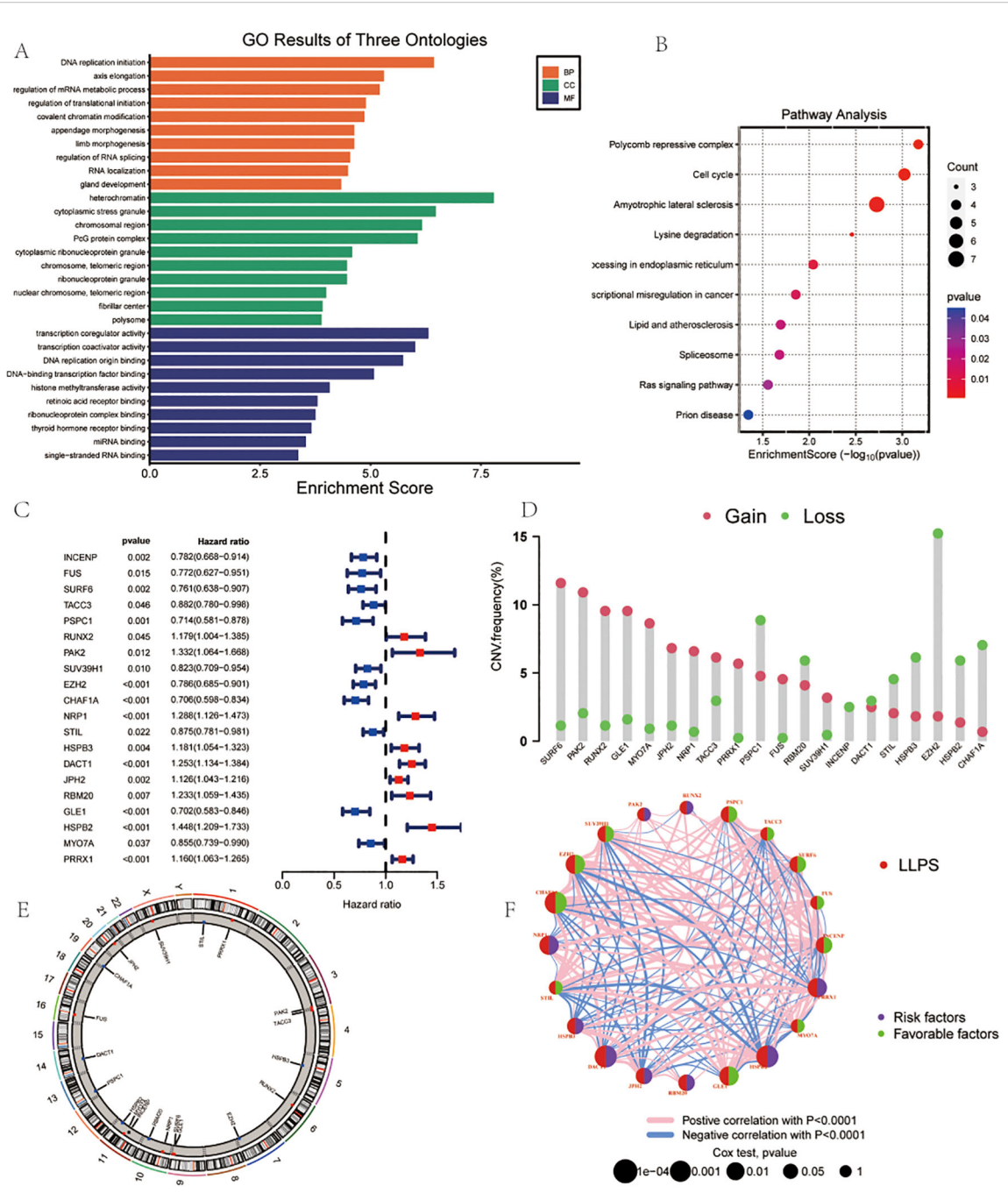

FIGURE 2
Landscape of LLPS-related Genes in Gastric Cancer. **(A)** GO Analysis. **(B)** Pathway Analysis. **(C)** Univariate COX regression analysis of the hazard ratio between 20 LLPS genes. **(D)** Frequency of CNVs in LLPS genes.**(E)** The location of CNV alteration of 14 model genes on 23 chromosomes. **(F)** Correlation network of the 20 LLPS genes.

intermediate stage group, and samples that had anysamples with distant metastases (M1) were categorized as the late group.This classification method is in line with the basic principle of AJCC staging, which takes into account the degree of local invasion, regional lymph node metastasis, and distant metastasis of the tumor. The GSE26899 dataset (n=108) had been preclassified into two groups, early (stage 1-2) and late (stage 3-4), according to the AJCC staging system, and we directly adopted its original grouping. Finally, based on the expression data of four gene markers (DACT1, EZH2, PAK2, PSPC1), we constructed a staging prediction model for 953 gastric cancer samples (319 early, 497 intermediate, and 137 advanced).

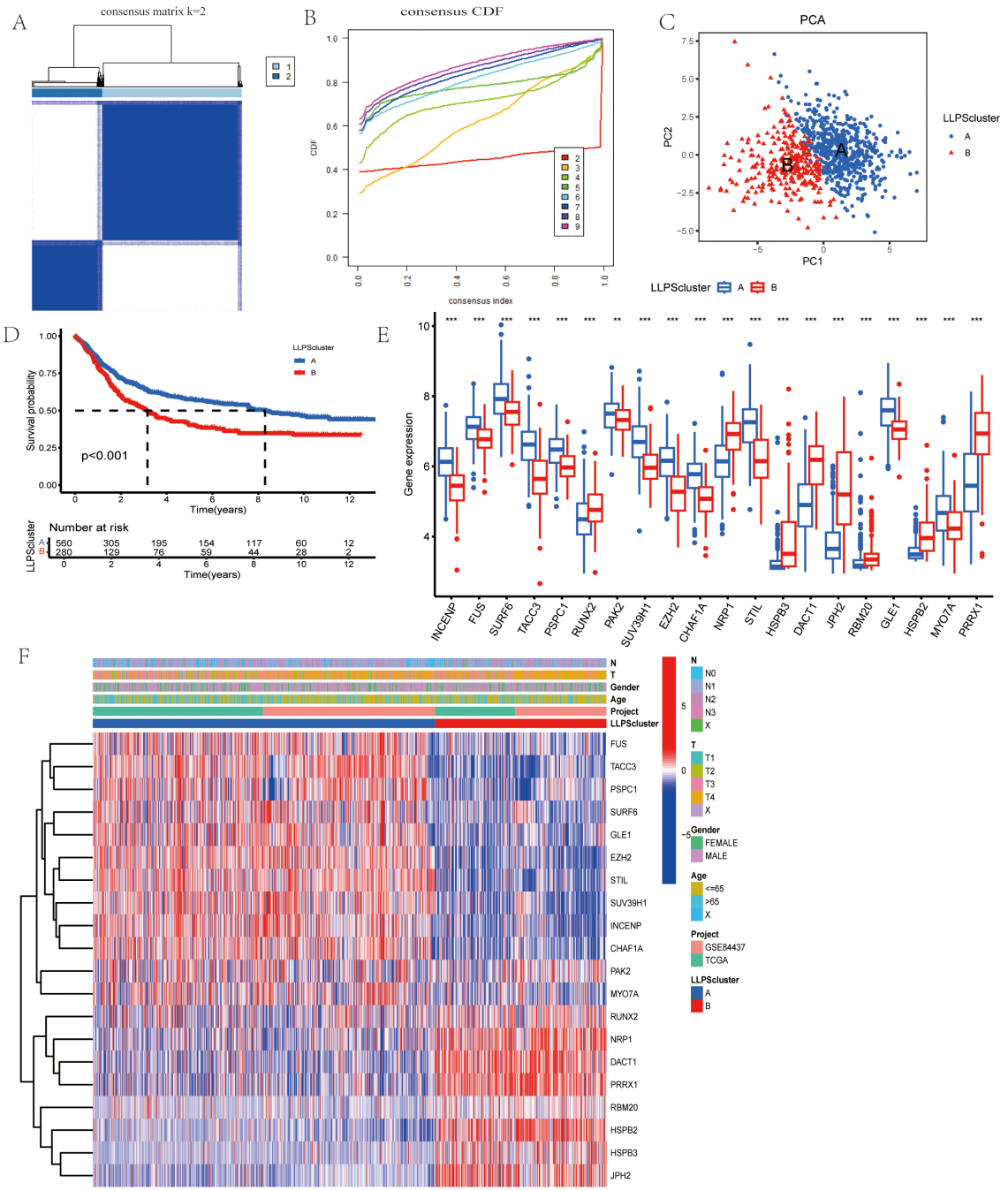

FIGURE 3
Identification of LLPS-related Gene Clusters in Gastric Cancer. **(A)** Consensus matrix showing the similarity, with k=2 indicating the division into two clusters. **(B)** Consensus cumulative distribution function (CDF) illustrating various cluster numbers (k values) to aid in determining the optimal number of clusters. **(C)** PCA of the two clusters. **(D)** Comparison of OS between the two clusters. **(E)** Gene expression boxplot comparing the expression levels of various genes between the two clusters. **(F)** Heatmap for the correlation between clinicopathologic features and the two clusters. **P*<0.05, ***P*<0.01, ****P*<0.001.

The results show that although deep learning and complex feature engineering demonstrate potential in certain aspects, the relatively simple three-gene combination (DACT1+EZH2+PSPC1) combined with the random forest model still achieves the best prediction performance (64.3% accuracy). The Bayesian approach, although slightly less accurate overall, excels in high-confidence prediction, providing an important capability for quantifying uncertainty in clinical applications.

Based on these findings, we further explored the expression patterns and functional significance of LLPS-related genes in gastric cancer. As shown in Supplementary Data 4-9, the differential expression patterns of key LLPS genes in different gastric cancer

stages were confirmed by integrative analysis, validating their potential value as staging prediction biomarkers.

3.3 Tumor–microenvironment features correlated with LLPS clusters

In order to rigorously investigate the contributions of LLPS-related genes to the gastric tumoral milieu, we implemented GSVA analysis. As illustrated in Figure 4A, a substantial enrichment of Cluster B was observed in multiple biological pathways, including muscle contraction, cation channel activity, and transporter activity regulation. In the KEGG Pathway analysis showed that Cluster A and Cluster B exhibited significant results. differences in gene expression. Genes in Cluster A were enriched in pathways connected to cell proliferation and DNA repair, including the "cell cycle" and "genome repair", while genes in Cluster B were enriched in pathways associated with cellular homeostasis, apoptosis, and other metabolic processes (Figure 4B). Moreover, using ssGSEA, Cluster B exhibited higher levels of myeloid-derived suppressor cells (MDSCs), activated B cell, regulatory T cells (Tregs), activated CD8 T cell, and macrophages compared to Cluster A (Figure 4C).

3.4 Construction and validation of the LLPS signature and associated prognostic scoring system

To explore the molecular basis of GC progression, we selected prognostic subtype-associated genes identified by Lasso-based Cox regression (Figures 5A, B). The risk index was created from four gene signatures linked to prognostic subtypes. This prognostic score was calculated using expression profiles of these genes, as explained below:

$$\text{Prognostic score} = 0.140 \times \text{DACT1} + 0.384 \times \text{PAK2} - 0.212 \times \text{EZH2} - 0.307 \times \text{PSPC1}$$

Risk score distribution across LLPS clusters was visualized (Figure 5C). The alluvial diagram showed how gastric cancer patients were allocated between the two LLPS clusters and the two prognostic-score groups (Supplementary Figure 2A). Survival analysis with the Kaplan-Meier method demonstrated significantly worse outcomes for patients in the high prognostic score group compared to those in the low group (Figure 5D). Additionally, the predictive ability of the LLPS-related differentially expressed gene signature was assessed through time-dependent ROC curve analysis, showing strong prognostic accuracy at 1, 3, and 5 years (Figure 5E).

Multivariable stratification of the high-risk group indicated a significant increase in mortality risk, as shown in the survival distribution plot (Figure 6A). In the multivariate Cox regression analysis, LRRS was associated with a hazard ratio of 1.84 (95% CI: 1.468–2.30, $P<0.001$; Figure 6B). The nomogram combined multiple variables, with the risk group serving as an important predictive factor (Figures 6C, D). The heat map revealed distinct expression patterns of the four genes, consistent with the prognostic score (Figure 6E). Moreover, the genes identified earlier were validated in two independent test sets (GSE19826 and GSE79973). The results showed high expression levels of DACT1, PAK2, PSPC1, and EZH2 in GC (Figures 7A, C). The ROC analysis confirmed the predictive power of these genes (Figures 7B, D).

3.5 Comprehensive evaluation of immunological activity and tumor mutational burden across distinct prognostic score categories

Cancer progression and immunotherapy response are heavily influenced by the immune microenvironment. Consequently, our research aimed to analyze the tumor microenvironment pattern among individuals with GC grouped into high- and low-risk categories. We evaluated differences in the immunophenotypic score. The low-risk group demonstrated an elevated immunophenotypic score, suggesting a more promising immunotherapeutic response potential (Figure 8A). The high-risk score group exhibited a strong positive correlation with the inhibitory immune checkpoints HAVCR2 and PDCD1 (Supplementary Figure 3A). The immune cell subpopulation correlation analysis indicated that prototypical immunosuppressive cells, including Tregs, MDSCs, and macrophages, are co-enriched within the high-risk score group, thereby further weakening the antitumor functions of effector T cells and NK cells (Supplementary Figure 3B). The heatmap displayed the distinctions between the two groups of immune cells (Figure 8B). Subsequent mutational profiling of the 20 most frequently altered genes demonstrated a significantly elevated mutational frequency in the low-risk group (Figures 8C, D). By analyzing the gene expression landscape, we determined stromal and immune scores for both cohorts (Figure 8E). A strong positive correlation was observed between the prognostic score and TMB, with significantly higher values in the low-risk cohort relative to the high-risk cohort (Figure 8F). Additionally, we observed that the TIDE score in the high-risk group was notably higher (Figure 8G). DACT1 showed strong positive correlations with Tregs, T helper cells (Th1 and Tfh). Conversely, it showed negative correlations with activated CD4 T cells and CD8 T cells (Figure 9A). EZH2 demonstrated significant positive correlations with activated CD4 T cells, memory B cells, and activated CD8 T cells, while showing negative relationships with monocytes and certain innate immune cells (Figure 9B). PAK2 exhibited prominent positive correlations with central memory CD4 T cells, immature dendritic cells, and plasmacytoid dendritic cells, while showing weak or even negative correlations with activated B cells and mast cells (Figure 9C). PSPC1 showed strong positive correlations with adaptive immune components such as activated CD4 T cells, memory B cells, and activated CD8 T cells, but demonstrates negative correlations with certain myeloid immune cells (such as MDSCs) (Figure 9D).

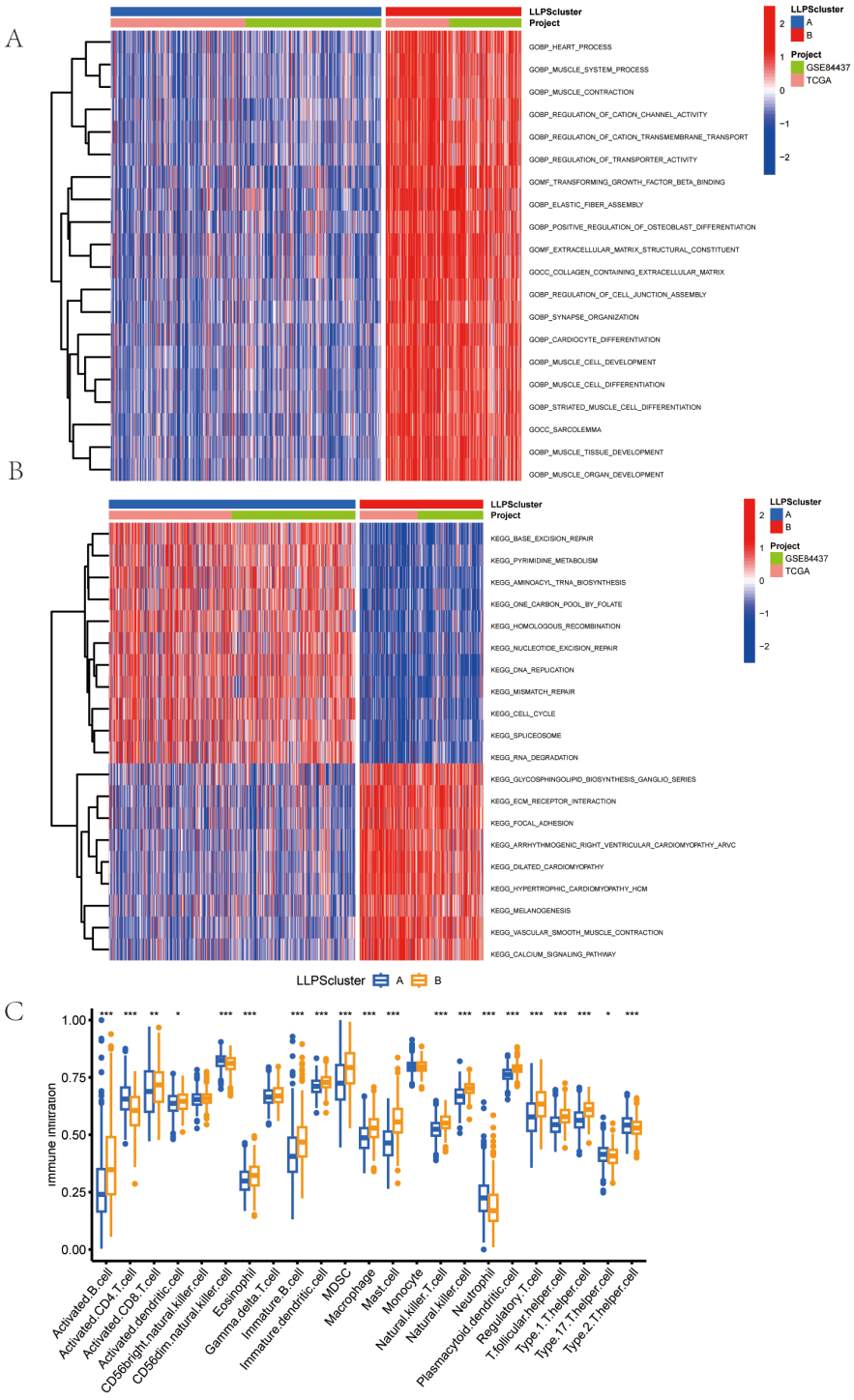

FIGURE 4
Features of the Tumor Microenvironment (TME) in the LLPS Clusters Identified in Gastric Cancer. **(A)** Comparison of the GSVA of Go Gene Ontology (GO) Terms between the two LLPS clusters in GC. **(B)** Comparison of the GSVA of biological pathways between the two LLPS clusters in GC. **(C)** Abundance of 23 infiltrating immune cell types in the two LLPS clusters.

3.6 Gene Expression and CRISPR Functional Dependency

We conducted multi-dimensional analyses focused on four candidate genes-*DACT1, EZH2, PAK2, and PSPC1*. Figure 10 showed the expression levels of these four genes in malignant (red) and normal (blue) tissues across multiple cancer types, including BRCA, COAD, LUAD, and KIRC. EZH2 and PSPC1 were significantly upregulated in the majority of cancers. DACT1 was notably downregulated in several cancer types. PAK2 exhibited

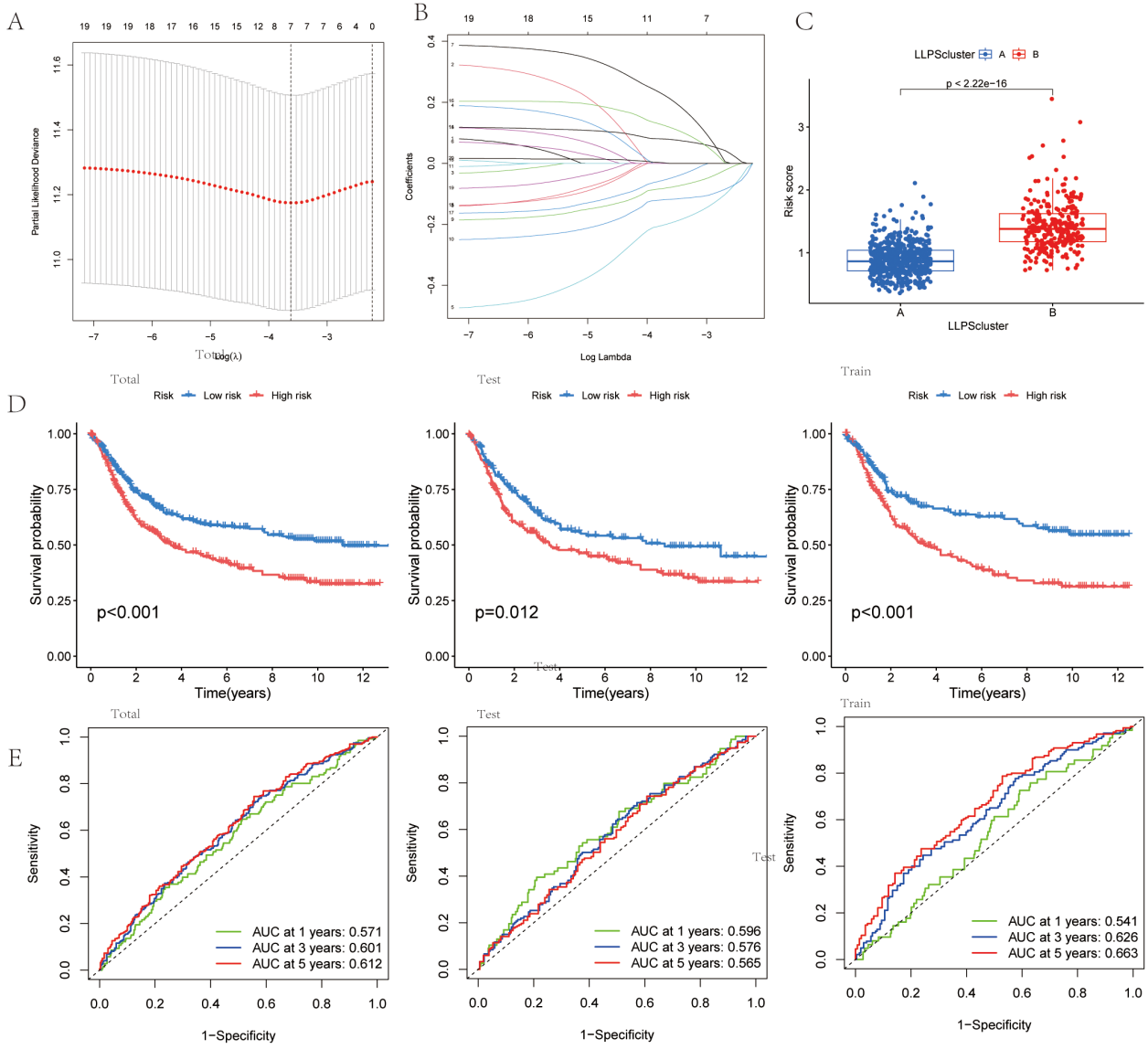

FIGURE 5
Identification of an LLPS-related Differentially Expressed Gene **(DEG)** Signature and Risk Model for Gastric Cancer. **(A)** LASSO regression for 7 candidate genes. **(B)** Cross-validation for 7 OS-related genes in the LASSO regression.**(C)** Risk score in the LLPS clusters.**(D)**Kaplan-Meier curve analysis for OS in total, test,and train Cohort. **(E)** The ROC curve analysis demonstrated the predictive efficiency of the prognostic score in total, test, and train Cohort.

cancer-type specificity: it was distinctly elevated in some cancers while showing no significant difference in others. Figure 11 presented dependency scores from the CERES algorithm-based genome-wide CRISPR knockout data in GC cell lines, indicating that these four genes are important for cancer survival. We used immunohistochemistry (IHC) slides from the Human Protein Atlas database to compare the protein abundance and localization of DACT1, EZH2, PAK2, and PSPC1 in normal and corresponding tumor tissues. DACT1 showed weak to moderate immunoreactivity in normal tissues and no significant change in tumor tissues (Figure 12A). In contrast, EZH2 displayed stronger, more widespread brownish staining in tumor tissues, suggesting overall upregulation in cancer cells (Figure 12B). PAK2 appeared to be expressed at moderate-to-low levels in normal tissues but showed partial elevation in tumor tissues, indicating its potential role in tumorigenesis (Figure 12C). PSPC1 demonstrated prominent staining in tumor tissues, with some regions showing strong positivity (Figure 12D).

3.7 Assessment of anticancer treatment efficacy in cohorts stratified by high versus low prognostic scores

We analyzed the drug responsiveness of groups with high or low prognostic scores to various chemotherapeutic and targeted

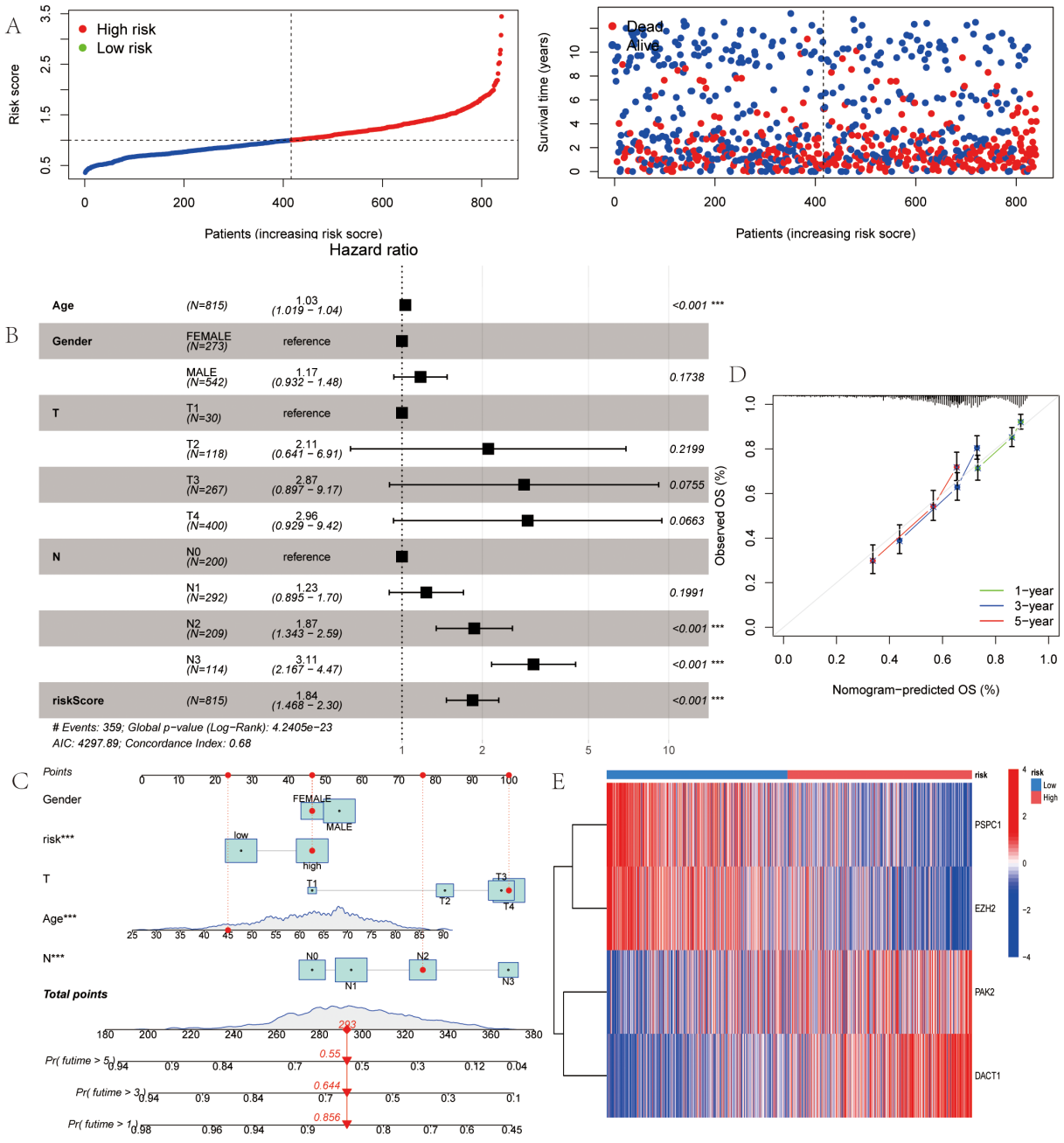

FIGURE 6
LLPS-Associated Risk Scoring System for Gastric Cancer. **(A)** Ranked dot of prognostic score distribution and patient survival status. **(B)** Multivariate independ- ent prgnostic analysis. **(C)** Nomogram was developed by integrating gender age, TNM stage, and LLPS risk. **(D)** Calibration plots to assess the accuracy of nomogram. **(E)** The Heatmap of the expression of the four OS-related genes. *P<0.05, **P<0.01, ***P<0.001.

agents (Figure 13). Boxplots clearly showed that the low score group exhibited heightened sensitivity to 5-Fluorouracil, Cisplatin, Paclitaxel, Oxaliplatin, Lapatinib, Erlotinib, Epirubicin, Galliblocquinazole, and Vinblastine compared with the high prognostic score group (P<0.001). Conversely, the high prognostic score cohort demonstrated increased sensitivity to Doramapimod, NU7441, AZD8055, AZD8186, and BMS-754807 (P<0.001).

3.8 Expression levels of LLPS genes expression in GC cell lines

As described earlier, this novel index was based on four LLPS genes (including DACT1, EZH2, PAK2, and PSPC1). Therefore, we next performed qRT-PCR to determine the mRNA expression levels of these target genes in GES, HGC-27, MKN-45, MKN-74, and AGS cell lines (Figure 14A). The experimental findings were similar to the

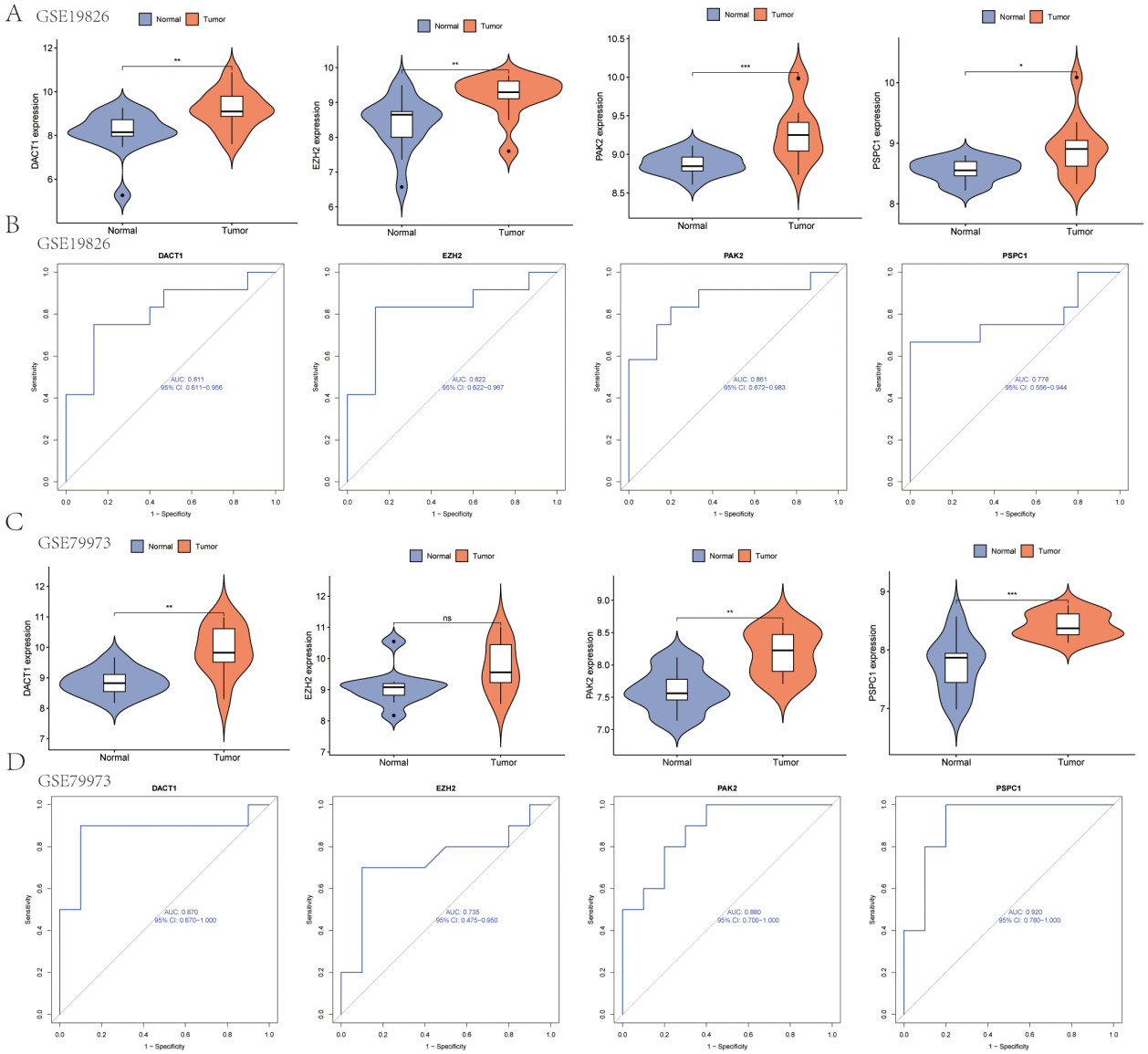

FIGURE 7
Gene Expression Analysis and ROC Curve Comparison in test sets (GSE19826 and GSE79973). **(A)** Expression analysis of the four genes in the GSE19826 data set. **(B)** ROC curve analysis of the four genes in the GSE19826 data set. **(C)** Expression analysis of the four genes in the GSE79973 data set. **(D)** ROC curve analysis of the four genes in the GSE79973 data set. *P<0.05, **P<0.01, ***P<0.001. Ns, Not Significant.

results from GEO and TCGA databases. IF analysis showed the localization of DACT1 and PSPC1 (Figure 14B, C). The Western Blot results demonstrated high protein expression in cancer cell lines (Figure 14D-G). Collectively, these results support the relevance of the identified LLPS genes in gastric cancer (GC) and their potential roles in tumor biology.

3.9 PSPC1 plays an important role in gastric cancer cell proliferation and migration

To verify the functional role of PSPC1 in gastric cancer progression, we performed loss-of-function experiments in two gastric cancer cell lines, HGC-27 and AGS.

First, we designed shRNAs (sh2 and sh3) targeting PSPC1 and established stable knockdown cell lines by lentiviral infection. RT-qPCR assay showed that in HGC-27 cells, both sh2 and sh3 significantly reduced the mRNA expression level of PSPC1 (**P < 0.01) (Figure 15A); in AGS cells, both shRNAs similarly effectively inhibited PSPC1 expression (***P <0.001) (Figure 15B). Western blot analysis further confirmed the knockdown effect at the protein level (Figure 15C, D). Based on the knockdown efficiency, we selected sh3 for subsequent functional experiments. To assess the effect of PSPC1 on cell proliferation, we performed CCK-8 and clone formation assays. CCK-8 results showed that PSPC1 knockdown significantly inhibited the proliferative ability of both gastric cancer cells. In HGC-27 cells, the difference in proliferation between the knockdown group and the control group reached a

10.3389/fimmu.2025.1620390

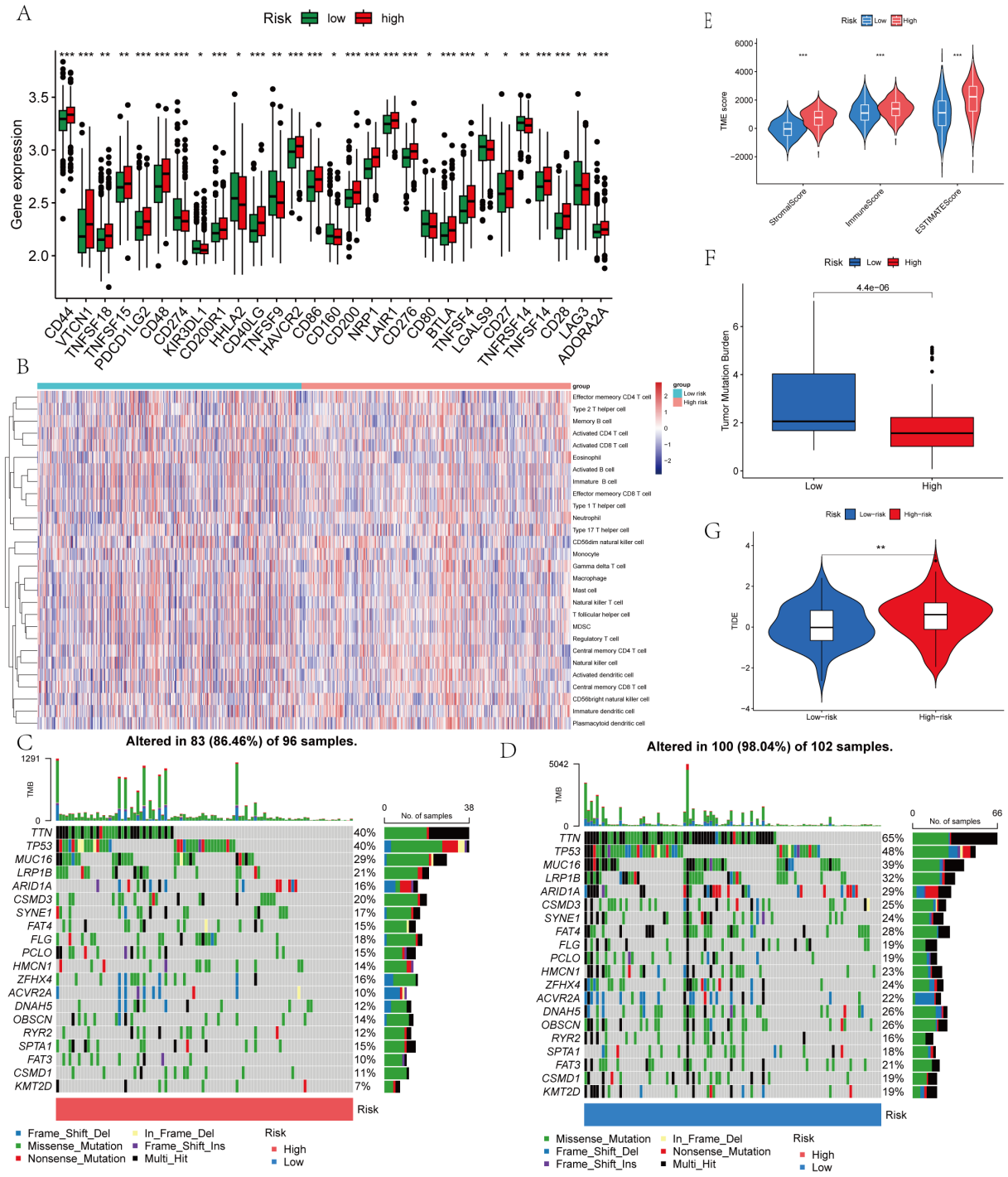

FIGURE 8
Immune Microenvironment and Tumor Mutational Burden (TMB) of Gastric Cancer Tissues with Different LLPS-Associated Prognostic Scores. **(A)** Expression levels of immune checkpoint genes of the two risk groups. **(B)** Correlation between LRRS and immune checkpoint genes. **(C)** The mutation frequency of the top 20 genes in the low LRRS group. **(D)** The mutation frequency of the top 20 genes in the high LRRS group. **(E)** TME score of the two risk groups. **(F)** TMB of the two risk groups. **(G)** TIDE of the two risk groups. *P<0.05, **P<0.01, ***P<0.001.

significant level at 48 hours of culture (***P<0.001) (Figure 15E); in AGS cells, this inhibition was more pronounced, with the proliferative capacity of the knockdown group decreasing to approximately 50% of that of the control group at 72 hours (***P<0.001) (Figure 15F). Clone formation assays further supported this finding: the number of clones formed in HGC-27 and AGS cells significantly decreased from approximately 400 and 300 to less than 100 after PSPC1 knockdown, respectively

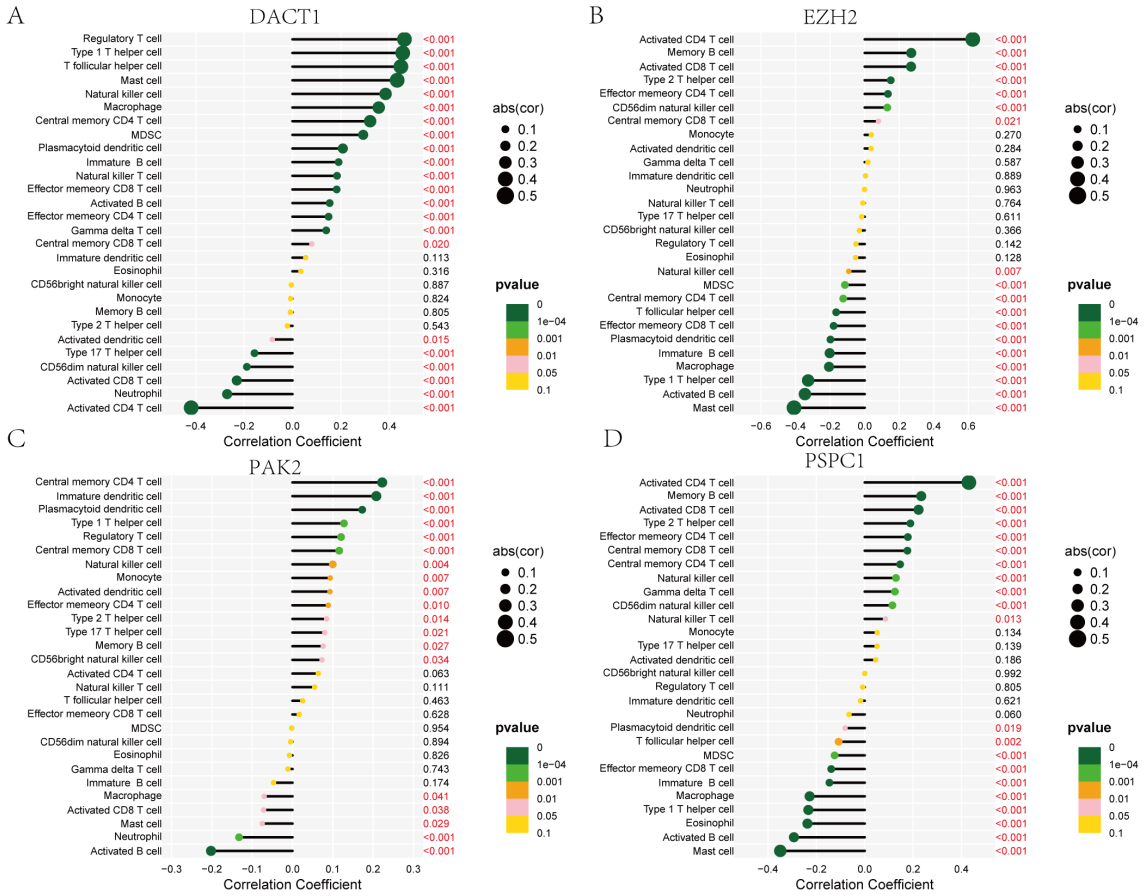

FIGURE 9
Correlation Analysis of DACT1, EZH2, PAK2, and PSPC1 with Immune Cell Types. **(A)** DACT1 with each type of infiltrating immune cell. **(B)** EZH2 with each type of infiltrating immune cell. **(C)** PAK2 with each type of infiltrating immune cell. **(D)** PSPC1with each type of infiltrating immune cell.

(****P<0.0001) (Figure 15G), suggesting that PSPC1 has an important role in the long-term proliferative capacity of gastric cancer cells.

In addition, we evaluated the effect of PSPC1 on cell migration ability by scratch healing assay. The results showed that PSPC1 knockdown significantly inhibited the migration ability of AGS cells.At each time point of 24, 48 and 72 hours, the migration area of the sh3 group was significantly lower than that of the control group (****P < 0.0001). In particular, at 72 hours, the scratches in the control group were essentially healed (100% of the migrated area), whereas the knockdown group migrated only about 50% (Figure 15H).

Taken together, these results indicate that PSPC1 plays an important role in promoting the proliferation and migration of gastric cancer cells, suggesting that it may act as a promoter of gastric cancer progression.

4 Discussion

Recent studies have shown that tumorigenesis and development are closely related to gene mutation, amplification, epigenetic abnormalities and signaling pathway imbalance (24, 25), in which LLPS plays an important role (26). In this study, the expression and mutation patterns of LLPS-related genes in gastric cancer were systematically analyzed for the first time, and gastric cancer patients were classified into two LLPS subtypes with different prognoses, clinicopathological features, and immune infiltration patterns by unsupervised clustering. A four-gene risk score model (LRRS) containing *DACT1, PAK2, EZH2, and PSPC1* was further constructed, which was significantly associated with patient survival, clinical features, and genomic alterations.

The four prognostic genes include two scaffold genes and two client genes. DACT1 showed heterogeneity in different tumors: it was downregulated in bladder (27), breast (28), and cervical (29) cancers and upregulated in colon and squamous cancers (30, 31). In the present study, DACT1 was found to be highly expressed in gastric cancer cells, suggesting its unique role in gastric cancer. PSPC1 is involved in RNA processing and transcriptional regulation, and is a key component of parafollicular plaque formation (32), which promotes the formation of intracellular LLPS structures by binding RNA (33). Although PSPC1 is associated with cell proliferation and metastasis in a variety of tumors (34–36), its specific mechanism in gastric cancer has not been previously elucidated. In the present study, we confirmed the critical role of PSPC1 in gastric cancer progression by functional

10.3389/fimmu.2025.1620390

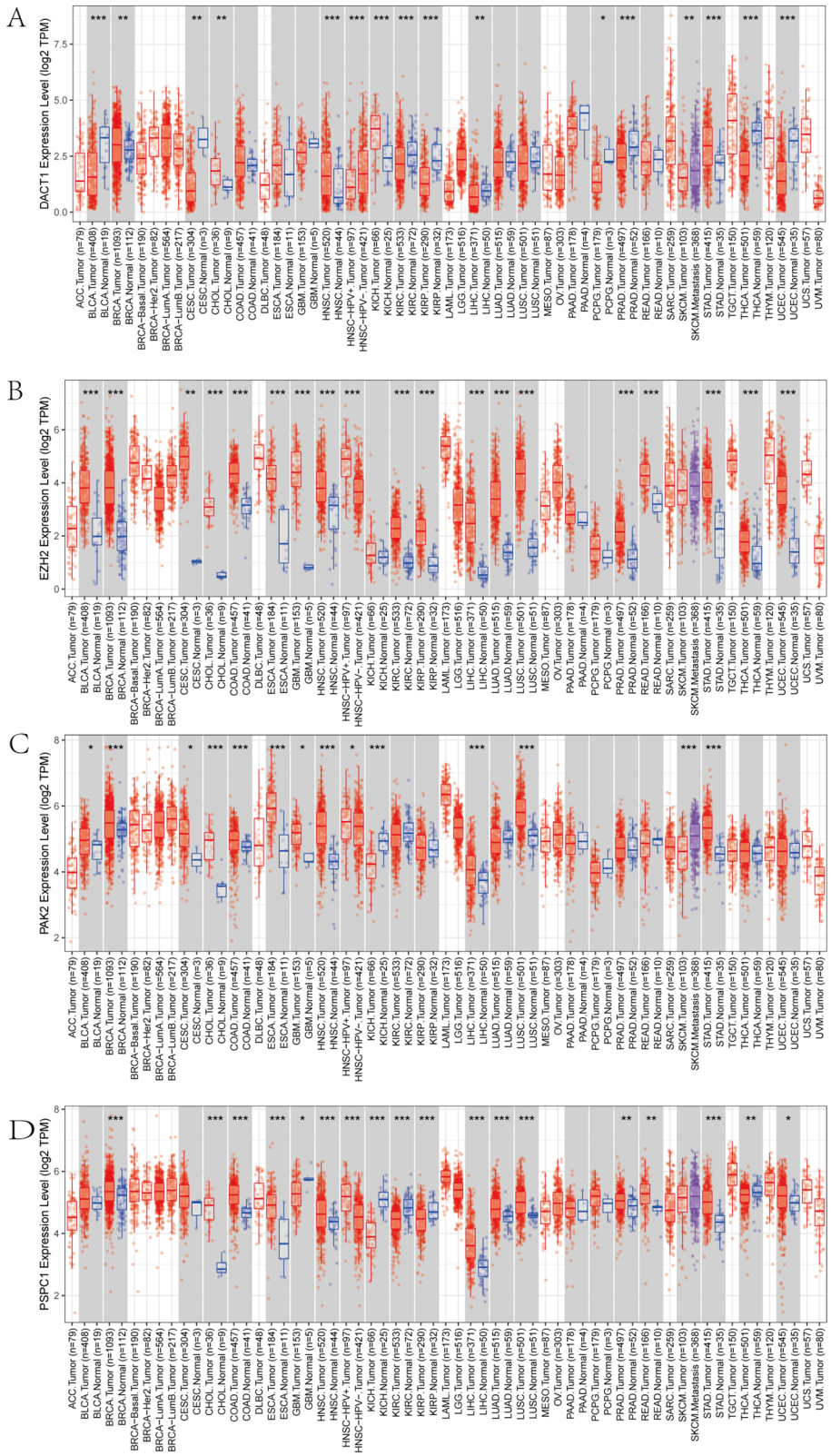

FIGURE 10
(A-D) Pan-cancer Analysis of Gene Expression Differences: DACT1, EZH2, PAK2, and PSPC1. **P*<0.05, ***P*<0.01, ****P*<0.001.

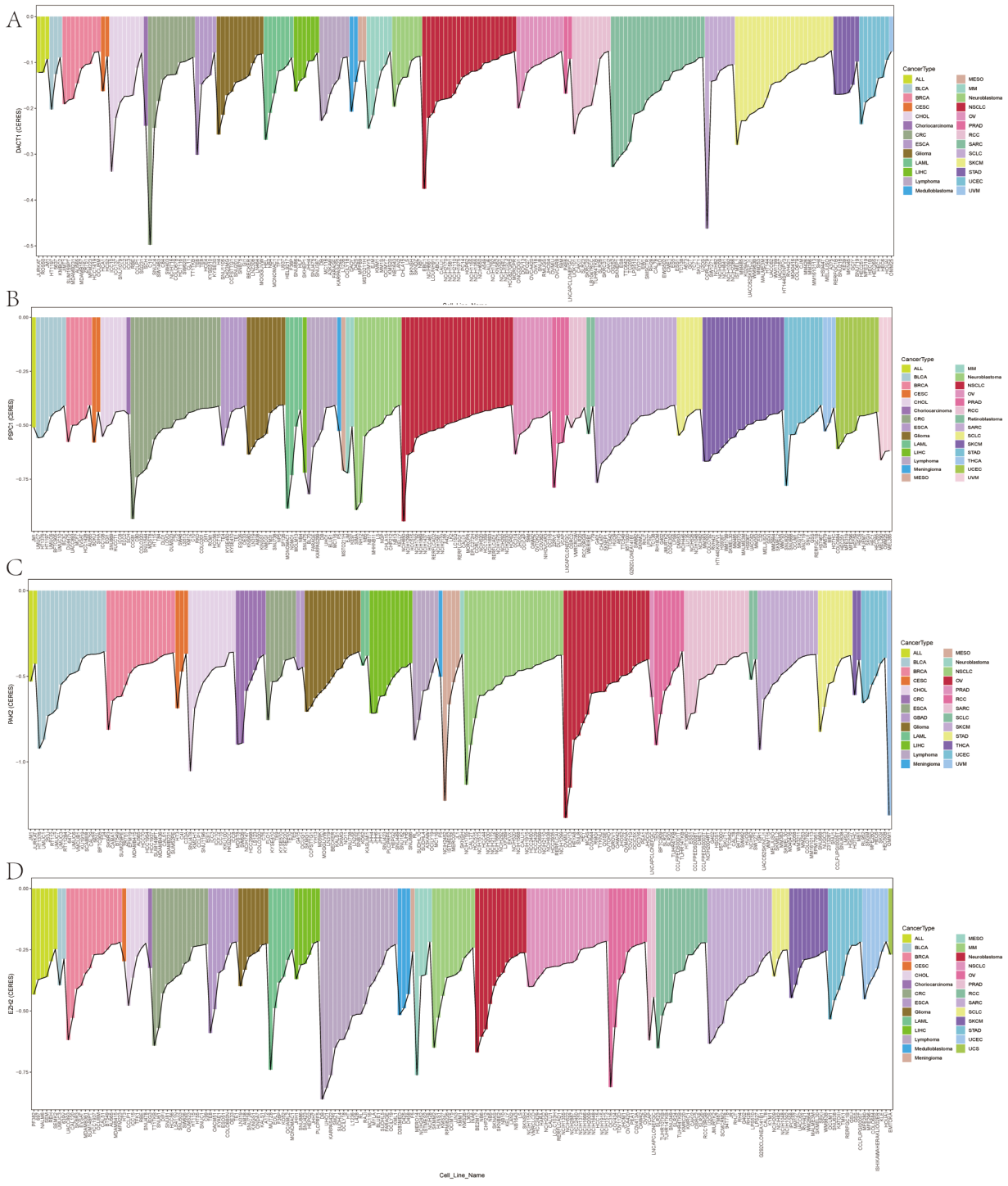

FIGURE 11
(A-D) Genome-Wide CRISPR Screening Dependency Scores in Gastric Cancer Using CERES Algorithm.

experiments, which is consistent with its report of promoting malignant phenotypes in other tumors (37–41), suggesting that PSPC1 may be involved in gastric cancer development by influencing the LLPS process, providing a theoretical basis for the development of targeted therapeutic strategies against PSPC1. EZH2, as an epigenetic regulator, affects gene expression by regulating histone methylation, and promotes tumor growth, metastasis, and drug resistance in a variety of malignancies (42, 43).In this study, we confirmed that EZH2 is highly expressed in gastric cancer, and CERES algorithm analysis showed that several gastric cancer cell lines were highly dependent on EZH2, supporting its potential as a therapeutic target. PAK2 is involved in cytoskeletal remodeling, migration, and cell cycle regulation, and in lung squamous carcinoma, it promotes proliferation and invasion

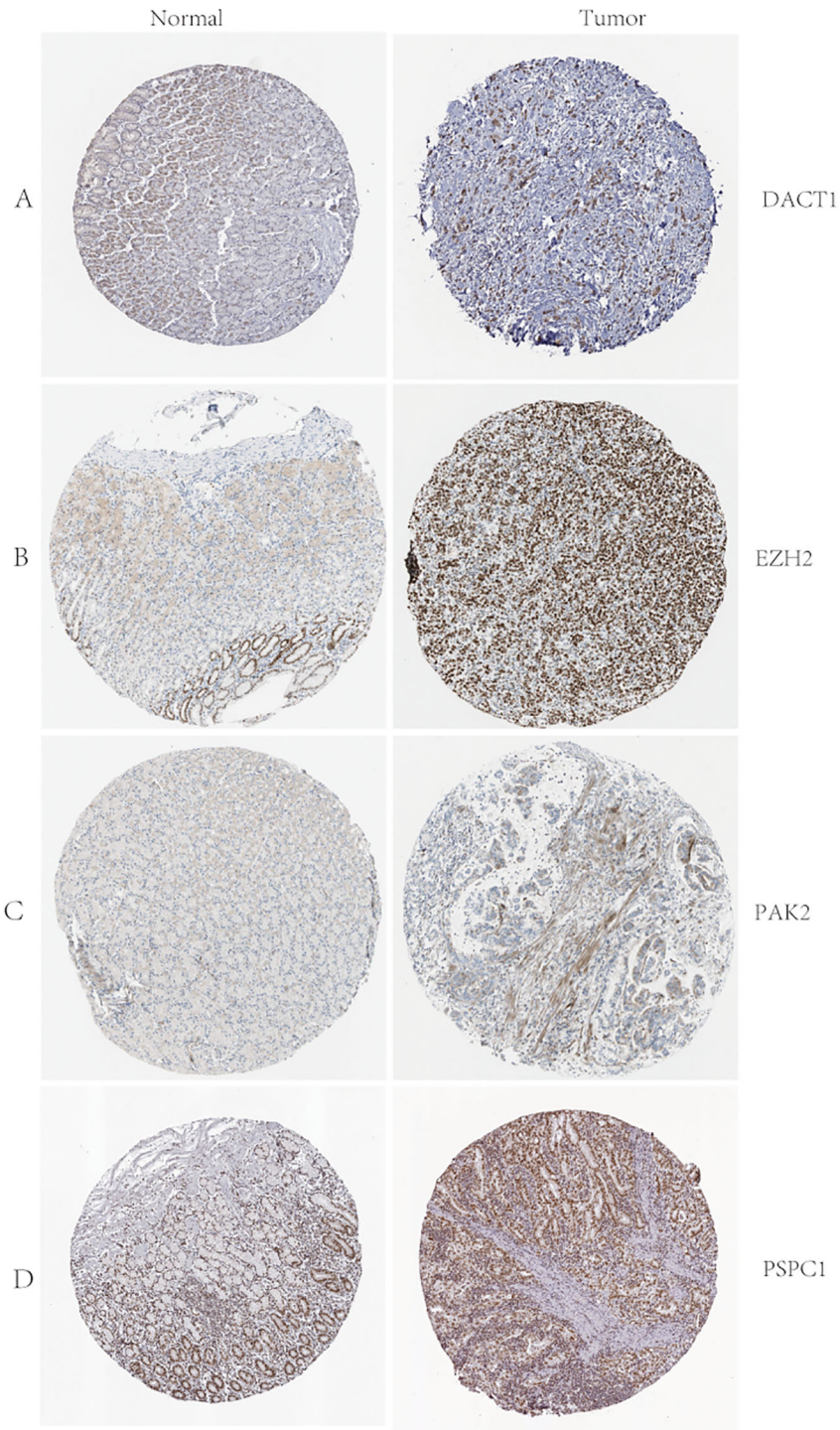

FIGURE 12
(A-D) D ACT1, EZH2, PAK2, and PSPC1 Protein Expression in Normal and Tumor Tissues: Immunohistochemistry Analysis from the Human Protein Atlas.

(44).We found that PAK2 was generally upregulated in gastric cancer tissues and highly dependent on it in certain cell lines, consistent with its critical role in maintaining tumor cell function.

Tumorigenesis is affected by both genetic mutations and immune dysregulation (45, 46).The high LRRS group showed a complex immune profile: increased immune cell infiltration, elevated stromal scores, immunity scores, and ESTIMATE scores, but greater immunosuppression. Genomic analysis revealed that TTN mutations induced CD8+ and CD4+ T cell infiltration (47); TP53 mutations affected cell cycle and DNA repair and remodeled the immune microenvironment (48); MUC16 mutations increased neoantigen production but may inhibit NK cell killing (49, 50); and ARID1A mutations regulated the tumor inflammatory

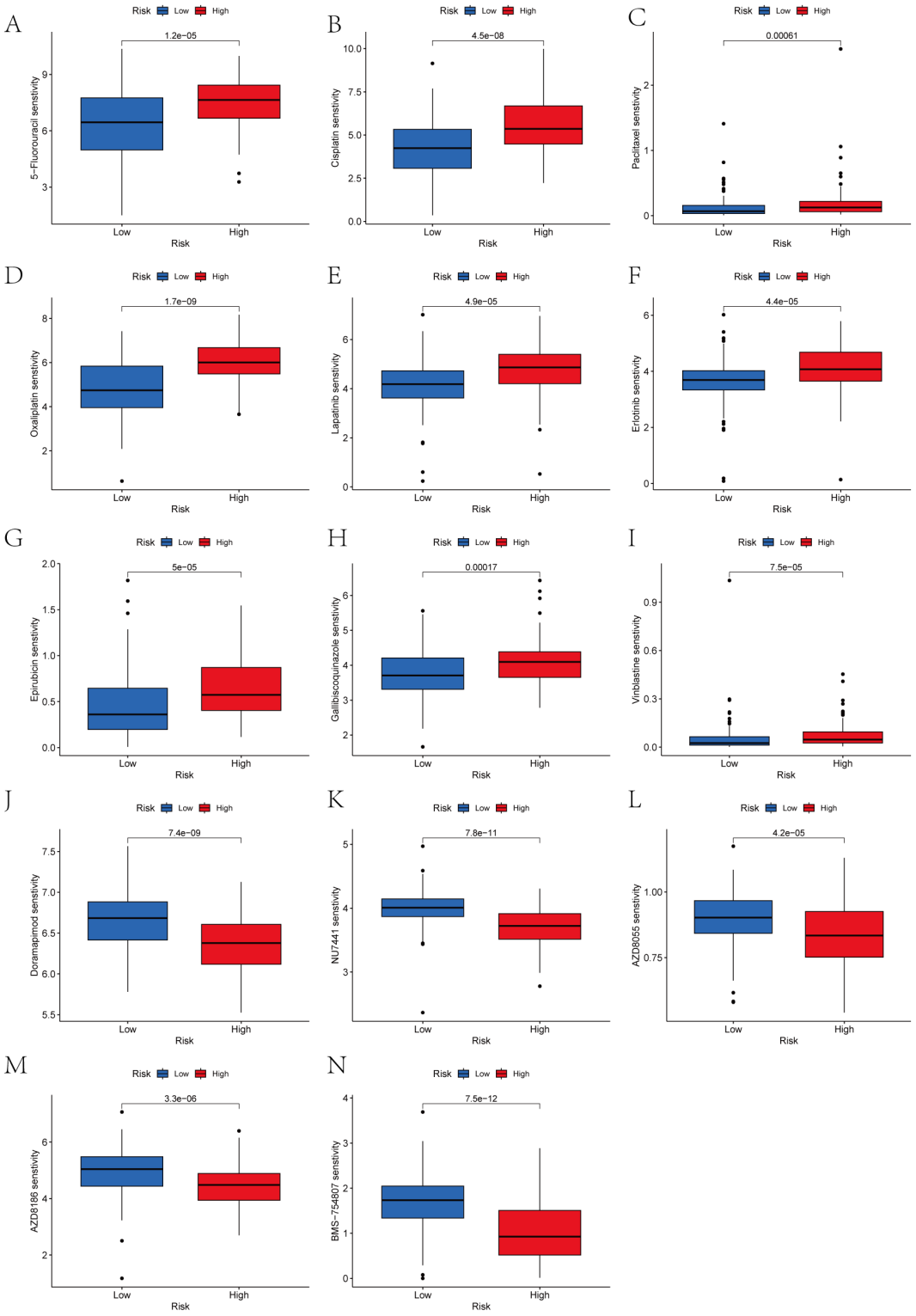

FIGURE 13
(A-N) Drug sensitivity analysis in gastric cancer: risk group comparison.

microenvironment and may enhance immunotherapy sensitivity (51). Low-risk groups may have more "benign" mutations, and high mutation loads enhance tumor antigenicity, promote immune recognition, and improve prognosis.

Drug sensitivity analysis revealed therapeutic strategies for different prognostic groups.The low-scoring group was more sensitive to first-line chemotherapeutic agents such as 5-fluorouracil, cisplatin, paclitaxel, oxaliplatin, and epirubicin

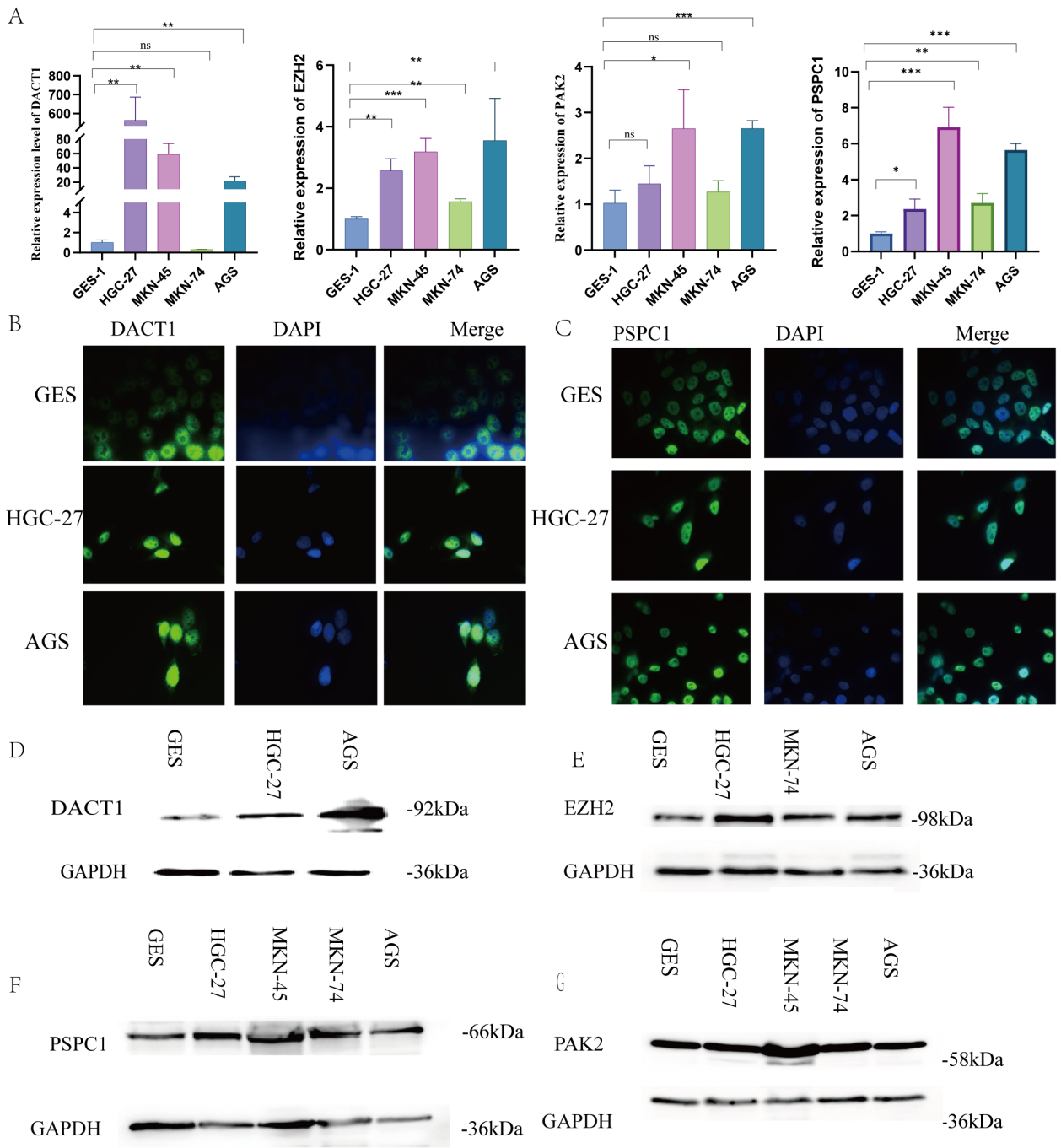

FIGURE 14
Verification Expression Levels of LLPS Genes Expression in GC Cell Lines. **(A)** The relative expression levels of DACT1, EZH2, PSPC, and PAK2 mRNA. **(B)** Immunofluorescence of DACT1. **(C)** Immunofluorescence of PSPC1. **(D-F)** Western Blot of DACT1, EZH2, PAK2 and PSPC1.***P* < 0.01, ****P* < 0.001. Ns: Not Significant.

(p<0.001) (52), as well as responded well to HER2/EGFR-targeted agents such as lapatinib and erlotinib, which was consistent with the results of clinical trials in HER2-positive or EGFR-highly-expressed gastric cancer (53, 54). The high-scoring group, on the other hand, was more sensitive to novel kinase inhibitors such as Doramapimod (p38 MAPK inhibitor), NU7441 (DNA-PK inhibitor), and AZD8055 (mTOR inhibitor) (55–57), which provides a rationale for individualized treatment.

In this study, LLPS gene was firstly used as a prognostic marker for gastric cancer, and its biological mechanism, immune characteristics and mutation spectrum were systematically explored, which provided a new idea for clinical individualized treatment.However, the study still has limitations: clinical samples are needed for further validation; the specific mechanisms of the four risk genes in LLPS and their interrelationships need to be explored in depth.Nevertheless, this study provides important candidate

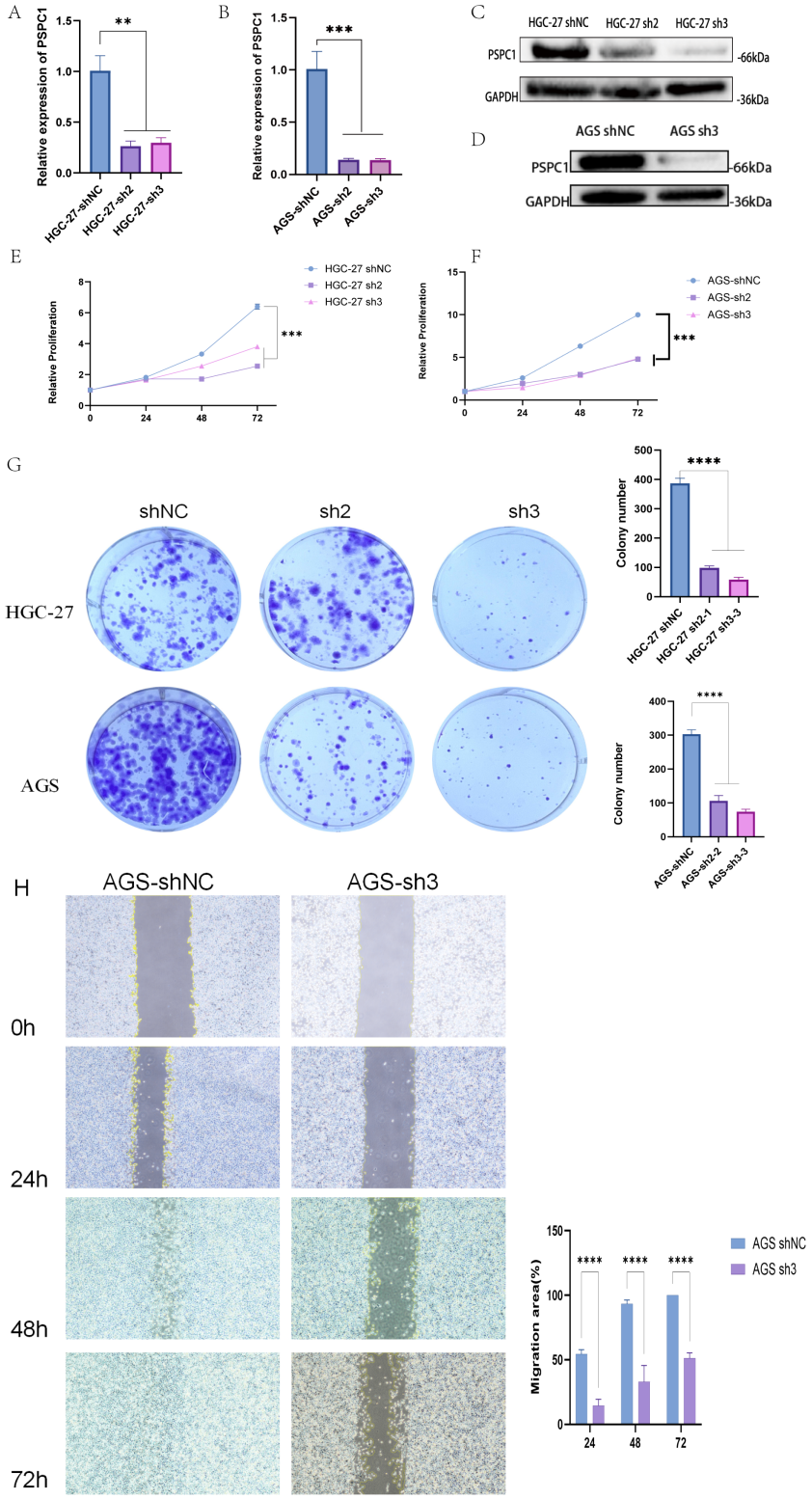

FIGURE 15
PSPC1 silencing inhibits the proliferation of GC *in vitro*. **(A)** RT-PCR verified the expression of depleted PSPC1 in the HGC-27. **(B)** RT-PCR verified the expression of depleted PSPC1 in the AGS. **(C)** Western blot showing depleted PSPC1 expression by two independent shRNA (sh2 and sh3) in HGC-27. **(D)** Western blot showing depleted PSPC1 expression by shRNA (sh3) in AGS. **(E)** Proliferation rates of PSPC1-depleted cells assessed by CCK8 assay in HGC-27. **(F)** Proliferation rates of PSPC1-depleted cells assessed by CCK8 assay in AGS. **(G)** Colony formation assay was performed on HGC-27 and AGS cells treated with PSPC1 silencing to validate the growth ability of the indicated cells *in vitro*. **(H)** Representative images and quantitative analysis of wound healing assay of AGS cells transfected with shRNA (sh3) and vector. $^{**}P < 0.01$, $^{***}P < 0.001$, $^{****}P < 0.0001$.

molecules for prognostic assessment and therapeutic target development in gastric cancer.

5 Conclusion

In conclusion, our research identified 20 genes related to LLPS that are linked to the prognosis of GC patients. By utilizing these genes, we effectively categorized patients into two distinct subtypes, which have different pathway activity, prognosis, clinicopathological features and immune cell infiltration. In addition,we created a prognostic model based on four of LLPS genes. Our results indicate that integrating scores based on LLPS genes applied in clinical practice could serve as a valuable instrument for predicting GC prognosis.

Data availability statement

The datasets presented in this study can be found in online repositories. The names of the repository/repositories and accession number(s) can be found in the article.

Ethics statement

Ethical approval and written informed consent were not required for the studies on humans because only commercially available cell lines were used.

Author contributions

XW: Conceptualization, Investigation, Data curation, Writing – review & editing, Formal analysis, Methodology, Writing – original draft. MC: Data curation, Writing – review & editing, Software. JZ: Writing – review & editing, Funding acquisition, Validation. HH: Writing – review & editing, Supervision, Funding acquisition, Validation, Visualization.

Funding

The author(s) declare financial support was received for the research and/or publication of this article. This research was funded by research grants from the National Natural Science Foundation of China [No.82060442], Natural Science Foundation of Hunan Province [NO.2023JJ30856] and Grant from Key Lab for Chronic Disease Biomarkers of Guizhou Medical University [No.2024fy004].

Acknowledgments

We express our gratitude to the staff members of the Cancer Genome Atlas for their valuable contribution to the cBioPortal for Cancer Genomics Program.

Conflict of interest

The authors declare that the research was conducted in the absence of any commercial or financial relationships that could be construed as a potential conflict of interest.

Generative AI statement

The author(s) declare that no Generative AI was used in the creation of this manuscript.

Any alternative text (alt text) provided alongside figures in this article has been generated by Frontiers with the support of artificial intelligence and reasonable efforts have been made to ensure accuracy, including review by the authors wherever possible. If you identify any issues, please contact us.

Publisher's note

Supplementary material

The Supplementary Material for this article can be found online at: https://www.frontiersin.org/articles/10.3389/fimmu.2025.1620390/full#supplementary-material

References

1. Sung H, Ferlay J, Siegel RL, Laversanne M, Soerjomataram I, Jemal A, et al. Global cancer statistics 2020: GLOBOCAN estimates of incidence and mortality worldwide for 36 cancers in 185 countries. *CA Cancer J Clin*. (2021) 71:209–49. doi: 10.3322/caac.21660

2. Qiu H, Cao S, Xu R. Cancer incidence, mortality, and burden in China: a time-trend analysis and comparison with the United States and United Kingdom based on the global epidemiological data released in 2020. *Cancer Commun (Lond)*. (2021) 41:1037–48. doi: 10.1002/cac2.12197

3. Li Y, Feng A, Zheng S, Chen C, Lyu J. Recent estimates and predictions of 5-year survival in patients with gastric cancer: A model-based period analysis. *Cancer Control*. (2022) 29:10732748221099227. doi: 10.1177/10732748221099227

4. Zheng LW, Liu CC, Yu KD. Phase separations in oncogenesis, tumor progressions and metastasis: a glance from hallmarks of cancer. *J Hematol Oncol*. (2023) 16:123. doi: 10.1186/s13045-023-01522-5

5. Alberti S, Gladfelter A, Mittag T. Considerations and challenges in studying liquid-liquid phase separation and biomolecular condensates. *Cell*. (2019) 176:419–34. doi: 10.1016/ j.cell. 2018. 12.035

6. Fan XJ, Wang YL, Zhao WW, Bai SM, Ma Y, Yin XK, et al. NONO phase separation enhances DNA damage repair by accelerating nuclear EGFR-induced DNA-PK activation. *Am J Cancer Res*. (2021) 11:2838–52.

7. Molliex A, Temirov J, Lee J, Coughlin M, Kanagaraj AP, Kim HJ, et al. Phase separation by low complexity domains promotes stress granule assembly and drives pathological fibrillization. *Cell*. (2015) 163:123–33. doi: 10.1016/j.cell.2015.09.015

8. Grabarz A, Barascu A, Guirouilh-Barbat J, Lopez BS. Initiation of DNA double strand break repair: signaling and single-stranded resection dictate the choice between homologous recombination, non-homologous end-joining and alternative end-joining. *Am J Cancer Res*. (2012) 2:249–68.

9. Liu Q, Li J, Zhang W, Xiao C, Zhang S, Nian C, et al. Glycogen accumulation and phase separation drives liver tumor initiation. *Cell*. (2021) 184:5559–76.e19. doi: 10.1016/j.cell.2021.10.001

10. Su X, Ditlev JA, Hui E, Xing W, Banjade S, Okrut J, et al. Phase separation of signaling molecules promotes T cell receptor signal transduction. *Science*. (2016) 352:595–9. doi: 10.1126/science.aad9964

11. Woo SR, Fuertes MB, Corrales L, Spranger S, Furdyna MJ, Leung MY, et al. STING-dependent cytosolic DNA sensing mediates innate immune recognition of immunogenic tumors. *Immunity*. (2014) 41:830–42. doi: 10.1016/j.immuni.2014.10.017

12. Deng L, Liang H, Xu M, Yang X, Burnette B, Arina A, et al. STING-dependent cytosolic DNA sensing promotes radiation-induced type I interferon-dependent antitumor immunity in immunogenic tumors. *Immunity*. (2014) 41:843–52. doi: 10.1016/j.immuni.2014.10.019

13. Jiang Y, Lei G, Lin T, Zhou N, Wu J, Wang Z, et al. 1,6-Hexanediol regulates angiogenesis via suppression of cyclin A1-mediated endothelial function. *BMC Biol*. (2023) 21:75. doi: 10.1186/s12915-023-01580-8

14. Shi Y, Liao Y, Liu Q, Ni Z, Zhang Z, Shi M, et al. BRD4-targeting PROTAC as a unique tool to study biomolecular condensates. *Cell Discov*. (2023) 9:47. doi: 10.1038/s41421-023-00544-0

15. Nakamura T, Hipp C, Santos Dias Mourão A, Borggräfe J, Aldrovandi M, Henkelmann B, et al. Phase separation of FSP1 promotes ferroptosis. *Nature*. (2023) 619:371–7. doi: 10.1038/s41586-023-06255-6

16. Lu Y, Wu T, Gutman O, Lu H, Zhou Q, Henis YI, et al. Phase separation of TAZ compartmentalizes the transcription machinery to promote gene expression. *Nat Cell Biol*. (2020) 22:453–64. doi: 10.1038/s41556-020-0485-0

17. Ahn JH, Davis ES, Daugird TA, Zhao S, Quiroga IY, Uryu H, et al. Phase separation drives aberrant chromatin looping and cancer development. *Nature*. (2021) 595:591–5. doi: 10.1038/s41586-021-03662-5

18. You K, Huang Q, Yu C, Shen B, Sevilla C, Shi M, et al. PhaSepDB: a database of liquid-liquid phase separation related proteins. *Nucleic Acids Res*. (2020) 48:D354–d9. doi: 10.1093/nar/gkz847

19. Tsiliki G, Munteanu CR, Seoane JA, Fernandez-Lozano C, Sarimveis H, Willighagen EL. RRegrs: an R package for computer-aided model selection with multiple regression models. *J Cheminform*. (2015) 7:46. doi: 10.1186/s13321-015-0094-2

20. Emura T, Matsui S, Chen HY. compound. *Cox: Univariate feature selection compound covariate predicting survival. Comput Methods Programs BioMed*. (2019) 168:21–37. doi: 10.1016/j.cmpb.2018.10.020

21. Yeh CT, Liao GY, Emura T. Sensitivity analysis for survival prognostic prediction with gene selection: A copula method for dependent censoring. *Biomedicines*. (2023) 11:797. doi: 10.3390/biomedicines11030797

22. Yang W, Soares J, Greninger P, Edelman EJ, Lightfoot H, Forbes S, et al. Genomics of Drug Sensitivity in Cancer (GDSC): a resource for therapeutic biomarker discovery in cancer cells. *Nucleic Acids Res*. (2013) 41:D955–61. doi: 10.1093/nar/gks1111

23. Meyers RM, Bryan JG, McFarland JM, Weir BA, Sizemore AE, Xu H, et al. Computational correction of copy number effect improves specificity of CRISPR-Cas9 essentiality screens in cancer cells. *Nat Genet*. (2017) 49:1779–84. doi: 10.1038/ng.3984

24. Sanjeevaiah A, Cheedella N, Hester C, Porembka MR. Gastric cancer: recent molecular classification advances, racial disparity, and management implications. *J Oncol Pract*. (2018) 14:217–24. doi: 10.1200/JOP.17.00025

25. Machlowska J, Baj J, Sitarz M, Maciejewski R, Sitarz R. Gastric cancer: epidemiology, risk factors, classification, genomic characteristics and treatment strategies. *Int J Mol Sci*. (2020) 21:4012. doi: 10.3390/ijms21114012

26. Nozawa RS, Yamamoto T, Takahashi M, Tachiwana H, Maruyama R, Hirota T, et al. Nuclear microenvironment in cancer: Control through liquid-liquid phase separation. *Cancer Sci*. (2020) 111:3155–63. doi: 10.1111/cas.14551

27. Cheng H, Deng Z, Wang Z, Zhang W, Su J. The role of aberrant promoter hypermethylation of DACT1 in bladder urothelial carcinoma. *J BioMed Res*. (2012) 26:319–24. doi: 10.7555/JBR.26.20110099

28. Yin X, Xiang T, Li L, Su X, Shu X, Luo X, et al. DACT1, an antagonist to Wnt/β-catenin signaling, suppresses tumor cell growth and is frequently silenced in breast cancer. *Breast Cancer Res*. (2013) 15:R23. doi: 10.1186/bcr3399

29. Shi X, Huo J, Gao X, Cai H, Zhu W. A newly identified lncRNA H1-AS1 targets DACT1 to inhibit cervical cancer via sponging miR-324-3p. *Cancer Cell Int*. (2020) 20:358. doi: 10.1186/s12935-020-01385-7

30. Ghasemian M, Rajabibazl M, Poodineh J, Sadeghi H, Razavi AE, Mirfakhraie R. Different expression of DACT1, DACT2, and CYCLIN D1 genes in human colorectal cancer tissues and its association with clinicopathological characteristics. *Nucleosides Nucleotides Nucleic Acids*. (2024) 43:203–13. doi: 10.1080/15257770.2023.2249052

31. Hou J, Li EM, Shen JH, Qing Z, Wu ZY, Xu XE, et al. Cytoplasmic HDPR1 is involved in regional lymph node metastasis and tumor development via beta-catenin accumulation in esophageal squamous cell carcinoma. *J Histochem Cytochem*. (2011) 59:711–8. doi: 10.1369/0022155411409941

32. Takeiwa T, Ikeda K, Horie K, Inoue S. Role of RNA binding proteins of the Drosophila behavior and human splicing (DBHS) family in health and cancer. *RNA Biol*. (2024) 21:1–17. doi: 10.1080/15476286.2024.2332855

33. Li J, Cui P, Sun Q, Du Z, Chen Z, Li Z, et al. PSPC1 regulates CHK1 phosphorylation through phase separation and participates in mouse oocyte maturation. *Acta Biochim Biophys Sin (Shanghai)*. (2021) 53:1527–37. doi: 10.1093/abbs/gmab123

34. Lemster AL, Weingart A, Bottner J, Perner S, Sailer V, Offermann A, et al. Elevated PSPC1 and KDM5C expression indicates poor prognosis in prostate cancer. *Hum Pathol*. (2023) 138:1–11. doi: 10.1016/j.humpath.2023.05.007

35. He H, Zhang L, Lin K, Huang Z, Zhou Y, Lin S, et al. The prognosis value of PSPC1 expression in nasopharyngeal cancer. *Cancer Manag Res*. (2021) 13:3281–91. doi: 10.2147/CMAR.S300567

36. Takeiwa T, Ikeda K, Suzuki T, Sato W, Iino K, Mitobe Y, et al. PSPC1 is a potential prognostic marker for hormone-dependent breast cancer patients and modulates RNA processing of ESR1 and SCFD2. *Sci Rep*. (2022) 12:9495. doi: 10.1038/s41598-022-13601-7

37. Hong J, Sui P, Li Y, Xu KY, Lee JH, Wang J, et al. PSPC1 exerts an oncogenic role in AML by regulating a leukemic transcription program in cooperation with PU. *1. Cell Stem Cell*. (2025) 32:463–78.e6. doi: 10.1016/j.stem.2025.01.010

38. Fox AH, Nakagawa S, Hirose T, Bond CS. Paraspeckles: where long noncoding RNA meets phase separation. *Trends Biochem Sci*. (2018) 43:124–35. doi: 10.1016/j.tibs.2017.12.001

39. Szabó AL, Sánta A, Pancsa R, Gáspári Z. Charged sequence motifs increase the propensity towards liquid-liquid phase separation. *FEBS Lett*. (2022) 596:1013–28. doi: 10.1002/1873-3468.14294

40. Zhao J, Xie W, Yang Z, Zhao M, Ke T, Xu C, et al. Identification and characterization of a special type of subnuclear structure: AGGF1-coated paraspeckles. *FASEB J*. (2022) 36:e22366. doi: 10.1096/fj.202101690RR

41. Shao W, Bi X, Pan Y, Gao B, Wu J, Yin Y, et al. Phase separation of RNA-binding protein promotes polymerase binding and transcription. *Nat Chem Biol*. (2022) 18:70–80. doi: 10.1038/s41589-021-00904-5

42. Guo HY, Tang SB, Li LJ, Lin J, Zhang TT, Chao S, et al. Gestational diabetes mellitus causes genome hyper-methylation of oocyte via increased EZH2. *Nat Commun*. (2025) 16:127. doi: 10.1038/s41467-024-55499-x

43. Ibraheem Shelash Al-Hawari S, Abdalkareem Jasim S, F MAA, Bansal P, Kaur H, Hjazi A, et al. An overview of lncRNA NEAT1 contribution in the pathogenesis of female cancers; from diagnosis to therapy resistance. *Gene*. (2025) 933:148975. doi: 10.1016/j.gene.2024.148975

44. Wang C, Wang J, Xu R, Huang X, Li Q, Zhang C, et al. PAK2 promotes proliferation, migration, and invasion of lung squamous cell carcinoma through LIMK1/cofilin signaling pathway. *J BioMed Res*. (2024) 39:184–97. doi: 10.7555/JBR.37.20230317

45. Chu PY, Tzeng YT, Chiu YH, Lin HY, Kuo CH, Hou MF, et al. Multi-omics reveals the immunological role and prognostic potential of mitochondrial ubiquitin ligase MARCH5 in human breast cancer. *Biomedicines*. (2021) 9:1329. doi: 10.3390/biomedicines9101329

46. Su Z, Guan M, Zhang L, Lian X. Factors associated with immune–related severe adverse events (Review). *Mol Clin Oncol*. (2025) 22:3. doi: 10.3892/mco.2024.2798

47. Liu H, Liu J, Guan X, Zhao Z, Cheng P, Chen H, et al. Titin gene mutations enhance radiotherapy efficacy via modulation of tumour immune microenvironment in rectum adenocarcinoma. *Clin Transl Med*. (2025) 15:e70123. doi: 10.1002/ctm2.70123

48. Qiu L, Ma Z, Wu X. Mutant p53-mediated tumor secretome: bridging tumor cells and stromal cells. *Genes (Basel)*. (2024) 15:1615. doi: 10.3390/genes15121615

49. Chen X, Sandrine IK, Yang M, Tu J, Yuan X. MUC1 and MUC16: critical for immune modulation in cancer therapeutics. *Front Immunol*. (2024) 15:1356913. doi: 10.3389/fimmu.2024.1356913

50. Gonzalez VD, Huang YW, Delgado-Gonzalez A, Chen SY, Donoso K, Sachs K, et al. High-grade serous ovarian tumor cells modulate NK cell function to create an immune-tolerant microenvironment. *Cell Rep*. (2021) 36:109632. doi: 10.1016/j.celrep.2021.109632

51. Fontana B, Gallerani G, Salamon I, Pace I, Roncarati R, Ferracin M. ARID1A in cancer: Friend or foe? *Front Oncol*. (2023) 13:1136248. doi: 10.3389/fonc.2023.1136248

52. Bang YJ, Van Cutsem E, Feyereislova A, Chung HC, Shen L, Sawaki A, et al. Trastuzumab in combination with chemotherapy versus chemotherapy alone for treatment of HER2-positive advanced gastric or gastro-oesophageal junction cancer (ToGA): a phase 3, open-label, randomised controlled trial. *Lancet*. (2010) 376:687–97. doi: 10.1016/S0140-6736(10)61121-X

53. Lordick F, Al-Batran SE, Dietel M, Gaiser T, Hofheinz RD, Kirchner T, et al. HER2 testing in gastric cancer: results of a German expert meeting. *J Cancer Res Clin Oncol*. (2017) 143:835–41. doi: 10.1007/s00432-017-2374-x

54. Satoh T, Xu RH, Chung HC, Sun GP, Doi T, Xu JM, et al. Lapatinib plus paclitaxel versus paclitaxel alone in the second-line treatment of HER2-amplified advanced gastric cancer in Asian populations: TyTAN–a randomized, phase III study. *J Clin Oncol*. (2014) 32:2039–49. doi: 10.1200/JCO.2013.53.6136

55. Geng W, Tian D, Wang Q, Shan S, Zhou J, Xu W, et al. DNA–PKcs inhibitor increases the sensitivity of gastric cancer cells to radiotherapy. *Oncol Rep*. (2019) 42:561–70. doi: 10.3892/or.2019.7187

56. Wei G, Wang Y, Liu R, Liu L. An integrated machine learning framework for developing and validating a prognostic risk model of gastric cancer based on endoplasmic reticulum stress-associated genes. *Biochem Biophys Rep*. (2025) 41:101891. doi: 10.1016/j.bbrep.2024.101891

57. Lei Z, Tan IB, Das K, Deng N, Zouridis H, Pattison S, et al. Identification of molecular subtypes of gastric cancer with different responses to PI3-kinase inhibitors and 5-fluorouracil. *Gastroenterology*. (2013) 145:554–65. doi: 10.1053/j.gastro.2013.05.010

frontiers | Frontiers in Immunology

TYPE Original Research
PUBLISHED 14 October 2025
DOI 10.3389/fimmu.2025.1618726

OPEN ACCESS

EDITED BY
Stavros P. Papadakos,
Laiko General Hospital of Athens, Greece

REVIEWED BY
Palash Mandal,
Charotar University of Science and Technology, India
Mehmet Emin Arayici,
Dokuz Eylül University, Türkiye

*CORRESPONDENCE
Wenwang Lang
290702062@qq.com

RECEIVED 26 April 2025
ACCEPTED 10 September 2025
PUBLISHED 14 October 2025

CITATION
Lang W, Mei L, Xiao Q, Zhou Z, Jiang H and Zhao X (2025) Cost-effectiveness of cadonilimab plus chemotherapy vs chemotherapy alone for advanced gastric cancer: evidence to inform drug pricing in the U.S. and China.
Front. Immunol. 16:1618726.
doi: 10.3389/fimmu.2025.1618726

Cost-effectiveness of cadonilimab plus chemotherapy vs chemotherapy alone for advanced gastric cancer: evidence to inform drug pricing in the U.S. and China

Wenwang Lang[1]*, Liuyong Mei[2], Qiang Xiao[3], Zujin Zhou[2], Huiqing Jiang[2] and Xianling Zhao[2]

[1]Department of Pharmacy, Nanxishan Hospital of Guangxi Zhuang Autonomous Region, Guilin, China, [2]Department of Oncology, Nanxishan Hospital of Guangxi Zhuang Autonomous Region, Guilin, China, [3]Department of Spine Surgery, Nanxishan Hospital of Guangxi Zhuang Autonomous Region, Guilin, China

Background: Cadonilimab, a bispecific antibody targeting programmed cell death protein 1 (PD-1) and cytotoxic T-lymphocyte-associated protein 4 (CTLA-4), was the first agent of its class to demonstrate promising therapeutic efficacy in combination with chemotherapy for patients diagnosed with advanced gastric or gastroesophageal junction adenocarcinoma (GC/GEJC). This economic evaluation aimed to determine whether cadonilimab plus chemotherapy offers cost-effective benefits compared to chemotherapy alone from both the U.S. and Chinese healthcare payer perspectives. In addition, we estimated the pricing thresholds at which cadonilimab would be considered economically viable as a first-line treatment.

Methods: We constructed a Markov model comprising three health states, progression-free survival (PFS), progressive disease (PD), and death, spanning a 10-year time horizon. The clinical efficacy data were sourced from the randomized phase 3 COMPASSION-15 trial. The cost and utility parameters were derived from existing literature. The model calculates total costs, quality-adjusted life-years (QALYs), and incremental cost-effectiveness ratios (ICERs). Subgroup, scenario, and sensitivity analyses were performed, and price simulations explored cost-effective thresholds at defined willingness-to-pay (WTP) levels.

Results: In the base-case analysis, the cadonilimab plus chemotherapy provided an incremental gain of 0.33 QALYs at an additional cost of $16,797.61, resulting in an ICER of $50,582.10 per QALY, above the WTP threshold of China of $40,354.27 per QALY. In the U.S. setting, although the combination therapy achieved a slightly higher incremental QALY gain of 0.35 QALYs, the substantial additional cost of $101,275.06 resulted in an unfavorable ICER of $290,498.45 per QALY, exceeding the U.S. WTP threshold of $150,000.00. Among Chinese patients with a PD-L1 combined positive score (CPS) ≥5, the ICER was lower at $37,499.27/QALY, rendering the therapy cost-effective. Simulations identified cadonilimab pricing below $209.54/125 mg (China) and $826.46/125 mg (the U.S.) as necessary for cost-effectiveness.

Conclusion: Cadonilimab combined with chemotherapy may be cost-effective in Chinese patients with elevated PD-L1 expression. However, its broader use in other patient subgroups or countries requires significant price reductions. These findings provide important guidance for future reimbursements and pricing decisions.

KEYWORDS

cost-effectiveness, cadonilimab, PD-1/CTLA-4, gastric cancer, Markov model

Introduction

Gastric cancer (GC), including tumors located at the gastroesophageal junction (GEJC), is the fourth most prevalent malignancy globally and is a major contributor to cancer-related mortality (1). In 2020, it accounted for approximately 1.1 million new cases and over 768,000 deaths worldwide (2). Epidemiological data reveal substantial regional disparities in disease burden: China reports roughly 358,700 new GC/GEJC cases and more than 260,400 annual deaths (3), while the United States reports around 30,300 new cases and over 10,780 deaths each year (4). A critical shared challenge in both regions is that most patients are diagnosed at an advanced stage, which severely restricts treatment options and undermines long-term prognosis. The most common histological type of gastric cancer is adenocarcinoma, with the majority being human epidermal growth factor receptor 2 (HER2)-negative (5, 6). Despite advances in medical technology, more than 50% of patients with gastric cancer present with metastatic and unresectable tumors at diagnosis. Anti-programmed cell death protein-1 (PD-1) and programmed death ligand 1 (PD-L1) inhibitors combined with chemotherapy have become the standard of care for first-line treatment of HER2-negative, unresectable locally advanced or metastatic gastric or gastroesophageal junction (GC/GEJ) adenocarcinoma (7–11). Although the addition of a PD-1 inhibitor to chemotherapy improves outcomes, survival benefits remain limited in patients with low PD-L1 expression.

Cadonilimab is a human tetravalent bispecific IgG1 antibody with a symmetric IgG single-chain variable fragment (scFv) structure and an Fc-null design to eliminate antibody-dependent cellular cytotoxicity (ADCC), antibody-dependent cellular phagocytosis (ADCP), complement-dependent cytotoxicity (CDC), and cytokine release. Fc receptor-mediated effector functions can eliminate or impair lymphocytes expressing PD-1 and cytotoxic T-lymphocyte-associated protein 4 (CTLA-4), thereby reducing their antitumor activity (Supplementary Figure 1). Moreover, immune-related adverse events (irAEs) induced by checkpoint inhibitors have been associated with the recruitment of immune cells bearing Fc receptors (12, 13). Cadonilimab has shown promising clinical activity and manageable safety in patients with gastric or GEJ adenocarcinoma, regardless of PD-L1 expression (14).

In the phase 3 COMPASSION-15 trial (15), both progression-free survival (PFS) and overall survival (OS) significantly improved in the cadonilimab group. In the intention-to-treat (ITT) population, the median OS was 15.0 months versus 10.8 months; in patients with PD-L1 combined positive score (CPS) ≥5, the median OS was not reached versus 10.6 months; and in those with PD-L1 CPS <5, it was 14.8 months versus 11.1 months. The median PFS was 7.0 months in the cadonilimab group compared to 5.3 months in the placebo group. Among patients with PD-L1 CPS ≥5, PFS was 6.9 months with cadonilimab and 4.6 months with placebo, while in the PD-L1 CPS <5 group, PFS was 6.9 months versus 5.5 months.

Cadonilimab is the world's first PD-1/CTLA-4 bispecific antibody tumor immunotherapy drug developed independently in China and provides critical evidence supporting updates to clinical practice guidelines for gastric cancer. Despite its clinical potential, there is no comprehensive evidence of its economic value. Cadonilimab has been granted orphan drug status and fast-track designation by the U.S. FDA and is expected to receive market approval as early as 2026. As a next-generation immunotherapy agent, it is projected to be a key component of the global oncology market, which is valued at nearly USD 100 billion. However, its high price triggered two rounds of price reductions in China, from $1,856.30 to $865.80, and then to $261.17 per 125 mg, raising concerns about affordability and cost-effectiveness. The absence of pricing information in the U.S. further complicates economic evaluations. Additionally, cadonilimab may soon be included in National Comprehensive Cancer Network (NCCN) Guidelines (16), underscoring the need for cost-effectiveness data to inform clinical and policy decisions in both regions.

This study aimed to assess the cost-effectiveness of cadonilimab in combination with chemotherapy versus chemotherapy alone as first-line treatment for advanced GC/GEJC from both U.S. and Chinese healthcare payer perspectives, thereby informing future drug pricing and reimbursement decisions.

Methods

Patient enrollment and intervention

This study followed the Consolidated Health Economic Evaluation Reporting Standards (CHEERS) guidelines (17).

Eligible patients were between 18 and 75 years of age and had histologically confirmed, locally advanced, unresectable, or metastatic GC/GEJC. None of the patients had previously received systemic therapy for advanced disease. Patient characteristics and inclusion criteria were consistent with those described in the COMPASSION-15 clinical trial.

The participants were randomly assigned to receive either cadonilimab (10 mg/kg, administered intravenously) or a placebo every 21 days for up to 24 months. Both groups received concurrent chemotherapy with capecitabine (1,000 mg/m² orally, twice daily on days 1–14) and oxaliplatin (130 mg/m² intravenously on day 1), repeated in 21-day cycles for up to six cycles (XELOX regimen). Following the combination phase, the patients continued with cadonilimab or placebo as monotherapy.

Subsequent treatments, including PD-1 inhibitors, targeted agents, chemotherapy, or best supportive care, were performed in accordance with the NCCN (16) and Chinese Society of Clinical Oncology (CSCO) guidelines for gastric cancer (18) and were consistent with post-treatment strategies used in the COMPASSION-15 trial (15). Tumor assessments were performed every six weeks during the first 54 weeks after enrollment and every nine weeks thereafter.

Adverse events (AEs) were monitored with a particular focus on severe (grade ≥3) events occurring in more than 3% of patients. These included anemia, neutropenia, thrombocytopenia, and hypokalemia (Table 1).

Model structure

A three-state Markov model was constructed using TreeAge Pro 2022 (Williamstown, MA, USA) and R version 4.2.4 (Vienna, Austria). Health states included PFS, progressive disease (PD), and death (Figure 1). The model employed a 3-week cycle length over a 10-year time horizon, representing the lifetime of the patient population and capturing over 99% mortality.

The analysis was conducted from the perspective of healthcare payers in both China and the United States. The Chinese model adopted a system-wide healthcare payer perspective, whereas the U.S. analysis focused on direct medical costs relevant to both public and private payers (25).

Outcomes

The model evaluated total life years, quality-adjusted life years (QALYs), incremental cost-effectiveness ratios (ICERs), incremental net health benefits (INHB), and incremental net monetary benefits (INMB). Annual discount rates were applied to both costs and utilities—3% for the U.S. and 5% for China—in accordance with established pharmacoeconomic guidelines (26, 27).

Chinese cost data were converted to 2024 U.S. dollars using an exchange rate of $1 = ¥7.1217 and were adjusted for inflation using the local consumer price index. The willingness-to-pay (WTP) thresholds were set at $40,354.27 per QALY in China (three times the national gross domestic product per capita) and $150,000 per QALY in the U.S., consistent with standards established by the WHO and U.S. healthcare payers (28).

Clinical data inputs

Probabilities for OS and PFS were extracted from Kaplan–Meier (KM) curves in the ASTRUM-005 trial using the GetData Graph

TABLE 1 Key clinical input data.

Parameters	Baseline value	Range		Distribution	Reference
		Minimum	Maximum		
Survival model for OS					
Cadonilimab plus chemotherapy	Meanlog=2.7363 Sdlog=0.9902			Lognormal	(15)
chemotherapy	Shape=2.0400 Scale=11.3080			Loglogistic	(15)
Survival model for PFS					
Cadonilimab plus chemotherapy	Mu=1.9580 Sigma=0.9908 Q=-0.4756			Generalized gamma	(15)
chemotherapy	Meanlog=1.6818 Sdlog=0.7658			Lognormal	(15)
Survival model for OS (CPS ≥5)					
Cadonilimab plus chemotherapy	Meanlog=2.8810 Sdlog=1.1670			Lognormal	(15)

(Continued)

TABLE 1 Continued

Parameters	Baseline value	Range		Distribution	Reference
		Minimum	Maximum		
Survival model for OS (CPS ≥5)					
chemotherapy	Shape=1.9017 Rate=0.1390			Gamma	(15)
Survival model for PFS (CPS ≥5)					
Cadonilimab plus chemotherapy	Meanlog=2.1741 Sdlog=0.9829			Lognormal	(15)
chemotherapy	Meanlog=1.6784 Sdlog=0.7388			Lognormal	(15)
Survival model for OS (CPS <5)					
Cadonilimab plus chemotherapy	Meanlog=2.6772 Sdlog=0.9669			Lognormal	(15)
chemotherapy	Meanlog=2.4639 Sdlog=0.8078			Lognormal	(15)
Survival model for PFS (CPS <5)					
Cadonilimab plus chemotherapy	Meanlog=2.0993 Sdlog=0.9096			Lognormal	(15)
chemotherapy	Meanlog=1.6956 Sdlog=0.7848			Lognormal	(15)
Drug cost, $/per cycle					
Cost of Cadonilimab	1305.87	1044.70	1567.04	Gamma	Local charge
Cost of Tislelizumab	352.03	281.62	422.44	Gamma	Local charge
Cost of Oxaliplatin	166.25	133.00	199.50	Gamma	Local charge
Cost of Capecitabine	44.06	35.25	52.87	Gamma	Local charge
Cost of 5-FU	126.87	101.50	152.24	Gamma	Local charge
Cost of Cisplatin	34.66	27.73	41.59	Gamma	Local charge
Cost of Paclitaxel	212.61	170.09	255.13	Gamma	Local charge
Cost of Ramucirumab	2106.24	1702.93	2554.39	Gamma	Local charge
Testing for PD-L1 protein biomarker	567.64	454.11	681.17	Gamma	Local charge
Cost of the laboratory test	106.61	85.29	127.93	Gamma	(19)
Enhanced CT	171.03	136.82	205.24	Gamma	Local charge
Cost of end-of-life	1460.30	1168.24	1752.36	Gamma	(20)
Best supportive care	164.57	92.16	138.24	Gamma	(20)
Cost of drug administration per unit	134.93	107.94	161.92	Gamma	(21, 22)
Proportion of receiving subsequent treatment in Cadonilimab plus chemotherapy group					
PD-L1/PD-1 Medication	11.50%	9.20%	13.80%	Beta	(15)
Chemotherapy Regimen	34.40%	27.52%	41.28%	Beta	(15)
Targeted therapy	11.10%	8.88%	13.32%	Beta	(15)
Proportion of receiving subsequent treatment in Chemotherapy group					
PD-L1/PD-1 Medication	22.30%	17.84%	26.76%	Beta	(15)

(Continued)

TABLE 1 Continued

Parameters	Baseline value	Range		Distribution	Reference
		Minimum	Maximum		
Proportion of receiving subsequent treatment in Chemotherapy group					
Chemotherapy Regimen	47.90%	38.32%	57.48%	Beta	(15)
Targeted therapy	20.30%	16.24%	24.36%	Beta	(15)
Cost of AEs, $					
Anemia	669.45	535.56	803.34	Gamma	(23)
Decreased platelet count	1054.22	843.38	1265.06	Gamma	(23)
Decreased neutrophil count	544.19	435.35	653.03	Gamma	(23)
Hypokalemia	3000.00	2400.00	3600.00	Gamma	(23)
Utilities					
Utility of PFS	0.797	0.638	0.956	Beta	(24)
Utility of PD	0.577	0.462	0.692	Beta	(24)
Disutility estimates					
Anemia	0.07	0.06	0.084	Beta	(23)
Decreased platelet count	0.11	0.09	0.132	Beta	(23)
Decreased neutrophil count	0.20	0.16	0.240	Beta	(23)
Hypokalemia	0.04	0.09	0.14	Beta	(23)
Risk for main AEs in Cadonilimab plus chemotherapy group					
Anemia	10.20%	8.16%	12.24%	Beta	(15)
Decreased platelet count	28.50%	22.80%	34.20%	Beta	(15)
Decreased neutrophil count	15.10%	12.08%	18.12%	Beta	(15)
Hypokalemia	5.90%	4.72%	7.08%	Beta	(15)
Risk for main AEs in Chemotherapy group					
Anemia	12.50%	10.00%	15.00%	Beta	(15)
Decreased platelet count	25.00%	20.00%	30.00%	Beta	(15)
Decreased neutrophil count	14.80%	11.84%	17.76%	Beta	(15)
Hypokalemia	1.00%	0.08%	0.12%	Beta	(15)
Discount rate	5%	4.00%	6.00%	Beta	
BMI/m2	1.72				
Weight/kg	65				
$1 = ¥7.0467	40,354.27				

OS, overall survival; PFS, progression-free survival; PD, progression disease; CPS, PD-L1 combined of positive score; AE, adverse event; BMI, body mass index.

Digitizer (http://getdata-graph-digitizer.com), and individual patient data were reconstructed following the method described by Guyot et al. (29).

Due to limited follow-up, extrapolation was required to extend survival estimates across the model's full time horizon (30). The reconstructed time-to-event data were then fitted with a series of parametric models, including classic models (exponential, Weibull, Gompertz, gamma, log-logistic, log-normal, and generalized gamma).

Model selection was guided by a combination of statistical goodness-of-fit based on the Akaike information criterion (AIC), extrapolation performance based on log likelihood (LogLik), and visual inspection. Using this framework, the most suitable parametric model was chosen to extrapolate KM curves for OS and PFS beyond the follow-up period of the COMPASSION-15 trial (consistent with the trial referenced earlier for treatment protocols) (Figures 2–4). Before implementing the Cox proportional hazards (PH) model, the PH assumption—a core prerequisite for valid

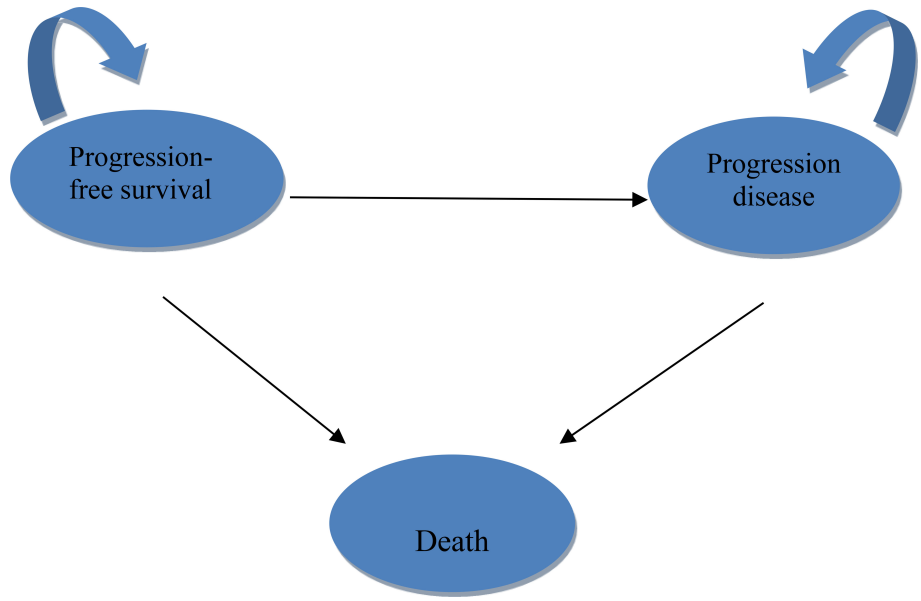

FIGURE 1
Markov model structure.

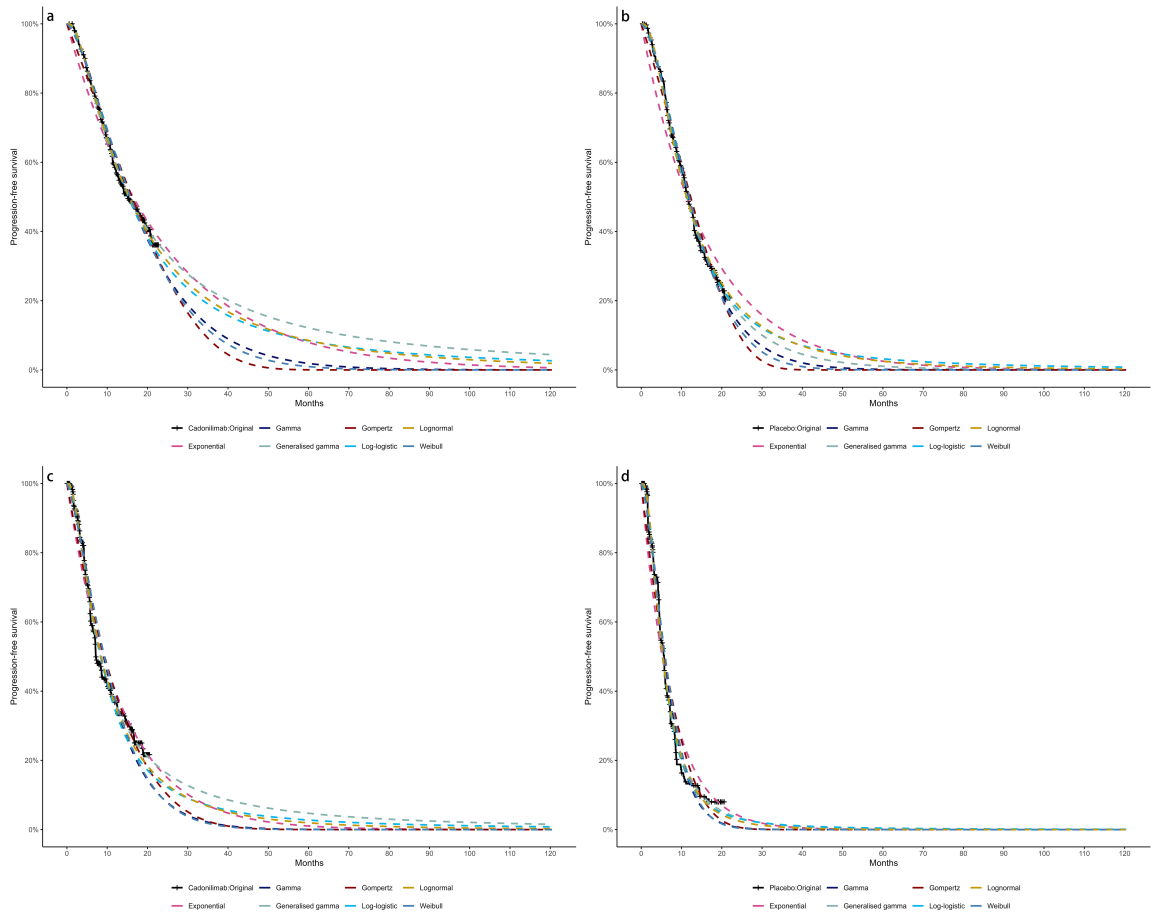

FIGURE 2
The Kaplan-Meier: **(A)** overall survival curves of Cadonilimab plus chemotherapy group, **(B)** overall survival curves of Chemotherapy group, **(C)** progression-free survival curves of Cadonilimab plus chemotherapy group, **(D)** progression-free survival curves of Chemotherapy group.

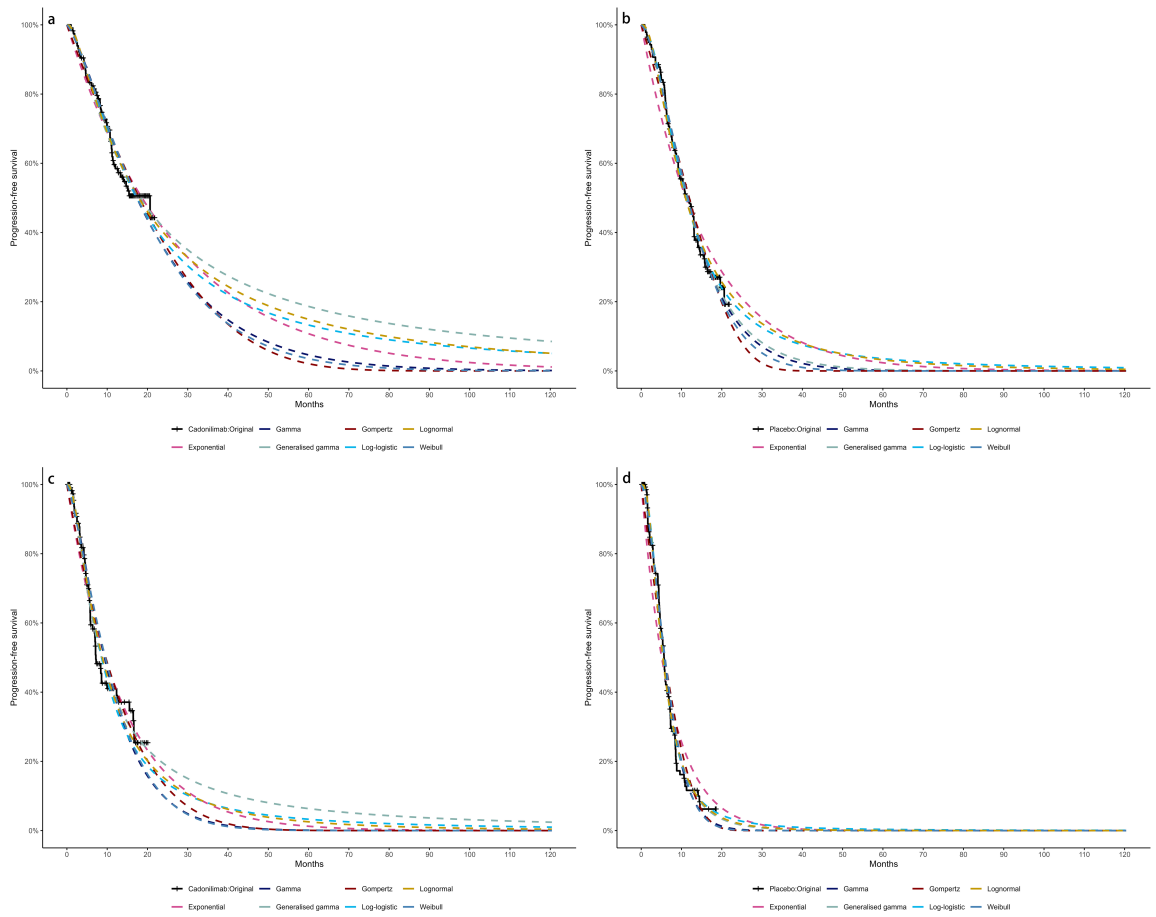

FIGURE 3
The Kaplan-Meier of CPS ≥ 5: **(A)** overall survival curves of Cadonilimab plus chemotherapy group, **(B)** overall survival curves of Chemotherapy group, **(C)** progression-free survival curves of Cadonilimab plus chemotherapy group, **(D)** progression-free survival curves of Chemotherapy group.

model inference—was validated using two complementary methods: visual inspection of log-log survival curves and quantitative assessment of Schoenfeld residuals (31, 32). While the PH assumption yielded p-values > 0.05 for both OS and PFS across all patient groups (nominally suggesting the assumption was satisfied), two critical observations indicated potential violation: crossing cumulative hazard curves between the treatment and control arms, and a non-horizontal trend in the smoothed Schoenfeld residuals. The variation in predicted hazards across different parameter distributions is shown in Figures 5–7. The corresponding survival function parameters are detailed in Tables 2–4.

Cost inputs

This analysis focused exclusively on the direct medical costs associated with the management of GC/GEJC. These costs include drug acquisition, laboratory testing, enhanced computed tomography (CT), intravenous drug administration, subsequent therapies, best supportive care, end-of-life care, and management of severe adverse events (grade 3 or 4). Medication prices were obtained from public Chinese databases and institutional pricing schedules, whereas other cost components were derived from published economic evaluations and relevant literature.

Owing to the absence of a listed market price for cadonilimab in the United States, its cost was estimated using a comparative approach. Specifically, pricing was approximated based on analogous immunotherapies such as toripalimab and tislelizumab (33). Drug prices for both China and the U.S. were converted to U.S. dollars and adjusted using a price index to ensure cross-national comparability. Tables 1 and 5 summarize the clinical and cost parameters used in this analysis (19–23, 28, 34, 35).

Quality-of-life inputs

Health outcomes in the model were adjusted using utility values obtained from previously published sources, as EQ-5D-5L (European Quality of Life-5 Dimension-5 Level) data were not

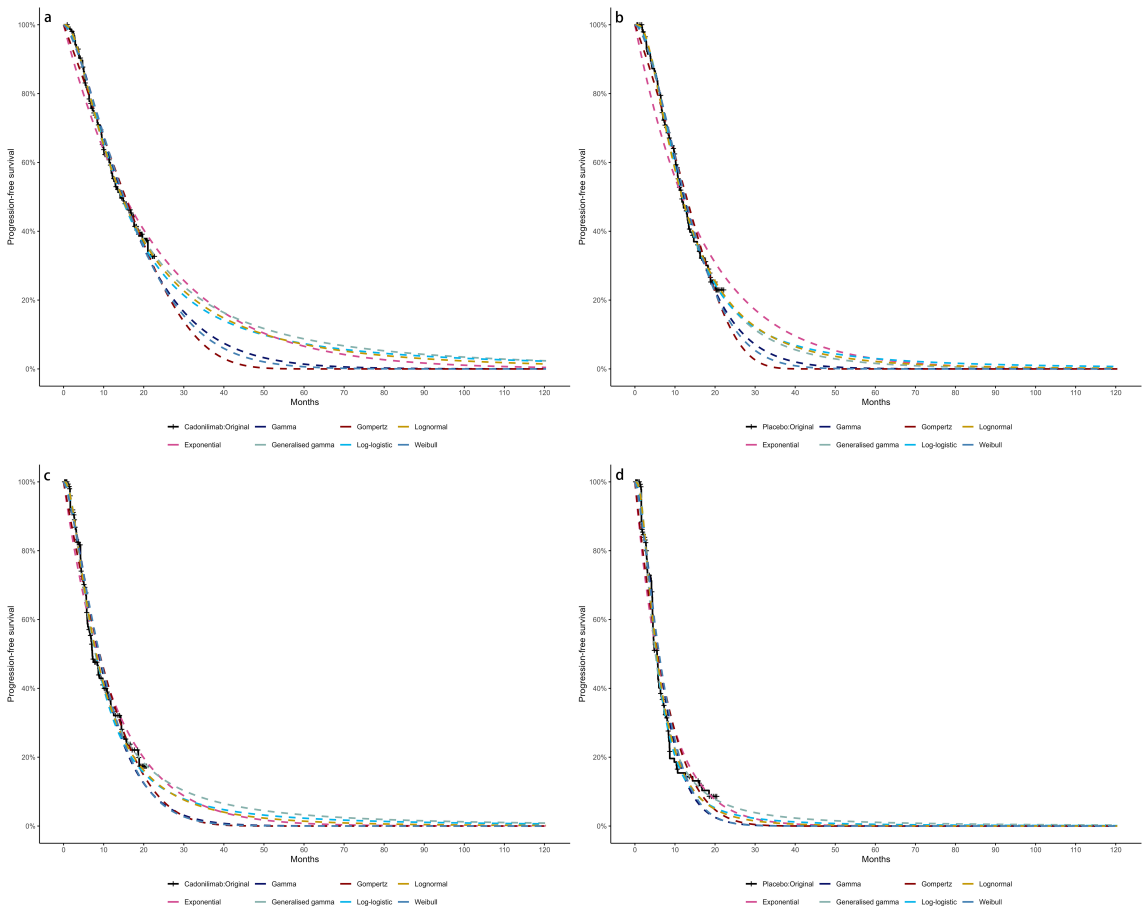

FIGURE 4
The Kaplan-Meier of CPS <5: **(A)** overall survival curves of Cadonilimab plus chemotherapy group, **(B)** overall survival curves of Chemotherapy group, **(C)** progression-free survival curves of Cadonilimab plus chemotherapy group, **(D)** progression-free survival curves of Chemotherapy group.

directly reported in the COMPASSION-15 trial. Utility values were anchored on a scale ranging from 0 (representing death) to 1 (representing perfect health).

For patients in the PFS state, the utility was set at 0.797 based on data from the TOGA trial and calculated using the Japanese EuroQol (EQ-5D) scoring algorithm (24). The utility for patients in the PD state was 0.577, derived from evaluations conducted by the National Institute for Health and Clinical Excellence (NICE). Quality-of-life decrements (disutilities) associated with severe adverse events, including anemia, thrombocytopenia, neutropenia, and hypokalemia, were also incorporated into the model (24). All AEs were assumed to occur during the initial treatment cycle, with detailed incidence rates provided in Table 1.

Subgroup analyses

To explore heterogeneity in cost-effectiveness outcomes, subgroup analyses were performed for patients with PD-L1 CPS ≥5 and CPS <5 in both China and the United States. These analyses employed the same modeling structure and assumptions as those used in the base-case scenario. Due to the lack of subgroup-specific data on follow-up treatments, adverse event rates, or healthcare resource utilization in the COMPASSION-15 trial, these parameters were assumed to be consistent with those observed in the overall study population.

Price simulation

Owing to uncertainties in the key input parameters, particularly drug pricing, scenario analyses were conducted to evaluate a range of potential pricing outcomes. In the Chinese context, cost-effectiveness was assessed with and without the inclusion of a patient assistance program. The price of cadonilimab varied between $0 and $2,000 per 625 mg dose, and outcomes were compared against the country-specific WTP threshold of $40,354.27 per QALY.

In the United States, where a formal list price for cadonilimab is currently unavailable, an estimated cost of $8,600 per 750 mg dose

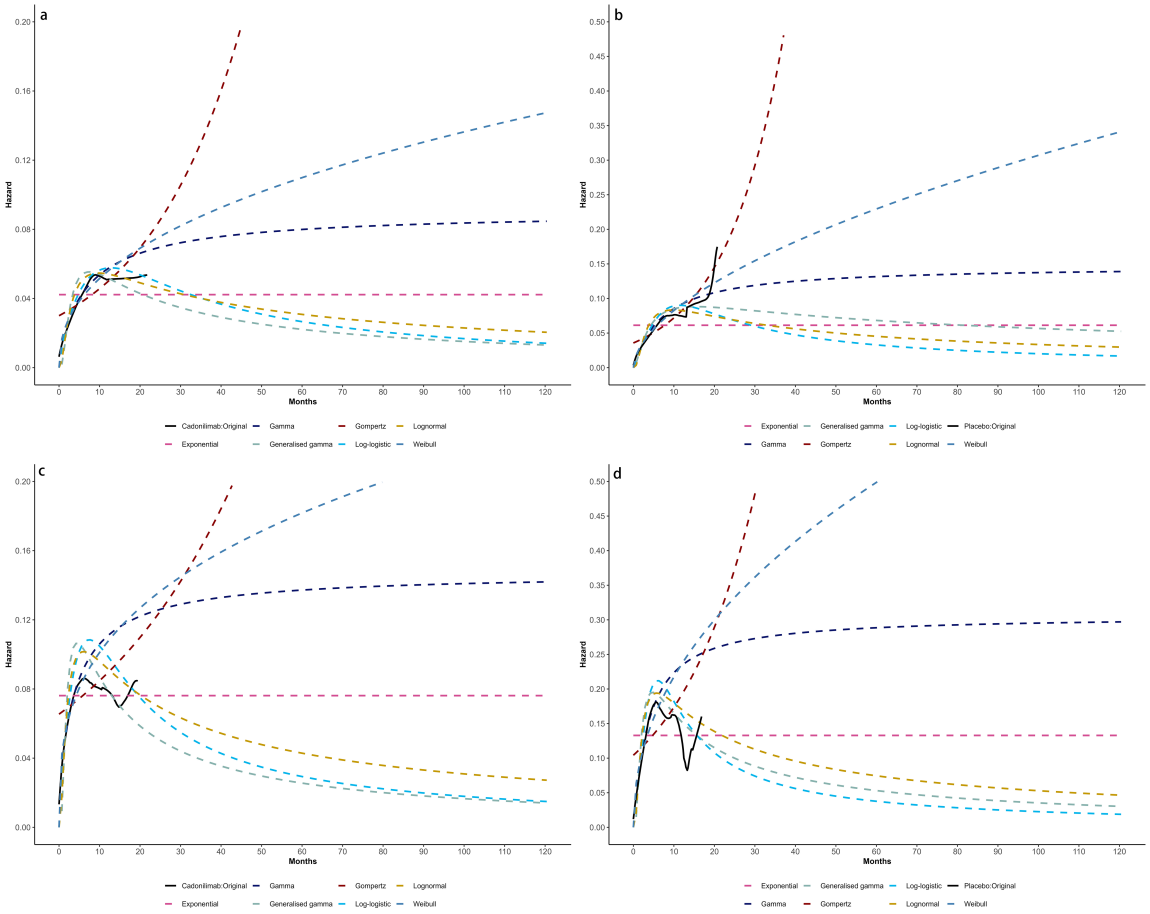

FIGURE 5
Comparison of fitted proportional hazards survival models with observed kaplan–meier curves: **(A)** overall survival curves of Cadonilimab plus chemotherapy group, **(B)** overall survival curves of Chemotherapy group, **(C)** progression-free survival curves of Cadonilimab plus chemotherapy group, **(D)** progression-free survival curves of Chemotherapy group.

was used. This estimate was based on price comparisons with other anti-PD-1 agents, including toripalimab and tislelizumab. Scenario analyses in the U.S. setting varied the price from $0 to $10,000 per dose to identify the maximum price at which cadonilimab would remain cost-effective under a $150,000 WTP threshold.

Scenario analysis

To address potential inconsistencies between the base-case discount rates (3% for the U.S., 5% for China) and World Health Organization (WHO) recommendations, an additional scenario was run where China's discount rate was lowered to 3% (matching the U.S. rate). This analysis evaluated how aligning discount rates across regions would impact cost-effectiveness conclusions, particularly for long-term survival outcomes. Given the volatility of the yuan–dollar exchange rate in 2024–2025, a second scenario incorporated Purchasing Power Parity (PPP) adjustments to currency conversion —replacing the base-case market exchange rate with 2024 International Monetary Fund (IMF) PPP values (¥1 = $0.2825, equivalent to ¥3.54 = $1). Concurrently, China's WTP threshold was adjusted to $20,243.85 per QALY to align with PPP-adjusted economic benchmarks, ensuring cross-country comparability of cost-effectiveness results under a standardized economic metric.

Sensitivity analysis

The robustness of the model outcomes was evaluated using one-way sensitivity analysis (OWSA) and probabilistic sensitivity analysis (PSA). In the OWSA, each key parameter was independently varied by ±20% from its base-case value to determine its influence on the ICER. The results were visualized using tornado diagrams to identify the most influential variables.

For the PSA, all model inputs were sampled simultaneously based on appropriate probability distributions, beta for probabilities and utility values, and gamma for cost parameters. A total of 10,000

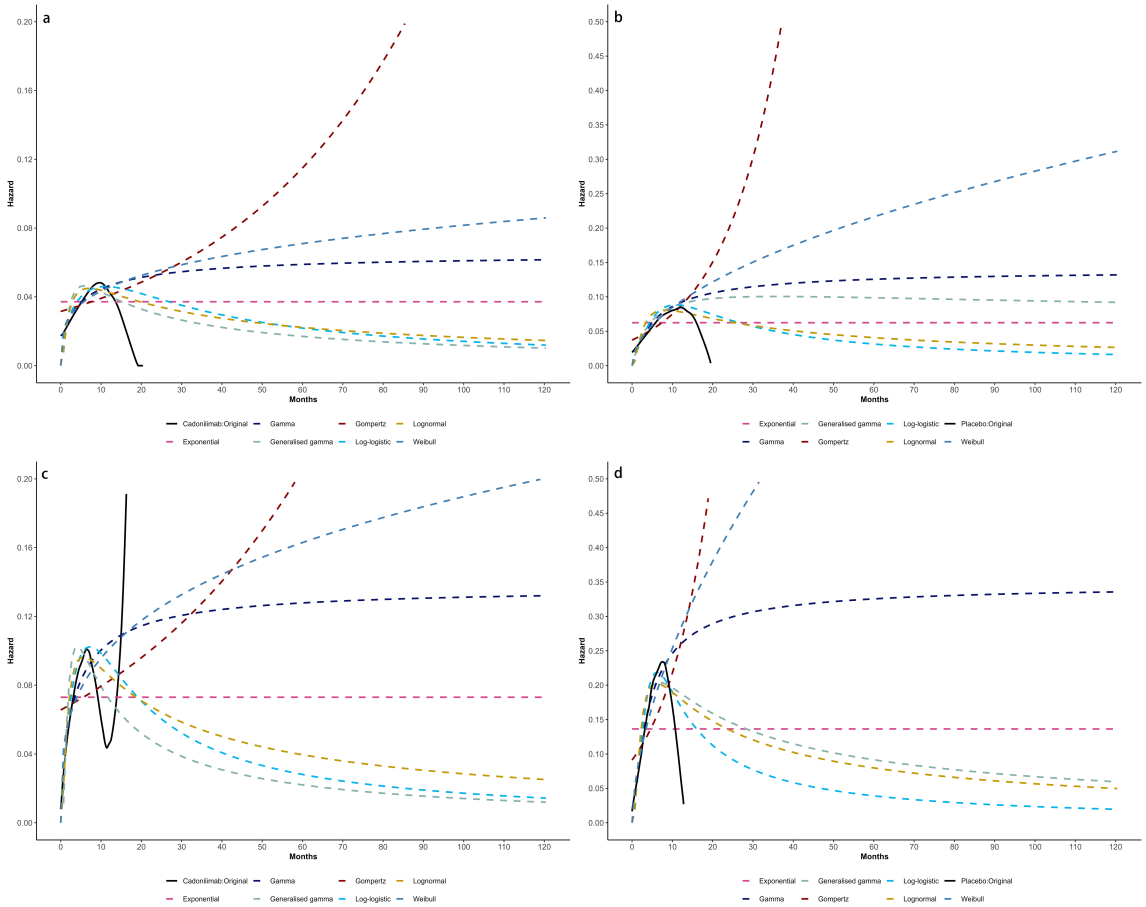

FIGURE 6
Comparison of fitted proportional hazards survival models with observed kaplan–meier curves of CPS ≥ 5: **(A)** overall survival curves of Cadonilimab plus chemotherapy group, **(B)** overall survival curves of Chemotherapy group, **(C)** progression-free survival curves of Cadonilimab plus chemotherapy group, **(D)** progression-free survival curves of Chemotherapy group.

Monte Carlo simulations were performed to quantify the uncertainty in ICER estimates and to calculate the likelihood that cadonilimab plus chemotherapy would be deemed cost-effective at different WTP thresholds.

Results

Base-case analysis

Over a 10-year time horizon, the base-case analysis indicated that patients receiving cadonilimab in combination with chemotherapy achieved 1.01 QALYs at a total cost of $28,528.60. In contrast, those treated with chemotherapy alone accrued 0.67 QALYs at a cost of $11,730.98. This resulted in an incremental gain of 0.33 QALYs and an additional cost of $16,797.61, yielding an ICER of $5,0582.10 per QALY for the combination therapy (Table 6).

When compared to China's WTP threshold of $40,354.27 per QALY, this ICER exceeded the acceptable limit. Consequently, the incremental net health benefit (INHB) was -0.08 QALYs, and the incremental net monetary benefit (INMB) was -$3,396.52, suggesting that cadonilimab plus chemotherapy is not cost-effective in the Chinese healthcare setting (Table 6).

In the U.S. scenario, the ICER for cadonilimab plus chemotherapy was estimated at $347,127.52 per QALY—well above the U.S. WTP threshold of $150,000.00. The corresponding INHB and INMB values were -0.41 QALYs and -$61,121.30, respectively, further supporting the conclusion that the combination regimen is not economically favorable under the current U.S. pricing assumptions (Table 6).

Subgroup analysis

Among patients with a PD-L1 CPS ≥5, the ICER for cadonilimab plus chemotherapy was $37,499.27 per QALY—

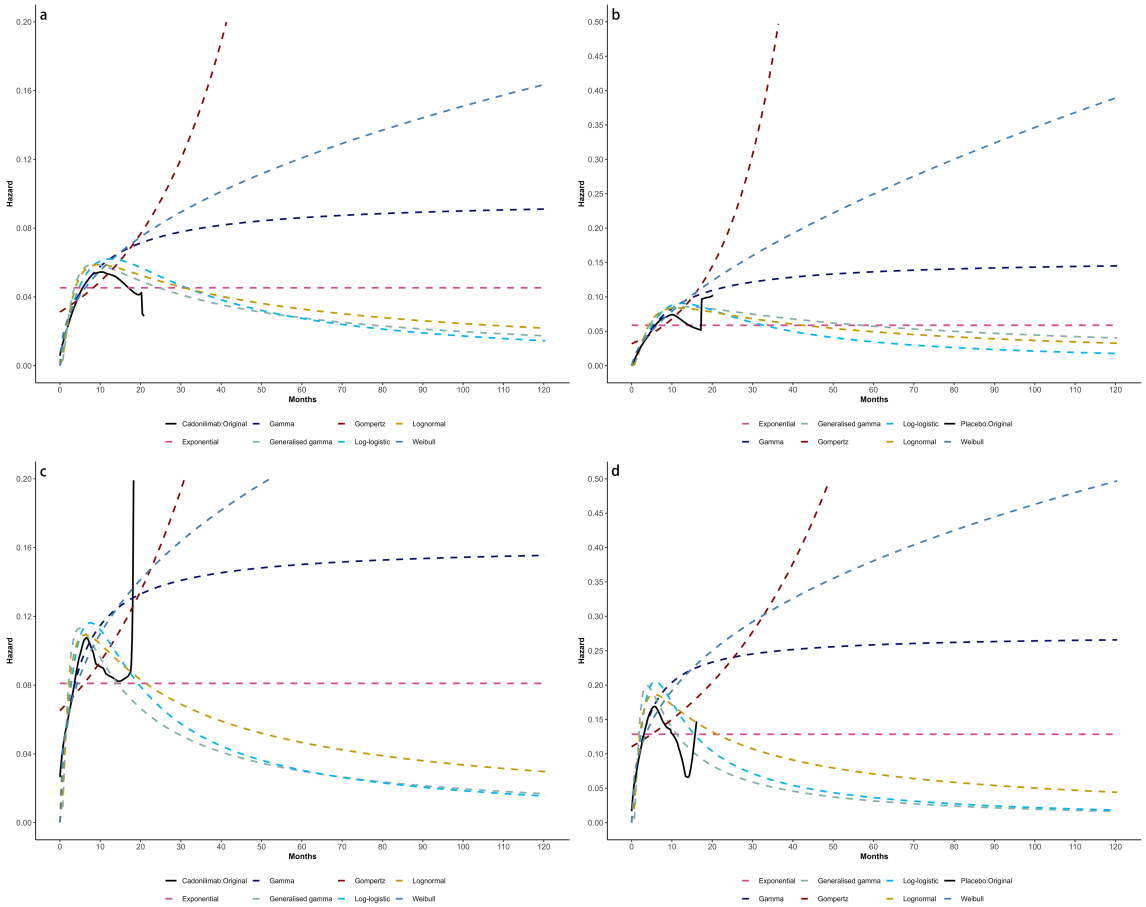

FIGURE 7
Comparison of fitted proportional hazards survival models with observed kaplan–meier curves of CPS <5: **(A)** overall survival curves of Cadonilimab plus chemotherapy group, **(B)** overall survival curves of Chemotherapy group, **(C)** progression-free survival curves of Cadonilimab plus chemotherapy group, **(D)** progression-free survival curves of Chemotherapy group.

below China's WTP threshold of $40,354.27 (Table 6). The corresponding INHB and INMB were 0.04 QALYs and $1,674.96, respectively, indicating that cadonilimab was cost-effective in this clinically responsive subgroup.

In contrast, for patients with a PD-L1 CPS <5, the ICER was $66,013.60 per QALY, exceeding the WTP threshold. The INHB was –0.16 QALYs and the INMB was –$6,355.16, suggesting that cadonilimab was not cost-effective in this lower PD-L1 expression group (Table 6).

In the U.S. setting, the ICER for cadonilimab plus chemotherapy reached $240,877.66 per QALY in the PD-L1 CPS ≥5 group and $398,852.61 per QALY in the CPS <5 group, both of which far exceeded the WTP threshold of $150,000.00 (Table 6). The corresponding INHBs were -0.38 and -0.43 QALYs, while the INMBs were -$56,677.19 and -$64,728.99, respectively. These findings indicate that cadonilimab was not cost-effective in either subgroup within the U.S. healthcare context, despite differential clinical responsiveness.

Price simulation

Figure 8 illustrated the results of the price simulation analysis across a range of cadonilimab pricing scenarios. In China, the ICER increased proportionally as the price varied from $0 to $2,000 per 625 mg dose. A similar trend was observed in the United States, where the price range examined ranged from $0 to $10,000 per 750 mg dose.

According to the respective WTP thresholds, cadonilimab would be considered cost-effective in China if the price was below $209.54 per 125 mg. In the U.S., the threshold for cost-effectiveness was $826.46 per 125 mg.

Scenario analysis

Scenario analysis evaluating a 3% discount rate for China showed the ICER of cadonilimab plus chemotherapy decreased to $48,678.70 per QALY, though the reduction was minimal (Table 7).

TABLE 2 The Akaike information criteria (AIC), Bayesian information criteria (BIC) and Log likelihood (LogLik).

Type of distribution	Cadonilimab plus chemotherapy (OS)			Chemotherapy (OS)			Cadonilimab plus chemotherapy (PFS)			Chemotherapy(PFS)		
	AIC	BIC	LogLik	AIC	BIC	LogLik	AIC	BIC	LogLik	AIC	BIC	LogLik
Exponential	1284.687	1288.407	-641.344	1488.312	1492.032	-743.156	1195.999	1199.719	-596.999	1360.303	1364.023	-679.151
Gamma	1260.438	1267.878	-628.219	1438.741	1446.182	-717.371	1171.728	1179.169	-583.864	1298.264	1305.705	-647.132
Generalized gamma	1252.248	1263.409	-623.124	1438.235	1449.395	-716.117	1152.010	1163.171	-573.005	1278.456	1289.617	-636.228
Gompertz	1278.451	1285.892	-637.226	1463.253	1470.693	-729.626	1195.445	1202.886	-595.722	1351.569	1359.010	-673.785
Weibull	1264.650	1272.091	-630.325	1443.448	1450.888	-719.724	1179.156	1186.597	-587.578	1314.639	1322.080	-655.319
Log-logistic	1256.508	1263.949	-626.254	1437.368	1444.808	-716.684	1158.399	1165.839	-577.199	1279.473	1286.913	-637.736
Lognormal	1251.234	1258.674	-623.617	1437.727	1445.168	-716.863	1152.9990	1160.440	-574.499	1277.656	1285.097	-636.828

OS, overall survival; PFS, progression-free survival; AIC, Akaike information criterion; BIC, Bayesian information criterion; LogLik, Log likelihood.

TABLE 3 The Akaike information criteria (AIC), Bayesian information criteria (BIC) and Log likelihood (LogLik) (CPS ≥5).

Type of distribution	Cadonilimab plus chemotherapy (OS)			Chemotherapy(OS)			Cadonilimab plus chemotherapy (PFS)			Chemotherapy (PFS)		
	AIC	BIC	LogLik	AIC	BIC	LogLik	AIC	BIC	LogLik	AIC	BIC	LogLik
Exponential	431.287	434.040	-214.620	673.620	676.562	-335.810	428.832	431.585	-213.416	630.366	633.307	-314.183
Gamma	429.017	434.525	-212.477	655.971	661.855	-325.986	422.720	428.227	-209.360	595.904	601.788	-295.952
Generalized gamma	427.851	436.112	-210.906	657.836	666.661	-325.918	416.104	424.365	-205.052	593.860	602.685	-293.930
Gompertz	432.654	438.161	-214.296	664.185	670.068	-330.092	430.376	435.884	-213.188	620.211	626.095	-308.106
Weibull	429.856	435.363	-212.895	657.056	662.939	-326.528	425.200	430.707	-210.600	601.944	607.828	-298.972
Log-logistic	427.599	433.106	-211.774	656.027	661.911	-326.014	417.733	423.240	-206.866	592.798	598.681	-294.399
Lognormal	426.077	431.584	-211.016	658.737	664.621	-327.369	415.505	421.012	-205.752	591.928	597.811	-293.964

OS, overall survival; PFS, progression-free survival; AIC, Akaike information criterion; BIC, Bayesian information criterion; LogLik, Log likelihood; CPS, PD-L1 combined of positive score.

TABLE 4 The Akaike information criteria (AIC), Bayesian information criteria (BIC) and Log likelihood (LogLik) (CPS <5).

Type of distribution	Cadonilimab plus chemotherapy (OS)			Chemotherapy (OS)			Cadonilimab plus chemotherapy (PFS)			Chemotherapy (PFS)		
	AIC	BIC	LogLik	AIC	BIC	LogLik	AIC	BIC	LogLik	AIC	BIC	LogLik
Exponential	698.054	701.110	-348.027	723.001	725.991	-360.500	648.459	651.515	-323.229	655.088	658.078	-326.544
Gamma	684.856	690.969	-340.428	695.367	701.348	-345.683	634.040	640.152	-315.020	631.682	637.663	-313.841
Generalized gamma	682.361	691.529	-338.180	695.279	704.250	-344.639	626.171	635.340	-310.086	614.320	623.291	-304.160
Gompertz	694.703	700.816	-345.352	709.257	715.238	-352.629	647.587	653.699	-321.793	655.037	661.018	-325.519
Weibull	687.161	693.274	-341.581	698.274	704.255	-347.137	638.087	644.200	-317.044	640.021	646.002	-321.793
Log-logistic	682.887	688.999	-339.443	694.586	700.567	-345.293	628.307	634.419	-312.153	618.165	624.146	-307.082
Lognormal	680.510	686.623	-338.255	693.371	699.352	-344.685	625.246	631.359	-310.623	616.300	622.280	-306.150

OS, overall survival; PFS, progression-free survival; AIC, Akaike information criterion; BIC, Bayesian information criterion; LogLik, Log likelihood; CPS, PD-L1 combined of positive score.

10.3389/fimmu.2025.1618726

TABLE 5 Key clinical input data (US).

Parameters	Baseline value	Range		Distribution	Reference
		Minimum	Maximum		
Drug cost, $/per cycle					
Cost of Cadonilimab	8640.00	6912.00	10368.00	Gamma	Estimated
Cost of Pembrolizumab	11520.60	9216.48	13824.72	Gamma	(34)
Cost of Oxaliplatin	40.95	31.45	47.17	Gamma	(34)
Cost of Capecitabine	56.00	87.92	131.88	Gamma	(34)
Cost of 5-FU	50.17	40.14	60.20	Gamma	(34)
Cost of Cisplatin	42.32	36.63	54.95	Gamma	(34)
Cost of Paclitaxel	40.06	32.36	48.54	Gamma	(34)
Cost of Ramucirumab	13124.36	10499.49	15749.23	Gamma	(34)
Cost of the laboratory test	111.65	89.32	133.98	Gamma	(34)
Enhanced CT	424.35	339.48	509.22	Gamma	(34)
Testing for PD-L1 protein biomarker	459.00	367.20	550.80	Gamma	(34)
Cost of end-of-life	21603.00	17282.40	25923.60	Gamma	(28)
Best supportive care	3049.00	2439.20	3658.80	Gamma	(28)
Cost of drug administration first hour	142.55	114.04	171.06	Gamma	(34)
Administration intravenous, additional hour	30.68	24.54	36.82	Gamma	(34)
Cost of AEs, $					
Anemia	20260.00	6352.80	9529.20	Gamma	(35)
Decreased platelet count	22698.00	10484.00	15726.00	Gamma	(35)
Decreased neutrophil count	17181.00	10484.00	15726.00	Gamma	(35)
Hypokalemia	25326.00	6705.75	10058.63	Gamma	(35)
Discount rate	3%	0.02	0.04	Beta	
BMI/m2	2.1				
Weight/kg	75				

AE, adverse event; BMI, body mass index.

For this scenario, PSA results indicated a 29.57% probability that the regimen would be cost-effective at China's defined WTP threshold. Under PPP-adjusted currency conversion, the ICER of the combination regimen was 25,374.68 per QALY—still exceeding the PPP–aligned WTP of 20,243.85 per QALY (Table 7). PSA findings for this scenario showed a 24.86% probability of cost-effectiveness at the defined WTP threshold.

Sensitivity analysis

The OWSA results for the overall population and all subgroups in both China and the U.S. are presented in Figures 9–11. The ICER was most sensitive to variations in the cost of cadonilimab, utility values for the PFS and PD health states, and the proportion of patients receiving targeted therapy during subsequent treatment. Despite these

TABLE 6 The base case analysis.

Treatment	Cost	QALY	Incremental cost	Incremental QALY	INHB	INMB	ICER
Cadonilimab plus chemotherapy(China)	28528.60	1.01	16797.61	0.33	-0.08	-3396.52	50582.10
Chemotherapy(China)	11730.98	0.67					
Cadonilimab plus chemotherapy(CPS ≥5)(China)	32039.12	1.18	21999.87	0.59	0.04	1674.96	37499.27
Chemotherapy(CPS ≥5)(China)	10039.25	0.59					
Cadonilimab plus chemotherapy(CPS <5)(China)	27699.35	0.91	16349.88	0.25	-0.16	-6355.16	66013.60
Chemotherapy(CPS <5)(China)	11349.47	0.66					
Cadonilimab plus chemotherapy(US)	191469.60	1.04	101275.06	0.35	-0.33	-48981.29	290498.45
Chemotherapy(US)	90194.54	0.69					
Cadonilimab plus chemotherapy(CPS ≥5)(US)	225496.39	1.22	150226.89	0.62	-0.38	-56677.19	240877.66
Chemotherapy(CPS ≥5)(US)	75269.50	0.60					
Cadonilimab plus chemotherapy(CPS <5)(US)	190095.49	0.93	103745.44	0.26	-0.43	-64728.99	398852.61
Chemotherapy(CPS <5)(US)	86350.04	0.67					

QALY, Quality-adjusted life year; ICER, Incremental cost-effectiveness ratio; INMB, the incremental net monetary benefits; INHB, the incremental net health benefits; CPS, PD-L1 combined of positive score.

sensitivities, the differences in health outcomes between treatment strategies were sufficiently large that parameter variations did not alter the overall conclusions, except in the CPS ≥5 subgroup in China, where the ICER was influenced by changes in drug cost and health state utilities.

The PSA findings are shown in Figures 12–17. In a Chinese setting, the probability that cadonilimab plus chemotherapy would be cost-effective at the defined WTP threshold was 23.35% for the overall cohort, 64.37% for the CPS ≥5 subgroup, and 3.20% for the CPS <5 subgroup. In the U.S., the corresponding probabilities were 2.30% for the overall cohort, 1.48% for the CPS ≥5 subgroup, and 0.09% for the CPS <5 subgroup. These results further support the conclusion that cadonilimab plus chemotherapy offers limited economic value at the current price.

Discussion

Cadonilimab, the first PD-1/CTLA-4 bispecific antibody approved for solid tumors, demonstrated notable clinical efficacy in improving both OS and PFS in patients with unresectable or metastatic GC/GEJC, as shown in the COMPASSION-15 trial. Results from a Bayesian network meta-analysis further supported its superiority: cadonilimab plus chemotherapy offered the greatest OS and PFS benefits among various ICI-based regimens, including nivolumab, pembrolizumab, sintilimab, tislelizumab, and sugemalimab, for HER2-negative GC/GEJC patients with positive PD-L1 CPS (36). This advancement marks a significant milestone in the era of bispecific antibodies for solid tumor immunotherapy and may reshape the global immunotherapy landscape.

Despite this clinical promise, our cost-effectiveness analysis revealed that cadonilimab plus chemotherapy is not economically viable as first-line treatment for most GC/GEJC patient groups in China under current or projected pricing. This conclusion was validated by scenario analyses: both PPP-adjusted currency conversion and a 3% discount rate (as a sensitivity check) confirmed the robustness of the base-case findings. Notably, however, the combination regimen was cost-effective in the PD-L1 CPS ≥5 subgroup—with an ICER of $37,499.27 per QALY, below China's WTP threshold of $40,354.27. Corresponding INHB and INMB values were also positive, further supporting the use of cadonilimab in this clinically responsive population.

This subgroup-specific value is particularly relevant in the Chinese healthcare context, where cadonilimab has already undergone significant price reductions: following the 2024 national medical insurance negotiations, it was included in the 2025 national medical insurance catalog for cervical cancer (effective January 1, 2025). While GC/GEJC were not included in this round due to timing constraints, the rapid approval and price reduction of cadonilimab offer meaningful hope for GC/GEJC patients. Our findings provide strong evidence to support its future inclusion in medical insurance for GC/GEJC. This aligns with the broader landscape of ICIs' cost-effectiveness analysis in China: nivolumab and pembrolizumab have been shown to be uneconomical (37–39), while the economic value of tislelizumab, sugemalimab, and sintilimab remains controversial (33, 40–44) — consistent with our results.

Conversely, in the United States, the ICERs were $290,498.45, $240,877.66, and $398,852.61 per QALY for the overall population,

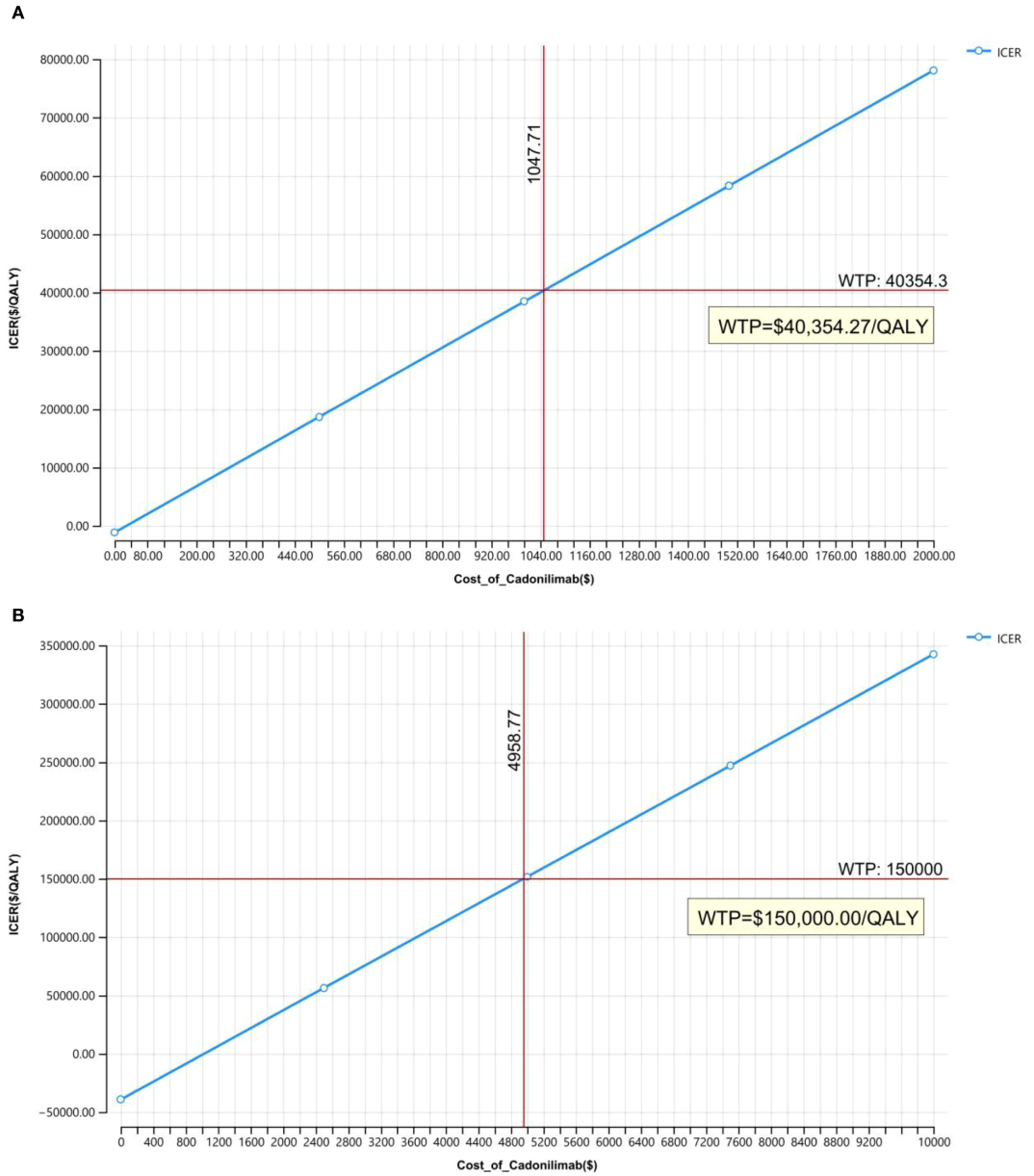

FIGURE 8
Price simulation: **(A)** China, **(B)** The U.S.

TABLE 7 Scenario analysis.

Treatment	Cost	QALY	Incremental cost	Incremental QALY	INHB	INMB	ICER
Cadonilimab plus chemotherapy(China)	29119.94	1.04	16970.62	0.35	-0.07	-2902.11	48678.70
Chemotherapy(China)	12149.32	0.69					
Cadonilimab plus chemotherapy(CPS ≥5) (China)	14311.46	1.01	8426.58	0.33	-0.08	-1703.88	25374.68
Chemotherapy(CPS ≥5)(China)	5884.89	0.67					

QALY, Quality-adjusted life year; ICER, Incremental cost-effectiveness ratio; INMB, the incremental net monetary benefits; INHB, the incremental net health benefits; CPS, PD-L1 combined of positive score.

FIGURE 9
The tornado diagram of one-way sensitivity analysis: **(A)** China, **(B)** The U.S.

CPS ≥5, and CPS <5 groups, respectively—all well above the $150,000.00 WTP threshold. This is consistent with prior findings that pembrolizumab, nivolumab, and tislelizumab also lack economic viability in the U.S. GC/GEJC setting (39, 45–47). Notably, our ICER for cadonilimab is relatively closer to the U.S. WTP threshold than other ICIs, suggesting that further Network Meta-analyses or real-world studies may help clarify its comparative economic value.

Although cadonilimab has already undergone significant price reductions in China, its price remains undetermined in many other markets. Ongoing global trade tensions and tariff policies, particularly between China and the U.S., add to pricing uncertainty, potentially

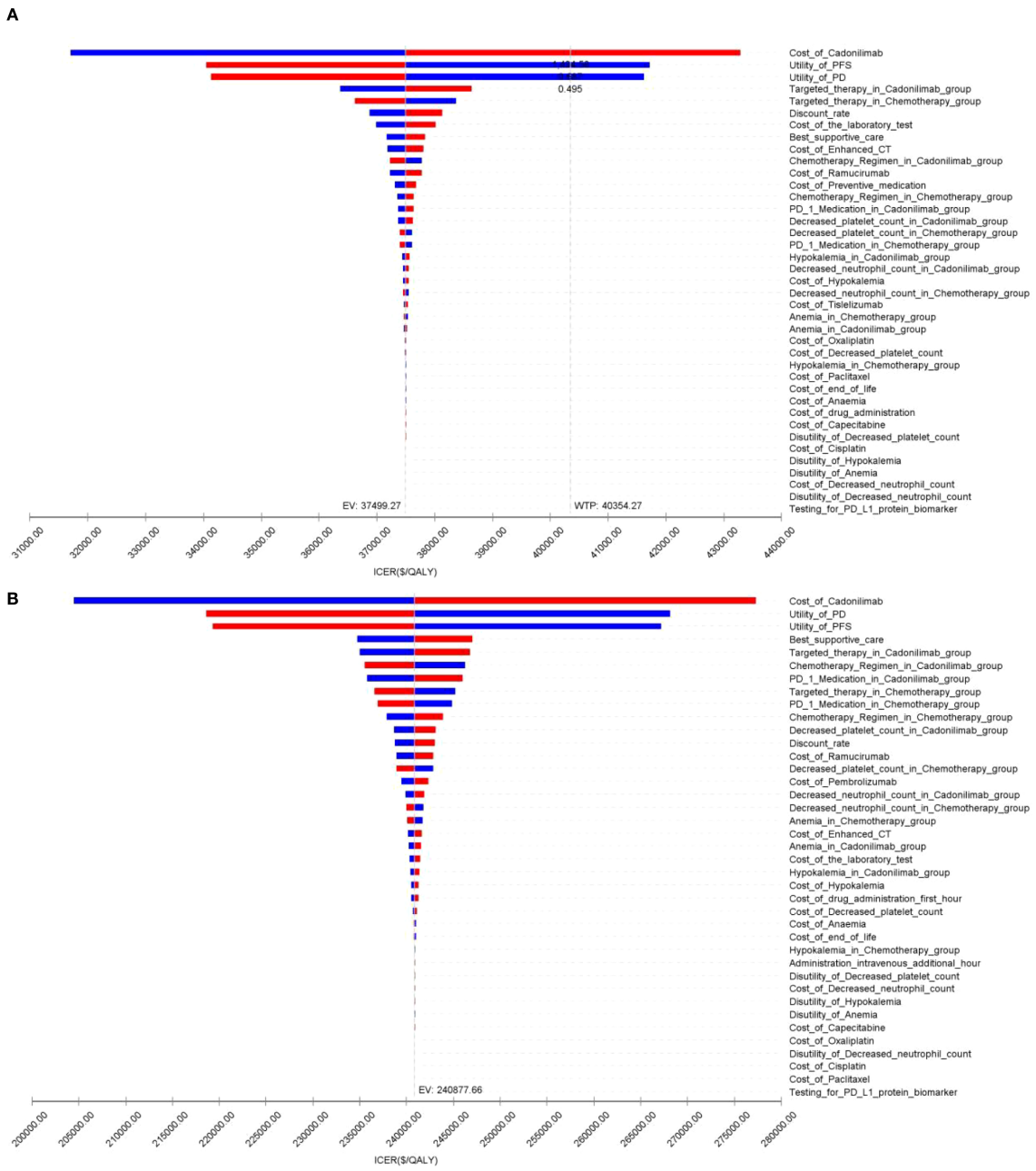

FIGURE 10
The tornado diagram of one-way sensitivity analysis in CPS ≥5 group: **(A)** China, **(B)** The U.S.

limiting access to high-value cancer therapies. Our price simulation provides important insights into pricing thresholds that could render cadonilimab cost-effective: below $1,047.71 per cycle in China and $4,958.77 per cycle in the U.S. Clinically, given its demonstrated safety and efficacy advantages (and lack of obvious economic disadvantages in select subgroups), we recommend that physicians tailor treatment plans to patients' disease profiles (e.g., PD-L1 status) and financial capacities—prioritizing the most effective regimens when affordable. These findings can inform health insurance reimbursement adjustments and guide drug tiering in clinical practice guidelines.

Sensitivity analyses identified the cost of cadonilimab and utility values for PFS and PD as the most influential parameters on the ICER, highlighting the critical role of drug pricing and patient

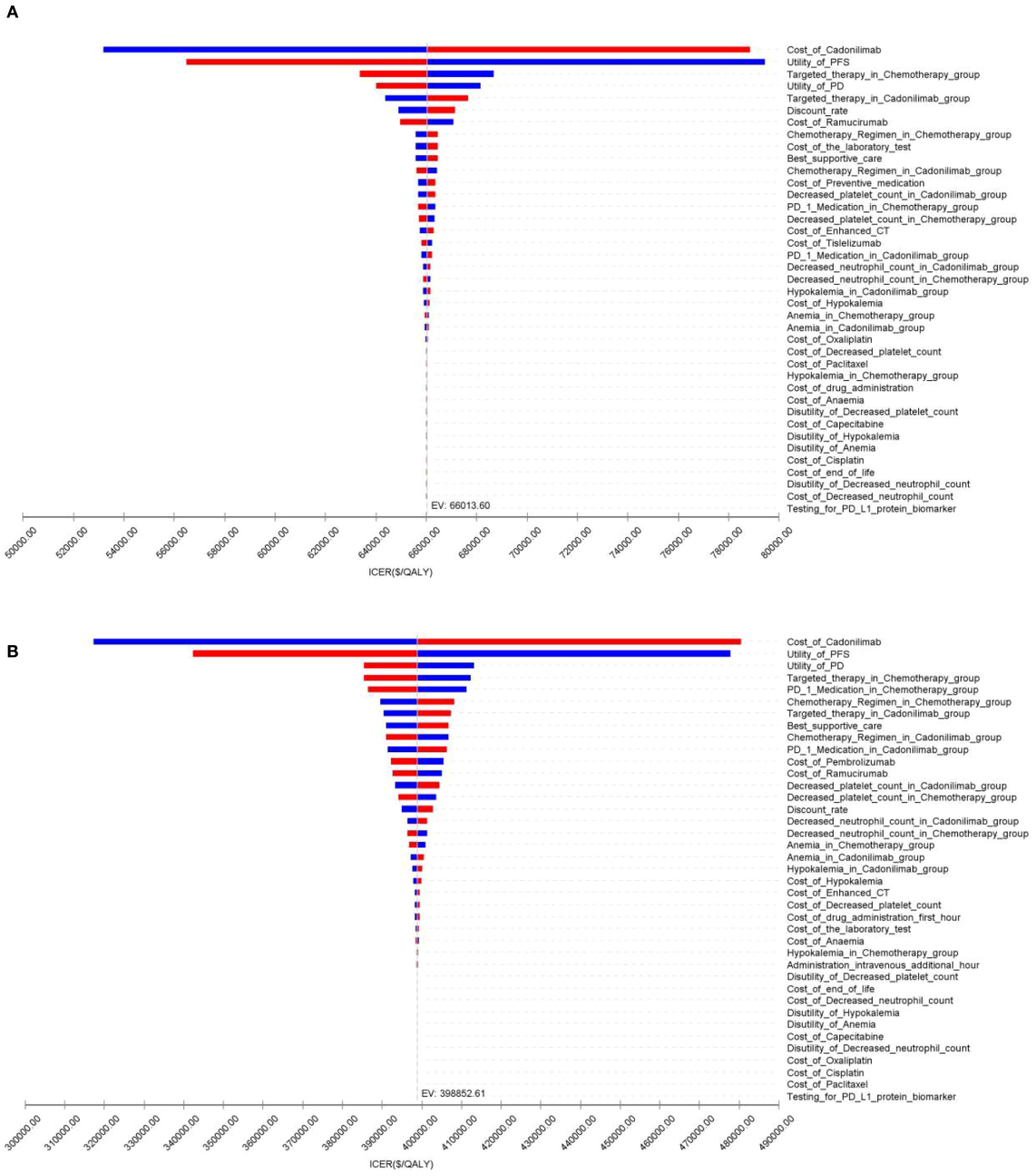

FIGURE 11
The tornado diagram of one-way sensitivity analysis in CPS <5 group: **(A)** China, **(B)** The U.S.

quality of life in determining economic value. The very low cost-effectiveness probabilities observed in the PSA further validated the robustness of our base-case conclusions.

To our knowledge, this study is the first to assess the cost-effectiveness of cadonilimab, a second-generation PD-1 inhibitor, combined with chemotherapy as a first-line therapy for GC/GEJC from both the U.S. and Chinese payer perspectives. Importantly, key model parameters (e.g., utility values, costs of best supportive care, and end-of-life care) were derived from GC/GEJC-specific studies to minimize input uncertainty.

Nonetheless, this study has several limitations that must be acknowledged. First, the clinical trial data used for modeling were derived exclusively from a Chinese population, which may limit their applicability to U.S. healthcare systems. Second, the model was based on data from a controlled clinical trial, which introduced inherent uncertainty. Although real-world patients

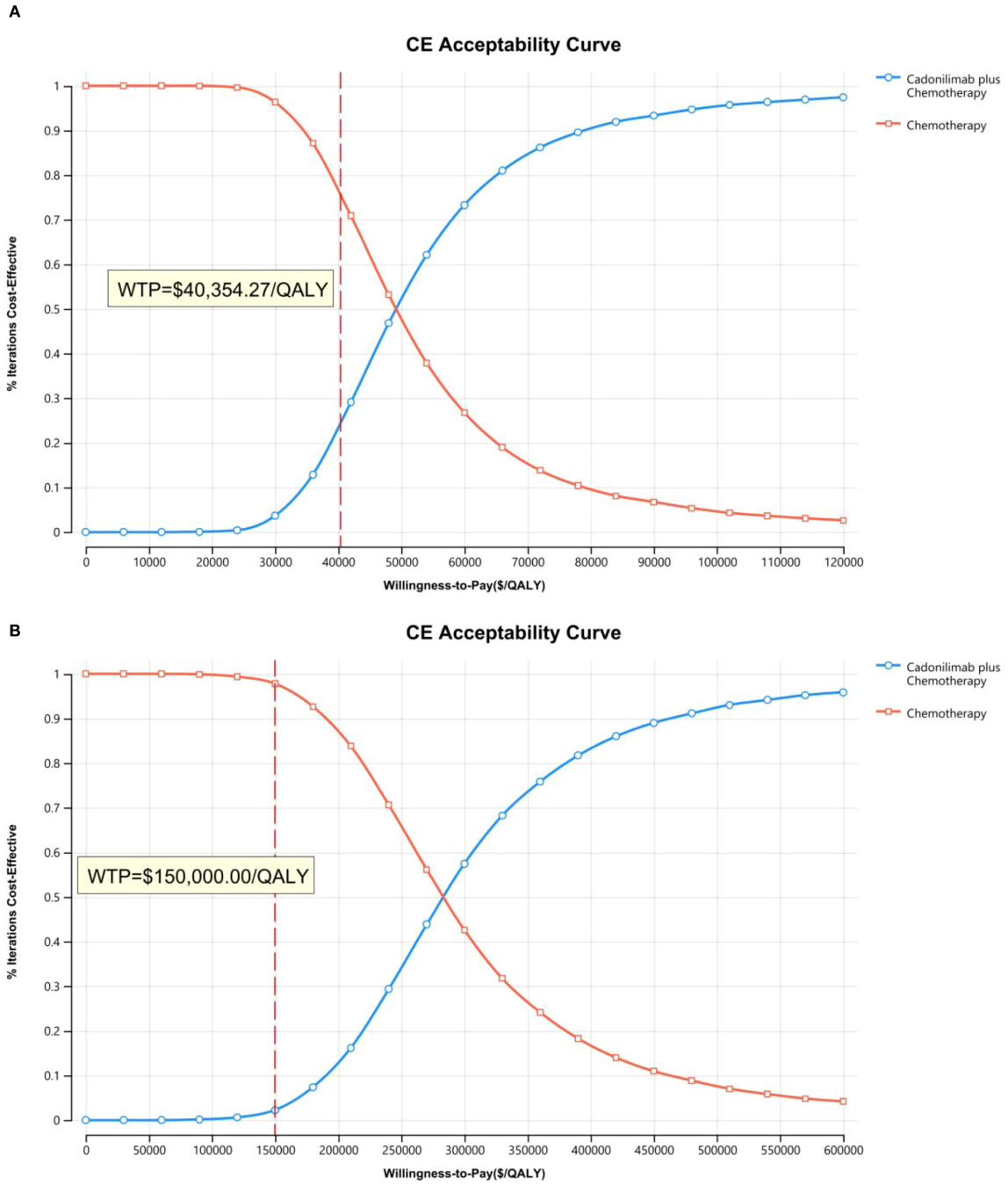

FIGURE 12
The cost-effectiveness acceptability curve: **(A)** China, **(B)** The U.S.

often receive multiple lines of therapy, our model incorporates only up to second-line treatment, potentially introducing bias. Lastly, subsequent treatment proportions were reported at the single-agent level, which may have affected the accuracy of the post-progression cost estimates. Future studies that incorporate broader real-world data are required to validate and refine these findings.

Conclusions

In China, cadonilimab combined with chemotherapy was cost-effective in patients with PD-L1 CPS ≥5, with an ICER of $37,499.27 per QALY—below the national WTP threshold of $40,354.27 per QALY. However, at current or projected prices, the therapy exceeded the WTP thresholds for all other subgroups in both

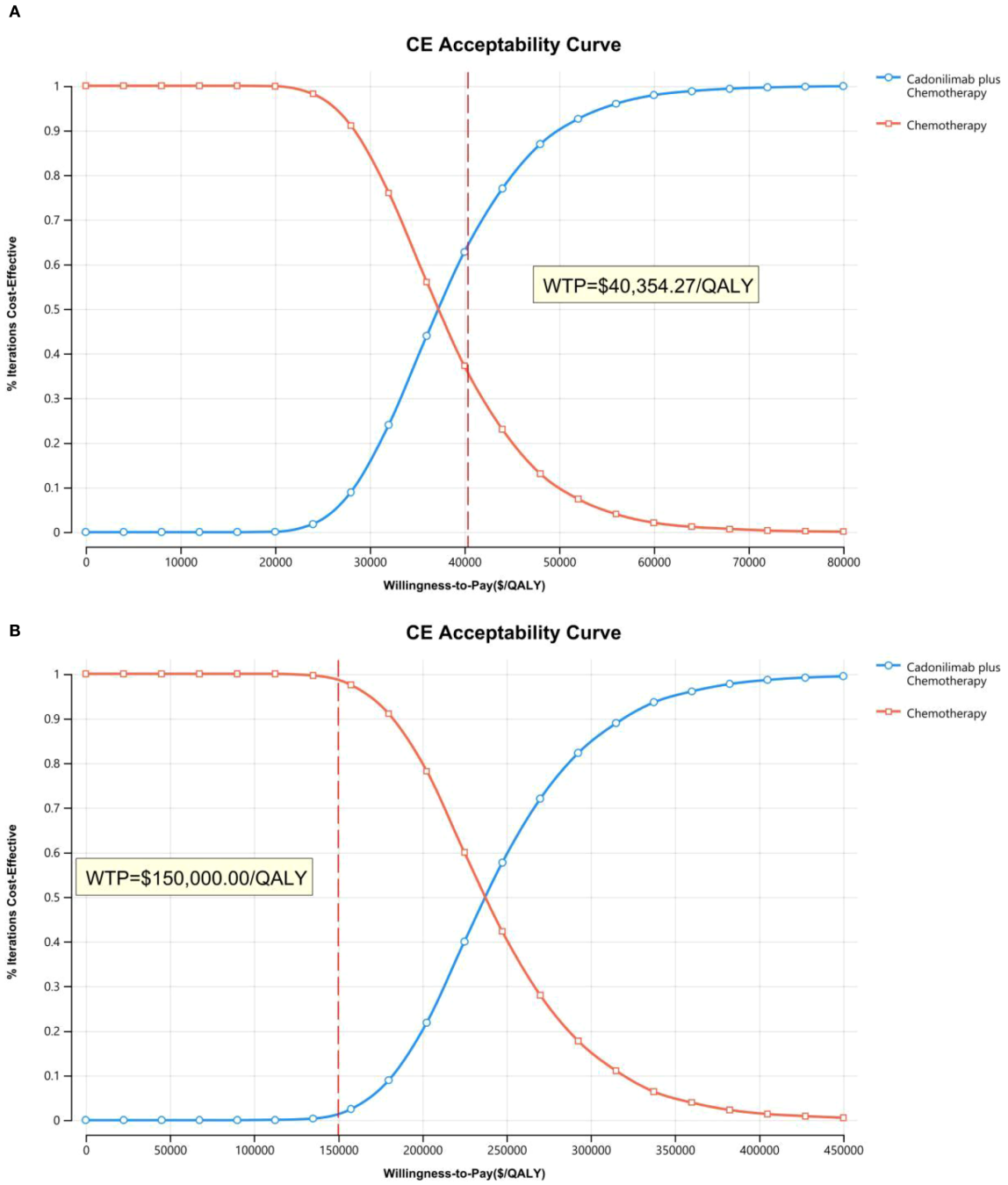

FIGURE 13
The cost-effectiveness acceptability curve in CPS ≥5 group: **(A)** China, **(B)** The U.S.

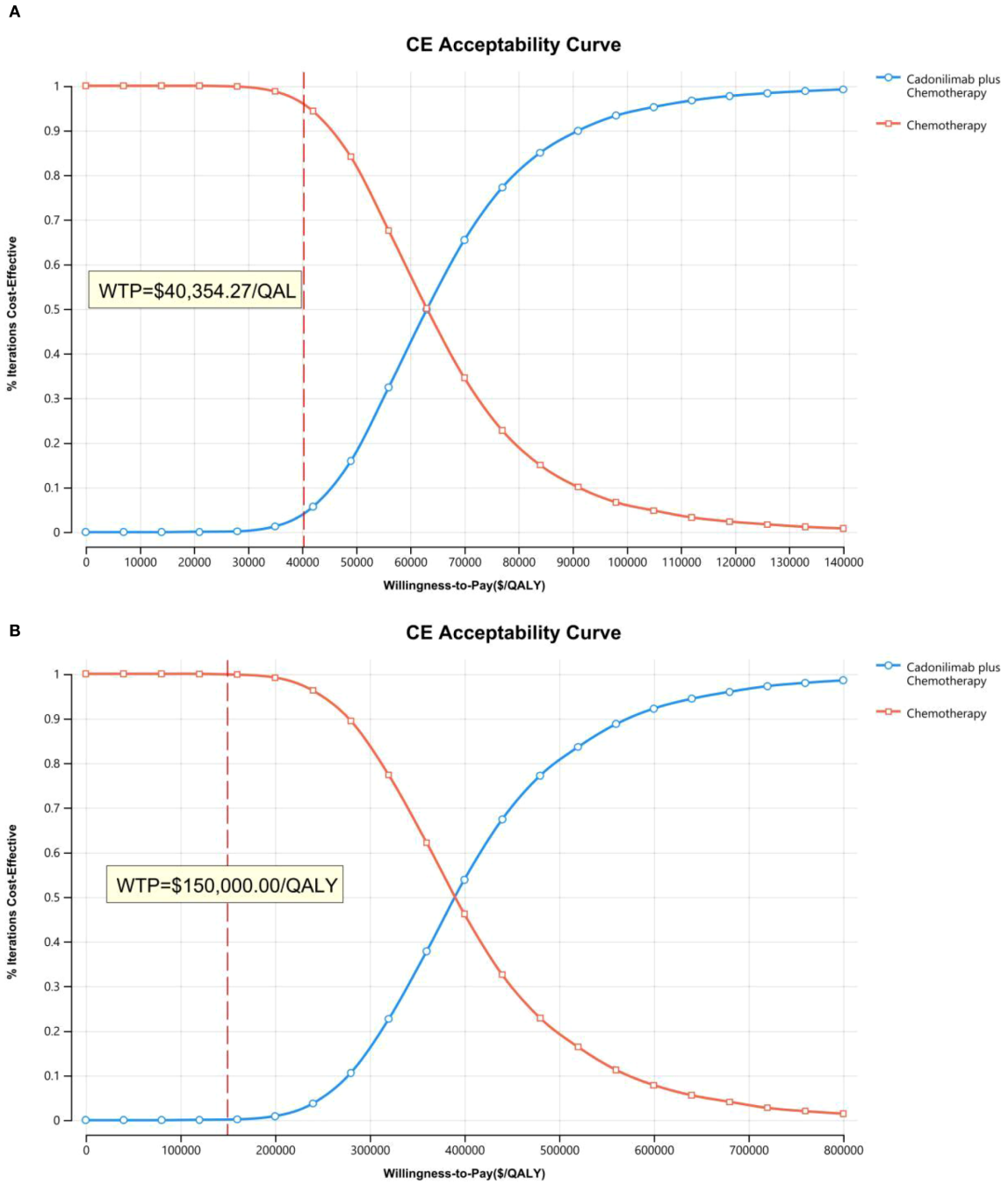

FIGURE 14
The cost-effectiveness acceptability curve in CPS <5 group: **(A)** China, **(B)** The U.S.

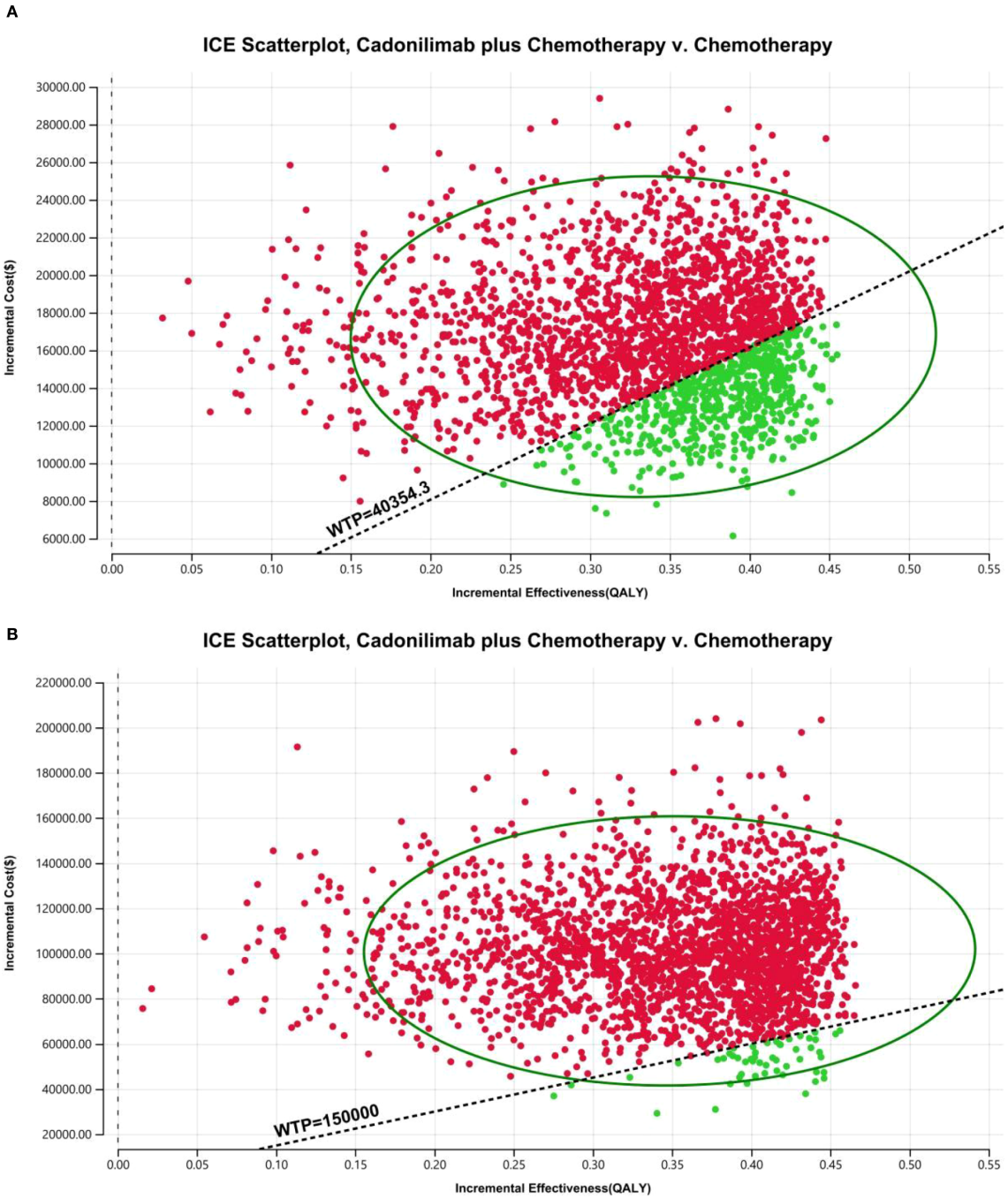

FIGURE 15
The cost-effectiveness probabilistic scatter plot: **(A)** China, **(B)** The U.S.

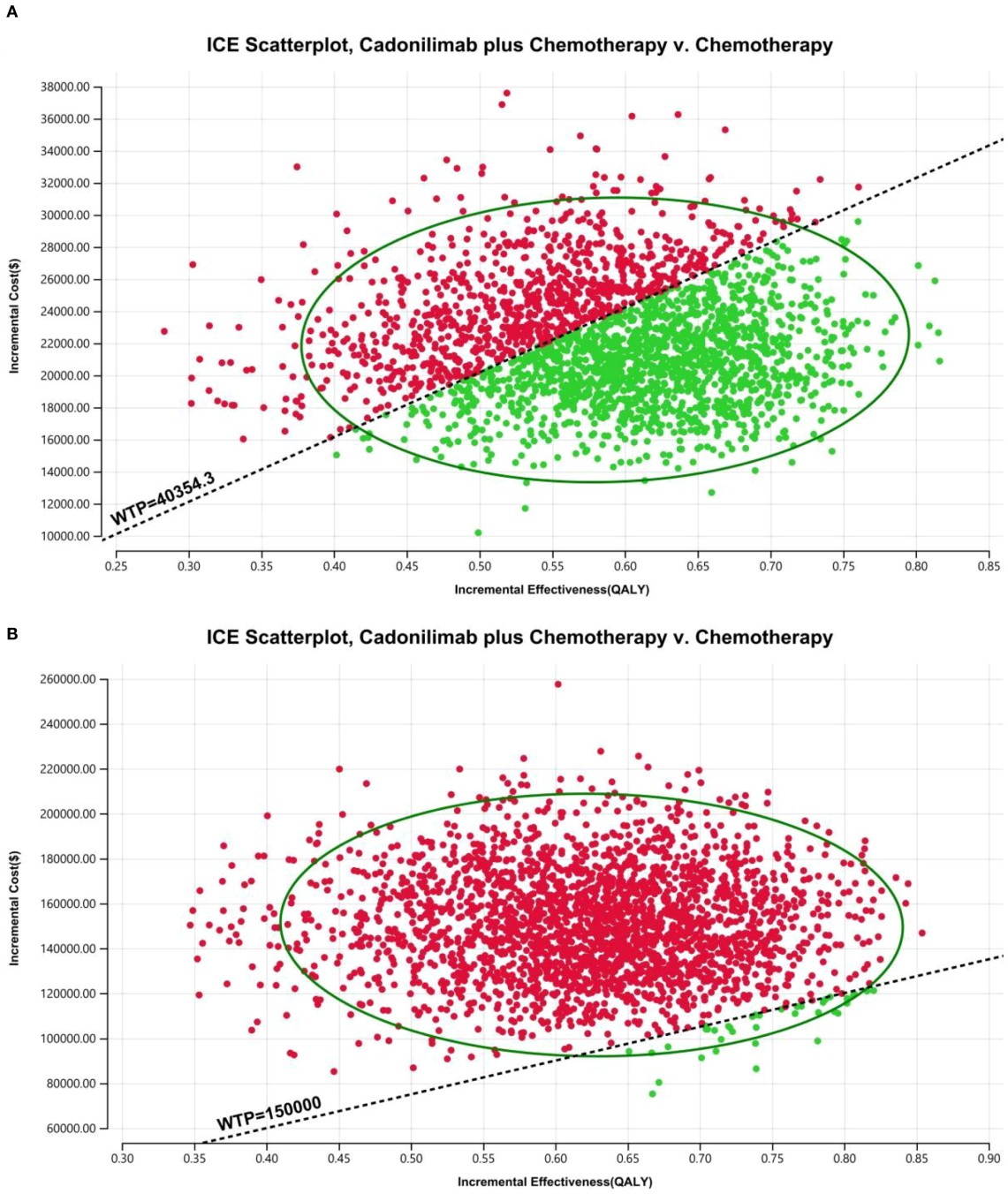

FIGURE 16
The cost-effectiveness probabilistic scatter plot in CPS ≥5 group: **(A)** China, **(B)** The U.S.

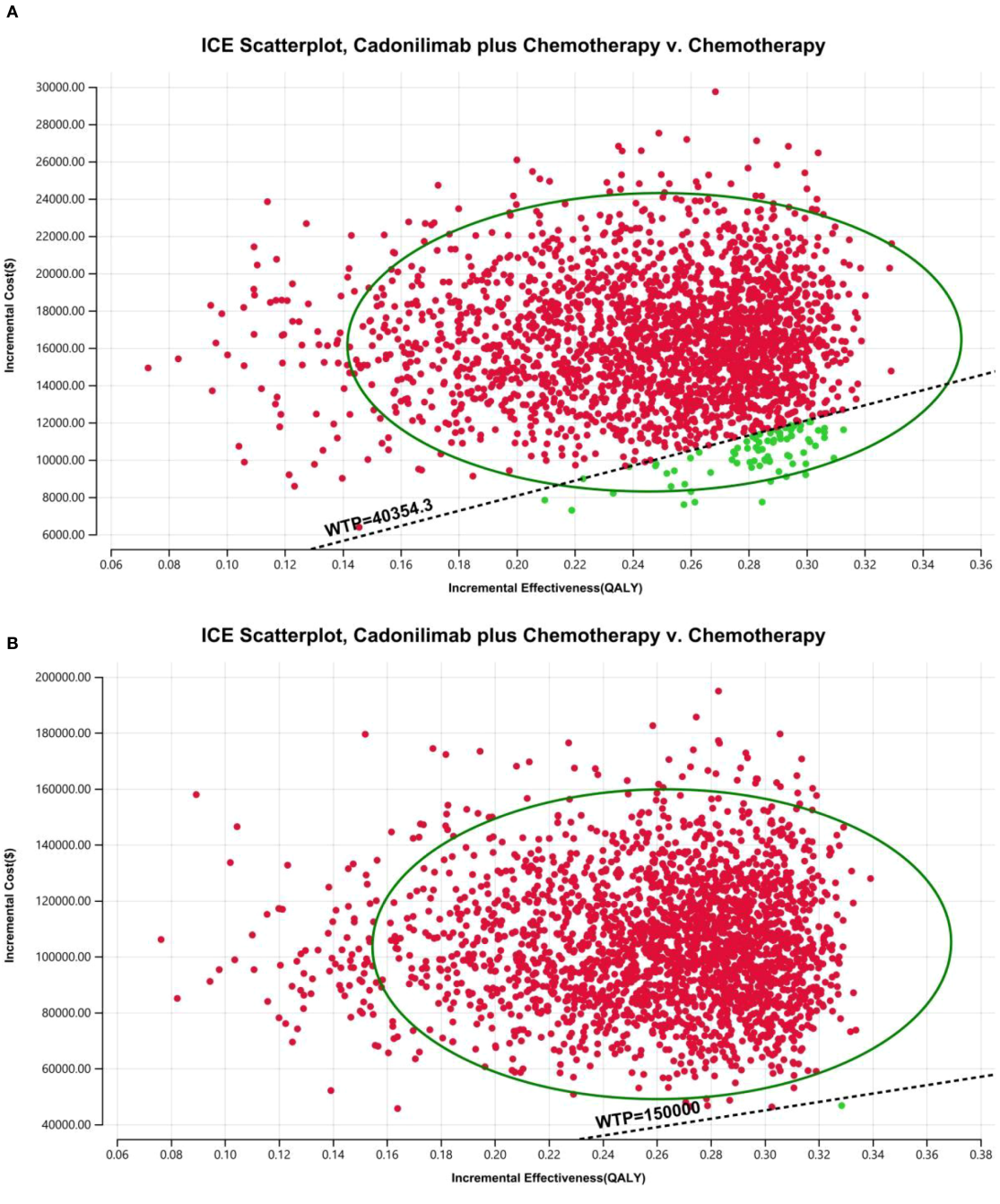

FIGURE 17
The cost-effectiveness probabilistic scatter plot in CPS <5 group: **(A)** China, **(B)** The U.S.

China and the United States. These findings highlight the need to align clinical innovations with economic value to inform rational and equitable oncological treatment decisions.

Data availability statement

The raw data supporting the conclusions of this article will be made available by the authors, without undue reservation.

Author contributions

WL: Writing – review & editing, Supervision, Investigation, Data curation, Methodology, Software, Conceptualization, Writing – original draft, Resources, Project administration, Validation, Funding acquisition, Formal analysis, Visualization. LM: Conceptualization, Software, Writing – original draft, Data curation. QX: Conceptualization, Writing – original draft, Data curation, Methodology. ZZ: Visualization, Conceptualization, Writing – review & editing, Data curation, Supervision. HJ: Conceptualization, Writing – original draft, Methodology, Formal analysis, Data curation. XZ: Methodology, Data curation, Software, Conceptualization, Writing – original draft.

Funding

The author(s) declare that no financial support was received for the research and/or publication of this article.

Conflict of interest

The authors declare that the research was conducted in the absence of any commercial or financial relationships that could be construed as a potential conflict of interest.

Generative AI statement

The author(s) declare that no Generative AI was used in the creation of this manuscript.

Any alternative text (alt text) provided alongside figures in this article has been generated by Frontiers with the support of artificial intelligence and reasonable efforts have been made to ensure accuracy, including review by the authors wherever possible. If you identify any issues, please contact us.

Publisher's note

Supplementary material

The Supplementary Material for this article can be found online at: https://www.frontiersin.org/articles/10.3389/fimmu.2025.1618726/full#supplementary-material

References

1. Smyth EC, Nilsson M, Grabsch HI, van Grieken NC, Lordick F. Gastric cancer. *Lancet*. (2020) 396:635–48. doi: 10.1016/s0140-6736(20)31288-5

2. Sung H, Ferlay J, Siegel RL, Laversanne M, Soerjomataram I, Jemal A, et al. Global cancer statistics 2020: globocan estimates of incidence and mortality worldwide for 36 cancers in 185 countries. *CA Cancer J Clin*. (2021) 71:209–49. doi: 10.3322/caac.21660

3. Han B, Zheng R, Zeng H, Wang S, Sun K, Chen R, et al. Cancer incidence and mortality in China, 2022. *J Natl Cancer Cent*. (2024) 4:47–53. doi: 10.1016/j.jncc.2024.01.006

4. Siegel RL, Kratzer TB, Giaquinto AN, Sung H, Jemal A. Cancer statistics, 2025. *CA Cancer J Clin*. (2025) 75:10–45. doi: 10.3322/caac.21871

5. Van Cutsem E, Bang YJ, Feng-Yi F, Xu JM, Lee KW, Jiao SC, et al. Her2 screening data from toga: targeting her2 in gastric and gastroesophageal junction cancer. *Gastric Cancer*. (2015) 18:476–84. doi: 10.1007/s10120-014-0402-y

6. Abrahao-MaChado LF, Scapulatempo-Neto C. Her2 testing in gastric cancer: an update. *World J Gastroenterol*. (2016) 22:4619–25. doi: 10.3748/wjg.v22.i19.4619

7. Rha SY, Oh DY, Yañez P, Bai Y, Ryu MH, Lee J, et al. Pembrolizumab plus chemotherapy versus placebo plus chemotherapy for her2-negative advanced gastric cancer (Keynote-859): A multicentre, randomised, double-blind, phase 3 trial. *Lancet Oncol*. (2023) 24:1181–95. doi: 10.1016/s1470-2045(23)00515-6

8. Qiu MZ, Oh DY, Kato K, Arkenau T, Tabernero J, Correa MC, et al. Tislelizumab plus chemotherapy versus placebo plus chemotherapy as first line treatment for advanced gastric or gastro-oesophageal junction adenocarcinoma: rationale-305 randomised, double blind, phase 3 trial. *Bmj*. (2024) 385:e078876. doi: 10.1136/bmj-2023-078876

9. Zhang X, Wang J, Wang G, Zhang Y, Fan Q, Lu C, et al. First-line sugemalimab plus chemotherapy for advanced gastric cancer: the gemstone-303 randomized clinical trial. *Jama*. (2025) 333:1305–14. doi: 10.1001/jama.2024.28463

10. Janjigian YY, Shitara K, Moehler M, Garrido M, Salman P, Shen L, et al. First-line nivolumab plus chemotherapy versus chemotherapy alone for advanced gastric, gastro-oesophageal junction, and oesophageal adenocarcinoma (Checkmate 649): A randomised, open-label, phase 3 trial. *Lancet*. (2021) 398:27–40. doi: 10.1016/s0140-6736(21)00797-2

11. Xu J, Jiang H, Pan Y, Gu K, Cang S, Han L, et al. Sintilimab plus chemotherapy for unresectable gastric or gastroesophageal junction cancer: the orient-16 randomized clinical trial. *Jama*. (2023) 330:2064–74. doi: 10.1001/jama.2023.19918

12. Pang X, Huang Z, Zhong T, Zhang P, Wang ZM, Xia M, et al. Cadonilimab, a tetravalent pd-1/ctla-4 bispecific antibody with trans-binding and enhanced target binding avidity. *MAbs*. (2023) 15:2180794. doi: 10.1080/19420862.2023.2180794

13. Gao X, Xu N, Li Z, Shen L, Ji K, Zheng Z, et al. Safety and antitumour activity of cadonilimab, an anti-pd-1/ctla-4 bispecific antibody, for patients with advanced solid tumours (Compassion-03): A multicentre, open-label, phase 1b/2 trial. *Lancet Oncol*. (2023) 24:1134–46. doi: 10.1016/s1470-2045(23)00411-4

14. Gao X, Ji K, Jia Y, Shan F, Chen Y, Xu N, et al. Cadonilimab with chemotherapy in her2-negative gastric or gastroesophageal junction adenocarcinoma: the phase 1b/2 compassion-04 trial. *Nat Med*. (2024) 30:1943–51. doi: 10.1038/s41591-024-03007-5

15. Shen L, Zhang Y, Li Z, Zhang X, Gao X, Liu B, et al. First-line cadonilimab plus chemotherapy in her2-negative advanced gastric or gastroesophageal junction adenocarcinoma: A randomized, double-blind, phase 3 trial. *Nat Med*. (2025) 31:1163–70. doi: 10.1038/s41591-024-03450-4

16. Ajani JA, D'Amico TA, Bentrem DJ, Corvera CU, Das P, Enzinger PC, et al. Gastric cancer, version 2.2025, nccn clinical practice guidelines in oncology. *J Natl Compr Canc Netw*. (2025) 23:169–91. doi: 10.6004/jnccn.2025.0022

17. Husereau D, Drummond M, Augustovski F, de Bekker-Grob E, Briggs AH, Carswell C, et al. Consolidated health economic evaluation reporting standards 2022

(Cheers 2022) statement: updated reporting guidance for health economic evaluations. *Clin Ther*. (2022) 44:158–68. doi: 10.1016/j.clinthera.2022.01.011

18. Wang FH, Zhang XT, Tang L, Wu Q, Cai MY, Li YF, et al. The chinese society of clinical oncology (Csco): clinical guidelines for the diagnosis and treatment of gastric cancer, 2023. *Cancer Commun (Lond)*. (2024) 44:127–72. doi: 10.1002/cac2.12516

19. Zhang M, Wen F, He X, Zhang W, Hu J, Li Q. Adjuvant chemoradiotherapy for gastric cancer: efficacy and cost-effectiveness analysis. *Front Oncol*. (2019) 9:1357. doi: 10.3389/fonc.2019.01357

20. Wu B, Li T, Cai J, Xu Y, Zhao G. Cost-effectiveness analysis of adjuvant chemotherapies in patients presenting with gastric cancer after D2 gastrectomy. *BMC Cancer*. (2014) 14:984. doi: 10.1186/1471-2407-14-984

21. Liu L, Wang L, Chen L, Ding Y, Zhang Q, Shu Y. Cost-effectiveness of sintilimab plus chemotherapy versus chemotherapy alone as first-line treatment of locally advanced or metastatic oesophageal squamous cell carcinoma. *Front Immunol*. (2023) 14:1092385. doi: 10.3389/fimmu.2023.1092385

22. Zhu Y, Liu K, Zhu H, Wu H. Immune checkpoint inhibitors plus chemotherapy for her2-negative advanced gastric/gastroesophageal junction cancer: A cost-effectiveness analysis. *Therap Adv Gastroenterol*. (2023) 16:17562848231207200. doi: 10.1177/17562848231207200

23. Meng R, Zhang X, Zhou T, Luo M, Qiu Y. Cost-effectiveness analysis of donafenib versus lenvatinib for first-line treatment of unresectable or metastatic hepatocellular carcinoma. *Expert Rev Pharmacoecon Outcomes Res*. (2022) 22:1079–86. doi: 10.1080/14737167.2022.2079498

24. Shiroiwa T, Fukuda T, Shimozuma K. Cost-effectiveness analysis of trastuzumab to treat her2-positive advanced gastric cancer based on the randomised toga trial. *Br J Cancer*. (2011) 105:1273–8. doi: 10.1038/bjc.2011.390

25. Dieleman JL, Cao J, Chapin A, Chen C, Li Z, Liu A, et al. Us health care spending by payer and health condition, 1996-2016. *Jama*. (2020) 323:863–84. doi: 10.1001/jama.2020.0734

26. Su D, Wu B, Shi L. Cost-effectiveness of atezolizumab plus bevacizumab vs sorafenib as first-line treatment of unresectable hepatocellular carcinoma. *JAMA Netw Open*. (2021) 4:e210037. doi: 10.1001/jamanetworkopen.2021.0037

27. Yue X, Li Y, Wu J, Guo JJ. Current development and practice of pharmacoeconomic evaluation guidelines for universal health coverage in China. *Value Health Reg Issues*. (2021) 24:1–5. doi: 10.1016/j.vhri.2020.07.580

28. Shao T, Zhao M, Liang L, Tang W. Serplulimab plus chemotherapy vs chemotherapy for treatment of us and chinese patients with extensive-stage small-cell lung cancer: A cost-effectiveness analysis to inform drug pricing. *BioDrugs*. (2023) 37:421–32. doi: 10.1007/s40259-023-00586-6

29. Murray CJ, Evans DB, Acharya A, Baltussen RM. Development of who guidelines on generalized cost-effectiveness analysis. *Health Econ*. (2000) 9:235–51. doi: 10.1002/(sici)1099-1050(200004)9:3<235::aid-hec502>3.0.co;2-o

30. Latimer NR. Survival analysis for economic evaluations alongside clinical trials–extrapolation with patient-level data: inconsistencies, limitations, and a practical guide. *Med Decis Making*. (2013) 33:743–54. doi: 10.1177/0272989x12472398

31. Rulli E, Ghilotti F, Biagioli E, Porcu L, Marabese M, D'Incalci M, et al. Assessment of proportional hazard assumption in aggregate data: A systematic review on statistical methodology in clinical trials using time-to-event endpoint. *Br J Cancer*. (2018) 119:1456–63. doi: 10.1038/s41416-018-0302-8

32. Chueh CH, Tsai YW, Chen ZR, Shiu MN, Wen YW, Chiang NJ. Cost-effectiveness analysis of a new second-line treatment regimen for advanced intrahepatic cholangiocarcinoma: biomarker-driven targeted therapy of pemigatinib versus 5-fu chemotherapy. *Pharmacoeconomics*. (2023) 41:307–19. doi: 10.1007/s40273-022-01227-6

33. Lang W, Ai Q, Zhang W, Jiang Q, He Y, Ouyang M. Cost-effectiveness analysis of tislelizumab plus chemotherapy versus placebo plus chemotherapy as first-line treatment for advanced gastric or gastroesophageal junction adenocarcinoma: perspectives from the United States and China. *Front Pharmacol*. (2024) 15:1461571. doi: 10.3389/fphar.2024.1461571

34. Centers_for_Medicare_and_Medicaid_Services. Medicare Physician Fee Schedule Look-up Tool: Centers for Medicare and Medicaid Services (2025). Available online at: https://www.cms.gov/medicare/physicianfee-schedule/search (Accessed January 17, 2025).

35. Wong W, Yim YM, Kim A, Cloutier M, Gauthier-Loiselle M, Gagnon-Sanschagrin P, et al. Assessment of costs associated with adverse events in patients with cancer. *PLoS One*. (2018) 13:e0196007. doi: 10.1371/journal.pone.0196007

36. Zhang W, Guo K, Zheng S. Immunotherapy combined with chemotherapy in the first-line treatment of advanced gastric cancer: systematic review and bayesian network meta-analysis based on specific pd-L1 cps. *Curr Oncol*. (2025) 32(2):Epub 20250216. doi: 10.3390/curroncol32020112

37. Jiang Y, Li Y, Wang LXW. Cost-effectiveness analysis of nivolumab plus standard chemotherapy versus chemotherapy alone for the first-line treatment of unresectable advanced or metastatic gastric cancer, gastroesophageal junction cancer, and esophageal adenocarcinoma. *Int J Clin Pharm*. (2022) 44:499–506. doi: 10.1007/s11096-021-01372-6

38. Lang Y, Lin Y, Li D, Liu J, Liu X. Pembrolizumab alone or in combination with chemotherapy versus chemotherapy for advanced gastric cancer: A cost-effectiveness analysis. *Cancer Med*. (2023) 12:18447–59. doi: 10.1002/cam4.6389

39. Lang W, Deng L, Lu M, Ouyang M. Cost-effectiveness analysis of pembrolizumab plus chemotherapy versus placebo plus chemotherapy for her2-negative advanced gastric/gastroesophageal junction cancer in the chinese healthcare system. *Expert Rev Pharmacoecon Outcomes Res*. (2024) 24:1027–42. doi: 10.1080/14737167.2024.2378983

40. Li W, Wan L, Zhang J. Cost-effectiveness of tislelizumab plus chemotherapy vs chemotherapy as first-line treatment of pd-L1 positive advanced gastric or gastroesophageal junction adenocarcinoma from a chinese perspective. *Expert Rev Gastroenterol Hepatol*. (2024) 18:293–301. doi: 10.1080/17474124.2024.2373730

41. Tang L, Zhu L, Zhan S, Chen Y, Feng PF. Cost-effectiveness analysis of sugemalimab combined with chemotherapy as first-line treatment for advanced gastric cancer. *Front Public Health*. (2025) 13:1620663. doi: 10.3389/fpubh.2025.1620663

42. Xu L, Long Y, Yao L, Wang H, Ge W. Updated cost-effectiveness analysis of tislelizumab in combination with chemotherapy for the first-line treatment of advanced gastric cancer or gastroesophageal junction adenocarcinoma. *Front Oncol*. (2024) 14:1477722. doi: 10.3389/fonc.2024.1477722

43. Xiang Z, Ma L, Fu Y, Pan Y. Cost-effectiveness analysis of first-line sintilimab plus chemotherapy vs. Chemotherapy alone for unresectable advanced or metastatic gastric or gastroesophageal junction cancer in China. *Front Pharmacol*. (2024) 15:1411571. doi: 10.3389/fphar.2024.1411571

44. Zheng Z, Song X, Cai H, Zhu H. Pembrolizumab combined with chemotherapy versus placebo combined with chemotherapy for her2-negative advanced gastric cancer in China: A cost-effectiveness analysis. *Expert Rev Pharmacoecon Outcomes Res*. (2024) 24:1017–25. doi: 10.1080/14737167.2024.2378986

45. Cao X, Zhang M, Li N, Zheng B, Liu M, Song X, et al. First-line nivolumab plus chemotherapy versus chemotherapy alone for advanced gastric cancer, gastroesophageal junction cancer, and esophageal adenocarcinoma: A cost-effectiveness analysis. *Ther Adv Med Oncol*. (2023) 15:17588359231171038. doi: 10.1177/17588359231171038

46. Marupuru S, Arku D, Axon DR, Villa-Zapata L, Yaghoubi M, Slack MK, et al. Cost-effectiveness analysis of nivolumab-chemotherapy as first-line therapy for locally advanced/metastatic gastric cancer: A United States payer perspective. *Expert Rev Pharmacoecon Outcomes Res*. (2023) 23:831–41. doi: 10.1080/14737167.2023.2219448

47. Zhang PF, Shi XQ, Li Q. Nivolumab plus chemotherapy versus chemotherapy alone as first-line treatment for advanced gastric, gastroesophageal junction, and esophageal adenocarcinoma: A cost-effectiveness analysis. *Cost Eff Resour Alloc*. (2023) 21:65. doi: 10.1186/s12962-023-00476-2

Frontiers in Immunology

Explores novel approaches and diagnoses to treat immune disorders.

The official journal of the International Union of Immunological Societies (IUIS) and the most cited in its field, leading the way for research across basic, translational and clinical immunology.

Discover the latest Research Topics

See more →

Frontiers

Avenue du Tribunal-Fédéral 34
1005 Lausanne, Switzerland
frontiersin.org

Contact us

+41 (0)21 510 17 00
frontiersin.org/about/contact